

European Centre for Training and Research in Earthquake Engineering

Research Report EUCENTRE - 2014/01

**Characterising the Seismic Behaviour of Steel Beam-Column
Joints for Seismic Design**

Edited by

Timothy J. Sullivan

Gerard J. O'Reilly

EUCENTRE
via Ferrata 1, 27100 Pavia, Italy

November, 2014

ABSTRACT

Following their favourable performance during the 1906 San Francisco earthquake, moment resisting frames (MRFs) became a widely used lateral resisting system for seismic design. However, poor performance of MRF beam-column joints during the 1994 Northridge earthquake in the US led to widespread failures and huge economic losses, highlighting the need for proper detailing of beam-column joints in steel MRFs. The joint types permitted in Europe can be subdivided in terms of strength; being either full or partial strength, and in terms of their stiffness; being either rigid or flexible. However, there is currently relatively limited guidance available for engineers wishing to demonstrate that a partial-strength beam-column joint meets the code-specified performance criteria, and it may often be concluded that experimental testing is required in order for a partial-strength joint to be deemed acceptable. Considering the above remarks, the European Research Fund for Coal and Steel has provided financial support for the DiSTEEL project, which is aiming to deliver a set of practical performance-based design guidelines for steel MRF structures. The objective of this report is to characterise the seismic behaviour of beam-column joints employed in MRF structures and provide simplified design tools to permit the seismic design of the various joint typologies.

This report first collects a total of 76 sets of experimental data on both fully welded and extended end-plate connections available in the literature for the calibration of numerical models. Using these, a series of parametric studies are conducted, which has resulted in a series of simplified design tools being proposed. Among these are, simplified expressions to determine connection yield drift, plastic resistance and plastic rotation capacities of partial strength and flexible joints. In addition, a set of spectral displacement reduction expressions have been proposed to permit the displacement-based design of MRFs to take the variation in connection behaviour into account during the design process.

Overall, this report provides a valuable contribution to the state-of-the-art as it moves towards providing simplified tools and guidelines for the design and analysis of various beam-column joint types employed in steel MRFs and aims to incorporate the design of such joint details into the displacement-based design methodology.

ACKNOWLEDGEMENTS

The authors gratefully acknowledge that the research leading to these results has received funding from the European Community's Research Fund for Coal and Steel (RFCS) under grant agreement n° [RFSR-CT-2010-00029].

TABLE OF CONTENTS

ABSTRACT.....	i
ACKNOWLEDGEMENTS.....	iii
TABLE OF CONTENTS.....	v
LIST OF TABLES	ix
LIST OF FIGURES.....	xi
LIST OF SYMBOLS	xix
1. INTRODUCTION	1
1.1 IMPORTANCE OF BEAM-COLUMN JOINT BEHAVIOUR AS OBSERVED AFTER PAST EARTHQUAKES	1
1.2 STEEL BEAM-COLUMN JOINT CONSIDERATIONS IN EUROPE	2
1.3 OBJECTIVES AND SCOPE OF THIS REPORT	3
1.4 REFERENCES.....	4
2. DISPLACEMENT-BASED SEISMIC DESIGN	5
2.1 OVERVIEW OF THE BASIC METHODOLOGY.....	5
2.2 DISPLACEMENT-BASED DESIGN OF MDOF SYSTEMS.....	8
2.3 INFORMATION REQUIRED FOR THE DBD OF STEEL MOMENT RESISTING FRAME STRUCTURES.....	11
2.4 REFERENCES.....	12
3. REVIEW OF PREVIOUS EXPERIMENTAL INVESTIGATIONS	13
3.1 INTRODUCTION.....	13
3.2 FULLY WELDED BEAM-COLUMN JOINTS	14
3.3 BOLTED EXTENDED END-PLATE BEAM-COLUMN JOINTS.....	35
4. CHARACTERISING BEAM-COLUMN ASSEMBLAGES WITH FULL-STRENGTH JOINTS	171
4.1 INTRODUCTION.....	171
4.2 METHODOLOGY.....	177
4.3 PHENOMENOLOGICAL MODELS FOR FULL-STRENGTH RIGID JOINTS	180

4.4 EXAMINATION OF EXPERIMENTAL RESULTS	184
4.5 CALIBRATION OF THE RICHARD-ABBOT MODEL.....	187
4.6 NUMERICAL INVESTIGATION INTO THE EQUIVALENT VISCOS DAMPING OFFERED BY STEEL MRFs WITH FULL-STRENGTH RIGID JOINTS.....	193
4.6.1 Nonlinear SDOF Models.....	193
4.6.2 Definition of the ductility	197
4.6.3 Residual Displacement	197
4.6.4 Linear SDOF model	198
4.6.5 Summary of equivalent viscous damping results.....	206
4.7 INTERPRETING RESULTS OF EVD STUDY ON FULL-STRENGTH JOINTS	207
4.8 SUMMARY AND CONCLUSIONS.....	209
4.9 REFERENCES	209
5. CHARACTERISING BOLTED END-PLATE BEAM-COLUMN JOINTS USING THE COMPONENT METHOD	211
5.1 INTRODUCTION	211
5.2 REVIEW OF THE EUROCODE 3 COMPONENT METHOD	212
5.3 EXAMINATION OF EXPERIMENTAL RESULTS AND COMPARISON WITH THEORETICAL PREDICTIONS	216
5.3.1 Initial Stiffness and Plastic Resistance	216
5.3.1.1 Summary	221
5.3.2 Plastic Rotation Capacity	226
5.3.2.1 Overview.....	226
5.3.2.2 Experimental data on extended end-plate joints.....	228
5.3.2.3 Experimental data on flush end-plate joints	236
5.3.2.4 Plastic rotation capacity and failure modes	239
5.3.2.5 Strain-hardening of the column web panel in shear	244
5.3.2.6 Review and interpretation of experimental data.....	246
5.3.2.7 Total joint plastic rotation consider both the column web panel and connection plastic deformation.....	255
5.4 PARAMETRIC ANALYSIS USING THE COMPONENT METHOD.....	258
5.5 SIMPLIFIED DESIGN EXPRESSIONS.....	262
5.6 EQUATION FOR THE YIELD DRIFT OF STEEL FRAMES ACCOUNTING FOR THE JOINT CHARACTERISTICS	266

5.7 REFERENCES.....	272
6. CHARACTERISING PARTIAL-STRENGTH JOINTS USING FINITE ELEMENT ANALYSIS.....	275
6.1 INTRODUCTION.....	275
6.2 REVIEW OF PAST NUMERICAL STUDIES.....	278
6.3 SURVEY OF EXPERIMENTAL RESULTS.....	284
6.3.1 Beam-to-Column Joints Tests	284
6.3.1.1 Bernuzzi et al. [1996]	284
6.3.1.2 Kim and Yang [2007]	285
6.3.1.3 Dubina et al. [2002]	286
6.3.1.4 Dubina et al. [2002]	287
6.3.1.5 Nogueiro [2009]	288
6.3.2 Organisation and Data Processing.....	289
6.3.2.1 Relevant Properties.....	289
6.3.2.2 Stiffness Comparison	290
6.3.2.3 Strength Comparison	292
6.3.2.4 Rotation Capacity Comparison.....	294
6.3.2.5 Ductility Capacity.....	297
6.3.2.6 Final Remarks.....	298
6.4 CALIBRATION OF THE FINITE-ELEMENT MODELS.....	300
6.4.1 Description of the Finite Element Models.....	300
6.4.2 T-stub Models	302
6.4.2.1 Material Modelling.....	304
6.4.2.2 Results of the T-stub Numerical Models	309
6.4.3 Full Connection Models	313
6.4.3.1 Material Modelling.....	314
6.4.3.2 Loading Protocol	315
6.4.3.3 Data Collection and Treatment	315
6.4.3.4 Results of the J1 Series Specimens.....	318
6.4.3.5 Results of the J3 Series Specimens.....	321
6.4.3.6 Further Validation of the FE Models	325

6.4.3.7	Final Remarks	327
6.5	PARAMETRIC STUDY OF PARTIAL-STRENGTH JOINTS USING FE ANALYSIS.....	327
6.5.1	Analytical Calculations.....	330
6.5.2	Numerical Calculations	331
6.5.3	Numerical Results	331
6.5.3.1	Final Remarks of the Parametric Study	337
6.6	DERIVATION OF EQUIVALENT VISCOUS DAMPING AND DISPLACEMENT REDUCTION FACTORS.....	338
6.6.1	Procedure Developed for the EVD Assessment	339
6.6.2	Joints Properties Adopted for the EVD Assessment.....	342
6.6.3	Records Adopted in the NLTH Analyses	344
6.6.4	Results from the NLTH Analyses and EVD Assessment.....	349
6.6.4.1	Equivalent Viscous Damping.....	350
6.6.4.2	Modification Factor for the Spectral Displacement Response	358
6.7	INTERPRETATION OF THE RESULTS OF THE EVD STUDY	366
6.8	SUMMARY AND CONCLUSIONS.....	369
6.9	REFERENCES	370
7.	SUMMARY OF THE DISTEEL PROJECT RECOMMENDATIONS FOR THE CHARACTERISATION OF STEEL BEAM-COLUMN JOINTS.....	379
7.1	SUMMARY	379
7.2	EXPRESSION FOR THE INITIAL STIFFNESS AND PLASTIC RESISTANCE OF STEEL BEAM-COLUMN ASSEMBLAGES	381
7.3	DESIGN EXPRESSION FOR THE DEFORMATION CAPACITY OF STEEL BEAM-COLUMN ASSEMBLAGES	382
7.4	DESIGN EXPRESSION FOR THE YIELD DRIFT OF STEEL BEAM-COLUMN ASSEMBLAGES ..	383
7.5	EQUIVALENT VISCOUS DAMPING EXPRESSIONS AND SPECTRAL DISPLACEMENT REDUCTION FACTORS.....	384
7.6	UNCERTAINTIES AND AREAS FOR FUTURE RESEARCH.....	386

LIST OF TABLES

Table 3.1. Summary details for fully welded beam-column joints.....	14
Table 3.2. Summary details for bolted extended end-plate beam-column joints.....	35
Table 4.1. Geometrical characteristics of the welded joints selected.....	175
Table 4.2. Geometrical characteristics of the extended end plate joints selected.....	176
Table 4.3. Evaluated parameters for the calibration of the phenomenological model.....	189
Table 4.4. Maximum rotation, associated moment and secant stiffness for ground motion recording ALP1 and scale factor from 0.025 to 0.25.....	196
Table 4.5. Maximum rotation, associated moment and secant stiffness for ground motion recording ALP1 and scale factor from 0.275 to 0.50.....	196
Table 4.6. Evaluation of the yielding rotation.....	197
Table 4.7. Maximum rotation and associated EVD factor for all the joints considered, ground motion ALP1 and scale factor from 0.025 to 0.250.....	200
Table 4.8. Maximum rotation and associated EVD factor for all the joints considered, ground motion ALP1 and scale factor from 0.275 to 0.500.....	200
Table 6.1. Initial stiffness comparison.....	291
Table 6.2. Strength comparison for the envelope maximum moments achieved.....	293
Table 6.3. Rotation comparison.....	296
Table 6.4. Ductility capacity.....	297
Table 6.5. Joints ranking table.....	299
Table 6.6. Measured geometrical properties of tested specimens.....	303
Table 6.7. Measured mechanical properties of tested specimens.....	304
Table 6.8. Kinematic hardening determination for the A2 test.....	308
Table 6.9. Material properties for the J1 and J3 series.....	315
Table 6.10. Equations for the M- θ curves determination.....	317
Table 6.11. Modified Richard-Abbott model parameters for the J1-3 connection.....	325
Table 6.12. Connections description.....	328
Table 6.13. FE model geometric properties.....	329

Table 6.14. Joint geometrical properties.....	329
Table 6.15. Analytical calculation main results.....	330
Table 6.16. Analytical results summary.....	334
Table 6.17. Numerical results summary	335
Table 6.18. Connections properties for the EVD assessment.....	343
Table 6.19. Record set for the soil type A (LA).....	345
Table 6.20. Record set for the soil type C (LC).....	345
Table 6.21. C-values determined for various joint typologies.....	366
Table 6.22. C_n -values determined for various joint typologies.....	367
Table 6.23. C and C_n -values determined for the several dissipative plastic mechanisms found in the end plate partial-strength joints.	368
Table 7.1. Ratio of component method predicted to experimental values of stiffness and resistance.....	380
Table 7.2. Design plastic rotation capacity for different beam-column joint typologies.....	383
Table 7.3. C_n -values determined for various joint typologies.....	386

LIST OF FIGURES

Figure 2.1. Key steps of DBD (Adapted from Priestley et al. [2007]).....	7
Figure 4.1. Joint stiffness classification boundaries.....	172
Figure 4.2. Joint stiffness classification based on span length.....	172
Figure 4.3. Steel frame sub-structure containing the beam-to-column joint considered.	173
Figure 4.4.Components influencing joint stiffness for Fully Welded (left) and Extended-End-Plate (right).	174
Figure 4.5. General workflow for the DBD procedure calibration for steel MRFs with full strength rigid joints.	178
Figure 4.6. Step 1: Collection of experimental data and model calibration.	179
Figure 4.7. Step 2: Nonlinear Time History Analyses on a SDOF element representing a sub-assemblage of the MRF structure.	179
Figure 4.8. Step 3: Nonlinear Time History Analyses on a linear model characterised by varying values of the EVD factor.	180
Figure 4.9. Moment rotation curve proposed by Della Corte et al. [1999].	182
Figure 4.10. Hardening asymptote translation.	183
Figure 4.11. Schematisation of the joint rotation.	184
Figure 4.12. Example of test results regularisation: (a) test setup of FW1 joint; (b) scan of test results; (c) digitised test results; (d) moment-rotation curve.	185
Figure 4.13. Moment-rotation curves of the selected tests on fully welded beam-to-column joints.	187
Figure 4.14. Example of calibration of k_o and k_h (joint FW1).....	188
Figure 4.15. Plastic and post-buckling curves used to determine the available rotation capacity..	189
Figure 4.16. Comparison between the experimental curve and model of joint : (a) FW1 (b) FW2 (c) FW3.	190
Figure 4.17. Comparison between the experimental curve and model of joint: (d) FW4 (e) FW5 (f) FW6.....	191
Figure 4.18. Comparison between the experimental curve and model of joint : (g) FW7, (h) FW8, (i) FW9.	192
Figure 4.19. Comparison between the experimental curve and model of joint :(j) FW10.....	193

Figure 4.20. Moment - rotation response of FW1 joint to ALP1 ground motion recording and a scale factor equal to 0.025 : (a) total reaction; (b) hysteretic reaction (without the damping contribution).....	194
Figure 4.21. Moment - rotation response of FW1 joint to ALP1 ground motion recording and a scale factor equal to 0.25 :(a) total reaction; (b) hysteretic reaction (without the damping contribution).....	195
Figure 4.22. Residual rotation for the considered joints when subjected to ALP1 ground motion recording	198
Figure 4.23. Residual rotation for joint FW1 when subjected to each of the selected ground motion recording (with scale factor varying from 0.025 to 0.50).....	198
Figure 4.24. Moment - rotation response of linear equivalent model of FW1 joint to ALP1 ground motion recording and a scale factor equal to 0.025: (a) total reaction; (b) elastic reaction (without the damping contribution).....	199
Figure 4.25. Moment - rotation response of linear equivalent model of FW1 joint to ALP1 ground motion recording and a scale factor equal to 0.25: (a) total reaction; (b) elastic reaction (without the damping contribution).....	199
Figure 4.26. Equivalent Viscous Damping (EVD) factor for the joint FW1 and calibrated equation ($C=0.795$).....	201
Figure 4.27. Equivalent Viscous Damping (EVD) factor for the joint FW2 and calibrated equation ($C=0.810$).....	202
Figure 4.28. Equivalent Viscous Damping (EVD) factor for the joint FW3 and calibrated equation ($C=0.8550$)	202
Figure 4.29. Equivalent Viscous Damping (EVD) factor for the joint FW4 and calibrated equation ($C=1.040$).....	203
Figure 4.30. Equivalent Viscous Damping (EVD) factor for the joint FW5 and calibrated equation ($C=0.750$).....	203
Figure 4.31. Equivalent Viscous Damping (EVD) factor for the joint FW6 and calibrated equation ($C=0.840$).....	204
Figure 4.32. Equivalent Viscous Damping (EVD) factor for the joint FW7 and calibrated equation ($C=0.815$).....	204
Figure 4.33. Equivalent Viscous Damping (EVD) factor for the joint FW8 and calibrated equation ($C=0.835$).....	205
Figure 4.34. Equivalent Viscous Damping (EVD) factor for the joint FW9 and calibrated equation ($C=0.440$).....	205
Figure 4.35. Equivalent Viscous Damping (EVD) factor for the joint FW10 and calibrated equation ($C=0.435$).....	206
Figure 4.36. Equivalent Viscous Damping (EVD) factor for joints from FW1 to FW8 and the relative calibrated equation ($C=0.810$).	207

Figure 5.1. Components of (a) flush end-plate joints and (b) extended end-plate joints.....	212
Figure 5.2. Mechanical models of end-plate joints.....	213
Figure 5.3. Moment rotation curve idealisations: (a) nonlinear and (b) bilinear.....	215
Figure 5.4. Theoretical vs. experimental results for specimen A-3 tested by Ghobarah et al. [1990].....	216
Figure 5.5. Theoretical vs. experimental results for specimen EPC-2 tested by Shi et al. [2007a].	217
Figure 5.6. Theoretical vs. experimental results for specimen JD-2 tested by Shi et al. [2007b]..	217
Figure 5.7. Theoretical vs. experimental results for series FS2 tested by Coelho et al. [2004].....	218
Figure 5.8. Theoretical vs. experimental results for specimen BC4 tested by Abidelah et al. [2012].....	218
Figure 5.9. Theoretical vs. experimental results for specimen EP2 tested by Broderick and Thomson [2002].	219
Figure 5.10. Theoretical vs. experimental results for specimen EP4 tested by Broderick and Thomson [2002].	220
Figure 5.11. Theoretical vs. experimental results for specimen FP2 tested by Broderick and Thomson [2005].	220
Figure 5.12. Theoretical vs. experimental results for specimen FP4 tested by Broderick and Thomson [2005].	221
Figure 5.13. Experimental value of initial stiffness and plastic resistance.	222
Figure 5.14. Theoretical vs. experimental results for extended end-plate joints: (a) initial stiffness (b) plastic resistance.	222
Figure 5.15. Theoretical vs. experimental results for extended end-plate joints: the role of joints.	223
Figure 5.16. Theoretical vs. experimental results for flush end-plate joints: (a) initial stiffness; (b) plastic resistance.	224
Figure 5.17. Theoretical vs. experimental results for flush end-plate joints: the role of joints.	224
Figure 5.18. Theoretical vs. experimental results for end-plate joints: (a) initial stiffness (b) plastic resistance.....	225
Figure 5.19. Theoretical vs. experimental results for end-plate joints: the role of joints.	225
Figure 5.20. Definitions of rotation capacity and ultimate rotation.	226
Figure 5.21. Analysis criteria for rotation capacity.	227
Figure 5.22. Plastic rotation capacities for Ghobarah et al. [1990] specimens.....	229
Figure 5.23. Plastic rotation capacities for Sumner and Murray [2002, 2003] specimens.	229
Figure 5.24. Plastic rotation capacities for Coelho et al. [2004] specimens.....	230
Figure 5.25. Plastic rotation capacities for Nogueiro et al. [2006] specimens.....	231

Figure 5.26. Plastic rotation capacities for Coelho and Bijlaard [2007] specimens.....	231
Figure 5.27. Plastic rotation capacities for Shi et al.[2007a] specimens.....	232
Figure 5.28. Plastic rotation capacities for Shi et al. [2007b] specimens.	233
Figure 5.29. Comparison of plastic rotation capacities of Shi et al. [2007a, 2007b] specimens.....	233
Figure 5.30. Plastic rotation capacities for Tahir and Hussein [2008] specimens.	234
Figure 5.31. Plastic rotation capacities for Iannone et al. [2011] specimens.	235
Figure 5.32. Plastic rotation capacities for Abidelah et al. [2012] specimens.	235
Figure 5.33. Plastic rotation capacities for Broderick and Thomson [2002] specimens.....	237
Figure 5.34. Plastic rotation capacity for da silva et al. [2004] specimen.....	237
Figure 5.35. Plastic rotation capacities for Broderick and Thomson [2005] specimens.	238
Figure 5.36. Plastic rotation capacity for Shi et al. [2007b] specimen.....	238
Figure 5.37. Plastic rotation capacity in case of bolt failure.	240
Figure 5.38. Plastic rotation capacity in case of the T-Stub mode 1 mechanism.....	241
Figure 5.39. Plastic rotation capacity in case of T-Stub mode 2 mechanism.	242
Figure 5.40. Plastic rotation capacity in case of shear buckling.....	243
Figure 5.41. Plastic rotation capacity in case of beam plastic hinge.....	243
Figure 5.42. Plastic rotation capacity for other particular cases.....	244
Figure 5.43. Bilinear modelling of shear force-deformation behaviour of the column web panel (test results from Shi et al. [2007a, 2007b]).....	245
Figure 5.44. Normalised bilinear modelling of column web panel in shear: (a) monotonic loading; (b) cyclic loading.	245
Figure 5.45. Example comparisons of approximate models.....	246
Figure 5.46. Plastic rotation capacity as a function of the internal lever arm in case of an equivalent T-stub plastic mechanism 1.	250
Figure 5.47. Plastic rotation capacity as a function of the internal lever arm in case of an equivalent T-stub plastic mechanism 3.	251
Figure 5.48. Plastic rotation capacity as a function of the internal lever arm (a) and the ratio d/t_p (b) in case of an equivalent T-stub plastic mechanism 2.	252
Figure 5.49. Plastic rotation capacity as a function of the internal lever arm in case of an equivalent T-stub plastic mechanism 1 – Interpolating data with a function of type $a\zeta^1$	253
Figure 5.50. Plastic rotation capacity as a function of the internal lever arm in case of an equivalent T-stub plastic mechanism 3 – Interpolating data with a function of type $a\zeta^1$	253

Figure 5.51. Plastic rotation capacity as a function of the internal lever arm (a) and the ratio d/t_p (b) in case of an equivalent T-stub plastic mechanism 2.....	254
Figure 5.52. Plastic rotations associated to column web panel deformations in shear and developed up to failure in the joint sub-assemblages tested by Shi et al. [2007a and 2007b].	255
Figure 5.53. Plastic rotations of joints where yielding starts in column web panels and ultimate failure occurs in connections.....	256
Figure 5.54. Summary of assumptions about the geometry of joints for parametric analyses.....	259
Figure 5.55. Variation of normalised stiffness (a), normalised resistance (b), yield rotation (c), failure mode (d) for extended end plate joints with: IPE 550 beam, HEB 280 column, continuity plates, no rib stiffener, no column web panel stiffener.	260
Figure 5.56. Variation of connection failure mode for the example case of Figure 12: (a) first bolt row; (b) second bolt row.....	261
Figure 5.57. Variation of normalised stiffness (a), normalised resistance (b), yield rotation (c), failure mode (d) for flush end plate joints with: IPE 550 beam, HEB 280 column, continuity plates, no rib stiffener, no column web panel stiffener.....	262
Figure 5.58. (a) m_b vs. d/t_{fc} and (b) k_b vs. d/t_{fc} relationships for beam-to-column combinations having HEM 200 column shape.....	264
Figure 5.59. Accuracy of approximate closed-form Equations: m_b	265
Figure 5.60. Accuracy of approximate closed-form Equations: k_b	266
Figure 5.61. Drift ratio (or angle).....	267
Figure 5.62. Plastic drift.....	268
Figure 6.1. Joints moment-rotation behaviour.....	276
Figure 6.2. Common partial strength joints configurations: (a) end-plate connections; (b) top and seat angle connection.....	276
Figure 6.3. Strength classification.....	277
Figure 6.4. Initial stiffness comparison.....	290
Figure 6.5. Strength comparison for the envelope maximum positive moments achieved.....	292
Figure 6.6. Strength comparison for the envelope maximum negative moments achieved.....	293
Figure 6.7. Rotation comparison for the positive envelope.....	295
Figure 6.8. Rotation comparison for the negative envelope.....	295
Figure 6.9. Ductility capacity.....	297
Figure 6.10. T-stub meshed parts of the FE model.....	302
Figure 6.11. End-plate joint meshed parts of the FE model.....	302
Figure 6.12. Failure modes of bolted T-stubs.....	303

Figure 6.13. Geometry of bolted T-Stubs (Adapted from Piluso and Rizzano [2008]).....	303
Figure 6.14. Menegotto-Pinto model.....	306
Figure 6.15. The case of $E_0 = E$ and $E_r=0$	306
Figure 6.16. Stress-strain relationships for the A1 test.....	306
Figure 6.17. Stress-strain relationships for the B1 test.....	307
Figure 6.18. Stress-strain relationships for the D1 test	307
Figure 6.19. Chaboche model for kinematic hardening for the A2 test.....	308
Figure 6.20. Chaboche model for kinematic hardening for the B7 test	309
Figure 6.21. Monotonic force-displacement experimental results [Piluso and Rizzano, 2008].	309
Figure 6.22. A1 test – Von Mises stress results for a 20mm displacement.....	310
Figure 6.23. A1 model results comparison with different material characterisations.	310
Figure 6.24. B1 test – Von Mises stress results for a 20mm displacement.....	311
Figure 6.25. B1 model results comparison with different material characterisations.....	311
Figure 6.26. D1 test – Von Mises stress results for a 20mm displacement.	311
Figure 6.27. D1 model results comparison with different material characterisations.....	312
Figure 6.28. A2 model results comparison, on the left only cycles 2 to 5 and on the right the complete results.	313
Figure 6.29. B7 model results comparison, on the left the first 3 cycles and on the right the complete results.	313
Figure 6.30. Experimental test setup (Adapted from Nogueiro <i>et al.</i> [2006b]).	314
Figure 6.31. Experimental test setup for J1.1 (Adapted from Nogueiro <i>et al.</i> [2006b]).	316
Figure 6.32. Points where the data is collected.....	317
Figure 6.33. J1 Nogueiro's test series – scheme of the connections (Adapted from Nogueiro <i>et al.</i> [2006b]).....	318
Figure 6.34. J1.1 Joint moment-rotation comparisons.....	319
Figure 6.35. J1.1 Von Mises stress field.....	319
Figure 6.36. J1.3 Connection moment-rotation comparisons, (a) total rotation of the sub-assemblage, (b) rotation of the component column web, (c) rotation of the component end-plate.	320
Figure 6.37. Energy dissipation comparison for the monotonic loaded model.....	321
Figure 6.38. Cumulative energy dissipation comparison for the cyclic loaded model	321
Figure 6.39. J3 Nogueiro's test series – scheme of the connections (Adapted from Nogueiro <i>et al.</i> [2006b]).....	322

Figure 6.40. J3.1 Joint moment-rotation comparisons.....	322
Figure 6.41. J3.1 Von Mises stress field.....	323
Figure 6.42. J3.2 Connection moment-rotation comparisons, (a) total rotation of the sub-assemblage, (b) rotation of the component column web, (c) rotation of the component end-plate.....	323
Figure 6.43. Energy dissipation comparison for the monotonic loaded model.....	324
Figure 6.44. Cumulated energy dissipation comparison for the cyclic loaded model.....	324
Figure 6.45. (a) SeismoStruct model for the J1.3; (b) analysis representation.....	325
Figure 6.46. Record used in the validation of the NLTH analyses.....	326
Figure 6.47. NLTH analysis of the sub-assemblage.....	326
Figure 6.48. (a) Sub-assemblage geometric properties for the FE models (b) Joint geometry.....	329
Figure 6.49. Monotonic results for the C1 to C5 joints.....	332
Figure 6.50. Monotonic results for the C1 to C5 components.....	333
Figure 6.51. Von Mises stress representation for the identified situations.....	333
Figure 6.52. Comparison of strength and stiffness results.....	335
Figure 6.53. ECCS load protocol.....	336
Figure 6.54. Assessment of the θ_y according to the ECCS procedure for the C1 joint.....	336
Figure 6.55. Cyclic response comparison for the joints C1 to C5.....	337
Figure 6.56. NLTH analysis of the sub-assemblage.....	339
Figure 6.57. Determination ductility and yield moment.....	340
Figure 6.58. EVD assessment in the elastic displacement spectra.....	341
Figure 6.59. Example of μ -EVD relationship chart.....	342
Figure 6.60. Frequency analyses for $T_{el} = 1.0s$	344
Figure 6.61. (a) Acceleration response spectra for LA set (b) Displacement response spectra for LA set.....	345
Figure 6.62. (a) Acceleration response spectra for LC set (b) Displacement response spectra for LC set.....	346
Figure 6.63. Records for the soil type A.....	347
Figure 6.64. Records for the soil type C.....	348
Figure 6.65. (a) Equal-displacement rule; (b) Elasto-plastic idealised behaviour for the sub-assemblage components, column, beam and joint.....	349
Figure 6.66. EVD results using the NLTHA (CCED).....	351
Figure 6.67. EVD results using the NLTHA (NCED).....	351

Figure 6.68. Ductility-EVD relationships (CCED)	354
Figure 6.69. Ductility-EVD relationships (NCED).....	355
Figure 6.70. Coefficients for the derived equations CCED	356
Figure 6.71. Coefficients for the derived equations NCED.....	356
Figure 6.72. Derived ductility-EVD relationships, CCED.....	357
Figure 6.73. Derived ductility-EVD relationships, NCED	358
Figure 6.74. Damping modifier comparison (CCED).	360
Figure 6.75. Deviation from the “real” and analytical reduction factors (CCED)	361
Figure 6.76. Damping modifier comparison (NCED).....	362
Figure 6.77. Deviation from the “real” and analytical reduction factors (NCED).....	363
Figure 6.78. Proposition for an improvement in the expression for the damping modifier: (a) CCED (b) NCED.....	364
Figure 6.79. Deviation from the “real” and analytical reduction factors: (a) CCED (b) NCED ..	364
Figure 6.80. Comparing the combined new EVD expressions with the new damping modifier expressions to the NLTH analyses ductility demands: (a) CCED (b) NCED.....	365
Figure 6.81. NLTH analyses to elastic displacement ratio: (a) CCED (b) NCED.....	365
Figure 6.82. (a) Derived equivalent viscous damping factors; and (b) derived modification factors for the spectral displacement response for the several joints plastic mechanisms....	368

LIST OF SYMBOLS

CHAPTER 1

E	Young's Modulus
I	Second Moment of Area
L	Length of beam

CHAPTER 2

F_i	Design lateral force at floor i
h_i	Interstorey height of floor i
h_1	Interstorey height of floor 1
H_n	Total building height
I_{zz}	Second moment of area about zz axis
K_e	Effective Stiffness
L_b	Bay width
m_e	Effective mass
n	Number of floors
T_e	Effective Period
V_b	Design base shear
V_i	Design storey shear at storey i

$W_{pl,zz}$	Plastic modulus about z axis
Δ_d	Design displacement
ϵ_y	Yield strain
θ_i	Design drift of floor i
θ_c	Drift Capacity
μ_i	Ductility of floor i
μ_{sys}	System ductility
ξ_i	Equivalent viscous damping of floor i
ξ_{sys}	Equivalent viscous damping of equivalent system
$\phi_{y,b}$	Yield curvature of a beam section
$\phi_{y,c}$	Yield curvature of a column section
ω_θ	Higher mode drift reduction factor

CHAPTER 4

CI	Collapse index
C	EVD calibration coefficient
E	Young's modulus
E_h	Hysteretic energy dissipated
F	Force
f_u	Ultimate strength
H_h	Plastic hardening factor

I_b	Beam second moment of area
I_c	Column second moment of area
k_0	Initial tangent stiffness
k_h	Richard-Abbott monotonic model asymptotic line parameter
L_{\min}	Span length
M	Moment
M_0	Richard-Abbott monotonic model asymptotic line parameter
M_u	Bending strength
$M_{u,\text{mon}}$	Ultimate monotonic bending strength
n	Hysteresis “smoothness” parameter
R_ξ	EC8 spectral reduction factor
$S_{j,\text{ini}}$	Initial rotational stiffness
W_{pl}	Plastic section modulus
β	Cyclic deterioration factor
Δ_v	Vertical displacement of test specimen
Φ	Rotation
$\bar{\phi}$	Maximum rotation reached
$\bar{\phi}_{u,0}$	Deformation capacity of the joint under monotonic loading
$\Phi_{u,\text{mon}}$	Ultimate monotonic plastic rotation
η	Displacement reduction factor

ξ_{visc}	Viscous damping
$\sigma_{z,\text{max}}$	Maximum stress in beam
μ	Ductility

CHAPTER 5

A_{vb}	Beam shear area
A_{vc}	Column shear area
d	Bolt diameter
E	Young's modulus
$F_{tr,Rd}$	Effective design resistance of bolt row r
G	Shear modulus
h	Lever arm
h_c	Column section height
h_r	Distance of bolt row r from the centre of compression
h_b	Beam section height
h	Distance between the two points of zero moment along the column length
I_b	Beam second moment of area
I_c	Column second moment of area
k_{eq}	Equivalent spring stiffness
$k_{\text{eff},r}$	Effective stiffness of bolt row r
k_i	Stiffness coefficient for the i^{th} basic joint component

$k_{wp,sh}$	Post-yield stiffness of column web panel in shear
$k_{wp,e}$	Pre-yield stiffness of column web panel in shear
k_b	Normalised stiffness
k_{ref}	Reference coefficient which depends on the column and beam shape
k_{jb}	Beam flexural deformability contribution
L_{vb}	Distance from the beam end to the point of zero moment along the beam
L_b	Beam length
M	Bending moment
$M_{conn,R}$	Plastic resistance of connection
$M_{wp,R}$	Plastic resistance of column web panel
$M_{j,Ed}$	Applied design moment
$M_{j,Rd}$	Design moment resistance
$M_{R,exp}$	Experimental value of the plastic resistance
$M_{R,th}$	Theoretical plastic resistance
$M_{b,R}$	Plastic resistance at the beam end
m_b	Normalised moment resistance
m_{ref}	Reference resistance
$m_{b,R}$	Resistance of the joint relative to the beam cross section
p	Vertical spacing of bolts in the tension zone
$S_{j,ini}$	Initial joint stiffness

$S_{\text{ini,exp}}$	Experimental value of the initial stiffness
$S_{\text{ini,th}}$	Theoretical value of the initial stiffness
$S_{\text{conn,ini,th}}$	Theoretical value of the initial stiffness of connection
$S_{\text{wp,ini}}$	Initial rotational stiffness due to the column web panel in shear
$S_{\text{conn,ini}}$	Initial rotational stiffness of the connection
s_h	Ratio of strain-hardening to initial (elastic) rotational stiffness
t_p	End-plate thickness
t_{fc}	Column flange thickness
t_{wc}	Column web thickness
w	Horizontal spacing of bolts in the tension zone
z_{eq}	Equivalent lever arm
δ_2	Gradient of the plastic rotation capacity in case of a plastic mechanism 2
Φ	Rotation
$\Phi_{j,c}$	Joint rotation capacity
$\Phi_{j,u}$	Ultimate rotation
$\Phi_{j,pc}$	Plastic rotation capacity
$\Phi_{j,pu}$	Ultimate plastic rotation
$\Phi_{j,y,\text{exp}}$	Experimental yield rotation
$\Phi_{\text{wp,p}}$	Plastic rotation due to the column web panel shear deformations
$\Phi_{\text{conn,pc}}$	Plastic rotation capacity of the connection;

$\Phi_{\text{conn,pC},1}$	Plastic rotation capacity of the connection for plastic mechanism 1
$\Phi_{\text{conn,pC},2}$	Plastic rotation capacity of the connection for plastic mechanism 2
$\Phi_{\text{conn,pC},3}$	Plastic rotation capacity of the connection for plastic mechanism 3
ψ	Connection type coefficient
μ	Stiffness ratio
θ_y	Yield drift
θ_p	Plastic drift ratio
θ	Total drift

CHAPTER 6

a	Fillet weld throat
A_0	Initial area
b	Empirical constant (in the equation of the equivalent viscous damping)
b	Width of the T-stub flange
b	Hardening stiffness ratio in the bilinear stress strain material definition
b_{classe}	Bolt steel grade
b_{iso}	Rate at which the size of the yield surface changes as plastic strain increases (Chaboche)
b_p	Width of the end-plate
B	Length of the T-stub flange
c	Damping coefficient (in the dynamic equation of equilibrium)
c	Empirical constant (in the equation of the equivalent viscous damping)

C	Empirical constant (equivalent damping expression)
C_{kin}	Kinematic hardening constant (Chaboche) E
d	Distance between the column flange and the actuator (force / displacement application point)
d_{bolt}	Bolts diameter
eph1	Bolts horizontal edge distance left side
eph2	Bolts horizontal edge distance right side
epv1	Bolts vertical edge distance
ext	Extended portion of the end-plate
E	Young's modulus
E_m	Average Young's modulus
E_0	Initial tangent modulus (Menegotto-Pinto)
E_∞	Secondary tangent modulus (Menegotto-Pinto)
e_u	Ultimate displacement
e_y	Elastic displacement limit
f_u	Ultimate strength
f_{utm}	Average tension ultimate strength
f_r	Strength at failure
f_y	Yield strength
f_{ytm}	Average tension yield strength
$F_{c,\text{fb,Rd}}$	Design resistance of the beam flange and web in compression

$F_{c,wc,Rd}$	Design resistance of the column web in compression
$F_{t1,Rd}$	Design resistance of the first row of bolts
h_p	Height of the end-plate
I_b	Second moment of area of the beam
I_y	Second moment of area around the y axis
K	Empirical constant (in the equation of the equivalent viscous damping)
K	Strength coefficient (Ramberg-Osgood)
k_e	Effective stiffness (in the procedure to assess the equivalent viscous damping)
K_0	Initial stiffness
L	Length of the column between supports
L_b	Length of the beam
L_2	Position of the beam relative to the axis of the bottom column support
m	Mass
M_E	Internal moment in the connection
$M_{j,Rd}$	Design moment resistance of a joint
M_{max}	Max moment
$M_{pl,Rd,b}$	Design plastic moment resistance of the beam
$M_{pl,Rd,c}$	Design plastic moment resistance of the column
$M_{rd,b,c}$	Design plastic moment resistance of the beam or column
M_y	Bending moment at yielding

M_{\max}	Moment associated to the max rotation (in the procedure to assess the equivalent viscos damping)
n	Strain hardening exponent (Ramberg-Osgood)
ph	Bolt horizontal spacing
$ppv1$	Bolts vertical spacing between the first and second row of bolts
$ppv2$	Bolts vertical spacing between the second and third row of bolts
$Ppv3$	Bolts vertical spacing between the third and fourth row of bolts
Q_∞	Maximum change in the size of the yield surface (Chaboche)
r	Radius between flanges and web
R	Material constant (Menegotto-Pinto)
R_s	Elastic displacement spectra modification factor
$S_{j,ini}$	The initial rotational stiffness of a joint
t_f	Flange thickness
t_p	End-plate thickness
t_s	Stiffeners thickness
t_w	Web thickness
$t_{(wp)}$	Supplementary web plate thickness
T_D	Corner period (value defining the beginning of the constant displacement response range of the spectrum)
T_e	Effective vibration period
T_{el}	Elastic vibration period

x	Response relative displacement (of the dynamic equation of equilibrium)
x	Empirical constant (in the damping modifier expression)
$\dot{\ddot{x}}_g$	Ground acceleration
α	Backstress (Chaboche)
β_k	Stiffness-proportional Rayleigh damping coefficient
Δ_d	Target displacement (in the procedure to assess the equivalent viscous damping)
$\Delta_{el,Te}$	Elastic displacement for the effective period
Δ_{in}	Maximum inelastic displacement in the NLTHA
Δ_{max}	Maximum displacement
Δ_y	Displacement of the beam tip at yielding
ϵ	Total strain (Ramberg-Osgood)
ϵ_0	Theoretical yielding strain (Menegotto-Pinto)
ϵ_e	True elastic strain
ϵ_p	True plastic strain
ϵ^p	Equivalent plastic strain (Chaboche)
ϵ_u	Ultimate strain
ϵ_{utm}	Average tension ultimate strain
ϵ_r	Elongation at failure
$\epsilon_{r(min)}$	Minimum elongation at failure

ϵ_{rtm}	Average elongation at failure in tension
ϵ_y	Yielding strain
ϵ_{ytm}	Average tension yielding strain
η	Displacement reduction factor
γ_{MP}	Partial safety factors
γ_{MP}	Material constant (Menegotto-Pinto)
γ	Material constant in the definition of the maximum backstress (Chaboche)
μ	Ductility factor
θ	Connection rotation
θ_{Column_web}	Connection rotation component associated to the column web panel deformation
θ_{elast_beam}	Connection rotation component associated to the beam elastic deformation
θ_{elast_column}	Connection rotation component associated to the column elastic deformation
$\theta_{End-plate}$	Connection rotation component associated to the end-plate deformation
θ_{max}	Maximum rotation
θ_u	Ultimate rotation
θ_{Total}	Global joint rotation
θ_y	Elastic rotation limit
σ	True stress (Ramberg-Osgood)

$\sigma_{0(MP)}$	Theoretical stress point (Menegotto-Pinto)
σ^0	Yield surface (Chaboche)
$\sigma _0$	Yield stress at zero equivalent plastic strain (Chaboche)
ξ	Fraction of the critical damping
ξ_{el}	Elastic part of the equivalent viscous damping
ξ_{eq}	Equivalent viscous damping
ξ_{hyst}	Hysteretic damping

CHAPTER 7

k_b	Initial stiffness
d	Bolt diameter
t_{fc}	Column flange thickness
h_b	Beam section height
h_c	Column section height
m_b	Plastic moment resistance
θ_p	Plastic rotation capacity
θ_y	Yield drift
$M_{b,R}$	Ratio between the minimum connection resistance and the beam section plastic resistance
I_b	Beam second moment of area
I_c	Column second moment of area
h	Distance between the two points of zero moment along the column length

L_b	Distance from the beam end to the point of zero moment along the beam
$S_{j,ini}$	Initial stiffness of the beam-to-column joint
E	Young's modulus
ξ	Fraction of critical damping
ξ_{el}	Elastic damping coefficient
ξ_{hyst}	Hysteretic damping coefficient
μ	Ductility
C	EVD coefficient
η	Displacement reduction factor
C_η	Displacement reduction factor calibration coefficient

1. INTRODUCTION

Timothy J. Sullivan & Gerard J. O'Reilly

1.1 IMPORTANCE OF BEAM-COLUMN JOINT BEHAVIOUR AS OBSERVED AFTER PAST EARTHQUAKES

The excellent performance of steel structures during the 1906 San Francisco earthquake led its acquisition of an excellent reputation for a lateral load resisting system among engineers at the time. This connection detail was gradually developed from a riveted connection into bolt-type connection in the 1950's, as well as the introduction of field welding in the 1960's, as reported by Malley *et al.* [2004]. The welded connection detail was developed further as it was relatively cheap and easy to construct, with full penetration welds required on just the beam flanges and a bolted shear tab required on the beam webs. This represented a significant deviation from the heavily riveted connection detail used in the US in 1906, where MRFs initially gained popularity [Bruneau *et al.*, 1998]. Experimental testing of this welded connection detail by Popov and Stephen [1970] showed reasonable ductility and this resulted in it being adopted into the 1988 UBC and it soon became the industry standard for moment frame connections [Malley *et al.*, 2004].

However, further experimental investigation by Engelhardt and Husain [1993] showed that this connection detail displayed an alarming lack of ductility and desirable connection behaviour, and this concern was justified following the occurrence of the 1994 Northridge earthquake in California. Youssef *et al.* [1995] reported that over 130 MRFs were observed to have experienced brittle connection fracture, with cracking observed in both column flanges and beam flanges at the connections [Mahin, 1998]. Most of the damage during this earthquake went largely unnoticed at first, as connections were often hidden behind architectural cladding [Mahin, 1998], and concern was raised when elevators in MRF structures did not work upon building re-occupancy due to residual deformations caused by the connection failures [Bruneau *et al.*, 1998]. The resulting inspections on these structures uncovered the widespread connection failures that have now become a well-known lesson learned from past events in the seismic design community. In addition to the damage observed in Northridge in 1994, subsequent investigations of some of the MRF structures affected by the 1989 Loma Prieta event in Northern California reported similar fractures that had gone unnoticed for over 5 years.

From the above comments regarding the widespread damage to MRF connections in the US that had become standard design practice prior to 1994, it is clear that the impact of inadequate connection detailing was significant. It is therefore essential that connections used in steel structures can be characterised fully such that future structures exhibit stable hysteresis with adequate ductility. In addition, it is also important to ensure that connection design and verification is a relatively straightforward process such that it remains an attractive option for design engineers, which is a factor that arguably made the MRF system popular prior to 1994. This report aims to review experimental testing and numerical studies of a variety of connection types in such a way that simplified design procedures can be proposed such that connection details that have been fully characterised experimentally and numerically can be designed with ease.

1.2 STEEL BEAM-COLUMN JOINT CONSIDERATIONS IN EUROPE

In Europe steel frame buildings can be realised with a range of beam-column joint typologies. Engineers are relatively free to choose a connection detail they prefer, provided that they can satisfy relatively general requirements specified in the Eurocode 3 [CEN, 2005]. This approach is in stark contrast to engineering practice in the United States where engineers are practically constrained to use a number of pre-qualified connection details, that have been thoroughly tested and assessed in a number of University laboratories. The requirements provided in Eurocode 3 state that steel beam-column joints should be classified as being either:

- Full-strength or partial strength, whereby a full strength beam-column joint is able to resist 1.2 times the design plastic resistance of the beams; or
- Rigid or semi-rigid, whereby a rigid joint possess a rotational stiffness greater than $25EI/L$ where E is Young's modulus, I is the second moment of inertia and L is the length of the beam framing into the joint.

In the event that full-strength rigid beam-column joints are provided, it is anticipated that flexural hinging will occur in beams and that joint deformations will not be particularly significant to the seismic response. In this case, designers only need to confirm that joints possess adequate strength and stiffness, after which point the frame can be analysed and designed essentially ignoring the influence the joints might have on the predicted response. It should be pointed out, however, that beam-column joints that failed in the 1994 Northridge earthquake were expected to be full-strength prior to the earthquake and hence, uninformed engineers in Europe today may unknowingly propose a connection detail that is partial-strength, as occurred in the U.S. some 20 years ago. In the case that partial-strength joints are desired and specified, these are permitted by the European code provided certain force-deformation characteristics are ensured. However, there is

currently relatively limited guidance available for engineers wishing to demonstrate that a partial-strength beam-column joint meets the code-specified performance criteria, and it may often be concluded that experimental testing is required in order for a partial-strength connection to be deemed acceptable.

1.3 OBJECTIVES AND SCOPE OF THIS REPORT

The previous sections have clearly highlighted the importance of being able to characterise the behaviour of beam-column joints for seismic design and also the apparent lack of guidance that exists in Europe for this task. As such, the objectives of this report are the following:

- Identify and review experimental test data relevant for the characterisation of steel beam-column sub-assemblages. In addition to considering the strength and stiffness offered by the steel beam-column sub-assemblages, the review will focus of the deformation capacity of the systems.
- Use existing experimental test data to assist in characterising the behaviour of welded full-strength rigid MRF systems. The objective will be to permit quantification of the yield and ultimate deformation capacity of steel MRF systems will full-strength rigid joints. In addition, experimental results will be used to calibrate numerical models so that analytical investigations can be undertaken with the objective of calibrating expressions for the spectral displacement reduction factors for steel MRF structures.
- Use existing experimental test data to assist in characterising the behaviour of bolted partial-strength rigid MRF systems. This review will again have the objective of characterising the yield and ultimate deformation capacity of steel MRF systems will full-strength rigid joints and also the equivalent viscous damping they offer.
- Provide guidance for the application of the Eurocode 3 component-method for the characterisation of partial-strength beam column joints.
- Provide guidance for the use of the finite-element analyses for the characterisation of the cyclic nonlinear behaviour of partial-strength beam column joints.

By achieving the above objectives, this report will make a valuable contribution to the state-of-the-art not only for what regards displacement-based seismic design (introduced

in the next chapter), but also generally for the characterisation of steel MRF systems in seismic regions.

The subject of beam-column joint behaviour clearly offers a broad scope for research, particularly considering the large number of different beam-column joint typologies that are found in practice. To this extent, this work will focus on fully welded or bolted end-plate joints, whereas other joint typologies are outside the scope of the research. Column base connections are also expected to influence the behaviour of steel MRF systems but these are also outside the scope of the current research. Finally, note that new experimental testing is also not within the scope of this research, which instead will make reference to experimental test results available in the literature.

1.4 REFERENCES

CEN, European Committee for Standardisation, [2005]. *Eurocode 3: Design of steel structures - Part 1-1*.

Bruneau, M., Uang, C.M. and Whittaker, A. [1998] *Ductile Design of Steel Structures*. McGraw-Hill, New York.

Engelhardt, M.D. and Husain, A.S. [1993] Cyclic Loading Performance of Welded Flange-Bolted Web Connections. *Journal of Structural Engineering, ASCE*, Vol. 119, pp. 3537-3550, No.12.

Mahin, S.A., [1998] Lessons from damage to steel buildings during the Northridge earthquake. *Engineering Structures*, 20(4-6), pp.261–270.

Malley, J.O., Yu, Q.S. and Moore, K. [2004] Seismic design of steel moment frames. In Y. Bozorgnia and V.V. Bertero, editors, *Earthquake Engineering: From Engineering Seismology to Performance Based Engineering*. CRC Press.

Popov, E.P. and Stephen, R.M. [1970] Cyclic loading of full-size steel connections. Technical Report UCB/EERC-70/03, Earthquake Engineering Research Center.

Youssef, N.F.G., Bonowitz, D. and Gross, J.L. [1995] A Survey of Steel Moment Resisting Frame Buildings Affected by the 1994 Northridge Earthquake. Technical Report NISTIR 5625, National Institute of Standards and Technology.

2. DISPLACEMENT-BASED SEISMIC DESIGN

Timothy J. Sullivan & Gerard J. O'Reilly

2.1 OVERVIEW OF THE BASIC METHODOLOGY

Since the inception of modern design codes aiming to control the response of structures subjected to seismic loading, these codes have typically represented the seismic action as an equivalent lateral force modified by some behaviour factor to account for the ductility in the system. This results in a design methodology that is driven by forces and ordinates such as material strains and interstorey drift limits become a secondary check in the design process. Numerous conceptual drawbacks to this method were highlighted by Priestley [1993, 2003], demonstrating that current code provisions for seismic design possess some fundamental shortcomings regarding system ductility when considering mixed systems among other issues. Some of these shortcomings most relevant to this report are listed in Sullivan *et al.* [2010] as follows:

- Difficulty in defining force behaviour factors for mixed structural systems – Codes typically force modification factors for mixed systems as the lower of the two structural systems being employed. In addition, it is assumed that the ductility capacity of a system is a function only of the structural typologies and not the member proportions or connection characteristics. This is highlighted in Sullivan *et al.* [2010] as lacking rationale and poses problems particularly when one of these systems is responding elastically, as in the case of a mixed BRB-MRF system.
- Distribution of lateral forces based on initial stiffness – As outlined by Sullivan *et al.* [2010], this approach to the distribution of lateral systems based on their initial elastic stiffness results in more load being carried by the stiffer system and subsequently the structure becomes poorly conditioned in terms of its lateral force distribution.
- Relating inelastic displacement response to elastic displacement – Design codes typically relate the inelastic displacements to the elastic spectral displacements using the so-called equal displacements rule, which is used in the US (for certain structural typologies) and Europe. However, in Japan the inelastic displacements are related using an equal energy approach which results in higher inelastic displacement response compared to that of the equal displacements rule. As noted by Priestley *et al.* [2007], the actual response displacements of the structure

are equal to neither as they depend on hysteretic properties and fundamental period for the case of tall buildings.

The above comments regarding some of the shortcomings of current code based seismic design approaches are not exhaustive and further discussion can be found in Priestley [1993, 2003] and Priestley *et al.* [2007]. Making reference to the final point listed above; this is of particular interest to this report as it states that current codes do not acknowledge the dependence of actual response displacements on the hysteretic behaviour of structures. As will be encountered in later sections, this will be related by equivalent viscous damping (EVD) ratios for a structure, which can be tailored for each individual structural configuration. This offers the distinct advantage of being able to account explicitly for, in the case of this project, the difference in response offered by using different connection details for a MRF system, such as partial strength or semi-rigid connections. The first of the points made above is also relevant to the current report since the joint flexibility will affect the frame yield and ultimate drift capacity, thereby affecting the apparent ductility capacity. Furthermore, in the case of partial strength joints, the deformation capacity of the joint itself will dictate the available drift capacity of the whole frame. In this report, expressions calibrated to results of experimental testing will be developed for yield drift and drift capacity of beam column sub-assemblages such that more accurate considerations of ductility demand and capacity can be made during the design process.

Acknowledging the above comments on the shortcomings of current code-based design approaches, an alternative approach termed displacement-based design (DBD) for structures has been proposed Priestley *et al.* [2007]. This method differs from current force based design approach in that the displacements at maximum response are the driving ordinate throughout the design method as opposed to lateral forces. This provides a more logical approach to design in that the displacement is being controlled, as opposed to checked, in the design process which enables the designer to respect limits such as interstorey drift for the case of non-structural elements and material strain and chord rotation limits for the case of structural elements. Maley *et al.* [2013] discusses the design of and behaviour of steel MRF structures using the DBD methodology and presented a step-by-step case study design of a number of structures. The following section will introduce the method in general and highlight the steps involved for the case of a single degree of freedom (SDOF) system.

The DBD methodology [Priestley *et al.*, 2007] allows for the design to a specific displacement level and thus, a specific performance level that can be related to material strain and storey drift limits. The key steps of DBD are summarised in Figure 2.1 where a SDOF system is used to represent an MDOF system at maximum displacement in its first fundamental mode of response (Figure 2.1(a)), which for the specific case of MRFs

will be discussed in the following section. Figure 2.1(b) shows the SDOF representation of the structure as an equivalent linear system with secant stiffness to the maximum displacement, which is characterised by an EVD ratio to account for the hysteretic damping of the actual system when using an equivalent linear representation. Using the EVD expressions for the particular type of structure being considered, the EVD for the equivalent structure can be determined for the target displacement ductility, as outlined in Figure 2.1(c). This target displacement ductility is a function of the system yield displacement and target displacement. The yield displacement can be typically found from geometry and material strain definitions, whereas the target displacements are determined from material strain limit states (plastic hinge rotation) or interstorey drift limits, which means that the structure's displacements is a key definition of the design process that can be adjusted to control certain limit states. The design displacement is then used in conjunction with the EVD ratio to enter the EVD-reduced spectral displacement spectrum for the given site's seismic hazard in order to determine the effective period of the system, as outlined in Figure 2.1(d).

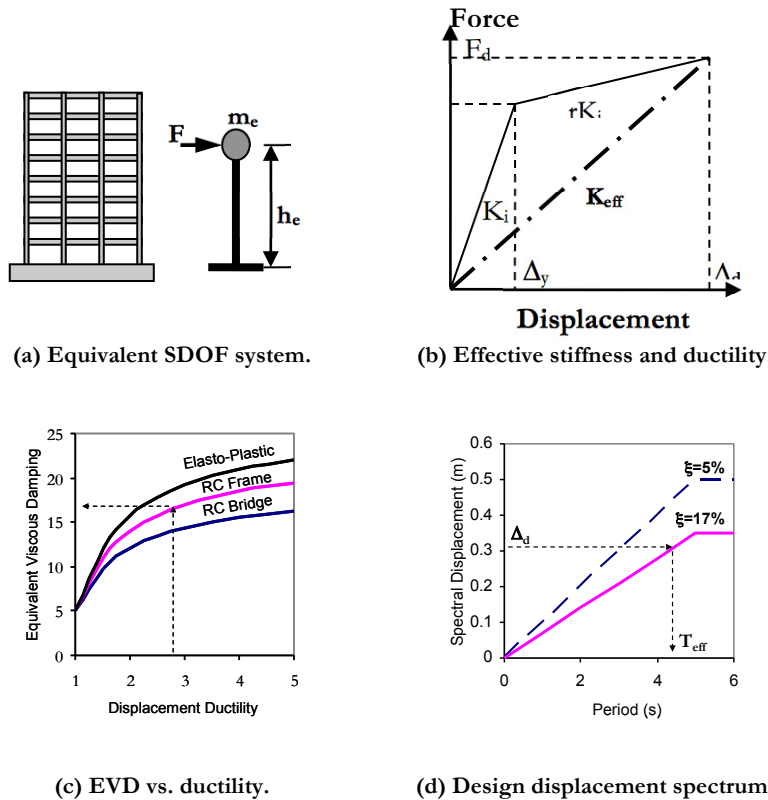


Figure 2.1. Key steps of DBD (Adapted from Priestley et al. [2007]).

Using the effective period, T_e , determined in Figure 2.1, the effective stiffness, K_e , of the SDOF system at the target displacement is determined from the following expression:

$$K_e = \frac{4\pi^2 m_e}{T_e^2} \quad (2.1)$$

where m_e is the effective mass. Using this effective stiffness to the design displacement, Δ_d , the design base shear V_b can be determined as follows:

$$V_b = K_e \Delta_d \quad (2.2)$$

2.2 DISPLACEMENT-BASED DESIGN OF MDOF SYSTEMS

The DBD of a SDOF system was presented in the previous section where it was seen how a nonlinear SDOF system could be represented as a linear SDOF oscillator characterised by an EVD value to account for nonlinear behaviour. This was then used with a design spectrum to determine the design base shear at the target design displacement. This section discusses how a MDOF system can be transformed into a SDOF system using a substitute structure approach. Once this SDOF representation is made, the DBD process is as previously outlined.

To extend the DBD approach to MDOF structures, the substitute structure concept by Gulkan and Sozen [1974] and Shibata and Sozen [1976] is used to identify the SDOF properties of an MDOF system assuming a certain displaced shape at maximum response. This is used to find the design target displacement, Δ_d , of the structure and its effective mass, m_e , that is used in the DBD process outlined previously. These are given as:

$$\Delta_d = \frac{\sum_{i=1}^n m_i \Delta_i^2}{\sum_{i=1}^n m_i \Delta_i} \quad (2.3)$$

$$m_e = \frac{\sum_{i=1}^n m_i \Delta_i^2}{\Delta_d} \quad (2.4)$$

where n is the number storeys in the structure and Δ_i comes from the assumed displacement profile for the structure, as outlined in Priestley et al. [2007]. For the case of steel MRFs, the assumed shape for the DBD of MRFs is given by Sullivan *et al.* [2012] as follows:

$$\Delta_i = \omega_\theta \theta_c h_i \left(\frac{4H_n - h_i}{4H_n - h_1} \right) \quad (2.5)$$

where θ_c is the design storey drift, h_i is the height to storey i , h_1 is the height of the storey, H_n is the total system height and n the number of storeys. ω_θ is a higher mode drift reduction factor that varies between 1.0 (for low-rise buildings) and 0.85 (for tall MRFs). For further details on the ω_θ factor, see Maley *et al.* [2013].

Once the displaced shape of the structure at its maximum response has been set, the yield displacement of the frame is needed in order to determine the storey-by-storey ductility demands. Maley *et al.* [2013] discuss that the calculation of yield storey drift in a steel MRF with full strength beam-column joints is a function of the section sizes chosen and it is possible to estimate the yield drift of the frame using either Equation 2.6 [Priestley *et al.*, 2007] or Equation 2.7 [Reyes *et al.*, 2008].

$$\theta_y = 0.65 \varepsilon_y \frac{L_b}{h_b} \quad (2.6)$$

$$\theta_y = \frac{\phi_{y,b} L_b + 0.9 \phi_{y,c} h_s}{6} \quad (2.7)$$

where L_b is the bay length, h_s is the inter-storey height, and $\phi_{y,b}$ and $\phi_{y,c}$ are the yield curvatures of the beam and column sections respectively. The yield curvature of a section can be obtained as the ratio of $\varepsilon_y W_{pl} / I_{zz}$ where ε_y is the yield strain of the steel, W_{pl} is the plastic section modulus and I_{zz} is the second moment of inertia, for the direction of bending being considered. Equations 2.6 and 2.7 are attractive since they are quite simple. However, the expressions have not been verified with the results of experimental testing.

As such, this report will aim to examine experimental testing and develop new expressions for the yield drift that also accounts for the beam-column joint typology.

Once the individual storey ductilities are defined, the EVD for each storey can be calculated using the relevant EVD relationship for the structural system being employed. For the case of MRFs, this is where the distinction between the different connection types may play a big role, as each connection could alter the hysteretic characteristics of the system and subsequently the EVD being provided.

With storey values of ductility and EVD defined, values for the system ductility and system EVD can be found by weighting by the design storey shear V_i and storey drift θ_i using work done considerations as given in Equation 2.8 and Equation 2.9.

$$\mu_{sys} = \frac{\sum V_i \theta_i \mu_i}{\sum V_i \theta_i} \quad (2.8)$$

$$\xi_{sys} = \frac{\sum V_i \theta_i \xi_i}{\sum V_i \theta_i} \quad (2.9)$$

To this extent, note that in DBD the equivalent lateral force distribution for a given design base shear force (V_b) is given by Equation 2.10 and the design storey shear by Equation 2.11.

$$F_i = \frac{m_i \Delta_i}{\sum_{j=i}^n m_j \Delta_j} V_b \quad (2.10)$$

$$V_i = \sum_{j=i}^{j=n} F_j \quad (2.11)$$

where n is the number of storeys. Note that the actual design storey shear need not be known to do this, only the profile of the shear distribution. Given that the MDOF system is now being represented as a SDOF with the above design displacement, EVD and effective mass, the DBD process as described can now be carried out as usual and the design base shear determined and distributed up the height to allow structural analysis and final member sizing.

2.3 INFORMATION REQUIRED FOR THE DBD OF STEEL MOMENT RESISTING FRAME STRUCTURES

As discussed in the previous section, the design of MRF structures using the DBD methodology is a relatively straightforward process. It was seen that the MDOF frame system is transformed into an equivalent SDOF system using an assumed displaced shape of the structure at the design deformation level. As such, one of the first pieces of information required when undertaking the DBD of steel MRF structures is an expression for the design displacement profile. The expression given by Equation 2.5 actually originates from the DBD of reinforced concrete frame structures but it has also been concluded (see Maley *et al.* [2013]) that it is suitable for the design of steel MRF structures. Expressions for the higher mode drift reduction factor, ω_θ in Equation 2.5 can also be found in Maley *et al.* [2013]. The other unknown in Equation 2.5 is the design story drift limit, θ_c , which may be governed by code-prescribed limits (assumed to limit the damage of non-structural elements) or by structural deformation limits. The structural deformation capacity of a steel MRF structure will essentially depend on the rotation capacity of plastic hinge regions, which implies that information is required on joint rotation capacity in the case of MRFs with partial strength joints, or the beam (or column base) plastic hinge rotation capacity in the case of MRFs with full-strength joints. An important focus of this report will therefore be to examine the deformation that characterises both the yield and ultimate limit states of steel MRF structures with either full-strength or partial-strength joints. Such information will be very useful for the finalisation of a DBD procedure for steel MRF structures.

Another aspect of the design procedure that needs further investigation is the subject of equivalent viscous damping. As shown earlier in Figure 2.1(c), the EVD is a function of the structural typology (or, more precisely, the hysteretic properties of a structure) and the ductility demand. In existing DBD guidelines [Priestley *et al.* 2007, Sullivan *et al.* 2012, Maley *et al.* 2013] that consider only full-strength rigid joints, use is made of equivalent viscous damping expressions corresponding to either the Ramberg-Osgood or the bilinear hysteretic models. An objective of this report will be to investigate, through advanced numerical analyses using hysteretic models calibrated to experimental results, whether such models are indeed appropriate for steel MRF structures with full-strength rigid joints. Furthermore, it is well known (and will be shown later in this report) that the beam-column joint typology can affect the hysteretic properties of a steel MRF. As such, another important objective of this report will be to develop equivalent viscous damping expressions that can be used for steel MRFs with partial-strength joints (and the focus will be on bolted extended end-plate joints). Finally, note that the EVD is a function of the ductility demand, which is in turn a function of the estimated yield drift for the frame. Equations 2.6 and 2.7 were developed through simplified analytical considerations of beam-column assemblages but have not been checked against extensive experimental testing results and nor are they applicable for MRFs with partial-strength joints. As such, this

report will aim to develop calibrated expressions for the yield drift of steel MRF structures that can account for the beam-column joint typology.

The points above represent the focus of the work in this report, where a review into existing experimental data is carried out with special attention to deformation capacity and to the validation of numerical models for further parametric studies on these connection types. These models can then be used to characterise various beam-column assemblages for future design.

2.4 REFERENCES

Gulkan, P. and Sozen, M.A., [1974] "Inelastic Response of Reinforced Concrete Structures to Earthquake Motions". ACI Journal, December, pp. 604-610.

Maley, T., Sullivan, T., Lago, A., Roldan, R. and Calvi, G.M. [2013] Characterising the Seismic Behaviour of Steel Structures, EUCENTRE Report No. 2013/02, Pavia, Italy.

Priestley, M. J. N., [1993] Myths and fallacies in earthquake engineering – Conflicts Between Design and Reality, Bull. NZ National Society for Earthquake Engineering, Vol. 26.n.3, 328-341.

Priestley, M. J. N., [2003] Myths and fallacies in earthquake engineering – Revisited, Mallet-Milne Lecture, IUSS Press, Pavia, Italy.

Priestley, M. J. N., Calvi, G. M., and Kowalski M. J., [2007] *Displacement based seismic design of structures*, IUSS Press, Pavia.

Reyes, G., Sullivan, T.J., Della Corte, G. [2008] "Development of a displacement based design method for steel frame-RC wall buildings," *Journal of Earthquake Engineering*, Vol. 14: 2, pp. 252-277

Shibata, A., Sozen, M. [1976] "Substitute Structure Method for Seismic Design in Reinforced Concrete", *ASCE Journal of Structural Engineering*, Vol. 102, No. 1, pp. 1-18.

Sullivan, T.J., Priestley, M.J.N. and Calvi, G.M., [2010] "Introduction to a Model Code for Displacement-Based Seismic Design" in Advances in Performance-Based Earthquake Engineering, Edited by Fardis M., Springer, ISBN 978-90-481-8745-4, pp.137-148.

Sullivan, T.J., Priestley, M.J.N., Calvi, G.M., Editors [2012]. *A Model Code for the Displacement-Based Seismic Design of Structures, DBD12*, IUSS Press, Pavia.

3. REVIEW OF PREVIOUS EXPERIMENTAL INVESTIGATIONS

Francesco Morelli, Walter Salvatore, Gaetano Della Corte, Giusy Terraciano, Gianmaria Di Lorenzo, Raffaele Landolfo, Hugo Augusto, José Miguel Castro, Carlos Rebelo & Luís Simões da Silva

3.1 INTRODUCTION

This chapter presents a concise overview of the current state of knowledge on the cyclic inelastic behaviour of full-strength, partial-strength, rigid or semi-rigid joints. Experimental data collected in the context of the DiSTEEL project is presented in a set of standardised forms that contain the detailed information regarding each experimental campaign.

Several experimental investigations into joint behaviour have already been undertaken and Nogueiro *et al.* [2007] recently observed that since the 1980s there have been 39 projects undertaken to investigate joint behaviour of steel structures with a total of 216 tests performed on different beam-to-column steel joint typologies. Two years later Nogueiro [2009] updated that information to 56 research projects and 288 experimental tests including the ones undertaken to investigate composite steel-concrete joint behaviour. Amongst other authors the collected data include the experimental campaigns conducted by Popov [1987], Korol *et al.* [1990], Plumier and Schleich [1993], Bernuzzi *et al.* [1996], Dubina *et al.* [2001], and Dunai *et al.* [2004].

In the next sub-sections a detailed description is made of the most relevant experimental tests performed on beam-to-column steel connections subjected to monotonic and/or cyclic loading conditions. The presentation is made in a systematic way by using easy and intuitive forms to describe the most relevant features of each test. The data is organised according to the publications produced by the various authors. The forms are divided into four parts. A first part dedicated to the identification of the publication and corresponding authors. A second part, where the geometry of the sub-assemblages and connection is illustrated. The third part is related to the material properties of the elements involved in the tested specimen. The last part is dedicated to the test set up and loading protocol (monotonic or cyclic), and also to the relevant data obtained with the test instrumentation. A field is included in the forms in which additional notes are provided regarding the most relevant data related to the test results, in particular the

resistance, mode of failure and ductility, when this information was provided by the authors.

It is important to refer that the experimental tests described here include results for fully welded beam-column connections and for bolted extended end-plate connections. Other connection typologies have clearly been tested but they are not reported here as the focus has been placed on the extended end-plate connection, which is quite common in Europe and can be detailed to be either full strength or partial strength, rigid or semi-rigid.

3.2 FULLY WELDED BEAM-COLUMN JOINTS

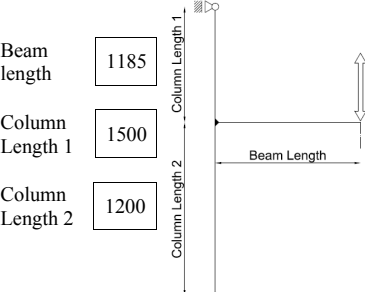
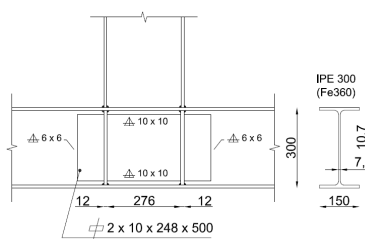
This section provides summary details for the experimental testing of fully welded beam-column joints, which are listed in Table 3.1.

Table 3.1. Summary details for fully welded beam-column joints.

Reference	Joint ID	Page
Ballio <i>et al.</i> [1987]	D1	15
Ballio <i>et al.</i> [1987]	D2	17
Dubina <i>et al.</i> [2001]	XS-W1	19
Dubina <i>et al.</i> [2001]	XU-W2	21
Ballio and Youquan [1993]	E1	23
Mele <i>et al.</i> [1999]	BCC5C	25
Mele <i>et al.</i> [1999]	BCC6C	27
Mele <i>et al.</i> [1999]	BCC8D	29
Beg <i>et al.</i> [2000]	SW1	31
Beg <i>et al.</i> [2000]	SW2	33

Test ID FW1																												
Paper																												
Title: <i>Cyclic behavior of steel beam-to-column joints experimental research</i>																												
Authors:																												
Ballio G.	Calado L.	De Martino A.	Faella C.	Mazzolani F.M.																								
Source	Volume:	Issue:	Pages:	Year:																								
Costruzioni Metalliche	2		69-90	1987																								
Test ID (with reference to the paper): D1																												
Geometry (mm)																												
Scheme:	Exterior Joint																											
Beam length	1185	Column Length 1																										
Column Length 1	1500		Beam Length																									
Column Length 2	1200	Column Length 2																										
<table border="1" style="width: 100%; border-collapse: collapse;"> <thead> <tr> <th colspan="2">Beam</th> </tr> </thead> <tbody> <tr> <td>Shape:</td> <td>IPE 300</td> </tr> <tr> <td>Height:</td> <td>300</td> <td>Width:</td> <td>150</td> </tr> <tr> <td>Flange Thickness:</td> <td>10.7</td> <td>Web Thickness:</td> <td>7.1</td> </tr> <tr> <td>Root radius:</td> <td></td> <td>Flange to web welds:</td> <td></td> </tr> </tbody> </table>					Beam		Shape:	IPE 300	Height:	300	Width:	150	Flange Thickness:	10.7	Web Thickness:	7.1	Root radius:		Flange to web welds:									
Beam																												
Shape:	IPE 300																											
Height:	300	Width:	150																									
Flange Thickness:	10.7	Web Thickness:	7.1																									
Root radius:		Flange to web welds:																										
Joint details <table border="1" style="width: 100%; border-collapse: collapse;"> <thead> <tr> <th colspan="2">Column</th> </tr> </thead> <tbody> <tr> <td>Shape:</td> <td>IPE300</td> </tr> <tr> <td>Heighth:</td> <td>300</td> <td>Width:</td> <td>150</td> </tr> <tr> <td>Flange Thickness:</td> <td>10.7</td> <td>Web Thickness:</td> <td>7.1</td> </tr> <tr> <td>Root radius:</td> <td></td> <td>Flange to web welds:</td> <td></td> </tr> <tr> <td>Supplementary web plates</td> <td></td> <td>Thickness:</td> <td></td> </tr> <tr> <td>Continuity plates</td> <td>X</td> <td>Thickness:</td> <td>12</td> </tr> </tbody> </table>					Column		Shape:	IPE300	Heighth:	300	Width:	150	Flange Thickness:	10.7	Web Thickness:	7.1	Root radius:		Flange to web welds:		Supplementary web plates		Thickness:		Continuity plates	X	Thickness:	12
Column																												
Shape:	IPE300																											
Heighth:	300	Width:	150																									
Flange Thickness:	10.7	Web Thickness:	7.1																									
Root radius:		Flange to web welds:																										
Supplementary web plates		Thickness:																										
Continuity plates	X	Thickness:	12																									
<small>NOTE: The beam length provided is the distance between the point of application of the force and the column flange.</small>																												

Test ID FW1		Material Properties (MPa)	
Beam Nominal grade <input type="checkbox"/> Measured values <input checked="" type="checkbox"/> 314 Flange yield strength <input type="checkbox"/> 288 Web yield strength <input type="checkbox"/> 339 (mean value)		Column Nominal grade <input type="checkbox"/> Measured values <input checked="" type="checkbox"/> 288 Flange yield strength <input type="checkbox"/> 339 (mean value) Supplementary web plate Nominal grade <input type="checkbox"/> Measured values <input type="checkbox"/> Yield strength <input type="checkbox"/>	
Continuity Plates Nominal grade <input type="checkbox"/> Measured values <input type="checkbox"/> Yield strength <input type="checkbox"/>			
Note: Type of test <input checked="" type="checkbox"/> Cyclic Loading protocol <input type="checkbox"/> ECCS [85] Data provided: <input type="checkbox"/>			
Test setup, loading protocol and test results Type of response curve Force <input checked="" type="checkbox"/> <input type="checkbox"/> Moment <input type="checkbox"/> Displacement <input checked="" type="checkbox"/> <input type="checkbox"/> Rotation <input type="checkbox"/>			
<u>Loading axis</u> 			

Test ID FW2				
Paper				
Title: <i>Cyclic behavior of steel beam-to-column joints experimental research</i>				
Authors:	Ballio G.	Calado L.	De Martino A.	Faella C. Mazzolani F.M.
Source	Costruzioni Metalliche	Volume:	2	Issue: Pages: Year: 69-90 1987
Test ID (with reference to the paper): D2				
Geometry (mm)				
Scheme:	Exterior Joint			
Beam length	1185			
Column Length 1	1500	Column Length 1	1500	Beam Length
Column Length 2	1200	Column Length 2	1200	
				
Beam Shape: IPE 300 Height: 300 Width: 150 Flange Thickness: 10.7 Web Thickness: 7.1 Root radius: Flange to web welds:				
Joint details				
				
Column Shape: IPE300 Height: 300 Width: 150 Flange Thickness: 10.7 Web Thickness: 7.1 Root radius: Flange to web welds: Supplementary web plates X Thickness 10 Continuity plates X Thickness 12				
NOTE: The beam length provided is the distance between the point of application of the force and the column flange.				

Test ID FW2

Material Properties (MPa)	
Beam	Column
Nominal grade	<input type="checkbox"/>
Measured values	<input checked="" type="checkbox"/>
Flange yield strength	304
Web yield strength	
Continuity Plates	
Nominal grade	<input type="checkbox"/>
Measured values	<input type="checkbox"/>
Yield strength	
Supplementary web plate	
Nominal grade	<input type="checkbox"/>
Measured values	<input type="checkbox"/>
Yield strength	

Note:

Type of test	Cyclic	Test setup, loading protocol and test results
Loading protocol	ECCS [85]	Type of response curve
Data provided:	<input type="checkbox"/>	Force <input checked="" type="checkbox"/>
		Moment <input type="checkbox"/>
		Displacement <input checked="" type="checkbox"/>
		Rotation <input type="checkbox"/>

Loading axis

Dimensions shown in the diagram:

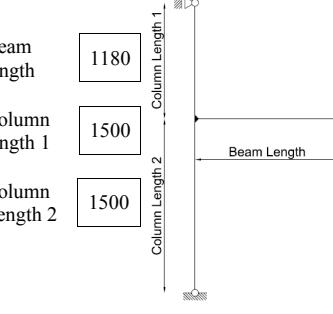
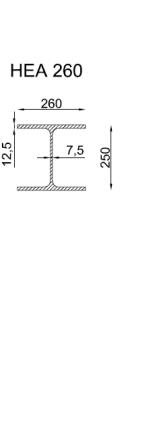
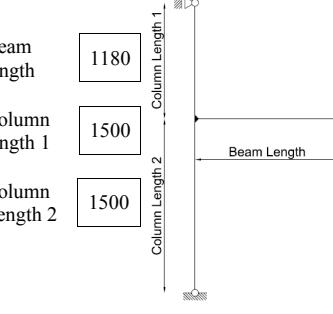
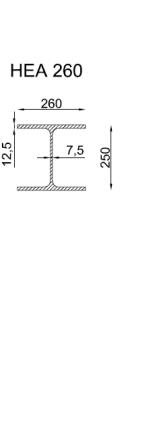
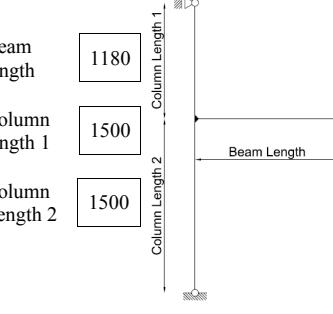
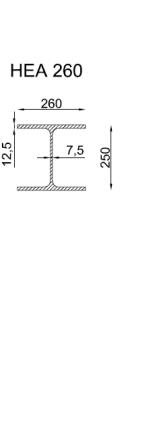
- Total height: 300 mm
- Flange width: 150 mm
- Base plate thickness: 6 mm
- Central vertical plate thickness: 10 mm
- Total length: 2725 mm
- Distance between supports: 1500 mm
- Distance from base to top of column: 1185 mm
- Eccentricity of eccentric base plates: 12 mm

Test ID FW3	
Paper	
Title: <i>Cyclic tests of double-sided beam-to-column joints</i>	
Authors: Dubina D. Ciutina A. Stratian A.	
Source Journal of Structural Engineering	
Volume: 127 Issue: 129-136 Pages: 129-136 Year: 2001	
Test ID (with reference to the paper): XS W2	
Geometry (mm)	
Scheme: Interior Joint	
Beam length 950	Height: 360
Beam length 2 950	Width: 170
Column Length 1225	Flange Thickness: 12.7
	Web Thickness: 8.0
	Root radius: <input type="text"/>
	Flange to web welds: <input type="text"/>
Beam	
Shape: IPE 360	
Height: 360	Width: 170
Flange Thickness: 12.7	Web Thickness: 8.0
Root radius: <input type="text"/>	Flange to web welds: <input type="text"/>
Joint details	
Column Shape: HEB 300 Height: 300 Width: 300 Flange Thickness: 18.4 Web Thickness: 11.4 Root radius: <input type="text"/> Flange to web welds: <input type="text"/> Supplementary web plates: <input type="text"/> Thickness: <input type="text"/> Continuity plates: X Thickness: 15	
NOTE: The beam length provided is the distance between the point of application of the force and the column flange. In the article, also the tensile strength and the elongation to maximum load are provided. Other information on the same test can be found in: Dubina D., Grecea D., Ciutina A., Stratian A., "Influence of Connection Topology and Loading Asymmetry", in Moment Resistant Connections of Steel Frames in Seismic Areas, edited by F.M. Mazzolani.	

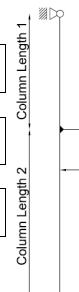
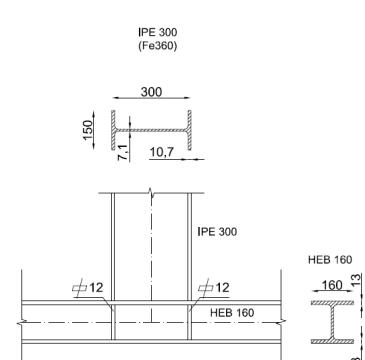
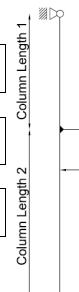
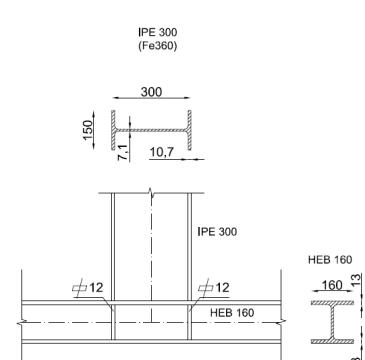
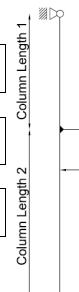
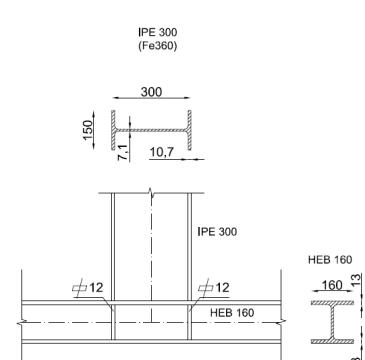
Test ID FW3	
Material Properties (MPa)	
Beam	
Nominal grade	<input type="checkbox"/>
Measured values	<input checked="" type="checkbox"/>
Flange yield strength	329.8
Web yield strength	348.4
Continuity Plates	
Nominal grade	<input type="checkbox"/>
Measured values	<input checked="" type="checkbox"/>
Yield strength	273.2
Column	
Nominal grade	<input type="checkbox"/>
Measured values	<input checked="" type="checkbox"/>
Flange yield strength	313.0
Web yield strength	341.8
Supplementary web plate	
Nominal grade	<input type="checkbox"/>
Measured values	<input type="checkbox"/>
Yield strength	
Note:	
Type of test	Cyclic/ Monotonic
Loading protocol	ECCS simpl.
Data provided:	
Test setup, loading protocol and test results	
Type of response curve	
Force	<input type="checkbox"/>
Moment	<input checked="" type="checkbox"/>
Displacement	<input type="checkbox"/>
Rotation	<input checked="" type="checkbox"/>
<p>Applied force symmetrical loading</p> <p>- Strain gauge □ Inclinometer ↓ Displacement transducer</p>	

Test ID FW4																			
Paper																			
Title: <i>Cyclic tests of doubled sided beam-to-column joints</i>																			
Authors: Dubina D. Ciutina A. Stratian A.																			
Source Journal of Structural Engineering																			
Volume: 127 Issue: 129-136 Year: 2001																			
Test ID (with reference to the paper): XU W1																			
Geometry (mm)																			
Scheme: Interior Joint	<table border="1"> <thead> <tr> <th colspan="2">Beam</th> </tr> </thead> <tbody> <tr> <td>Shape:</td><td>IPE 360</td></tr> <tr> <td>Height:</td><td>360.9</td></tr> <tr> <td>Flange Thickness:</td><td>12.5</td></tr> <tr> <td>Root radius:</td><td></td></tr> <tr> <td>Flange to web welds:</td><td></td></tr> </tbody> </table>	Beam		Shape:	IPE 360	Height:	360.9	Flange Thickness:	12.5	Root radius:		Flange to web welds:							
Beam																			
Shape:	IPE 360																		
Height:	360.9																		
Flange Thickness:	12.5																		
Root radius:																			
Flange to web welds:																			
Beam length	950																		
Beam length 1	Column Length 2																		
Beam length 2	950																		
Column Length	1225																		
Column Length 1	Beam Length																		
Column Length 2	Beam Length																		
Joint details																			
	<table border="1"> <thead> <tr> <th colspan="2">Column</th> </tr> </thead> <tbody> <tr> <td>Shape:</td><td>HEB 300</td></tr> <tr> <td>Height:</td><td>297.7</td></tr> <tr> <td>Flange Thickness:</td><td>18.7</td></tr> <tr> <td>Root radius:</td><td></td></tr> <tr> <td>Flange to web welds:</td><td></td></tr> <tr> <td>Supplementary web plates:</td><td></td></tr> <tr> <td>Continuity plates:</td><td>X</td></tr> <tr> <td>Thickness:</td><td>15</td></tr> </tbody> </table>	Column		Shape:	HEB 300	Height:	297.7	Flange Thickness:	18.7	Root radius:		Flange to web welds:		Supplementary web plates:		Continuity plates:	X	Thickness:	15
Column																			
Shape:	HEB 300																		
Height:	297.7																		
Flange Thickness:	18.7																		
Root radius:																			
Flange to web welds:																			
Supplementary web plates:																			
Continuity plates:	X																		
Thickness:	15																		
NOTE: The beam length provided is the distance between the point of application of the force and the column flange. In the article, also the tensile strength and the elongation to maximum load are provided. Other information on the same test can be found in: Dubina D., Grecea D., Ciutina A., Stratian A., "Influence of Connection Typology and Loading Asymmetry", in Moment Resistant Connections of Steel Frames in Seismic Areas, edited by F.M. Mazzolani.																			

Test ID FW4		Material Properties (MPa)	
Beam Nominal grade <input type="checkbox"/> Measured values <input checked="" type="checkbox"/> X Flange yield strength 329.8 Web yield strength 348.4		Column Nominal grade <input type="checkbox"/> Measured values <input checked="" type="checkbox"/> X Flange yield strength 313.0 Web yield strength 341.8	
Continuity Plates Nominal grade <input type="checkbox"/> Measured values <input checked="" type="checkbox"/> X Yield strength 273.2		Supplementary web plate Nominal grade <input type="checkbox"/> Measured values <input type="checkbox"/> Yield strength <input type="checkbox"/>	
Note: Type of test <input type="checkbox"/> Loading protocol ECCS simpl. Data provided: <input type="checkbox"/>			
Test setup, loading protocol and test results Type of response curve Force <input type="checkbox"/> Moment <input checked="" type="checkbox"/> X Displacement <input type="checkbox"/> Rotation <input checked="" type="checkbox"/> The moment is computed at the column face Total joint rotation			

Test ID FW5																	
Paper <i>Title: An Experimental Research on Beam to Column Joints: Exterior Connections</i>																	
Authors: Ballio G. Youquan C.																	
Source Proceedings XIV C.T.A.	Volume: Issue: Pages: 110-132 Year: 1993																
Test ID (with reference to the paper): E1																	
<table border="1"> <thead> <tr> <th colspan="2">Geometry (mm)</th> </tr> <tr> <th colspan="2">Beam</th> </tr> </thead> <tbody> <tr> <td>Scheme: Exterior Joint</td> <td>Shape: HEA 260</td> </tr> <tr> <td>Beam length 1180</td> <td>Height: 250 Width: 260</td> </tr> <tr> <td>Column length 1 1500</td> <td>Flange Thickness: 12.5 Web Thickness: 7.5</td> </tr> <tr> <td>Column Length 2 1500</td> <td>Root radius: 24 Flange to web welds []</td> </tr> </tbody> </table>		Geometry (mm)		Beam		Scheme: Exterior Joint	Shape: HEA 260	Beam length 1180	Height: 250 Width: 260	Column length 1 1500	Flange Thickness: 12.5 Web Thickness: 7.5	Column Length 2 1500	Root radius: 24 Flange to web welds []				
Geometry (mm)																	
Beam																	
Scheme: Exterior Joint	Shape: HEA 260																
Beam length 1180	Height: 250 Width: 260																
Column length 1 1500	Flange Thickness: 12.5 Web Thickness: 7.5																
Column Length 2 1500	Root radius: 24 Flange to web welds []																
<table border="1"> <thead> <tr> <th colspan="2">Joint details</th> </tr> <tr> <th colspan="2">Column</th> </tr> </thead> <tbody> <tr> <td></td> <td>Shape: HEB 300</td> </tr> <tr> <td></td> <td>Height: 300 Width: 300</td> </tr> <tr> <td></td> <td>Flange Thickness: 19.0 Web Thickness: 11.0</td> </tr> <tr> <td></td> <td>Root radius: [] Flange to web welds: []</td> </tr> <tr> <td></td> <td>Supplementary web plates [] Thickness []</td> </tr> <tr> <td></td> <td>Continuity plates X Thickness [?]</td> </tr> </tbody> </table>		Joint details		Column			Shape: HEB 300		Height: 300 Width: 300		Flange Thickness: 19.0 Web Thickness: 11.0		Root radius: [] Flange to web welds: []		Supplementary web plates [] Thickness []		Continuity plates X Thickness [?]
Joint details																	
Column																	
	Shape: HEB 300																
	Height: 300 Width: 300																
	Flange Thickness: 19.0 Web Thickness: 11.0																
	Root radius: [] Flange to web welds: []																
	Supplementary web plates [] Thickness []																
	Continuity plates X Thickness [?]																
<small>NOTE: The beam length provided is the distance between the point of application of the force and the column flange.</small>																	

Test ID FW5		Material Properties (MPa)																					
<table border="1"> <thead> <tr> <th colspan="2">Beam</th> </tr> </thead> <tbody> <tr> <td>Nominal grade</td> <td><input type="checkbox"/></td> </tr> <tr> <td>Measured values</td> <td><input checked="" type="checkbox"/></td> </tr> <tr> <td>Flange yield strength</td> <td>302.0</td> </tr> <tr> <td>Web yield strength</td> <td>302.0</td> </tr> </tbody> </table>		Beam		Nominal grade	<input type="checkbox"/>	Measured values	<input checked="" type="checkbox"/>	Flange yield strength	302.0	Web yield strength	302.0	<table border="1"> <thead> <tr> <th colspan="2">Column</th> </tr> </thead> <tbody> <tr> <td>Nominal grade</td> <td><input type="checkbox"/></td> </tr> <tr> <td>Measured values</td> <td><input type="checkbox"/></td> </tr> <tr> <td>Flange yield strength</td> <td>?</td> </tr> <tr> <td>Web yield strength</td> <td>?</td> </tr> </tbody> </table>		Column		Nominal grade	<input type="checkbox"/>	Measured values	<input type="checkbox"/>	Flange yield strength	?	Web yield strength	?
Beam																							
Nominal grade	<input type="checkbox"/>																						
Measured values	<input checked="" type="checkbox"/>																						
Flange yield strength	302.0																						
Web yield strength	302.0																						
Column																							
Nominal grade	<input type="checkbox"/>																						
Measured values	<input type="checkbox"/>																						
Flange yield strength	?																						
Web yield strength	?																						
<table border="1"> <thead> <tr> <th colspan="2">Continuity Plates</th> </tr> </thead> <tbody> <tr> <td>Nominal grade</td> <td><input type="checkbox"/></td> </tr> <tr> <td>Measured values</td> <td><input type="checkbox"/></td> </tr> <tr> <td>Yield strength</td> <td>?</td> </tr> </tbody> </table>		Continuity Plates		Nominal grade	<input type="checkbox"/>	Measured values	<input type="checkbox"/>	Yield strength	?	<table border="1"> <thead> <tr> <th colspan="2">Supplementary web plate</th> </tr> </thead> <tbody> <tr> <td>Nominal grade</td> <td><input type="checkbox"/></td> </tr> <tr> <td>Measured values</td> <td><input type="checkbox"/></td> </tr> <tr> <td>Yield strength</td> <td></td> </tr> </tbody> </table>		Supplementary web plate		Nominal grade	<input type="checkbox"/>	Measured values	<input type="checkbox"/>	Yield strength					
Continuity Plates																							
Nominal grade	<input type="checkbox"/>																						
Measured values	<input type="checkbox"/>																						
Yield strength	?																						
Supplementary web plate																							
Nominal grade	<input type="checkbox"/>																						
Measured values	<input type="checkbox"/>																						
Yield strength																							
<p>Note:</p> <table border="1"> <tr> <td>Type of test</td> <td colspan="3">Test setup, loading protocol and test results</td> </tr> <tr> <td>Loading protocol</td> <td>ECCS</td> <td>Type of response curve</td> <td></td> </tr> <tr> <td>Data provided:</td> <td colspan="3"></td> </tr> </table> <table border="1"> <tr> <td>Force</td> <td><input type="checkbox"/></td> </tr> <tr> <td>Moment</td> <td><input checked="" type="checkbox"/></td> </tr> <tr> <td>Displacement</td> <td><input type="checkbox"/></td> </tr> <tr> <td>Rotation</td> <td><input checked="" type="checkbox"/></td> </tr> </table>				Type of test	Test setup, loading protocol and test results			Loading protocol	ECCS	Type of response curve		Data provided:				Force	<input type="checkbox"/>	Moment	<input checked="" type="checkbox"/>	Displacement	<input type="checkbox"/>	Rotation	<input checked="" type="checkbox"/>
Type of test	Test setup, loading protocol and test results																						
Loading protocol	ECCS	Type of response curve																					
Data provided:																							
Force	<input type="checkbox"/>																						
Moment	<input checked="" type="checkbox"/>																						
Displacement	<input type="checkbox"/>																						
Rotation	<input checked="" type="checkbox"/>																						

Test ID FW6																																
Paper Title: <i>Experimental Behavior of Beam-to-Column Welded Connections: Effect of the Panel Zone Design</i>																																
Authors: Mele E. Calado L. De Luca A.																																
Source Proceedings XVII C.T.A. Volume: Issue: Pages: Year: 1999																																
Test ID (with reference to the paper): BCC5C																																
<table border="1"> <thead> <tr> <th colspan="3">Geometry (mm)</th></tr> </thead> <tbody> <tr> <td colspan="3"> Scheme: Exterior Joint </td></tr> <tr> <td>Beam length</td><td>862</td><td>Column Length 1</td></tr> <tr> <td>Column length 1</td><td>905</td><td>Column Length 2</td></tr> <tr> <td>Column Length 2</td><td>905</td><td>Beam Length</td></tr> <tr> <td colspan="3">  </td></tr> <tr> <td colspan="3"> Beam Shape: IPE 300 Height: 300 Width: 150 Flange Thickness: 10.7 Web Thickness: 7.1 Root radius: Flange to web welds: </td></tr> <tr> <td colspan="3"> Joint details  </td></tr> <tr> <td colspan="3"> Column Shape: HEB 160 Height: 160 Width: 160 Flange Thickness: 13.0 Web Thickness: 8.0 Root radius: Flange to web welds: Supplementary web plates Thickness: Continuity plates X Thickness: 12 </td></tr> <tr> <td colspan="3"> NOTE: The beam length provided is the distance between the point of application of the force and the column flange. </td></tr> </tbody> </table>			Geometry (mm)			Scheme: Exterior Joint			Beam length	862	Column Length 1	Column length 1	905	Column Length 2	Column Length 2	905	Beam Length				Beam Shape: IPE 300 Height: 300 Width: 150 Flange Thickness: 10.7 Web Thickness: 7.1 Root radius: Flange to web welds:			Joint details 			Column Shape: HEB 160 Height: 160 Width: 160 Flange Thickness: 13.0 Web Thickness: 8.0 Root radius: Flange to web welds: Supplementary web plates Thickness: Continuity plates X Thickness: 12			NOTE: The beam length provided is the distance between the point of application of the force and the column flange.		
Geometry (mm)																																
Scheme: Exterior Joint																																
Beam length	862	Column Length 1																														
Column length 1	905	Column Length 2																														
Column Length 2	905	Beam Length																														
																																
Beam Shape: IPE 300 Height: 300 Width: 150 Flange Thickness: 10.7 Web Thickness: 7.1 Root radius: Flange to web welds:																																
Joint details 																																
Column Shape: HEB 160 Height: 160 Width: 160 Flange Thickness: 13.0 Web Thickness: 8.0 Root radius: Flange to web welds: Supplementary web plates Thickness: Continuity plates X Thickness: 12																																
NOTE: The beam length provided is the distance between the point of application of the force and the column flange.																																

Test ID FW6	
Material Properties (MPa)	
Beam	Column
Nominal grade <input type="checkbox"/>	Nominal grade <input type="checkbox"/>
Measured values <input checked="" type="checkbox"/>	Measured values <input checked="" type="checkbox"/>
Flange yield strength 274.78	Flange yield strength 323.13
Web yield strength 305.54	Web yield strength 395.56
Continuity Plates	
Nominal grade <input type="checkbox"/>	Nominal grade <input type="checkbox"/>
Measured values <input type="checkbox"/>	Measured values <input type="checkbox"/>
Yield strength <input type="checkbox"/>	Yield strength <input type="checkbox"/>
Note:	
Type of test	Test setup, loading protocol and test results
Loading protocol	Type of response curve
(4 different tests) Constant amplitude (37.5mm) Constant amplitude (50.0mm) Constant amplitude (75.0mm) ECCS	Force <input checked="" type="checkbox"/> <input type="checkbox"/> Moment <input type="checkbox"/> <input checked="" type="checkbox"/> Displacement <input checked="" type="checkbox"/> <input type="checkbox"/> Rotation <input type="checkbox"/> <input type="checkbox"/>

Test ID FW7																							
Paper																							
Title: <i>Experimental Behavior of Beam-to-Column Welded Connections: Effect of the Panel Zone Design</i>																							
Authors:	Mele E.	Calado L.																					
Source	Calado L.	De Luca A.																					
Proceedings XVII C.T.A.	Volume:	Issue:																					
	Pages:	Year:																					
	1999																						
Test ID (with reference to the paper): BCC6																							
Geometry (mm)																							
Scheme:	Exterior Joint																						
Beam length	862	Column Length 1																					
Column length 1	905	Column Length 2																					
Column Length 2	905	Beam Length																					
<table border="1"> <thead> <tr> <th colspan="3">Beam</th></tr> </thead> <tbody> <tr> <td>Shape:</td><td colspan="2">IPE 300</td></tr> <tr> <td>Height:</td><td>300</td><td>Width: 150</td></tr> <tr> <td>Flange Thickness:</td><td>10.7</td><td>Web Thickness: 7.1</td></tr> <tr> <td>Root radius:</td><td></td><td>Flange to web welds</td></tr> </tbody> </table>			Beam			Shape:	IPE 300		Height:	300	Width: 150	Flange Thickness:	10.7	Web Thickness: 7.1	Root radius:		Flange to web welds						
Beam																							
Shape:	IPE 300																						
Height:	300	Width: 150																					
Flange Thickness:	10.7	Web Thickness: 7.1																					
Root radius:		Flange to web welds																					
Joint details																							
<table border="1"> <thead> <tr> <th colspan="3">Column</th></tr> </thead> <tbody> <tr> <td>Shape:</td><td colspan="2">HEB 200</td></tr> <tr> <td>Height:</td><td>200</td><td>Width: 200</td></tr> <tr> <td>Flange Thickness:</td><td>15.0</td><td>Web Thickness: 9.0</td></tr> <tr> <td>Root radius:</td><td></td><td>Flange to web welds</td></tr> <tr> <td>Supplementary web plates</td><td></td><td>Thickness</td></tr> <tr> <td>Continuity plates</td><td>X</td><td>Thickness 12</td></tr> </tbody> </table>			Column			Shape:	HEB 200		Height:	200	Width: 200	Flange Thickness:	15.0	Web Thickness: 9.0	Root radius:		Flange to web welds	Supplementary web plates		Thickness	Continuity plates	X	Thickness 12
Column																							
Shape:	HEB 200																						
Height:	200	Width: 200																					
Flange Thickness:	15.0	Web Thickness: 9.0																					
Root radius:		Flange to web welds																					
Supplementary web plates		Thickness																					
Continuity plates	X	Thickness 12																					
<p>NOTE: The beam length provided is the distance between the point of application of the force and the column flange. Other information on the same test can be found in: Calado L., "Influence of Column Size", in Moment Resistant Connections of Steel Frames in Seismic Areas, edited by F.M. Mazzolani.</p>																							

Test ID FW7																																					
Material Properties (MPa)																																					
<table border="1" style="width: 100%; border-collapse: collapse;"> <tr> <th colspan="2" style="text-align: center;">Beam</th> </tr> <tr> <td>Nominal grade</td> <td><input type="checkbox"/></td> </tr> <tr> <td>Measured values</td> <td><input checked="" type="checkbox"/></td> </tr> <tr> <td>Flange yield strength</td> <td>278.62</td> </tr> <tr> <td>Web yield strength</td> <td>304.62</td> </tr> <tr> <td colspan="2" style="text-align: center;">Continuity Plates</td> </tr> <tr> <td>Nominal grade</td> <td><input type="checkbox"/></td> </tr> <tr> <td>Measured values</td> <td><input type="checkbox"/></td> </tr> <tr> <td>Yield strength</td> <td><input type="checkbox"/></td> </tr> <tr> <th colspan="2" style="text-align: center;">Column</th> </tr> <tr> <td>Nominal grade</td> <td><input type="checkbox"/></td> </tr> <tr> <td>Measured values</td> <td><input checked="" type="checkbox"/></td> </tr> <tr> <td>Flange yield strength</td> <td>312.56</td> </tr> <tr> <td>Web yield strength</td> <td>401.62</td> </tr> <tr> <th colspan="2" style="text-align: center;">Supplementary web plate</th> </tr> <tr> <td>Nominal grade</td> <td><input type="checkbox"/></td> </tr> <tr> <td>Measured values</td> <td><input type="checkbox"/></td> </tr> <tr> <td>Yield strength</td> <td><input type="checkbox"/></td> </tr> </table>		Beam		Nominal grade	<input type="checkbox"/>	Measured values	<input checked="" type="checkbox"/>	Flange yield strength	278.62	Web yield strength	304.62	Continuity Plates		Nominal grade	<input type="checkbox"/>	Measured values	<input type="checkbox"/>	Yield strength	<input type="checkbox"/>	Column		Nominal grade	<input type="checkbox"/>	Measured values	<input checked="" type="checkbox"/>	Flange yield strength	312.56	Web yield strength	401.62	Supplementary web plate		Nominal grade	<input type="checkbox"/>	Measured values	<input type="checkbox"/>	Yield strength	<input type="checkbox"/>
Beam																																					
Nominal grade	<input type="checkbox"/>																																				
Measured values	<input checked="" type="checkbox"/>																																				
Flange yield strength	278.62																																				
Web yield strength	304.62																																				
Continuity Plates																																					
Nominal grade	<input type="checkbox"/>																																				
Measured values	<input type="checkbox"/>																																				
Yield strength	<input type="checkbox"/>																																				
Column																																					
Nominal grade	<input type="checkbox"/>																																				
Measured values	<input checked="" type="checkbox"/>																																				
Flange yield strength	312.56																																				
Web yield strength	401.62																																				
Supplementary web plate																																					
Nominal grade	<input type="checkbox"/>																																				
Measured values	<input type="checkbox"/>																																				
Yield strength	<input type="checkbox"/>																																				
<p>Note:</p> <table border="1" style="width: 100%; border-collapse: collapse;"> <tr> <td rowspan="5" style="vertical-align: top; width: 30%;"> Type of test Loading protocol <ul style="list-style-type: none"> <input checked="" type="checkbox"/> (4 different tests) Constant amplitude (37.5mm) Constant amplitude (50.0mm) Constant amplitude (75.0mm) ECCS </td> <td colspan="2" style="text-align: center;">Test setup, loading protocol and test results</td> </tr> <tr> <td colspan="2" style="text-align: center;">Type of response curve</td> </tr> <tr> <td>Force</td> <td><input checked="" type="checkbox"/></td> </tr> <tr> <td>Moment</td> <td><input type="checkbox"/></td> </tr> <tr> <td>Displacement</td> <td><input checked="" type="checkbox"/></td> </tr> <tr> <td>Rotation</td> <td><input type="checkbox"/></td> </tr> </table>		Type of test Loading protocol <ul style="list-style-type: none"> <input checked="" type="checkbox"/> (4 different tests) Constant amplitude (37.5mm) Constant amplitude (50.0mm) Constant amplitude (75.0mm) ECCS 	Test setup, loading protocol and test results		Type of response curve		Force	<input checked="" type="checkbox"/>	Moment	<input type="checkbox"/>	Displacement	<input checked="" type="checkbox"/>	Rotation	<input type="checkbox"/>																							
Type of test Loading protocol <ul style="list-style-type: none"> <input checked="" type="checkbox"/> (4 different tests) Constant amplitude (37.5mm) Constant amplitude (50.0mm) Constant amplitude (75.0mm) ECCS 	Test setup, loading protocol and test results																																				
	Type of response curve																																				
	Force		<input checked="" type="checkbox"/>																																		
	Moment		<input type="checkbox"/>																																		
	Displacement	<input checked="" type="checkbox"/>																																			
Rotation	<input type="checkbox"/>																																				

Test ID FW8		
Paper		
Title: <i>Experimental Behavior of Beam-to-Column Welded Connections: Effect of the Panel Zone Design</i>		
Authors:		
Mele E.	Calado L.	De Luca A.
Source	Volume:	Issue:
Proceedings XVII C.T.A.		Pages:
		Year: 1999
Test ID (with reference to the paper): BCC8		
Geometry (mm)		
Scheme: Exterior Joint		
Beam length	862	Column Length 1
Column length 1	905	Column Length 2
Column Length 2	905	Beam Length
Beam Shape: IPE 300 Height: 300 Width: 150 Flange Thickness: 10.7 Web Thickness: 7.1 Root radius: [] Flange to web welds: []		
Joint details		
Column Shape: HEB 240 Height: 240 Width: 240 Flange Thickness: 17.0 Web Thickness: 10.0 Root radius: [] Flange to web welds: [] Supplementary web plates: [] Thickness: [] Continuity plates: X Thickness: 12		
NOTE: The beam length provided is the distance between the point of application of the force and the column flange. Other information on the same test can be found in: Calado L., "Influence of Column Size", in Moment Resistant Connections of Steel Frames in Seismic Areas, edited by F.M. Mazzolani.		

Test ID FW8		Material Properties (MPa)																					
<table border="1"> <thead> <tr> <th colspan="2">Beam</th> </tr> </thead> <tbody> <tr> <td>Nominal grade</td> <td><input type="checkbox"/></td> </tr> <tr> <td>Measured values</td> <td><input checked="" type="checkbox"/></td> </tr> <tr> <td>Flange yield strength</td> <td>292.00</td> </tr> <tr> <td>Web yield strength</td> <td>299.50</td> </tr> </tbody> </table>		Beam		Nominal grade	<input type="checkbox"/>	Measured values	<input checked="" type="checkbox"/>	Flange yield strength	292.00	Web yield strength	299.50	<table border="1"> <thead> <tr> <th colspan="2">Column</th> </tr> </thead> <tbody> <tr> <td>Nominal grade</td> <td><input type="checkbox"/></td> </tr> <tr> <td>Measured values</td> <td><input checked="" type="checkbox"/></td> </tr> <tr> <td>Flange yield strength</td> <td>300.50</td> </tr> <tr> <td>Web yield strength</td> <td>309.00</td> </tr> </tbody> </table>		Column		Nominal grade	<input type="checkbox"/>	Measured values	<input checked="" type="checkbox"/>	Flange yield strength	300.50	Web yield strength	309.00
Beam																							
Nominal grade	<input type="checkbox"/>																						
Measured values	<input checked="" type="checkbox"/>																						
Flange yield strength	292.00																						
Web yield strength	299.50																						
Column																							
Nominal grade	<input type="checkbox"/>																						
Measured values	<input checked="" type="checkbox"/>																						
Flange yield strength	300.50																						
Web yield strength	309.00																						
<table border="1"> <thead> <tr> <th colspan="2">Continuity Plates</th> </tr> </thead> <tbody> <tr> <td>Nominal grade</td> <td><input type="checkbox"/></td> </tr> <tr> <td>Measured values</td> <td><input type="checkbox"/></td> </tr> <tr> <td>Yield strength</td> <td><input type="checkbox"/></td> </tr> </tbody> </table>		Continuity Plates		Nominal grade	<input type="checkbox"/>	Measured values	<input type="checkbox"/>	Yield strength	<input type="checkbox"/>	<table border="1"> <thead> <tr> <th colspan="2">Supplementary web plate</th> </tr> </thead> <tbody> <tr> <td>Nominal grade</td> <td><input type="checkbox"/></td> </tr> <tr> <td>Measured values</td> <td><input type="checkbox"/></td> </tr> <tr> <td>Yield strength</td> <td><input type="checkbox"/></td> </tr> </tbody> </table>		Supplementary web plate		Nominal grade	<input type="checkbox"/>	Measured values	<input type="checkbox"/>	Yield strength	<input type="checkbox"/>				
Continuity Plates																							
Nominal grade	<input type="checkbox"/>																						
Measured values	<input type="checkbox"/>																						
Yield strength	<input type="checkbox"/>																						
Supplementary web plate																							
Nominal grade	<input type="checkbox"/>																						
Measured values	<input type="checkbox"/>																						
Yield strength	<input type="checkbox"/>																						
<p>Note:</p> <table border="1"> <tr> <td>Type of test</td> <td colspan="3">Test setup, loading protocol and test results</td> </tr> <tr> <td>Loading protocol</td> <td colspan="3"> Type of response curve Force <input checked="" type="checkbox"/> Moment <input type="checkbox"/> Displacement <input checked="" type="checkbox"/> Rotation <input type="checkbox"/> </td> </tr> <tr> <td>(4 different tests) Constant amplitude (37.5mm) Constant amplitude (50.0mm) Constant amplitude (75.0mm) ECCS</td> <td></td> <td></td> <td></td> </tr> </table>				Type of test	Test setup, loading protocol and test results			Loading protocol	Type of response curve Force <input checked="" type="checkbox"/> Moment <input type="checkbox"/> Displacement <input checked="" type="checkbox"/> Rotation <input type="checkbox"/>			(4 different tests) Constant amplitude (37.5mm) Constant amplitude (50.0mm) Constant amplitude (75.0mm) ECCS											
Type of test	Test setup, loading protocol and test results																						
Loading protocol	Type of response curve Force <input checked="" type="checkbox"/> Moment <input type="checkbox"/> Displacement <input checked="" type="checkbox"/> Rotation <input type="checkbox"/>																						
(4 different tests) Constant amplitude (37.5mm) Constant amplitude (50.0mm) Constant amplitude (75.0mm) ECCS																							

Test ID FW9																						
Paper																						
Title: <i>Cyclic Behavior of Beam-to-Column Bare Steel Connections: Influence of Strain Rate</i>																						
Authors:																						
Beg D.	Plumier A.	Reme C.	Sanchez L.																			
Source																						
Moment Resistant Connections of Steel Frames in Seismic Areas, Edited by F.M. Mazolani	Pages: 167-216	Year: 2000																				
Test ID (with reference to the paper): SW1																						
<table border="1"> <thead> <tr> <th colspan="2">Geometry (mm)</th></tr> </thead> <tbody> <tr> <td>Scheme: Exterior Joint</td><td>Beam</td></tr> <tr> <td>Beam length: 862</td><td>Shape: IPE 300</td></tr> <tr> <td>Column length 1: 600</td><td>Height: 300</td><td>Width: 150</td></tr> <tr> <td>Column length 2: 600</td><td>Flange Thickness: 10.7</td><td>Web Thickness: 7.1</td></tr> <tr> <td></td><td>Root radius: []</td><td>Flange to web welds: []</td></tr> </tbody> </table>		Geometry (mm)		Scheme: Exterior Joint	Beam	Beam length: 862	Shape: IPE 300	Column length 1: 600	Height: 300	Width: 150	Column length 2: 600	Flange Thickness: 10.7	Web Thickness: 7.1		Root radius: []	Flange to web welds: []						
Geometry (mm)																						
Scheme: Exterior Joint	Beam																					
Beam length: 862	Shape: IPE 300																					
Column length 1: 600	Height: 300	Width: 150																				
Column length 2: 600	Flange Thickness: 10.7	Web Thickness: 7.1																				
	Root radius: []	Flange to web welds: []																				
<table border="1"> <thead> <tr> <th colspan="2">Joint details</th></tr> </thead> <tbody> <tr> <td> </td><td>Column</td></tr> <tr> <td> </td><td>Shape: HEB 200</td></tr> <tr> <td> </td><td>Height: 200</td><td>Width: 200</td></tr> <tr> <td></td><td>Flange Thickness: 15.0</td><td>Web Thickness: 9.0</td></tr> <tr> <td></td><td>Root radius: []</td><td>Flange to web welds: []</td></tr> <tr> <td></td><td>Supplementary web plates: []</td><td>Thickness: []</td></tr> <tr> <td></td><td>Continuity plates: X</td><td>Thickness: 12</td></tr> </tbody> </table>		Joint details			Column		Shape: HEB 200		Height: 200	Width: 200		Flange Thickness: 15.0	Web Thickness: 9.0		Root radius: []	Flange to web welds: []		Supplementary web plates: []	Thickness: []		Continuity plates: X	Thickness: 12
Joint details																						
	Column																					
	Shape: HEB 200																					
	Height: 200	Width: 200																				
	Flange Thickness: 15.0	Web Thickness: 9.0																				
	Root radius: []	Flange to web welds: []																				
	Supplementary web plates: []	Thickness: []																				
	Continuity plates: X	Thickness: 12																				
<small>NOTE: The beam length provided is the distance between the point of application of the force and the column flange. The two test are carried out with different loading frequencies.</small>																						

Test ID FW9											
Material Properties (MPa)											
<table border="1"> <thead> <tr> <th colspan="2">Beam</th> </tr> </thead> <tbody> <tr> <td>Nominal grade</td> <td><input type="checkbox"/></td> </tr> <tr> <td>Measured values</td> <td><input checked="" type="checkbox"/></td> </tr> <tr> <td>Flange yield strength</td> <td>306</td> </tr> <tr> <td>Web yield strength</td> <td>366</td> </tr> </tbody> </table>		Beam		Nominal grade	<input type="checkbox"/>	Measured values	<input checked="" type="checkbox"/>	Flange yield strength	306	Web yield strength	366
Beam											
Nominal grade	<input type="checkbox"/>										
Measured values	<input checked="" type="checkbox"/>										
Flange yield strength	306										
Web yield strength	366										
<table border="1"> <thead> <tr> <th colspan="2">Column</th> </tr> </thead> <tbody> <tr> <td>Nominal grade</td> <td><input type="checkbox"/></td> </tr> <tr> <td>Measured values</td> <td><input checked="" type="checkbox"/></td> </tr> <tr> <td>Flange yield strength</td> <td>305</td> </tr> <tr> <td>Web yield strength</td> <td>313</td> </tr> </tbody> </table>		Column		Nominal grade	<input type="checkbox"/>	Measured values	<input checked="" type="checkbox"/>	Flange yield strength	305	Web yield strength	313
Column											
Nominal grade	<input type="checkbox"/>										
Measured values	<input checked="" type="checkbox"/>										
Flange yield strength	305										
Web yield strength	313										
<table border="1"> <thead> <tr> <th colspan="2">Continuity Plates</th> </tr> </thead> <tbody> <tr> <td>Nominal grade</td> <td><input type="checkbox"/></td> </tr> <tr> <td>Measured values</td> <td><input type="checkbox"/></td> </tr> <tr> <td>Yield strength</td> <td><input type="checkbox"/></td> </tr> </tbody> </table>		Continuity Plates		Nominal grade	<input type="checkbox"/>	Measured values	<input type="checkbox"/>	Yield strength	<input type="checkbox"/>		
Continuity Plates											
Nominal grade	<input type="checkbox"/>										
Measured values	<input type="checkbox"/>										
Yield strength	<input type="checkbox"/>										
<table border="1"> <thead> <tr> <th colspan="2">Supplementary web plate</th> </tr> </thead> <tbody> <tr> <td>Nominal grade</td> <td><input type="checkbox"/></td> </tr> <tr> <td>Measured values</td> <td><input type="checkbox"/></td> </tr> <tr> <td>Yield strength</td> <td><input type="checkbox"/></td> </tr> </tbody> </table>		Supplementary web plate		Nominal grade	<input type="checkbox"/>	Measured values	<input type="checkbox"/>	Yield strength	<input type="checkbox"/>		
Supplementary web plate											
Nominal grade	<input type="checkbox"/>										
Measured values	<input type="checkbox"/>										
Yield strength	<input type="checkbox"/>										
<p>Note:</p>											
Type of test											
Loading protocol	Constant amplitude; Frequency 0.3 Hz										
Test setup, loading protocol and test results											
Type of response curve											
Force	<input type="checkbox"/>										
Moment	<input checked="" type="checkbox"/>										
Displacement	<input type="checkbox"/>										
Rotation	<input checked="" type="checkbox"/>										

Test ID FW10																		
Paper Title: <i>Cyclic Behavior of Beam-to-Column Bare Steel Connections: Influence of Strain Rate</i>																		
Authors: Beg D. Plumier A. Remec C. Sanchez L.																		
Source Moment Resistant Connections of Steel Frames in Seismic Areas, Edited by F.M. Mazolani	Pages: 167-216	Year: 2000																
Test ID (with reference to the paper): SW2																		
<table border="1"> <thead> <tr> <th colspan="2">Geometry (mm)</th> </tr> </thead> <tbody> <tr> <td>Scheme: Exterior Joint</td><td>Beam</td></tr> <tr> <td>Beam length: 862</td><td>Shape: IPE 300</td></tr> <tr> <td>Column length 1: 600</td><td>Height: 300 Width: 150</td></tr> <tr> <td>Column length 2: 600</td><td>Flange Thickness: 10.7 Web Thickness: 7.1</td></tr> <tr> <td></td><td>Root radius: [] Flange to web welds: []</td></tr> </tbody> </table>			Geometry (mm)		Scheme: Exterior Joint	Beam	Beam length: 862	Shape: IPE 300	Column length 1: 600	Height: 300 Width: 150	Column length 2: 600	Flange Thickness: 10.7 Web Thickness: 7.1		Root radius: [] Flange to web welds: []				
Geometry (mm)																		
Scheme: Exterior Joint	Beam																	
Beam length: 862	Shape: IPE 300																	
Column length 1: 600	Height: 300 Width: 150																	
Column length 2: 600	Flange Thickness: 10.7 Web Thickness: 7.1																	
	Root radius: [] Flange to web welds: []																	
<table border="1"> <thead> <tr> <th colspan="2">Joint details</th> </tr> </thead> <tbody> <tr> <td></td><td>Column</td></tr> <tr> <td></td><td>Shape: HEB 200</td></tr> <tr> <td></td><td>Height: 200 Width: 200</td></tr> <tr> <td></td><td>Flange Thickness: 15.0 Web Thickness: 9.0</td></tr> <tr> <td></td><td>Root radius: [] Flange to web welds: []</td></tr> <tr> <td></td><td>Supplementary web plates: [] Thickness: []</td></tr> <tr> <td></td><td>Continuity plates: X Thickness: 12</td></tr> </tbody> </table>			Joint details			Column		Shape: HEB 200		Height: 200 Width: 200		Flange Thickness: 15.0 Web Thickness: 9.0		Root radius: [] Flange to web welds: []		Supplementary web plates: [] Thickness: []		Continuity plates: X Thickness: 12
Joint details																		
	Column																	
	Shape: HEB 200																	
	Height: 200 Width: 200																	
	Flange Thickness: 15.0 Web Thickness: 9.0																	
	Root radius: [] Flange to web welds: []																	
	Supplementary web plates: [] Thickness: []																	
	Continuity plates: X Thickness: 12																	
NOTE: The beam length provided is the distance between the point of application of the force and the column flange. The two test are carried out with different loading frequencies.																		

Test ID FW10											
Material Properties (MPa)											
<table border="1"> <thead> <tr> <th colspan="2">Beam</th> </tr> </thead> <tbody> <tr> <td>Nominal grade</td> <td><input type="checkbox"/></td> </tr> <tr> <td>Measured values</td> <td><input checked="" type="checkbox"/></td> </tr> <tr> <td>Flange yield strength</td> <td>306</td> </tr> <tr> <td>Web yield strength</td> <td>366</td> </tr> </tbody> </table>		Beam		Nominal grade	<input type="checkbox"/>	Measured values	<input checked="" type="checkbox"/>	Flange yield strength	306	Web yield strength	366
Beam											
Nominal grade	<input type="checkbox"/>										
Measured values	<input checked="" type="checkbox"/>										
Flange yield strength	306										
Web yield strength	366										
<table border="1"> <thead> <tr> <th colspan="2">Column</th> </tr> </thead> <tbody> <tr> <td>Nominal grade</td> <td><input type="checkbox"/></td> </tr> <tr> <td>Measured values</td> <td><input checked="" type="checkbox"/></td> </tr> <tr> <td>Flange yield strength</td> <td>305</td> </tr> <tr> <td>Web yield strength</td> <td>313</td> </tr> </tbody> </table>		Column		Nominal grade	<input type="checkbox"/>	Measured values	<input checked="" type="checkbox"/>	Flange yield strength	305	Web yield strength	313
Column											
Nominal grade	<input type="checkbox"/>										
Measured values	<input checked="" type="checkbox"/>										
Flange yield strength	305										
Web yield strength	313										
<table border="1"> <thead> <tr> <th colspan="2">Continuity Plates</th> </tr> </thead> <tbody> <tr> <td>Nominal grade</td> <td><input type="checkbox"/></td> </tr> <tr> <td>Measured values</td> <td><input type="checkbox"/></td> </tr> <tr> <td>Yield strength</td> <td><input type="checkbox"/></td> </tr> </tbody> </table>		Continuity Plates		Nominal grade	<input type="checkbox"/>	Measured values	<input type="checkbox"/>	Yield strength	<input type="checkbox"/>		
Continuity Plates											
Nominal grade	<input type="checkbox"/>										
Measured values	<input type="checkbox"/>										
Yield strength	<input type="checkbox"/>										
<table border="1"> <thead> <tr> <th colspan="2">Supplementary web plate</th> </tr> </thead> <tbody> <tr> <td>Nominal grade</td> <td><input type="checkbox"/></td> </tr> <tr> <td>Measured values</td> <td><input type="checkbox"/></td> </tr> <tr> <td>Yield strength</td> <td><input type="checkbox"/></td> </tr> </tbody> </table>		Supplementary web plate		Nominal grade	<input type="checkbox"/>	Measured values	<input type="checkbox"/>	Yield strength	<input type="checkbox"/>		
Supplementary web plate											
Nominal grade	<input type="checkbox"/>										
Measured values	<input type="checkbox"/>										
Yield strength	<input type="checkbox"/>										
<p>Note:</p>											
Type of test											
Loading protocol	Constant amplitude; Frequency 0.3 Hz										
Test setup, loading protocol and test results											
Type of response curve											
Force	<input type="checkbox"/>										
Moment	<input checked="" type="checkbox"/>										
Displacement	<input type="checkbox"/>										
Rotation	<input checked="" type="checkbox"/>										

3.3 BOLTED EXTENDED END-PLATE BEAM-COLUMN JOINTS

This section provides summary details for the experimental testing of bolted end-plate beam-column joints, which are listed in Table 3.2.

Table 3.2. Summary details for bolted extended end-plate beam-column joints.

Reference	Joint ID	Page
Abidelah <i>et al.</i> [2012]	BC2	37
Abidelah <i>et al.</i> [2012]	BC3	39
Abidelah <i>et al.</i> [2012]	BC4	41
Coelho <i>et al.</i> [2004]	FS1a	43
Coelho <i>et al.</i> [2004]	FS1b	45
Coelho <i>et al.</i> [2004]	FS2a	47
Coelho <i>et al.</i> [2004]	FS2b	49
Coelho <i>et al.</i> [2004]	FS3a	51
Coelho <i>et al.</i> [2004]	FS3b	53
Coelho <i>et al.</i> [2004]	FS4a	55
Coelho <i>et al.</i> [2004]	FS4b	57
Coelho and Bijlaard [2007]	EEP-10-2a	59
Coelho and Bijlaard [2007]	EEP-10-2b	61
Coelho and Bijlaard [2007]	EEP-15-2	63
Ghobarah <i>et al.</i> [1990]	A-1	65
Ghobarah <i>et al.</i> [1990]	A-2	67
Ghobarah <i>et al.</i> [1990]	A-3	69
Ghobarah <i>et al.</i> [1990]	A-4	71
Ghobarah <i>et al.</i> [1990]	A-5	73
Iannone <i>et al.</i> [2011]	EEP-CYC-01	75
Iannone <i>et al.</i> [2011]	EEP-CYC-02	77
Nogueiro <i>et al.</i> [2006]	J-1.1	79
Nogueiro <i>et al.</i> [2006]	J-1.2	81
Nogueiro <i>et al.</i> [2006]	J-1.3	83
Nogueiro <i>et al.</i> [2006]	J-3.1	85
Nogueiro <i>et al.</i> [2006]	J-3.2	87
Nogueiro <i>et al.</i> [2006]	J-3.3	89
Shi <i>et al.</i> [2007a]	EPC-1	91
Shi <i>et al.</i> [2007a]	EPC-2	93
Shi <i>et al.</i> [2007a]	EPC-3	95
Shi <i>et al.</i> [2007a]	EPC-4	97
Shi <i>et al.</i> [2007a]	EPC-5	99

Shi <i>et al.</i> [2007b]	JD2	101
Shi <i>et al.</i> [2007b]	JD3	103
Shi <i>et al.</i> [2007b]	JD4	105
Shi <i>et al.</i> [2007b]	JD5	107
Shi <i>et al.</i> [2007b]	JD6	109
Shi <i>et al.</i> [2007b]	JD7	111
Shi <i>et al.</i> [2007b]	JD8	113
Sumner <i>et al.</i> [2002]	4E-1.25-1.5-2	115
Tahir and Hussein [2008]	EEP6	117
Tahir and Hussein [2008]	EEP7	119
Tahir and Hussein [2008]	EEP8	121
Tahir and Hussein [2008]	EEP9	123
Bernuzzi <i>et al.</i> [1996]	EPBC1	125
Bernuzzi <i>et al.</i> [1996]	EPBC2	127
Bernuzzi <i>et al.</i> [1996]	EPC	129
Bursi <i>et al.</i> [2002]	JB1-3A	131
Bursi <i>et al.</i> [2002]	JB1-3M	133
Zandonini and Bursi [2002]	JA1-2M	135
Zandonini and Bursi [2002]	JA1-2A	137
Zandonini and Bursi [2002]	JA1-2B	139
Zandonini and Bursi [2002]	JA1-3B	141
Dubina <i>et al.</i> [2001]	XS-EP1	143
Dubina <i>et al.</i> [2001]	XS-EP2	145
Dubina <i>et al.</i> [2001]	XU-EP1	147
Dubina <i>et al.</i> [2001]	XU-EP2	149
Dubina <i>et al.</i> [2002]	BX-SS-M	151
Dubina <i>et al.</i> [2002]	BX-SS-C1	153
Dubina <i>et al.</i> [2002]	BX-SS-C2	155
Dubina <i>et al.</i> [2002]	BX-SU-M	157
Dubina <i>et al.</i> [2002]	BX-SU-C1	159
Dubina <i>et al.</i> [2002]	BX-SU-C2	161
Nogueiro [2009]	J-4.1	163
Nogueiro [2009]	J-4.2	165
Nogueiro [2009]	J-4.3	167

Paper

Title: Experimental and analytical behavior of bolted end-plate connections with or without stiffeners

Authors: Abidelah A. Bouchair A. Kerdal D. E.

Source: Journal of Constructional Steel Research

Volume: 76 **Issue:** 13-27 **Pages:** 13-27 **Year:** 2012

Test BC2

Geometry (mm)

Scheme: Interior joint

Beam length: 1711
Beam position: n.a.
Column length: n.a.

Beam

Shape: IPE 240

Height: 240 Width: 120
Flange thickness: 9.8 Web thickness: 6.2
Root radius: Flange-to-web welds:

Column

Shape: HEA 120

Height: 114 Width: 120
Flange thickness: 8 Web thickness: 5
Root radius: 12 Flange-to-web welds:
 Supplementary web plate Thickness:
 Continuity plates Thickness:

End-plate

hp:	340								
bp:	150	ep:	37.5	exs:	40	mx1:	45.1	p1:	131
tp:	15	w:	75	exl:	14.1	mx2:	45.1	p2:	0
<input type="checkbox"/> Rib stiffener					mx3:	45.1			
Thickness: <input type="text"/>					mx4:	<input type="text"/>			

Bolts

Rows in tension: 2 Bolts per row: 2
Diameter: 16 Tensile stress area: 157

Beam-to-plate welds

Throat thickness
 Leg thickness
Flange
 Full penetration
 Fillet welds 6
Web
 Full penetration
 Fillet welds 6

Notes:

Test BC2

		Material properties	
		(MPa)	
Beam		Column	
<input type="checkbox"/> Nominal grade S235 <input checked="" type="checkbox"/> Measured values fy,f: 356 fy,w: 343 fu,f: 480 fu,w: 456		<input type="checkbox"/> Nominal grade S235 <input checked="" type="checkbox"/> Measured values fy,f: 338 fy,w: 345 fu,f: 435 fu,w: 456	
Young's modulus		Young's modulus	
<input checked="" type="checkbox"/> Nominal Ef: 210000 <input type="checkbox"/> Measured Ew: 21000		<input checked="" type="checkbox"/> Nominal Ef: 210000 <input type="checkbox"/> Measured Ew: 210000	
Bolts		Continuity plate	
<input type="checkbox"/> Nominal grade 8.8 <input checked="" type="checkbox"/> Measured values Yield strength: 893 Ultimate strength: 1010 Young's modulus <input checked="" type="checkbox"/> Nominal <input type="checkbox"/> Measured E: 210000		<input type="checkbox"/> Nominal grade <input type="checkbox"/> Measured values Yield strength: Ultimate strength: Young's modulus <input type="checkbox"/> Nominal <input type="checkbox"/> Measured E:	
End-plate		Supplementary web plate	
<input type="checkbox"/> Nominal grade S235 <input checked="" type="checkbox"/> Measured values Yield strength: 310 Ultimate strength: 464 Young's modulus <input checked="" type="checkbox"/> Nominal <input type="checkbox"/> Measured E: 210000		<input type="checkbox"/> Nominal grade <input type="checkbox"/> Measured values Yield strength: Ultimate strength: Young's modulus <input type="checkbox"/> Nominal <input type="checkbox"/> Measured E:	
Notes:		End-plate rib stiffener	
<input type="checkbox"/> Nominal grade <input type="checkbox"/> Measured value Yield strength: Ultimate strength: Young's modulus <input type="checkbox"/> Nominal <input type="checkbox"/> Measured E:			
Test set up and loading protocol			
Type of test:	Monotonic		
Loading protocol:			
Data provided:	Inclinometer and displacement transducers		
Type of response curve:			
<input type="checkbox"/> Force <input checked="" type="checkbox"/> Moment <input type="checkbox"/> Displacement <input checked="" type="checkbox"/> Rotation	Connection rotation		

Paper

Title: Experimental and analytical behavior of bolted end-plate connections with or without stiffeners

Authors: Abidelah A. Bouchair A. Kerdal D. E.

Source: Journal of Constructional Steel Research

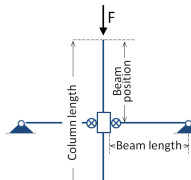
Volume: 76 **Issue:** 13-27 **Pages:** 13-27 **Year:** 2012

Test BC3

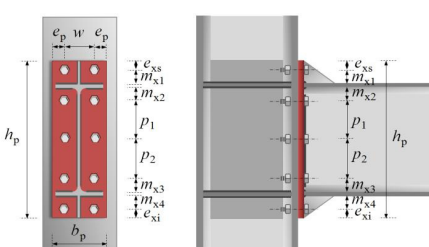
Geometry (mm)

Scheme: Internal joint

Beam length: 1711
Beam position: n.a.
Column length: n.a.



End-plate



hp: 340	bp: 150	ep: 37.5	exs: 40	mx1: 45.1	p1: 131
tp: 15	w: 75		exl: 14.1	mx2: 45.1	p2: 0
<input checked="" type="checkbox"/> Rib stiffener				mx3: 45.1	
Thickness: 10				mx4:	

Notes:

Geometry (mm)

Beam

Shape: IPE 240

Height: 240 Width: 120
Flange thickness: 9.8 Web thickness: 6.2
Root radius: 15 Flange-to-web welds:

Column

Shape: HEA 120

Height: 114 Width: 120
Flange thickness: 8 Web thickness: 5
Root radius: 12 Flange-to-web welds:

End-plate

Rows in tension: 2 Bolts per row: 2
Diameter: 16 Tensile stress area: 157

Head washer Nut washer

Bolts

Throat thickness Leg thickness

Beam-to-plate welds

Full penetration Fillet welds 6

Head washer Nut washer

Full penetration Fillet welds 6

Test BC3		Material properties	
		(MPa)	
Beam <input type="checkbox"/> Nominal grade S235 <input checked="" type="checkbox"/> Measured values fy,f: 356 fy,w: 343 fu,f: 480 fu,w: 456		Column <input type="checkbox"/> Nominal grade S235 <input checked="" type="checkbox"/> Measured values fy,f: 338 fy,w: 345 fu,f: 435 fu,w: 456	
Young's modulus <input checked="" type="checkbox"/> Nominal Ef: 210000 <input type="checkbox"/> Measured Ew: 210000		Young's modulus <input checked="" type="checkbox"/> Nominal Ef: 210000 <input type="checkbox"/> Measured Ew: 210000	
Bolts <input type="checkbox"/> Nominal grade 8.8 <input checked="" type="checkbox"/> Measured values Yield strength: 893 Ultimate strength: 1010 Young's modulus <input checked="" type="checkbox"/> Nominal <input type="checkbox"/> Measured E: 210000		Continuity plate <input type="checkbox"/> Nominal grade <input type="checkbox"/> Measured values Yield strength: Ultimate strength: Young's modulus <input type="checkbox"/> Nominal <input type="checkbox"/> Measured E:	
End-plate <input type="checkbox"/> Nominal grade S235 <input checked="" type="checkbox"/> Measured values Yield strength: 310 Ultimate strength: 464 Young's modulus <input checked="" type="checkbox"/> Nominal <input type="checkbox"/> Measured E: 210000		Supplementary web plate <input type="checkbox"/> Nominal grade <input type="checkbox"/> Measured values Yield strength: Ultimate strength: Young's modulus <input type="checkbox"/> Nominal <input type="checkbox"/> Measured E:	
<p>Notes:</p> <div style="border: 1px solid black; height: 100px; width: 100%;"></div>			
End-plate rib stiffener <input type="checkbox"/> Nominal grade S235 <input checked="" type="checkbox"/> Measured value Yield strength: 343 Ultimate strength: 456 Young's modulus <input checked="" type="checkbox"/> Nominal <input type="checkbox"/> Measured E: 210000			
Test set up and loading protocol			
Type of test:	Monotonic		
Loading protocol:			
Data provided:	Inclinometer and displacement transducers		
Type of response curve:			
<input type="checkbox"/> Force			
<input checked="" type="checkbox"/> Moment			
<input type="checkbox"/> Displacement	Connection rotation		
<input checked="" type="checkbox"/> Rotation			

Paper

Title: Experimental and analytical behavior of bolted end-plate connections with or without stiffeners

Authors: Abidelah A. Bouchair A. Kerdal D. E.

Source: Journal of Constructional Steel Research

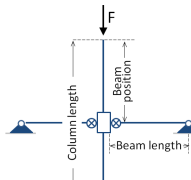
Volume: 76 **Issue:** 13-27 **Pages:** 13-27 **Year:** 2012

Test BC4

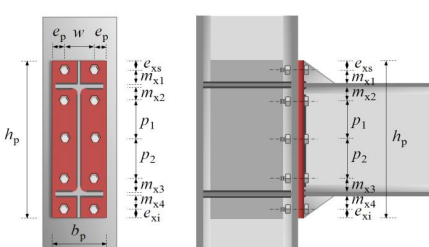
Geometry (mm)

Scheme: Internal joint

Beam length: 1711
Beam position: n.a.
Column length: n.a.



End-plate



hp: 410	bp: 150	ep: 37.5	exs: 40	mx1: 45.1	p1: 131
tp: 15	w: 75	exi: 39		mx2: 45.1	p2: 0
<input checked="" type="checkbox"/> Rib stiffener				mx3: 45.1	
Thickness: 10				mx4: 45.1	

Notes:

Beam

Shape: IPE 240

Height: 240 Width: 120
Flange thickness: 9.8 Web thickness: 6.2
Root radius: 15 Flange-to-web welds:

Column

Shape: HEA 120

Height: 114 Width: 120
Flange thickness: 8 Web thickness: 5
Root radius: 12 Flange-to-web welds:
 Supplementary web plate Thickness:
 Continuity plates Thickness:

Bolts

Rows in tension: 2 Bolts per row: 2
Diameter: 16 Tensile stress area: 157

Head washer
 Nut washer

Beam-to-plate welds

Throat thickness
 Leg thickness
Flange
 Full penetration
 Fillet welds 6
Web
 Full penetration
 Fillet welds 6

Test BC4

		Material properties	
		(MPa)	
Beam		Column	
<input type="checkbox"/> Nominal grade	S235	<input type="checkbox"/> Nominal grade	S235
<input checked="" type="checkbox"/> Measured values		<input type="checkbox"/> Measured values	
fy,f: 356	fy,w: 343	fy,f: 338	fy,w: 345
fu,f: 480	fu,w: 456	fu,f: 435	fu,w: 456
Young's modulus		Young's modulus	
<input checked="" type="checkbox"/> Nominal	Ef: 210000	<input checked="" type="checkbox"/> Nominal	Ef: 210000
<input type="checkbox"/> Measured	Ew: 210000	<input type="checkbox"/> Measured	Ew: 210000
Bolts		Continuity plate	
<input type="checkbox"/> Nominal grade	8.8	<input type="checkbox"/> Nominal grade	
<input checked="" type="checkbox"/> Measured values		<input type="checkbox"/> Measured values	
Yield strength:	893	Yield strength:	
Ultimate strength:	1010	Ultimate strength:	
Young's modulus		Young's modulus	
<input checked="" type="checkbox"/> Nominal		<input type="checkbox"/> Nominal	
<input type="checkbox"/> Measured	E: 210000	<input type="checkbox"/> Measured	E:
End-plate		Supplementary web plate	
<input type="checkbox"/> Nominal grade	S235	<input type="checkbox"/> Nominal grade	
<input checked="" type="checkbox"/> Measured values		<input type="checkbox"/> Measured values	
Yield strength:	310	Yield strength:	
Ultimate strength:	464	Ultimate strength:	
Young's modulus		Young's modulus	
<input checked="" type="checkbox"/> Nominal		<input type="checkbox"/> Nominal	
<input type="checkbox"/> Measured	E: 210000	<input type="checkbox"/> Measured	E:
Notes:		End-plate rib stiffener	
<input type="checkbox"/> Nominal grade		S235	
<input checked="" type="checkbox"/> Measured value			
Yield strength:		343	
Ultimate strength:		456	
Young's modulus			
<input checked="" type="checkbox"/> Nominal		<input type="checkbox"/> Nominal	
<input type="checkbox"/> Measured	E: 210000	<input type="checkbox"/> Measured	E:
Test set up and loading protocol			
Type of test:	Monotonic		
Loading protocol:			
Data provided:	Inclinometer and displacement transducers		
Type of response curve:			
<input type="checkbox"/> Force			
<input checked="" type="checkbox"/> Moment			
<input type="checkbox"/> Displacement	Connection rotation		
<input checked="" type="checkbox"/> Rotation			

Paper

Title: Experimental assessment of the ductility of extended end plate connections

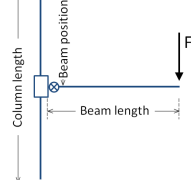
Authors: Coelho A. M. G. Bijlaard F. S. K. da Silva L. S.

Source: Engineering Structures **Volume:** 26 **Issue:** 9 **Pages:** 1185-1206 **Year:** 2004

Test FS1a

Scheme: Exterior joint

Beam length: 1053.11 **Beam position:** 600 **Column length:** 1200



Geometry (mm)

Beam			
Shape:	IPE 300		
Height:	300.45	Width:	150.50
Flange thickness:	10.76	Web thickness:	7.2
Root radius:	15	Flange-to-web welds:	

Column			
Shape:	HEM 340		
Height:	376	Width:	307.50
Flange thickness:	40.21	Web thickness:	21
Root radius:	27	Flange-to-web welds:	
<input type="checkbox"/> Supplementary web plate		Thickness:	
<input type="checkbox"/> Continuity plates		Thickness:	

End-plate

hp:	401.04								
bp:	149.84	ep:	30.01	exs:	29.90	mx1:	39.64	p1:	205.90
tp:	10.40	w:	89.91	exi:	76.45	mx2:	39.64	p2:	0
<input type="checkbox"/> Rib stiffener					mx3:	39.64			
Thickness:					mx4:	0			

Bolts	
Rows in tension:	2
Bolts per row:	2
Diameter:	20
Tensile stress area:	245
<input type="checkbox"/> Head washer	
<input type="checkbox"/> Nut washer	

Beam-to-plate welds	
<input checked="" type="checkbox"/> Throat thickness	
<input type="checkbox"/> Leg thickness	
Flange	
<input type="checkbox"/> Full penetration	
<input checked="" type="checkbox"/> Fillet welds	6
Web	
<input type="checkbox"/> Full penetration	
<input checked="" type="checkbox"/> Fillet welds	4

Notes:

Authors provide actual values of: column height, column flange width and thickness, beam height, beam flange width and thickness, beam web thickness, end-plate height, width, thickness and layout.

Test FS1a

		Material properties			
		(MPa)			
Beam		Column		End-plate	
<input type="checkbox"/> Nominal grade S235 <input checked="" type="checkbox"/> Measured values fy,f: 316.24 fy,w: 299.12 fu,f: 462.28 fu,w: 446.25		<input checked="" type="checkbox"/> Nominal grade S355 <input type="checkbox"/> Measured values fy,f: 355 fy,w: 355 fu,f: 510 fu,w: 510		<input type="checkbox"/> Nominal grade S355 <input checked="" type="checkbox"/> Measured values Yield strength: 340.12 Ultimate strength: 480.49 Young's modulus <input type="checkbox"/> Nominal Ef: 210000 <input checked="" type="checkbox"/> Measured Ew: 210000	
Young's modulus <input type="checkbox"/> Nominal Ef: 209496 <input checked="" type="checkbox"/> Measured Ew: 208332					
Bolts		Continuity plate		Supplementary web plate	
<input type="checkbox"/> Nominal grade 8.8 <input checked="" type="checkbox"/> Measured values Yield strength: 857.33 Ultimate strength: 913.78 Young's modulus <input type="checkbox"/> Nominal <input checked="" type="checkbox"/> Measured E: 223166		<input type="checkbox"/> Nominal grade <input type="checkbox"/> Measured values Yield strength: Ultimate strength: Young's modulus <input type="checkbox"/> Nominal <input type="checkbox"/> Measured E:		<input type="checkbox"/> Nominal grade <input type="checkbox"/> Measured values Yield strength: Ultimate strength: Young's modulus <input type="checkbox"/> Nominal <input type="checkbox"/> Measured E:	
Notes: <div style="border: 1px solid black; height: 100px; width: 100%;"></div>					
End-plate rib stiffener					
<input type="checkbox"/> Nominal grade <input type="checkbox"/> Measured value Yield strength: Ultimate strength: Young's modulus <input type="checkbox"/> Nominal <input type="checkbox"/> Measured E:					
Test set up and loading protocol					
Type of test:	Monotonic				
Loading protocol:					
Data provided:	Transducer DT1				
Type of response curve:	<input type="checkbox"/> Force <input checked="" type="checkbox"/> Moment Evaluated on the end-plate <input type="checkbox"/> Displacement <input checked="" type="checkbox"/> Rotation				

Paper

Title: Experimental assessment of the ductility of extended end plate connections

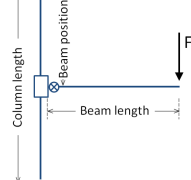
Authors: Coelho A. M. G. Bijlaard F. S. K. da Silva L. S.

Source: Engineering Structures **Volume:** 26 **Issue:** 9 **Pages:** 1185-1206 **Year:** 2004

Test FS1b

Scheme: Exterior joint

Beam length: 1053.11
Beam position: 600
Column length: 1200



Geometry (mm)

Beam			
Shape:	IPE 300		
Height:	300.45	Width:	150.50
Flange thickness:	10.76	Web thickness:	7.2
Root radius:	15	Flange-to-web welds:	

Column			
Shape:	HEM 340		
Height:	376	Width:	307.50
Flange thickness:	40.21	Web thickness:	21
Root radius:	27	Flange-to-web welds:	
<input type="checkbox"/> Supplementary web plate	Thickness:		
<input type="checkbox"/> Continuity plates	Thickness:		

End-plate

hp: 401.04	bp: 149.84	ep: 30.01	exs: 29.90	mx1: 39.64	p1: 205.9
tp: 10.40	w: 89.91	exi: 76.45	mx2: 39.64	p2: 0	mx3: 39.64
<input type="checkbox"/> Rib stiffener	Thickness:		mx4: 0		

Bolts

Rows in tension:	2
Bolts per row:	2
Diameter:	20
Tensile stress area:	245
<input type="checkbox"/> Head washer	
<input type="checkbox"/> Nut washer	

Beam-to-plate welds

<input checked="" type="checkbox"/> Throat thickness
<input type="checkbox"/> Leg thickness
Flange
<input type="checkbox"/> Full penetration
<input checked="" type="checkbox"/> Fillet welds 6
Web
<input type="checkbox"/> Full penetration
<input checked="" type="checkbox"/> Fillet welds 4

Notes:

Authors provide actual values of: column height, column flange width and thickness, beam height, beam flange width and thickness, beam web thickness, end-plate height, width, thickness and layout.

Test FS1b

		Material properties			
		(MPa)			
Beam		Column		End-plate	
<input type="checkbox"/> Nominal grade S235 <input checked="" type="checkbox"/> Measured values fy,f: 316.24 fy,w: 299.15 fu,f: 462.28 fu,w: 446.25		<input checked="" type="checkbox"/> Nominal grade S355 <input type="checkbox"/> Measured values fy,f: 355 fy,w: 355 fu,f: 510 fu,w: 510		<input type="checkbox"/> Nominal grade S355 <input checked="" type="checkbox"/> Measured values Yield strength: 340.12 Ultimate strength: 480.49 Young's modulus <input type="checkbox"/> Nominal Ef: 210000 <input checked="" type="checkbox"/> Measured Ew: 210000	
Young's modulus <input type="checkbox"/> Nominal Ef: 209496 <input checked="" type="checkbox"/> Measured Ew: 208332					
Bolts		Continuity plate		Supplementary web plate	
<input type="checkbox"/> Nominal grade 8.8 <input checked="" type="checkbox"/> Measured values Yield strength: 857.33 Ultimate strength: 913.78 Young's modulus <input type="checkbox"/> Nominal <input checked="" type="checkbox"/> Measured E: 223166		<input type="checkbox"/> Nominal grade <input type="checkbox"/> Measured values Yield strength: Ultimate strength: Young's modulus <input type="checkbox"/> Nominal <input type="checkbox"/> Measured E:		<input type="checkbox"/> Nominal grade <input type="checkbox"/> Measured values Yield strength: Ultimate strength: Young's modulus <input type="checkbox"/> Nominal <input type="checkbox"/> Measured E:	
Notes: <div style="border: 1px solid black; height: 100px; width: 100%;"></div>					
End-plate rib stiffener					
<input type="checkbox"/> Nominal grade <input type="checkbox"/> Measured value Yield strength: Ultimate strength: Young's modulus <input type="checkbox"/> Nominal <input type="checkbox"/> Measured E:					
Test set up and loading protocol					
Type of test:	Monotonic				
Loading protocol:					
Data provided:	Transducer DT1				
Type of response curve:	<input type="checkbox"/> Force <input checked="" type="checkbox"/> Moment Evaluated on the end-plate <input type="checkbox"/> Displacement <input checked="" type="checkbox"/> Rotation				

Paper

Title: Experimental assessment of the ductility of extended end plate connections

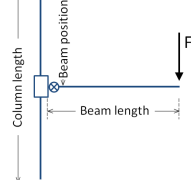
Authors: Coelho A. M. G. Bijlaard F. S. K. da Silva L. S.

Source: Engineering Structures **Volume:** 26 **Issue:** 9 **Pages:** 1185-1206 **Year:** 2004

Test FS2a

Scheme: Exterior joint

Beam length: 1055.47
Beam position: 600
Column length: 1200



Geometry (mm)

Beam			
Shape:	IPE 300		
Height:	301.40	Width:	149.60
Flange thickness:	10.67	Web thickness:	7.01
Root radius:	15	Flange-to-web welds:	

Column			
Shape:	HEM 340		
Height:	376	Width:	307.50
Flange thickness:	40.21	Web thickness:	21
Root radius:	27	Flange-to-web welds:	
<input type="checkbox"/> Supplementary web plate	Thickness:		
<input type="checkbox"/> Continuity plates	Thickness:		

End-plate

hp:	400.84								
bp:	149.41	ep:	29.76	exs:	30.10	mx1:	39.66	p1:	205.04
tp:	15.01	w:	89.89	exi:	74.44	mx2:	39.66	p2:	0
<input type="checkbox"/> Rib stiffener	Thickness:		mx3:	39.66					
Thickness:		mx4:	0						

Bolts

Rows in tension:	2
Bolts per row:	2
Diameter:	20
Tensile stress area:	245
<input type="checkbox"/> Head washer	
<input type="checkbox"/> Nut washer	

Beam-to-plate welds

<input checked="" type="checkbox"/> Throat thickness	
<input type="checkbox"/> Leg thickness	
Flange	
<input type="checkbox"/> Full penetration	
<input checked="" type="checkbox"/> Fillet welds	6
Web	
<input type="checkbox"/> Full penetration	
<input checked="" type="checkbox"/> Fillet welds	4

Notes:
Authors provide actual values of: column height, column flange width and thickness, beam height, beam flange width and thickness, beam web thickness, end-plate height, width, thickness and layout.

Test FS2a		Material properties			
		(MPa)			
Beam <input type="checkbox"/> Nominal grade S235 <input checked="" type="checkbox"/> Measured values fy,f: 316.24 fy,w: 299.12 fu,f: 462.28 fu,w: 466.25 Young's modulus <input type="checkbox"/> Nominal Ef: 209496 <input checked="" type="checkbox"/> Measured Ew: 208332		Column <input checked="" type="checkbox"/> Nominal grade S355 <input type="checkbox"/> Measured values fy,f: 355 fy,w: 355 fu,f: 510 fu,w: 510 Young's modulus <input checked="" type="checkbox"/> Nominal Ef: 210000 <input type="checkbox"/> Measured Ew: 210000		End-plate <input type="checkbox"/> Nominal grade S355 <input checked="" type="checkbox"/> Measured values Yield strength: 342.82 Ultimate strength: 507.85 Young's modulus <input type="checkbox"/> Nominal <input checked="" type="checkbox"/> Measured E: 208538	
Bolts <input type="checkbox"/> Nominal grade 8.8 <input checked="" type="checkbox"/> Measured values Yield strength: 857.33 Ultimate strength: 913.78 Young's modulus <input type="checkbox"/> Nominal <input checked="" type="checkbox"/> Measured E: 223166		Continuity plate <input type="checkbox"/> Nominal grade <input type="checkbox"/> Measured values Yield strength: Ultimate strength: Young's modulus <input type="checkbox"/> Nominal <input type="checkbox"/> Measured E:		Supplementary web plate <input type="checkbox"/> Nominal grade <input type="checkbox"/> Measured values Yield strength: Ultimate strength: Young's modulus <input type="checkbox"/> Nominal <input checked="" type="checkbox"/> Measured E:	
<p>Notes:</p> <div style="border: 1px solid black; height: 150px; width: 100%;"></div>					
End-plate rib stiffener <input type="checkbox"/> Nominal grade <input type="checkbox"/> Measured value Yield strength: Ultimate strength: Young's modulus <input type="checkbox"/> Nominal <input type="checkbox"/> Measured E:					
Test set up and loading protocol					
Type of test:	Monotonic				
Loading protocol:					
Data provided:	Transducer DT1				
Type of response curve:					
<input type="checkbox"/> Force	Evaluated on the end-plate				
<input checked="" type="checkbox"/> Moment					
<input type="checkbox"/> Displacement	Joint rotation				
<input checked="" type="checkbox"/> Rotation					

Paper

Title: Experimental assessment of the ductility of extended end plate connections

Authors: Coelho A. M. G. Bijlaard F. S. K. da Silva L. S.

Source: Engineering Structures **Volume:** 26 **Issue:** 9 **Pages:** 1185-1206 **Year:** 2004

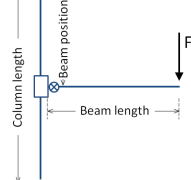
Test FS2b

Scheme: Exterior joint

Beam length: 1055.47

Beam position: 600

Column length: 1200



Geometry (mm)

Beam	
Shape:	IPE 300
Height:	301.40
Flange thickness:	10.67
Root radius:	15
Width:	149.60
Web thickness:	7.01
Flange-to-web welds:	

Column	
Shape:	HEM 340
Height:	376
Flange thickness:	40.21
Root radius:	27
Width:	307.50
Web thickness:	21
Flange-to-web welds:	
<input type="checkbox"/> Supplementary web plate	Thickness:
<input type="checkbox"/> Continuity plates	Thickness:

End-plate

hp:	400.84								
bp:	149.41	ep:	29.76	exs:	30.10	mx1:	39.66	p1:	205.04
tp:	15.01	w:	89.89	exi:	75.44	mx2:	39.66	p2:	0
<input type="checkbox"/> Rib stiffener					mx3:	39.66			
Thickness:					mx4:	0			

Bolts

Rows in tension:	2
Bolts per row:	2
Diameter:	20
Tensile stress area:	245

Beam-to-plate welds

<input checked="" type="checkbox"/> Throat thickness	
<input type="checkbox"/> Leg thickness	
Flange	
<input type="checkbox"/> Full penetration	
<input checked="" type="checkbox"/> Fillet welds	6
Web	
<input type="checkbox"/> Full penetration	
<input checked="" type="checkbox"/> Fillet welds	4

Notes:

Authors provide actual values of: column height, column flange width and thickness, beam height, beam flange width and thickness, beam web thickness, end-plate height, width, thickness and layout.

Test FS2b

		Material properties			
		(MPa)			
Beam		Column		End-plate	
<input type="checkbox"/> Nominal grade S235 <input checked="" type="checkbox"/> Measured values fy,f: 316.24 fy,w: 299.12 fu,f: 462.28 fu,w: 446.25		<input checked="" type="checkbox"/> Nominal grade S355 <input type="checkbox"/> Measured values fy,f: 355 fy,w: 355 fu,f: 510 fu,w: 510		<input type="checkbox"/> Nominal grade S355 <input checked="" type="checkbox"/> Measured values Yield strength: 342.82 Ultimate strength: 507.85 Young's modulus <input type="checkbox"/> Nominal Ef: 210000 <input checked="" type="checkbox"/> Measured Ew: 210000	
Young's modulus <input type="checkbox"/> Nominal Ef: 209496 <input checked="" type="checkbox"/> Measured Ew: 208332					
Bolts		Continuity plate		Supplementary web plate	
<input type="checkbox"/> Nominal grade 8.8 <input checked="" type="checkbox"/> Measured values Yield strength: 857.33 Ultimate strength: 913.78 Young's modulus <input type="checkbox"/> Nominal <input checked="" type="checkbox"/> Measured E: 223166		<input type="checkbox"/> Nominal grade <input type="checkbox"/> Measured values Yield strength: Ultimate strength: Young's modulus <input type="checkbox"/> Nominal <input type="checkbox"/> Measured E:		<input type="checkbox"/> Nominal grade <input type="checkbox"/> Measured values Yield strength: Ultimate strength: Young's modulus <input type="checkbox"/> Nominal <input type="checkbox"/> Measured E:	
Notes: <div style="border: 1px solid black; height: 100px; width: 100%;"></div>					
End-plate rib stiffener					
<input type="checkbox"/> Nominal grade <input type="checkbox"/> Measured value Yield strength: Ultimate strength: Young's modulus <input type="checkbox"/> Nominal <input type="checkbox"/> Measured E:					
Test set up and loading protocol					
Type of test:	Monotonic				
Loading protocol:					
Data provided:	Transducer DT1				
Type of response curve:	<input type="checkbox"/> Force <input checked="" type="checkbox"/> Moment Evaluated on the end-plate <input type="checkbox"/> Displacement <input checked="" type="checkbox"/> Rotation				

Paper

Title: Experimental assessment of the ductility of extended end plate connections

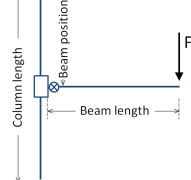
Authors: Coelho A. M. G. Bijlaard F. S. K. da Silva L. S.

Source: Engineering Structures **Volume:** 26 **Issue:** 9 **Pages:** 1185-1206 **Year:** 2004

Test FS3a

Scheme: Exterior joint

Beam length: 1052.86 **Beam position:** 600 **Column length:** 1200



Geometry (mm)

Beam			
Shape:	IPE 300		
Height:	301.46	Width:	149.75
Flange thickness:	10.57	Web thickness:	7.03
Root radius:	15	Flange-to-web welds:	

Column			
Shape:	HEM 340		
Height:	376	Width:	307.50
Flange thickness:	40.21	Web thickness:	21
Root radius:	27	Flange-to-web welds:	
<input type="checkbox"/> Supplementary web plate		Thickness:	
<input type="checkbox"/> Continuity plates		Thickness:	

End-plate

hp:	401.40								
bp:	150.47	ep:	30.27	exs:	29.74	mx1:	39.78	p1:	204.84
tp:	20.02	w:	89.93	exi:	30.35	mx2:	39.78	p2:	0
<input type="checkbox"/> Rib stiffener					mx3:	39.78			
Thickness:					mx4:	0			

Bolts

Rows in tension:	2
Bolts per row:	2
Diameter:	20
Tensile stress area:	245
<input type="checkbox"/> Head washer	
<input type="checkbox"/> Nut washer	

Beam-to-plate welds

<input checked="" type="checkbox"/> Throat thickness	
<input type="checkbox"/> Leg thickness	
Flange	
<input type="checkbox"/> Full penetration	
<input checked="" type="checkbox"/> Fillet welds	6
Web	
<input type="checkbox"/> Full penetration	
<input checked="" type="checkbox"/> Fillet welds	4

Notes:

Authors provide actual values of: column height, column flange width and thickness, beam height, beam flange width and thickness, beam web thickness, end-plate height, width, thickness and layout.

Test FS3a

		Material properties			
		(MPa)			
Beam		Column		End-plate	
<input type="checkbox"/> Nominal grade S235 <input checked="" type="checkbox"/> Measured values fy,f: 316.24 fy,w: 299.12 fu,f: 462.28 fu,w: 446.25		<input checked="" type="checkbox"/> Nominal grade S355 <input type="checkbox"/> Measured values fy,f: 355 fy,w: 355 fu,f: 510 fu,w: 510		<input type="checkbox"/> Nominal grade S355 <input checked="" type="checkbox"/> Measured values Yield strength: 342.62 Ultimate strength: 502.59 Young's modulus <input type="checkbox"/> Nominal Ef: 210000 <input checked="" type="checkbox"/> Measured Ew: 210000	
Young's modulus <input type="checkbox"/> Nominal Ef: 209496 <input checked="" type="checkbox"/> Measured Ew: 208332					
Bolts		Continuity plate		Supplementary web plate	
<input type="checkbox"/> Nominal grade 8.8 <input checked="" type="checkbox"/> Measured values Yield strength: 857.33 Ultimate strength: 913.78 Young's modulus <input type="checkbox"/> Nominal <input checked="" type="checkbox"/> Measured E: 223166		<input type="checkbox"/> Nominal grade <input type="checkbox"/> Measured values Yield strength: Ultimate strength: Young's modulus <input type="checkbox"/> Nominal <input type="checkbox"/> Measured E:		<input type="checkbox"/> Nominal grade <input type="checkbox"/> Measured values Yield strength: Ultimate strength: Young's modulus <input type="checkbox"/> Nominal <input type="checkbox"/> Measured E:	
Notes: <div style="border: 1px solid black; height: 100px; width: 100%;"></div>					
End-plate rib stiffener					
<input type="checkbox"/> Nominal grade <input type="checkbox"/> Measured value Yield strength: Ultimate strength: Young's modulus <input type="checkbox"/> Nominal <input type="checkbox"/> Measured E:					
Test set up and loading protocol					
Type of test:	Monotonic				
Loading protocol:					
Data provided:	Transducer DT1				
Type of response curve:	<input type="checkbox"/> Force <input checked="" type="checkbox"/> Moment Evaluated on the end-plate <input type="checkbox"/> Displacement <input checked="" type="checkbox"/> Rotation				

Paper

Title: Experimental assessment of the ductility of extended end plate connections

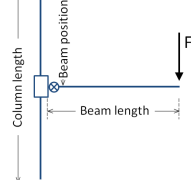
Authors: Coelho A. M. G. Bijlaard F. S. K. da Silva L. S.

Source: Engineering Structures **Volume:** 26 **Issue:** 9 **Pages:** 1185-1206 **Year:** 2004

Test FS3b

Scheme: Exterior joint

Beam length: 1052.86
Beam position: 600
Column length: 1200



Geometry (mm)

Beam	
Shape:	IPE 300
Height:	301.46
Flange thickness:	10.57
Web thickness:	7.03
Root radius:	15
Flange-to-web welds:	

Column	
Shape:	HEM 340
Height:	376
Flange thickness:	40.21
Web thickness:	21
Root radius:	27
Supplementary web plate:	<input type="checkbox"/>
Continuity plates:	<input type="checkbox"/>
Thickness:	
Thickness:	

End-plate

hp:	401.40
bp:	150.47
tp:	20.02
ep:	30.27
w:	89.93
exs:	29.74
exi:	76.82
mx1:	39.78
mx2:	39.78
mx3:	39.78
mx4:	0
Rib stiffener:	<input type="checkbox"/>
Thickness:	

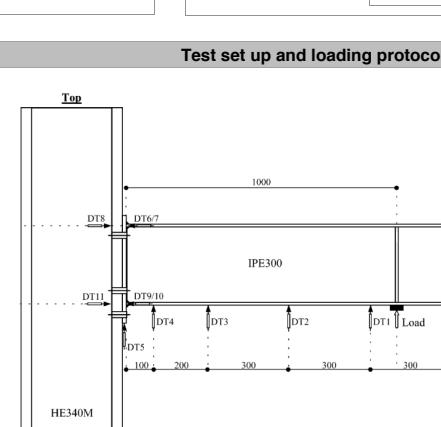
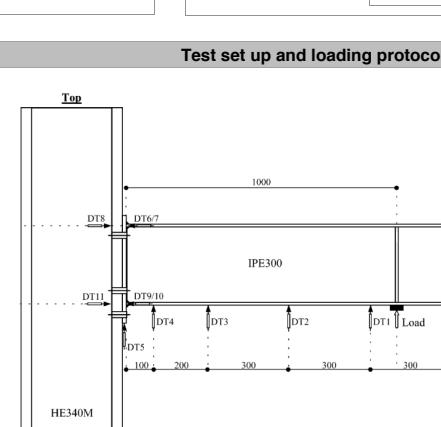
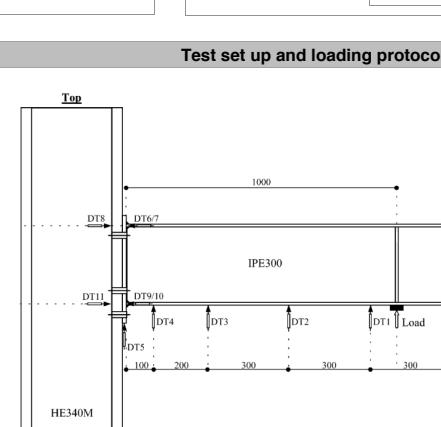
Bolts

Rows in tension:	2
Bolts per row:	2
Diameter:	20
Tensile stress area:	245
Head washer:	<input type="checkbox"/>
Nut washer:	<input type="checkbox"/>

Beam-to-plate welds

<input checked="" type="checkbox"/> Throat thickness
<input type="checkbox"/> Leg thickness
Flange
<input type="checkbox"/> Full penetration
<input checked="" type="checkbox"/> Fillet welds 6
Web
<input type="checkbox"/> Full penetration
<input checked="" type="checkbox"/> Fillet welds 4

Notes:
Authors provide actual values of: column height, column flange width and thickness, beam height, beam flange width and thickness, beam web thickness, end-plate height, width, thickness and layout.

Test FS3b		Material properties													
		(MPa)													
Beam <input type="checkbox"/> Nominal grade S235 <input checked="" type="checkbox"/> Measured values fy,f: 316.24 fy,w: 299.12 fu,f: 462.28 fu,w: 446.25 Young's modulus <input type="checkbox"/> Nominal Ef: 209496 <input checked="" type="checkbox"/> Measured Ew: 208332		Column <input checked="" type="checkbox"/> Nominal grade S355 <input type="checkbox"/> Measured values fy,f: 355 fy,w: 355 fu,f: 510 fu,w: 510 Young's modulus <input checked="" type="checkbox"/> Nominal Ef: 210000 <input type="checkbox"/> Measured Ew: 210000		End-plate <input type="checkbox"/> Nominal grade S355 <input checked="" type="checkbox"/> Measured values Yield strength: 342.62 Ultimate strength: 502.59 Young's modulus <input type="checkbox"/> Nominal <input checked="" type="checkbox"/> Measured E: 208622											
Bolts <input type="checkbox"/> Nominal grade 8.8 <input checked="" type="checkbox"/> Measured values Yield strength: 854.31 Ultimate strength: 916.81 Young's modulus <input type="checkbox"/> Nominal <input checked="" type="checkbox"/> Measured E: 222982		Continuity plate <input type="checkbox"/> Nominal grade <input type="checkbox"/> Measured values Yield strength: Ultimate strength: Young's modulus <input type="checkbox"/> Nominal <input type="checkbox"/> Measured E:		Supplementary web plate <input type="checkbox"/> Nominal grade <input type="checkbox"/> Measured values Yield strength: Ultimate strength: Young's modulus <input type="checkbox"/> Nominal <input checked="" type="checkbox"/> Measured E:											
<p>Notes:</p> <div style="border: 1px solid black; height: 100px; width: 100%;"></div>															
Test set up and loading protocol <table border="1"> <tr> <td>Type of test:</td> <td>Monotonic</td> </tr> <tr> <td>Loading protocol:</td> <td></td> </tr> <tr> <td>Data provided:</td> <td>Transducer DT1</td> </tr> <tr> <td>Type of response curve:</td> <td> <input type="checkbox"/> Force <input checked="" type="checkbox"/> Moment <input type="checkbox"/> Displacement <input checked="" type="checkbox"/> Rotation </td> </tr> <tr> <td colspan="2">  </td> </tr> </table>						Type of test:	Monotonic	Loading protocol:		Data provided:	Transducer DT1	Type of response curve:	<input type="checkbox"/> Force <input checked="" type="checkbox"/> Moment <input type="checkbox"/> Displacement <input checked="" type="checkbox"/> Rotation		
Type of test:	Monotonic														
Loading protocol:															
Data provided:	Transducer DT1														
Type of response curve:	<input type="checkbox"/> Force <input checked="" type="checkbox"/> Moment <input type="checkbox"/> Displacement <input checked="" type="checkbox"/> Rotation														
															

Paper

Title: Experimental assessment of the ductility of extended end plate connections

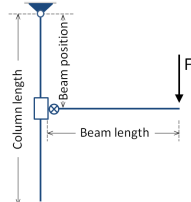
Authors: Coelho A. M. G. Bijlaard F. S. K. da Silva L. S.

Source: Engineering Structures **Volume:** 26 **Issue:** 9 **Pages:** 1185-1206 **Year:** 2004

Test FS4a

Scheme: Exterior joint

Beam length: 1042.51
Beam position: 600
Column length: 1200



Geometry (mm)

Beam	
Shape:	IPE 300
Height:	300.66
Flange thickness:	11.86
Root radius:	15
Width:	149.54
Web thickness:	7.03
Flange-to-web welds:	

Column	
Shape:	HEM 340
Height:	376
Flange thickness:	40.21
Root radius:	27
Width:	307.50
Web thickness:	21
Flange-to-web welds:	
<input type="checkbox"/> Supplementary web plate	Thickness:
<input type="checkbox"/> Continuity plates	Thickness:

End-plate

hp:	401.69								
bp:	149.76	ep:	29.94	exs:	29.83	mx1:	39.04	p1:	205.28
tp:	10.06	w:	89.88	exi:	76.13	mx2:	39.04	p2:	0
<input type="checkbox"/> Rib stiffener					mx3:	39.04			
Thickness:					mx4:	0			

Bolts	
Rows in tension:	2
Bolts per row:	2
Diameter:	20
Tensile stress area:	245
<input type="checkbox"/> Head washer	
<input type="checkbox"/> Nut washer	

Beam-to-plate welds	
<input checked="" type="checkbox"/> Throat thickness	
<input type="checkbox"/> Leg thickness	
Flange	
<input type="checkbox"/> Full penetration	
<input checked="" type="checkbox"/> Fillet welds	6
Web	
<input type="checkbox"/> Full penetration	
<input checked="" type="checkbox"/> Fillet welds	4

Notes:
Authors provide actual values of: column height, column flange width and thickness, beam height, beam flange width and thickness, beam web thickness, end-plate height, width, thickness and layout.

Test FS4a

		Material properties			
		(MPa)			
Beam		Column		End-plate	
<input type="checkbox"/> Nominal grade S235 <input checked="" type="checkbox"/> Measured values fy,f: 316.24 fy,w: 299.12 fu,f: 462.28 fu,w: 446.28		<input checked="" type="checkbox"/> Nominal grade S355 <input type="checkbox"/> Measured values fy,f: 355 fy,w: 355 fu,f: 510 fu,w: 510		<input type="checkbox"/> Nominal grade S690 <input checked="" type="checkbox"/> Measured values Yield strength: 698.55 Ultimate strength: 741.28 Young's modulus <input type="checkbox"/> Nominal Ef: 210000 <input checked="" type="checkbox"/> Measured Ew: 210000	
Young's modulus <input type="checkbox"/> Nominal Ef: 209496 <input checked="" type="checkbox"/> Measured Ew: 208332		Young's modulus <input checked="" type="checkbox"/> Nominal Ef: 210000 <input type="checkbox"/> Measured Ew: 210000		Young's modulus <input type="checkbox"/> Nominal <input checked="" type="checkbox"/> Measured E: 204462	
Bolts		Continuity plate		Supplementary web plate	
<input type="checkbox"/> Nominal grade 8.8 <input checked="" type="checkbox"/> Measured values Yield strength: 854.31 Ultimate strength: 916.81 Young's modulus <input type="checkbox"/> Nominal <input checked="" type="checkbox"/> Measured E: 222982		<input type="checkbox"/> Nominal grade <input type="checkbox"/> Measured values Yield strength: Ultimate strength: Young's modulus <input type="checkbox"/> Nominal <input type="checkbox"/> Measured E:		<input type="checkbox"/> Nominal grade <input type="checkbox"/> Measured values Yield strength: Ultimate strength: Young's modulus <input type="checkbox"/> Nominal <input type="checkbox"/> Measured E:	
Notes: <div style="border: 1px solid black; height: 100px; width: 100%;"></div>					
End-plate rib stiffener					
<input type="checkbox"/> Nominal grade <input type="checkbox"/> Measured value Yield strength: Ultimate strength: Young's modulus <input type="checkbox"/> Nominal <input type="checkbox"/> Measured E:					
Test set up and loading protocol					
Type of test:	Monotonic				
Loading protocol:					
Data provided:	Transducer DT1				
Type of response curve:	<input type="checkbox"/> Force <input checked="" type="checkbox"/> Moment Evaluated on the end-plate <input type="checkbox"/> Displacement <input checked="" type="checkbox"/> Rotation				

Paper

Title: Experimental assessment of the ductility of extended end plate connections

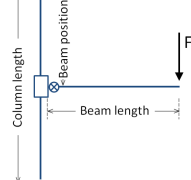
Authors: Coelho A. M. G. Bijlaard F. S. K. da Silva L. S.

Source: Engineering Structures **Volume:** 26 **Issue:** 9 **Pages:** 1185-1206 **Year:** 2004

Test FS4b

Scheme: Exterior joint

Beam length: 1042.51
Beam position: 600
Column length: 1200



Geometry (mm)

Beam			
Shape:	IPE 300		
Height:	300.66	Width:	149.54
Flange thickness:	11.86	Web thickness:	7.03
Root radius:	15	Flange-to-web welds:	

Column			
Shape:	HEM 340		
Height:	376	Width:	307.50
Flange thickness:	40.21	Web thickness:	21
Root radius:	27	Flange-to-web welds:	
<input type="checkbox"/> Supplementary web plate	Thickness:		
<input type="checkbox"/> Continuity plates	Thickness:		

End-plate

hp:	401.69								
bp:	149.76	ep:	29.94	exs:	29.83	mx1:	39.04	p1:	205.28
tp:	10.06	w:	89.88	exi:	76.13	mx2:	39.04	p2:	0
<input type="checkbox"/> Rib stiffener	Thickness:		mx3:	39.04					
	Thickness:		mx4:	0					

Bolts

Rows in tension:	2
Bolts per row:	2
Diameter:	20
Tensile stress area:	245
<input type="checkbox"/> Head washer	
<input type="checkbox"/> Nut washer	

Beam-to-plate welds

<input checked="" type="checkbox"/> Throat thickness	
<input type="checkbox"/> Leg thickness	
Flange	
<input type="checkbox"/> Full penetration	
<input checked="" type="checkbox"/> Fillet welds	6
Web	
<input type="checkbox"/> Full penetration	
<input checked="" type="checkbox"/> Fillet welds	4

Notes:
Authors provide actual values of: column height, column flange width and thickness, beam height, beam flange width and thickness, beam web thickness, end-plate height, width, thickness and layout.

Test FS4b

Material properties		
(MPa)		
Beam	Column	End-plate
<input type="checkbox"/> Nominal grade S235 <input checked="" type="checkbox"/> Measured values fy,f: 316.24 fy,w: 299.12 fu,f: 462.28 fu,w: 446.25	<input checked="" type="checkbox"/> Nominal grade S355 <input type="checkbox"/> Measured values fy,f: 355 fy,w: 355 fu,f: 510 fu,w: 510	<input type="checkbox"/> Nominal grade S690 <input checked="" type="checkbox"/> Measured values Yield strength: 698.55 Ultimate strength: 741.28 Young's modulus <input type="checkbox"/> Nominal Ef: 210000 <input checked="" type="checkbox"/> Measured Ew: 210000
Bolts	Continuity plate	Supplementary web plate
<input type="checkbox"/> Nominal grade 8.8 <input checked="" type="checkbox"/> Measured values Yield strength: 854.31 Ultimate strength: 916.81 Young's modulus <input type="checkbox"/> Nominal <input checked="" type="checkbox"/> Measured E: 222982	<input type="checkbox"/> Nominal grade <input type="checkbox"/> Measured values Yield strength: Ultimate strength: Young's modulus <input type="checkbox"/> Nominal <input type="checkbox"/> Measured E:	<input type="checkbox"/> Nominal grade <input type="checkbox"/> Measured values Yield strength: Ultimate strength: Young's modulus <input type="checkbox"/> Nominal <input type="checkbox"/> Measured E:
Notes:		
End-plate rib stiffener <input type="checkbox"/> Nominal grade <input type="checkbox"/> Measured value Yield strength: Ultimate strength: Young's modulus <input type="checkbox"/> Nominal <input type="checkbox"/> Measured E:		
Test set up and loading protocol		
Type of test:	Monotonic	
Loading protocol:		
Data provided:	Transducer DT1	
Type of response curve:	<input type="checkbox"/> Force <input checked="" type="checkbox"/> Moment <input type="checkbox"/> Displacement <input checked="" type="checkbox"/> Rotation	
	Evaluated on the end-plate 	

Paper

Title: Experimental behaviour of high strength steel end-plate connections

Authors: Coelho A. M. G. Bijlaard F. S. K.

Source: Journal of constructional steel research

Volume: 63 **Issue:** 1228-1240 **Year:** 2007

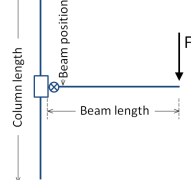
Test EEP-10-2a

Scheme: Exterior joint

Beam length: 1349.10

Beam position: n.a.

Column length: 1540



Geometry (mm)

Beam	
Height:	310
Flange thickness:	15.5
Root radius:	27
Web thickness:	9
Flange-to-web welds:	

Column	
Height:	340
Flange thickness:	39
Root radius:	27
Width:	310
Web thickness:	21
Thickness:	
Flange-to-web welds:	
Thickness:	

End-plate

hp:	435								
bp:	300	ep:	75	exs:	40	mx1:	59.75	p1:	160
tp:	10.10	w:	150	exi:	25	mx2:	59.75	p2:	0
<input type="checkbox"/> Rib stiffener					mx3:	59.75			
Thickness:					mx4:				

Bolts	
Rows in tension:	2
Bolts per row:	2
Diameter:	24
Tensile stress area:	353

Beam-to-plate welds	
<input checked="" type="checkbox"/> Throat thickness	
<input type="checkbox"/> Leg thickness	
Flange	
<input type="checkbox"/> Full penetration	
<input checked="" type="checkbox"/> Fillet welds	10
Web	
<input type="checkbox"/> Full penetration	
<input checked="" type="checkbox"/> Fillet welds	8

Notes:

The beam position is not specified.

Test EEP-10-2a

		Material properties	
		(MPa)	
Beam		Column	
<input checked="" type="checkbox"/> Nominal grade S355 <input type="checkbox"/> Measured values		<input checked="" type="checkbox"/> Nominal grade S355 <input type="checkbox"/> Measured values	
fy,f: 355 fy,w: 355		fy,f: 355 fy,w: 355	
fu,f: 510 fu,w: 510		fu,f: 510 fu,w: 510	
Young's modulus		Young's modulus	
<input checked="" type="checkbox"/> Nominal Ef: 210000 <input type="checkbox"/> Measured Ew: 210000		<input checked="" type="checkbox"/> Nominal Ef: 210000 <input type="checkbox"/> Measured Ew: 210000	
Bolts		Continuity plate	
<input type="checkbox"/> Nominal grade 8.8 <input checked="" type="checkbox"/> Measured values		<input type="checkbox"/> Nominal grade <input type="checkbox"/> Measured values	
Yield strength: 640		Yield strength:	
Ultimate strength: 939.9		Ultimate strength:	
Young's modulus		Young's modulus	
<input checked="" type="checkbox"/> Nominal <input type="checkbox"/> Measured E:		<input type="checkbox"/> Nominal <input type="checkbox"/> Measured E:	
End-plate		Supplementary web plate	
<input type="checkbox"/> Nominal grade S690 <input checked="" type="checkbox"/> Measured values		<input type="checkbox"/> Nominal grade <input type="checkbox"/> Measured values	
Yield strength: 698		Yield strength:	
Ultimate strength: 749		Ultimate strength:	
Young's modulus		Young's modulus	
<input type="checkbox"/> Nominal <input checked="" type="checkbox"/> Measured E: 205900		<input type="checkbox"/> Nominal <input checked="" type="checkbox"/> Measured E:	
Notes:		End-plate rib stiffener	
Concerning bolts, Authors provide only the measured ultimate strength. Consequently the yield strength is assumed equal to the nominal value.		<input type="checkbox"/> Nominal grade <input type="checkbox"/> Measured value	
		Yield strength:	
		Ultimate strength:	
Young's modulus		Young's modulus	
<input type="checkbox"/> Nominal <input type="checkbox"/> Measured E:		<input type="checkbox"/> Nominal <input type="checkbox"/> Measured E:	
Test set up and loading protocol			
Type of test:	Monotonic		
Loading protocol:			
Data provided:	Transducer DT1		
Type of response curve:			
<input type="checkbox"/> Force <input checked="" type="checkbox"/> Moment <input type="checkbox"/> Displacement <input checked="" type="checkbox"/> Rotation	Evaluated on the end-plate joint rotation		

Paper

Title: Experimental behaviour of high strength steel end-plate connections

Authors: Coelho A. M. G. Bijlaard F. S. K.

Source: Journal of constructional steel research

Volume:	63	Issue:		Pages:	1228-1240	Year:	2007
---------	----	--------	--	--------	-----------	-------	------

Test EEP-10-2b

Geometry (mm)

Scheme: Exterior joint

Beam length: 1349.1

Beam position: n.a.

Column length: 1540

Beam

Shape: HEA 320

Height:	310	Width:	300
Flange thickness:	15.5	Web thickness:	9
Root radius:	27	Flange-to-web welds:	

Column

Shape: HEM 300

Height:	340	Width:	310
Flange thickness:	39	Web thickness:	21
Root radius:	27	Flange-to-web welds:	

End-plate

hp:	435								
bp:	300	ep:	75	exs:	40	mx1:	59.75	p1:	160
tp:	10.10	w:	150	exi:	25	mx2:	59.75	p2:	0
<input type="checkbox"/> Rib stiffener				mx3:	59.75				
Thickness:				mx4:	0				

Bolts

Rows in tension:	2
Bolts per row:	2
Diameter:	24
Tensile stress area:	353

Beam-to-plate welds

<input checked="" type="checkbox"/> Throat thickness
<input type="checkbox"/> Leg thickness
Flange
<input type="checkbox"/> Full penetration
<input checked="" type="checkbox"/> Fillet welds 10
Web
<input type="checkbox"/> Full penetration
<input checked="" type="checkbox"/> Fillet welds 8

Notes:

The beam position is not specified.

Test EEP-10-2b

		Material properties			
		(MPa)			
Beam		Column		End-plate	
<input checked="" type="checkbox"/> Nominal grade S355 <input type="checkbox"/> Measured values		<input checked="" type="checkbox"/> Nominal grade S355 <input type="checkbox"/> Measured values		<input type="checkbox"/> Nominal grade S690 <input checked="" type="checkbox"/> Measured values	
fy,f: 355 fy,w: 355		fy,f: 355 fy,w: 355		Yield strength: 698	
fu,f: 510 fu,w: 510		fu,f: 510 fu,w: 510		Ultimate strength: 749	
Young's modulus		Young's modulus		Young's modulus	
<input checked="" type="checkbox"/> Nominal Ef: 210000 <input type="checkbox"/> Measured Ew: 210000		<input checked="" type="checkbox"/> Nominal Ef: 210000 <input type="checkbox"/> Measured Ew: 210000		<input type="checkbox"/> Nominal <input checked="" type="checkbox"/> Measured E: 205900	
Bolts		Continuity plate		Supplementary web plate	
<input type="checkbox"/> Nominal grade 8.8 <input checked="" type="checkbox"/> Measured values		<input type="checkbox"/> Nominal grade <input type="checkbox"/> Measured values		<input type="checkbox"/> Nominal grade <input type="checkbox"/> Measured values	
Yield strength: 640		Yield strength:		Yield strength:	
Ultimate strength: 939.9		Ultimate strength:		Ultimate strength:	
Young's modulus		Young's modulus		Young's modulus	
<input type="checkbox"/> Nominal <input checked="" type="checkbox"/> Measured E: 210000		<input type="checkbox"/> Nominal <input type="checkbox"/> Measured E:		<input type="checkbox"/> Nominal <input type="checkbox"/> Measured E:	
Notes:					
Concerning bolts, Authors provide only the measured ultimate strength. Consequently the yield strength is assumed equal to the nominal value.					
End-plate rib stiffener					
<input type="checkbox"/> Nominal grade <input type="checkbox"/> Measured value Yield strength: Ultimate strength: Young's modulus <input type="checkbox"/> Nominal <input type="checkbox"/> Measured E:					
Test set up and loading protocol					
Type of test:	Monotonic				
Loading protocol:					
Data provided:	Transducer DT1				
Type of response curve:					
<input type="checkbox"/> Force <input checked="" type="checkbox"/> Moment <input type="checkbox"/> Displacement <input checked="" type="checkbox"/> Rotation	Evaluated on the end-plate joint rotation				

Paper

Title: Experimental behaviour of high strength steel end-plate connections

Authors: Coelho A. M. G. Bijlaard F. S. K.

Source: Journal of constructional steel research

Volume:	63	Issue:		Pages:	1228-1240	Year:	2007
---------	----	--------	--	--------	-----------	-------	------

Test EEP-15-2

Geometry (mm)

Scheme: Exterior joint

Beam length: 1353.62

Beam position: n.a.

Column length: 1540

Beam

Shape: HEA 320

Height:	310	Width:	300
Flange thickness:	15.5	Web thickness:	9
Root radius:	27	Flange-to-web welds:	

Column

Shape: HEM 300

Height:	340	Width:	310
Flange thickness:	39	Web thickness:	21
Root radius:	27	Flange-to-web welds:	
<input type="checkbox"/> Supplementary web plate	Thickness:		
<input type="checkbox"/> Continuity plates	Thickness:		

End-plate

hp:	435								
bp:	150	ep:	75	exs:	40	mx1:	59.75	p1:	160
tp:	14.62	w:	150	exi:	25	mx2:	59.75	p2:	0
<input type="checkbox"/> Rib stiffener	Thickness:		mx3:	59.75					
Thickness:		mx4:	0						

Bolts

Rows in tension:	2
Bolts per row:	2
Diameter:	24
Tensile stress area:	353

Beam-to-plate welds

<input checked="" type="checkbox"/> Throat thickness	
<input type="checkbox"/> Leg thickness	
Flange	
<input type="checkbox"/> Full penetration	
<input checked="" type="checkbox"/> Fillet welds	10
Web	
<input type="checkbox"/> Full penetration	
<input checked="" type="checkbox"/> Fillet welds	8

Notes:

The beam position is not specified.

Test EEP-15-2		Material properties													
		(MPa)													
Beam <input checked="" type="checkbox"/> Nominal grade S355 <input type="checkbox"/> Measured values fy,f: 355 fy,w: 355 fu,f: 355 fu,w: 355 Young's modulus <input checked="" type="checkbox"/> Nominal Ef: 210000 <input type="checkbox"/> Measured Ew: 210000		Column <input checked="" type="checkbox"/> Nominal grade S355 <input type="checkbox"/> Measured values fy,f: 355 fy,w: 355 fu,f: 510 fu,w: 510 Young's modulus <input checked="" type="checkbox"/> Nominal Ef: 210000 <input type="checkbox"/> Measured Ew: 210000		End-plate <input type="checkbox"/> Nominal grade <input checked="" type="checkbox"/> Measured values S690 Yield strength: 774 Ultimate strength: 814 Young's modulus <input type="checkbox"/> Nominal <input checked="" type="checkbox"/> Measured E: 206400											
Bolts <input type="checkbox"/> Nominal grade <input checked="" type="checkbox"/> Measured values 12.9 Yield strength: 1080 Ultimate strength: 1412.8 Young's modulus <input checked="" type="checkbox"/> Nominal <input type="checkbox"/> Measured E: 210000		Continuity plate <input type="checkbox"/> Nominal grade <input type="checkbox"/> Measured values Yield strength: Ultimate strength: Young's modulus <input type="checkbox"/> Nominal <input type="checkbox"/> Measured E:		Supplementary web plate <input type="checkbox"/> Nominal grade <input type="checkbox"/> Measured values Yield strength: Ultimate strength: Young's modulus <input type="checkbox"/> Nominal <input checked="" type="checkbox"/> Measured E:											
<p>Notes:</p> <p>Concerning bolts, Authors provide only the measured ultimate strength. Consequently the yield strength is assumed equal to the nominal value.</p>															
Test set up and loading protocol <table border="1"> <tr> <td>Type of test:</td> <td>Monotonic</td> </tr> <tr> <td>Loading protocol:</td> <td></td> </tr> <tr> <td>Data provided:</td> <td>Trandcucer DT1</td> </tr> <tr> <td>Type of response curve:</td> <td> <input type="checkbox"/> Force <input checked="" type="checkbox"/> Moment <input type="checkbox"/> Displacement <input checked="" type="checkbox"/> Rotation </td> </tr> <tr> <td colspan="2"> <input type="checkbox"/> Evaluated on the end-plate <input type="checkbox"/> Evaluated on the beam </td> </tr> </table>						Type of test:	Monotonic	Loading protocol:		Data provided:	Trandcucer DT1	Type of response curve:	<input type="checkbox"/> Force <input checked="" type="checkbox"/> Moment <input type="checkbox"/> Displacement <input checked="" type="checkbox"/> Rotation	<input type="checkbox"/> Evaluated on the end-plate <input type="checkbox"/> Evaluated on the beam	
Type of test:	Monotonic														
Loading protocol:															
Data provided:	Trandcucer DT1														
Type of response curve:	<input type="checkbox"/> Force <input checked="" type="checkbox"/> Moment <input type="checkbox"/> Displacement <input checked="" type="checkbox"/> Rotation														
<input type="checkbox"/> Evaluated on the end-plate <input type="checkbox"/> Evaluated on the beam															

Paper

Title: Behaviour of extended end-plate connections under cyclic loading

Authors: Ghobarah A., Osman A., Korol R. M.

Source: Engineering Structures

Volume:	12	Issue:	1	Pages:	15-27
Year:	1990				

Test A-1

Geometry (mm)

Beam

Shape: W360x170x45 (W14x30)

Height:	352	Width:	171
Flange thickness:	9.8	Web thickness:	6.9
Root radius:	10	Flange-to-web welds:	

Column

Shape: W360x200x64 (W14x43)

Height:	347	Width:	203
Flange thickness:	13.5	Web thickness:	7.7
Root radius:	15	Flange-to-web welds:	
<input checked="" type="checkbox"/> Supplementary web plate	Thickness:	8	
<input type="checkbox"/> Continuity plates	Thickness:		

End-plate

hp:	558								
bp:	203	ep:	n.a.	exs:	n.a.	mx1:	n.a.	p1:	n.a.
tp:	25.4	w:	n.a.	xi:	n.a.	mx2:	n.a.	p2:	n.a.
<input type="checkbox"/> Rib stiffener					mx3:	n.a.			
Thickness:					mx4:	n.a.			

Bolts

Rows in tension:	2
Bolts per row:	2
Diameter:	25
Tensile stress area:	390.9

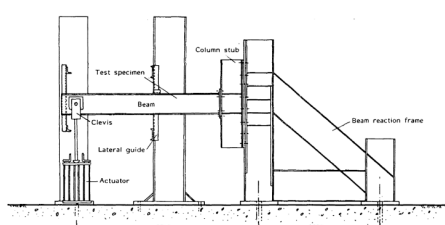
Beam-to-plate welds

<input type="checkbox"/> Throat thickness	
<input checked="" type="checkbox"/> Leg thickness	
Flange	
<input type="checkbox"/> Full penetration	
<input checked="" type="checkbox"/> Fillet welds	10
Web	
<input type="checkbox"/> Full penetration	
<input checked="" type="checkbox"/> Fillet welds	7

Notes:

The beam length provided is the distance between the point of application of the force and the column axis. The paper does not provide any bolts arrangement. The column web was reinforced by doubler plates.

Test A-1

		Material properties	
		(MPa)	
Beam		Column	
<input type="checkbox"/> Nominal grade <input checked="" type="checkbox"/> Measured values		<input checked="" type="checkbox"/> Nominal grade G40.21-M300W <input type="checkbox"/> Measured values	
f _{y,f} :	310.9	f _{y,w} :	315.7
f _{u,f} :	500.0	f _{u,w} :	480.7
Young's modulus		Young's modulus	
<input checked="" type="checkbox"/> Nominal	E _f : 210000	<input checked="" type="checkbox"/> Nominal	E _f : 210000
<input type="checkbox"/> Measured	E _w : 210000	<input type="checkbox"/> Measured	E _w : 210000
Bolts		Continuity plate	
<input checked="" type="checkbox"/> Nominal grade A490M <input type="checkbox"/> Measured values		<input type="checkbox"/> Nominal grade <input type="checkbox"/> Measured values	
Yield strength:	940	Yield strength:	
Ultimate strength:	1040	Ultimate strength:	
Young's modulus		Young's modulus	
<input checked="" type="checkbox"/> Nominal	E: 210000	<input type="checkbox"/> Nominal	E: 210000
<input type="checkbox"/> Measured	E: 210000	<input type="checkbox"/> Measured	E: 210000
End-plate		Supplementary web plate	
<input type="checkbox"/> Nominal grade G40.21-M300W <input checked="" type="checkbox"/> Measured values		<input checked="" type="checkbox"/> Nominal grade G40.21-M300W <input type="checkbox"/> Measured values	
Yield strength:	300	Yield strength:	300
Ultimate strength:	450	Ultimate strength:	450
Young's modulus		Young's modulus	
<input checked="" type="checkbox"/> Nominal	E: 210000	<input type="checkbox"/> Nominal	E: 210000
<input type="checkbox"/> Measured	E: 210000	<input type="checkbox"/> Measured	E: 210000
Notes:		End-plate rib stiffener	
<input type="checkbox"/> Nominal grade <input type="checkbox"/> Measured value		<input type="checkbox"/> Nominal grade <input type="checkbox"/> Measured value	
Yield strength:		Yield strength:	
Ultimate strength:		Ultimate strength:	
Young's modulus		Young's modulus	
<input type="checkbox"/> Nominal	E: 210000	<input type="checkbox"/> Nominal	E: 210000
<input type="checkbox"/> Measured	E: 210000	<input type="checkbox"/> Measured	E: 210000
Test set up and loading protocol			
Type of test:	Cyclic		
Loading protocol:	Tailor made protocol		
Partial ductility	0.5-1-1.5-2-2.5-3-3.5-4-5-6		
Data provided:			
Type of response curve:			
<input checked="" type="checkbox"/> Force	The force is applied to the beam tip		
<input type="checkbox"/> Moment			
<input checked="" type="checkbox"/> Displacement	Beam tip displacement due to the elastic and inelastic deformation of the beam, column flanges, end-plate and bolts		
<input type="checkbox"/> Rotation			

Paper

Title: Behaviour of extended end-plate connections under cyclic loading

Authors: Ghobarah A., Osman A., Korol R. M.

Source: Engineering Structures

Volume:	12	Issue:	1	Pages:	15-27
Year:	1990				

Test A-2

Geometry (mm)

Scheme: Exterior joint

Beam length: 2162

Beam position: 610

Column length: 1220

Beam

Shape: W360x170x45 (W14x30)

Height: 352

Flange thickness: 9.8

Root radius: 10

Width: 171

Web thickness: 6.9

Flange-to-web welds: []

Column

Shape: W360x200x64 (W14x43)

Height: 347

Flange thickness: 13.5

Root radius: 15

Width: 203

Web thickness: 7.7

Thickness: 8

Supplementary web plate:

Continuity plates:

Thickness: 9

End-plate

hp: 558

bp: 203

tp: 25.4

ep: n.a.

w: n.a.

exs: n.a.

exi: n.a.

mx1: n.a.

mx2: n.a.

p1: n.a.

p2: n.a.

mx3: n.a.

mx4: n.a.

Rib stiffener:

Thickness: []

Bolts

Rows in tension: 2

Bolts per row: 2

Diameter: 25

Tensile stress area: 390.9

Beam-to-plate welds

Throat thickness

Leg thickness

Flange

Full penetration

Fillet welds 10

Web

Full penetration

Fillet welds 7

Notes:

The beam length provided is the distance between the point of application of the force and the column axis. The paper does not provide any bolts arrangement. The column web was reinforced by doubler plates.

Test A-2

		Material properties	
		(MPa)	
Beam		Column	
<input type="checkbox"/> Nominal grade <input checked="" type="checkbox"/> Measured values		<input type="checkbox"/> Nominal grade G40.21-M300W <input type="checkbox"/> Measured values	
fy,f: 316.1 fy,w: 322.1 fu,f: 503.3 fu,w: 480.6		fy,f: 300 fy,w: 300 fu,f: 450 fu,w: 450	
Young's modulus		Young's modulus	
<input checked="" type="checkbox"/> Nominal Ef: 210000 <input type="checkbox"/> Measured Ew: 210000		<input checked="" type="checkbox"/> Nominal Ef: 210000 <input type="checkbox"/> Measured Ew: 210000	
Bolts		Continuity plate	
<input checked="" type="checkbox"/> Nominal grade A490M <input type="checkbox"/> Measured values		<input checked="" type="checkbox"/> Nominal grade G40.21-M300W <input type="checkbox"/> Measured values	
Yield strength: 940 Ultimate strength: 1040		Yield strength: 300 Ultimate strength: 450	
Young's modulus		Young's modulus	
<input checked="" type="checkbox"/> Nominal E: 210000 <input type="checkbox"/> Measured		<input checked="" type="checkbox"/> Nominal E: 210000 <input type="checkbox"/> Measured	
End-plate		Supplementary web plate	
<input type="checkbox"/> Nominal grade G40.21-M300W <input checked="" type="checkbox"/> Measured values		<input type="checkbox"/> Nominal grade G40.21-M300W <input checked="" type="checkbox"/> Measured values	
Yield strength: 300 Ultimate strength: 450		Yield strength: 300 Ultimate strength: 450	
Young's modulus		Young's modulus	
<input checked="" type="checkbox"/> Nominal E: 210000 <input type="checkbox"/> Measured		<input checked="" type="checkbox"/> Nominal E: 210000 <input type="checkbox"/> Measured	
Notes:		End-plate rib stiffener	
<input type="checkbox"/> Nominal grade <input type="checkbox"/> Measured value		<input type="checkbox"/> Nominal grade <input type="checkbox"/> Measured value	
Yield strength:		Yield strength:	
Ultimate strength:		Ultimate strength:	
Young's modulus		Young's modulus	
<input type="checkbox"/> Nominal <input type="checkbox"/> Measured E:		<input type="checkbox"/> Nominal <input type="checkbox"/> Measured E:	
Test set up and loading protocol			
Type of test:	Cyclic		
Loading protocol:	Tailor made protocol		
Partial ductility	0.5-1-1.5-2-2.5-3-3.5-4-5-6		
Data provided:			
Type of response curve:	<input checked="" type="checkbox"/> Force The force is applied to the beam tip <input type="checkbox"/> Moment <input checked="" type="checkbox"/> Displacement Beam tip displacement due to the elastic and inelastic deformation of the beam, column flanges, end-plate and bolts <input type="checkbox"/> Rotation		

Paper

Title: Behaviour of extended end-plate connections under cyclic loading

Authors: Ghobarah A., Osman A., Korol R. M.

Source: Engineering Structures

Volume:	12	Issue:	1	Pages:	15-27
Year:	1990				

Test A-3

Geometry (mm)

Beam

Shape: W360x170x45 (W14x30)

Height:	352	Width:	171
Flange thickness:	9.8	Web thickness:	6.9
Root radius:	10	Flange-to-web welds:	

Column

Shape: W360x200x79 (W14x53)

Height:	354	Width:	205
Flange thickness:	16.8	Web thickness:	9.4
Root radius:	15	Flange-to-web welds:	
<input checked="" type="checkbox"/> Supplementary web plate	Thickness:	8	
<input checked="" type="checkbox"/> Continuity plates	Thickness:	9	

End-plate

hp:	558								
bp:	203	ep:	n.a.	exs:	n.a.	mx1:	n.a.	p1:	n.a.
tp:	19	w:	n.a.	xi:	n.a.	mx2:	n.a.	p2:	n.a.
<input checked="" type="checkbox"/> Rib stiffener					mx3:	n.a.			
Thickness:	9				mx4:	n.a.			

Bolts

Rows in tension:	2
Bolts per row:	2
Diameter:	25
Tensile stress area:	390.9

Beam-to-plate welds

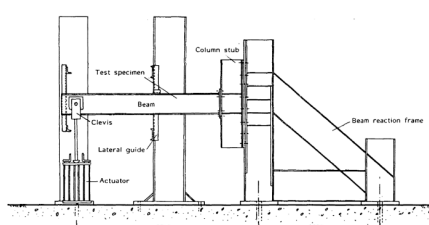
<input checked="" type="checkbox"/> Throat thickness	
<input type="checkbox"/> Leg thickness	
Flange	
<input type="checkbox"/> Full penetration	
<input checked="" type="checkbox"/> Fillet welds	10
Web	
<input type="checkbox"/> Full penetration	
<input checked="" type="checkbox"/> Fillet welds	7

Notes:

The beam length provided is the distance between the point of application of the force and the column axis. The paper does not provide any bolts arrangement.

Test A-3

		Material properties	
		(MPa)	
Beam		Column	
<input type="checkbox"/> Nominal grade <input checked="" type="checkbox"/> Measured values		<input checked="" type="checkbox"/> Nominal grade G40.21-M300W <input type="checkbox"/> Measured values	
f _{y,f} :	310.9	f _{y,w} :	315.7
f _{u,f} :	500.0	f _{u,w} :	480.7
Young's modulus		Young's modulus	
<input checked="" type="checkbox"/> Nominal	E _f : 210000	<input checked="" type="checkbox"/> Nominal	E _f : 210000
<input type="checkbox"/> Measured	E _w : 210000	<input type="checkbox"/> Measured	E _w : 210000
Bolts		Continuity plate	
<input checked="" type="checkbox"/> Nominal grade A490M <input type="checkbox"/> Measured values		<input checked="" type="checkbox"/> Nominal grade G40.21-M300W <input type="checkbox"/> Measured values	
Yield strength:	940	Yield strength:	300
Ultimate strength:	1040	Ultimate strength:	450
Young's modulus		Young's modulus	
<input checked="" type="checkbox"/> Nominal	E: 210000	<input checked="" type="checkbox"/> Nominal	E: 210000
<input type="checkbox"/> Measured	E: 210000	<input type="checkbox"/> Measured	E: 210000
End-plate		Supplementary web plate	
<input checked="" type="checkbox"/> Nominal grade G40.21-M300W <input type="checkbox"/> Measured values		<input checked="" type="checkbox"/> Nominal grade G40.21-M300W <input type="checkbox"/> Measured values	
Yield strength:	300	Yield strength:	300
Ultimate strength:	450	Ultimate strength:	450
Young's modulus		Young's modulus	
<input checked="" type="checkbox"/> Nominal	E: 210000	<input checked="" type="checkbox"/> Nominal	E: 210000
<input type="checkbox"/> Measured	E: 210000	<input type="checkbox"/> Measured	E: 210000
Notes:		End-plate rib stiffener	
<input checked="" type="checkbox"/> Nominal grade G40.21-M300W <input type="checkbox"/> Measured value		<input checked="" type="checkbox"/> Nominal grade G40.21-M300W <input type="checkbox"/> Measured value	
Yield strength:	300	Yield strength:	300
Ultimate strength:	450	Ultimate strength:	450
Young's modulus		Young's modulus	
<input checked="" type="checkbox"/> Nominal	E: 210000	<input checked="" type="checkbox"/> Nominal	E: 210000
<input type="checkbox"/> Measured	E: 210000	<input type="checkbox"/> Measured	E: 210000
Test set up and loading protocol			
Type of test:	Cyclic		
Loading protocol:	Tailor made protocol		
Partial ductility	0.5-1-1.5-2-2.5-3-3.5-4-5-6		
Data provided:			
Type of response curve:			
<input checked="" type="checkbox"/> Force	The force is applied to the beam tip		
<input type="checkbox"/> Moment			
<input checked="" type="checkbox"/> Displacement	Beam tip displacement due to the elastic and inelastic deformation of the beam, column flanges, end-plate and bolts		
<input type="checkbox"/> Rotation			



Paper

Title: Behaviour of extended end-plate connections under cyclic loading

Authors: Ghobarah A., Osman A., Korol R. M.

Source: Engineering Structures

Volume:	12	Issue:	1	Pages:	15-27
Year:	1990				

Test A-4

Geometry (mm)

Scheme: Exterior joint

Beam length: 2165 **Beam position:** 610 **Column length:** 1220

Beam

Shape: W360x170x45 (W14x30)

Height:	352	Width:	171
Flange thickness:	9.8	Web thickness:	6.9
Root radius:	10	Flange-to-web welds:	

Column

Shape: W360x200x79 (W14x53)

Height:	354	Width:	205
Flange thickness:	16.8	Web thickness:	9.4
Root radius:	15	Flange-to-web welds:	
<input checked="" type="checkbox"/> Supplementary web plate	Thickness:	8	
<input type="checkbox"/> Continuity plates	Thickness:		

End-plate

hp:	558								
bp:	203	ep:	n.a.	exs:	n.a.	mx1:	n.a.	p1:	n.a.
tp:	19	w:	n.a.	xi:	n.a.	mx2:	n.a.	p2:	n.a.
<input type="checkbox"/> Rib stiffener					mx3:	n.a.			
Thickness:					mx4:	n.a.			

Bolts

Rows in tension:	2
Bolts per row:	2
Diameter:	25
Tensile stress area:	390.9

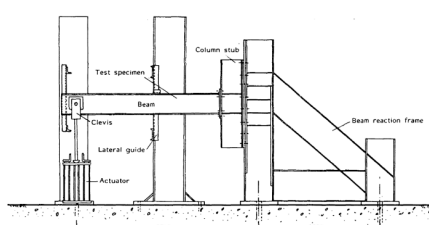
Beam-to-plate welds

<input checked="" type="checkbox"/> Throat thickness	
<input type="checkbox"/> Leg thickness	
Flange	
<input type="checkbox"/> Full penetration	
<input checked="" type="checkbox"/> Fillet welds	10
Web	
<input type="checkbox"/> Full penetration	
<input checked="" type="checkbox"/> Fillet welds	7

Notes:

The beam length provided is the distance between the point of application of the force and the column axis. The paper does not provide any bolts arrangement.

Test A-4

		Material properties	
		(MPa)	
Beam		Column	
<input type="checkbox"/> Nominal grade <input checked="" type="checkbox"/> Measured values		<input checked="" type="checkbox"/> Nominal grade G40.21-M300W <input type="checkbox"/> Measured values	
fy,f: 310.9 fy,w: 315.7 fu,f: 500.0 fu,w: 480.7		fy,f: 300 fy,w: 300 fu,f: 450 fu,w: 450	
Young's modulus		Young's modulus	
<input checked="" type="checkbox"/> Nominal Ef: 210000 <input type="checkbox"/> Measured Ew: 210000		<input checked="" type="checkbox"/> Nominal Ef: 210000 <input type="checkbox"/> Measured Ew: 210000	
Bolts		Continuity plate	
<input checked="" type="checkbox"/> Nominal grade A490M <input type="checkbox"/> Measured values		<input type="checkbox"/> Nominal grade <input type="checkbox"/> Measured values	
Yield strength: 940 Ultimate strength: 1040		Yield strength: Ultimate strength:	
Young's modulus		Young's modulus	
<input checked="" type="checkbox"/> Nominal E: 210000 <input type="checkbox"/> Measured E: 210000		<input type="checkbox"/> Nominal <input type="checkbox"/> Measured E: 210000	
End-plate		Supplementary web plate	
<input type="checkbox"/> Nominal grade G40.21-M300W <input checked="" type="checkbox"/> Measured values		<input checked="" type="checkbox"/> Nominal grade G40.21-M300W <input type="checkbox"/> Measured values	
Yield strength: 300 Ultimate strength: 450		Yield strength: 300 Ultimate strength: 450	
Young's modulus		Young's modulus	
<input checked="" type="checkbox"/> Nominal E: 210000 <input type="checkbox"/> Measured E: 210000		<input checked="" type="checkbox"/> Nominal E: 210000 <input type="checkbox"/> Measured E: 210000	
Notes:		End-plate rib stiffener	
<input type="checkbox"/> Nominal grade <input type="checkbox"/> Measured value		<input type="checkbox"/> Nominal grade <input type="checkbox"/> Measured value	
Yield strength: Ultimate strength:		Yield strength: Ultimate strength:	
Young's modulus		Young's modulus	
<input type="checkbox"/> Nominal <input type="checkbox"/> Measured E: 210000		<input type="checkbox"/> Nominal <input type="checkbox"/> Measured E: 210000	
Test set up and loading protocol			
Type of test:	Cyclic		
Loading protocol:	Tailor made protocol		
Partial ductility	0.5-1-1.5-2-2.5-3-3.5-4-5-6		
Data provided:			
Type of response curve:	<input checked="" type="checkbox"/> Force The force is applied to the beam tip <input type="checkbox"/> Moment <input checked="" type="checkbox"/> Displacement Beam tip displacement due to the elastic and inelastic deformation of the beam, column flanges, end-plate and bolts <input type="checkbox"/> Rotation		
			

Paper

Title: Behaviour of extended end-plate connections under cyclic loading

Authors: Ghobarah A., Osman A., Korol R. M.

Source: Engineering Structures

Volume:	12	Issue:	1	Pages:	15-27
Year:	1990				

Test A-5

Geometry (mm)

Scheme: Exterior joint

Beam length: 2165 **Beam position:** 610 **Column length:** 1220

Beam

Shape: W360x170x45 (W14x30)

Height:	352	Width:	171
Flange thickness:	9.8	Web thickness:	6.9
Root radius:	10	Flange-to-web welds:	

Column

Shape: W360x200x79 (W14x53)

Height:	354	Width:	205
Flange thickness:	16.8	Web thickness:	9.4
Root radius:	15	Flange-to-web welds:	
<input checked="" type="checkbox"/> Supplementary web plate	Thickness:	8	
<input checked="" type="checkbox"/> Continuity plates	Thickness:	9	

End-plate

hp:	558	bp:	203	ep:	n.a.	exs:	n.a.	mx1:	n.a.	p1:	n.a.
tp:	16	w:	n.a.	xi:	n.a.	mx2:	n.a.	p2:	n.a.		
<input checked="" type="checkbox"/> Rib stiffener					mx3:	n.a.					
Thickness:	9				mx4:	n.a.					

Bolts

Rows in tension:	2	Bolts per row:	2
Diameter:	25	Tensile stress area:	390.9

Beam-to-plate welds

<input checked="" type="checkbox"/> Throat thickness	
<input type="checkbox"/> Leg thickness	
Flange	
<input type="checkbox"/> Full penetration	
<input checked="" type="checkbox"/> Fillet welds	10
Web	
<input type="checkbox"/> Full penetration	
<input checked="" type="checkbox"/> Fillet welds	7

Notes:

The beam length provided is the distance between the point of application of the force and the column axis. The paper does not provide any bolts arrangement.

Test A-5

		Material properties	
		(MPa)	
Beam		Column	
<input type="checkbox"/> Nominal grade <input checked="" type="checkbox"/> Measured values		<input checked="" type="checkbox"/> Nominal grade G40.21-M300W <input type="checkbox"/> Measured values	
f _{y,f} :	316.1	f _{y,w} :	322.1
f _{u,f} :	503.3	f _{u,w} :	480.6
Young's modulus		Young's modulus	
<input checked="" type="checkbox"/> Nominal	E _f : 210000	<input checked="" type="checkbox"/> Nominal	E _f : 210000
<input type="checkbox"/> Measured	E _w :	<input type="checkbox"/> Measured	E _w : 210000
Bolts		Continuity plate	
<input checked="" type="checkbox"/> Nominal grade A490M <input type="checkbox"/> Measured values		<input checked="" type="checkbox"/> Nominal grade G40.21-M300W <input type="checkbox"/> Measured values	
Yield strength:	940	Yield strength:	300
Ultimate strength:	1040	Ultimate strength:	450
Young's modulus		Young's modulus	
<input checked="" type="checkbox"/> Nominal	E: 210000	<input checked="" type="checkbox"/> Nominal	E: 210000
<input type="checkbox"/> Measured	E:	<input type="checkbox"/> Measured	E: 210000
End-plate		Supplementary web plate	
<input checked="" type="checkbox"/> Nominal grade G40.21-M300W <input type="checkbox"/> Measured values		<input checked="" type="checkbox"/> Nominal grade G40.21-M300W <input type="checkbox"/> Measured values	
Yield strength:	300	Yield strength:	300
Ultimate strength:	450	Ultimate strength:	450
Young's modulus		Young's modulus	
<input checked="" type="checkbox"/> Nominal	E: 210000	<input checked="" type="checkbox"/> Nominal	E: 210000
<input type="checkbox"/> Measured	E:	<input type="checkbox"/> Measured	E: 210000
Notes:		End-plate rib stiffener	
<input checked="" type="checkbox"/> Nominal grade G40.21-M300W <input type="checkbox"/> Measured value		<input checked="" type="checkbox"/> Nominal grade G40.21-M300W <input type="checkbox"/> Measured value	
Yield strength:	300	Yield strength:	300
Ultimate strength:	450	Ultimate strength:	450
Young's modulus		Young's modulus	
<input checked="" type="checkbox"/> Nominal	E: 210000	<input checked="" type="checkbox"/> Nominal	E: 210000
<input type="checkbox"/> Measured	E:	<input type="checkbox"/> Measured	E: 210000
Test set up and loading protocol			
Type of test:	Cyclic		
Loading protocol:	Tailor made protocol		
Partial ductility	0.5-1-1.5-2-2.5-3-3.5-4-5-6		
Data provided:			
Type of response curve:	<input checked="" type="checkbox"/> Force <input type="checkbox"/> Moment <input checked="" type="checkbox"/> Displacement <input type="checkbox"/> Rotation		
	The force is applied to the beam tip Beam tip displacement due to the elastic and inelastic deformation of the beam, column flanges, end-plate and bolts		
<p>The diagram illustrates the test setup. A central vertical column stub supports a horizontal beam specimen. The beam is held in place by lateral guides and is connected to a reaction frame at its right end. An actuator is positioned at the left end of the beam to apply cyclic loading. The total width of the setup is indicated as 2745 mm, and the distance from the center of the column stub to the reaction frame is 1830 mm.</p>			

Paper

Title: Experimental analysis of bolted steel beam-to-column connections: Component identification

Authors: Iannone F., Latour M., Piluso V., Rizzano G.

Source: Journal of Earthquake Engineering

Volume:	Issue:	Pages:	Year:
15	2	214-244	2011

Test EEP-CYC 01

Geometry (mm)

Scheme: Exterior joint

Beam length: 1474.8

Beam position: 1350

Column length: 2700

Beam

Shape: IPE 270

Height: 268 **Width:** 134

Flange thickness: 10.9 **Web thickness:** 6.6

Root radius: 15 **Flange-to-web welds:** []

Column

Shape: HEB 200

Height: 201 **Width:** 201

Flange thickness: 15.3 **Web thickness:** 9.2

Root radius: 18 **Flange-to-web welds:** []

Thickness: [] **Thickness:** []

End-plate

hp: 449 **bp:** 153.6 **ep:** 30.5 **exs:** 42.2 **mx1:** 44.25 **p1:** 160.1

tp: 20.1 **w:** 91.6 **exi:** 42.2 **mx2:** 44.25 **p2:** 0

Rib stiffener **Thickness:** [] **mx3:** 44.25 **mx4:** 44.25

Bolts

Rows in tension: 2 **Bolts per row:** 2

Diameter: 20 **Tensile stress area:** 245

Head washer Nut washer

Beam-to-plate welds

Throat thickness Leg thickness

Flange

Full penetration Fillet welds []

Web

Full penetration Fillet welds []

Notes:

Details about washers and beam-to-plate welds are not provided.

Test EEP-CYC 01

		Material properties	
		(MPa)	
Beam		Column	
<input type="checkbox"/> Nominal grade S355 <input checked="" type="checkbox"/> Measured values		<input type="checkbox"/> Nominal grade S355 <input checked="" type="checkbox"/> Measured values	
fy,f: 405 fy,w: 387		fy,f: 430 fy,w: 382.5	
fu,f: 546 fu,w: 534		fu,f: 523 fu,w: 522	
Young's modulus		Young's modulus	
<input checked="" type="checkbox"/> Nominal Ef: 210000 <input type="checkbox"/> Measured Ew: 210000		<input checked="" type="checkbox"/> Nominal Ef: 210000 <input type="checkbox"/> Measured Ew: 210000	
Bolts		Continuity plate	
<input checked="" type="checkbox"/> Nominal grade 10.9 <input type="checkbox"/> Measured values		<input type="checkbox"/> Nominal grade <input type="checkbox"/> Measured values	
Yield strength: 900		Yield strength:	
Ultimate strength: 1000		Ultimate strength:	
Young's modulus		Young's modulus	
<input checked="" type="checkbox"/> Nominal <input type="checkbox"/> Measured E: 210000		<input type="checkbox"/> Nominal <input type="checkbox"/> Measured E:	
End-plate		Supplementary web plate	
<input type="checkbox"/> Nominal grade <input checked="" type="checkbox"/> Measured values S275		<input type="checkbox"/> Nominal grade <input type="checkbox"/> Measured values	
Yield strength: 290		Yield strength:	
Ultimate strength: 493.7		Ultimate strength:	
Young's modulus		Young's modulus	
<input type="checkbox"/> Nominal <input checked="" type="checkbox"/> Measured E: 207288		<input type="checkbox"/> Nominal <input checked="" type="checkbox"/> Measured E:	
Notes:		End-plate rib stiffener	
<input type="checkbox"/> Nominal grade <input type="checkbox"/> Measured value		<input type="checkbox"/> Nominal grade <input type="checkbox"/> Measured values	
Yield strength:		Yield strength:	
Ultimate strength:		Ultimate strength:	
Young's modulus		Young's modulus	
<input type="checkbox"/> Nominal <input type="checkbox"/> Measured E:		<input type="checkbox"/> Nominal <input type="checkbox"/> Measured E:	
Test set up and loading protocol			
Type of test:	Cyclic		
Loading protocol:	AISC protocol		
Data provided:	LVDT 1-2, LVDT 3-6, transducers 1,2		
Type of response curve:	<input type="checkbox"/> Force <input checked="" type="checkbox"/> Moment <input type="checkbox"/> Displacement <input checked="" type="checkbox"/> Rotation		
	<input type="checkbox"/> Joint rotation, web panel distortion		

Paper

Title: Experimental analysis of bolted steel beam-to-column connections: Component identification

Authors: Iannone F., Latour M., Piluso V., Rizzano G.

Source: Journal of Earthquake Engineering

Volume:	Issue:	Pages:	Year:
15	2	214-244	2011

Test EEP-CYC 02

Geometry (mm)

Scheme: Exterior joint

Beam length: 1476.5
Beam position: 1350
Column length: 2700

Column length
beam position
Beam length

Beam

Shape: IPE 270

Height:	271	Width:	131
Flange thickness:	10.7	Web thickness:	6.8
Root radius:	15	Flange-to-web welds:	

Column

Shape: HEB 200

Height:	198	Width:	198
Flange thickness:	15.5	Web thickness:	9.2
Root radius:	18	Flange-to-web welds:	
<input checked="" type="checkbox"/> Supplementary web plate		Thickness:	10
<input checked="" type="checkbox"/> Continuity plates		Thickness:	10

End-plate

hp:	474.4								
bp:	156.7	ep:	31.2	exs:	40.5	mx1:	61.45	p1:	126.2
tp:	20.7	w:	94.3	exi:	40.5	mx2:	61.45	p2:	0
<input type="checkbox"/> Rib stiffener					mx3:	61.45			
Thickness:					mx4:	61.45			

Bolts

Rows in tension:	2
Bolts per row:	2
Diameter:	20
Tensile stress area:	245

Beam-to-plate welds

<input type="checkbox"/> Throat thickness
<input type="checkbox"/> Leg thickness
Flange
<input type="checkbox"/> Full penetration
<input checked="" type="checkbox"/> Fillet welds
Web
<input type="checkbox"/> Full penetration
<input checked="" type="checkbox"/> Fillet welds

Notes:

The column web panel is reinforced by means two 10 mm supplementary web plates. Details about washers and beam-to-plate welds are not provided.

Test EEP-CYC 02

		Material properties			
		(MPa)			
Beam		Column		End-plate	
<input type="checkbox"/> Nominal grade S355 <input checked="" type="checkbox"/> Measured values		<input type="checkbox"/> Nominal grade S355 <input checked="" type="checkbox"/> Measured values		<input type="checkbox"/> Nominal grade S275 <input checked="" type="checkbox"/> Measured values	
fy,f: 405 fy,w: 387 fu,f: 546 fu,w: 534		fy,f: 430 fy,w: 382.5 fu,f: 523 fu,w: 522		Yield strength: 290 Ultimate strength: 493.7	
Young's modulus <input checked="" type="checkbox"/> Nominal Ef: 210000 <input type="checkbox"/> Measured Ew: 210000		Young's modulus <input checked="" type="checkbox"/> Nominal Ef: 210000 <input type="checkbox"/> Measured Ew: 210000		Young's modulus <input type="checkbox"/> Nominal <input checked="" type="checkbox"/> Measured E: 207288	
Bolts		Continuity plate		Supplementary web plate	
<input type="checkbox"/> Nominal grade <input checked="" type="checkbox"/> Measured values		<input type="checkbox"/> Nominal grade <input type="checkbox"/> Measured values		<input type="checkbox"/> Nominal grade <input type="checkbox"/> Measured values	
Yield strength: Ultimate strength: Young's modulus <input checked="" type="checkbox"/> Nominal <input type="checkbox"/> Measured E:		Yield strength: Ultimate strength: Young's modulus <input type="checkbox"/> Nominal <input type="checkbox"/> Measured E:		Yield strength: Ultimate strength: Young's modulus <input type="checkbox"/> Nominal <input type="checkbox"/> Measured E:	
Notes: The material properties of the continuity plates and supplementary web plates are not available					
End-plate rib stiffener					
<input type="checkbox"/> Nominal grade <input type="checkbox"/> Measured value Yield strength: Ultimate strength: Young's modulus <input type="checkbox"/> Nominal <input type="checkbox"/> Measured E:					
Test set up and loading protocol					
Type of test:	Cyclic				
Loading protocol:	AISC protocol				
Data provided:	LVDT 1-2, LVDT 3-6, transducers 1,2				
Type of response curve:	<input type="checkbox"/> Force <input checked="" type="checkbox"/> Moment <input type="checkbox"/> Displacement <input checked="" type="checkbox"/> Rotation				
	Joint rotation, web panel distortion				

Paper

Title:
Experimental behaviour of standardised european end-plate beam-to-column steel joints under arbitrary cycling loading

Authors:
Nogueiro P. da Silva L. S. Bento R. Simoes R.

Source: Proceedings of **Volume:** **Issue:** **Pages:** **Year:** 2006

Test J-1.1

Geometry (mm)

Beam

Shape: IPE 360

Height:	360	Width:	170
Flange thickness:	12.7	Web thickness:	8
Root radius:	18	Flange-to-web welds:	

Column

Shape: HEA 320

Height:	310	Width:	300
Flange thickness:	15.5	Web thickness:	9
Root radius:	27	Flange-to-web welds:	
<input type="checkbox"/> Supplementary web plate		Thickness:	
<input checked="" type="checkbox"/> Continuity plates		Thickness:	15

Scheme: Exterior joint

Beam length: 1147

Beam position: 1755

Column length: 3000

Geometry (mm)

Beam

Shape: IPE 360

Height:	360	Width:	170
Flange thickness:	12.7	Web thickness:	8
Root radius:	18	Flange-to-web welds:	

Column

Shape: HEA 320

Height:	310	Width:	300
Flange thickness:	15.5	Web thickness:	9
Root radius:	27	Flange-to-web welds:	
<input type="checkbox"/> Supplementary web plate		Thickness:	
<input checked="" type="checkbox"/> Continuity plates		Thickness:	15

End-plate

hp:	540								
bp:	220	ep:	55	exs:	50	mx1:	40	p1:	240
tp:	18	w:	110	exi:	50	mx2:	47.3	p2:	0
<input type="checkbox"/> Rib stiffener		Thickness:		mx3:	47.3				
		Thickness:		mx4:	40				

Bolts

Rows in tension:	2
Bolts per row:	2
Diameter:	24
Tensile stress area:	353

Beam-to-plate welds

<input checked="" type="checkbox"/> Throat thickness
<input type="checkbox"/> Leg thickness
Flange
<input type="checkbox"/> Full penetration
<input type="checkbox"/> Fillet welds
15
Web
<input type="checkbox"/> Full penetration
<input checked="" type="checkbox"/> Nut washer
8

Notes:

Test J-1.1

		Material properties	
		(MPa)	
Beam		Column	
<input checked="" type="checkbox"/> Nominal grade S355 <input type="checkbox"/> Measured values		<input checked="" type="checkbox"/> Nominal grade S355 <input type="checkbox"/> Measured values	
$f_y,f:$ 355 $f_y,w:$ 355 $f_u,f:$ 510 $f_u,w:$ 510		$f_y,f:$ 355 $f_y,w:$ 355 $f_u,f:$ 510 $f_u,w:$ 510	
Young's modulus		Young's modulus	
<input checked="" type="checkbox"/> Nominal $E_f:$ 210000 <input type="checkbox"/> Measured $E_w:$ 210000		<input checked="" type="checkbox"/> Nominal $E_f:$ 210000 <input type="checkbox"/> Measured $E_w:$ 21000	
Bolts		Continuity plate	
<input checked="" type="checkbox"/> Nominal grade 10.9 <input type="checkbox"/> Measured values		<input checked="" type="checkbox"/> Nominal grade S355 <input type="checkbox"/> Measured values	
Yield strength: 900		Yield strength: 355	
Ultimate strength: 1000		Ultimate strength: 510	
Young's modulus		Young's modulus	
<input checked="" type="checkbox"/> Nominal $E:$ 210000 <input type="checkbox"/> Measured		<input checked="" type="checkbox"/> Nominal $E:$ 210000 <input type="checkbox"/> Measured	
End-plate		Supplementary web plate	
<input checked="" type="checkbox"/> Nominal grade S355 <input type="checkbox"/> Measured values		<input type="checkbox"/> Nominal grade [] <input type="checkbox"/> Measured values []	
Yield strength: 355		Yield strength: []	
Ultimate strength: 510		Ultimate strength: []	
Young's modulus		Young's modulus	
<input checked="" type="checkbox"/> Nominal $E:$ 210000 <input type="checkbox"/> Measured		<input type="checkbox"/> Nominal $E:$ [] <input type="checkbox"/> Measured	
Notes:		End-plate rib stiffener	
<input type="checkbox"/> Nominal grade [] <input type="checkbox"/> Measured value []		<input type="checkbox"/> Nominal grade [] <input type="checkbox"/> Measured value []	
Yield strength: []		Yield strength: []	
Ultimate strength: []		Ultimate strength: []	
Young's modulus		Young's modulus	
<input type="checkbox"/> Nominal $E:$ [] <input type="checkbox"/> Measured		<input type="checkbox"/> Nominal $E:$ [] <input type="checkbox"/> Measured	
Test set up and loading protocol			
Type of test:	Monotonic		
Loading protocol:	<input type="checkbox"/> [] <input type="checkbox"/> []		
Data provided:	Displacement transducers DT1, DT2, DT3, DT4		
Type of response curve:			
<input type="checkbox"/> Force Evaluated on the column flange <input checked="" type="checkbox"/> Moment			
<input type="checkbox"/> Displacement Joint rotation <input checked="" type="checkbox"/> Rotation			

Paper

Title:
Experimental behaviour of standardised european end-plate beam-to-column steel joints under arbitrary cycling loading

Authors:
Nogueiro P. da Silva L. S. Bento R. Simoes R.

Source: Proceedings of **Volume:** **Issue:** **Pages:** **Year:** 2006

Test J-1.2

Geometry (mm)

Beam

Shape: IPE 360
Height: 360 Width: 170
Flange thickness: 12.7 Web thickness: 8
Root radius: 18 Flange-to-web welds:

Column

Shape: HEA 320
Height: 310 Width: 300
Flange thickness: 15.5 Web thickness: 9
Root radius: 27 Flange-to-web welds:
 Supplementary web plate Thickness:
 Continuity plates Thickness: 15

Scheme: Exterior joint

Beam length: 1147 Column length: 3000 Beam position: 1755

End-plate

hp:	540								
bp:	220	ep:	55	exs:	50	mx1:	40	p1:	240
tp:	18	w:	110	exi:	50	mx2:	47.3	p2:	0
<input type="checkbox"/> Rib stiffener					mx3:	47.3			
Thickness:					mx4:	40			

Bolts

Rows in tension: 2 Bolts per row: 2
Diameter: 24 Tensile stress area: 353

Beam-to-plate welds

Throat thickness
 Leg thickness
Flange
 Full penetration
 Fillet welds 15
Web
 Full penetration
 Fillet welds 8

Notes:

Test J-1.2

		Material properties	
		(MPa)	
Beam		Column	
<input checked="" type="checkbox"/> Nominal grade S355 <input type="checkbox"/> Measured values		<input checked="" type="checkbox"/> Nominal grade S355 <input type="checkbox"/> Measured values	
fy,f: 355 fy,w: 355		fy,f: 355 fy,w: 355	
fu,f: 510 fu,w: 510		fu,f: 510 fu,w: 510	
Young's modulus		Young's modulus	
<input checked="" type="checkbox"/> Nominal Ef: 210000 <input type="checkbox"/> Measured Ew: 210000		<input checked="" type="checkbox"/> Nominal Ef: 210000 <input type="checkbox"/> Measured Ew: 210000	
Bolts		Continuity plate	
<input checked="" type="checkbox"/> Nominal grade 10.9 <input type="checkbox"/> Measured values		<input checked="" type="checkbox"/> Nominal grade S355 <input type="checkbox"/> Measured values	
Yield strength: 900		Yield strength: 355	
Ultimate strength: 1000		Ultimate strength: 510	
Young's modulus		Young's modulus	
<input checked="" type="checkbox"/> Nominal E: 210000 <input type="checkbox"/> Measured		<input checked="" type="checkbox"/> Nominal E: 210000 <input type="checkbox"/> Measured	
End-plate		Supplementary web plate	
<input checked="" type="checkbox"/> Nominal grade S355 <input type="checkbox"/> Measured values		<input type="checkbox"/> Nominal grade <input type="checkbox"/> Measured values	
Yield strength: 355		Yield strength:	
Ultimate strength: 510		Ultimate strength:	
Young's modulus		Young's modulus	
<input checked="" type="checkbox"/> Nominal E: 210000 <input type="checkbox"/> Measured		<input type="checkbox"/> Nominal E: <input type="checkbox"/> Measured	
Notes:		End-plate rib stiffener	
<input type="checkbox"/> Nominal grade <input type="checkbox"/> Measured value		<input type="checkbox"/> Nominal grade <input type="checkbox"/> Measured value	
Yield strength:		Yield strength:	
Ultimate strength:		Ultimate strength:	
Young's modulus		Young's modulus	
<input type="checkbox"/> Nominal <input type="checkbox"/> Measured		<input type="checkbox"/> Nominal <input type="checkbox"/> Measured E:	
Test set up and loading protocol			
Type of test:	Cyclic		
Loading protocol:	???????		
Data provided:	Displacement transducers DT1, DT2, DT3, DT4		
Type of response curve:			
<input type="checkbox"/> Force <input checked="" type="checkbox"/> Moment	Evaluated on the column flange		
<input type="checkbox"/> Displacement <input checked="" type="checkbox"/> Rotation	Joint rotation		

Paper

Title:
Experimental behaviour of standardised european end-plate beam-to-column steel joints under arbitrary cycling loading

Authors:
Nogueiro P. da Silva L. S. Bento R. Simoes R.

Source: Proceedings of **Volume:** **Issue:** **Pages:** **Year:** 2006

Test J-1.3

Geometry (mm)

Beam

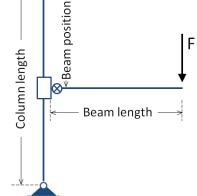
Shape: IPE 360

Height:	360	Width:	170
Flange thickness:	12.7	Web thickness:	8
Root radius:	18	Flange-to-web welds:	

Column

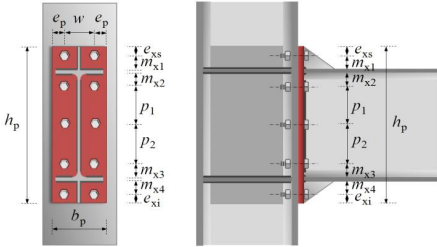
Shape: HEA 320

Height:	310	Width:	300
Flange thickness:	15.5	Web thickness:	9
Root radius:	27	Flange-to-web welds:	
<input type="checkbox"/> Supplementary web plate		Thickness:	
<input checked="" type="checkbox"/> Continuity plates		Thickness:	18



Scheme: Exterior joint

Beam length: 1147
Beam position: 1755
Column length: 3000



End-plate

hp:	540								
bp:	220	ep:	55	exs:	50	mx1:	40	p1:	240
tp:	18	w:	110	exi:	50	mx2:	47.3	p2:	0
<input type="checkbox"/> Rib stiffener				mx3: 47.3		mx4: 40			
Thickness:									

Bolts

Rows in tension:	2
Bolts per row:	2
Diameter:	24
Tensile stress area:	353

Beam-to-plate welds

<input type="checkbox"/> Throat thickness
<input checked="" type="checkbox"/> Leg thickness
Flange
<input type="checkbox"/> Full penetration
<input checked="" type="checkbox"/> Fillet welds 15
Web
<input type="checkbox"/> Full penetration
<input checked="" type="checkbox"/> Fillet welds 8

Notes:

Test J-1.3

		Material properties	
		(MPa)	
Beam		Column	
<input checked="" type="checkbox"/> Nominal grade S355 <input type="checkbox"/> Measured values		<input checked="" type="checkbox"/> Nominal grade S355 <input type="checkbox"/> Measured values	
$f_y,f:$ 355 $f_y,w:$ 355 $f_u,f:$ 510 $f_u,w:$ 510		$f_y,f:$ 355 $f_y,w:$ 355 $f_u,f:$ 510 $f_u,w:$ 510	
Young's modulus		Young's modulus	
<input checked="" type="checkbox"/> Nominal $E_f:$ 210000 <input type="checkbox"/> Measured $E_w:$ 210000		<input checked="" type="checkbox"/> Nominal $E_f:$ 210000 <input type="checkbox"/> Measured $E_w:$ 210000	
Bolts		Continuity plate	
<input checked="" type="checkbox"/> Nominal grade 10.9 <input type="checkbox"/> Measured values		<input checked="" type="checkbox"/> Nominal grade S355 <input type="checkbox"/> Measured values	
Yield strength: 900		Yield strength: 355	
Ultimate strength: 1000		Ultimate strength: 510	
Young's modulus		Young's modulus	
<input checked="" type="checkbox"/> Nominal $E:$ 210000 <input type="checkbox"/> Measured		<input checked="" type="checkbox"/> Nominal $E:$ 210000 <input type="checkbox"/> Measured	
End-plate		Supplementary web plate	
<input checked="" type="checkbox"/> Nominal grade S355 <input type="checkbox"/> Measured values		<input type="checkbox"/> Nominal grade [] <input type="checkbox"/> Measured values []	
Yield strength: 355		Yield strength: []	
Ultimate strength: 510		Ultimate strength: []	
Young's modulus		Young's modulus	
<input checked="" type="checkbox"/> Nominal $E:$ 210000 <input type="checkbox"/> Measured		<input type="checkbox"/> Nominal $E:$ [] <input type="checkbox"/> Measured	
Notes:		End-plate rib stiffener	
<input type="checkbox"/> Nominal grade [] <input type="checkbox"/> Measured value []		<input type="checkbox"/> Nominal grade [] <input type="checkbox"/> Measured value []	
Yield strength: []		Yield strength: []	
Ultimate strength: []		Ultimate strength: []	
Young's modulus		Young's modulus	
<input type="checkbox"/> Nominal $E:$ [] <input type="checkbox"/> Measured		<input type="checkbox"/> Nominal $E:$ [] <input type="checkbox"/> Measured	
Test set up and loading protocol			
Type of test:	Cyclic		
Loading protocol:	?????		
Data provided:	Displacement transducers DT1, DT2, DT3, DT4		
Type of response curve:			
<input type="checkbox"/> Force Evaluated on the column flange <input checked="" type="checkbox"/> Moment			
<input type="checkbox"/> Displacement Joint rotation <input checked="" type="checkbox"/> Rotation			

Paper

Title:
Experimental behaviour of standardised european end-plate beam-to-column steel joints under arbitrary cycling loading

Authors:
Nogueiro P. da Silva L. S. Bento R. Simoes R.

Source: Proceedings of **Volume:** **Issue:** **Pages:** **Year:** 2006

Test J-3.1

Geometry (mm)

Beam

Shape: IPE 360
Height: 360 Width: 170
Flange thickness: 12.7 Web thickness: 8
Root radius: 18 Flange-to-web welds:

Column

Shape: HEB 320
Height: 320 Width: 300
Flange thickness: 20.5 Web thickness: 11.5
Root radius: 27 Flange-to-web welds:
 Supplementary web plate Thickness:
 Continuity plates Thickness: 18

End-plate

hp: 540
bp: 220 ep: 55 exs: 50 mx1: 40 p1: 240
tp: 18 w: 110 exi: 50 mx2: 47.3 p2:
 Rib stiffener mx3: 47.3
Thickness: mx4: 40

Bolts

Rows in tension: 2 Bolts per row: 2
Diameter: 24 Tensile stress area: 353

Beam-to-plate welds

Throat thickness
 Leg thickness
Flange
 Full penetration
 Fillet welds 12
Web
 Full penetration
 Fillet welds 8

Notes:

Test J-3.1

		Material properties	
		(MPa)	
Beam		Column	
<input checked="" type="checkbox"/> Nominal grade S355 <input type="checkbox"/> Measured values		<input checked="" type="checkbox"/> Nominal grade S355 <input type="checkbox"/> Measured values	
fy,f: 355 fy,w: 355		fy,f: 355 fy,w: 355	
fu,f: 510 fu,w: 510		fu,f: 510 fu,w: 510	
Young's modulus		Young's modulus	
<input checked="" type="checkbox"/> Nominal Ef: 210000 <input type="checkbox"/> Measured Ew: 210000		<input checked="" type="checkbox"/> Nominal Ef: 210000 <input type="checkbox"/> Measured Ew: 210000	
Bolts		Continuity plate	
<input checked="" type="checkbox"/> Nominal grade 10.9 <input type="checkbox"/> Measured values		<input checked="" type="checkbox"/> Nominal grade S355 <input type="checkbox"/> Measured values	
Yield strength: 900		Yield strength: 355	
Ultimate strength: 1000		Ultimate strength: 510	
Young's modulus		Young's modulus	
<input checked="" type="checkbox"/> Nominal E: 210000 <input type="checkbox"/> Measured		<input checked="" type="checkbox"/> Nominal E: 210000 <input type="checkbox"/> Measured	
End-plate		Supplementary web plate	
<input checked="" type="checkbox"/> Nominal grade S355 <input type="checkbox"/> Measured values		<input type="checkbox"/> Nominal grade [] <input type="checkbox"/> Measured values []	
Yield strength: 355		Yield strength: []	
Ultimate strength: 510		Ultimate strength: []	
Young's modulus		Young's modulus	
<input checked="" type="checkbox"/> Nominal E: 210000 <input type="checkbox"/> Measured		<input type="checkbox"/> Nominal E: [] <input type="checkbox"/> Measured	
Notes:		End-plate rib stiffener	
<input type="checkbox"/> Nominal grade [] <input type="checkbox"/> Measured value []		<input type="checkbox"/> Nominal grade [] <input type="checkbox"/> Measured value []	
Yield strength: []		Yield strength: []	
Ultimate strength: []		Ultimate strength: []	
Young's modulus		Young's modulus	
<input type="checkbox"/> Nominal E: [] <input type="checkbox"/> Measured		<input type="checkbox"/> Nominal E: [] <input type="checkbox"/> Measured	
Test set up and loading protocol			
Type of test:	Monotonic		
Loading protocol:	<input type="checkbox"/> [] <input type="checkbox"/> []		
Data provided:	Displacement transducers DT1, DT2, DT3, DT4		
Type of response curve:	<input type="checkbox"/> Force Evaluated on the column flange <input checked="" type="checkbox"/> Moment <input type="checkbox"/> Displacement Joint rotation <input checked="" type="checkbox"/> Rotation		

Paper

Title:
Experimental behaviour of standardised european end-plate beam-to-column steel joints under arbitrary cycling loading

Authors:
Nogueiro P. da Silva L. S. Bento R. Simoes R.

Source: Proceedings of **Volume:** **Issue:** **Pages:** **Year:** 2006

Test J-3.2

Geometry (mm)

Beam

Shape: IPE 360

Height:	360	Width:	170
Flange thickness:	12.7	Web thickness:	8
Root radius:	18	Flange-to-web welds:	

Column

Shape: HEB 320

Height:	320	Width:	300
Flange thickness:	20.5	Web thickness:	11.5
Root radius:	27	Flange-to-web welds:	
<input type="checkbox"/> Supplementary web plate		Thickness:	
<input checked="" type="checkbox"/> Continuity plates		Thickness:	18

Scheme: Exterior joint

Beam length: 1147

Beam position: 1755

Column length: 3000

Dimensions for the end-plate: $h_p = 540$, $b_p = 220$, $e_p = 55$, $e_{xi} = 50$, $m_{x1} = 40$, $p_1 = 240$, $tp = 18$, $w = 110$, $exs = 50$, $mx2 = 47.3$, $p2 = 0$, $mx3 = 47.3$, $mx4 = 40$.
 Rib stiffener
 Thickness: _____

Notes:

End-plate

hp: 540

bp: 220 ep: 55 exs: 50 mx1: 40 p1: 240

tp: 18 w: 110 exi: 50 mx2: 47.3 p2: 0

Rib stiffener
 Thickness: _____

Bolts

Rows in tension: 2

Bolts per row: 2

Diameter: 24

Tensile stress area: 353

Head washer
 Nut washer

Beam-to-plate welds

Throat thickness
 Leg thickness

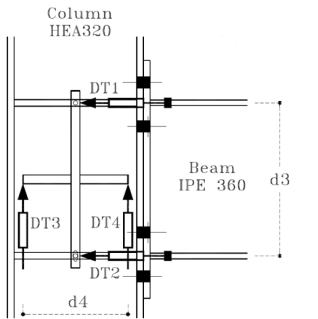
Flange

Full penetration
 Fillet welds 12

Web

Full penetration
 Fillet welds 8

Test J-3.2

		Material properties			
		(MPa)			
Beam		Column		End-plate	
<input checked="" type="checkbox"/> Nominal grade S355 <input type="checkbox"/> Measured values		<input checked="" type="checkbox"/> Nominal grade S355 <input type="checkbox"/> Measured values		<input checked="" type="checkbox"/> Nominal grade [] <input type="checkbox"/> Measured values	
fy,f: 355 fy,w: 355		fy,f: 355 fy,w: 355		Yield strength: []	
fu,f: 510 fu,w: 510		fu,f: 510 fu,w: 510		Ultimate strength: []	
Young's modulus		Young's modulus		Young's modulus	
<input checked="" type="checkbox"/> Nominal Ef: 210000 <input type="checkbox"/> Measured Ew: 210000		<input checked="" type="checkbox"/> Nominal Ef: 210000 <input type="checkbox"/> Measured Ew: 210000		<input checked="" type="checkbox"/> Nominal E: [] <input type="checkbox"/> Measured E: []	
Bolts		Continuity plate		Supplementary web plate	
<input checked="" type="checkbox"/> Nominal grade 10.9 <input type="checkbox"/> Measured values		<input checked="" type="checkbox"/> Nominal grade S355 <input type="checkbox"/> Measured values		<input type="checkbox"/> Nominal grade [] <input type="checkbox"/> Measured values	
Yield strength: 900		Yield strength: 355		Yield strength: []	
Ultimate strength: 1000		Ultimate strength: 510		Ultimate strength: []	
Young's modulus		Young's modulus		Young's modulus	
<input checked="" type="checkbox"/> Nominal E: 210000 <input type="checkbox"/> Measured E: []		<input checked="" type="checkbox"/> Nominal E: 210000 <input type="checkbox"/> Measured E: []		<input type="checkbox"/> Nominal E: [] <input type="checkbox"/> Measured E: []	
Notes:					
<input type="checkbox"/> Nominal grade <input type="checkbox"/> Measured value Yield strength: Ultimate strength: Young's modulus <input type="checkbox"/> Nominal E: [] <input type="checkbox"/> Measured E: []					
Test set up and loading protocol					
Type of test:	Cyclic		Column	HEA320	
Loading protocol:	????				
Data provided:	Displacement transducers DT1, DT2, DT3, DT4				
Type of response curve:	<input type="checkbox"/> Force Evaluated on the column flange <input checked="" type="checkbox"/> Moment <input type="checkbox"/> Displacement Joint rotation <input checked="" type="checkbox"/> Rotation				

Paper

Title:
Experimental behaviour of standardised european end-plate beam-to-column steel joints under arbitrary cycling loading

Authors:
Nogueiro P. da Silva L. S. Bento R. Simoes R.

Source: Proceedings of **Volume:** **Issue:** **Pages:** **Year:** 2006

Test J-3.3

Geometry (mm)

Beam

Shape: IPE 360
Height: 360 Width: 170
Flange thickness: 12.7 Web thickness: 8
Root radius: 18 Flange-to-web welds:

Column

Shape: HEB 320
Height: 320 Width: 300
Flange thickness: 20.5 Web thickness: 11.5
Root radius: 27 Flange-to-web welds:
 Supplementary web plate Thickness:
 Continuity plates Thickness: 18

Scheme: Exterior joint

Beam length: 1147
Beam position: 1755
Column length: 3000

End-plate

hp:	540								
bp:	220	ep:	55	exs:	50	mx1:	40	p1:	240
tp:	18	w:	110	exi:	50	mx2:	47.3	p2:	0
<input type="checkbox"/> Rib stiffener					mx3:	47.3			
Thickness:					mx4:	40			

Bolts

Rows in tension: 2
Bolts per row: 2
Diameter: 24
Tensile stress area: 353

Beam-to-plate welds

Throat thickness
 Leg thickness
Flange
 Full penetration
 Fillet welds 12
Web
 Full penetration
 Fillet welds 8

Notes:

Test J-3.3

		Material properties			
		(MPa)			
Beam		Column		End-plate	
<input checked="" type="checkbox"/> Nominal grade S355 <input type="checkbox"/> Measured values		<input checked="" type="checkbox"/> Nominal grade S355 <input type="checkbox"/> Measured values		<input checked="" type="checkbox"/> Nominal grade S355 <input type="checkbox"/> Measured values	
fy,f: 355 fy,w: 355		fy,f: 355 fy,w: 355		Yield strength: 355	
fu,f: 510 fu,w: 510		fu,f: 510 fu,w: 510		Ultimate strength: 510	
Young's modulus		Young's modulus		Young's modulus	
<input checked="" type="checkbox"/> Nominal Ef: 210000 <input type="checkbox"/> Measured Ew: 210000		<input checked="" type="checkbox"/> Nominal Ef: 210000 <input type="checkbox"/> Measured Ew: 210000		<input checked="" type="checkbox"/> Nominal E: 210000 <input type="checkbox"/> Measured	
Bolts		Continuity plate		Supplementary web plate	
<input checked="" type="checkbox"/> Nominal grade 10.9 <input type="checkbox"/> Measured values		<input checked="" type="checkbox"/> Nominal grade S355 <input type="checkbox"/> Measured values		<input type="checkbox"/> Nominal grade <input type="checkbox"/> Measured values	
Yield strength: 900		Yield strength: 355		Yield strength:	
Ultimate strength: 1000		Ultimate strength: 510		Ultimate strength:	
Young's modulus		Young's modulus		Young's modulus	
<input checked="" type="checkbox"/> Nominal E: 210000 <input type="checkbox"/> Measured		<input checked="" type="checkbox"/> Nominal E: 210000 <input type="checkbox"/> Measured		<input type="checkbox"/> Nominal <input type="checkbox"/> Measured E:	
Notes:					
<input type="checkbox"/> Nominal grade <input type="checkbox"/> Measured value Yield strength: Ultimate strength: Young's modulus <input type="checkbox"/> Nominal <input type="checkbox"/> Measured E:					
Test set up and loading protocol					
Type of test:	Cyclic				
Loading protocol:	???				
Data provided:	Displacement transducers DT1, DT2, DT3, DT4				
Type of response curve:					
<input type="checkbox"/> Force <input checked="" type="checkbox"/> Moment <input type="checkbox"/> Displacement <input checked="" type="checkbox"/> Rotation	Evaluated on the column flange Joint rotation				

Paper

Title:
Experimental and theoretical analysis of the moment–rotation behaviour of stiffened extended end-plate connections

Authors:
Shi Y. Shi G. Wang Y.

Source: Journal of Constructional Steel Research Volume: 63 Issue: 9 Pages: 1279–1293 Year: 2007

Test EPC-1

Geometry (mm)

Beam

Shape: Built-up I-shaped

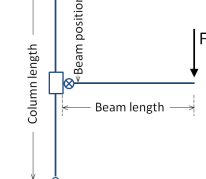
Height:	300	Width:	200
Flange thickness:	12	Web thickness:	8
Root radius:		Flange-to-web welds:	FP

Column

Shape: Built-up I-shaped

Height:	300	Width:	250
Flange thickness:	12	Web thickness:	8
Root radius:		Flange-to-web welds:	FP
<input type="checkbox"/> Supplementary web plate		Thickness:	
<input checked="" type="checkbox"/> Continuity plates		Thickness:	12

Scheme: Exterior joint



End-plate

hp:	500								
bp:	200	ep:	46	exs:	50	mx1:	50	p1:	176
tp:	20	w:	108	exi:	50	mx2:	50	p2:	0
<input checked="" type="checkbox"/> Rib stiffener		Thickness:	10	mx3:	50				
		Thickness:	10	mx4:	50				

Bolts

Rows in tension:	2
Bolts per row:	2
Diameter:	20
Tensile stress area:	245

Beam-to-plate welds

<input type="checkbox"/> Throat thickness
<input checked="" type="checkbox"/> Leg thickness
Flange
<input checked="" type="checkbox"/> Full penetration
<input type="checkbox"/> Fillet welds
Web
<input type="checkbox"/> Full penetration
<input checked="" type="checkbox"/> Fillet welds
8

Notes:
The column flange thickness is equal to the end-plate thickness within the range of 100 mm above and below the extension edge of the end-plate.

Test EPC-1

		Material properties			
		(MPa)			
Beam		Column		End-plate	
<input type="checkbox"/> Nominal grade Q345 <input checked="" type="checkbox"/> Measured values fy,f: 391 fy,w: 391 fu,f: 559 fu,w: 559		<input type="checkbox"/> Nominal grade Q345 <input checked="" type="checkbox"/> Measured values fy,f: 363 fy,w: 391 fu,f: 537 fu,w: 559		<input type="checkbox"/> Nominal grade Q345 <input checked="" type="checkbox"/> Measured values Yield strength: 363 Ultimate strength: 537	
Young's modulus		Young's modulus		Young's modulus	
<input type="checkbox"/> Nominal Ef: 190707 <input checked="" type="checkbox"/> Measured Ew: 190707		<input type="checkbox"/> Nominal Ef: 204228 <input checked="" type="checkbox"/> Measured Ew: 190707		<input type="checkbox"/> Nominal <input checked="" type="checkbox"/> Measured E: 204228	
Bolts		Continuity plate		Supplementary web plate	
<input type="checkbox"/> Nominal grade 10.9 <input checked="" type="checkbox"/> Measured values Yield strength: 995 Ultimate strength: 1160 Young's modulus <input type="checkbox"/> Nominal <input checked="" type="checkbox"/> Measured E: 206000		<input type="checkbox"/> Nominal grade Q345 <input checked="" type="checkbox"/> Measured values Yield strength: 391 Ultimate strength: 559 Young's modulus <input type="checkbox"/> Nominal <input checked="" type="checkbox"/> Measured E: 190707		<input type="checkbox"/> Nominal grade <input type="checkbox"/> Measured values Yield strength: Ultimate strength: Young's modulus <input type="checkbox"/> Nominal <input checked="" type="checkbox"/> Measured E:	
Notes:					
<input type="checkbox"/> Nominal grade Q345 <input checked="" type="checkbox"/> Measured value Yield strength: 391 Ultimate strength: 559 Young's modulus <input type="checkbox"/> Nominal <input checked="" type="checkbox"/> Measured E: 190707					
Test set up and loading protocol					
Type of test:	Monotonic				
Loading protocol:					
Data provided:	Transducers No.13-14 and No.4				
Type of response curve:					
<input type="checkbox"/> Force <input checked="" type="checkbox"/> Moment	Evaluated on the column flange				
<input type="checkbox"/> Displacement <input checked="" type="checkbox"/> Rotation	Panel zone shearing rotation, relative deformation between the column flange and the end-plate				

Paper

Title:
Experimental and theoretical analysis of the moment-rotation behaviour of stiffened extended end-plate connections

Authors:
Shi Y. Shi G. Wang Y.

Source: Journal of Constructional Steel Research Volume: 63 Issue: 9 Pages: 1279–1293 Year: 2007

Test EPC-2

Geometry (mm)

Beam

Scheme: Exterior joint

Beam length: 1175

Beam position: 1000

Column length: 2000

Column length

Beam position

Beam length

End-plate

hp: 500

bp: 200 ep: 46 exs: 50 mx1: 50 p1: 176

tp: 25 w: 108 exi: 50 mx2: 50 p2: 0

Rib stiffener

Thickness: 10

mx3: 50

mx4: 50

Geometry (mm)

Beam

Shape: Built-up I-shaped

Height: 300 Width: 200

Flange thickness: 12 Web thickness: 8

Root radius: Flange-to-web welds: FP

Column

Shape: Built-up I-shaped

Height: 300 Width: 250

Flange thickness: 12 Web thickness: 8

Root radius: Flange-to-web welds: FP

Supplementary web plate

Continuity plates

Thickness: Thickness: 12

Bolts

Rows in tension: 2

Bolts per row: 2

Diameter: 20

Tensile stress area: 245

Head washer

Nut washer

Beam-to-plate welds

Throat thickness

Leg thickness

Flange

Full penetration

Fillet welds

Web

Full penetration

Fillet welds 8

Notes:

The column flange thickness is equal to the end-plate thickness within the range of 100 mm above and below the extension edge of the end-plate.

Test EPC-2		Material properties											
		(MPa)											
Beam <input type="checkbox"/> Nominal grade Q345 <input checked="" type="checkbox"/> Measured values fy,f: 391 fy,w: 391 fu,f: 559 fu,w: 559 Young's modulus <input type="checkbox"/> Nominal Ef: 190707 <input checked="" type="checkbox"/> Measured Ew: 190707		Column <input type="checkbox"/> Nominal grade Q345 <input checked="" type="checkbox"/> Measured values fy,f: 363 fy,w: 391 fu,f: 537 fu,w: 559 Young's modulus <input type="checkbox"/> Nominal Ef: 204228 <input checked="" type="checkbox"/> Measured Ew: 190707		End-plate <input type="checkbox"/> Nominal grade Q345 <input checked="" type="checkbox"/> Measured values Yield strength: 363 Ultimate strength: Young's modulus <input type="checkbox"/> Nominal E: 204228 <input checked="" type="checkbox"/> Measured E: 190707									
Bolts <input type="checkbox"/> Nominal grade 10.9 <input checked="" type="checkbox"/> Measured values Yield strength: 995 Ultimate strength: 1160 Young's modulus <input type="checkbox"/> Nominal <input checked="" type="checkbox"/> Measured E: 206000		Continuity plate <input type="checkbox"/> Nominal grade Q345 <input checked="" type="checkbox"/> Measured values Yield strength: 391 Ultimate strength: 559 Young's modulus <input type="checkbox"/> Nominal <input checked="" type="checkbox"/> Measured E: 190707		Supplementary web plate <input type="checkbox"/> Nominal grade <input type="checkbox"/> Measured values Yield strength: Ultimate strength: Young's modulus <input type="checkbox"/> Nominal <input type="checkbox"/> Measured E:									
<p>Notes:</p> <div style="border: 1px solid black; height: 100px; width: 100%;"></div>													
Test set up and loading protocol <table border="1"> <tr> <td>Type of test:</td> <td>Monotonic</td> </tr> <tr> <td>Loading protocol:</td> <td></td> </tr> <tr> <td>Data provided:</td> <td>Transducers No.13-14 and No.4</td> </tr> <tr> <td>Type of response curve:</td> <td> <input type="checkbox"/> Force <input checked="" type="checkbox"/> Moment <input type="checkbox"/> Displacement <input checked="" type="checkbox"/> Rotation Evaluated on the column flange Panel zone shearing rotation, relative deformation between the column flange and the end-plate </td> </tr> </table>						Type of test:	Monotonic	Loading protocol:		Data provided:	Transducers No.13-14 and No.4	Type of response curve:	<input type="checkbox"/> Force <input checked="" type="checkbox"/> Moment <input type="checkbox"/> Displacement <input checked="" type="checkbox"/> Rotation Evaluated on the column flange Panel zone shearing rotation, relative deformation between the column flange and the end-plate
Type of test:	Monotonic												
Loading protocol:													
Data provided:	Transducers No.13-14 and No.4												
Type of response curve:	<input type="checkbox"/> Force <input checked="" type="checkbox"/> Moment <input type="checkbox"/> Displacement <input checked="" type="checkbox"/> Rotation Evaluated on the column flange Panel zone shearing rotation, relative deformation between the column flange and the end-plate												

Paper
Title:

Experimental and theoretical analysis of the moment–rotation behaviour of stiffened extended end-plate connections

Authors:

Shi Y. Shi G. Wang Y.

Source:

Journal of Constructional Steel Research 63 9 1279–1293 2007

Test EPC-3

Geometry (mm)			
Beam			
Shape:	Built-up I-shaped		
Height:	300	Width:	200
Flange thickness:	12	Web thickness:	8
Root radius:		Flange-to-web welds:	FP
Column			
Shape:	Built-up I-shaped		
Height:	300	Width:	250
Flange thickness:	12	Web thickness:	8
Root radius:		Flange-to-web welds:	FP
<input type="checkbox"/> Supplementary web plate		Thickness:	
<input checked="" type="checkbox"/> Continuity plates		Thickness:	12
End-plate		Bolts	
hp: 500	Rows in tension: 2		
bp: 200	Bolts per row: 2		
ep: 46	Diameter: 24		
exs: 50	Tensile stress area: 353		
mx1: 50			
p1: 176	Beam-to-plate welds		
tp: 20	<input type="checkbox"/> Throat thickness		
w: 108	<input checked="" type="checkbox"/> Leg thickness		
exi: 50	Flange		
mx2: 50	<input checked="" type="checkbox"/> Full penetration		
p2: 0	<input type="checkbox"/> Fillet welds		
<input checked="" type="checkbox"/> Rib stiffener	Web		
Thickness: 10	<input type="checkbox"/> Head washer		
mx3: 50	<input checked="" type="checkbox"/> Nut washer		
mx4: 50	<input checked="" type="checkbox"/> Fillet welds 8		
Notes:			
The column flange thickness is equal to the end-plate thickness within the range of 100 mm above and below the extension edge of the end-plate.			

Test EPC-3

		Material properties			
		(MPa)			
Beam		Column		End-plate	
<input type="checkbox"/> Nominal grade Q345 <input checked="" type="checkbox"/> Measured values fy,f: 391 fy,w: 391 fu,f: 559 fu,w: 559		<input type="checkbox"/> Nominal grade Q345 <input checked="" type="checkbox"/> Measured values fy,f: 363 fy,w: 391 fu,f: 537 fu,w: 559		<input type="checkbox"/> Nominal grade Q345 <input checked="" type="checkbox"/> Measured values Yield strength: 363 Ultimate strength: 537	
Young's modulus		Young's modulus		Young's modulus	
<input type="checkbox"/> Nominal Ef: 190707 <input checked="" type="checkbox"/> Measured Ew: 190707		<input type="checkbox"/> Nominal Ef: 204228 <input checked="" type="checkbox"/> Measured Ew: 190707		<input type="checkbox"/> Nominal <input checked="" type="checkbox"/> Measured E: 204228	
Bolts		Continuity plate		Supplementary web plate	
<input type="checkbox"/> Nominal grade 10.9 <input checked="" type="checkbox"/> Measured values Yield strength: 975 Ultimate strength: 1188 Young's modulus <input type="checkbox"/> Nominal <input checked="" type="checkbox"/> Measured E: 206000		<input type="checkbox"/> Nominal grade Q345 <input checked="" type="checkbox"/> Measured values Yield strength: 391 Ultimate strength: 559 Young's modulus <input type="checkbox"/> Nominal <input checked="" type="checkbox"/> Measured E: 190707		<input type="checkbox"/> Nominal grade <input type="checkbox"/> Measured values Yield strength: Ultimate strength: Young's modulus <input type="checkbox"/> Nominal <input checked="" type="checkbox"/> Measured E:	
Notes:					
<input type="checkbox"/> Nominal grade Q345 <input checked="" type="checkbox"/> Measured value Yield strength: 391 Ultimate strength: 559 Young's modulus <input type="checkbox"/> Nominal <input checked="" type="checkbox"/> Measured E: 190707					
Test set up and loading protocol					
Type of test:	Monotonic				
Loading protocol:					
Data provided:	Transducers No.13-14 and No.4				
Type of response curve:					
<input type="checkbox"/> Force <input checked="" type="checkbox"/> Moment <input type="checkbox"/> Displacement <input checked="" type="checkbox"/> Rotation	Evaluated on the column flange Panel zone shearing rotation, relative deformation between the column flange and the end-plate				

Paper

Title:
Experimental and theoretical analysis of the moment–rotation behaviour of stiffened extended end-plate connections

Authors:
Shi Y. Shi G. Wang Y.

Source: Journal of Constructional Steel Research Volume: 63 Issue: 9 Pages: 1279–1293 Year: 2007

Test EPC-4

Geometry (mm)

Beam

Shape: Built-up I-shaped

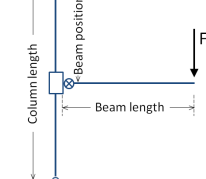
Height:	300	Width:	200
Flange thickness:	12	Web thickness:	8
Root radius:		Flange-to-web welds:	FP

Column

Shape: Built-up I-shaped

Height:	300	Width:	250
Flange thickness:	12	Web thickness:	8
Root radius:		Flange-to-web welds:	FP
<input type="checkbox"/> Supplementary web plate		Thickness:	
<input checked="" type="checkbox"/> Continuity plates		Thickness:	12

Scheme: Exterior joint



End-plate

hp:	500								
bp:	200	ep:	46	exs:	50	mx1:	50	p1:	176
tp:	25	w:	108	exi:	50	mx2:	50	p2:	0
<input checked="" type="checkbox"/> Rib stiffener									
Thickness:	10	mx3:	50						
mx4:	50								

Bolts

Rows in tension:	2
Bolts per row:	2
Diameter:	24
Tensile stress area:	353

Beam-to-plate welds

- Throat thickness
- Leg thickness
- Flange**
- Full penetration
- Fillet welds
- Web**
- Full penetration
- Fillet welds

Notes:

The column flange thickness is equal to the end-plate thickness within the range of 100 mm above and below the extension edge of the end-plate.

Test EPC-4

		Material properties			
		(MPa)			
Beam		Column		End-plate	
<input type="checkbox"/> Nominal grade Q345 <input checked="" type="checkbox"/> Measured values fy,f: 391 fy,w: 391 fu,f: 559 fu,w: 559		<input type="checkbox"/> Nominal grade Q345 <input checked="" type="checkbox"/> Measured values fy,f: 363 fy,w: 391 fu,f: 537 fu,w: 559		<input type="checkbox"/> Nominal grade Q345 <input checked="" type="checkbox"/> Measured values Yield strength: 363 Ultimate strength: 537	
Young's modulus		Young's modulus		Young's modulus	
<input type="checkbox"/> Nominal Ef: 190707 <input checked="" type="checkbox"/> Measured Ew: 190707		<input type="checkbox"/> Nominal Ef: 204228 <input checked="" type="checkbox"/> Measured Ew: 190707		<input type="checkbox"/> Nominal <input checked="" type="checkbox"/> Measured E: 190707	
Bolts		Continuity plate		Supplementary web plate	
<input type="checkbox"/> Nominal grade 10.9 <input checked="" type="checkbox"/> Measured values Yield strength: 975 Ultimate strength: 1188 Young's modulus <input type="checkbox"/> Nominal <input checked="" type="checkbox"/> Measured E: 206000		<input type="checkbox"/> Nominal grade Q345 <input checked="" type="checkbox"/> Measured values Yield strength: 391 Ultimate strength: 559 Young's modulus <input type="checkbox"/> Nominal <input checked="" type="checkbox"/> Measured E: 190707		<input type="checkbox"/> Nominal grade <input type="checkbox"/> Measured values Yield strength: Ultimate strength: Young's modulus <input type="checkbox"/> Nominal <input checked="" type="checkbox"/> Measured E:	
Notes:					
<input type="checkbox"/> Nominal grade Q345 <input checked="" type="checkbox"/> Measured value Yield strength: 391 Ultimate strength: 559 Young's modulus <input type="checkbox"/> Nominal <input checked="" type="checkbox"/> Measured E: 190707					
Test set up and loading protocol					
Type of test:	Monotonic				
Loading protocol:	<input type="checkbox"/> <input type="checkbox"/>				
Data provided:	Transducers No.13-14 and No.4				
Type of response curve:					
<input type="checkbox"/> Force <input checked="" type="checkbox"/> Moment <input type="checkbox"/> Displacement <input checked="" type="checkbox"/> Rotation	Evaluated on the column flange Panel zone shearing rotation, relative deformation between the column flange and the end-plate				

Paper

Title:
Experimental and theoretical analysis of the moment–rotation behaviour of stiffened extended end-plate connections

Authors:
Shi Y. Shi G. Wang Y.

Source: Journal of Constructional Steel Research Volume: 63 Issue: 9 Pages: 1279–1293 Year: 2007

Test EPC-5

Geometry (mm)

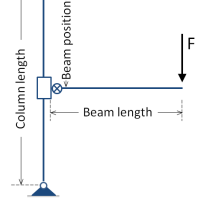
Beam

Scheme: Exterior joint

Beam length: 1184

Beam position: 1000

Column length: 2000



Column

Shape: Built-up I-shaped

Height: 300

Flange thickness: 12

Root radius: []

Web thickness: 8

Flange-to-web welds: FP

End-plate

hp: 500

bp: 200

tp: 16

ep: 46

w: 108

exs: 50

exi: 50

mx1: 50

mx2: 50

p1: 176

p2: 0

Thickness: 10

Rib stiffener

Thickness: 10

mx3: 50

mx4: 50

Bolts

Rows in tension: 2

Bolts per row: 2

Diameter: 20

Tensile stress area: 245

Beam-to-plate welds

Throat thickness

Leg thickness

Flange

Full penetration

Fillet welds []

Web

Full penetration

Fillet welds 8

Geometry (mm)

Beam

Shape: Built-up I-shaped

Height: 300

Flange thickness: 12

Root radius: []

Width: 200

Web thickness: 8

Flange-to-web welds: FP

Column

Shape: Built-up I-shaped

Height: 300

Flange thickness: 12

Root radius: []

Width: 250

Web thickness: 8

Flange-to-web welds: FP

Supplementary web plate

Continuity plates

Thickness: []

Thickness: 12

Notes:
The column flange thickness is equal to the end-plate thickness within the range of 100 mm above and below the extension edge of the end-plate.

Test EPC-5

		Material properties			
		(MPa)			
Beam		Column		End-plate	
<input type="checkbox"/> Nominal grade Q345 <input checked="" type="checkbox"/> Measured values fy,f: 391 fy,w: 391 fu,f: 559 fu,w: 559		<input type="checkbox"/> Nominal grade Q345 <input checked="" type="checkbox"/> Measured values fy,f: 391 fy,w: 391 fu,f: 559 fu,w: 559		<input type="checkbox"/> Nominal grade Q345 <input checked="" type="checkbox"/> Measured values Yield strength: 391 Ultimate strength: 559	
Young's modulus		Young's modulus		Young's modulus	
<input type="checkbox"/> Nominal Ef: 190707 <input checked="" type="checkbox"/> Measured Ew: 190707		<input type="checkbox"/> Nominal Ef: 190707 <input checked="" type="checkbox"/> Measured Ew: 190707		<input type="checkbox"/> Nominal E: <input checked="" type="checkbox"/> Measured E: 190707	
Bolts		Continuity plate		Supplementary web plate	
<input type="checkbox"/> Nominal grade 10.9 <input checked="" type="checkbox"/> Measured values Yield strength: 995 Ultimate strength: 1160 Young's modulus <input type="checkbox"/> Nominal <input checked="" type="checkbox"/> Measured E: 206000		<input type="checkbox"/> Nominal grade Q345 <input checked="" type="checkbox"/> Measured values Yield strength: 391 Ultimate strength: 559 Young's modulus <input type="checkbox"/> Nominal <input checked="" type="checkbox"/> Measured E: 190707		<input type="checkbox"/> Nominal grade <input type="checkbox"/> Measured values Yield strength: Ultimate strength: Young's modulus <input type="checkbox"/> Nominal <input checked="" type="checkbox"/> Measured E:	
Notes:					
<input type="checkbox"/> Nominal grade Q345 <input checked="" type="checkbox"/> Measured value Yield strength: 391 Ultimate strength: 559 Young's modulus <input type="checkbox"/> Nominal <input checked="" type="checkbox"/> Measured E: 190707					
Test set up and loading protocol					
Type of test:	Monotonic				
Loading protocol:	<input type="checkbox"/> <input type="checkbox"/>				
Data provided:	Transducers No.13-14 and No.4				
Type of response curve:					
<input type="checkbox"/> Force <input checked="" type="checkbox"/> Moment <input type="checkbox"/> Displacement <input checked="" type="checkbox"/> Rotation	Evaluated on the column flange Panel zone shearing rotation, relative deformation between the column flange and the end-plate				
<img alt="Diagram of the test setup showing a beam connected to a column through an end-plate. A hydraulic jack applies a load to the beam, and a pressure transducer is connected to it. The column has stiffeners and a thicker flange. The end-plate is supported by a backing plate. Dimensions shown are 1000 mm width, 130 mm height, and various thicknesses labeled 2, 5, 6, 8, 10, 11, 12, 13, 14, 15, 16, 17, 18, 19, 20, 21, 22, 23, 24, 25, 26, 27, 28, 29, 30, 31, 32, 33, 34, 35, 36, 37, 38, 39, 40, 41, 42, 43, 44, 45, 46, 47, 48, 49, 50, 51, 52, 53, 54, 55, 56, 57, 58, 59, 60, 61, 62, 63, 64, 65, 66, 67, 68, 69, 70, 71, 72, 73, 74, 75, 76, 77, 78, 79, 80, 81, 82, 83, 84, 85, 86, 87, 88, 89, 90, 91, 92, 93, 94, 95, 96, 97, 98, 99, 100, 101, 102, 103, 104, 105, 106, 107, 108, 109, 110, 111, 112, 113, 114, 115, 116, 117, 118, 119, 120, 121, 122, 123, 124, 125, 126, 127, 128, 129, 130, 131, 132, 133, 134, 135, 136, 137, 138, 139, 140, 141, 142, 143, 144, 145, 146, 147, 148, 149, 150, 151, 152, 153, 154, 155, 156, 157, 158, 159, 160, 161, 162, 163, 164, 165, 166, 167, 168, 169, 170, 171, 172, 173, 174, 175, 176, 177, 178, 179, 180, 181, 182, 183, 184, 185, 186, 187, 188, 189, 190, 191, 192, 193, 194, 195, 196, 197, 198, 199, 200, 201, 202, 203, 204, 205, 206, 207, 208, 209, 210, 211, 212, 213, 214, 215, 216, 217, 218, 219, 220, 221, 222, 223, 224, 225, 226, 227, 228, 229, 230, 231, 232, 233, 234, 235, 236, 237, 238, 239, 240, 241, 242, 243, 244, 245, 246, 247, 248, 249, 250, 251, 252, 253, 254, 255, 256, 257, 258, 259, 260, 261, 262, 263, 264, 265, 266, 267, 268, 269, 270, 271, 272, 273, 274, 275, 276, 277, 278, 279, 280, 281, 282, 283, 284, 285, 286, 287, 288, 289, 290, 291, 292, 293, 294, 295, 296, 297, 298, 299, 300, 301, 302, 303, 304, 305, 306, 307, 308, 309, 310, 311, 312, 313, 314, 315, 316, 317, 318, 319, 320, 321, 322, 323, 324, 325, 326, 327, 328, 329, 330, 331, 332, 333, 334, 335, 336, 337, 338, 339, 340, 341, 342, 343, 344, 345, 346, 347, 348, 349, 350, 351, 352, 353, 354, 355, 356, 357, 358, 359, 360, 361, 362, 363, 364, 365, 366, 367, 368, 369, 370, 371, 372, 373, 374, 375, 376, 377, 378, 379, 380, 381, 382, 383, 384, 385, 386, 387, 388, 389, 390, 391, 392, 393, 394, 395, 396, 397, 398, 399, 400, 401, 402, 403, 404, 405, 406, 407, 408, 409, 410, 411, 412, 413, 414, 415, 416, 417, 418, 419, 420, 421, 422, 423, 424, 425, 426, 427, 428, 429, 430, 431, 432, 433, 434, 435, 436, 437, 438, 439, 440, 441, 442, 443, 444, 445, 446, 447, 448, 449, 450, 451, 452, 453, 454, 455, 456, 457, 458, 459, 460, 461, 462, 463, 464, 465, 466, 467, 468, 469, 470, 471, 472, 473, 474, 475, 476, 477, 478, 479, 480, 481, 482, 483, 484, 485, 486, 487, 488, 489, 490, 491, 492, 493, 494, 495, 496, 497, 498, 499, 500, 501, 502, 503, 504, 505, 506, 507, 508, 509, 510, 511, 512, 513, 514, 515, 516, 517, 518, 519, 520, 521, 522, 523, 524, 525, 526, 527, 528, 529, 530, 531, 532, 533, 534, 535, 536, 537, 538, 539, 540, 541, 542, 543, 544, 545, 546, 547, 548, 549, 550, 551, 552, 553, 554, 555, 556, 557, 558, 559, 560, 561, 562, 563, 564, 565, 566, 567, 568, 569, 570, 571, 572, 573, 574, 575, 576, 577, 578, 579, 580, 581, 582, 583, 584, 585, 586, 587, 588, 589, 5810, 5811, 5812, 5813, 5814, 5815, 5816, 5817, 5818, 5819, 5820, 5821, 5822, 5823, 5824, 5825, 5826, 5827, 5828, 5829, 5830, 5831, 5832, 5833, 5834, 5835, 5836, 5837, 5838, 5839, 58310, 58311, 58312, 58313, 58314, 58315, 58316, 58317, 58318, 58319, 58320, 58321, 58322, 58323, 58324, 58325, 58326, 58327, 58328, 58329, 58330, 58331, 58332, 58333, 58334, 58335, 58336, 58337, 58338, 58339, 583310, 583311, 583312, 583313, 583314, 583315, 583316, 583317, 583318, 583319, 583320, 583321, 583322, 583323, 583324, 583325, 583326, 583327, 583328, 583329, 5833210, 5833211, 5833212, 5833213, 5833214, 5833215, 5833216, 5833217, 5833218, 5833219, 5833220, 5833221, 5833222, 5833223, 5833224, 5833225, 5833226, 5833227, 5833228, 5833229, 58332210, 58332211, 58332212, 58332213, 58332214, 58332215, 58332216, 58332217, 58332218, 58332219, 58332220, 58332221, 58332222, 58332223, 58332224, 58332225, 58332226, 58332227, 58332228, 58332229, 583322210, 583322211, 583322212, 583322213, 583322214, 583322215, 583322216, 583322217, 583322218, 583322219, 583322220, 583322221, 583322222, 583322223, 583322224, 583322225, 583322226, 583322227, 583322228, 583322229, 5833222210, 5833222211, 5833222212, 5833222213, 5833222214, 5833222215, 5833222216, 5833222217, 5833222218, 5833222219, 5833222220, 5833222221, 5833222222, 5833222223, 5833222224, 5833222225, 5833222226, 5833222227, 5833222228, 5833222229, 58332222210, 58332222211, 58332222212, 58332222213, 58332222214, 58332222215, 58332222216, 58332222217, 58332222218, 58332222219, 58332222220, 58332222221, 58332222222, 58332222223, 58332222224, 58332222225, 58332222226, 58332222227, 58332222228, 58332222229, 583322222210, 583322222211, 583322222212, 583322222213, 583322222214, 583322222215, 583322222216, 583322222217, 583322222218, 583322222219, 583322222220, 583322222221, 583322222222, 583322222223, 583322222224, 583322222225, 583322222226, 583322222227, 583322222228, 583322222229, 5833222222210, 5833222222211, 5833222222212, 5833222222213, 5833222222214, 5833222222215, 5833222222216, 5833222222217, 5833222222218, 5833222222219, 5833222222220, 5833222222221, 5833222222222, 5833222222223, 5833222222224, 5833222222225, 5833222222226, 5833222222227, 5833222222228, 5833222222229, 58332222222210, 58332222222211, 58332222222212, 58332222222213, 58332222222214, 58332222222215, 58332222222216, 58332222222217, 58332222222218, 58332222222219, 58332222222220, 58332222222221, 58332222222222, 58332222222223, 58332222222224, 58332222222225, 58332222222226, 58332222222227, 58332222222228, 58332222222229, 583322222222210, 583322222222211, 583322222222212, 583322222222213, 583322222222214, 583322222222215, 583322222222216, 583322222222217, 583322222222218, 583322222222219, 583322222222220, 583322222222221, 583322222222222, 583322222222223, 583322222222224, 583322222222225, 583322222222226, 583322222222227, 583322222222228, 583322222222229, 5833222222222210, 5833222222222211, 5833222222222212, 5833222222222213, 5833222222222214, 5833222222222215, 5833222222222216, 5833222222222217, 5833222222222218, 5833222222222219, 5833222222222220, 5833222222222221, 5833222222222222, 5833222222222223, 5833222222222224, 5833222222222225, 5833222222222226, 5833222222222227, 5833222222222228, 5833222222222229, 58332222222222210, 58332222222222211, 58332222222222212, 58332222222222213, 58332222222222214, 58332222222222215, 58332222222222216, 58332222222222217, 58332222222222218, 58332222222222219, 58332222222222220, 58332222222222221, 58332222222222222, 58332222222222223, 58332222222222224, 58332222222222225, 58332222222222226, 58332222222222227, 58332222222222228, 58332222222222229, 583322222222222210, 583322222222222211, 583322222222222212, 583322222222222213, 583322222222222214, 583322222222222215, 583322222222222216, 583322222222222217, 583322222222222218, 583322222222222219, 583322222222222220, 583322222222222221, 583322222222222222, 583322222222222223, 583322222222222224, 583322222222222225, 583322222222222226, 583322222222222227, 583322222222222228, 583322222222222229, 5833222222222222210, 5833222222222222211, 5833222222222222212, 5833222222222222213, 5833222222222222214, 5833222222222222215, 5833222222222222216, 5833222222222222217, 5833222222222222218, 5833222222222222219, 5833222222222222220, 5833222222222222221, 5833222222222222222, 5833222222222222223, 5833222222222222224, 5833222222222222225, 5833222222222222226, 5833222222222222227, 5833222222222222228, 5833222222222222229, 58332222222222222210, 58332222222222222211, 58332222222222222212, 58332222222222222213, 58332222222222222214, 58332222222222222215, 58332222222222222216, 58332222222222222217, 58332222222222222218, 58332222222222222219, 58332222222222222220, 58332222222222222221, 58332222222222222222, 58332222222222222223, 58332222222222222224, 58332222222222222225, 58332222222222222226, 58332222222222222227, 58332222222222222228, 58332222222222222229, 583322222222222222210, 583322222222222222211, 583322222222222222212, 583322222222222222213, 583322222222222222214, 583322222222222222215, 583322222222222222216, 583322222222222222217, 583322222222222222218, 583322222222222222219, 583322222222222222220, 583322222222222222221, 583322222222222222222, 583322222222222222223, 583322222222222222224, 583322222222222222225, 583322222222222222226, 583322222222222222227, 583322222222222222228, 583322222222222222229, 5833222222222222222210, 5833222222222222222211, 5833222222222222222212, 5833222222222222222213, 5833222222222222222214, 5833222222222222222215, 5833222222222222222216, 5833222222222222222217, 5833222222222222222218, 5833222222222222222219, 5833222222222222222220, 5833222222222222222221, 5833222222222222222222, 5833222222222222222223, 5833222222222222222224, 5833222222222222222225, 5833222222222222222226, 5833222222222222222227, 5833222222222222222228, 5833222222222222222229, 58332222222222222222210, 58332222222222222222211, 58332222222222222222212, 58332222222222222222213, 58332222222222222222214, 58332222222222222222215, 58332222222222222222216, 58332222222222222222217, 58332222222222222222218, 58332222222222222222219, 58332222222222222222220, 58332222222222222222221, 58332222222222222222222, 58332222222222222222223, 58332222222222222222224, 58332222222222222222225, 58332222222222222222226, 58332222222222222222227, 58332222222222222222228, 58332222222222222222229, 583322222222222222222210, 583322222222222222222211, 583322222222222222222212, 583322222222222222222213, 583322222222222222222214, 583322222222222222222215, 583322222222222222222216, 583322222222222222222217, 583322222222222222222218, 583322222222222222222219, 583322222222222222222220, 583322222222222222222221, 583322222222222222222222, 583322222222222222222223, 583322222222222222222224, 583322222222222222222225, 583322222222222222222226, 583322222222222222222227, 583322222222222222222228, 583322222222222222222229, 5833222222222222222222210, 5833222222222222222222211, 5833222222222222222222212, 5833222222222222222222213, 5833222222222222222222214, 5833222222222					

Paper

Title: Behaviour of end-plate moment connections under earthquake loading

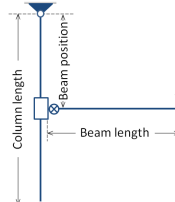
Authors: Shi G. Shi Y. Wang Y.

Source: Engineering Structures **Volume:** 29 **Issue:** 5 **Pages:** 703-716 **Year:** 2007

Test JD2

Scheme: Exterior joint

Beam length: 1180
Beam position: 1000
Column length: 2000



Geometry (mm)

Beam	
Height:	300
Flange thickness:	12
Root radius:	
Web thickness:	8
Flange-to-web welds:	FP

Column	
Height:	300
Flange thickness:	12
Root radius:	
Width:	250
Web thickness:	8
Flange-to-web welds:	FP
<input type="checkbox"/> Supplementary web plate	
<input checked="" type="checkbox"/> Continuity plates	
Thickness:	
Thickness:	12

End-plate

hp:	500								
bp:	200	ep:	46	exs:	50	mx1:	50	p1:	176
tp:	20	w:	108	exi:	50	mx2:	50	p2:	0
mx3: 50									
Thickness: 10									
mx4: 50									

Bolts

Rows in tension:	2
Bolts per row:	2
Diameter:	20
Tensile stress area:	245

Beam-to-plate welds

<input type="checkbox"/> Throat thickness	
<input checked="" type="checkbox"/> Leg thickness	
Flange	
<input checked="" type="checkbox"/> Full penetration	
<input type="checkbox"/> Fillet welds	
Web	
<input type="checkbox"/> Full penetration	
<input checked="" type="checkbox"/> Fillet welds	8

Notes:

The column flange thickness is equal to the end-plate thickness within the range of 100 mm above and below the extension edge of the end-plate.

Test JD2

		Material properties (MPa)
Beam		
<input type="checkbox"/> Nominal grade	Q345	
<input checked="" type="checkbox"/> Measured values		
fy,f: 409.0	fy,w: 409.0	
fu,f: 536.6	fu,w: 536.6	
Young's modulus		
<input type="checkbox"/> Nominal	Ef: 195452	
<input checked="" type="checkbox"/> Measured	Ew: 195452	
Column		
<input type="checkbox"/> Nominal grade	Q345	
<input checked="" type="checkbox"/> Measured values		
fy,f: 372.6	fy,w: 409.0	
fu,f: 537.0	fu,w: 536.6	
Young's modulus		
<input type="checkbox"/> Nominal	Ef: 188671	
<input checked="" type="checkbox"/> Measured	Ew: 195452	
End-plate		
<input type="checkbox"/> Nominal grade	Q345	
<input checked="" type="checkbox"/> Measured values		
Yield strength:	372.6	
Ultimate strength:	537.0	
Young's modulus		
<input type="checkbox"/> Nominal	E: 188671	
<input checked="" type="checkbox"/> Measured	E: 188671	
Bolts		
<input type="checkbox"/> Nominal grade	10.9	
<input checked="" type="checkbox"/> Measured values		
Yield strength:	995	
Ultimate strength:	1160	
Young's modulus		
<input type="checkbox"/> Nominal	E: 206000	
<input checked="" type="checkbox"/> Measured	E: 195452	
Continuity plate		
<input type="checkbox"/> Nominal grade	Q345	
<input checked="" type="checkbox"/> Measured values		
Yield strength:	409.0	
Ultimate strength:	536.6	
Young's modulus		
<input type="checkbox"/> Nominal	E: 195452	
<input checked="" type="checkbox"/> Measured	E: 195452	
Supplementary web plate		
<input type="checkbox"/> Nominal grade		
<input type="checkbox"/> Measured values		
Yield strength:		
Ultimate strength:		
Young's modulus		
<input type="checkbox"/> Nominal		
<input type="checkbox"/> Measured		
End-plate rib stiffener		
<input type="checkbox"/> Nominal grade	Q345	
<input checked="" type="checkbox"/> Measured value		
Yield strength:	409.0	
Ultimate strength:	536.6	
Young's modulus		
<input type="checkbox"/> Nominal		
<input checked="" type="checkbox"/> Measured	E: 195452	
Notes:		
<p> </p> <p> </p>		
Test set up and loading protocol		
Type of test:	Monotonic	
Loading protocol:		
Data provided:	Trasducers No.13,14 and No.4,8	
Type of response curve:		
<input type="checkbox"/> Force	Evaluated on the column flange	
<input checked="" type="checkbox"/> Moment		
<input type="checkbox"/> Displacement	Panel zone shearing rotation, relative deformation between the column flange and the end-plate	
<input checked="" type="checkbox"/> Rotation		

Paper

Title: Behaviour of end-plate moment connections under earthquake loading

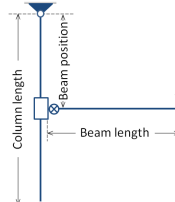
Authors: Shi G. Shi Y. Wang Y.

Source: Engineering Structures **Volume:** 29 **Issue:** 5 **Pages:** 703-716 **Year:** 2007

Test JD3

Scheme: Exterior joint

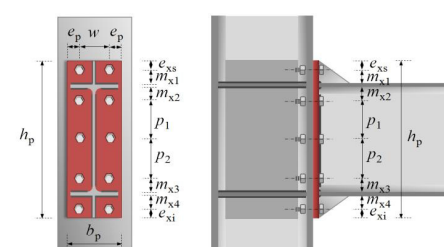
Beam length: 1180
Beam position: 1000
Column length: 2000



Geometry (mm)

Beam	
Height:	300
Flange thickness:	12
Root radius:	FP
Web thickness:	8
Flange-to-web welds:	FP

Column	
Height:	300
Flange thickness:	12
Root radius:	FP
Width:	250
Web thickness:	8
Flange-to-web welds:	FP
Thickness:	12



End-plate

hp: 500
bp: 200 ep: 46 exs: 50 mx1: 50 p1: 176
tp: 20 w: 108 exi: 50 mx2: 50 p2: 0
 Rib stiffener
Thickness: mx3: 50
mx4: 50

Bolts

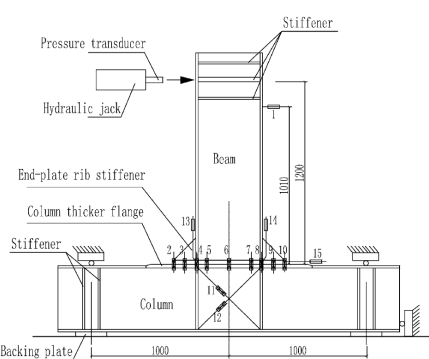
Rows in tension: 2
Bolts per row: 2
Diameter: 20
Tensile stress area: 245

Beam-to-plate welds

Throat thickness
 Leg thickness
Flange
 Full penetration
 Fillet welds
Web
 Full penetration
 Nut washer

Notes:
The column flange thickness is equal to the end-plate thickness within the range of 100 mm above and below the extension edge of the end-plate.

Test JD3

		Material properties			
		(MPa)			
Beam		Column		End-plate	
<input type="checkbox"/> Nominal grade Q345 <input checked="" type="checkbox"/> Measured values fy,f: 409.0 fy,w: 409.0 fu,f: 536.6 fu,w: 536.6		<input type="checkbox"/> Nominal grade Q345 <input checked="" type="checkbox"/> Measured values fy,f: 372.6 fy,w: 409.0 fu,f: 537.0 fu,w: 436.6		<input type="checkbox"/> Nominal grade Q345 <input checked="" type="checkbox"/> Measured values Yield strength: 372.6 Ultimate strength: 537.0 Young's modulus <input type="checkbox"/> Nominal Ef: 188671 <input checked="" type="checkbox"/> Measured Ew: 195452	
Bolts <input type="checkbox"/> Nominal grade 10.9 <input checked="" type="checkbox"/> Measured values Yield strength: 995 Ultimate strength: 1160 Young's modulus <input type="checkbox"/> Nominal <input checked="" type="checkbox"/> Measured E: 206000		Continuity plate <input type="checkbox"/> Nominal grade Q345 <input checked="" type="checkbox"/> Measured values Yield strength: 409.0 Ultimate strength: 536.6 Young's modulus <input type="checkbox"/> Nominal <input checked="" type="checkbox"/> Measured E: 195452		Supplementary web plate <input type="checkbox"/> Nominal grade <input type="checkbox"/> Measured values Yield strength: Ultimate strength: Young's modulus <input type="checkbox"/> Nominal <input type="checkbox"/> Measured E:	
Notes: <div style="border: 1px solid black; height: 100px; width: 100%;"></div>					
End-plate rib stiffener <input type="checkbox"/> Nominal grade <input type="checkbox"/> Measured value Yield strength: Ultimate strength: Young's modulus <input type="checkbox"/> Nominal <input type="checkbox"/> Measured E:					
Test set up and loading protocol					
Type of test:	Monotonic				
Loading protocol:					
Data provided:	Trasducers No.13,14 and No.4,8				
Type of response curve:	<input type="checkbox"/> Force <input checked="" type="checkbox"/> Moment <input type="checkbox"/> Displacement <input checked="" type="checkbox"/> Rotation		Evaluated on the column flange Panel zone shearing rotation, relative deformation between the column flange and the end-plate		

Paper

Title: Behaviour of end-plate moment connections under earthquake loading

Authors: Shi G. Shi Y. Wang Y.

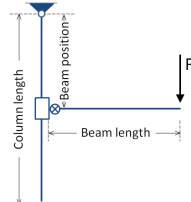
Source: Engineering Structures **Volume:** 29 **Issue:** 5 **Pages:** 703-716 **Year:** 2007

Test JD4

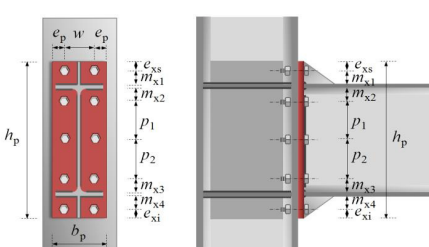
Geometry (mm)

Scheme: Exterior joint

Beam length: 1180
Beam position: 1000
Column length: 2000



End-plate



hp:	500
bp:	200
tp:	20
ep:	46
w:	108
exi:	50
Thickness:	10
exs:	50
mx1:	50
mx2:	50
mx3:	50
mx4:	50
p1:	176
p2:	0

Rib stiffener

Beam

Shape: Built-up I-shaped

Height:	300
Flange thickness:	12
Root radius:	FP
Width:	200
Web thickness:	8
Flange-to-web welds:	FP

Column

Shape: Built-up I-shaped

Height:	300
Flange thickness:	12
Root radius:	FP
Width:	250
Web thickness:	8
Flange-to-web welds:	FP
<input type="checkbox"/> Supplementary web plate	
<input type="checkbox"/> Continuity plates	
Thickness:	
Thickness:	

Bolts

Rows in tension:	2
Bolts per row:	2
Diameter:	20
Tensile stress area:	245

Beam-to-plate welds

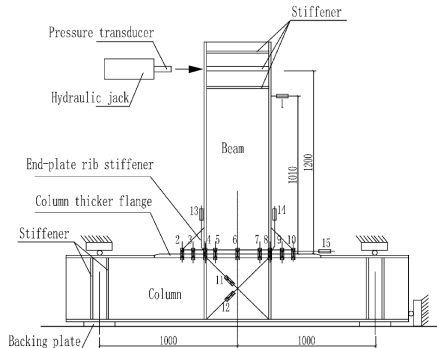
- Throat thickness
- Leg thickness
- Flange**
- Full penetration
- Fillet welds
- Web**
- Full penetration
- Fillet welds

Thickness: 8

Notes:

The column flange thickness is equal to the end-plate thickness within the range of 100 mm above and below the extension edge of the end-plate.

Test JD4

		Material properties	
		(MPa)	
Beam	Column	End-plate	
<input type="checkbox"/> Nominal grade Q345 <input checked="" type="checkbox"/> Measured values fy,f: 409.0 fy,w: 409.0 fu,f: 536.6 fu,w: 536.6	<input type="checkbox"/> Nominal grade Q345 <input checked="" type="checkbox"/> Measured values fy,f: 372.6 fy,w: 409.0 fu,f: 537.0 fu,w: 536.6	<input type="checkbox"/> Nominal grade Q345 <input checked="" type="checkbox"/> Measured values Yield strength: 372.6 Ultimate strength: 537.0 Young's modulus <input type="checkbox"/> Nominal Ef: 188671 <input checked="" type="checkbox"/> Measured Ew: 195452	
Bolts	Continuity plate	Supplementary web plate	
<input type="checkbox"/> Nominal grade 10.9 <input checked="" type="checkbox"/> Measured values Yield strength: 995 Ultimate strength: 1160 Young's modulus <input type="checkbox"/> Nominal <input checked="" type="checkbox"/> Measured E: 206000	<input type="checkbox"/> Nominal grade <input type="checkbox"/> Measured values Yield strength: Ultimate strength: Young's modulus <input type="checkbox"/> Nominal <input type="checkbox"/> Measured E:	<input type="checkbox"/> Nominal grade <input type="checkbox"/> Measured values Yield strength: Ultimate strength: Young's modulus <input type="checkbox"/> Nominal <input type="checkbox"/> Measured E:	
Notes: <div style="border: 1px solid black; height: 100px; width: 100%;"></div>			
End-plate rib stiffener <input type="checkbox"/> Nominal grade Q345 <input checked="" type="checkbox"/> Measured value Yield strength: 409.0 Ultimate strength: 536.6 Young's modulus <input type="checkbox"/> Nominal <input checked="" type="checkbox"/> Measured E: 195452			
Test set up and loading protocol			
Type of test:	Monotonic		
Loading protocol:			
Data provided:	Trasducers No.13,14 and No.4,8		
Type of response curve:	<input type="checkbox"/> Force <input checked="" type="checkbox"/> Moment <input type="checkbox"/> Displacement <input checked="" type="checkbox"/> Rotation		
	Evaluated on the column flange Panel zone shearing rotation, relative deformation between the column flange and the end-plate		
			

Paper

Title: Behaviour of end-plate moment connections under earthquake loading

Authors: Shi G. Shi Y. Wang Y.

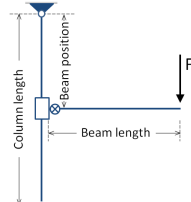
Source: Engineering Structures **Volume:** 29 **Issue:** 5 **Pages:** 703-716 **Year:** 2007

Test JD5

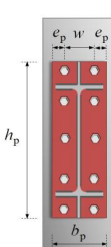
Geometry (mm)

Scheme: Exterior joint

Beam length: 1175
Beam position: 1000
Column length: 2000



End-plate



hp:	500
bp:	200
ep:	46
exs:	50
mx1:	50
p1:	176
tp:	25
w:	108
exi:	50
mx2:	50
p2:	0
<input checked="" type="checkbox"/> Rib stiffener	
Thickness:	10
mx3:	50
mx4:	50

Notes:
The column flange thickness is equal to the end-plate thickness within the range of 100 mm above and below the extension edge of the end-plate.

Geometry (mm)

Beam

Shape: Built-up I-shaped

Height:	300
Flange thickness:	12
Root radius:	[]
Width:	200
Web thickness:	8
Flange-to-web welds:	FP

Column

Shape: Built-up I-shaped

Height:	300
Flange thickness:	12
Root radius:	[]
Width:	250
Web thickness:	8
Flange-to-web welds:	FP
<input type="checkbox"/> Supplementary web plate	
<input checked="" type="checkbox"/> Continuity plates	
Thickness:	[]
Thickness:	12

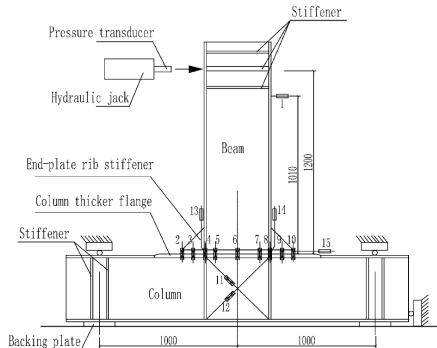
Bolts

Rows in tension:	2
Bolts per row:	2
Diameter:	20
Tensile stress area:	245

Beam-to-plate welds

<input type="checkbox"/> Throat thickness
<input checked="" type="checkbox"/> Leg thickness
Flange
<input type="checkbox"/> Full penetration
<input checked="" type="checkbox"/> Fillet welds []
Web
<input checked="" type="checkbox"/> Full penetration
<input checked="" type="checkbox"/> Nut washer []

Test JD5

		Material properties	
		(MPa)	
Beam	Column	End-plate	
<input type="checkbox"/> Nominal grade Q345 <input checked="" type="checkbox"/> Measured values fy,f: 409.0 fy,w: 409.0 fu,f: 536.6 fu,w: 536.6	<input type="checkbox"/> Nominal grade Q345 <input checked="" type="checkbox"/> Measured values fy,f: 372.6 fy,w: 409.0 fu,f: 537.0 fu,w: 536.6	<input type="checkbox"/> Nominal grade Q345 <input checked="" type="checkbox"/> Measured values Yield strength: 372.6 Ultimate strength: 537.0 Young's modulus <input type="checkbox"/> Nominal Ef: 188671 <input checked="" type="checkbox"/> Measured Ew: 195452	
Bolts	Continuity plate	Supplementary web plate	
<input type="checkbox"/> Nominal grade 10.9 <input checked="" type="checkbox"/> Measured values Yield strength: 995 Ultimate strength: 1160 Young's modulus <input type="checkbox"/> Nominal <input checked="" type="checkbox"/> Measured E: 195452	<input type="checkbox"/> Nominal grade Q345 <input checked="" type="checkbox"/> Measured values Yield strength: 409.0 Ultimate strength: 536.6 Young's modulus <input type="checkbox"/> Nominal <input checked="" type="checkbox"/> Measured E: 195452	<input type="checkbox"/> Nominal grade <input type="checkbox"/> Measured values Yield strength: Ultimate strength: Young's modulus <input type="checkbox"/> Nominal <input type="checkbox"/> Measured E:	
Notes: <div style="border: 1px solid black; height: 100px; width: 100%;"></div>			
End-plate rib stiffener <input type="checkbox"/> Nominal grade Q345 <input checked="" type="checkbox"/> Measured value Yield strength: 409.0 Ultimate strength: 536.6 Young's modulus <input type="checkbox"/> Nominal <input checked="" type="checkbox"/> Measured E: 195452			
Test set up and loading protocol			
Type of test:	Monotonic		
Loading protocol:			
Data provided:	Trasducers No.13,14 and No.4,8		
Type of response curve:	<input type="checkbox"/> Force <input checked="" type="checkbox"/> Moment <input type="checkbox"/> Displacement <input checked="" type="checkbox"/> Rotation		
	Evaluated on the column flange Panel zone shearing rotation, relative deformation between the column flange and the end-plate		
			

Paper

Title: Behaviour of end-plate moment connections under earthquake loading

Authors: Shi G. Shi Y. Wang Y.

Source: Engineering Structures **Volume:** 29 **Issue:** 5 **Pages:** 703-716 **Year:** 2007

Test JD6

Geometry (mm)

Scheme: Exterior joint

Beam length: 1180
Beam position: 1000
Column length: 2000

End-plate

hp: 500	bp: 200	ep: 46	exs: 50	mx1: 50	p1: 176
tp: 20	w: 108	exi: 50	mx2: 50	p2: 0	
<input checked="" type="checkbox"/> Rib stiffener			mx3: 50		
Thickness: 10			mx4: 50		

Notes:
The column flange thickness is equal to the end-plate thickness within the range of 100 mm above and below the extension edge of the end-plate.

Geometry (mm)

Beam

Shape: Built-up I-shaped
Height: 300 Width: 200
Flange thickness: 12 Web thickness: 8
Root radius: Flange-to-web welds: FP

Column

Shape: Built-up I-shaped
Height: 300 Width: 250
Flange thickness: 12 Web thickness: 8
Root radius: Flange-to-web welds: FP
 Supplementary web plate Thickness:
 Continuity plates Thickness: 12

Bolts

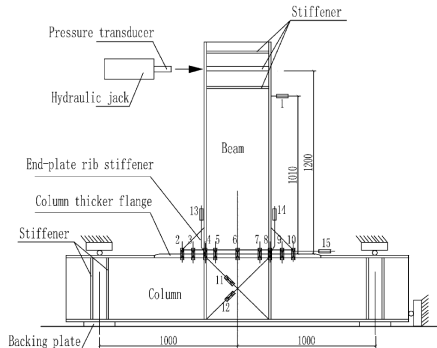
Rows in tension: 2 Bolts per row: 2
Diameter: 24 Tensile stress area: 353
 Head washer
 Nut washer

Beam-to-plate welds

Throat thickness
 Leg thickness
Flange
 Full penetration
 Fillet welds
Web
 Full penetration
 Fillet welds 8

Test JD6

		Material properties	
		(MPa)	
Beam		Column	
<input type="checkbox"/> Nominal grade <input checked="" type="checkbox"/> Measured values		<input type="checkbox"/> Nominal grade <input checked="" type="checkbox"/> Measured values	
fy,f: 409.0		fy,w: 409.0	
fu,f: 536.6		fu,w: 536.6	
Young's modulus		Young's modulus	
<input type="checkbox"/> Nominal Ef: 195452 <input checked="" type="checkbox"/> Measured Ew: 195452		<input type="checkbox"/> Nominal Ef: 188671 <input checked="" type="checkbox"/> Measured Ew: 195452	
Bolts		Continuity plate	
<input type="checkbox"/> Nominal grade 10.9 <input checked="" type="checkbox"/> Measured values		<input type="checkbox"/> Nominal grade Q345 <input checked="" type="checkbox"/> Measured values	
Yield strength: 975		Yield strength: 409.0	
Ultimate strength: 1188		Ultimate strength: 536.6	
Young's modulus		Young's modulus	
<input type="checkbox"/> Nominal E: 206000 <input checked="" type="checkbox"/> Measured E: 195452		<input type="checkbox"/> Nominal E: <input checked="" type="checkbox"/> Measured E: 195452	
End-plate		Supplementary web plate	
<input type="checkbox"/> Nominal grade <input checked="" type="checkbox"/> Measured values		<input type="checkbox"/> Nominal grade <input type="checkbox"/> Measured values	
Yield strength: 409.0		Yield strength:	
Ultimate strength: 536.6		Ultimate strength:	
Young's modulus		Young's modulus	
<input type="checkbox"/> Nominal E: <input checked="" type="checkbox"/> Measured E: 195452		<input type="checkbox"/> Nominal E: <input type="checkbox"/> Measured E:	
Notes:		End-plate rib stiffener	
<input type="checkbox"/> Nominal grade Q345 <input checked="" type="checkbox"/> Measured value		<input type="checkbox"/> Nominal grade <input checked="" type="checkbox"/> Measured value	
Yield strength: 409.0		Yield strength: 409.0	
Ultimate strength: 536.6		Ultimate strength: 536.6	
Young's modulus		Young's modulus	
<input type="checkbox"/> Nominal E: <input checked="" type="checkbox"/> Measured E: 195452		<input type="checkbox"/> Nominal E: <input checked="" type="checkbox"/> Measured E: 195452	
Test set up and loading protocol			
Type of test:	Monotonic		
Loading protocol:			
Data provided:	Trasducers No.13,14 and No.4,8		
Type of response curve:			
<input type="checkbox"/> Force <input checked="" type="checkbox"/> Moment	Evaluated on the column flange		
<input type="checkbox"/> Displacement <input checked="" type="checkbox"/> Rotation	Panel zone shearing rotation, relative deformation between the column flange and the end-plate		



Paper

Title: Behaviour of end-plate moment connections under earthquake loading

Authors: Shi G. Shi Y. Wang Y.

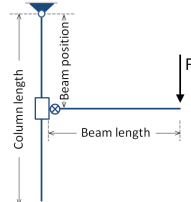
Source: Engineering Structures **Volume:** 29 **Issue:** 5 **Pages:** 703-716 **Year:** 2007

Test JD7

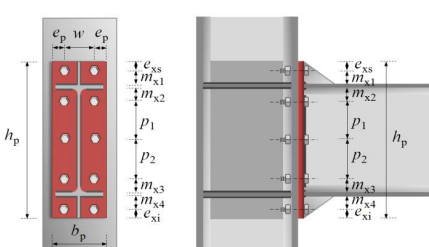
Geometry (mm)

Scheme: Exterior joint

Beam length: 1175
Beam position: 1000
Column length: 2000



End-plate



hp:	500
bp:	200
tp:	25
ep:	46
w:	108
exi:	50
mx1:	50
p1:	176
mx2:	50
p2:	0
Thickness:	10
mx3:	50
mx4:	50

Notes:
The column flange thickness is equal to the end-plate thickness within the range of 100 mm above and below the extension edge of the end-plate.

Geometry (mm)

Beam

Shape: Built-up I-shaped

Height:	300
Flange thickness:	12
Root radius:	FP
Width:	200
Web thickness:	8
Flange-to-web welds:	FP

Column

Shape: Built-up I-shaped

Height:	300
Flange thickness:	12
Root radius:	FP
Width:	250
Web thickness:	8
Flange-to-web welds:	FP
<input type="checkbox"/> Supplementary web plate	Thickness:
<input checked="" type="checkbox"/> Continuity plates	Thickness: 12

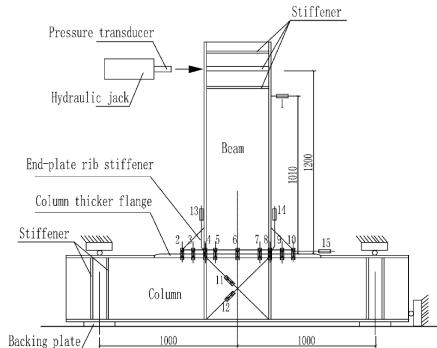
Bolts

Rows in tension:	2
Bolts per row:	2
Diameter:	24
Tensile stress area:	353

Beam-to-plate welds

<input type="checkbox"/> Throat thickness
<input checked="" type="checkbox"/> Leg thickness
Flange
<input checked="" type="checkbox"/> Full penetration
<input type="checkbox"/> Fillet welds
Web
<input type="checkbox"/> Full penetration
<input checked="" type="checkbox"/> Fillet welds
Thickness: 8

Test JD7

		Material properties	
		(MPa)	
Beam	Column	End-plate	
<input type="checkbox"/> Nominal grade Q345 <input checked="" type="checkbox"/> Measured values fy,f: 409.0 fy,w: 409.0 fu,f: 536.6 fu,w: 536.6	<input type="checkbox"/> Nominal grade Q345 <input checked="" type="checkbox"/> Measured values fy,f: 372.6 fy,w: 409.0 fu,f: 537.0 fu,w: 536.6	<input type="checkbox"/> Nominal grade Q345 <input checked="" type="checkbox"/> Measured values Yield strength: 372.6 Ultimate strength: 537.0 Young's modulus <input type="checkbox"/> Nominal Ef: 188671 <input checked="" type="checkbox"/> Measured Ew: 195452	
Bolts	Continuity plate	Supplementary web plate	
<input type="checkbox"/> Nominal grade 10.9 <input checked="" type="checkbox"/> Measured values Yield strength: 975 Ultimate strength: 1188 Young's modulus <input type="checkbox"/> Nominal <input checked="" type="checkbox"/> Measured E: 195452	<input type="checkbox"/> Nominal grade Q345 <input checked="" type="checkbox"/> Measured values Yield strength: 409.0 Ultimate strength: 536.6 Young's modulus <input type="checkbox"/> Nominal <input checked="" type="checkbox"/> Measured E: 195452	<input type="checkbox"/> Nominal grade <input type="checkbox"/> Measured values Yield strength: Ultimate strength: Young's modulus <input type="checkbox"/> Nominal <input type="checkbox"/> Measured E:	
Notes: <div style="border: 1px solid black; height: 100px; width: 100%;"></div>			
End-plate rib stiffener <input type="checkbox"/> Nominal grade Q345 <input checked="" type="checkbox"/> Measured value Yield strength: 409.0 Ultimate strength: 536.6 Young's modulus <input type="checkbox"/> Nominal <input checked="" type="checkbox"/> Measured E: 195452			
Test set up and loading protocol			
Type of test:	Monotonic		
Loading protocol:			
Data provided:	Trasducers No.13,14 and No.4,8		
Type of response curve:	<input type="checkbox"/> Force <input checked="" type="checkbox"/> Moment <input type="checkbox"/> Displacement <input checked="" type="checkbox"/> Rotation		
	Evaluated on the column flange Panel zone shearing rotation, relative deformation between the column flange and the end-plate		
			

Paper

Title: Behaviour of end-plate moment connections under earthquake loading

Authors: Shi G. Shi Y. Wang Y.

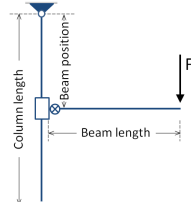
Source: Engineering Structures **Volume:** 29 **Issue:** 5 **Pages:** 703-716 **Year:** 2007

Test JD8

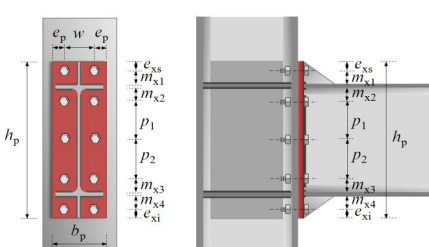
Geometry (mm)

Scheme: Exterior joint

Beam length: 1182
Beam position: 1000
Column length: 2000



End-plate



hp:	500
bp:	200
tp:	16
ep:	46
exi:	50
mx1:	50
p1:	176
w:	108
mx2:	50
p2:	0
Thickness:	10
mx3:	50
mx4:	50

Notes:
The column flange thickness is equal to the end-plate thickness within the range of 100 mm above and below the extension edge of the end-plate.

Geometry (mm)

Beam

Shape: Built-up I-shaped

Height:	300
Flange thickness:	12
Root radius:	FP
Width:	200
Web thickness:	8
Flange-to-web welds:	FP

Column

Shape: Built-up I-shaped

Height:	300
Flange thickness:	12
Root radius:	FP
Width:	250
Web thickness:	8
Flange-to-web welds:	FP
Thickness:	12
Supplementary web plate:	<input type="checkbox"/>
Continuity plates:	<input checked="" type="checkbox"/>

Bolts

Rows in tension:	2
Bolts per row:	2
Diameter:	20
Tensile stress area:	245

Beam-to-plate welds

Throat thickness:	<input type="checkbox"/>
Leg thickness:	<input checked="" type="checkbox"/>
Flange	
Full penetration:	<input checked="" type="checkbox"/>
Fillet welds:	<input type="checkbox"/>
Web	
Full penetration:	<input type="checkbox"/>
Fillet welds:	<input checked="" type="checkbox"/>
Thickness:	8

Test JD8

		Material properties			
		(MPa)			
Beam		Column		End-plate	
<input type="checkbox"/> Nominal grade Q345 <input checked="" type="checkbox"/> Measured values fy,f: 409.0 fy,w: 409.0 fu,f: 536.6 fu,w: 536.6		<input type="checkbox"/> Nominal grade Q345 <input checked="" type="checkbox"/> Measured values fy,f: 372.6 fy,w: 409.0 fu,f: 537.0 fu,w: 536.6		<input type="checkbox"/> Nominal grade Q345 <input checked="" type="checkbox"/> Measured values Yield strength: 409.0 Ultimate strength: 536.6 Young's modulus <input type="checkbox"/> Nominal Ef: 188671 <input checked="" type="checkbox"/> Measured Ew: 195452	
Bolts		Continuity plate		Supplementary web plate	
<input type="checkbox"/> Nominal grade 10.9 <input type="checkbox"/> Measured values Yield strength: 995 Ultimate strength: 1160 Young's modulus <input type="checkbox"/> Nominal <input checked="" type="checkbox"/> Measured E: 206000		<input type="checkbox"/> Nominal grade Q345 <input checked="" type="checkbox"/> Measured values Yield strength: 409.0 Ultimate strength: 536.6 Young's modulus <input type="checkbox"/> Nominal <input checked="" type="checkbox"/> Measured E: 195452		<input type="checkbox"/> Nominal grade <input type="checkbox"/> Measured values Yield strength: Ultimate strength: Young's modulus <input type="checkbox"/> Nominal <input checked="" type="checkbox"/> Measured E:	
Notes: <div style="border: 1px solid black; height: 100px; width: 100%;"></div>					
End-plate rib stiffener					
<input type="checkbox"/> Nominal grade Q345 <input checked="" type="checkbox"/> Measured value Yield strength: 409.0 Ultimate strength: 536.6 Young's modulus <input type="checkbox"/> Nominal <input checked="" type="checkbox"/> Measured E: 195452					
Test set up and loading protocol					
Type of test:	Monotonic				
Loading protocol:					
Data provided:	Trasducers No.13,14 and No.4,8				
Type of response curve:	<input type="checkbox"/> Force <input checked="" type="checkbox"/> Moment <input type="checkbox"/> Displacement <input checked="" type="checkbox"/> Rotation Evaluated on the column flange Panel zone shearing rotation, relative deformation between the column flange and the end-plate				

Paper

Title: Behavior of extended end-plate moment connections subject to cyclic loading

Authors: Sumner E. A. Murray T. M.

Source: Journal of Structural Engineering Volume: 128 Issue: 4 Pages: 501-508 Year: 2002

Test 4E-1.25-1.5-2

Geometry (inch)

Beam

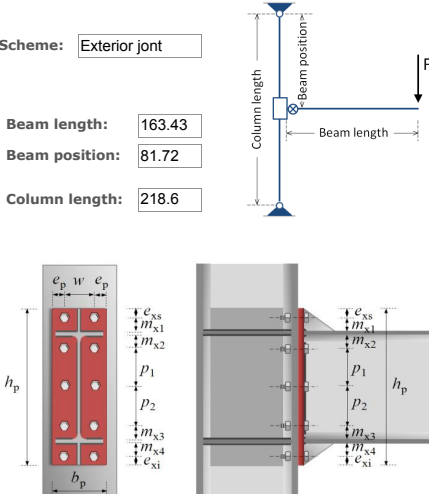
Shape: W610x230x101 (W24x68)

Height:	23.87	Width:	9.16
Flange thickness:	0.583	Web thickness:	0.438
Root radius:	0.521	Flange-to-web welds:	

Column

Shape: W360x370x179 (W14x120)

Height:	14.5	Width:	14.75
Flange thickness:	0.933	Web thickness:	0.601
Root radius:	0.591	Flange-to-web welds:	
<input checked="" type="checkbox"/> Supplementary web plate		Thickness:	0.375
<input checked="" type="checkbox"/> Continuity plates		Thickness:	0.63



End-plate

hp:	33.75								
bp:	10	ep:	2.01	exs:	3.04	mx1:	1.71	p1:	24.25
tp:	1.535	w:	5.98	exi:	3.04	mx2:	1.71	p2:	0
<input type="checkbox"/> Rib stiffener		Thickness:		mx3:	2.093				
				mx4:	2.093				

Bolts

Rows in tension:	2
Bolts per row:	2
Diameter:	1.25
Tensile stress area:	0.969

Beam-to-plate welds

<input checked="" type="checkbox"/> Throat thickness
<input type="checkbox"/> Leg thickness
Flange
<input checked="" type="checkbox"/> Full penetration
<input type="checkbox"/> Fillet welds
Web
<input type="checkbox"/> Full penetration
<input checked="" type="checkbox"/> Fillet welds
Thickness: 0.3

Notes:

Test 4E-1.25-1.5-2

		Material properties			
		(ksi)			
Beam		Column		End-plate	
<input type="checkbox"/> Nominal grade ASTM <input checked="" type="checkbox"/> Measured values A572		<input type="checkbox"/> Nominal grade ASTM <input checked="" type="checkbox"/> Measured values A572		<input type="checkbox"/> Nominal grade ASTM <input checked="" type="checkbox"/> Measured values A36	
f_y, f_c : 53.6 f_y, w : 53.6 f_u, f_c : 70.7 f_u, w : 70.7		f_y, f_c : 52 f_y, w : 52 f_u, f_c : 70.6 f_u, w : 70.6		f_y, f_c : 38.1 f_u, w : 68.8	
Young's modulus <input checked="" type="checkbox"/> Nominal E_f : 29000 <input type="checkbox"/> Measured E_w : 29000		Young's modulus <input checked="" type="checkbox"/> Nominal E_f : 29000 <input type="checkbox"/> Measured E_w : 29000		Young's modulus <input checked="" type="checkbox"/> Nominal E : 29000 <input type="checkbox"/> Measured E : 29000	
Bolts		Continuity plate		Supplementary web plate	
<input checked="" type="checkbox"/> Nominal grade A490 <input type="checkbox"/> Measured values		<input type="checkbox"/> Nominal grade ASTM <input checked="" type="checkbox"/> Measured values A36		<input type="checkbox"/> Nominal grade ASTM <input checked="" type="checkbox"/> Measured values A36	
Yield strength: 130 Ultimate strength: 150		Yield strength: 36 Ultimate strength: 58		Yield strength: 42.1 Ultimate strength: 64.95	
Young's modulus <input checked="" type="checkbox"/> Nominal E : 29000 <input type="checkbox"/> Measured E : 29000		Young's modulus <input checked="" type="checkbox"/> Nominal E_f : 29000 <input type="checkbox"/> Measured E_w : 29000		Young's modulus <input checked="" type="checkbox"/> Nominal E : 29000 <input type="checkbox"/> Measured E : 29000	
Notes: The paper provides the nominal values of material properties, while the PhD thesis the measured ones. The measured values are reported.					
End-plate rib stiffener					
<input type="checkbox"/> Nominal grade <input type="checkbox"/> Measured value Yield strength: Ultimate strength: Young's modulus <input type="checkbox"/> Nominal <input type="checkbox"/> Measured E : _____					
Test set up and loading protocol					
Type of test:	Cyclic				
Loading protocol:	SAC loading protocol				
Drift angle (%)	0.375-0.5-0.75-1-1.5-2-3...				
Data provided:					
Type of response curve:	<input type="checkbox"/> Force <input checked="" type="checkbox"/> Moment <input type="checkbox"/> Displacement <input checked="" type="checkbox"/> Rotation		At the column centreline Rotation of the specimen		

Paper

Title: Experimental tests on extended end-plate connections with variable parameters

Authors: Tahir M. M. Hussein M. A.

Source: Steel Structures Volume: 8 Issue: 369-381 Pages: 369-381 Year: 2008

Test EEP 6

Geometry (mm)

Beam

Shape: HB 450X200X65.1

Height:	446	Width:	199
Flange thickness:	12	Web thickness:	8
Root radius:	13	Flange-to-web welds:	

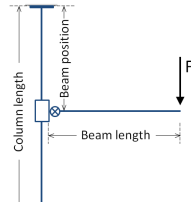
Column

Shape: HB 250X250X63.8

Height:	244	Width:	252
Flange thickness:	11	Web thickness:	11
Root radius:	13	Flange-to-web welds:	
<input type="checkbox"/> Supplementary web plate		Thickness:	
<input type="checkbox"/> Continuity plates		Thickness:	

Scheme: Exterior joint

Beam length: 1500
Beam position: n.a.
Column length: 3000



End-plate

hp: 561
bp: 200 ep: 55 exs: 50 mx1: 40 p1: 326
tp: 12 w: 90 exi: 25 mx2: 48 p2: 0
 Rib stiffener
Thickness: mx3: 48
mx4: 0

Bolts

Rows in tension: 2
Bolts per row: 2
Diameter: 20
Tensile stress area: 245

Beam-to-plate welds

Throat thickness
 Leg thickness
Flange
 Full penetration
 Fillet welds 10
Web
 Full penetration
 Fillet welds 8

Notes:
The position of the beam is not specified. Details concerning washers are not provided.

Test EEP 6

Material properties		
Beam	Column	End-plate
<input type="checkbox"/> Nominal grade S275 <input checked="" type="checkbox"/> Measured values fy,f: 313 fy,w: 318 fu,f: 472 fu,w: 500 Young's modulus <input type="checkbox"/> Nominal Ef: 199000 <input checked="" type="checkbox"/> Measured Ew: 200000	<input type="checkbox"/> Nominal grade S275 <input checked="" type="checkbox"/> Measured values fy,f: 351 fy,w: 351 fu,f: 510 fu,w: 540 Young's modulus <input type="checkbox"/> Nominal Ef: 193000 <input checked="" type="checkbox"/> Measured Ew: 192000	<input type="checkbox"/> Nominal grade S275 <input checked="" type="checkbox"/> Measured values Yield strength: 307.3 Ultimate strength: 476 Young's modulus <input type="checkbox"/> Nominal <input checked="" type="checkbox"/> Measured E: 204000
Bolts	Continuity plate	Supplementary web plate
<input checked="" type="checkbox"/> Nominal grade 8.8 <input type="checkbox"/> Measured values Yield strength: 640 Ultimate strength: 800 Young's modulus <input checked="" type="checkbox"/> Nominal <input type="checkbox"/> Measured E: 210000	<input type="checkbox"/> Nominal grade <input type="checkbox"/> Measured values Yield strength: Ultimate strength: Young's modulus <input type="checkbox"/> Nominal <input type="checkbox"/> Measured E:	<input type="checkbox"/> Nominal grade <input type="checkbox"/> Measured values Yield strength: Ultimate strength: Young's modulus <input type="checkbox"/> Nominal <input type="checkbox"/> Measured E:
Notes:		
<input type="checkbox"/> End-plate rib stiffener <input type="checkbox"/> Nominal grade <input type="checkbox"/> Measured value Yield strength: Ultimate strength: Young's modulus <input type="checkbox"/> Nominal <input type="checkbox"/> Measured E:		
Test set up and loading protocol		
Type of test:	Monotonic	
Loading protocol:		
Data provided:	Inclinometers on the beam and column centrelines	
Type of response curve:	<input type="checkbox"/> Force Evaluated on the column flange <input checked="" type="checkbox"/> Moment <input type="checkbox"/> Displacement <input checked="" type="checkbox"/> Rotation	
		

Paper

Title: Experimental tests on extended end-plate connections with variable parameters

Authors: Tahir M. M. Hussein M. A.

Source: Steel Structures Volume: 8 Issue: 369-381 Pages: 369-381 Year: 2008

Test EEP 7

Geometry (mm)

Beam

Shape: HB 450X200X65.1

Height:	446	Width:	119
Flange thickness:	12	Web thickness:	8
Root radius:	13	Flange-to-web welds:	

Column

Shape: HB 250X250X63.8

Height:	244	Width:	252
Flange thickness:	11	Web thickness:	11
Root radius:	13	Flange-to-web welds:	
<input type="checkbox"/> Supplementary web plate		Thickness:	
<input type="checkbox"/> Continuity plates		Thickness:	

Scheme: Exterior joint

Beam length: 1300
Beam position: n.a.
Column length: 3000

End-plate

hp:	561								
bp:	250	ep:	80	exs:	50	mx1:	40	p1:	326
tp:	12	w:	90	exi:	25	mx2:	48	p2:	0
<input type="checkbox"/> Rib stiffener		Thickness:		mx3:	48				
		Thickness:		mx4:	0				

Notes:
The position of the beam is not specified. Details concerning washers are not provided.

Bolts

Rows in tension: 2
Bolts per row: 2
Diameter: 20
Tensile stress area: 245

Head washer
 Nut washer

Beam-to-plate welds

Throat thickness
 Leg thickness
Flange
 Full penetration
 Fillet welds 10
Web
 Full penetration
 Fillet welds 8

Test EEP 7

Material properties		
Beam <input type="checkbox"/> Nominal grade S275 <input checked="" type="checkbox"/> Measured values fy,f: 313 fy,w: 318 fu,f: 472 fu,w: 500 Young's modulus <input type="checkbox"/> Nominal Ef: 199000 <input checked="" type="checkbox"/> Measured Ew: 200000	Column <input type="checkbox"/> Nominal grade S275 <input checked="" type="checkbox"/> Measured values fy,f: 351 fy,w: 351 fu,f: 510 fu,w: 540 Young's modulus <input type="checkbox"/> Nominal Ef: 193000 <input checked="" type="checkbox"/> Measured Ew: 192000	End-plate <input type="checkbox"/> Nominal grade S275 <input checked="" type="checkbox"/> Measured values Yield strength: 307.3 Ultimate strength: 476 Young's modulus <input type="checkbox"/> Nominal <input checked="" type="checkbox"/> Measured E: 204000
Bolts <input checked="" type="checkbox"/> Nominal grade 8.8 <input type="checkbox"/> Measured values Yield strength: 640 Ultimate strength: 800 Young's modulus <input checked="" type="checkbox"/> Nominal <input type="checkbox"/> Measured E: 210000	Continuity plate <input type="checkbox"/> Nominal grade <input type="checkbox"/> Measured values Yield strength: Ultimate strength: Young's modulus <input type="checkbox"/> Nominal <input checked="" type="checkbox"/> Measured E:	Supplementary web plate <input type="checkbox"/> Nominal grade <input type="checkbox"/> Measured values Yield strength: Ultimate strength: Young's modulus <input type="checkbox"/> Nominal <input checked="" type="checkbox"/> Measured E:
Notes: <div style="border: 1px solid black; height: 100px; width: 100%;"></div>		
End-plate rib stiffener <input type="checkbox"/> Nominal grade <input type="checkbox"/> Measured value Yield strength: Ultimate strength: Young's modulus <input type="checkbox"/> Nominal <input checked="" type="checkbox"/> Measured E:		
Test set up and loading protocol		
Type of test: Monotonic Loading protocol: <div style="border: 1px solid black; height: 40px; width: 100%;"></div>	Data provided: Inclinometers on the beam and column centrelines <div style="border: 1px solid black; height: 40px; width: 100%;"></div>	
Type of response curve: <input type="checkbox"/> Force Evaluated on the column flange <input checked="" type="checkbox"/> Moment <input type="checkbox"/> Displacement <input checked="" type="checkbox"/> Rotation <div style="border: 1px solid black; height: 40px; width: 100%;"></div>		

Paper

Title: Experimental tests on extended end-plate connections with variable parameters

Authors: Tahir M. M. Hussein M. A.

Source: Steel Structures Volume: 8 Issue: 369-381 Pages: 369-381 Year: 2008

Test EEP 8

Geometry (mm)

Beam

Shape: HB 450X200X65.1

Height:	446	Width:	119
Flange thickness:	12	Web thickness:	8
Root radius:	13	Flange-to-web welds:	

Column

Shape: HB250x250x63.8

Height:	244	Width:	252
Flange thickness:	11	Web thickness:	11
Root radius:	13	Flange-to-web welds:	
<input type="checkbox"/> Supplementary web plate		Thickness:	
<input type="checkbox"/> Continuity plates		Thickness:	

Scheme: Exterior joint

Beam length: 1500
Beam position: n.a.
Column length: 3000

End-plate

hp: 561
bp: 200 ep: 55 exs: 50 mx1: 48 p1: 326
tp: 15 w: 90 exi: 25 mx2: 48 p2: 0
 Rib stiffener Thickness: mx3: 48
Thickness: mx4: 0

Bolts

Rows in tension: 2
Bolts per row: 2
Diameter: 24
Tensile stress area: 353
 Head washer
 Nut washer

Beam-to-plate welds

Throat thickness
 Leg thickness
Flange
 Full penetration
 Fillet welds 10
Web
 Full penetration
 Fillet welds 8

Notes:
The position of the beam is not specified. Details concerning washers are not provided.

Test EEP 8

Material properties		
Beam <input type="checkbox"/> Nominal grade S275 <input checked="" type="checkbox"/> Measured values fy,f: 313 fy,w: 318 fu,f: 472 fu,w: 500 Young's modulus <input type="checkbox"/> Nominal Ef: 199000 <input checked="" type="checkbox"/> Measured Ew: 200000	Column <input type="checkbox"/> Nominal grade S275 <input checked="" type="checkbox"/> Measured values fy,f: 351 fy,w: 351 fu,f: 510 fu,w: 540 Young's modulus <input type="checkbox"/> Nominal Ef: 193000 <input checked="" type="checkbox"/> Measured Ew: 192000	End-plate <input type="checkbox"/> Nominal grade S275 <input checked="" type="checkbox"/> Measured values Yield strength: 309.7 Ultimate strength: 515.3 Young's modulus <input type="checkbox"/> Nominal <input checked="" type="checkbox"/> Measured E: 204000
Bolts <input checked="" type="checkbox"/> Nominal grade 8.8 <input type="checkbox"/> Measured values Yield strength: 640 Ultimate strength: 800 Young's modulus <input checked="" type="checkbox"/> Nominal <input type="checkbox"/> Measured E: 210000	Continuity plate <input type="checkbox"/> Nominal grade <input type="checkbox"/> Measured values Yield strength: Ultimate strength: Young's modulus <input type="checkbox"/> Nominal <input type="checkbox"/> Measured E:	Supplementary web plate <input type="checkbox"/> Nominal grade <input type="checkbox"/> Measured values Yield strength: Ultimate strength: Young's modulus <input type="checkbox"/> Nominal <input type="checkbox"/> Measured E:
Notes: <div style="border: 1px solid black; height: 100px; width: 100%;"></div>		
End-plate rib stiffener <input type="checkbox"/> Nominal grade <input type="checkbox"/> Measured value Yield strength: Ultimate strength: Young's modulus <input type="checkbox"/> Nominal <input type="checkbox"/> Measured E:		
Test set up and loading protocol		
Type of test: Monotonic Loading protocol: <div style="border: 1px solid black; height: 40px; width: 100%;"></div>		Data provided: Inclinometers on the beam and column centrelines Type of response curve: <input type="checkbox"/> Force Evaluated on the column flange <input checked="" type="checkbox"/> Moment <input type="checkbox"/> Displacement Connection rotation <input checked="" type="checkbox"/> Rotation

Paper

Title: Experimental tests on extended end-plate connections with variable parameters

Authors: Tahir M. M. Hussein M. A.

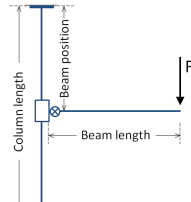
Source: Steel Structures Volume: 8 Issue: 369-381 Pages: 369-381 Year: 2008

Test EEP 9

Geometry (mm)

Scheme: Exterior joint

Beam length: 1500
Beam position: n.a.
Column length: 3000



Beam

Shape: HB 450X200X65.1

Height:	446	Width:	119
Flange thickness:	12	Web thickness:	8
Root radius:	13	Flange-to-web welds:	

Column

Shape: HB 250x250x63.8

Height:	244	Width:	252
Flange thickness:	11	Web thickness:	11
Root radius:	13	Flange-to-web welds:	
<input type="checkbox"/> Supplementary web plate		Thickness:	
<input type="checkbox"/> Continuity plates		Thickness:	

End-plate

hp:	561								
bp:	250	ep:	80	exs:	50	mx1:	40	p1:	326
tp:	15	w:	90	exi:	25	mx2:	48	p2:	0
<input type="checkbox"/> Rib stiffener					mx3:	48			
Thickness:					mx4:				

Bolts

Rows in tension:	2
Bolts per row:	2
Diameter:	24
Tensile stress area:	353
<input type="checkbox"/> Head washer	
<input type="checkbox"/> Nut washer	

Beam-to-plate welds

<input type="checkbox"/> Throat thickness
<input checked="" type="checkbox"/> Leg thickness
Flange
<input type="checkbox"/> Full penetration
<input checked="" type="checkbox"/> Fillet welds 10
Web
<input type="checkbox"/> Full penetration
<input checked="" type="checkbox"/> Fillet welds 8

Notes:

The position of the beam is not specified. Details concerning washers are not provided.

Test EEP 9

Material properties		
Beam <input type="checkbox"/> Nominal grade S275 <input checked="" type="checkbox"/> Measured values fy,f: 313 fy,w: 318 fu,f: 472 fu,w: 500 Young's modulus <input type="checkbox"/> Nominal Ef: 199000 <input checked="" type="checkbox"/> Measured Ew: 200000	Column <input type="checkbox"/> Nominal grade S275 <input checked="" type="checkbox"/> Measured values fy,f: 351 fy,w: 351 fu,f: 510 fu,w: 540 Young's modulus <input type="checkbox"/> Nominal Ef: 193000 <input checked="" type="checkbox"/> Measured Ew: 192000	End-plate <input type="checkbox"/> Nominal grade S275 <input checked="" type="checkbox"/> Measured values Yield strength: 309.7 Ultimate strength: 515.3 Young's modulus <input type="checkbox"/> Nominal <input checked="" type="checkbox"/> Measured E: 204000
Bolts <input checked="" type="checkbox"/> Nominal grade 8.8 <input type="checkbox"/> Measured values Yield strength: 640 Ultimate strength: 800 Young's modulus <input checked="" type="checkbox"/> Nominal <input type="checkbox"/> Measured E: 210000	Continuity plate <input type="checkbox"/> Nominal grade <input type="checkbox"/> Measured values Yield strength: Ultimate strength: Young's modulus <input type="checkbox"/> Nominal <input checked="" type="checkbox"/> Measured E:	Supplementary web plate <input type="checkbox"/> Nominal grade <input type="checkbox"/> Measured values Yield strength: Ultimate strength: Young's modulus <input type="checkbox"/> Nominal <input checked="" type="checkbox"/> Measured E:
Notes: <div style="border: 1px solid black; height: 100px; width: 100%;"></div>		
End-plate rib stiffener <input type="checkbox"/> Nominal grade <input type="checkbox"/> Measured value Yield strength: Ultimate strength: Young's modulus <input type="checkbox"/> Nominal <input checked="" type="checkbox"/> Measured E:		
Test set up and loading protocol		
Type of test: Monotonic test Loading protocol: <div style="border: 1px solid black; height: 40px; width: 100%;"></div>	<div style="border: 1px solid black; height: 100px; width: 100%;"></div>	
Data provided: Inclinometers on the beam and column centrelines		
Type of response curve: <input type="checkbox"/> Force Evaluated on the column flange <input checked="" type="checkbox"/> Moment <input type="checkbox"/> Displacement <input checked="" type="checkbox"/> Rotation <div style="border: 1px solid black; height: 40px; width: 100%;"></div>		

Paper

Title:
Experimental Analysis and Modelling of Semi-rigid Steel Joints Under Cyclic Reversal Loading

Authors:
Bernuzzi, C. Zandonini, R. Zanon, P.

Source:
Journal of Constructional Steel Research
Volume: 38 **Issue:** 2 **Pages:** 95-123 **Year:** 1996

Test EPBC1

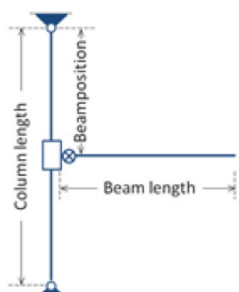
Geometry (mm)

Scheme: External joint; Extended end-plate

Beam length: -

Beam position: -

Column length: -



Beam

Shape: IPE300

Height: [] Width: []

Flange thickness: [] Web thickness: []

Root radius: [] Flange-to-web welds: []

Column

Shape: Rigid counterbeam

Height: [] Width: []

Flange thickness: [] Web thickness: []

Root radius: [] Flange-to-web welds: []

Supplementary web plate Continuity Thickness: []

End-plate

hp:	520
bp:	180
tp:	11.9
ep:	38
w:	105
exs:	50
mx1:	60.0
p1:	180
exi:	50
mx2:	49.3
p2:	[]
mx3:	49.3
mx4:	60.0

Rib Thickness []

Bolts

Rows in tension: 3 Throat

Bolts per row: 2 Leg thickness

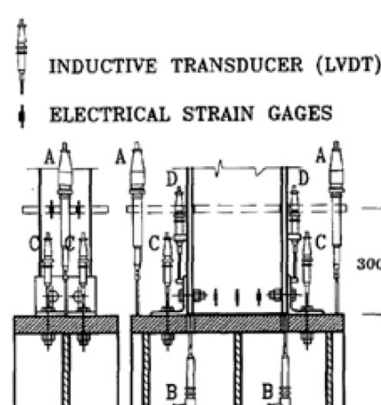
Diameter: 20 Flange: []

Tensile stress: 245 Web: []

Washer Washer nut

Notes:

Test EPBC1

Material properties (MPa)		
Beam	Column	End-plate
<input checked="" type="checkbox"/> Nominal values S355 <input type="checkbox"/> Measured values fy,f: [] fy,w: [] fu,f: [] fu,w: [] Young's modulus <input checked="" type="checkbox"/> Nominal Ef: [] <input type="checkbox"/> Measured Ew: []	<input type="checkbox"/> Nominal values [] <input type="checkbox"/> Measured values [] fy,f: [] fy,w: [] fu,f: [] fu,w: [] Young's modulus <input type="checkbox"/> Nominal Ef: [] <input checked="" type="checkbox"/> Measured Ew: []	<input type="checkbox"/> Nominal values [] <input checked="" type="checkbox"/> Measured values Yield strength: 321 Ultimate strength: 465 Young's modulus <input checked="" type="checkbox"/> Nominal E: [] <input type="checkbox"/> Measured E: []
Bolts	Continuity plate	Supplementary web plate
<input checked="" type="checkbox"/> Nominal values 8.8 <input type="checkbox"/> Measured values Yield strength: [] Ultimate strength: [] Young's modulus <input checked="" type="checkbox"/> Nominal E: [] <input type="checkbox"/> Measured E: []	<input type="checkbox"/> Nominal values [] <input type="checkbox"/> Measured values [] Yield strength: [] Ultimate strength: [] Young's modulus <input type="checkbox"/> Nominal E: [] <input checked="" type="checkbox"/> Measured E: []	<input type="checkbox"/> Nominal values [] <input type="checkbox"/> Measured values [] Yield strength: [] Ultimate strength: [] Young's modulus <input type="checkbox"/> Nominal E: [] <input checked="" type="checkbox"/> Measured E: []
Notes: <p>"The material properties of the beam stubs have a very low scatter within the same group of specimens. Mean values can hence be adopted for the elastic and plastic moments resistances; they are: (...), $M_{c,b} = 244 \text{ kNm}$ and $M_{p,b} = 284 \text{ kNm}$ for the second" series of tests. // Yielding mode - Plate yield. After weld crack at $18\phi_y$ // Failure mode - Plate fracture</p>		
End-plate rib stiffener		
<input type="checkbox"/> Nominal values [] <input type="checkbox"/> Measured values [] Yield strength: [] Ultimate strength: [] Young's modulus <input type="checkbox"/> Nominal E: [] <input checked="" type="checkbox"/> Measured E: []		
Test set up and loading protocol		
Type of test: Cyclic		
Loading protocol: Modified ECCS		
Amplitude inc. = e_y and 2 cycles per level.		
Data provided: Initial stiffnesses, moments and rotations		
Type of response:		
<input type="checkbox"/> Force		
<input checked="" type="checkbox"/> Moment		
<input type="checkbox"/> Displacement		
<input checked="" type="checkbox"/> Rotation	Rotation of the joint = beam + end-plate	
		

Paper

Title:
Experimental Analysis and Modelling of Semi-rigid Steel Joints Under Cyclic Reversal Loading

Authors:
Bernuzzi, C. Zandonini, R. Zanon, P.

Source:
Journal of Constructional Steel Research
Volume: 38 **Issue:** 2 **Pages:** 95-123 **Year:** 1996

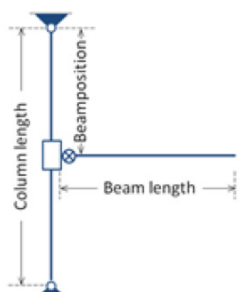
Test EPBC2

Scheme: External joint; Extended end-plate

Beam length: -

Beam position: -

Column length: -



Geometry (mm)

Beam			
Shape:	IPE300		
Height:	[]	Width:	[]
Flange thickness:	[]	Web thickness:	[]
Root radius:	[]	Flange-to-web welds:	[]

Column			
Shape:	Rigid counterbeam		
Height:	[]	Width:	[]
Flange thickness:	[]	Web thickness:	[]
Root radius:	[]	Flange-to-web welds:	[]
<input type="checkbox"/> Supplementary web plate	<input type="checkbox"/> Thickness: []		
<input checked="" type="checkbox"/> Continuity	<input type="checkbox"/> Thickness: []		

End-plate

hp:	520								
bp:	180	ep:	38	exs:	50	mx1:	60.0	p1:	180
tp:	17.5	w:	105	exi:	50	mx2:	49.3	p2:	[]
					mx3:	49.3			
<input type="checkbox"/> Rib					mx4:	60.0			
Thickness:	[]								

Bolts

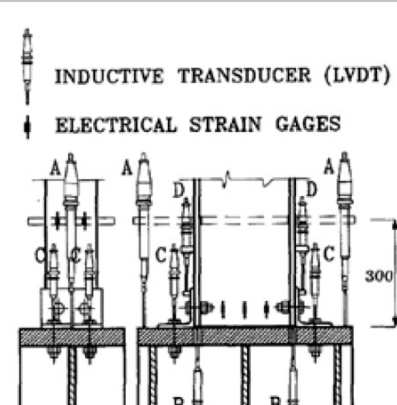
Rows in tension:	3
Bolts per row:	2
Diameter:	20
Tensile stress:	245
<input checked="" type="checkbox"/> Washer	<input type="checkbox"/> Throat
<input checked="" type="checkbox"/> Washer nut	<input type="checkbox"/> Leg thickness

Beam to plate welds

Flange:	[]
Web:	[]

Notes:

Test EPBC2

Material properties (MPa)					
Beam		Column		End-plate	
<input checked="" type="checkbox"/> Nominal values S355 <input type="checkbox"/> Measured values		<input type="checkbox"/> Nominal values <input type="checkbox"/> Measured values		<input type="checkbox"/> Nominal values <input checked="" type="checkbox"/> Measured values	
fy,f: [] fy,w: []		fy,f: [] fy,w: []		Yield strength: 339	
fu,f: [] fu,w: []		fu,f: [] fu,w: []		Ultimate strength: 513	
Young's modulus		Young's modulus		Young's modulus	
<input checked="" type="checkbox"/> Nominal Ef: [] <input type="checkbox"/> Measured Ew: []		<input type="checkbox"/> Nominal Ef: [] <input type="checkbox"/> Measured Ew: []		<input checked="" type="checkbox"/> Nominal E: [] <input type="checkbox"/> Measured E: []	
Bolts		Continuity plate		Supplementary web plate	
<input checked="" type="checkbox"/> Nominal values 8.8 <input type="checkbox"/> Measured values		<input type="checkbox"/> Nominal values <input type="checkbox"/> Measured values		<input type="checkbox"/> Nominal values <input type="checkbox"/> Measured values	
Yield strength: []		Yield strength: []		Yield strength: []	
Ultimate strength: []		Ultimate strength: []		Ultimate strength: []	
Young's modulus		Young's modulus		Young's modulus	
<input checked="" type="checkbox"/> Nominal E: [] <input type="checkbox"/> Measured E: []		<input type="checkbox"/> Nominal E: [] <input type="checkbox"/> Measured E: []		<input type="checkbox"/> Nominal E: [] <input type="checkbox"/> Measured E: []	
Notes: "The material properties of the beam stubs have a very low scatter within the same group of specimens. Mean values can hence be adopted for the elastic and plastic moments resistances; they are: (...), $M_{c,b} = 244$ kNm and $M_{p,b} = 284$ kNm for the second" series of tests. /// Failure mode - Bolt rupture					
Test set up and loading protocol					
Type of test: Cyclic Loading protocol: Modified ECCS Amplitude inc. = e_y and 2 cycles per level.			 INDUCTIVE TRANSDUCER (LVDT) ELECTRICAL STRAIN GAGES		
Data provided: Initial stiffnesses, moments and rotations					
Type of response: <input type="checkbox"/> Force <input checked="" type="checkbox"/> Moment <input type="checkbox"/> Displacement <input checked="" type="checkbox"/> Rotation					
Rotation of the joint = beam + end-plate					

Paper**Title:**

Experimental Analysis and Modelling of Semi-rigid Steel Joints Under Cyclic Reversal Loading

Authors:

Bernuzzi, C. Zandonini, R. Zanon, P.

Source:

Journal of Constructional Steel Research

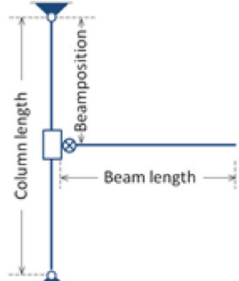
Volume 38

Issue 2

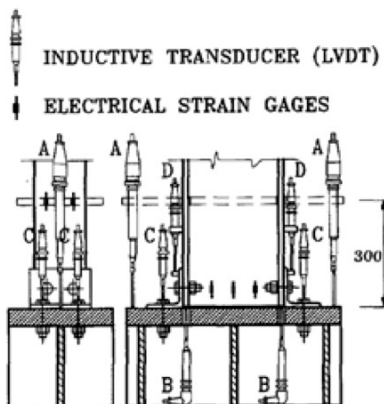
Pages 95-123

Year: 1996

Test EPC

Geometry (mm)	
Scheme: External joint; Extended end-plate one side	
Beam length: -	Column length: -
Beam position: -	Beam length: -
Column length: -	
Beam Shape: IPE300 Height: <input type="text"/> Flange thickness: <input type="text"/> Root radius: <input type="text"/> Width: <input type="text"/> Web thickness: <input type="text"/> Flange-to-web welds: <input type="text"/>	
Column Shape: Rigid counterbeam Height: <input type="text"/> Flange thickness: <input type="text"/> Root radius: <input type="text"/> Width: <input type="text"/> Web thickness: <input type="text"/> Flange-to-web welds: <input type="text"/> <input type="checkbox"/> Supplementary web plate <input checked="" type="checkbox"/> Continuity Thickness: <input type="text"/>	
End-plate hp: 520 bp: 180 ep: 38 exs: 50 mx1: 60.0 p1: 180 tp: 17.5 w: 105 exi: 10 mx2: 49.3 p2: <input type="text"/> mx3: 49.3 mx4: <input type="text"/> <input type="checkbox"/> Rib Thickness: <input type="text"/>	
Bolts Rows in tension: 3 Bolts per row: 2 Diameter: 20 Tensile stress: 245 <input checked="" type="checkbox"/> Washer <input checked="" type="checkbox"/> Washer nut	
Beam to plate welds <input type="checkbox"/> Throat <input type="checkbox"/> Leg thickness Flange: <input type="text"/> Web: <input type="text"/>	
Notes: <input type="text"/>	

Test EPC

Material properties (MPa)		
Beam	Column	End-plate
<input checked="" type="checkbox"/> Nominal values S355 <input type="checkbox"/> Measured values fy,f: [] fy,w: [] fu,f: [] fu,w: [] Young's modulus <input checked="" type="checkbox"/> Nominal Ef: [] <input type="checkbox"/> Measured Ew: []	<input type="checkbox"/> Nominal values [] <input type="checkbox"/> Measured values [] fy,f: [] fy,w: [] fu,f: [] fu,w: [] Young's modulus <input type="checkbox"/> Nominal Ef: [] <input type="checkbox"/> Measured Ew: []	<input type="checkbox"/> Nominal values [] <input checked="" type="checkbox"/> Measured values Yield strength: 339 Ultimate strength: 513 Young's modulus <input checked="" type="checkbox"/> Nominal E: [] <input type="checkbox"/> Measured E: []
Bolts	Continuity plate	Supplementary web plate
<input checked="" type="checkbox"/> Nominal values 8.8 <input type="checkbox"/> Measured values Yield strength: [] Ultimate strength: [] Young's modulus <input checked="" type="checkbox"/> Nominal E: [] <input type="checkbox"/> Measured E: []	<input type="checkbox"/> Nominal values [] <input type="checkbox"/> Measured values [] Yield strength: [] Ultimate strength: [] Young's modulus <input type="checkbox"/> Nominal E: [] <input type="checkbox"/> Measured E: []	<input type="checkbox"/> Nominal values [] <input type="checkbox"/> Measured values [] Yield strength: [] Ultimate strength: [] Young's modulus <input type="checkbox"/> Nominal E: [] <input type="checkbox"/> Measured E: []
Notes:		
<p>"The material properties of the beam stubs have a very low scatter within the same group of specimens. Mean values can hence be adopted for the elastic and plastic moments resistances; they are: (...), $M_{c,b} = 244$ kNm and $M_{p,b} = 284$ kNm for the second" series of tests. /// Failure mode - Bolt rupture at $6e_y$</p>		
Test set up and loading protocol		
Type of test: Cyclic		
Loading protocol: Modified ECCS		
Amplitude inc. = e_y and 2 cycles per level.		
Data provided: Initial stiffnesses, moments and rotations		
Type of response:		
<input type="checkbox"/> Force		
<input checked="" type="checkbox"/> Moment		
<input type="checkbox"/> Displacement		
<input checked="" type="checkbox"/> Rotation	Rotation of the joint = beam + end-plate	
		

Paper**Title:**

Non-linear analysis of the low-cycle fracture behaviour of isolated tee stub connections

Authors:

Bursi, O.S. | Ferrario, F. | Fontanari, V.

Source:

Computers and Structures

Volume

Issue:

Pages:

Year:

80

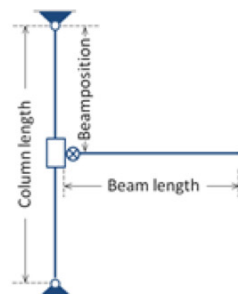
-

2333-2360

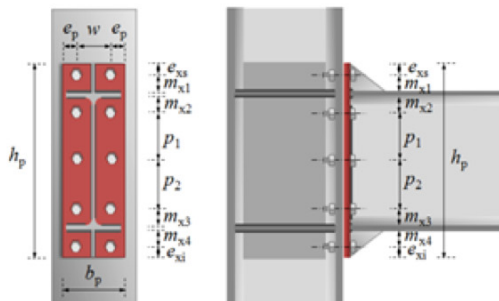
2002

Test JB1-3A**Geometry (mm)**

Scheme: External double extended end-plate joint
Beam length: 1304
Beam position: 999.5
Column length: 1999



Beam
Shape: IPE300
Height: [] **Width:** []
Flange thickness: [] **Web thickness:** []
Root radius: [] **Flange-to-web welds:** []



Column
Shape: HEB180
Height: [] **Width:** []
Flange thickness: [] **Web thickness:** []
Root radius: [] **Flange-to-web welds:** []
 Supplementary web plate **Thickness:** []
 Continuity **Thickness:** []

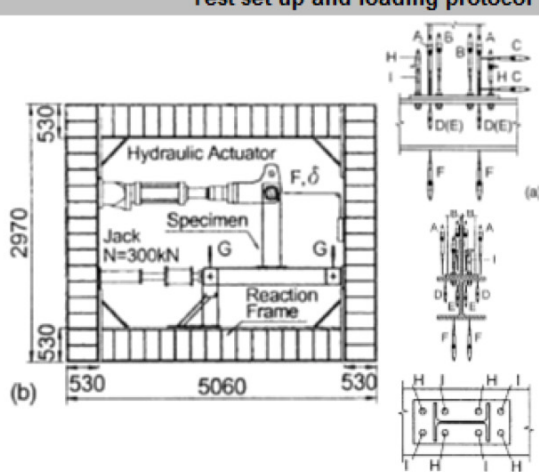
End-plate
hp: 520 **bp:** 180 **ep:** 37.5 **exs:** 50 **mx1:** 50.0 **p1:** 180
tp: 18.6 **w:** 105 **exi:** 50 **mx2:** 49.3 **p2:** []
 Rib **Thickness:** [] **mx3:** 49.3 **mx4:** 50.0

Bolts
Rows in tension: 3 **Bolts per row:** 2
Diameter: 20 **Tensile stress:** 245
 Washer
 Washer nut
 Throat
 Leg thickness
Flange: 7.5 **Web:** -

Notes:

The beam length provided is the distance between the point of application of the force and the column support axis. The beam length is 1350mm and the column length is 2220mm [Deng *et al.*, 2000].

Test JB1-3A

Material properties (MPa)		
Beam <input type="checkbox"/> Nominal values S275 <input checked="" type="checkbox"/> Measured values $f_y, f_u:$ 307.0 $f_y, w:$ 328.0 $f_u, f_u:$ 471.0 $f_u, w:$ 477.0 Young's modulus <input type="checkbox"/> Nominal Ef: 191875 <input checked="" type="checkbox"/> Measured Ew: 192941	Column <input type="checkbox"/> Nominal values S275 <input checked="" type="checkbox"/> Measured values $f_y, f_u:$ 292.0 $f_y, w:$ 316.0 $f_u, f_u:$ 478.0 $f_u, w:$ 493.0 Young's modulus <input type="checkbox"/> Nominal Ef: 243333 <input checked="" type="checkbox"/> Measured Ew: 185882	End-plate <input type="checkbox"/> Nominal values S275 <input checked="" type="checkbox"/> Measured values Yield strength: 318.0 Ultimate strength: 441.0 Young's modulus <input type="checkbox"/> Nominal E: 198750 <input checked="" type="checkbox"/> Measured E: 198750
Bolts <input type="checkbox"/> Nominal values 8.8 <input checked="" type="checkbox"/> Measured values Yield strength: 888.0 Ultimate strength: 948.0 Young's modulus <input type="checkbox"/> Nominal E: 206512 <input checked="" type="checkbox"/> Measured E: 206512	Continuity plate <input type="checkbox"/> Nominal values <input type="checkbox"/> Measured values Yield strength: Ultimate strength: Young's modulus <input type="checkbox"/> Nominal E: <input type="checkbox"/> Measured E:	Supplementary web plate <input type="checkbox"/> Nominal values <input type="checkbox"/> Measured values Yield strength: Ultimate strength: Young's modulus <input type="checkbox"/> Nominal E: <input type="checkbox"/> Measured E:
Notes: <p>"With regard to the cyclic response, one can observe that total rotations of CJ reach values greater than 45 mrad, implying a suitable ductile behaviour for high ductile (class H) structures [CEN, 2001]. These joints exhibited failure at weld toes in the end plate part outside the beam section owing to fragile crack propagation." // Energy dissipation: Over 165 kJ [Zandonini, Bursi, 2002]</p>		
End-plate rib stiffener <input type="checkbox"/> Nominal values <input type="checkbox"/> Measured values Yield strength: Ultimate strength: Young's modulus <input type="checkbox"/> Nominal E: <input type="checkbox"/> Measured E:		
Test set up and loading protocol		
Type of test: Cyclic Loading protocol: SDTP-1 [ECCS, 1986]		Data provided: Initial stiff., moments, rotat and energy diss. Type of response: <input type="checkbox"/> Force <input checked="" type="checkbox"/> Moment <input type="checkbox"/> Displacemen <input checked="" type="checkbox"/> Rotation N and M Joint Web panel Connection

Paper**Title:**

Non-linear analysis of the low-cycle fracture behaviour of isolated tee stub connections

Authors:

Bursi, O.S. | Ferrario, F. | Fontanari, V.

Source:

Computers and Structures

Volume

Issue:

Pages:

Year:

80

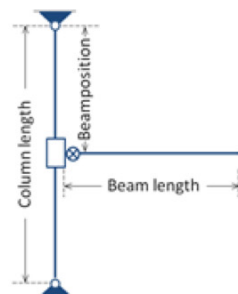
-

2333-2360

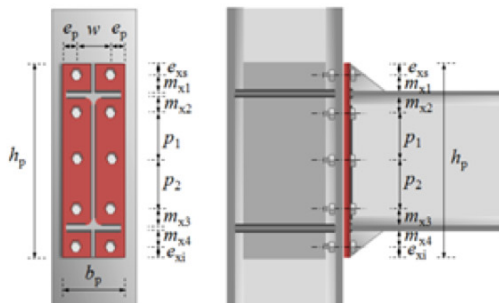
2002

Test JB1-3M**Geometry (mm)**

Scheme: External double extended end-plate joint
Beam length: 1304
Beam position: 999.5
Column length: 1999



Beam
Shape: IPE300
Height: [] **Width:** []
Flange thickness: [] **Web thickness:** []
Root radius: [] **Flange-to-web welds:** []



Column
Shape: HEB180
Height: [] **Width:** []
Flange thickness: [] **Web thickness:** []
Root radius: [] **Flange-to-web welds:** []
 Supplementary web plate **Thickness:** []
 Continuity **Thickness:** []

End-plate
hp: 520 **bp:** 180 **ep:** 37.5 **exs:** 50 **mx1:** 50.0 **p1:** 180
tp: 18.6 **w:** 105 **exi:** 50 **mx2:** 49.3 **p2:** []
 Rib **Thickness:** [] **mx3:** 49.3 **mx4:** 50.0

Bolts
Rows in tension: 3 **Bolts per row:** 2
Diameter: 20 **Tensile stress:** 245
 Washer
 Washer nut
Beam to plate welds
 Throat
 Leg thickness
Flange: 7.5 **Web:** -

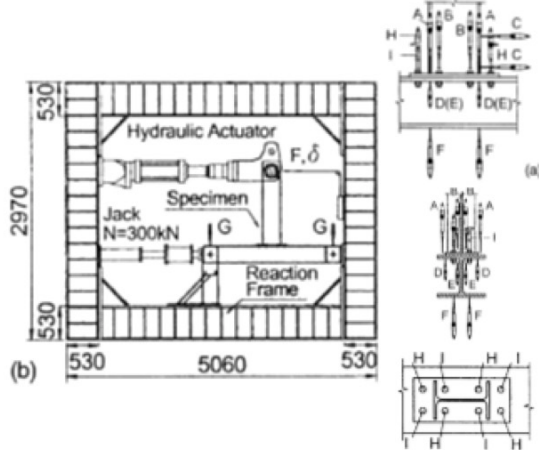
Notes:

The beam length provided is the distance between the point of application of the force and the column support axis. The beam length is 1350mm and the column length is 2220mm [Deng et al., 2000].

Test JB1-3M

Material properties (MPa)		
Beam	Column	End-plate
<input type="checkbox"/> Nominal values S275 <input checked="" type="checkbox"/> Measured values fy,f: 307.0 fy,w: 328.0 fu,f: 471.0 fu,w: 477.0 Young's modulus <input type="checkbox"/> Nominal Ef: 191875 <input checked="" type="checkbox"/> Measured Ew: 192941	<input type="checkbox"/> Nominal values S275 <input checked="" type="checkbox"/> Measured values fy,f: 292.0 fy,w: 316.0 fu,f: 478.0 fu,w: 493.0 Young's modulus <input type="checkbox"/> Nominal Ef: 243333 <input checked="" type="checkbox"/> Measured Ew: 185882	<input type="checkbox"/> Nominal values S275 <input checked="" type="checkbox"/> Measured values Yield strength: 318.0 Ultimate strength: 441.0 Young's modulus <input type="checkbox"/> Nominal E: 198750 <input checked="" type="checkbox"/> Measured E: 198750
Bolts	Continuity plate	Supplementary web plate
<input type="checkbox"/> Nominal values 8.8 <input checked="" type="checkbox"/> Measured values Yield strength: 888.0 Ultimate strength: 948.0 Young's modulus <input type="checkbox"/> Nominal E: 206512 <input checked="" type="checkbox"/> Measured E: 206512	<input type="checkbox"/> Nominal values <input type="checkbox"/> Measured values Yield strength: Ultimate strength: Young's modulus <input type="checkbox"/> Nominal E: <input type="checkbox"/> Measured E:	<input type="checkbox"/> Nominal values <input type="checkbox"/> Measured values Yield strength: Ultimate strength: Young's modulus <input type="checkbox"/> Nominal E: <input type="checkbox"/> Measured E:
Notes:		
<p>"The monotonic response is characterized by inelastic phenomena activated in the end plate, the column flange and the column web panel in shear." // The joint reached an overall rotation near to the 100mrad.</p>		
End-plate rib stiffener		
<input type="checkbox"/> Nominal values <input type="checkbox"/> Measured values Yield strength: Ultimate strength: Young's modulus <input type="checkbox"/> Nominal E: <input type="checkbox"/> Measured E:		

Test set up and loading protocol

Type of test:	Monotonic
Loading protocol:	
Data provided:	Initial stiff., moments, rotat.
Type of response:	<input type="checkbox"/> Force <input checked="" type="checkbox"/> Moment <input type="checkbox"/> Displacemen <input checked="" type="checkbox"/> Rotation
	N and M Joint Web panel Connection
	

Paper

Title:
Monotonic and hysteretic behaviour of bolted endplate beam-to-column joints

Authors:
Zandonini, R. Bursi, O.S.

Source:
Proc. of Advanced in Steel Structures, Hong Kong, China

Volume	Issue:	Pages:	Year:
1	-	81-94	2002

Test JA1-2M

Geometry (mm)

Scheme: External double extended end-plate joint

Beam length: 1298
Beam position: 1000
Column length: 2000

Beam

Shape: IPE300
Height: [] Width: []
Flange thickness: [] Web thickness: []
Root radius: [] Flange-to-web welds: []

Column

Shape: HEA180
Height: [] Width: []
Flange thickness: [] Web thickness: []
Root radius: [] Flange-to-web welds: []
 Supplementary web plate Thickness: []
 Continuity Thickness: []

End-plate

hp:	520
bp:	180
tp:	12.5
ep:	37.5
w:	105
exs:	50
mx1:	50.0
p1:	180
exi:	50
mx2:	49.3
p2:	[]
mx3:	49.3
mx4:	50.0

Rib
 Thickness []

Bolts

Rows in tension:	3
Bolts per row:	2
Diameter:	20
Tensile stress:	245

Washer
 Washer nut

Beam to plate welds

Throat	<input type="checkbox"/>
Leg thickness	<input checked="" type="checkbox"/>
Flange:	7.5
Web:	-

Notes:
The beam length provided is the distance between the point of application of the force and the column support axis. The beam length is 1350mm and the column length is 2220mm [Deng et al., 2000].

Test JA1-2M

		Material properties (MPa)	
Beam		Column	
<input type="checkbox"/> Nominal values S275 <input checked="" type="checkbox"/> Measured values fy,f: 307.0 fy,w: 328.0 fu,f: 471.0 fu,w: 477.0 Young's modulus <input type="checkbox"/> Nominal Ef: 191875 <input checked="" type="checkbox"/> Measured Ew: 192941		<input type="checkbox"/> Nominal values S275 <input checked="" type="checkbox"/> Measured values fy,f: 317.0 fy,w: 373.0 fu,f: 471.0 fu,w: 494.0 Young's modulus <input type="checkbox"/> Nominal Ef: 176111 <input checked="" type="checkbox"/> Measured Ew: 207222	
Bolts		Continuity plate	
<input type="checkbox"/> Nominal values 8.8 <input checked="" type="checkbox"/> Measured values Yield strength: 888.0 Ultimate strength: 948.0 Young's modulus <input type="checkbox"/> Nominal E: 206512 <input checked="" type="checkbox"/> Measured E: 206512		<input type="checkbox"/> Nominal values <input type="checkbox"/> Measured values Yield strength: Ultimate strength: Young's modulus <input type="checkbox"/> Nominal E: <input checked="" type="checkbox"/> Measured E:	
End-plate		Supplementary web plate	
<input type="checkbox"/> Nominal values S275 <input checked="" type="checkbox"/> Measured values Yield strength: 260.0 Ultimate strength: 442.0 Young's modulus <input type="checkbox"/> Nominal E: <input checked="" type="checkbox"/> Measured E: 200000		<input type="checkbox"/> Nominal values <input type="checkbox"/> Measured values Yield strength: Ultimate strength: Young's modulus <input type="checkbox"/> Nominal E: <input checked="" type="checkbox"/> Measured E:	
Notes:		<p>"The monotonic tests confirmed the high rotation capacity coupled with extensive yield of the main joint components." // The joint reached an overall rotation over the 100mrad.</p>	
		End-plate rib stiffener	
		<input type="checkbox"/> Nominal values <input type="checkbox"/> Measured values Yield strength: Ultimate strength: Young's modulus <input type="checkbox"/> Nominal E: <input checked="" type="checkbox"/> Measured E:	
Test set up and loading protocol			
Type of test:	Monotonic		
Loading protocol:	<input type="checkbox"/> <input type="checkbox"/>		
Data provided:	Initial stiff., moments, rotat.		
Type of response:	<input type="checkbox"/> Force <input checked="" type="checkbox"/> Moment <input type="checkbox"/> Displacemen <input checked="" type="checkbox"/> Rotation		

Paper

Title:
Monotonic and hysteretic behaviour of bolted endplate beam-to-column joints

Authors:
Zandonini, R. Bursi, O.S.

Source:
Proc. of Advanced in Steel Structures, Hong Kong, China

Volume	Issue:	Pages:	Year:
1	-	81-94	2002

Test JA1-2A

Geometry (mm)

Scheme: External double extended end-plate joint

Beam length: 1298
Beam position: 1000
Column length: 2000

Beam

Shape: IPE300
Height: [] Width: []
Flange thickness: [] Web thickness: []
Root radius: [] Flange-to-web welds: []

Column

Shape: HEA180
Height: [] Width: []
Flange thickness: [] Web thickness: []
Root radius: [] Flange-to-web welds: []

Supplementary web plate Thickness: []
 Continuity Thickness: []

End-plate

hp:	520
bp:	180
tp:	12.5
ep:	37.5
w:	105
exs:	50
mx1:	50.0
p1:	180
exi:	50
mx2:	49.3
p2:	[]
mx3:	49.3
mx4:	50.0

Rib
 Thickness []

Bolts

Rows in tension: 3
Bolts per row: 2
Diameter: 20
Tensile stress: 245

Washer
 Washer nut

Beam to plate welds

Throat
 Leg thickness
Flange: 7.5
Web: []

Notes:

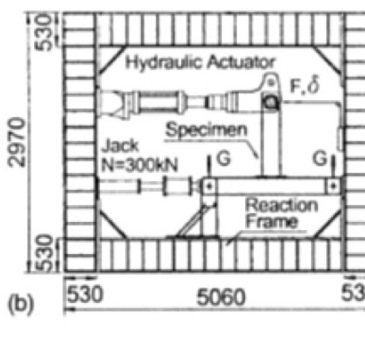
The beam length provided is the distance between the point of application of the force and the column support axis. The beam length is 1350mm and the column length is 2220mm [Deng et al., 2000].

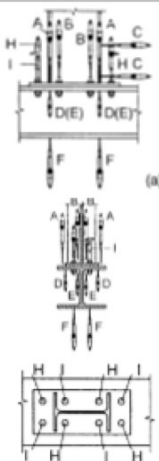
Test JA1-2A

Material properties (MPa)		
Beam <input type="checkbox"/> Nominal values S275 <input checked="" type="checkbox"/> Measured values fy,f: 307.0 fy,w: 328.0 fu,f: 471.0 fu,w: 477.0 Young's modulus <input type="checkbox"/> Nominal Ef: 191875 <input checked="" type="checkbox"/> Measured Ew: 192941	Column <input type="checkbox"/> Nominal values S275 <input checked="" type="checkbox"/> Measured values fy,f: 317.0 fy,w: 373.0 fu,f: 471.0 fu,w: 494.0 Young's modulus <input type="checkbox"/> Nominal Ef: 176111 <input checked="" type="checkbox"/> Measured Ew: 207222	End-plate <input type="checkbox"/> Nominal values S275 <input checked="" type="checkbox"/> Measured values Yield strength: 260.0 Ultimate strength: 442.0 Young's modulus <input type="checkbox"/> Nominal E: 200000 <input checked="" type="checkbox"/> Measured E: 200000
Bolts <input type="checkbox"/> Nominal values 8.8 <input checked="" type="checkbox"/> Measured values Yield strength: 888.0 Ultimate strength: 948.0 Young's modulus <input type="checkbox"/> Nominal E: 206512 <input checked="" type="checkbox"/> Measured E: 206512	Continuity plate <input type="checkbox"/> Nominal values <input type="checkbox"/> Measured values Yield strength: Ultimate strength: Young's modulus <input type="checkbox"/> Nominal E: <input checked="" type="checkbox"/> Measured E:	Supplementary web plate <input type="checkbox"/> Nominal values <input type="checkbox"/> Measured values Yield strength: Ultimate strength: Young's modulus <input type="checkbox"/> Nominal E: <input checked="" type="checkbox"/> Measured E:
Notes: <p>"(...) response of joint JA1-2A is plotted in Fig. 10. Similar behavioural features were observed for the joint JB1-3A, and for the twin specimens JA1-2B and JB1-3B. These joints achieve values of plastic rotation greater than 35 mrad, implying a satisfactory ductile behavior for seismic applications (...) (...) the contribution of the column web panel is in all cases significant (...) Failure of all specimens occurred at weld toes in the extension of the end plate by fragile crack propagation." // Energy dissipation: Over 90 kJ.</p>		
End-plate rib stiffener <input type="checkbox"/> Nominal values <input type="checkbox"/> Measured values Yield strength: Ultimate strength: Young's modulus <input type="checkbox"/> Nominal E: <input checked="" type="checkbox"/> Measured E:		

Test set up and loading protocol

Type of test:	Cyclic
Loading protocol:	SDIP-1 [ECCS, 1986]
Data provided:	Initial stiff., moments, rotat and energy diss.
Type of response:	<input type="checkbox"/> Force <input checked="" type="checkbox"/> Moment <input type="checkbox"/> Displacemen <input checked="" type="checkbox"/> Rotation
	N and M Joint Web panel Connection





Paper

Title:
Monotonic and hysteretic behaviour of bolted endplate beam-to-column joints

Authors:
Zandonini, R. Bursi, O.S.

Source:
Proc. of Advanced in Steel Structures, Hong Kong, China

Volume	Issue:	Pages:	Year:
1	-	81-94	2002

Test JA1-2B

Geometry (mm)

Scheme: External double extended end-plate joint

Beam length: 1298
Beam position: 1000
Column length: 2000

Beam

Shape: IPE300
Height: [] Width: []
Flange thickness: [] Web thickness: []
Root radius: [] Flange-to-web welds: []

Column

Shape: HEA180
Height: [] Width: []
Flange thickness: [] Web thickness: []
Root radius: [] Flange-to-web welds: []
 Supplementary web plate Thickness: []
 Continuity Thickness: []

End-plate

hp:	520
bp:	180
tp:	12.5
ep:	37.5
w:	105
exs:	50
mx1:	50.0
p1:	180
exi:	50
mx2:	49.3
p2:	[]
mx3:	49.3
mx4:	50.0

Rib
 Thickness []

Bolts

Rows in tension:	3
Bolts per row:	2
Diameter:	20
Tensile stress:	245

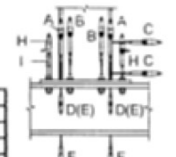
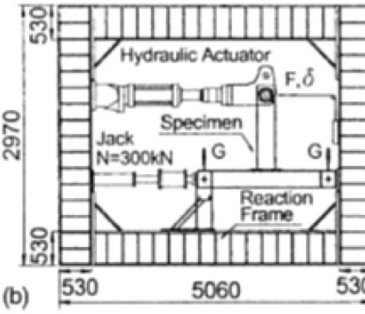
Washer
 Washer nut

Beam to plate welds

Throat	<input type="checkbox"/>
Leg thickness	<input checked="" type="checkbox"/>
Flange:	7.5
Web:	-

Notes:
The beam length provided is the distance between the point of application of the force and the column support axis. The beam length is 1350mm and the column length is 2220mm [Deng et al., 2000].

Test JA1-2B

Material properties (MPa)		
Beam <input type="checkbox"/> Nominal values S275 <input checked="" type="checkbox"/> Measured values fy,f: 307.0 fy,w: 328.0 fu,f: 471.0 fu,w: 477.0 Young's modulus <input type="checkbox"/> Nominal Ef: 191875 <input checked="" type="checkbox"/> Measured Ew: 192941	Column <input type="checkbox"/> Nominal values S275 <input checked="" type="checkbox"/> Measured values fy,f: 317.0 fy,w: 373.0 fu,f: 471.0 fu,w: 494.0 Young's modulus <input type="checkbox"/> Nominal Ef: 176111 <input checked="" type="checkbox"/> Measured Ew: 207222	End-plate <input type="checkbox"/> Nominal values S275 <input checked="" type="checkbox"/> Measured values Yield strength: 260.0 Ultimate strength: 442.0 Young's modulus <input type="checkbox"/> Nominal E: 200000 <input checked="" type="checkbox"/> Measured E: 200000
Bolts <input type="checkbox"/> Nominal values 8.8 <input checked="" type="checkbox"/> Measured values Yield strength: 888.0 Ultimate strength: 948.0 Young's modulus <input type="checkbox"/> Nominal E: 206512 <input checked="" type="checkbox"/> Measured E: 206512	Continuity plate <input type="checkbox"/> Nominal values <input type="checkbox"/> Measured values Yield strength: Ultimate strength: Young's modulus <input type="checkbox"/> Nominal E: <input checked="" type="checkbox"/> Measured E:	Supplementary web plate <input type="checkbox"/> Nominal values <input type="checkbox"/> Measured values Yield strength: Ultimate strength: Young's modulus <input type="checkbox"/> Nominal E: <input checked="" type="checkbox"/> Measured E:
Notes: <p>"(...) response of joint JA1-2A is plotted in Fig. 10. Similar behavioural features were observed for the joint JB1-3A, and for the twin specimens JA1-2B and JB1-3B. These joints achieve values of plastic rotation greater than 35 mrad, implying a satisfactory ductile behavior for seismic applications (...) (...) the contribution of the column web panel is in all cases significant (...) Failure of all specimens occurred at weld toes in the extension of the end plate by fragile crack propagation."</p>		
Test set up and loading protocol		
Type of test: Cyclic Loading protocol: SDIP-1 [ECCS, 1986]		
Data provided: Initial stiff., moments, rotat and energy diss.	Type of response: <input type="checkbox"/> Force <input checked="" type="checkbox"/> Moment <input type="checkbox"/> Displacemen <input checked="" type="checkbox"/> Rotation	<input type="checkbox"/> N and M Joint Web panel Connection

Paper**Title:**

Monotonic and hysteretic behaviour of bolted endplate beam-to-column joints

Authors:

Zandonini, R. Bursi, O.S.

Source:

Proc. of Advanced in Steel Structures, Hong Kong, China

Volume**Issue:****Pages:**

1 - 81-94

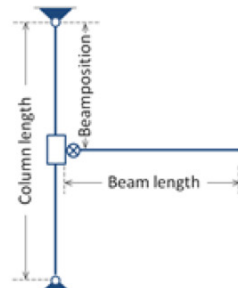
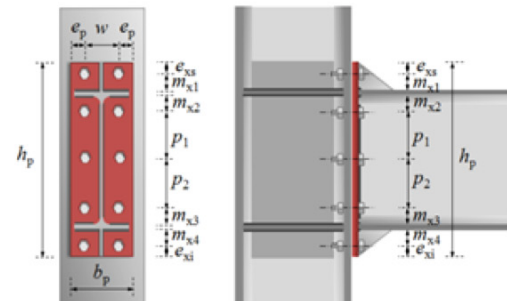
Year:

2002

Test JB1-3B**Geometry**

(mm)

Scheme: External double extended end-plate joint

Beam length: 1304**Beam position:** 999.5**Column length:** 1999**Beam****Shape:** IPE300**Height:** []**Width:** []**Flange thickness:** []**Web thickness:** []**Root radius:** []**Flange-to-web welds:** []**Column****Shape:** HEB180**Height:** []**Width:** []**Flange thickness:** []**Web thickness:** []**Root radius:** []**Flange-to-web welds:** []

Supplementary web plate
 Continuity

Thickness: []
Thickness: []

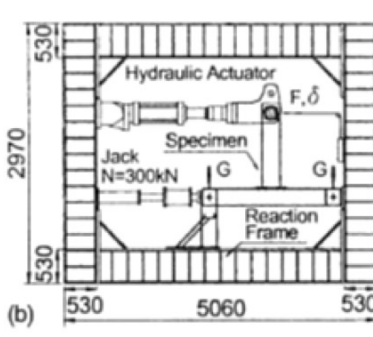
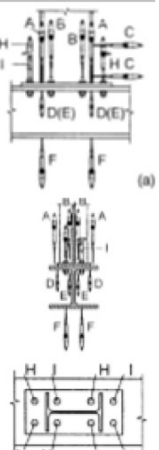
End-plate					
hp:	520	bp:	180	ep:	37.5
tp:	18.6	w:	105	exs:	50
Thickness		mx1:	50.0	p1:	180
<input type="checkbox"/> Rib		mx2:	49.3	mx3:	49.3
		mx4:	50.0		

Bolts		Beam to plate welds	
Rows in tension:	3	<input type="checkbox"/> Throat	
Bolts per row:	2	<input checked="" type="checkbox"/> Leg thickness	
Diameter:	20	Flange:	7.5
Tensile stress:	245	Web:	-
<input checked="" type="checkbox"/> Washer			
<input checked="" type="checkbox"/> Washer nut			

Notes:

The beam length provided is the distance between the point of application of the force and the column support axis. The beam length is 1350mm and the column length is 2220mm [Deng et al., 2000].

Test JB1-3B

		Material properties (MPa)	
Beam		Column	
<input type="checkbox"/> Nominal values S275 <input checked="" type="checkbox"/> Measured values fy,f: 307.0 fy,w: 328.0 fu,f: 471.0 fu,w: 477.0 Young's modulus <input type="checkbox"/> Nominal Ef: 191875 <input checked="" type="checkbox"/> Measured Ew: 192941		<input type="checkbox"/> Nominal values S275 <input checked="" type="checkbox"/> Measured values fy,f: 292.0 fy,w: 316.0 fu,f: 478.0 fu,w: 493.0 Young's modulus <input type="checkbox"/> Nominal Ef: 243333 <input checked="" type="checkbox"/> Measured Ew: 185882	
Bolts		Continuity plate	
<input type="checkbox"/> Nominal values 8.8 <input checked="" type="checkbox"/> Measured values Yield strength: 888.0 Ultimate strength: 948.0 Young's modulus <input type="checkbox"/> Nominal E: 206512 <input checked="" type="checkbox"/> Measured E: 192941		<input type="checkbox"/> Nominal values <input type="checkbox"/> Measured values Yield strength: Ultimate strength: Young's modulus <input type="checkbox"/> Nominal E: <input checked="" type="checkbox"/> Measured E:	
End-plate		Supplementary web plate	
<input type="checkbox"/> Nominal values S275 <input checked="" type="checkbox"/> Measured values Yield strength: 318.0 Ultimate strength: 441.0 Young's modulus <input type="checkbox"/> Nominal E: <input checked="" type="checkbox"/> Measured E: 198750		<input type="checkbox"/> Nominal values <input type="checkbox"/> Measured values Yield strength: Ultimate strength: Young's modulus <input type="checkbox"/> Nominal E: <input checked="" type="checkbox"/> Measured E:	
Notes:		<p>" Similar behavioural features were observed for the joint JB1-3A, and for the twin specimens JAI-2B and JB1-3B. These joints achieve values of plastic rotation greater than 35 mrad, implying a satisfactory ductile behavior for seismic applications(...). It should be noted that the contribution of the column web panel is in all cases significant (...). Failure of all specimens occurred at weld toes in the extension of the end plate by fragile crack propagation."</p>	
Test set up and loading protocol			
Type of test:	Cyclic		
Loading protocol:	SDIP-1 [ECCS, 1986]		
Data provided:	Initial stiffness and energy dissipation.		
Type of response:	<input type="checkbox"/> Force <input checked="" type="checkbox"/> Moment <input type="checkbox"/> Displacement <input checked="" type="checkbox"/> Rotation		
			

Paper**Title:**

Cyclic tests of double-sided beam-to-column joints

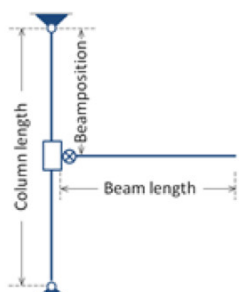
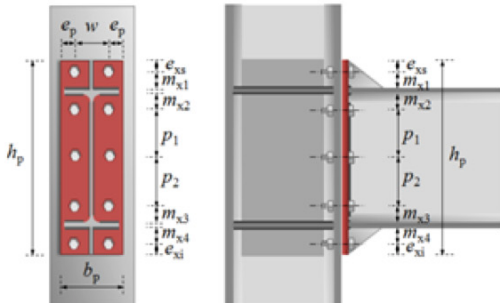
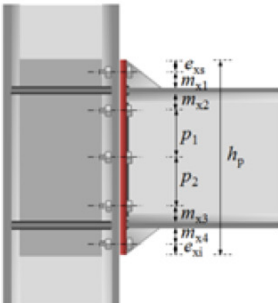
Authors:

Dubina, D. Ciutina, A. Stratan, A.

Source:

Journal of Structural Engineering Volume 127 Issue 2 Pages 129-136 Year: 2001

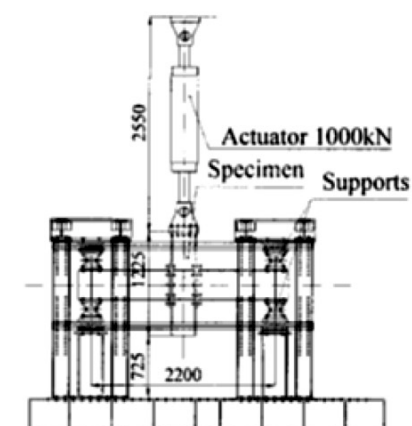
Test XS-EP1

Geometry (mm)	
Scheme: Internal joint symmetric load; Ext. end-plate	
Beam length: 950	Height: <input type="text"/>
Beam position: 612.5	Width: <input type="text"/>
Column length: 1225	Flange thickness: <input type="text"/> Web thickness: <input type="text"/> Root radius: <input type="text"/> Flange-to-web welds: <input type="text"/>
	Shape: IPE360
	Shape: HEB300
End-plate	Column
hp: 530	Height: <input type="text"/>
bp: 220	Width: <input type="text"/>
tp: 20	Flange thickness: <input type="text"/> Web thickness: <input type="text"/> Root radius: <input type="text"/> Flange-to-web welds: <input type="text"/>
ep: 40	Supplementary web plate: <input type="checkbox"/> Thickness: <input type="text"/>
exi: 45	Continuity: <input checked="" type="checkbox"/> Thickness: 15
mx1: 40.0	Diameter: 20
mx2: 47.3	Tensile stress: 245
mx3: 47.3	Bolts per row: 2
mx4: 40.0	Rows in tension: 4
<input type="checkbox"/> Rib	Bolts: <input type="checkbox"/> Throat
Thickness: <input type="text"/>	<input type="checkbox"/> Leg thickness
	Beam to plate welds:
	<input type="checkbox"/> Flange: FP
	<input type="checkbox"/> Web: FW
	<input checked="" type="checkbox"/> Washer
	<input checked="" type="checkbox"/> Washer nut

Notes:

The beam length provided is the distance between the axis of the beam support to the column flange. FP stands for full-penetration welds and FW fillet welds.

Test XS-EP1

Material properties (MPa)		
Beam	Column	End-plate
<input type="checkbox"/> Nominal values S235 <input checked="" type="checkbox"/> Measured values fy,f: 329.8 fy,w: 348.4 fu,f: 463.2 fu,w: 464.0 Young's modulus <input checked="" type="checkbox"/> Nominal Ef: <input type="text"/> <input type="checkbox"/> Measured Ew: <input type="text"/>	<input type="checkbox"/> Nominal values S235 <input checked="" type="checkbox"/> Measured values fy,f: 313.0 fy,w: 341.8 fu,f: 449.8 fu,w: 464.4 Young's modulus <input checked="" type="checkbox"/> Nominal Ef: <input type="text"/> <input type="checkbox"/> Measured Ew: <input type="text"/>	<input type="checkbox"/> Nominal values S235 <input checked="" type="checkbox"/> Measured values Yield strength: 248.3 Ultimate strength: 416.0 Young's modulus <input checked="" type="checkbox"/> Nominal E: <input type="text"/> <input type="checkbox"/> Measured E: <input type="text"/>
Bolts	Continuity plate	Supplementary web plate
<input checked="" type="checkbox"/> Nominal values 10.9 <input type="checkbox"/> Measured values Yield strength: <input type="text"/> Ultimate strength: <input type="text"/> Young's modulus <input checked="" type="checkbox"/> Nominal E: <input type="text"/> <input type="checkbox"/> Measured E: <input type="text"/>	<input type="checkbox"/> Nominal values <input type="text"/> <input type="checkbox"/> Measured values Yield strength: <input type="text"/> Ultimate strength: <input type="text"/> Young's modulus <input type="checkbox"/> Nominal E: <input type="text"/> <input checked="" type="checkbox"/> Measured E: <input type="text"/>	<input type="checkbox"/> Nominal values <input type="text"/> <input type="checkbox"/> Measured values Yield strength: <input type="text"/> Ultimate strength: <input type="text"/> Young's modulus <input type="checkbox"/> Nominal E: <input type="text"/> <input checked="" type="checkbox"/> Measured E: <input type="text"/>
Notes: <p>"The specified welds of the beam flanges/cover plates to the column flanges/end plate are of full-penetration type, while the beam web is welded with fillet welds." (...) "The yield stress of the tested elements is higher than the specified one, the actual steel grade of beam and column being rather grade S275." // Yielding mode: Plate yield + -2e_y // Failure mode: Weld rupture bottom beam flange at + -4e_y</p>		
Test set up and loading protocol		
Type of test: Cyclic		
Loading protocol: ECCS procedure		
Amplitude inc. = e _y		
Data provided: Initial stiff., moments, rotations and energy d.		
Type of response:		
<input type="checkbox"/> Force		
<input checked="" type="checkbox"/> Moment		
<input type="checkbox"/> Displacemen		
<input checked="" type="checkbox"/> Rotation		
		

Paper

Title:
Cyclic tests of double-sided beam-to-column joints

Authors:
Dubina, D. Ciutina, A. Stratan, A.

Source:
Journal of Structural Engineering

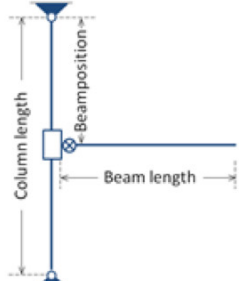
Volume	Issue:	Pages:	Year:
127	2	129-136	2001

Test XS-EP2

Geometry (mm)

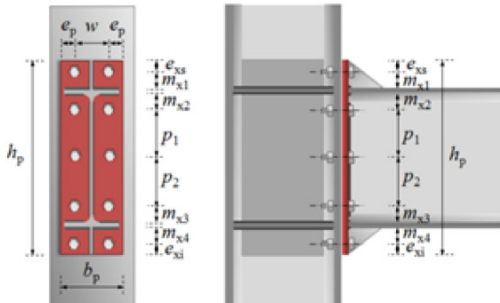
Scheme: Internal joint symmetric load.; Ext. end-plate

Beam length: 950
Beam position: 612.5
Column length: 1225



Beam

Shape: IPE360
Height: [] Width: []
Flange thickness: [] Web thickness: []
Root radius: [] Flange-to-web welds: []



Column

Shape: HEB300
Height: [] Width: []
Flange thickness: [] Web thickness: []
Root radius: [] Flange-to-web welds: []

Supplementary web plate Thickness: []
 Continuity Thickness: 15

End-plate

hp: 530
bp: 220 ep: 40 exs: 45 mx1: 40.0 p1: 120
tp: 20 w: 140 exi: 45 mx2: 47.3 p2: 120
mx3: 47.3 mx4: 40.0

Rib
 Thickness []

Bolts

Rows in tension: 4 Bolts per row: 2
Diameter: 20 Tensile stress: 245

Washer
 Washer nut

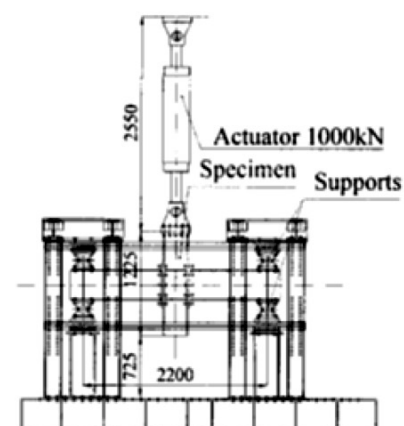
Beam to plate welds

Throat
 Leg thickness
Flange: FP
Web: FW

Notes:

The beam length provided is the distance between the axis of the beam support to the column flange. FP stands for full-penetration welds and FW fillet welds.

Test XS-EP2

Material properties (MPa)		
Beam <input type="checkbox"/> Nominal values S235 <input checked="" type="checkbox"/> Measured values fy,f: 329.8 fy,w: 348.4 fu,f: 463.2 fu,w: 464.0 Young's modulus <input checked="" type="checkbox"/> Nominal Ef: <input type="text"/> <input type="checkbox"/> Measured Ew: <input type="text"/>	Column <input type="checkbox"/> Nominal values S235 <input checked="" type="checkbox"/> Measured values fy,f: 313.0 fy,w: 341.8 fu,f: 449.8 fu,w: 464.4 Young's modulus <input checked="" type="checkbox"/> Nominal Ef: <input type="text"/> <input type="checkbox"/> Measured Ew: <input type="text"/>	End-plate <input type="checkbox"/> Nominal values S235 <input checked="" type="checkbox"/> Measured values Yield strength: 248.3 Ultimate strength: 416.0 Young's modulus <input checked="" type="checkbox"/> Nominal E: <input type="text"/> <input type="checkbox"/> Measured E: <input type="text"/>
Bolts <input checked="" type="checkbox"/> Nominal values 10.9 <input type="checkbox"/> Measured values Yield strength: <input type="text"/> Ultimate strength: <input type="text"/> Young's modulus <input checked="" type="checkbox"/> Nominal E: <input type="text"/> <input type="checkbox"/> Measured E: <input type="text"/>	Continuity plate <input type="checkbox"/> Nominal values <input type="text"/> <input type="checkbox"/> Measured values Yield strength: <input type="text"/> Ultimate strength: <input type="text"/> Young's modulus <input type="checkbox"/> Nominal E: <input type="text"/> <input type="checkbox"/> Measured E: <input type="text"/>	Supplementary web plate <input type="checkbox"/> Nominal values <input type="text"/> <input type="checkbox"/> Measured values Yield strength: <input type="text"/> Ultimate strength: <input type="text"/> Young's modulus <input type="checkbox"/> Nominal E: <input type="text"/> <input type="checkbox"/> Measured E: <input type="text"/>
Notes: <p>"The specified welds of the beam flanges to the end plate are of full-penetration type, while the beam web is welded with fillet welds." (...) "The yield stress of the tested elements is higher than the specified one, the actual steel grade of beam and column being rather grade S275." // Yielding / failure mode: Plate yield + 1bolt rupture of the fourth row, degradation of stiffness and energy dissip from + - 4e_y to 8e_y and + - 4e_y to 6e_y, respectively.</p>		
Test set up and loading protocol		
Type of test: Cyclic Loading protocol: ECCS procedure Amplitude inc. = e_y	Data provided: Initial stiff., moments, rotations and energy d.	
Type of response: <input type="checkbox"/> Force <input checked="" type="checkbox"/> Moment <input type="checkbox"/> Displacement <input checked="" type="checkbox"/> Rotation		

Paper**Title:**

Cyclic tests of double-sided beam-to-column joints

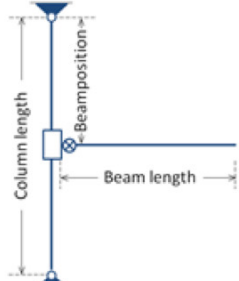
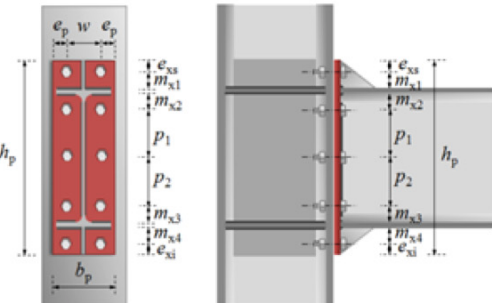
Authors:

Dubina, D. Ciutina, A. Stratan, A.

Source:

Journal of Structural Engineering Volume 127 Issue 2 Pages 129-136 Year: 2001

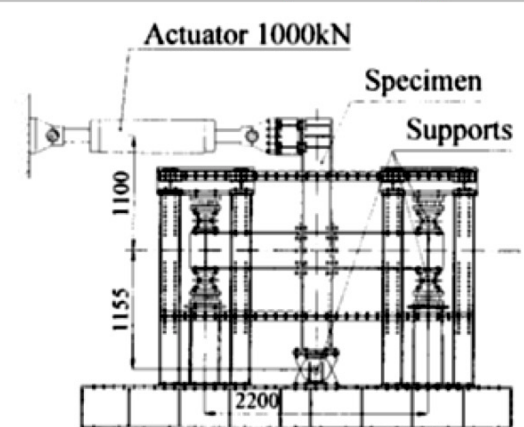
Test XU-EP1

Geometry (mm)	
Scheme: Internal joint antisymmetric; Ext. end-plate	
Beam length: 950	Height: []
Beam position: 1100	Width: []
Column length: 2255	Flange thickness: []
	Web thickness: []
	Root radius: []
	Flange-to-web welds: []
	Shape: IPE360
End-plate:	Column
hp: 530	Shape: HEB300
bp: 220	Height: []
ep: 40	Width: []
exs: 45	Flange thickness: []
mx1: 40.0	Root radius: []
p1: 120	Supplementary web plate: <input type="checkbox"/>
tp: 20	Continuity: <input checked="" type="checkbox"/>
w: 140	Thickness: []
exi: 45	Thickness: 15
mx2: 47.3	
p2: 120	
mx3: 47.3	
<input type="checkbox"/> Rib	
Thickness: []	
mx4: 40.0	
Bolts	Beam to plate welds
Rows in tension: 4	<input type="checkbox"/> Throat
Bolts per row: 2	<input type="checkbox"/> Leg thickness
Diameter: 20	Flange: FP
Tensile stress: 245	Web: FW
<input checked="" type="checkbox"/> Washer	
<input checked="" type="checkbox"/> Washer nut	

Notes:

The beam length provided is the distance between the axis of the beam support to the column flange. FP stands for full-penetration welds and FW fillet welds.

Test XU-EP1

Material properties (MPa)		
Beam <input type="checkbox"/> Nominal values S235 <input checked="" type="checkbox"/> Measured values fy,f: 329.8 fy,w: 348.4 fu,f: 463.2 fu,w: 464.0 Young's modulus <input checked="" type="checkbox"/> Nominal Ef: <input type="text"/> <input type="checkbox"/> Measured Ew: <input type="text"/>	Column <input type="checkbox"/> Nominal values S235 <input checked="" type="checkbox"/> Measured values fy,f: 313.0 fy,w: 341.8 fu,f: 449.8 fu,w: 464.4 Young's modulus <input checked="" type="checkbox"/> Nominal Ef: <input type="text"/> <input type="checkbox"/> Measured Ew: <input type="text"/>	End-plate <input type="checkbox"/> Nominal values S235 <input checked="" type="checkbox"/> Measured values Yield strength: 248.3 Ultimate strength: 416.0 Young's modulus <input checked="" type="checkbox"/> Nominal E: <input type="text"/> <input type="checkbox"/> Measured E: <input type="text"/>
Bolts <input checked="" type="checkbox"/> Nominal values 10.9 <input type="checkbox"/> Measured values Yield strength: <input type="text"/> Ultimate strength: <input type="text"/> Young's modulus <input checked="" type="checkbox"/> Nominal E: <input type="text"/> <input type="checkbox"/> Measured E: <input type="text"/>	Continuity plate <input type="checkbox"/> Nominal values <input type="text"/> <input type="checkbox"/> Measured values Yield strength: <input type="text"/> Ultimate strength: <input type="text"/> Young's modulus <input type="checkbox"/> Nominal E: <input type="text"/> <input type="checkbox"/> Measured E: <input type="text"/>	Supplementary web plate <input type="checkbox"/> Nominal values <input type="text"/> <input type="checkbox"/> Measured values Yield strength: <input type="text"/> Ultimate strength: <input type="text"/> Young's modulus <input type="checkbox"/> Nominal E: <input type="text"/> <input type="checkbox"/> Measured E: <input type="text"/>
Notes: <p>"The specified welds of the beam flanges/cover plates to the column flanges/end plate are of full-penetration type, while the beam web is welded with fillet welds." (...) "The yield stress of the tested elements is higher than the specified one, the actual steel grade of beam and column being rather grade S275." /// Yielding mode: panel zone at $+e_y$; end-plate yield $+2e_y$; crack welds at $+6e_y$ /// Failure mode: end-plate rupture at $+8e_y$</p>		
Test set up and loading protocol		
Type of test: Cyclic Loading protocol: ECCS procedure Amplitude inc. = e_y Data provided: Initial stiff., moments, rotations and energy d. Type of response: <input type="checkbox"/> Force <input checked="" type="checkbox"/> Moment <input type="checkbox"/> Displacement <input checked="" type="checkbox"/> Rotation		

Paper

Title:
Cyclic tests of double-sided beam-to-column joints

Authors:
Dubina, D. Ciutina, A. Stratan, A.

Source:
Journal of Structural Engineering

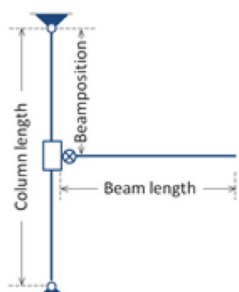
Volume	Issue:	Pages:	Year:
127	2	129-136	2001

Test XU-EP2

Geometry (mm)

Scheme: Internal joint antisymmetric; Ext. end-plate

Beam length: 950
Beam position: 1100
Column length: 2255



Beam

Shape: IPE360
Height: [] Width: []
Flange thickness: [] Web thickness: []
Root radius: [] Flange-to-web welds: []

Column

Shape: HEB300
Height: [] Width: []
Flange thickness: [] Web thickness: []
Root radius: [] Flange-to-web welds: []

Supplementary web plate Thickness: []
 Continuity Thickness: 15

End-plate

hp:	530
bp:	220
tp:	20
ep:	40
w:	140
exs:	45
mx1:	40.0
exi:	45
mx2:	47.3
p1:	120
mx3:	47.3
mx4:	40.0

Rib
 Thickness []

Bolts

Rows in tension: 4
Bolts per row: 2
Diameter: 20
Tensile stress: 245

Washer
 Washer nut

Beam to plate welds

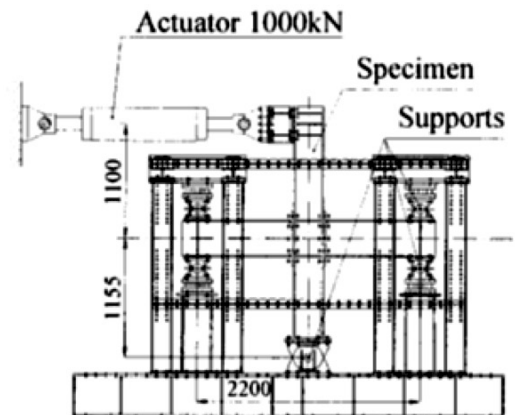
Throat
 Leg thickness

Flange: FP
Web: FW

Notes:

The beam length provided is the distance between the axis of the beam support to the column flange. FP stands for full-penetration welds and FW fillet welds.

Test XU-EP2

Material properties (MPa)		
Beam <input type="checkbox"/> Nominal values S235 <input checked="" type="checkbox"/> Measured values fy,f: 329.8 fy,w: 348.4 fu,f: 463.2 fu,w: 464.0 Young's modulus <input checked="" type="checkbox"/> Nominal Ef: <input type="text"/> <input type="checkbox"/> Measured Ew: <input type="text"/>	Column <input type="checkbox"/> Nominal values S235 <input checked="" type="checkbox"/> Measured values fy,f: 313.0 fy,w: 341.8 fu,f: 449.8 fu,w: 464.4 Young's modulus <input checked="" type="checkbox"/> Nominal Ef: <input type="text"/> <input type="checkbox"/> Measured Ew: <input type="text"/>	End-plate <input type="checkbox"/> Nominal values S235 <input checked="" type="checkbox"/> Measured values Yield strength: 248.3 Ultimate strength: 416.0 Young's modulus <input checked="" type="checkbox"/> Nominal E: <input type="text"/> <input type="checkbox"/> Measured E: <input type="text"/>
Bolts <input checked="" type="checkbox"/> Nominal values 10.9 <input type="checkbox"/> Measured values Yield strength: <input type="text"/> Ultimate strength: <input type="text"/> Young's modulus <input checked="" type="checkbox"/> Nominal E: <input type="text"/> <input type="checkbox"/> Measured E: <input type="text"/>	Continuity plate <input type="checkbox"/> Nominal values <input type="text"/> <input type="checkbox"/> Measured values Yield strength: <input type="text"/> Ultimate strength: <input type="text"/> Young's modulus <input type="checkbox"/> Nominal E: <input type="text"/> <input type="checkbox"/> Measured E: <input type="text"/>	Supplementary web plate <input type="checkbox"/> Nominal values <input type="text"/> <input type="checkbox"/> Measured values Yield strength: <input type="text"/> Ultimate strength: <input type="text"/> Young's modulus <input type="checkbox"/> Nominal E: <input type="text"/> <input type="checkbox"/> Measured E: <input type="text"/>
Notes: <p>"The specified welds of the beam flanges/cover plates to the column flanges/end plate are of full-penetration type, while the beam web is welded with fillet welds." (...) "The yield stress of the tested elements is higher than the specified one, (...)." // Yielding mode: panel zone at $+e_y$; plate yield $+2e_y$; crack welds at $+4e_y$ and bolt rupture// Failure mode: complete fracture of beam web + top flange.</p>		
Test set up and loading protocol		
Type of test: Cyclic Loading protocol: ECCS procedure <input type="checkbox"/> Amplitude inc. = e_y		Actuator 1000kN Specimen Supports 1100 1155 2200
Data provided: <input type="checkbox"/> Initial stiff., moments, rotations and energy d.		
Type of response: <input type="checkbox"/> Force <input checked="" type="checkbox"/> Moment <input type="checkbox"/> Displacement <input checked="" type="checkbox"/> Rotation		

Paper**Title:**

Cyclic tests on bolted steel and composite double-sided beam-to-column joints

Authors:

Dubina, D. Ciutina, A. Stratan, A.

Source:

Journal of Steel and Composite Structures

Volume

Issue:

Pages:

2

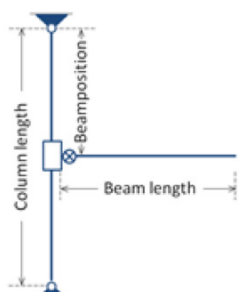
2

147-160

Year:

2002

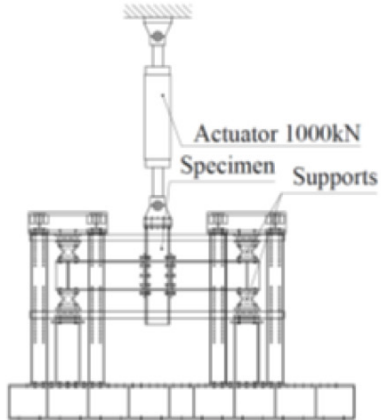
Test BX-SS-M

Geometry (mm)		
Scheme: Internal joint symmetric load; Ext. end-plate		
Beam	Shape: I	
Height: 290	Width: 150	
Flange thickness: 12	Web thickness: 8	
Root radius: []	Flange-to-web welds: [-]	
Column	Shape: I	
Height: 360	Width: 170	
Flange thickness: 14	Web thickness: 8	
Root radius: []	Flange-to-web welds: [-]	
<input type="checkbox"/> Supplementary web plate	Thickness: []	
<input checked="" type="checkbox"/> Continuity	Thickness: 12	
End-plate	Bolts	Beam to plate welds
hp: 440	Rows in tension: 3	<input type="checkbox"/> Throat
bp: 170 ep: 35 exs: 45 mx1: 30.0 p1: 190	Bolts per row: 2	<input type="checkbox"/> Leg thickness
tp: 20 w: 100 exi: 45 mx2: 38.0 p2: []	Diameter: 20	Flange: FP
mx3: 38.0	Tensile stress: 245	Web: FW
<input type="checkbox"/> Rib	<input checked="" type="checkbox"/> Washer	
Thickness: []	<input checked="" type="checkbox"/> Washer nut	

Notes:

The beam length provided is the distance between the axis of the beam support to the column flange. FP stands for full-penetration welds and FW fillet welds.

Test BX-SS-M

Material properties (MPa)					
Beam		Column		End-plate	
<input type="checkbox"/> Nominal values OL37 <input checked="" type="checkbox"/> Measured values fy,f: 310.1 fy,w: 316.2 fu,f: 470.6 fu,w: 455.7 Young's modulus <input checked="" type="checkbox"/> Nominal Ef: <input type="text"/> <input type="checkbox"/> Measured Ew: <input type="text"/>		<input type="checkbox"/> Nominal values OL37 <input checked="" type="checkbox"/> Measured values fy,f: 295.2 fy,w: 361.2 fu,f: 444.2 fu,w: 455.7 Young's modulus <input checked="" type="checkbox"/> Nominal Ef: <input type="text"/> <input type="checkbox"/> Measured Ew: <input type="text"/>		<input type="checkbox"/> Nominal values OL37 <input checked="" type="checkbox"/> Measured values Yield strength: 295.5 Ultimate strength: 484.3 Young's modulus <input checked="" type="checkbox"/> Nominal E: <input type="text"/> <input type="checkbox"/> Measured E: <input type="text"/>	
Bolts		Continuity plate		Supplementary web plate	
<input checked="" type="checkbox"/> Nominal values 10.9 <input type="checkbox"/> Measured values Yield strength: <input type="text"/> Ultimate strength: <input type="text"/> Young's modulus <input checked="" type="checkbox"/> Nominal E: <input type="text"/> <input type="checkbox"/> Measured E: <input type="text"/>		<input type="checkbox"/> Nominal values <input type="text"/> <input checked="" type="checkbox"/> Measured values Yield strength: 310.1 Ultimate strength: 470.6 Young's modulus <input checked="" type="checkbox"/> Nominal E: <input type="text"/> <input type="checkbox"/> Measured E: <input type="text"/>		<input type="checkbox"/> Nominal values <input type="text"/> <input type="checkbox"/> Measured values Yield strength: <input type="text"/> Ultimate strength: <input type="text"/> Young's modulus <input type="checkbox"/> Nominal E: <input type="text"/> <input type="checkbox"/> Measured E: <input type="text"/>	
Notes: <p>"The (...) results of the coupon tests match fairly well to the mill certificates for beam flanges, column flanges and stiffeners, while the yield strength for the end plates, beam and column webs display important differences." // Yielding mode: end-plate displacement 3e_y, column flanges 6-8e_y // Failure mode: extended bolt rupture 9.5e_y, general loss of stability 12e_y.</p>					
Test set up and loading protocol					
Type of test:	Monotonic				
Loading protocol:	<input type="text"/> <input type="text"/>				
Data provided:	Initial stiff., moments, rotations and energy d.				
Type of response:	<input type="checkbox"/> Force <input checked="" type="checkbox"/> Moment <input type="checkbox"/> Displacemen <input checked="" type="checkbox"/> Rotation				
					

Paper**Title:**

Cyclic tests on bolted steel and composite double-sided beam-to-column joints

Authors:

Dubina, D. Ciutina, A. Stratan, A.

Source:

Journal of Steel and Composite Structures

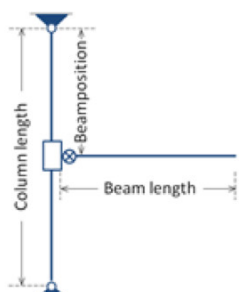
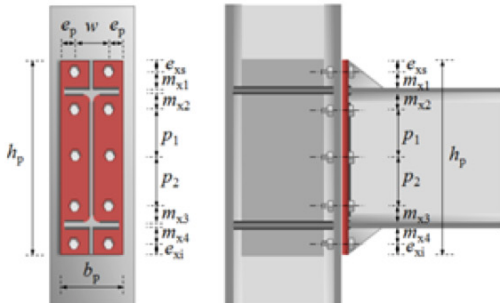
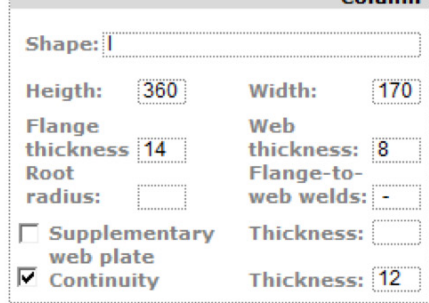
Volume 2

Issue: 2

Pages: 147-160

Year: 2002

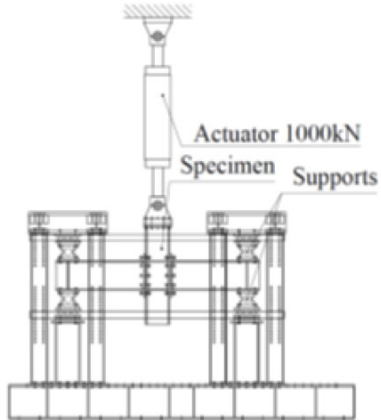
Test BX-SS-C1

Geometry (mm)		
Scheme: Internal joint symmetric load; Ext. end-plate		
Beam length: 950	Height: 290	
Beam position: 612.5	Width: 150	
Column length: 1225	Flange thickness: 12	
	Web thickness: 8	
	Root radius: -	
	Flange-to-web welds: -	
	Beam	
	Shape: I	
	Height: 290	
	Width: 150	
	Flange thickness: 12	
	Web thickness: 8	
	Root radius: -	
	Flange-to-web welds: -	
	Column	
	Shape: I	
	Height: 360	
	Width: 170	
	Flange thickness: 14	
	Web thickness: 8	
	Root radius: -	
<input type="checkbox"/> Supplementary web plate	Thickness: -	
<input checked="" type="checkbox"/> Continuity	Thickness: 12	
End-plate	Bolts	Beam to plate welds
hp: 440	Rows in tension: 3	<input type="checkbox"/> Throat
bp: 170 ep: 35 exs: 45 mx1: 30.0 p1: 190	Bolts per row: 2	<input type="checkbox"/> Leg thickness
tp: 20 w: 100 exi: 45 mx2: 38.0 p2:	Diameter: 20	Flange: FP
	Tensile stress: 245	Web: FW
<input type="checkbox"/> Rib	<input checked="" type="checkbox"/> Washer	
Thickness:	<input checked="" type="checkbox"/> Washer nut	

Notes:

The beam length provided is the distance between the axis of the beam support to the column flange. FP stands for full-penetration welds and FW fillet welds.

Test BX-SS-C1

Material properties (MPa)		
Beam <input type="checkbox"/> Nominal values OL37 <input checked="" type="checkbox"/> Measured values fy,f: 310.1 fy,w: 316.2 fu,f: 470.6 fu,w: 455.7 Young's modulus <input checked="" type="checkbox"/> Nominal Ef: <input type="text"/> <input type="checkbox"/> Measured Ew: <input type="text"/>	Column <input type="checkbox"/> Nominal values OL37 <input checked="" type="checkbox"/> Measured values fy,f: 295.2 fy,w: 361.2 fu,f: 444.2 fu,w: 455.7 Young's modulus <input checked="" type="checkbox"/> Nominal Ef: <input type="text"/> <input type="checkbox"/> Measured Ew: <input type="text"/>	End-plate <input type="checkbox"/> Nominal values OL37 <input checked="" type="checkbox"/> Measured values Yield strength: 295.5 Ultimate strength: 484.3 Young's modulus <input checked="" type="checkbox"/> Nominal E: <input type="text"/> <input type="checkbox"/> Measured E: <input type="text"/>
Bolts <input checked="" type="checkbox"/> Nominal values 10.9 <input type="checkbox"/> Measured values Yield strength: <input type="text"/> Ultimate strength: <input type="text"/> Young's modulus <input checked="" type="checkbox"/> Nominal E: <input type="text"/> <input type="checkbox"/> Measured E: <input type="text"/>	Continuity plate <input type="checkbox"/> Nominal values <input type="text"/> <input checked="" type="checkbox"/> Measured values Yield strength: 310.1 Ultimate strength: 470.6 Young's modulus <input checked="" type="checkbox"/> Nominal E: <input type="text"/> <input type="checkbox"/> Measured E: <input type="text"/>	Supplementary web plate <input type="checkbox"/> Nominal values <input type="text"/> <input type="checkbox"/> Measured values Yield strength: <input type="text"/> Ultimate strength: <input type="text"/> Young's modulus <input type="checkbox"/> Nominal E: <input type="text"/> <input type="checkbox"/> Measured E: <input type="text"/>
Notes: <p>"The (...) results of the coupon tests match fairly well to the mill certificates for beam flanges, column flanges and stiffeners, while the yield strength for the end plates, beam and column webs display important differences." // Yielding mode: end-plate+column flange yield 4-6e_y // Failure mode: Brittle failure of the lower left beam flange weld +8e_y</p>		
Test set up and loading protocol		
Type of test: <input type="text"/> Cyclic Loading protocol: <input type="text"/> ECCS procedure <input type="text"/> Amplitude inc. = e_y		Data provided: <input type="text"/> Initial stiff., moments, rotations and energy d. Type of response: <input type="checkbox"/> Force <input checked="" type="checkbox"/> Moment <input type="checkbox"/> Displacement <input checked="" type="checkbox"/> Rotation

Paper**Title:**

Cyclic testes on bolted steel and composite double-sided beam-to-column joints

Authors:

Dubina, D.

Ciutina, A.

Stratan, A.

Source:

Journal of Steel and Composite Structures

Volume

Issue:

Pages:

2

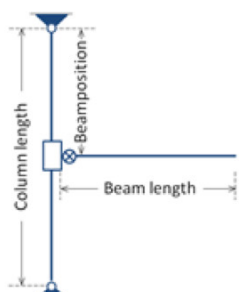
2

147-160

Year:

2002

Test BX-SS-C2

Geometry (mm)		
Scheme: Internal joint symmetric load; Ext. end-plate		
Beam		
Shape: []		
Height: 290	Width: 150	
Flange thickness: 12	Web thickness: 8	
Root radius: []	Flange-to-web welds: [-]	
Column		
Shape: []		
Height: 360	Width: 170	
Flange thickness: 14	Web thickness: 8	
Root radius: []	Flange-to-web welds: [-]	
<input type="checkbox"/> Supplementary web plate	Thickness: []	
<input checked="" type="checkbox"/> Continuity	Thickness: 12	
End-plate	Bolts Beam to plate welds	
hp: 440	Rows in tension: 3	<input type="checkbox"/> Throat
bp: 170	Bolts per row: 2	<input type="checkbox"/> Leg thickness
ep: 35	Diameter: 20	Flange: FP
exs: 45	Tensile stress: 245	Web: FW
mx1: 30.0	<input type="checkbox"/> Washer	
p1: 190	<input checked="" type="checkbox"/> Washer nut	
tp: 20		
w: 100		
exi: 45		
mx2: 38.0		
p2: []		
	mx3: 38.0	
<input type="checkbox"/> Rib	mx4: 30.0	
Thickness: []		
Notes:	The beam length provided is the distance between the axis of the beam support to the column flange. FP stands for full-penetration welds and FW fillet welds.	

Test BX-SS-C2

		Material properties (MPa)			
Beam		Column		End-plate	
<input type="checkbox"/> Nominal values OL37 <input checked="" type="checkbox"/> Measured values fy,f: 310.1 fy,w: 316.2 fu,f: 470.6 fu,w: 455.7 Young's modulus <input checked="" type="checkbox"/> Nominal Ef: <input type="text"/> <input checked="" type="checkbox"/> Measured Ew: <input type="text"/>		<input type="checkbox"/> Nominal values OL37 <input checked="" type="checkbox"/> Measured values fy,f: 295.2 fy,w: 361.2 fu,f: 444.2 fu,w: 455.7 Young's modulus <input checked="" type="checkbox"/> Nominal Ef: <input type="text"/> <input checked="" type="checkbox"/> Measured Ew: <input type="text"/>		<input type="checkbox"/> Nominal values OL37 <input checked="" type="checkbox"/> Measured values Yield strength: 295.5 Ultimate strength: 484.3 Young's modulus <input checked="" type="checkbox"/> Nominal E: <input type="text"/> <input checked="" type="checkbox"/> Measured E: <input type="text"/>	
Bolts		Continuity plate		Supplementary web plate	
<input checked="" type="checkbox"/> Nominal values 10.9 <input type="checkbox"/> Measured values Yield strength: <input type="text"/> Ultimate strength: <input type="text"/> Young's modulus <input checked="" type="checkbox"/> Nominal E: <input type="text"/> <input type="checkbox"/> Measured E: <input type="text"/>		<input type="checkbox"/> Nominal values <input type="text"/> <input checked="" type="checkbox"/> Measured values Yield strength: 310.1 Ultimate strength: 470.6 Young's modulus <input checked="" type="checkbox"/> Nominal E: <input type="text"/> <input checked="" type="checkbox"/> Measured E: <input type="text"/>		<input type="checkbox"/> Nominal values <input type="text"/> <input type="checkbox"/> Measured values Yield strength: <input type="text"/> Ultimate strength: <input type="text"/> Young's modulus <input type="checkbox"/> Nominal E: <input type="text"/> <input type="checkbox"/> Measured E: <input type="text"/>	
Notes: <p>"The (...) results of the coupon tests match fairly well to the mill certificates for beam flanges, column flanges and stiffeners, while the yield strength for the end plates, beam and column webs display important differences." // Yielding mode: end-plate + column flange yield $4-6e_y$ // Failure mode: brittle failure of the lower beam flange weld + cracking beam web $6e_y$.</p>					
Test set up and loading protocol					
Type of test:	Cyclic				
Loading protocol:	ECCS procedure				
	Amplitude inc. = e_y				
Data provided:	Initial stiff., moments, rotations and energy d.				
Type of response:	<input type="checkbox"/> Force <input checked="" type="checkbox"/> Moment <input type="checkbox"/> Displacemen <input checked="" type="checkbox"/> Rotation				

Paper**Title:**

Cyclic tests on bolted steel and composite double-sided beam-to-column joints

Authors:

Dubina, D. Ciutina, A. Stratan, A.

Source:

Journal of Steel and Composite Structures

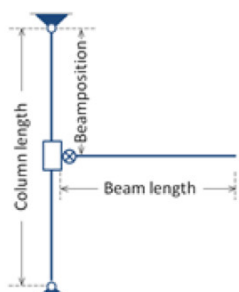
Volume 2

Issue: 2

Pages: 147-160

Year: 2002

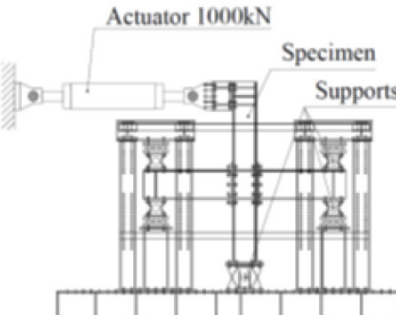
Test BX-SU-M

Geometry (mm)	
Scheme: Internal joint symmetric load; Ext. end-plate	
Beam length: 950	Height: 290
Beam position: 1100	Width: 150
Column length: 2255	Flange thickness: 12
	Web thickness: 8
	Root radius: -
	Flange-to-web welds: -
Beam	
Shape: I	
Height: 290	Width: 150
Flange thickness: 12	Web thickness: 8
Root radius: -	Flange-to-web welds: -
Column	
Shape: I	
Height: 360	Width: 170
Flange thickness: 14	Web thickness: 8
Root radius: -	Flange-to-web welds: -
<input type="checkbox"/> Supplementary web plate	Thickness: -
<input checked="" type="checkbox"/> Continuity	Thickness: 12
End-plate	
hp: 440	Bolts
bp: 170	Rows in tension: 3
ep: 35	Bolts per row: 2
exs: 45	Diameter: 20
mx1: 30.0	Tensile stress: 245
p1: 190	<input type="checkbox"/> Throat
tp: 20	<input type="checkbox"/> Leg thickness
w: 100	Flange: FP
exi: 45	Web: FW
<input type="checkbox"/> Rib	
Thickness: -	
mx2: 38.0	
mx3: 38.0	
mx4: 30.0	
Beam to plate welds	
<input type="checkbox"/> Washer	
<input checked="" type="checkbox"/> Washer nut	

Notes:

The beam length provided is the distance between the axis of the beam support to the column flange. FP stands for full-penetration welds and FW fillet welds.

Test BX-SU-M

Material properties (MPa)					
Beam		Column		End-plate	
<input type="checkbox"/> Nominal values OL37 <input checked="" type="checkbox"/> Measured values fy,f: 310.1 fy,w: 316.2 fu,f: 470.6 fu,w: 455.7 Young's modulus <input checked="" type="checkbox"/> Nominal Ef: <input type="text"/> <input type="checkbox"/> Measured Ew: <input type="text"/>		<input type="checkbox"/> Nominal values OL37 <input checked="" type="checkbox"/> Measured values fy,f: 295.2 fy,w: 361.2 fu,f: 444.2 fu,w: 455.7 Young's modulus <input checked="" type="checkbox"/> Nominal Ef: <input type="text"/> <input type="checkbox"/> Measured Ew: <input type="text"/>		<input type="checkbox"/> Nominal values OL37 <input checked="" type="checkbox"/> Measured values Yield strength: 295.5 Ultimate strength: 484.3 Young's modulus <input checked="" type="checkbox"/> Nominal E: <input type="text"/> <input type="checkbox"/> Measured E: <input type="text"/>	
Bolts		Continuity plate		Supplementary web plate	
<input checked="" type="checkbox"/> Nominal values 10.9 <input type="checkbox"/> Measured values Yield strength: <input type="text"/> Ultimate strength: <input type="text"/> Young's modulus <input checked="" type="checkbox"/> Nominal E: <input type="text"/> <input type="checkbox"/> Measured E: <input type="text"/>		<input type="checkbox"/> Nominal values <input type="text"/> <input checked="" type="checkbox"/> Measured values Yield strength: 310.1 Ultimate strength: 470.6 Young's modulus <input checked="" type="checkbox"/> Nominal E: <input type="text"/> <input type="checkbox"/> Measured E: <input type="text"/>		<input type="checkbox"/> Nominal values <input type="text"/> <input type="checkbox"/> Measured values Yield strength: <input type="text"/> Ultimate strength: <input type="text"/> Young's modulus <input type="checkbox"/> Nominal E: <input type="text"/> <input checked="" type="checkbox"/> Measured E: <input type="text"/>	
Notes: <p>"The (...) results of the coupon tests match fairly well to the mill certificates for beam flanges, column flanges and stiffeners, while the yield strength for the end plates, beam and column webs display important differences." // Yielding mode: web panel at 1-2e_y, end-plate + column flanges 4e_y, flange buckled at 5e_y // Failure mode: ext. bolt failure at 10.5e_y, second ext. bolt f. 11.5e_y.</p>					
Test set up and loading protocol					
Type of test:	Monotonic				
Loading protocol:	<input type="text"/> <input type="text"/>				
Data provided:	Initial stiff., moments, rotations and energy d.				
Type of response:	<input type="checkbox"/> Force <input checked="" type="checkbox"/> Moment <input type="checkbox"/> Displacemen <input checked="" type="checkbox"/> Rotation				
					

Paper**Title:**

Cyclic testes on bolted steel and composite double-sided beam-to-column joints

Authors:

Dubina, D.

Ciutina, A.

Stratan, A.

Source:

Journal of Steel and Composite Structures

Volume

Issue:

Pages:

2

2

147-160

Year:

2002

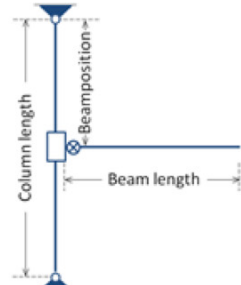
Test BX-SU-C1**Geometry (mm)**

Scheme: Internal joint
symmetric load;
Ext. end-plate

Beam length: 950

Beam position: 1100

Column length: 2255

**Beam****Shape:** []

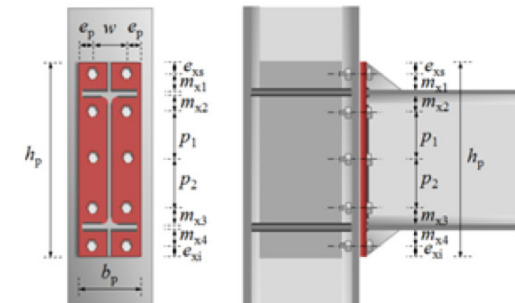
Height: 290 Width: 150

Flange thickness: 12

Web thickness: 8

Root radius: []

Flange-to-web welds: [-]

**Column****Shape:** []

Height: 360 Width: 170

Flange thickness: 14

Web thickness: 8

Root radius: []

Flange-to-web welds: [-]

 Supplementary web plate Thickness: [] Continuity Thickness: 12

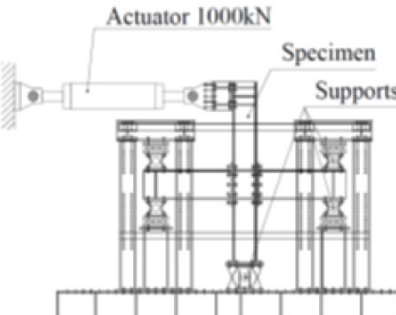
End-plate							
hp:	440						
bp:	170	ep:	35	exs:	45	mx1:	8.5 p1:
tp:	20	w:	100	exi:	45	mx2:	38.0 p2: []
						mx3:	38.0
<input type="checkbox"/> Rib						mx4:	30.0
Thickness:	[]						

Bolts		Beam to plate welds	
Rows in tension:	3	<input type="checkbox"/> Throat	
Bolts per row:	2	<input type="checkbox"/> Leg thickness	
Diameter:	20	Flange: FP	
Tensile stress:	245	Web: FW	
<input checked="" type="checkbox"/> Washer			
<input checked="" type="checkbox"/> Washer nut			

Notes:

The beam length provided is the distance between the axis of the beam support to the column flange. FP stands for full-penetration welds and FW fillet welds.

Test BX-SU-C1

Material properties (MPa)		
Beam <input type="checkbox"/> Nominal values OL37 <input checked="" type="checkbox"/> Measured values fy,f: 310.1 fy,w: 316.2 fu,f: 470.6 fu,w: 455.7 Young's modulus <input checked="" type="checkbox"/> Nominal Ef: <input type="text"/> <input type="checkbox"/> Measured Ew: <input type="text"/>	Column <input type="checkbox"/> Nominal values OL37 <input checked="" type="checkbox"/> Measured values fy,f: 295.2 fy,w: 361.2 fu,f: 444.2 fu,w: 455.7 Young's modulus <input checked="" type="checkbox"/> Nominal Ef: <input type="text"/> <input type="checkbox"/> Measured Ew: <input type="text"/>	End-plate <input type="checkbox"/> Nominal values OL37 <input checked="" type="checkbox"/> Measured values Yield strength: 295.5 Ultimate strength: 484.3 Young's modulus <input checked="" type="checkbox"/> Nominal E: <input type="text"/> <input type="checkbox"/> Measured E: <input type="text"/>
Bolts <input checked="" type="checkbox"/> Nominal values 10.9 <input type="checkbox"/> Measured values Yield strength: <input type="text"/> Ultimate strength: <input type="text"/> Young's modulus <input checked="" type="checkbox"/> Nominal E: <input type="text"/> <input type="checkbox"/> Measured E: <input type="text"/>	Continuity plate <input type="checkbox"/> Nominal values <input type="text"/> <input checked="" type="checkbox"/> Measured values Yield strength: 310.1 Ultimate strength: 470.6 Young's modulus <input checked="" type="checkbox"/> Nominal E: <input type="text"/> <input type="checkbox"/> Measured E: <input type="text"/>	Supplementary web plate <input type="checkbox"/> Nominal values <input type="text"/> <input type="checkbox"/> Measured values Yield strength: <input type="text"/> Ultimate strength: <input type="text"/> Young's modulus <input type="checkbox"/> Nominal E: <input type="text"/> <input type="checkbox"/> Measured E: <input type="text"/>
Notes: <p>"The (...) results of the coupon tests match fairly well to the mill certificates for beam flanges, column flanges and stiffeners, while the yield strength for the end plates, beam and column webs display important differences." // Yielding mode: end-plate + web panel+ column flanges at 4e_y // Failure mode: failure of the lower left beam flange weld, propagating into the end-plate until the end-plate failure 3rd 6e_y cycle.</p>		
Test set up and loading protocol		
Type of test: <input type="text"/> Cyclic Loading protocol: <input type="text"/> ECCS procedure <input type="text"/> Amplitude inc. = e_y		
Data provided: <input type="text"/> Initial stiff., moments, rotations and energy d.		
Type of response: <input type="checkbox"/> Force <input checked="" type="checkbox"/> Moment <input type="checkbox"/> Displacemen <input checked="" type="checkbox"/> Rotation		
		

Paper**Title:**

Cyclic tests on bolted steel and composite double-sided beam-to-column joints

Authors:

Dubina, D. Ciutina, A. Stratan, A.

Source:

Journal of Steel and Composite Structures

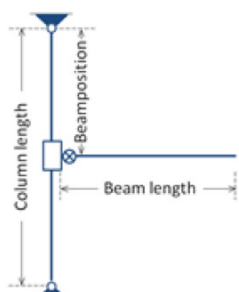
Volume 2

Issue: 2

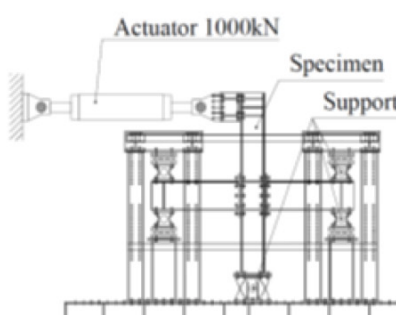
Pages: 147-160

Year: 2002

Test BX-SU-C2

Geometry (mm)	
Scheme: Internal joint symmetric load; Ext. end-plate	
Beam length: 950	Height: 290
Beam position: 1100	Width: 150
Column length: 2255	Flange thickness: 12
	Web thickness: 8
	Root radius: -
	Flange-to-web welds: -
Beam	
Shape: I	
Height: 290	Width: 150
Flange thickness: 12	Web thickness: 8
Root radius: -	Flange-to-web welds: -
Column	
Shape: I	
Height: 360	Width: 170
Flange thickness: 14	Web thickness: 8
Root radius: -	Flange-to-web welds: -
<input type="checkbox"/> Supplementary web plate	Thickness: -
<input checked="" type="checkbox"/> Continuity	Thickness: 12
End-plate	
hp: 440	Bolts
bp: 170	Rows in tension: 3
ep: 35	Bolts per row: 2
exs: 45	Diameter: 20
mx1: 30.0	Tensile stress: 245
p1: 190	<input type="checkbox"/> Throat
tp: 20	<input type="checkbox"/> Leg thickness
w: 100	Flange: FP
exi: 45	Web: FW
<input type="checkbox"/> Rib	
Thickness: -	
mx2: 38.0	
mx3: 38.0	
mx4: 30.0	
Beam to plate welds	
<input type="checkbox"/> Washer	
<input checked="" type="checkbox"/> Washer nut	
Notes:	
The beam length provided is the distance between the axis of the beam support to the column flange. FP stands for full-penetration welds and FW fillet welds.	

Test BX-SU-C2

Material properties (MPa)					
Beam		Column		End-plate	
<input type="checkbox"/> Nominal values OL37 <input checked="" type="checkbox"/> Measured values fy,f: 310.1 fy,w: 316.2 fu,f: 470.6 fu,w: 455.7 Young's modulus <input checked="" type="checkbox"/> Nominal Ef: <input type="text"/> <input type="checkbox"/> Measured Ew: <input type="text"/>		<input type="checkbox"/> Nominal values OL37 <input checked="" type="checkbox"/> Measured values fy,f: 295.2 fy,w: 361.2 fu,f: 444.2 fu,w: 455.7 Young's modulus <input checked="" type="checkbox"/> Nominal Ef: <input type="text"/> <input type="checkbox"/> Measured Ew: <input type="text"/>		<input type="checkbox"/> Nominal values OL37 <input checked="" type="checkbox"/> Measured values Yield strength: 295.5 Ultimate strength: 484.3 Young's modulus <input checked="" type="checkbox"/> Nominal E: <input type="text"/> <input type="checkbox"/> Measured E: <input type="text"/>	
Bolts		Continuity plate		Supplementary web plate	
<input checked="" type="checkbox"/> Nominal values 10.9 <input type="checkbox"/> Measured values Yield strength: <input type="text"/> Ultimate strength: <input type="text"/> Young's modulus <input checked="" type="checkbox"/> Nominal E: <input type="text"/> <input type="checkbox"/> Measured E: <input type="text"/>		<input type="checkbox"/> Nominal values <input type="text"/> <input checked="" type="checkbox"/> Measured values Yield strength: 310.1 Ultimate strength: 470.6 Young's modulus <input checked="" type="checkbox"/> Nominal E: <input type="text"/> <input type="checkbox"/> Measured E: <input type="text"/>		<input type="checkbox"/> Nominal values <input type="text"/> <input type="checkbox"/> Measured values Yield strength: <input type="text"/> Ultimate strength: <input type="text"/> Young's modulus <input type="checkbox"/> Nominal E: <input type="text"/> <input type="checkbox"/> Measured E: <input type="text"/>	
Notes: <p>"The (...) results of the coupon tests match fairly well to the mill certificates for beam flanges, column flanges and stiffeners, while the yield strength for the end plates, beam and column webs display important differences." // Yielding mode: end-plate + web pane I+ column flanges at $4e_y$ // Failure mode: weld cracks in one side, leading to end-plate rupture and consequently to 5 bolt rupture in the other side at $6e_y$.</p>					
Test set up and loading protocol					
Type of test:	<input type="checkbox"/> Cyclic				
Loading protocol:	<input type="checkbox"/> ECCS procedure <input type="checkbox"/> Amplitude inc. = e_y				
Data provided:	<input type="checkbox"/> Initial stiff., moments, rotations and energy d.				
Type of response:	<input type="checkbox"/> Force <input checked="" type="checkbox"/> Moment <input type="checkbox"/> Displacement <input checked="" type="checkbox"/> Rotation				
					

Paper

Title:
Comportamento Dinâmico de Ligações Metálicas ("Dinamic behaviour of steel joints")

Authors:
Nogueiro, P.

Source:
PhD Thesis, University of Coimbra, Portugal

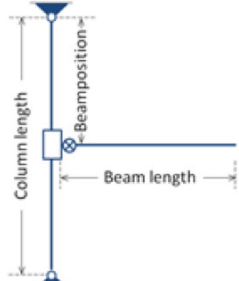
Volume Issue: -
Pages: -
Year: 2009

Test J.4.1

Geometry (mm)

Scheme: External double extended end-plate joint

Beam length: 1160
Beam position: 1775
Column length: 3260



Beam

Shape: HEA280
Height: [] Width: []
Flange thickness: [] Web thickness: []
Root radius: [] Flange-to-web welds: []

Column

Shape: HEA320
Height: [] Width: []
Flange thickness: [] Web thickness: []
Root radius: [] Flange-to-web welds: []
 Supplementary web plate Thickness: []
 Continuity Thickness: 15

End-plate

hp:	540
bp:	220
tp:	18
ep:	55
w:	110
exs:	50
mx1:	40.0
mx2:	48.5
mx3:	48.5
mx4:	40.0
<input type="checkbox"/> Rib	
<input type="checkbox"/> Thickness	

Bolts

Rows in tension:	3
Bolts per row:	2
Diameter:	24
Tensile stress:	353

Throat
 Leg thickness

Beam to plate welds

Flange:	12
Web:	8

Washer
 Washer nut

Notes:

The beam length provided is the distance between the point of application of the force and the column flange, and for the column is the distance between the pins connections supports, the real length of the column is 3000mm.

Test J-4.1

Material properties (MPa)		
Beam <input type="checkbox"/> Nominal values S355 <input checked="" type="checkbox"/> Measured values fy,f: 439.7 fy,w: 461.7 fu,f: 547.7 fu,w: 575.9 Young's modulus <input type="checkbox"/> Nominal Ef: 209400 <input checked="" type="checkbox"/> Measured Ew: 210200	Column <input type="checkbox"/> Nominal values S355 <input checked="" type="checkbox"/> Measured values fy,f: 414.8 fy,w: 449.6 fu,f: 531.4 fu,w: 553.4 Young's modulus <input type="checkbox"/> Nominal Ef: 204900 <input checked="" type="checkbox"/> Measured Ew: 207400	End-plate <input type="checkbox"/> Nominal values S355 <input checked="" type="checkbox"/> Measured values Yield strength: 405.1 Ultimate strength: 534.0 Young's modulus <input type="checkbox"/> Nominal E: 210300 <input checked="" type="checkbox"/> Measured E: 210300
Bolts <input type="checkbox"/> Nominal values 10.9 <input checked="" type="checkbox"/> Measured values Yield strength: - Ultimate strength: 1170.0 Young's modulus <input type="checkbox"/> Nominal E: 213000 <input checked="" type="checkbox"/> Measured E: 213000	Continuity plate <input type="checkbox"/> Nominal values S275 <input checked="" type="checkbox"/> Measured values Yield strength: 286.4 Ultimate strength: 451.8 Young's modulus <input type="checkbox"/> Nominal E: 205900 <input checked="" type="checkbox"/> Measured E: 205900	Supplementary web plate <input type="checkbox"/> Nominal values <input type="checkbox"/> Measured values Yield strength: Ultimate strength: Young's modulus <input type="checkbox"/> Nominal E: <input type="checkbox"/> Measured E:
Notes: Initial stiffness equal to approximately 50000 kNm/rad was obtained and a resistance approximately of 245 kNm. The observed yield rotation was 6.4 mrad and the ultimate rotation approximately 80 mrad. /// Failure mode: failure of 1 external bolt.		
End-plate rib stiffener <input type="checkbox"/> Nominal values <input type="checkbox"/> Measured values Yield strength: Ultimate strength: Young's modulus <input type="checkbox"/> Nominal E: <input type="checkbox"/> Measured E:		

Test set up and loading protocol

Type of test:	Monotonic
Loading protocol:	
Data provided:	Initial stiff., moments, rotat. and energy diss.
Type of response:	<input type="checkbox"/> Force <input checked="" type="checkbox"/> Moment <input type="checkbox"/> Displacemen <input checked="" type="checkbox"/> Rotation
	M = F.d Joint - DT11/DT12 Web panel - DT3/DT4 End-plate - DT1/DT2

The diagram illustrates the test setup for the beam-column joint. It shows a vertical column connected to a horizontal beam. Various displacement and force measurement points are indicated by labels such as DT1, DT2, DT3, DT4, DT5, DT6, DT7, DT8, DT9, DT10, DT11, DT12, DT13, DT14, DT15, and DT16. Points DT1 through DT4 are located at the joint, while points DT5 through DT16 are distributed along the beam and column sections. A coordinate system (x, y) is also shown.

Paper

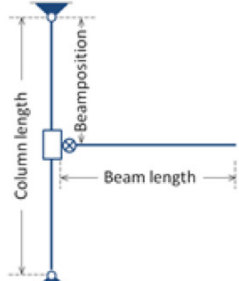
Title:
Comportamento Dinâmico de Ligações Metálicas ("Dinamic behaviour of steel joints")

Authors:
Nogueiro, P.

Source:
PhD Thesis, University of Coimbra, Portugal

Volume Issue: -
Pages: -
Year: 2009

Test J.4.2

Geometry (mm)	
Scheme: External double extended end-plate joint	
Beam length: 1170	Height: []
Beam position: 1775	Width: []
Column length: 3260	Flange thickness: []
	Web thickness: []
	Root radius: []
	Flange-to-web welds: []
Shape: HEA280	Beam
Height: []	Width: []
Flange thickness: []	Web thickness: []
Root radius: []	Flange-to-web welds: []

Column	
Shape: HEA320	Column
Height: []	Width: []
Flange thickness: []	Web thickness: []
Root radius: []	Flange-to-web welds: []
<input type="checkbox"/> Supplementary web plate	Thickness: []
<input checked="" type="checkbox"/> Continuity	Thickness: 15

End-plate	
hp: 540	Bolts
bp: 220	Rows in tension: 3
ep: 55	Bolts per row: 2
exs: 50	Diameter: 24
mx1: 40.0	Tensile stress: 353
p1: 240	<input type="checkbox"/> Throat
tp: 18	<input checked="" type="checkbox"/> Leg thickness
w: 110	Flange: 12
exi: 50	Web: 8
mx2: 48.5	
p2: []	
mx3: 48.5	
<input type="checkbox"/> Rib	<input checked="" type="checkbox"/> Washer
Thickness: []	<input checked="" type="checkbox"/> Washer nut
mx4: 40.0	

Notes:
The beam length provided is the distance between the point of application of the force and the column flange, and for the column is the distance between the pins connections supports, the real length of the column is 3000mm.

Test J4.2

Material properties					
(MPa)					
Beam			Column		
<input type="checkbox"/> Nominal values	S355		<input type="checkbox"/> Nominal values	S355	
<input checked="" type="checkbox"/> Measured values			<input checked="" type="checkbox"/> Measured values		
fy,f:	439.7	fy,w:	461.7	fy,f:	414.8
fu,f:	547.7	fu,w:	575.9	fu,f:	531.4
Young's modulus			Young's modulus		
<input type="checkbox"/> Nominal	Ef:	209400	<input type="checkbox"/> Nominal	Ef:	204900
<input checked="" type="checkbox"/> Measured	Ew:	210200	<input checked="" type="checkbox"/> Measured	Ew:	207400
Bolts					
<input type="checkbox"/> Nominal values	10.9		<input type="checkbox"/> Nominal values	S275	
<input checked="" type="checkbox"/> Measured values			<input checked="" type="checkbox"/> Measured values		
Yield strength:	-		Yield strength:	286.4	
Ultimate strength:	1170.0		Ultimate strength:	451.8	
Young's modulus			Young's modulus		
<input type="checkbox"/> Nominal	E:	213000	<input type="checkbox"/> Nominal	E:	205900
<input checked="" type="checkbox"/> Measured			<input checked="" type="checkbox"/> Measured		
Continuity plate					
<input type="checkbox"/> Nominal values	S275		<input type="checkbox"/> Nominal values	S275	
<input checked="" type="checkbox"/> Measured values			<input checked="" type="checkbox"/> Measured values		
Yield strength:	286.4		Yield strength:	286.4	
Ultimate strength:	451.8		Ultimate strength:	451.8	
Young's modulus			Young's modulus		
<input type="checkbox"/> Nominal	E:	205900	<input type="checkbox"/> Nominal	E:	205900
<input checked="" type="checkbox"/> Measured			<input checked="" type="checkbox"/> Measured		
Supplementary web plate					
<input type="checkbox"/> Nominal values			<input type="checkbox"/> Nominal values		
<input checked="" type="checkbox"/> Measured values			<input checked="" type="checkbox"/> Measured values		
Yield strength:			Yield strength:		
Ultimate strength:			Ultimate strength:		
Young's modulus			Young's modulus		
<input type="checkbox"/> Nominal	E:		<input type="checkbox"/> Nominal	E:	
<input checked="" type="checkbox"/> Measured			<input checked="" type="checkbox"/> Measured		
End-plate rib stiffener					
<input type="checkbox"/> Nominal values			<input type="checkbox"/> Nominal values		
<input checked="" type="checkbox"/> Measured values			<input checked="" type="checkbox"/> Measured values		
Yield strength:			Yield strength:		
Ultimate strength:			Ultimate strength:		
Young's modulus			Young's modulus		
<input type="checkbox"/> Nominal	E:		<input type="checkbox"/> Nominal	E:	
<input checked="" type="checkbox"/> Measured			<input checked="" type="checkbox"/> Measured		

Test set up and loading protocol

Paper

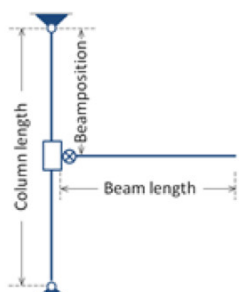
Title:
Comportamento Dinâmico de Ligações Metálicas ("Dinamic behaviour of steel joints")

Authors:
Nogueiro, P.

Source:
PhD Thesis, University of Coimbra, Portugal

Volume Issue: -
Pages: -
Year: 2009

Test J.4.3

Geometry (mm)		
Scheme: External double extended end-plate joint		
Beam length: 1170	Height: []	
Beam position: 1775	Width: []	
Column length: 3260	Flange thickness: []	
	Web thickness: []	
	Root radius: []	
	Flange-to-web welds: []	
	Beam	
	Shape: HEA280	
	Height: []	
	Width: []	
	Flange thickness: []	
	Web thickness: []	
	Root radius: []	
	Column	
	Shape: HEA320	
	Height: []	
	Width: []	
	Flange thickness: []	
	Web thickness: []	
	Root radius: []	
<input type="checkbox"/> Supplementary web plate	Thickness: []	
<input checked="" type="checkbox"/> Continuity	Thickness: 15	
End-plate	Bolts	Beam to plate welds
hp: 540	Rows in tension: 3	<input type="checkbox"/> Throat
bp: 220 ep: 55 exs: 50 mx1: 40.0 p1: 240	Bolts per row: 2	<input checked="" type="checkbox"/> Leg thickness
tp: 18 w: 110 exi: 50 mx2: 48.5 p2: []	Diameter: 24	Flange: 12
mx3: 48.5	Tensile stress: 353	Web: 8
<input type="checkbox"/> Rib	<input checked="" type="checkbox"/> Washer	
<input type="checkbox"/> Thickness []	<input checked="" type="checkbox"/> Washer nut	
Notes:	The beam length provided is the distance between the point of application of the force and the column flange, and for the column is the distance between the pins connections supports, the real length of the column is 3000mm.	

Test J-4.3

Material properties (MPa)		
Beam <input type="checkbox"/> Nominal values S355 <input checked="" type="checkbox"/> Measured values fy,f: 439.7 fy,w: 461.7 fu,f: 547.7 fu,w: 575.9 Young's modulus <input type="checkbox"/> Nominal Ef: 209400 <input checked="" type="checkbox"/> Measured Ew: 210200	Column <input type="checkbox"/> Nominal values S355 <input checked="" type="checkbox"/> Measured values fy,f: 414.8 fy,w: 449.6 fu,f: 531.4 fu,w: 553.4 Young's modulus <input type="checkbox"/> Nominal Ef: 204900 <input checked="" type="checkbox"/> Measured Ew: 207400	End-plate <input type="checkbox"/> Nominal values S355 <input checked="" type="checkbox"/> Measured values Yield strength: 405.1 Ultimate strength: 534.0 Young's modulus <input type="checkbox"/> Nominal E: 210300 <input checked="" type="checkbox"/> Measured E: 210300
Bolts <input type="checkbox"/> Nominal values 10.9 <input checked="" type="checkbox"/> Measured values Yield strength: Ultimate strength: 1170.0 Young's modulus <input type="checkbox"/> Nominal E: 213000 <input checked="" type="checkbox"/> Measured E: 213000	Continuity plate <input type="checkbox"/> Nominal values S275 <input checked="" type="checkbox"/> Measured values Yield strength: 286.4 Ultimate strength: 451.8 Young's modulus <input type="checkbox"/> Nominal E: 205900 <input checked="" type="checkbox"/> Measured E: 205900	Supplementary web plate <input type="checkbox"/> Nominal values <input type="checkbox"/> Measured values Yield strength: Ultimate strength: Young's modulus <input type="checkbox"/> Nominal E: <input type="checkbox"/> Measured E:
Notes: No prestress applied to the bolts. The joint failure occurred at the 34 th cycle, by the interface between the bottom beam flange weld to the end-plate. /// Energy dissipated: 505611 kN.mrad, maximum rotations: -34 to 32mrad, maximum bending moments: -300 to 280kNm.		
End-plate rib stiffener <input type="checkbox"/> Nominal values <input type="checkbox"/> Measured values Yield strength: Ultimate strength: Young's modulus <input type="checkbox"/> Nominal E: <input type="checkbox"/> Measured E:		

Test set up and loading protocol

Type of test:	Cyclic
Loading protocol:	Based on ECCS proc. I) $(6\phi_y)/4$; II) $2(6\phi_y)/4$; III) $3(6\phi_y)/4$; $6\phi_y$ until rupture.
Data provided:	Initial stiff., moments, rotat. and energy diss.
Type of response:	<input type="checkbox"/> Force <input checked="" type="checkbox"/> Moment <input type="checkbox"/> Displacemen <input checked="" type="checkbox"/> Rotation
	$M = F \cdot d$ Joint - DT11/DT12 Web panel - DT3/DT4 End-plate - DT1/DT2

The diagram illustrates the test setup for the beam-column joint. It shows a vertical column connected to a horizontal beam. Various displacement and force measurement points are indicated around the joint area, labeled DT1 through DT16. Points include DT1 (vertical displacement), DT2 (horizontal displacement), DT3 (vertical displacement), DT4 (horizontal displacement), DT5 (vertical displacement), DT6 (horizontal displacement), DT7 (vertical displacement), DT8 (horizontal displacement), DT9 (vertical displacement), DT10 (horizontal displacement), DT11 (vertical displacement), DT12 (horizontal displacement), DT13 (vertical displacement), DT14 (horizontal displacement), DT15 (vertical displacement), and DT16 (horizontal displacement). A coordinate system (x, y) is also shown.

4. CHARACTERISING BEAM-COLUMN ASSEMBLAGES WITH FULL-STRENGTH JOINTS

Francesco Morelli & Walter Salvatore

4.1 INTRODUCTION

Moment-resisting frames, also known as moment frames are in their simplest form, rectangular assemblages of beams and columns, with beam-to-column connections capable of transmitting bending moments. Resistance to lateral force is provided primarily by the development of bending moments and shear forces in the frame members and joints. Hence, the bending rigidity and strength of the frame members and joints are the primary source of lateral stiffness and strength for the entire frame [Bruneau *et al.* 1998].

Traditional models of moment frames do not explicitly consider the beam-to-column joint's effective stiffness, which provides an incomplete picture of the MRF behaviour. In fact, some modern codes such as Eurocode 3 [CEN, 2005] prescribe to model the deformational behaviour of a joint, taking into account the shear deformation of the web panel and the rotational deformation of the connection. Besides, Eurocode 3 prescribes that in order to model a joint in a way that closely reproduces the expected behaviour, the web panel in shear and each of the connections should be modelled separately, taking account of the internal moments and forces in the members, acting at the periphery of the web panel. Moreover, according to Eurocode 8 [CEN, 2005], "joints in dissipative zones should possess sufficient overstrength to allow for yielding of the ends of connected members" and "the adequacy of design should be supported by experimental evidence whereby strength and ductility of members and their connections under cyclic loading should be supported by experimental evidence, in order to conform to the specific requirements" for "each structural type and structural ductility class. This applies to partial and full strength connections in or adjacent to dissipative zones". However, dissipative semi-rigid and/or partial strength connections are permitted, provided that all of the following requirements are verified [CEN, 2005]:

- i) Connections have a rotation capacity consistent with the global deformations.
- ii) Members framing into the connections are demonstrated to be stable at the ultimate limit state (ULS).
- iii) Effects of connection deformation on global drift is taken into account using nonlinear static (pushover) global analysis or nonlinear time history analysis.

Therefore, according to European code full strength joints are more reliable than partial strength joints, whose application in seismic zones is not specifically prevented but in practice are strongly limited because of the requisite of experimental verification of their ductility capacity and the further requirements on nonlinear global analysis.

Within this chapter, fully welded and extended end plate joints are initially considered and classified following the provisions of the Eurocode 3 [CEN, 2005]. In this standard, joints are classified as full strength if the design resistance of the joint is not lower than the resistance of connected members and can be classified as rigid, pinned or semi-rigid by comparing their initial rotational stiffness, $S_{j,ini}$, with the classification boundaries shown in the Figure 4.1:

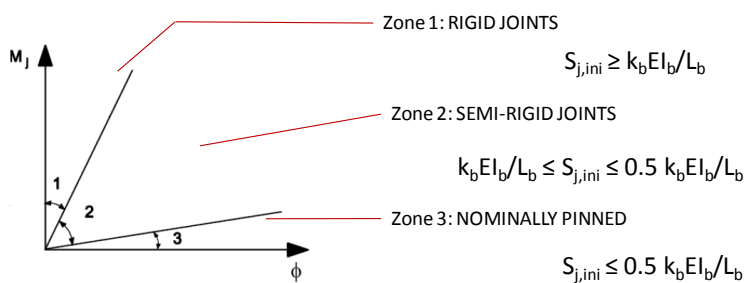


Figure 4.1. Joint stiffness classification boundaries.

where:

- $k_b = 25$ (for framed structures)
- E is the steel elastic Young's Modulus
- I_b is the second moment of area of the beam
- L_b is the span of the beam (centre-to-centre of columns)

It should be noted that a defined beam-to-column joint can be classified as rigid, semi-rigid or nominally pinned depending on the beam span as schematically shown in Figure 4.2.

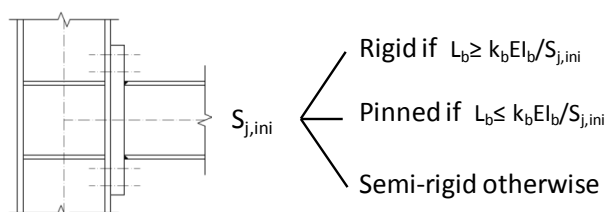


Figure 4.2. Joint stiffness classification based on span length.

Therefore, in order to evaluate if a given joint should be classified as rigid, semi-rigid or nominally pinned, a criterion assuming common loads and beams dimensions that can be found in practice is used. Assuming the considered joint as belonging to a steel frame sub-structures where (see Figure 4.3):

- a total vertical load equal to 8 kN/m² (considering dead, permanent and live loads) is applied to the floor
- the distance between the main beams is assumed equal to 5000 mm
- the span length L_{\min} is equal to the edge value between the rigid and semi-rigid fields:

$$L_{\min} = \frac{k_b \cdot E \cdot J_b}{S_{j,ini}} \quad (4.1)$$

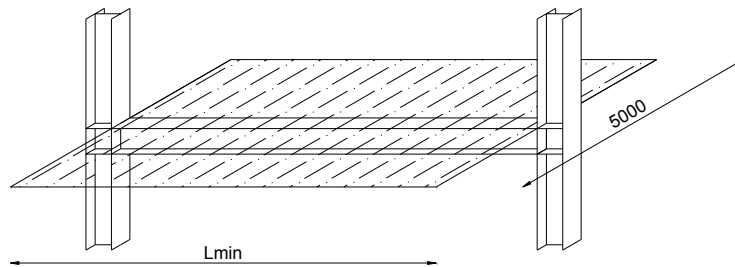


Figure 4.3. Steel frame sub-structure containing the beam-to-column joint considered.

then, the joint is assumed to be rigid if the maximum stress in the beam, evaluated as:

$$\sigma_{z\max} = \frac{q \cdot L_{int} \cdot L_{\min}^2}{16 \cdot W_z} \quad (4.2)$$

does not exceed 180 MPa, a value which is assumed to be an optimum working stress under vertical loads (not considering the seismic action). Among all the rigid joint typologies for which experimental data on cyclic behaviour are available, the fully welded and extended end plate typologies were initially selected, considering the solutions are reasonably practical and potentially cost-effective.

For these joint categories and following EC3 [EN 1993-1, 2005] provisions, the elements influencing the joint stiffness are schematically show in the Figure 4.4.

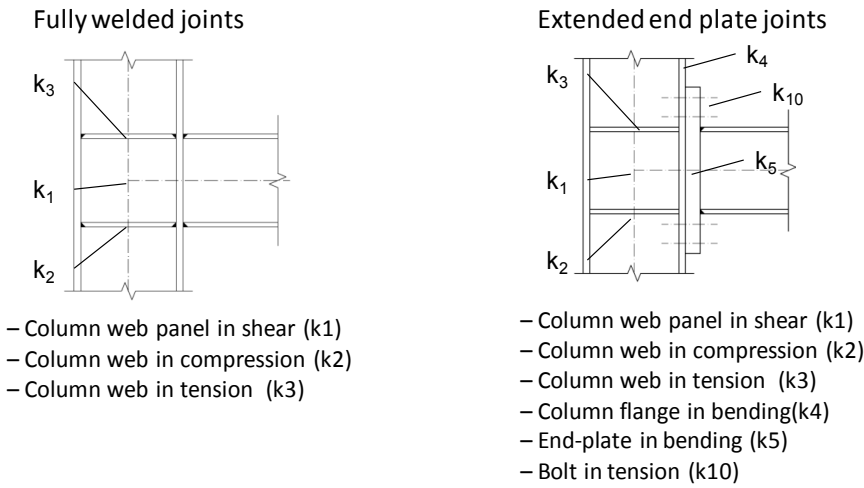


Figure 4.4. Components influencing joint stiffness for Fully Welded (left) and Extended-End-Plate (right).

In order to be classified as rigid with commonly used maximum span length, it was noted that both welded and extended end plate joints shall be at least provided with the column flange stiffeners for the web panel in tension and in compression. Without these stiffeners, the minimum span length of the beam connected needed to consider the joint as rigid would be too high and the case study would not be realistic.

For the welded joints identified among all the data collected, ten cases were selected whose main geometrical characteristics and testing information are summarised in the Table 4.1.

Table 4.1. Geometrical characteristics of the welded joints selected.

WELDED JOINTS							
Joint ID	References	Joint ID (within the reference)	Column	Beam	Web Stiff.	Shear web stiff.	Min. span length [mm]
FW1	Ballio et al. [1987]	D1	IPE 300	IPE 300	Y	N	7400
FW2	Ballio et al. [1987]	D2	IPE 300	IPE 300	Y	Y	4000
FW3	Dubina et al. [2000]	XSW2	HEB300	IPE 360	Y	N	6500
FW4	Dubina et al. [2000]	XUW1	HEB300	IPE 360	Y	N	6500
FW5	Ballio -Youquan [1993]	E1	HEB300	HEA260	Y	N	6400
FW6	Dubina et al. [2000]	BCC5	HEB160	IPE 300	Y	N	10500
FW7	Dubina et al. [2000]	BCC6	HEB200	IPE 300	Y	N	6600
FW8	Dubina et al. [2000]	BCC8	HEB240	IPE 300	Y	N	5700
FW9	Beg et al. [2000]	SW1	HEB200	IPE 300	Y	N	6600
FW10	Beg et al. [2000]	SW2	HEB200	IPE 300	Y	N	6600

It can be seen that most of the joints considered can be classified as rigid if the beam span length is lower than about 7000 mm. The joints FW1 and FW6 were however

studied in order to take into account the influence of the web stiffener (joint FW1 respect to joint FW2) and of the column size (joint FW6 respect to joints FW7 and FW8).

On the basis of the data collected, it is possible to take into account the influence of the following parameters on the behaviour of fully welded joints:

- i) Column size (HEB160, HEB200, HEB240, HEB300, IPE300)
- ii) Beam size (HEA260, IPE300, IPE360)
- iii) Column shear web stiffeners
- iv) Loading history

For the extended end-plate joint, the twelve cases that best represent rigid joints were selected among the available data with their main geometrical characteristics given in Table 4.2.

Table 4.2. Geometrical characteristics of the extended end plate joints selected.

Joint ID	Authors	Column	Beam	Flange/ Shear web Stiffener	End plate thick. [mm]	Bolts		Min. span length [mm]
						N°	Ø	
EP1	Ballio et al. [1993]	HEB300	HEA260	Y/N	44	8	24	8000
EP2	Ballio et al. [1993]	HEB300	HEA260	Y/N	26	4	30	9500
EP3	Ballio - et al. [1993]	HEB300	HEA260	Y/N	50	4	30	8800
EP4	Ballio et al. [1993]	HEB300	HEA260	N/Y	50	4	30	7400
EP5	Ballio et al. [1993]	HEB300	HEA260	Y/N	40	4	30	9000
EP6	Ballio et al. [1987]	Rigid	IPE 300	Y/Y	20	8	24	N.C.*

EP7	Ballio et al. [1987]	Rigid	IPE 300	Y/Y	20	8	24	N.C.*
EP8	Ballio et al. [1987]	Rigid	IPE 300	Y/Y	30	8	24	N.C.*
EP9	Ballio et al. [1987]	Rigid	IPE 300	Y/Y	30	8	24	N.C.*
EP10	Piluso et al. [2007]	HEB200	IPE 270	N/N	20	8	20	9600
EP11	Piluso et al. [2007]	HEB300	IPE 360	Y/Y	20	8	20	6000
EP12	Piluso et al. [2007]	HEB300	IPE 360	Y/Y	25	8	24	5800

*The considered joint is characterised by an uncommonly stiff column. See Ballio et al. [1987] for details.

From Table 4.2, it can be seen that in order to obtain an extended end plate rigid joint, a very expensive joint detailing would be needed (web stiffeners, thick end plates, large bolt diameter, etc.) and in the current literature, data concerning this joint typology is very rare, while there are a large amount of tests on full strength (or partial strength) semi-rigid joints. For this reason, only welded joint are considered within this work package.

In Chapter 3, test setup, loading history, geometrical information, beam and column sections and registered data have been summarised for the experimental tests selected on fully welded joints listed in Table 4.1. As such, this chapter focuses on the post-processing and interpretation of results provided so as to permit better characterisation of MRFs with full strength rigid joints.

4.2 METHODOLOGY

The development of a well-calibrated displacement-based design procedure for steel moment resisting frames characterised by full strength rigid joints is composed of two main parts:

- i) Study of the nonlinear cyclic behaviour of the main dissipative element (beam ends and beam-to-column joint).
- ii) Evaluation of an equivalent viscous damping factor of an elastic SDOF element as a function of the ductility demand.

For the steel MRFs with full strength rigid joints given, the elements which most influence the dissipative capacity of the structure, and therefore the calibration of the equivalent viscous damping, are the beam ends in which the inelastic behaviour concentrates and hence, the greatest amount of the energy dissipation takes place. The evaluation of the equivalent viscous damping factor started from the study of the experimental behaviour of full strength rigid joints, where several test campaigns were selected and data on joints classified as full strength rigid joints were collected. Different test configurations, element sizes, profiles, load patterns and beam-to-column joints were considered in order to cover as many cases as possible (see Chapter 3).

On the basis of the experimental data collected and given the simple shape of hysteretic curve of full-strength rigid joints, a phenomenological model was developed and calibrated that takes hardening and degradation effects into account. Once these analytical models were calibrated, several incremental dynamic analyses (IDA) were carried out on a single degree of freedom (SDOF) model characterised by the same hysteretic behaviour of the joints studied. For each intensity level, the maximum deformation experienced by the model and the residual displacements were recorded. In this way, it was possible to evaluate the secant stiffness associated with the maximum displacement and use it to calculate the equivalent viscous damping factor needed to reach the same maximum displacement with a linear SDOF model. The general workflow is schematically shown in Figure 4.5.

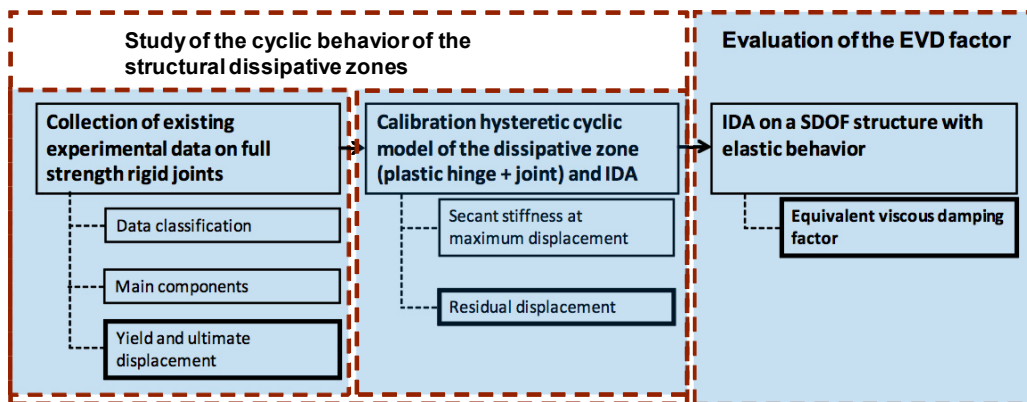


Figure 4.5. General workflow for the DBD procedure calibration for steel MRFs with full strength rigid joints.

The procedure can be carried out in three main steps, as schematically shown in the Figure 4.6, Figure 4.7 and Figure 4.8. In the first step, in order to take into account the effective nonlinear behaviour and dissipative capacity of the structural typology considered, several test campaigns were selected and data on joints, classified as full strength rigid joints, collected. Different test configurations, element sizes, profiles, load patterns and beam-to-column joints were considered in order to cover as many cases as

possible. On the basis of the experimental data collected, and given the simple shape of the hysteretic curve of full strength rigid joints, a phenomenological model was calibrated which takes hardening and degradation effects into account.

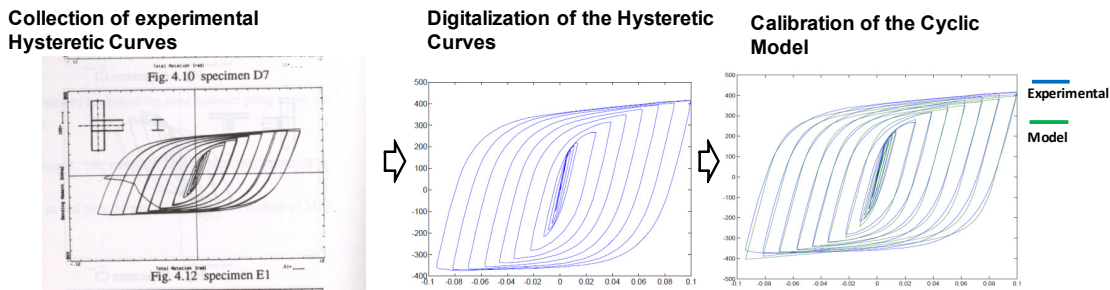


Figure 4.6. Step 1: Collection of experimental data and model calibration.

Once the numerical model of the joint is calibrated, several IDA were carried out on a SDOF model characterised by the same hysteretic behaviour of the joints studied. For each intensity level, the maximum deformation experienced by the model and associated secant stiffness associated recorded (see Figure 4.7).

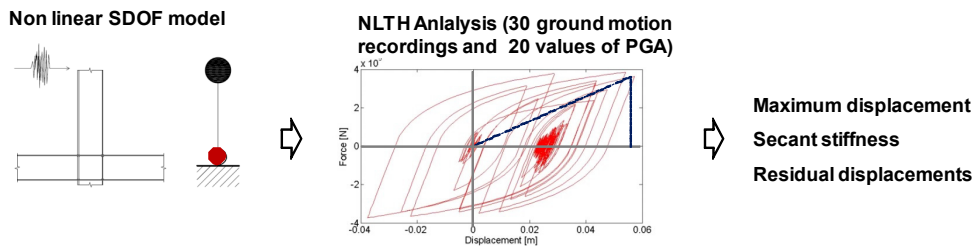


Figure 4.7. Step 2: Nonlinear Time History Analyses on a SDOF element representing a sub-assemblage of the MRF structure.

Once the maximum displacement of the nonlinear hysteretic model is evaluated, several IDA using a linear SDOF model, characterised by the secant stiffness found in Step 2, are carried out evaluating the EVD factor value that permit the linear model to achieve the same displacement of the nonlinear one. In this way, using a great amount of experimental and numerical data, it is possible to evaluate the relationship between the EVD factor and the displacement demand (or ductility demand).

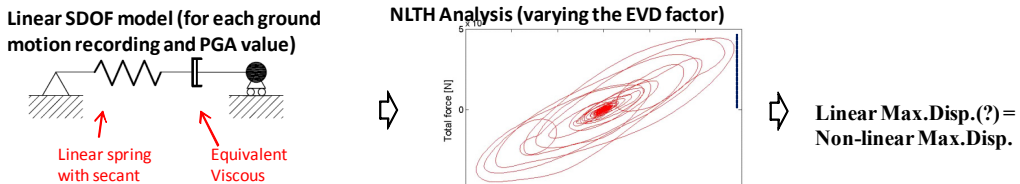


Figure 4.8. Step 3: Nonlinear Time History Analyses on a linear model characterised by varying values of the EVD factor.

4.3 PHENOMENOLOGICAL MODELS FOR FULL-STRENGTH RIGID JOINTS

Generally, three main types of analytical models can be used to describe the hysteretic behaviour of steel joints:

- Finite Element Models
- Phenomenological Models
- Physical Theory Models.

Finite Element Models

The finite element approach generally subdivides all the members of a joint into a series of segments, each of which may be subdivided again into a number of elements (beams, shells or solid elements discretisation). As demonstrated by recent studies, it is also possible to take the interaction between local and lateral buckling of slender elements (such as I beams) into account. However, in spite of providing the most realistic representation of the element behaviour, the finite element method usually demands a lot of computation time for each joint that have to be studied.

Phenomenological Models

Phenomenological models are based on simplified hysteretic rules that try to reproduce the observed hysteretic behaviour of the joints and represent currently the most common approach to the analysis of steel elements. Two of the most recent phenomenological models used to describe the hysteretic behaviour of steel joint are:

- Richard-Abbott model
- Ramberg-Osgood model

Even if the aforementioned models were originally developed as monotonic models, recent studies, such as Della Corte *et al.* [1999] based on Richard-Abbott monotonic model and Ballio *et al.* [1987] based on Ramberg-Osgood monotonic model, were developed in order to be used to describe the hysteretic behaviour of steel joints.

Physical Theory Models

Physical theory models incorporate simplified formulations based on physical considerations that allow the cyclic inelastic behaviour to be computed. While phenomenological models need empirical information on cyclic inelastic behaviour in order to be calibrated, the input data for physical theory models are based on the material properties and common geometric properties of a member. Moreover, the geometric representation of the element is considerably simpler than that used for a finite element model. In fact, physical models used to simulate the monotonic or cyclic behaviour of steel elements or joints consist of elastic or rigid bars connected by a deformable element. The correct calibration of the deformable element (usually nonlinear springs) properties is one of the key points to assure a good correspondence between the model and the experimental behaviour. One such physical theory model is the "component method" proposed by Eurocode 3 [CEN, 2005], where practical design rules are provided to determine the strength, stiffness and deformation capacity of individual components of the joints (for instance bolts in tension, column web in compression etc.). The overall joint behaviour may be assessed by assembling the mechanical characteristics the individual components together in order to determine the total global response of the connection.

As highlighted in the following paragraphs, the hysteretic behaviour of full strength rigid joints is quite simple if compared with semi-rigid ones or to pinned connections. In fact, they are not characterised by the presence of important pinching phenomenon because the majority of the plastic deformations is concentrated into the connected elements (usually the beams) and not into the joint components (i.e. the bolts). Even if some yielding occurs in the column web panel zone, it is characterised by very stable cycles. Hence, the phenomenological models seem to be the most appropriate in order to describe this joint typology.

Within this work, the model proposed by Della Corte *et al.* [1999] is used. As schematically shown in Figure 4.9, this model distinguishes the loading branch from the unloading one.

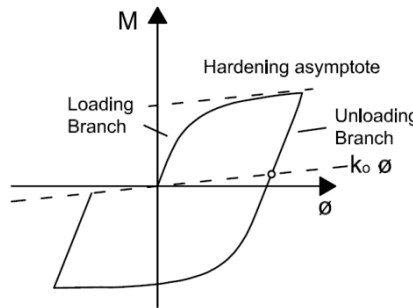


Figure 4.9. Moment rotation curve proposed by Della Corte et al. [1999].

The loading branch is based on Richard-Abbott monotonic model that, expressed in terms of moment-rotation functions, assumes the following expression:

$$M = \frac{(k_o - k_h) \cdot \phi}{\left[1 + \left| \frac{(k_o - k_h) \cdot \phi}{M_o} \right|^n \right]^{1/n}} + k_h \cdot \phi \quad (4.3)$$

where k_o represents the initial tangent stiffness, n is a parameter that influences the "smoothness" of the passage between the elastic and inelastic field (if n is great, the curve tends to be bilinear), M_o and k_h are parameters that define the asymptotic line whose equation is given by:

$$M = k_h \cdot \phi + M_o \quad (4.4)$$

The unloading branch is assumed to be linear with stiffness equal to the initial loading one. So the equation, in terms of moment-rotation, is expressed by:

$$M = k_o \phi \quad (4.5)$$

The cyclic hardening, which is assumed to be isotropic, is taken into account by the translation of the asymptotic line. The entity of this translation is a function of the maximum rotation ϕ_{max} (positive or negative) experienced by the joint, expressed in the following way:

$$M_{o,inc} = M_o \cdot \left(1 + H_h \frac{\phi_{max} - \phi_y}{\phi_y} \right) \quad \text{if } \phi_{max} \geq \phi_y \quad (4.6)$$

Therefore, when the joint rotation exceeds the yield value, the parameter M_o is updated and the asymptote translates, as shown in Figure 4.10.

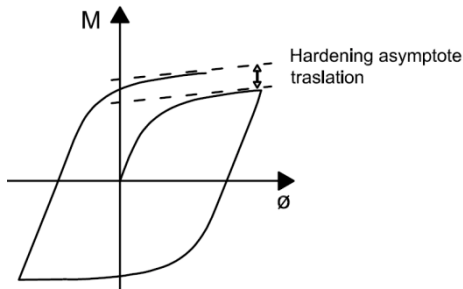


Figure 4.10. Hardening asymptote translation.

The deterioration of the mechanical characteristic due to the accumulation of plastic damage is taken into account by means of the collapse index proposed by Park and Ang that assumes the following expression:

$$IC = \frac{\bar{\phi}}{\bar{\phi}_{u,o}} + \beta \cdot \frac{E_h}{M_u \cdot \bar{\phi}_{u,o}} \quad (4.7)$$

where:

- $\bar{\phi}$ is the maximum rotation reached at the instant in which the index is evaluated
- $\bar{\phi}_{u,o}$ is the deformation capacity of the joint under monotonic loading conditions
- β is a coefficient to be determined from the experimental results
- E_h is the energy dissipated until the instant in which the index is evaluated
- M_u is the bending strength

As shown in Equation 4.7, the collapse index (IC) is given by the contribution of two terms. The first one takes the damage related to the maximum deformation $\bar{\phi}$ reached into account, while the second one takes the damage related to the hysteretic energy dissipated into account. The collapse of the joint takes place when the IC reaches a value equal to 1. Both terms of the IC equation are a function of $\bar{\phi}_{u,o}$ which is the maximum deformation of the joint under monotonic loading. This term should be evaluated considering that the maximum rotation capacity is often imposed by the possibility of local and global instability mechanisms of the beam. The application of the IC index is used within this work to evaluate the strength deterioration only, but it can be used to estimate also the variation of the other mechanical parameters (stiffness, etc.).

4.4 EXAMINATION OF EXPERIMENTAL RESULTS

As mentioned in the previous paragraphs, the cyclic force-displacement or moment-rotation curve for each joint was collected and digitised in order to simplify the calibration of the model and standardise the results. In fact, the collected data refers to different test campaigns and therefore different test setups were used. In order to make the results comparable and as homogeneous as possible, the digitised data was scaled in order to obtain the moment-rotation curve for each joint test. In particular, the evaluated moment is referred to the column axis, see Equation 4.8, while the rotation is defined as the ratio between the relative displacement of the beam end and the joint centre and the distance between the displacement measured point and the joint centre, see Equation 4.9, as schematically shown in the Figure 4.11.

$$M = F \cdot L_b \quad (4.8)$$

$$\theta = \frac{\Delta_{v2} - \Delta_{v1}}{L_b} \quad (4.9)$$

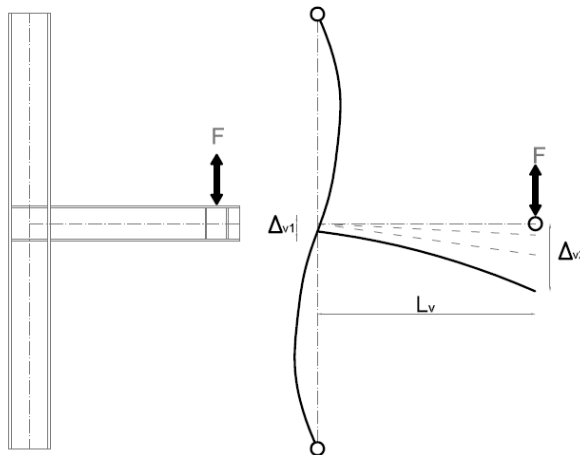


Figure 4.11. Schematisation of the joint rotation.

As an example of the procedure used, results are shown in Figure 4.12 for the FW1 test setup. The scan of force-displacement curve, the digitisation of the force-displacement curve and the derived moment-rotation curve are shown.

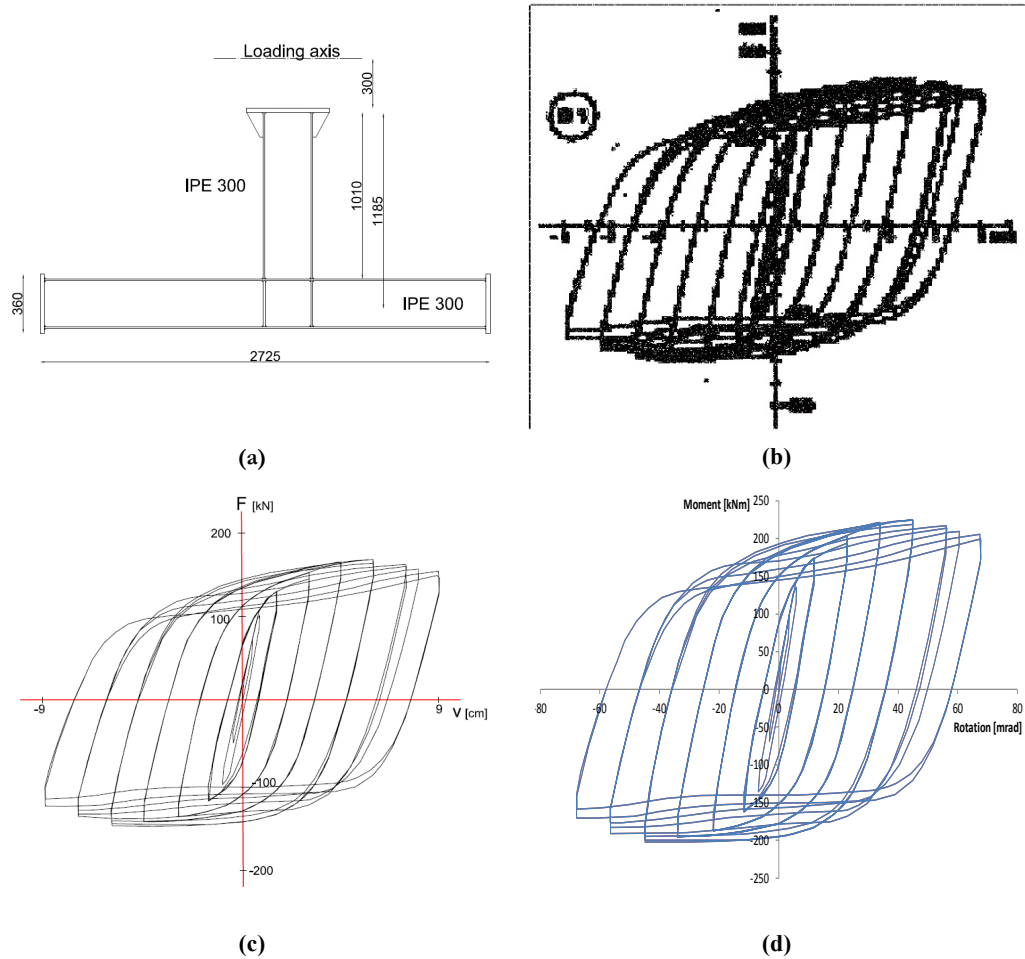
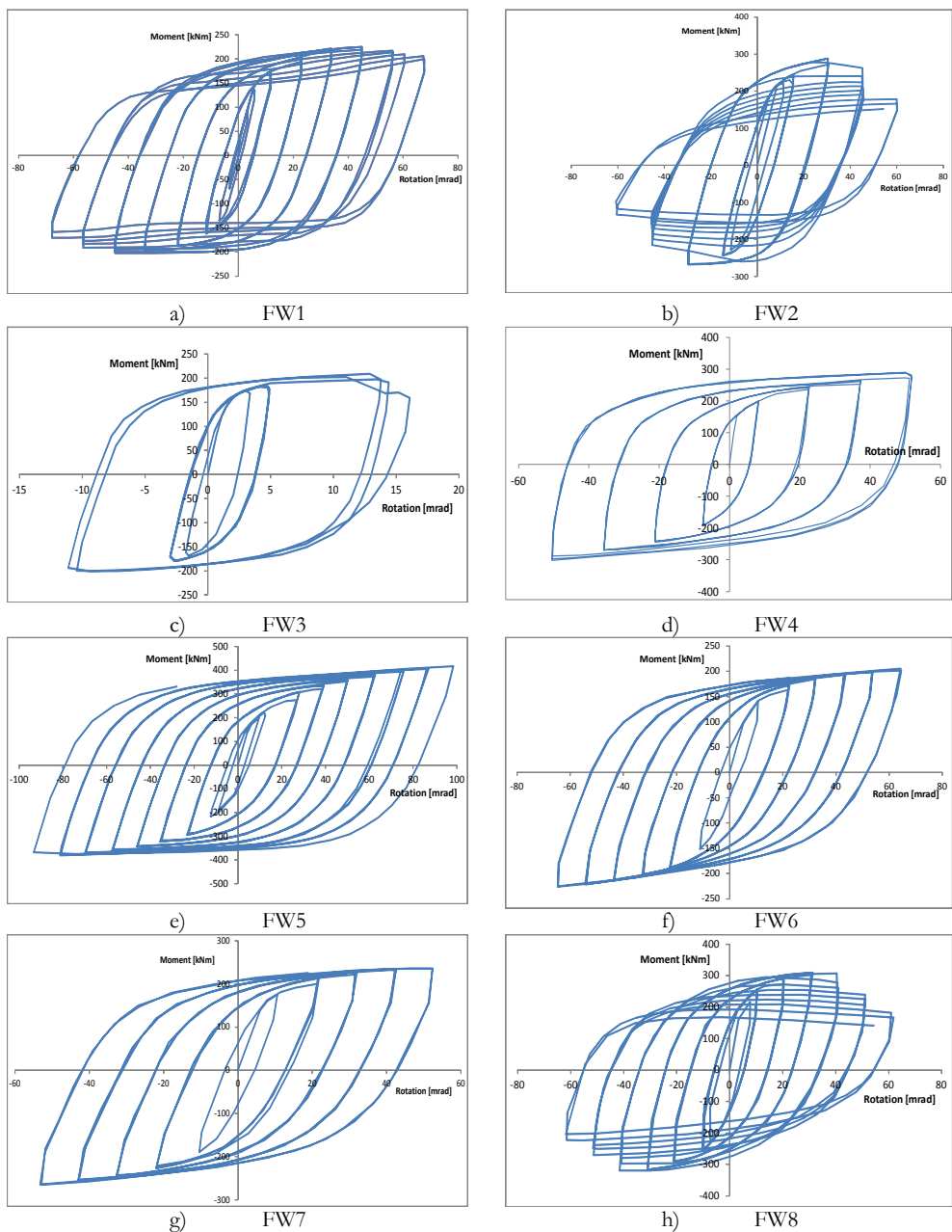


Figure 4.12. Example of test results regularisation: (a) test setup of FW1 joint; (b) scan of test results; (c) digitised test results; (d) moment-rotation curve.

This procedure has been applied to each collected datasets, which obtained a set of moment-rotation curves representative of different beam-to-column assemblages, loading histories, rotation range. In Figure 4.13, the moment-rotation curves relative to the selected test on welded joints are reported.



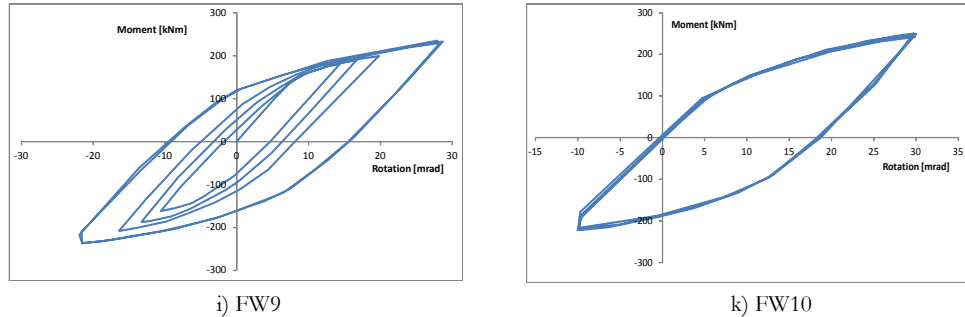


Figure 4.13. Moment-rotation curves of the selected tests on fully welded beam-to-column joints.

4.5 CALIBRATION OF THE RICHARD-ABBOT MODEL

Once all the collected data were digitised and the moment-rotation curves standardised, it was then possible to calibrate the phenomenological model described in the previous paragraphs. As previously mentioned in previous paragraphs, this is a cyclic application of the moment-rotation relationship proposed by Richard-Abbott monotonic model and for the current study, it is implemented to cyclically loaded specimens taking into account the cyclic hardening and the cyclic strength deterioration. The parameters to be defined for each cyclic curves are the following:

- k_o , initial elastic and unloading stiffness
- k_h , asymptotic post-elastic stiffness
- M_o , interception between the ordinate axis and the asymptote line
- n , factor influencing the “smoothness” between the elastic and post-elastic branches
- $M_{u,mon}$ and $\phi_{u,mon}$, ultimate bending strength and ultimate plastic rotation derived from a monotonic test
- H_h , plastic hardening factor
- β , cyclic strength deterioration factor

It can be seen that the unloading and post-elastic stiffness degradation, the variation of the “smoothness” due to the cyclic deterioration are not directly taken into account. The calibration of the aforementioned parameters, except for $M_{u,mon}$ and $\phi_{u,mon}$, has been conducted using the experimental data of the collected tests directly. For each test, k_o has been calibrated using the unloading stiffness of the moment-rotation curve, while k_h using the post elastic stiffness. In both cases, data of the first cycles after the first plasticisation were used for the calibration. This way, it is possible to evaluate the value of

k_o and k_h not influenced by the strain hardening or cyclic degradation, as shown in the Figure 4.14 for the FW1 joint.

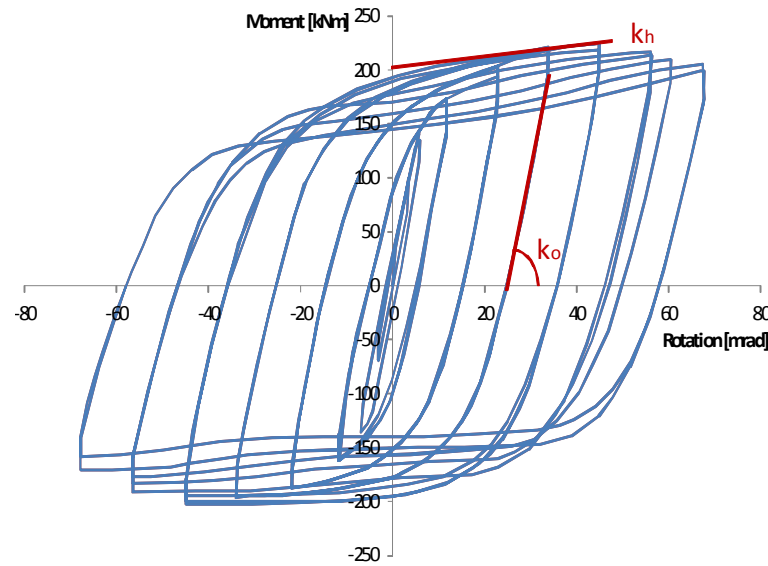


Figure 4.14. Example of calibration of k_o and k_h (joint FW1).

$M_{u,mon}$ and $\phi_{u,mon}$ should be defined using the results of monotonic tests conducted on the same beam-to-column sub-assemblage. However, for the experimental cases selected, there were no monotonic results and therefore $M_{u,mon}$ was defined as the product of the plastic section modulus, W_{pl} , and the ultimate material strength, f_u (if available, otherwise the nominal value was used), while $\phi_{u,mon}$ was evaluated using the “DuctRot” program developed by Victor Gioncu and Dana Petcu [Petcu *et al.*, 2003, Gioncu *et al.* 2012a, Gioncu *et al.* 2012b]. This program deals with the available rotation capacity of steel beams, using the local plastic mechanism methodology considering both the in-plane and out-of-plane plastic mechanisms, as well as the application of gradient or quasi-constant moments. In Figure 4.15, a screenshot of the DUCTROT-M program is shown.

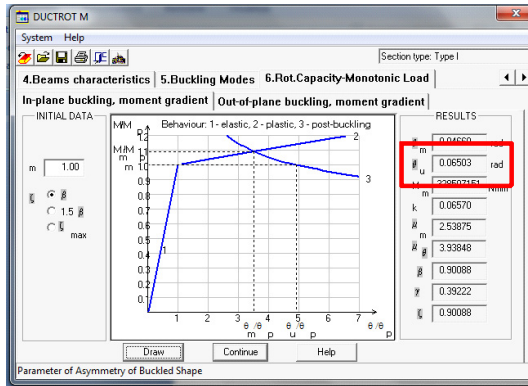


Figure 4.15. Plastic and post-buckling curves used to determine the available rotation capacity.

It should be noted that even if the $M_{u,mon}$ and $\phi_{u,mon}$ are only numerical estimation of the real values, their approximations does not influence the global cyclic curve in a significant way. The remaining parameters were evaluated directly using the collected experimental data, evaluating the values that minimise the sum of the absolute values of the distance between the experimental curve and the numerical one. In Table 4.3, the evaluated parameters for each considered joint are reported.

Table 4.3. Evaluated parameters for the calibration of the phenomenological model.

Joint ID	k_o	k_h/k_o	M_o	$M_{u,mon}$	$\phi_{u,mon}$	n	H_h	β
	[kNm]	-	[kNm]	[kNm]	[rad]	-	-	-
FW1	20700	0.004	200	270	0.088	1.15	0.11	0.03
FW2	26210	0.004	350	270	0.107	1.30	0.00	0.05
FW3	99050	0.004	300	438	0.128	1.40	0.01	0.00
FW4	80000	0.004	315	438	0.117	0.65	0.01	0.00
FW5	26270	0.004	350	395	0.085	1.15	0.03	0.00
FW6	18020	0.032	170	270	0.111	1.25	0.04	0.01
FW7	23570	0.023	210	270	0.111	1.30	0.04	0.01
FW8	44420	0.010	300	270	0.111	0.90	0.09	0.05
FW9	17720	0.05	250	270	0.111	1.45	0.01	0.00
FW10	18504	0.12	220	270	0.111	1.40	0.00	0.00

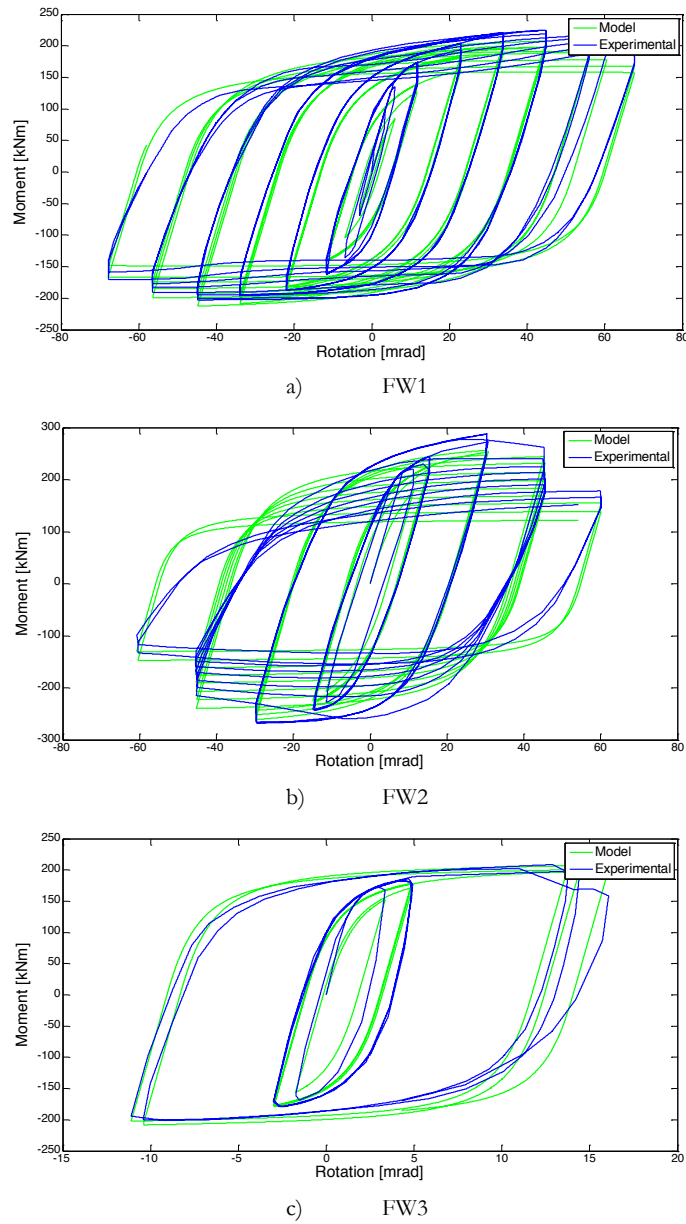


Figure 4.16. Comparison between the experimental curve and model of joint : (a) FW1 (b) FW2 (c) FW3.

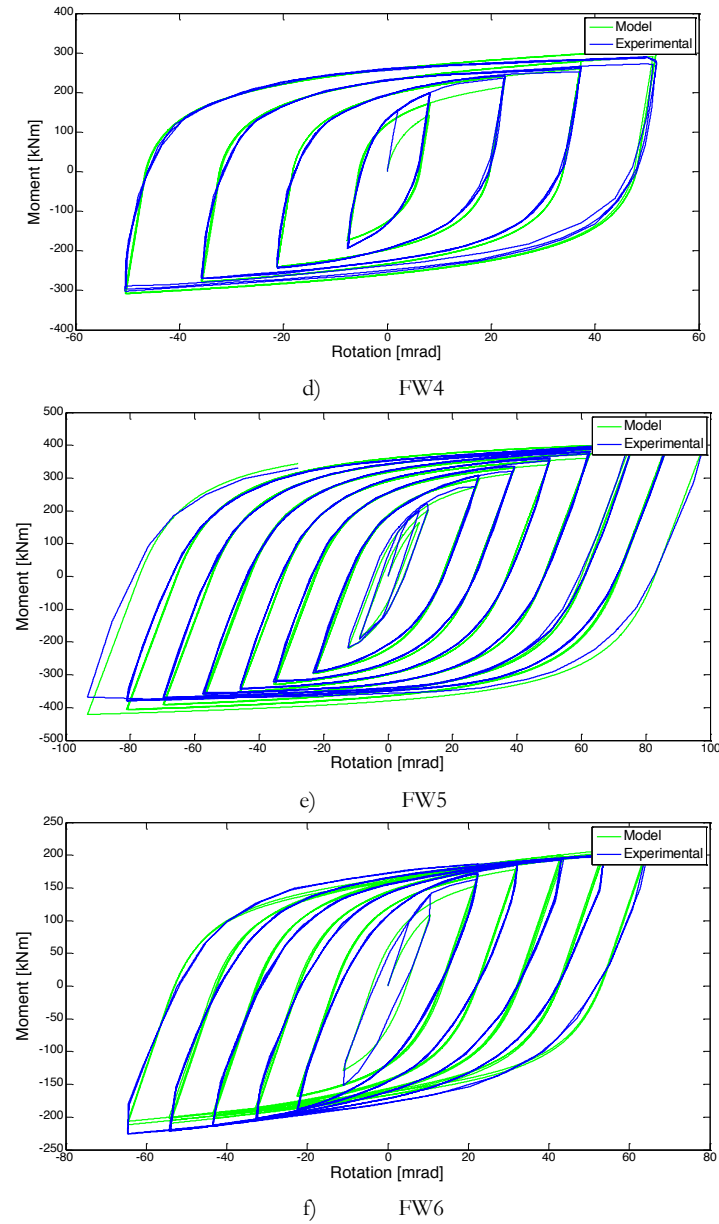


Figure 4.17. Comparison between the experimental curve and model of joint: (d) FW4 (e) FW5 (f) FW6.

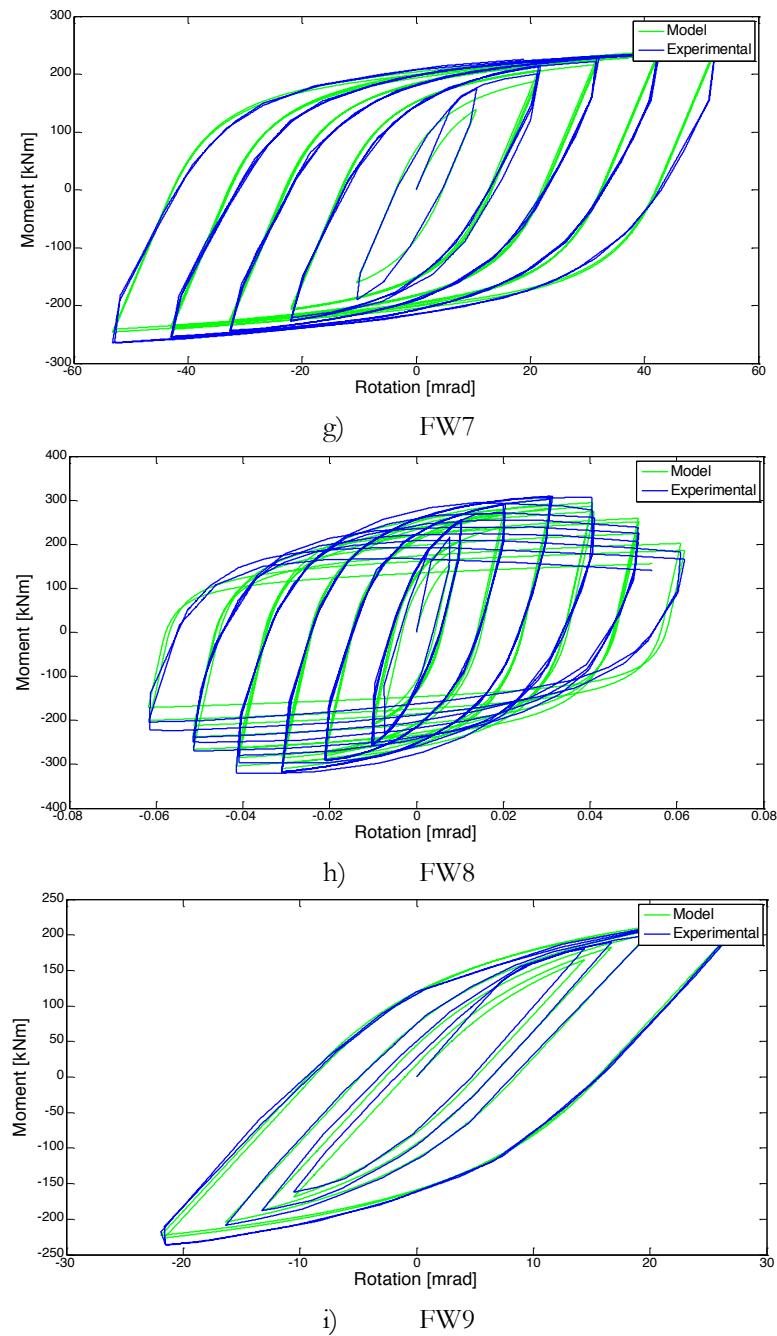


Figure 4.18. Comparison between the experimental curve and model of joint : (g) FW7, (h) FW8, (i) FW9.

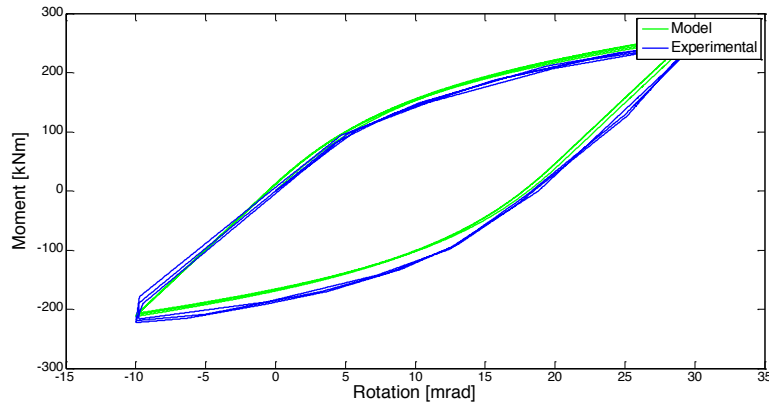


Figure 4.19. Comparison between the experimental curve and model of joint : (j) FW10.

4.6 NUMERICAL INVESTIGATION INTO THE EQUIVALENT VISCOUS DAMPING OFFERED BY STEEL MRFs WITH FULL-STRENGTH RIGID JOINTS

As previously described, once the phenomenological model is calibrated on the basis of the experimental results, the evaluation of the EVD factor – ductility relationship is carried out through two different analyses on two different models. The first ones are nonlinear time-history (NLTH) analyses carried out on a SDOF model representative of the joint cyclic behaviour. In this way, the maximum displacement demand associated to a given earthquake intensity level and the related secant stiffness can be evaluated. The second ones are linear time-history analyses carried out on a linear SDOF model characterised by the secant stiffness found in the previous analyses. They are used to evaluate the EVD factor value that permit the linear model to achieve the same displacement of the nonlinear one. This way, it is possible to evaluate the relationship between the EVD factor and the displacement demand (or ductility demand), which is subsequently used in the DBD method to relate the inelastic displacements of a connection to the equivalent linear system displacements by using an equivalent viscous damping term.

4.6.1 Nonlinear SDOF Models

The SDOF model representative of the nonlinear behaviour of the studied joint is composed by a nonlinear spring characterised by the hysteretic behaviour described in the previous paragraph, with an elastic damping equal to 5% of critical and a mass evaluated in order to assure an initial elastic period equal to 0.5s. Given that the purpose of this analyses is to compare the maximum displacement of the nonlinear model with the maximum displacement of the linear one and that the these displacements are evaluated

with the same seismic intensity input, it is actually independent of the mass chosen, as this is reflected in the period.

The NLTH analyses were carried out scaling the selected accelerograms with a scale-factor varying from 0.025 to 0.5 for a total of 20 nonlinear analyses for each selected joint. These records consisted of the ALP, LA, LC, CC, CA and LPC ground motion sets outlined in Maley *et al.* [2013], however, for brevity, the discussion herein only considers examples from the ALP ground motion set. For example, Figure 4.20 and Figure 4.21 show the hysteretic response of joint FW1 to ground motion ALP1 and a scale factor respectively equal to 0.025 and 0.5 are reported.

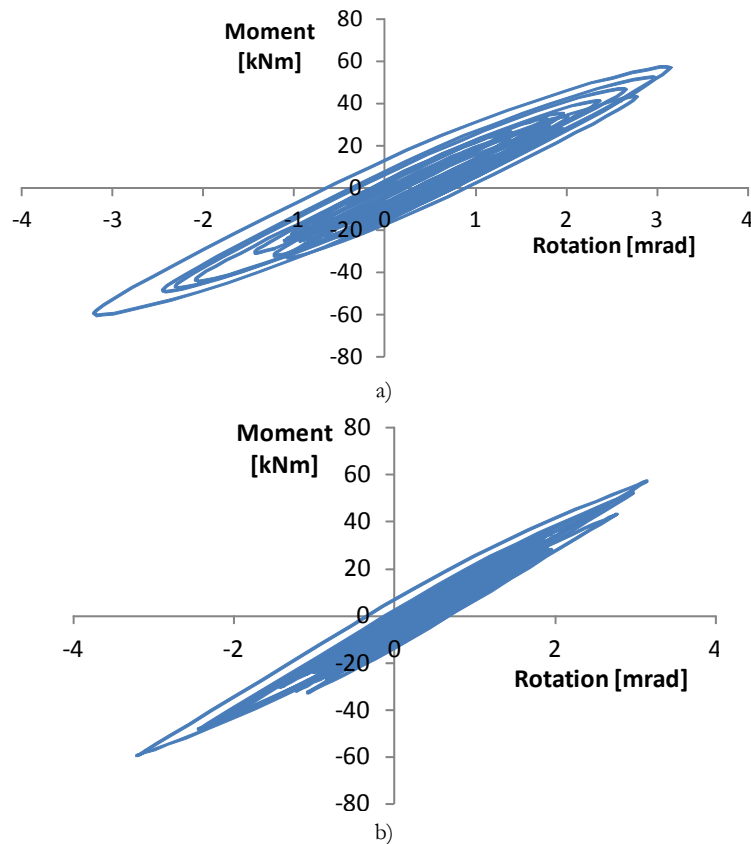


Figure 4.20. Moment - rotation response of FW1 joint to ALP1 ground motion recording and a scale factor equal to 0.025 : (a) total reaction; (b) hysteretic reaction (without the damping contribution).

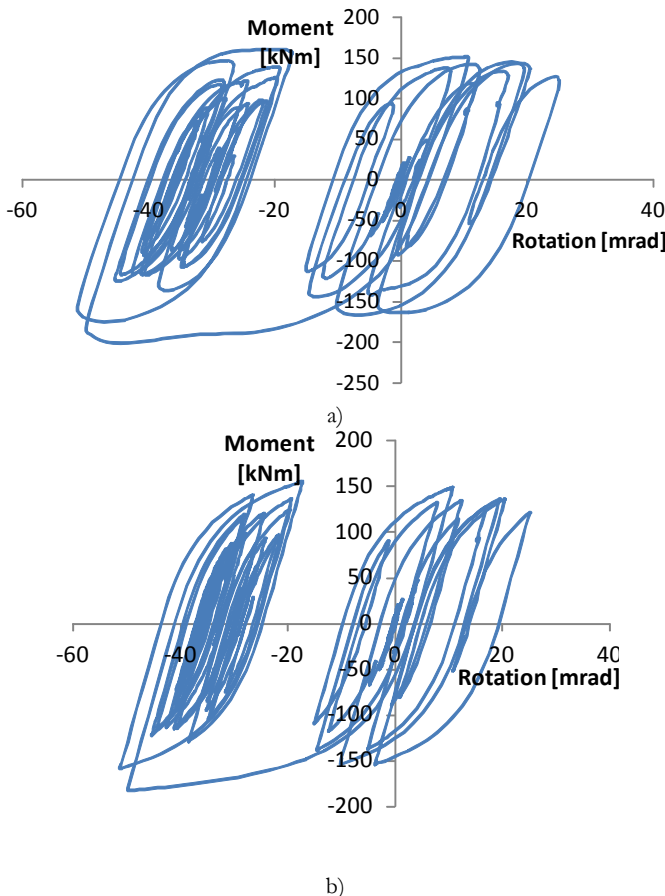


Figure 4.21. Moment - rotation response of FW1 joint to ALP1 ground motion recording and a scale factor equal to 0.25 : (a) total reaction; (b) hysteretic reaction (without the damping contribution).

From Figure 4.20(b) it can be noticed that even if the induced force on the SDOF model is very low, when compared to the yield moment, the model shows a dissipative hysteretic capacity. For this reason, even for low force level (and so for low ductility level), the EVD factor is expected to be greater than the 5% as there is a certain degree of hysteretic damping present in the system. For example, in Table 4.4 and Table 4.5, the maximum rotation, the associated moment and secant stiffness are reported for each considered joint, ground motion record ALP1 and scale-factor from 0.025 to 0.50.

Table 4.4. Maximum rotation, associated moment and secant stiffness for ground motion recording ALP1 and scale factor from 0.025 to 0.25.

Scale factor		0.025	0.05	0.075	0.100	0.125	0.150	0.175	0.200	0.225	0.250
Joint FW1	Max rotation [mrad]	3.2	5.6	7.9	9.7	11.2	15.5	23.3	32.1	41.4	51.3
	Associated Moment [kNm]	59	73	94	77	91	146	161	171	155	159
	Secant stiffness [kNm]	18604	13064	11874	7876	8134	9434	6896	5321	3748	3094
	Residual disp. [mrad]	0.6	1.9	3.4	4.6	4.3	1.0	6.7	16.3	25.9	35.9

Table 4.5. Maximum rotation, associated moment and secant stiffness for ground motion recording ALP1 and scale factor from 0.275 to 0.50.

Scale factor		0.275	0.300	0.325	0.350	0.375	0.400	0.425	0.450	0.475	0.500
Joint FW1	Max rotation [mrad]	61.1	71.0	80.8	91.7	102.9	114.7	126.4	138.5	149.5	162.4
	Associated Moment [kNm]	162	164	167	154	160	165	150	152	155	157
	Secant stiffness [kNm]	2647	2317	2065	1686	1559	1440	1186	1102	1037	968
	Residual disp. [mrad]	45.4	55.1	64.8	75.3	84.3	93.4	101.8	109.7	116.5	125.0

4.6.2 Definition of the ductility

It is clear that the EVD values associated with different ground motion recordings cannot be compared by relating it directly with the scale factors. In fact, mainly due to the different frequency content, ground motion recordings with the same nominal intensity can lead the same joint to very different maximum displacements. For this reason and in order to standardise the obtained results also for the different joints as much as possible, it is convenient to associate the EVD factors evaluated with the ductility demand. As mentioned in the previous chapters, the definition of the ductility for real hysteretic behaviour is not unique and a different assumption can lead to very scattered results. Within this work, the yielding rotation (required in order to define the ductility) is defined as the rotation associated with the yielding of the panel zone or that of the beam.

Table 4.6. Evaluation of the yielding rotation.

Joint ID	k_{oexp} [kNm]	k_{otheo} [kNm]	M_{ybeam} [kNm]	M_{ypanel} [kNm]	M_{ytheo} [kNm]	M_{oexp} [kNm]	$\theta_y = (M_{ytheo}/K_{otheo})$ [mrad]
FW1	20700	18320	175	106	106	200	5.78
FW2	26210	25350	175	530	175	350	6.90
FW3	99050	105000	298	--*	298	300	2.81
FW4	8000	45660	298	223	223	315	4.88
FW5	26270	37700	253	557	253	350	6.70
FW6	18020	9825	152	60	60	200	6.20
FW7	23570	14710	159	122	122	210	6.15
FW8	44420	25740	261	125	125	300	4.86
FW9	17720	19820	174	86	86	250	4.03
FW10	18504	19820	174	86	86	220	4.03

* the joint setup is symmetrical, so there is no shear force in the panel zone.

4.6.3 Residual Displacement

In Figure 4.22, the residual rotations for the considered joints subjected to the ALP1 ground motion recording (with the scale factor varying from 0.025 to 0.5) are reported. These residual displacements are determined from the average displacement from the last 5 seconds of the free vibration response. It can be seen that it is possible to establish some sort of relation between the ductility demand and the residual rotations. But when looking at Figure 4.23, where the residual rotations of joint FW1 subjected to the selected ground motion recordings are shown, it can be seen that the relation between the residual rotations (or displacement) and the ductility demand is strongly related to the ground motion recording characteristics.

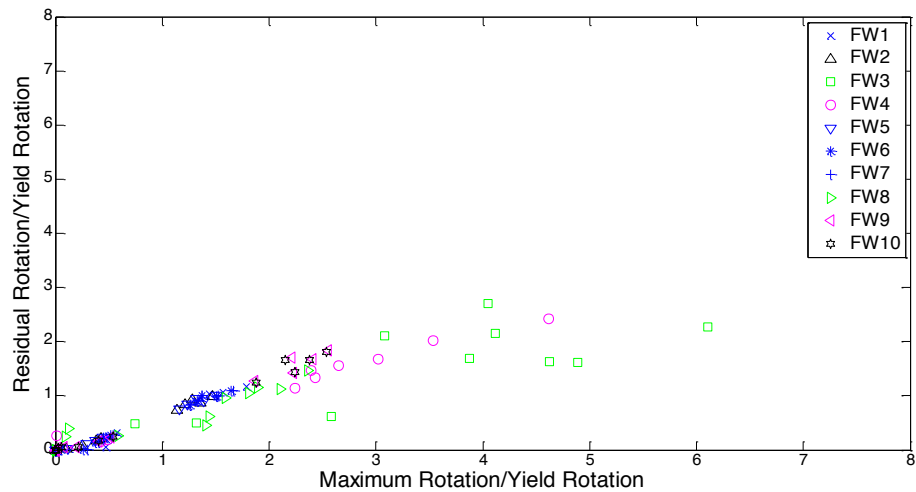


Figure 4.22. Residual rotation for the considered joints when subjected to ALP1 ground motion recording.

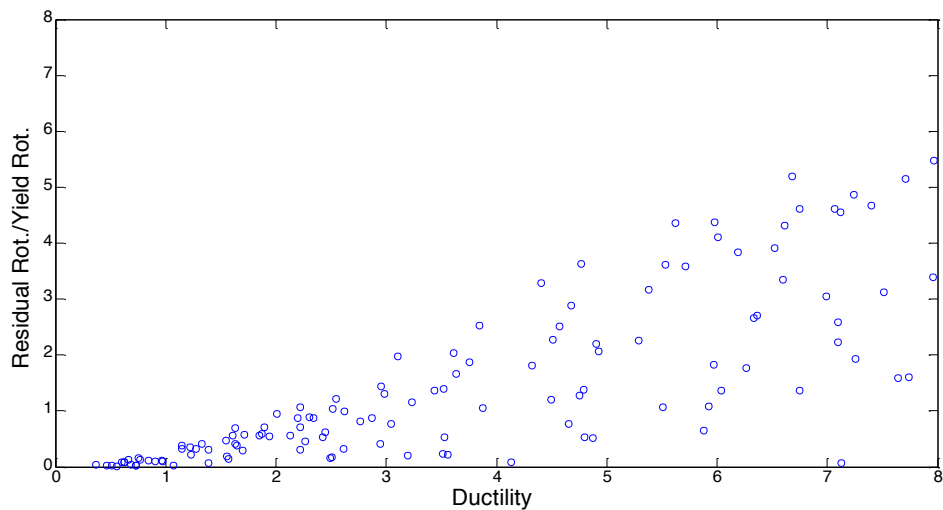


Figure 4.23. Residual rotation for joint FW1 when subjected to each of the selected ground motion recording (with scale factor varying from 0.025 to 0.50).

4.6.4 Linear SDOF model

Using the secant stiffness reported in Table 4.4 and Table 4.5, several analyses were carried out on a linear SDOF model, varying the equivalent viscous damping factor in order to evaluate the values that for a given ground motion record and a given scale

factor, permit the linear elastic model to reach the same maximum displacement of the nonlinear one. The equivalent viscous damping factor was varied from 5% to 55%, with an increment of 1%. So, for each NLTH analysis on the nonlinear model, 50 analyses were carried out on the linear one. To illustrate more clearly, Figure 4.24 and Figure 4.25 show the global response of the linear model equivalent to the hysteretic behaviour of joint FW1 to ground motion ALP1, a scale factor respectively equal to 0.025 and 0.5 are reported.

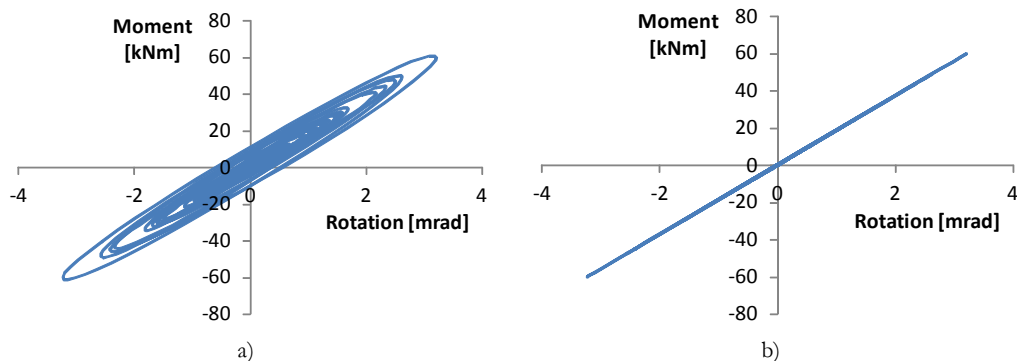


Figure 4.24. Moment - rotation response of linear equivalent model of FW1 joint to ALP1 ground motion recording and a scale factor equal to 0.025: (a) total reaction; (b) elastic reaction (without the damping contribution).

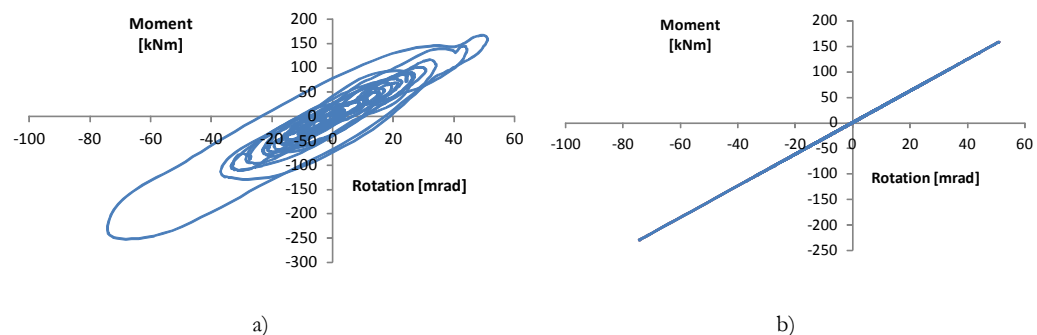


Figure 4.25. Moment - rotation response of linear equivalent model of FW1 joint to ALP1 ground motion recording and a scale factor equal to 0.25: (a) total reaction; (b) elastic reaction (without the damping contribution).

The elastic reaction is obviously linear and characterised by the secant stiffness obtained from the analyses on the nonlinear model. From the comparison of Figure 4.20 and Figure 4.24, and from Figure 4.21 and Figure 4.25, it can be seen that for both cases of scale factor equal to 0.025 and 0.25, the maximum displacement of the nonlinear model

and of the linear one is the same. From a displacement-based point of view, the two model can be so considered as equivalent. Obviously, even if the joint is the same (in this case the FW1 joint), the value of the EVD factor and of the secant stiffness depend on the maximum displacement. In Table 4.7 and Table 4.8, the value of the evaluated EVD factor for joint FW1, ground motion recording and scale factor are reported, together with the maximum rotation reached.

Table 4.7. Maximum rotation and associated EVD factor for all the joints considered, ground motion ALP1 and scale factor from 0.025 to 0.250.

Scale factor		0.025	0.05	0.075	0.100	0.125	0.150	0.175	0.200	0.225	0.250
Joint FW1	Max rotation [mrad]	3.2	5.6	7.9	9.7	11.2	15.5	23.3	32.1	41.4	51.3
	EVD factor [%]	9	13	17	28	30	23	23	22	18	18

Table 4.8. Maximum rotation and associated EVD factor for all the joints considered, ground motion ALP1 and scale factor from 0.275 to 0.500.

Scale factor		0.275	0.300	0.325	0.350	0.375	0.400	0.425	0.450	0.475	0.500
Joint FW1	Max rotation [mrad]	61.1	71.0	80.8	91.7	102.9	114.7	126.4	138.5	149.5	162.4
	EVD factor [%]	19	20	21	21	21	20	29	31	32	34

The results obtained from the two analyses on the nonlinear model and the equivalent linear one allowed for the calibration of a simplified expression of the EVD factor as a function of the ductility. In Figure 4.26 to Figure 4.35, the EVD factor obtained for the considered joints are reported together with the expression that better approximate them. This expression was calibrated evaluating the C coefficient of the equation originally proposed by Dwairi and Kowalsky [2007] and modified in order to take into account the viscous damping contribution ξ_{visc} set equal to 5%, see Equation 4.10. The C values were evaluated as the values that minimise the sum of the absolute distance between Equation 4.10 and the EVD factor values found by the linear analyses.

$$\xi_{tot} = \xi_{visc} + \xi_{hyst} = 0.05 + C \cdot \left(\frac{\mu - 1}{\mu \cdot \pi} \right) \quad (4.10)$$

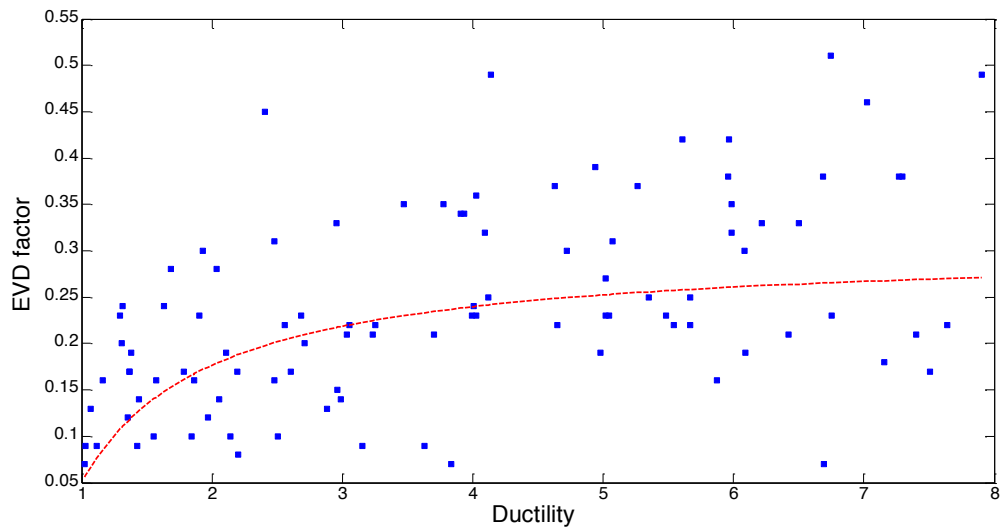


Figure 4.26. Equivalent Viscous Damping (EVD) factor for the joint FW1 and calibrated equation ($C=0.795$).

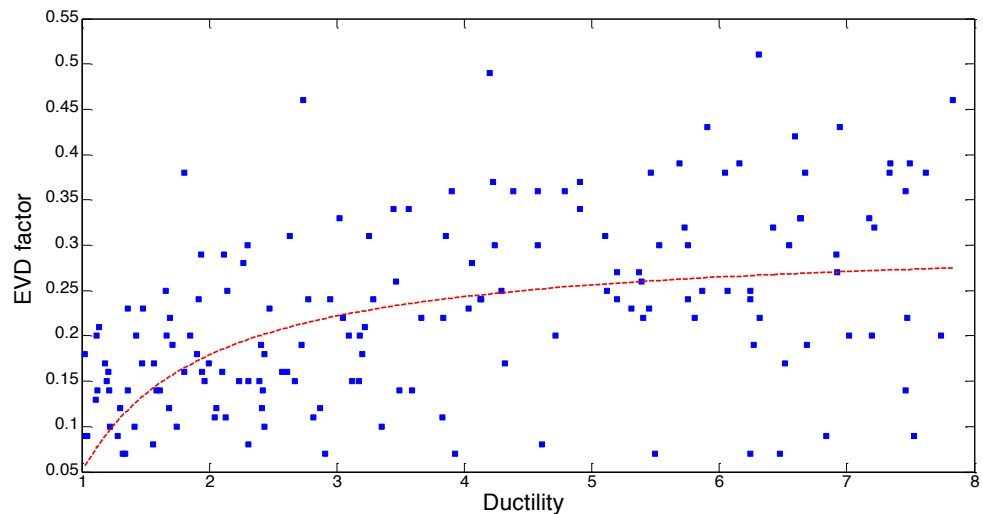


Figure 4.27. Equivalent Viscous Damping (EVD) factor for the joint FW2 and calibrated equation ($C=0.810$).

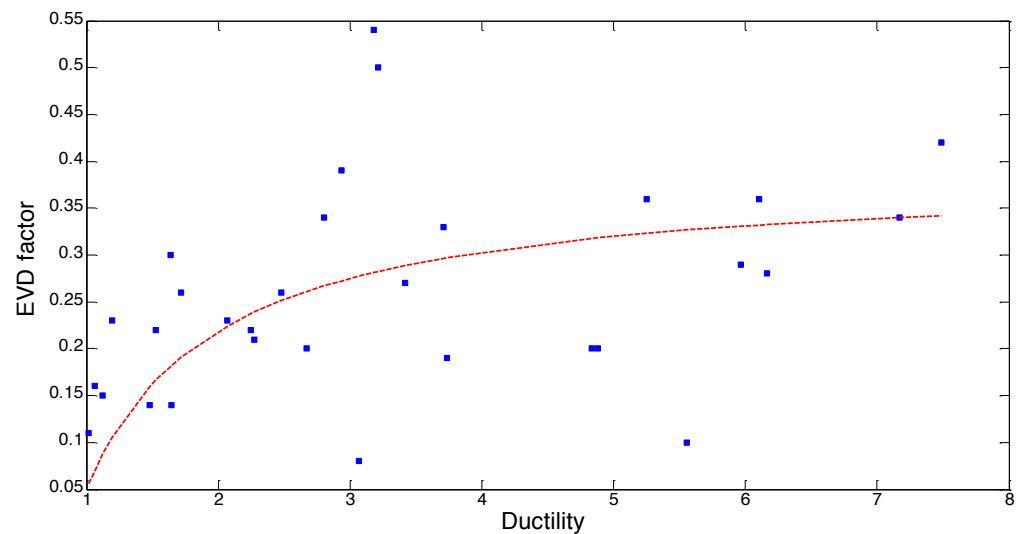


Figure 4.28. Equivalent Viscous Damping (EVD) factor for the joint FW3 and calibrated equation ($C=0.8550$).

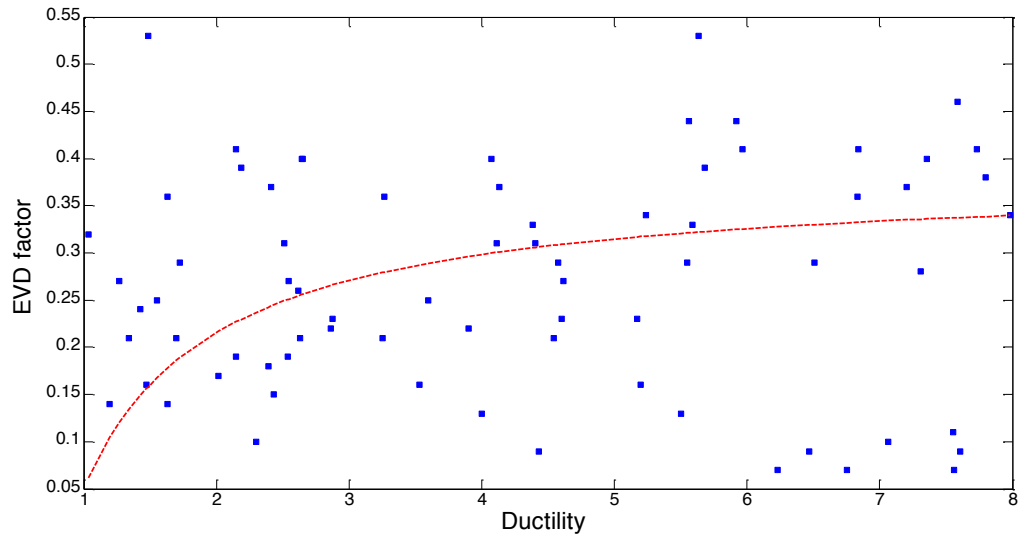


Figure 4.29. Equivalent Viscous Damping (EVD) factor for the joint FW4 and calibrated equation ($C=1.040$).

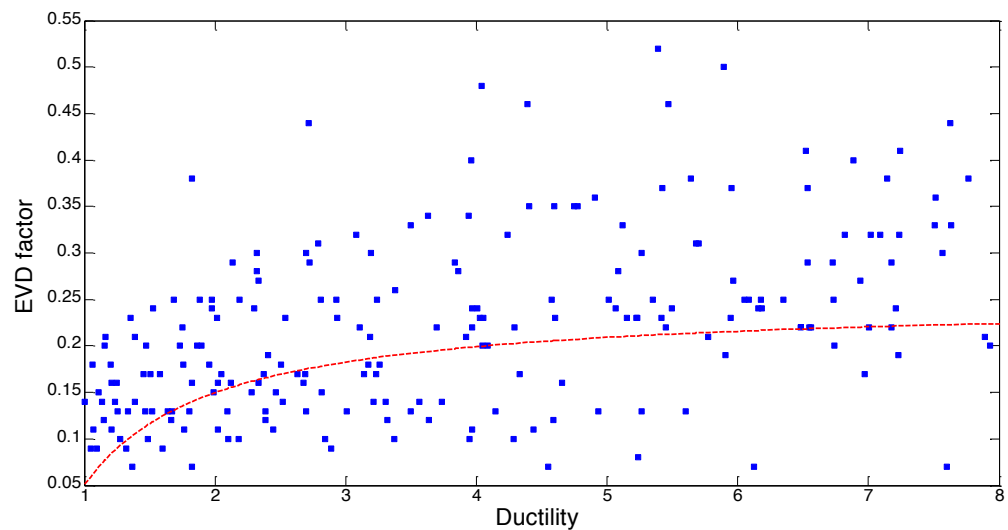


Figure 4.30. Equivalent Viscous Damping (EVD) factor for the joint FW5 and calibrated equation ($C=0.750$).

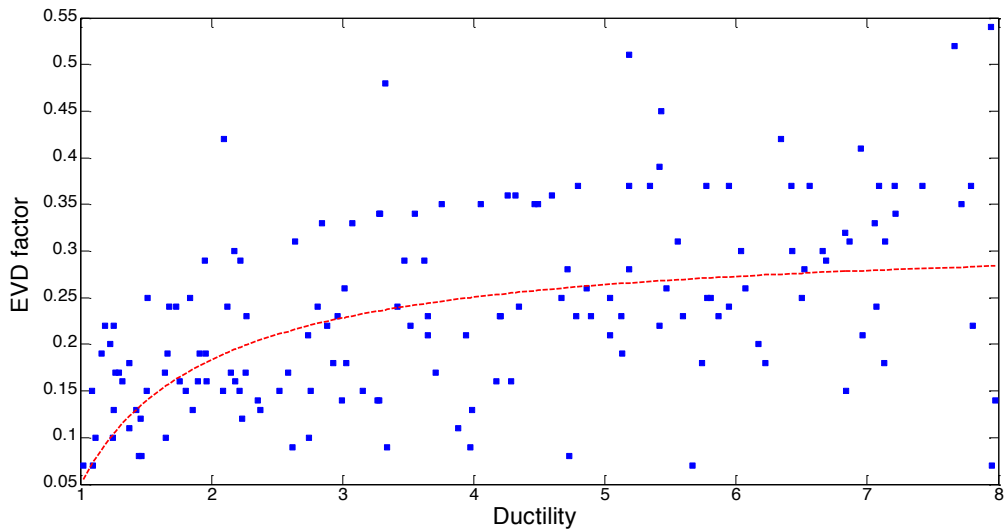


Figure 4.31. Equivalent Viscous Damping (EVD) factor for the joint FW6 and calibrated equation ($C=0.840$).

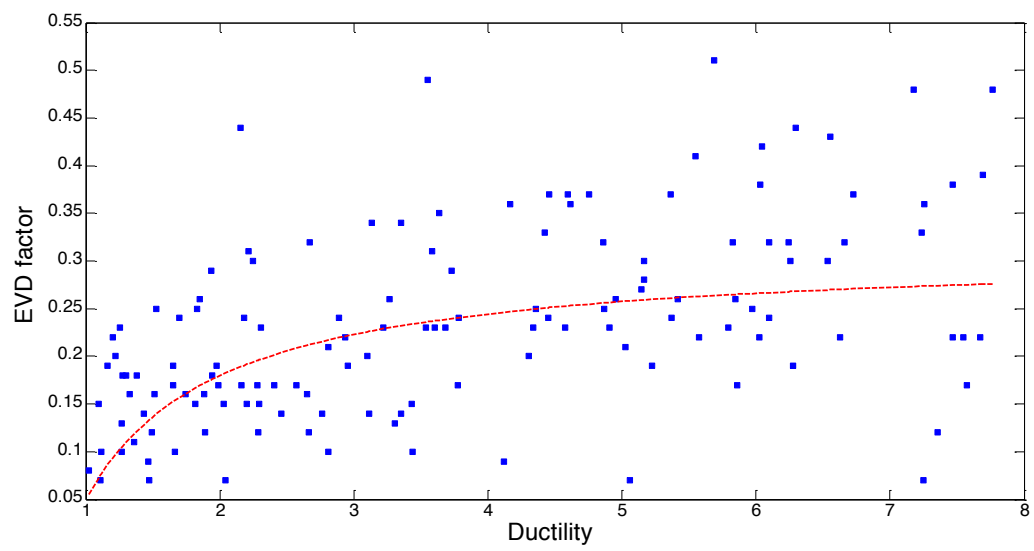


Figure 4.32. Equivalent Viscous Damping (EVD) factor for the joint FW7 and calibrated equation ($C=0.815$).

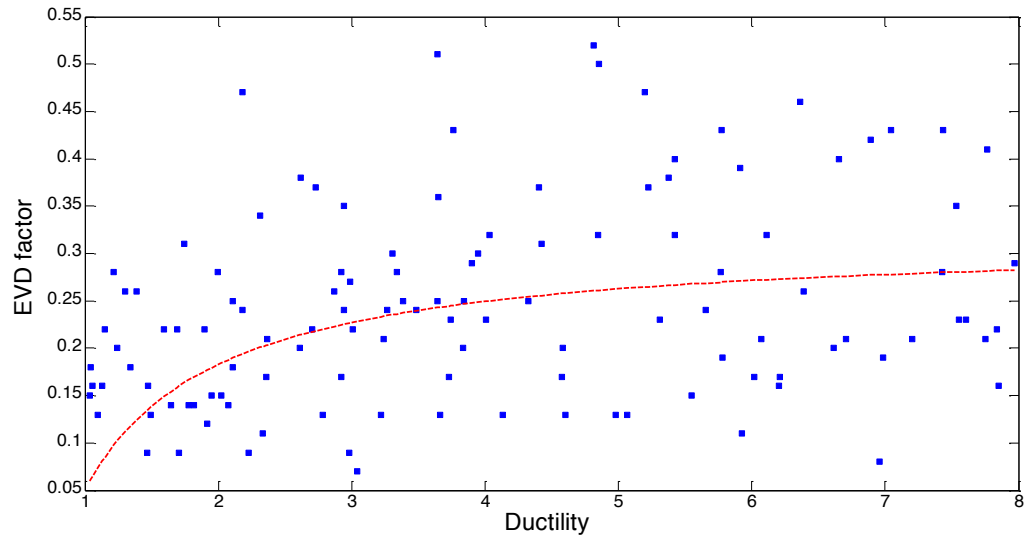


Figure 4.33. Equivalent Viscous Damping (EVD) factor for the joint FW8 and calibrated equation ($C=0.835$).

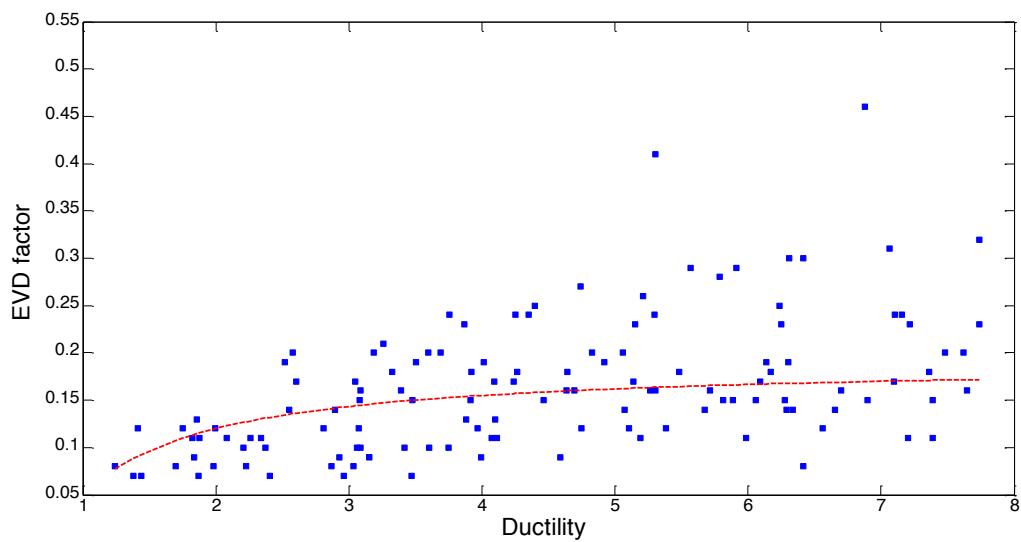


Figure 4.34. Equivalent Viscous Damping (EVD) factor for the joint FW9 and calibrated equation ($C=0.440$).

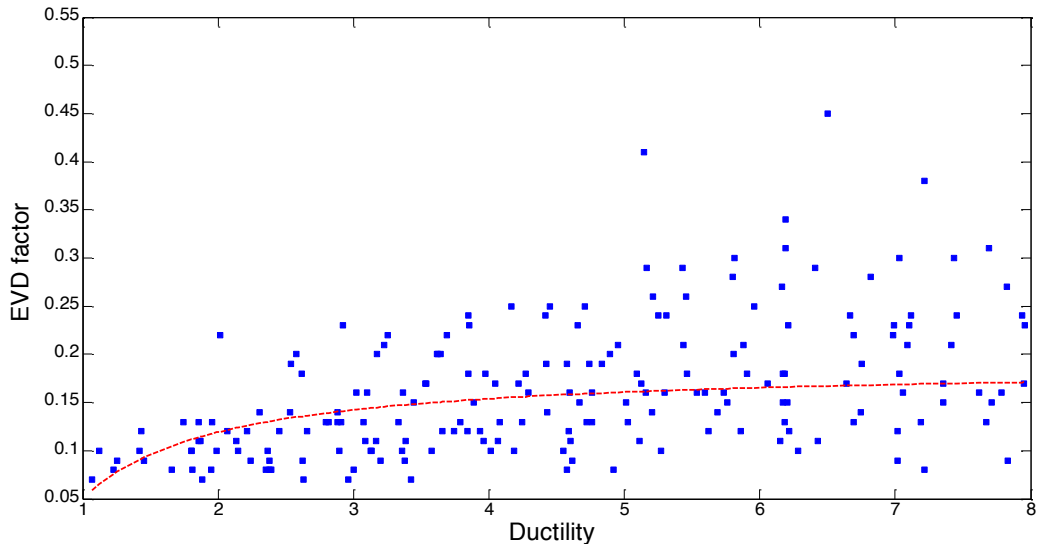


Figure 4.35. Equivalent Viscous Damping (EVD) factor for the joint FW10 and calibrated equation ($C=0.435$).

4.6.5 Summary of equivalent viscous damping results

From the comparison of Figure 4.26 to Figure 4.35, it can be noticed that even with the scattering, which is due to the very different ground motions recordings used, the relationship between the equivalent viscous damping (EVD) factors and the ductility, follows the shape previously observed by the equation proposed by Dwairi and Kowalsky [2007]. The number of results for the joint FW3 is lower if compared to the other joints due to numerical convergence problems. It can be noticed also that the dispersion of the data related to joints FW9 and FW10 is very low compared to the other joints studied. This can be mainly due to the fact that these two joints didn't show a significant hardening or damaging during the experimental tests, which is probably due to the low deformation limits imposed. In this way, the influence of the loading history is reduced and the data results are therefore less dispersed. From this, it can be seen that a very complicated hysteretic model, given its capacity to represent different physical effects such as hardening or cyclic damaging, can lead to very scattered results in NLTH analyses amplifying the dispersion due to the different ground motion recordings used. On the other hand, if the hysteretic model is well calibrated on the base of experimental data, the results obtained represent a good estimation of the real behaviour of the joint. In Figure 4.36, the EVD-ductility curve is calibrated using all the data from FW1 to FW8.

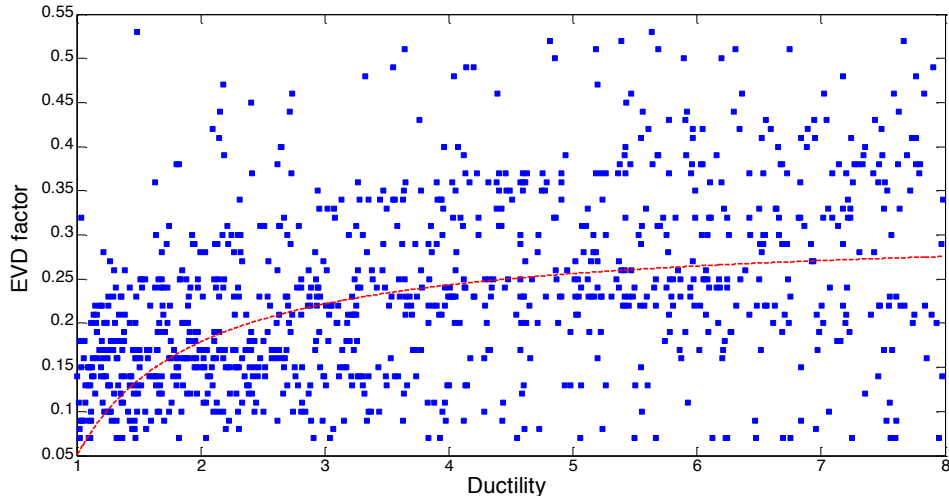


Figure 4.36. Equivalent Viscous Damping (EVD) factor for joints from FW1 to FW8 and the relative calibrated equation ($C=0.810$).

4.7 INTERPRETING RESULTS OF EVD STUDY ON FULL-STRENGTH JOINTS

This study has been conducted using a set of real ground motions. MRFs with full-strength welded connections have been examined, with the Richard-Abbott hysteretic model calibrated to the results of ten different experimental tests. After fitting EVD curves to the results of NLTH analyses, the following expression was proposed for the EVD of full-strength fully welded MRF systems:

$$\xi_{eq} = 0.05 + 0.81 \left(\frac{\mu - 1}{\mu \pi} \right) \quad (4.11)$$

As natural ground motions were used for the investigation and given that the NLTH analyses were conducted using 5% elastic damping, it could be assumed that the best elastic-damping spectrum scaling expression for the records is that given by the current EC8 expression:

$$R_\xi = (0.10 / (0.05 + \xi))^{0.5} \quad (4.12)$$

With the above in mind, the final displacement reduction factor expression can be found by substituting to be:

$$\eta = \left(0.10 / \left(0.10 + 0.81 \left(\frac{\mu - 1}{\mu \pi} \right) \right) \right)^{0.5} \quad (4.13)$$

$$\eta = \left(\frac{1}{\left(1 + 8.1 \left(\frac{\mu - 1}{\mu \pi} \right) \right)} \right)^{0.5} \quad (4.14)$$

It is also of interest to compare the above expression to existing expressions in the literature. In particular, the expression proposed in Priestley *et al.* [2007] for steel frame systems with Ramberg-Osgood behaviour is of interest given that the Richard-Abbott hysteretic model is relatively similar to the Ramberg-Osgood model. In Priestley *et al.* [2007], the equivalent viscous damping of a system with Ramberg-Osgood hysteretic properties can be computed as:

$$\xi_{eq} = 0.05 + 0.577 \left(\frac{\mu - 1}{\mu \pi} \right) \quad (4.15)$$

Priestley *et al.* [2007] also recommend that Equation 4.15 be used with the damping-dependent spectrum scaling expression given by:

$$R_\xi = (0.07 / (0.02 + \xi))^{0.5} \quad (4.16)$$

This implies that Priestley *et al.* [2007] are effectively proposing a displacement reduction factor given by:

$$\eta = \left(0.07 / \left(0.07 + 0.577 \left(\frac{\mu - 1}{\mu \pi} \right) \right) \right)^{0.5} \quad (4.17)$$

$$\eta = \left(\frac{1}{\left(1 + 8.2 \left(\frac{\mu - 1}{\mu \pi} \right) \right)} \right)^{0.5} \quad (4.18)$$

Encouragingly, it can be seen that there is very good correlation the displacement reduction factor expression proposed by Priestley *et al.* [2007] and that obtained in this work (Equation 4.14). Given that the work leading to the expression of Priestley *et al.* [2007] considered a much larger range of periods of vibration, and seeing as it is already quite well established in the literature, it is concluded that the existing expressions provided in Priestley *et al.* [2007] for steel frame systems are suitable for full-strength fully-welded steel MRF systems.

4.8 SUMMARY AND CONCLUSIONS

This chapter has reported on a detailed investigation into the behaviour of full-strength rigid joints with investigation of existing experimental data and execution of new numerical studies. The Richard-Abbot hysteretic model was calibrated to experimental test results for fully-welded beam column joints and the calibrated models were used to calibrate expressions for the equivalent viscous damping of steel frames by conducting NLTH analyses on SDOF systems subject to a number of accelerograms. Finally, by comparing displacement-reduction factors obtained from the new approach with the equivalent expression from Priestley *et al.* [2007] for steel MRFs, it was found that existing expressions for equivalent viscous damping of steel frames work well, provided they are used in conjunction with an appropriate spectral scaling expression.

4.9 REFERENCES

- Ballio, G., Calado, L., De Martino, A., Faella, C., Mazzolani, F.M. [1987] "Indagine sperimentale sul comportamento ciclico di nodi trave-colonna in acciaio", *Costruzioni Metalliche*, vol.II, 1987.
- Ballio, G., Youquan, C. [1993]: "An experimental research on beam to column joints: Exterior connections". *Proc. XIV C.T.A.*, Viareggio, Italia, Ottobre.
- Beg, D., Plumier, A., Remec, C., Sanchez, L., [2000]: "Influence of strain rate". In: *Mazzolani FM (ed.) Moment Resistant Connections of Steel Buildings Frames in Seismic Areas*, E. & F.N. Spon, London, UK.

Bruneau, M., Uang, C. M., Whittaker, A., [1998] *Ductile Design of Steel Structures*, McGraw-Hill, New York.

Calado, L. [2000] "Influence of column size" In: *Mazzolani FM (ed.). Moment Resistant Connections of Steel Buildings Frames in Seismic Areas*, E. & F.N. Spon, London, UK.

Della Corte, G., De Matteis, G., Landolfo, R. [1999] "A mathematical model interpreting the cyclic behaviour of steel-to-column joints". In *Proc. of XVII CTA Congress*, Naples 3-5 October.

Dwairi, H.M., Kowalsky, M.J., Nau, J.M., [2007], "Equivalent Viscous Damping in Support of Direct Displacement-Based Design", *Journal of Earthquake Engineering*, vol. 11, No.4.

Dubina, D., Grecea, D., Ciutina, A., Stratan A. [2000]: "Influence of connection typology and loading asymmetry". In: *Mazzolani FM (ed.). Moment Resistant Connections of Steel Buildings Frames in Seismic Areas*, E. & F.N. Spon, London, UK.

Gioncu V., Mosoarca, M., Anastasiadis, A. [2012, a]. "Prediction of available rotation capacity and ductility of wide-flange beams: Part 1: DUCTROT-M computer program". *Journal of Constructional Steel Research*, 69, pp. 8-19.

Gioncu V., Mosoarca, M., Anastasiadis, A. [2012, b]. Prediction of available rotation capacity and ductility of wide-flange beams: Part 2: Applications". *Journal of Constructional Steel Research*, 68, pp. 176-191.

Iannone, F., Piluso, V., Rizzano, G., [2007]: "Design of steel beam-to-column extended end plate joints: comparison between different solutions". *Proc. XXI C.T.A*, Catania, Italia, Ottobre.

Petcu, D., Gioncu, V. [2003] "Computer program for available ductility analysis of steel structures" *Computers & Structures*, vol. 81, Issues 22-23.

UNI EN 1993-1-8 [2005] "Design of steel structures: Design of joints," *EN 1993 part 1-8. Eurocode 3*, European Committee for Standardization, Brussels.

UNI EN 1998-1[2005] "Design of structures for earthquake resistance: General rules," *EN 1998 part 1. Eurocode 8*, European Committee for Standardization, Brussels.

5. CHARACTERISING BOLTED END-PLATE BEAM-COLUMN JOINTS USING THE COMPONENT METHOD

Gaetano Della Corte, Giusy Terracciano, Gianmaria Di Lorenzo & Raffaele Landolfo

5.1 INTRODUCTION

Bolted end-plate beam-to-column connections are frequently used as an alternative to fully welded connections. Bolted end-plate connections can either have sufficient rotational stiffness to allow for efficient moment frame action, or they can be significantly flexible. Bolted end-plate connections can be designed to be either full-strength or partial strength.

An investigation into the seismic response of bolted end-plate connections is worthy of consideration from the viewpoint of both the design of new buildings and the assessment of existing buildings. New buildings should meet requirements in terms of cost of construction and energy savings. Bolted end-plate connections offer advantages in these respects, especially if the possibility to dismount the building and recycle the materials at the end of the building's life is considered. Existing buildings frequently employ bolted end-plate partial-strength connections, either because of the lack of adequate structural design code provisions in the past, or the low intensity of the design seismic actions leading to relaxed seismic design rules. In addition, data available for characterising the seismic response of bolted end-plate connections is relatively poor when compared to data available for fully welded connections, for example.

This chapter presents an investigation into the moment-rotation response of bolted end-plate beam-to-column joints through an analysis of collected experimental results and a comparison with theoretical predictions. Eurocode 3's (EC3) [CEN, 2005] component method is applied to calculate the stiffness and the resistance of such joints. The theoretical predictions are then compared with the experimental testing results, which have been collected and reported in Chapter 3. Such a comparison allows a statistical assessment of the performance of the component method, in terms of the accuracy of prediction of both the initial stiffness and the plastic resistance to be carried out. Subsequently, simplified analysis tools are proposed and discussed.

5.2 REVIEW OF THE EUROCODE 3 COMPONENT METHOD

The method implemented into the EC3 [CEN, 2005] to evaluate the response of beam-to-column joints is known as the “component method” [Faella *et al.*, 2000; Jaspart, 2000; Lemonis and Gantes, 2009].

The application of the component method requires the following basic steps:

- i) Decomposing the joint into an assemblage of more elementary “components”.
- ii) Evaluation of the force-deformation response of each component (initial stiffness and plastic resistance).
- iii) Assemblage of the components to evaluate the mechanical characteristics of the whole joint (rotational stiffness, moment resistance).

Figure 5.1 shows the components composing the whole joint and included in the analysis of flush (a) and extended (b) end-plate joints according to EC3, which are listed as follows for both:

- i) *cws* - column web panel in shear.
- ii) *cwc* - column web in compression.
- iii) *cwt* - column web in tension.
- iv) *qfb* - column flange in bending.
- v) *epb* - end-plate in bending.
- vi) *bfc* - beam flange and web in compression.
- vii) *bwt* - beam web in tension.
- viii) *bt* - bolts in tension.

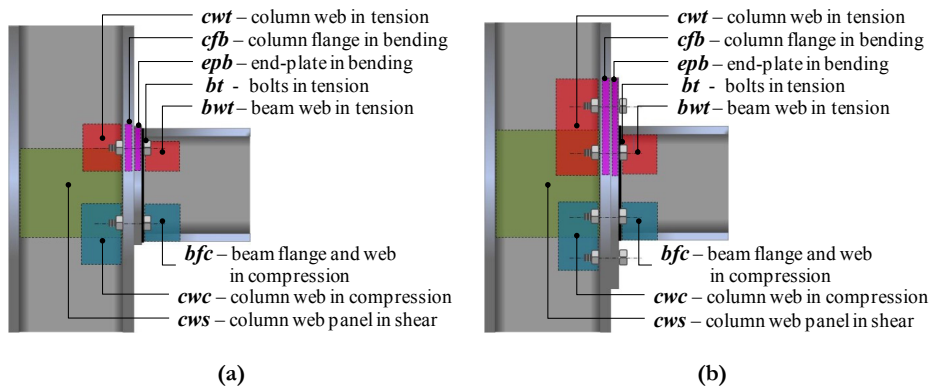


Figure 5.1. Components of (a) flush end-plate joints and (b) extended end-plate joints.

The joint components are then arranged into a mechanical model. EC3's models of both flush and extended end-plate joints are depicted in Figure 5.2. As shown, the components are represented by rigid and flexible springs arranged in series or parallel configurations. The model assumes that the tension springs are located at the bolt level, while the compressive springs are positioned at the compression centre, which is supposed to be located at the centreline of the compressed beam flange. The column web panel zone can be considered either together or separately from other components depending on the global modelling approach (either one single spring at the beam end including the panel zone deformation or two separate rotational flexibilities for the column web panel and the remaining connection elements).

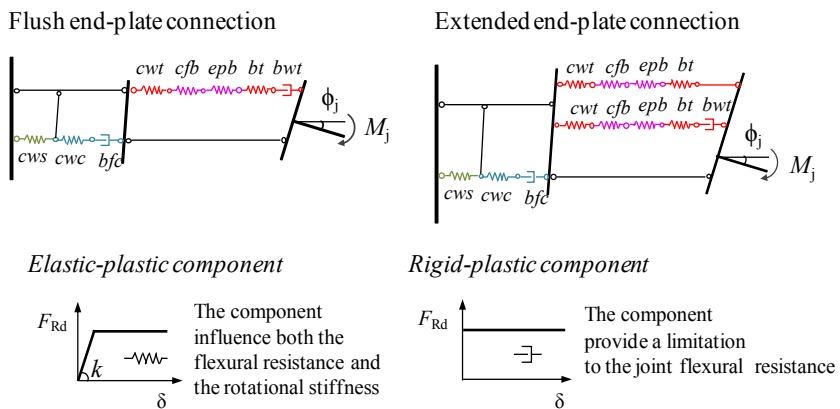


Figure 5.2. Mechanical models of end-plate joints.

In general, each component is characterised by a non-linear force-displacement response curve, where EC3 approximates the complex nonlinear component behaviour by means of simplified models, as presented in Figure 5.2. The elastic-perfectly plastic response, characterised by a plastic resistance and initial stiffness, is considered for components influencing both the joint resistance and stiffness, while a rigid-plastic behaviour is used to account for a limitation to the joint resistance but without a contribution to the joint flexibility.

The assemblage of the components permits the evaluation of the design moment resistance, $M_{j,Rd}$, and the initial rotational stiffness $S_{j,ini}$ of the whole joint. The flexural resistance of beam-to-column joints, $M_{j,Rd}$, is evaluated as follows:

$$M_{j,Rd} = \sum_r b_r F_{tr,Rd} \quad (5.1)$$

where $F_{tr,Rd}$ is the effective design resistance of bolt row r ; b_r is the distance of bolt row r from the centre of compression and r is the bolt row number. The values of $F_{tr,Rd}$ are calculated starting at the top row and working down. The effective tensile resistance of each bolt row is the smallest value of the tension resistance of the components at that bolt row, reduced if the total tensile resistance is greater than the design resistance of the column web panel in shear or if the compression resistance is exceeded. A complete and detailed description of the calculation procedure is provided by SCI [1995].

The column flange in bending and the end-plate in bending, including the relevant bolts in tension, are represented as two separate T-stubs with an equivalent width calculated using yield line patterns formerly evaluated by Zoetemeijer [1974]. The resistances of these components are equal to the resistances of the representative T-Stubs. Essentially, the component method is based on a plastic distribution of bolt forces, which is reasonable if the deformation of the column flange or end-plate can take place. A limit to the bolt row forces is used by EC3 to consider cases where the failure mode is not a ductile one [SCI 1995, CEN 2005].

The initial rotational stiffness, $S_{j,ini}$, of bolted joints is given by the following Equation:

$$S_{j,ini} = \frac{E \cdot b^2}{\sum_i \frac{1}{k_i}} \quad (5.2)$$

where E is the Young's modulus, b is the lever arm and k_i is the stiffness coefficient for the i^{th} basic joint component. In case of two or more bolt rows, the stiffness coefficients of the bolt rows in tension are represented by an equivalent spring of stiffness k_{eq} evaluated as follows:

$$k_{eq} = \frac{\sum_r k_{eff,r} b_r}{\tilde{\chi}_{eq}} \quad (5.3)$$

where $k_{eff,r}$ is the effective stiffness of bolt row r , determined from Equation 5.4 and $\tilde{\chi}_{eq}$ is the equivalent lever arm evaluated from Equation 5.5.

$$k_{eff,r} = \frac{1}{\sum_i k_{i,r}} \quad (5.4)$$

$$\tilde{z}_{eq} = \frac{\sum_r k_{eff,r} b_r^2}{\sum_r k_{eff,r} b_r} \quad (5.5)$$

According to the procedure described above, the assembly of tension springs in series and in parallel is replaced by an equivalent spring and the deformations of tensile springs are proportional to their distance to the compression centre.

Finally, the flexural behaviour of beam-to-column joints is represented by a moment-rotation curve ($M-\phi$) that describes the relationship between the applied bending moment (M) and the corresponding rotation between the members (ϕ). The idealisations of the $M-\phi$ curve proposed by Eurocode 3 are given in Figure 5.3. As depicted, the behaviour of beam-to-column joints is idealised by either a nonlinear (Figure 5.3(a)) or a simplified bilinear (elastic-plastic) (Figure 5.3(b)) $M-\phi$ response curve.

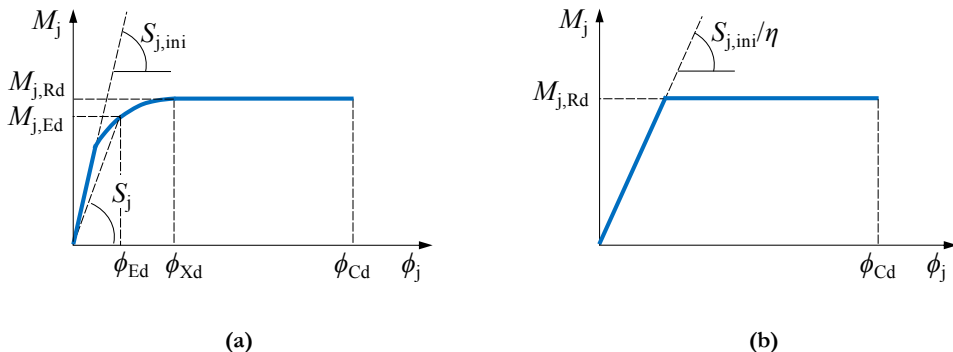


Figure 5.3. Moment rotation curve idealisations: (a) nonlinear and (b) bilinear.

The nonlinear part of the $M-\phi$ curve is identified by means of the stiffness ratio μ defined as follows:

$$\frac{S_{j,ini}}{S_j} = \mu = \left(\frac{1.5M_{j,Ed}}{M_{j,Rd}} \right)^{\psi} \quad (5.6)$$

where $M_{j,Ed}$ is the applied design moment, $M_{j,Rd}$ is the design moment resistance of the joint and ψ is a coefficient depending on the connection type. For bolted end-plate connections, this coefficient is taken as 2.7. The start of the plateau of plastic resistance, $M=M_{j,Rd}$, corresponds to a secant stiffness (slope of a straight line through the origin and the first point on the plateau) equal to $S_{j,ini}/3$ ($\mu = 1.5^{2.7} \approx 3$).

Using the component method, the moment resistance and the initial rotational stiffness of several end-plate connections were evaluated and these theoretical predictions were compared with experimental results, which are described in the following section.

5.3 EXAMINATION OF EXPERIMENTAL RESULTS AND COMPARISON WITH THEORETICAL PREDICTIONS

5.3.1 Initial Stiffness and Plastic Resistance

Some selected examples of comparisons between experimental and theoretical results for extended end-plate connections are shown in Figure 5.4 to Figure 5.8. Figure 5.4 is relevant to the experimental data provided by Ghobarah *et al.* [1990] for the specimen labelled A3 and tested under cyclic loading conditions. In those tests by Ghobarah *et al.* [1990], the column web panel was restrained from shear deformations, such that the results are relevant to the behaviour of the connection and beam only. Applying the EC3 component method, the tested extended end-plate connection has a predicted resistance larger than the beam plastic resistance, but smaller than the peak resistance actually reached during the test. Therefore, a beam plastic hinge is predicted to occur, which is confirmed by the experimental evidence shown in Figure 5.4. However, since the connection resistance is smaller than the peak system resistance, some plastic deformation is expected to occur in the connection also. Considering that the theoretical connection resistance is based on elastic-perfectly plastic material modelling (i.e. strain hardening of the connection is neglected in the theoretical model) a full development of the beam plastic hinge, observed in the experimental test, can be explained and understood.

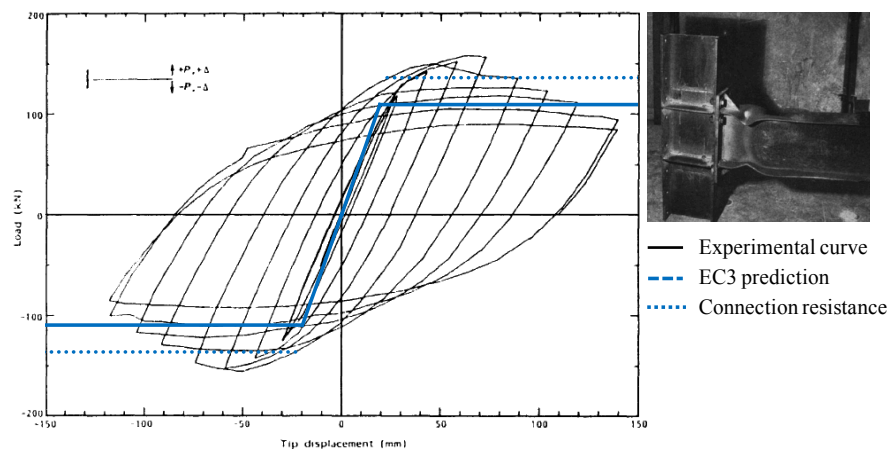


Figure 5.4. Theoretical vs. experimental results for specimen A-3 tested by Ghobarah *et al.* [1990].

Figure 5.5 illustrates the comparison between theoretical and experimental results for the specimen EPC-1 tested by Shi *et al.* [2007a]. This is one case of a partial-strength connection where the prediction by EC3 is particularly good, especially in terms of initial stiffness. For this specimen, yielding is predicted to occur because of the column web panel in shear. However, after the development of significant plastic deformations, significant strain hardening develops in the column web panel. This explains the significant increase of the actual resistance beyond the theoretical plastic resistance and also the ultimate failure mode, which was bolt rupture, as shown in Figure 5.5.

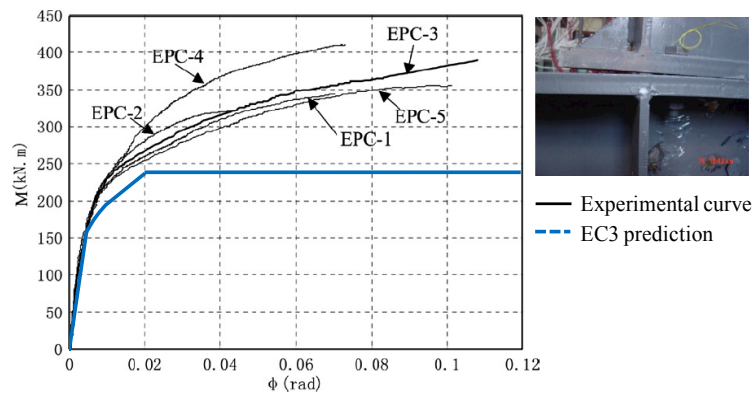


Figure 5.5. Theoretical vs. experimental results for specimen EPC-2 tested by Shi *et al.* [2007a].

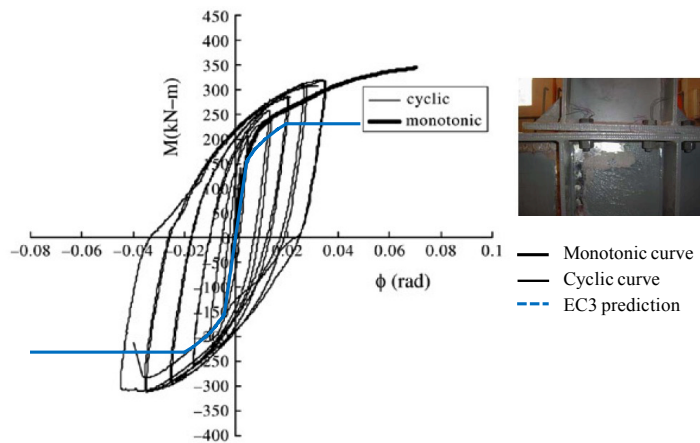


Figure 5.6. Theoretical vs. experimental results for specimen JD-2 tested by Shi *et al.* [2007b].

Figure 5.6 is also relevant to one extended end-plate connection, similar to the one shown in Figure 5.5 but tested under cyclic loading [Shi *et al.*, 2007b]. For this specimen, the agreement between theoretical predictions and experimental results is also reasonably good, where yielding is predicted to occur in the column web panel in shear in accordance with the observed response. The ultimate failure of the connection was due to bolt rupture, due to the large strain-hardening that took place in the column web panel in shear.

Figure 5.7 shows the comparison between theoretical predictions and experimental results for the specimens FS2 from the tests by Coelho *et al.* [2004]. Figure 5.7 shows that the initial stiffness predicted by the component method overestimates the experimental result in this case. Yielding is predicted to occur as a mixed mode of end-plate in bending and bolts in tension, which was also observed in the experimental test.

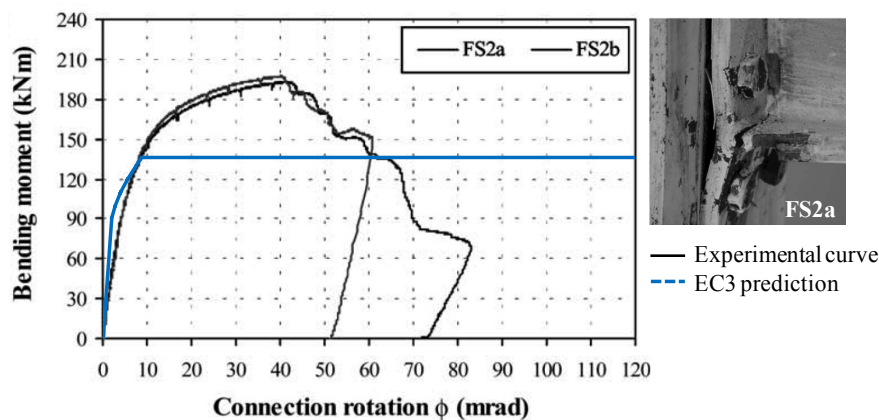


Figure 5.7. Theoretical vs. experimental results for series FS2 tested by Coelho *et al.* [2004].

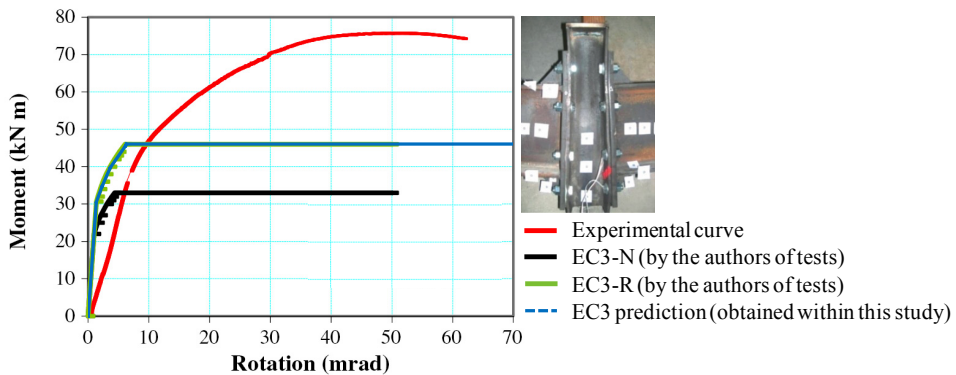


Figure 5.8. Theoretical vs. experimental results for specimen BC4 tested by Abidelah *et al.* [2012].

Figure 5.8 summarises the results from a test carried out by Abidelah *et al.* [2012]. The tested specimen was an internal joint with two identical extended end-plate connections subjected to a monotonically increasing load applied vertically to the column stub. Therefore, the column web panel is not contributing to the overall connection deformation. The comparison between the experimental response and the theoretical prediction shows clearly that the initial stiffness is largely overestimated by the component method. The calculated plastic resistance corresponds to complete column flange yielding, which is in agreement with the experimental results.

Some of the comparisons carried out for flush end-plate connections are shown in Figure 5.9 to Figure 5.12. Figure 5.9 shows the comparison of results for the specimen labelled EP2 and tested by Broderick and Thomson [2002]. This is one case where the theoretical prediction matches quite well the experimental results. However, the subsequent Figure 5.10 to Figure 5.12, which are relevant to other specimens tested by the same authors [Broderick and Thomson, 2002 and 2005] show that the predicted response can also significantly deviate from the observed moment-rotation curve. In particular, the theoretical initial stiffness is observed to be quite larger than the experimental result.

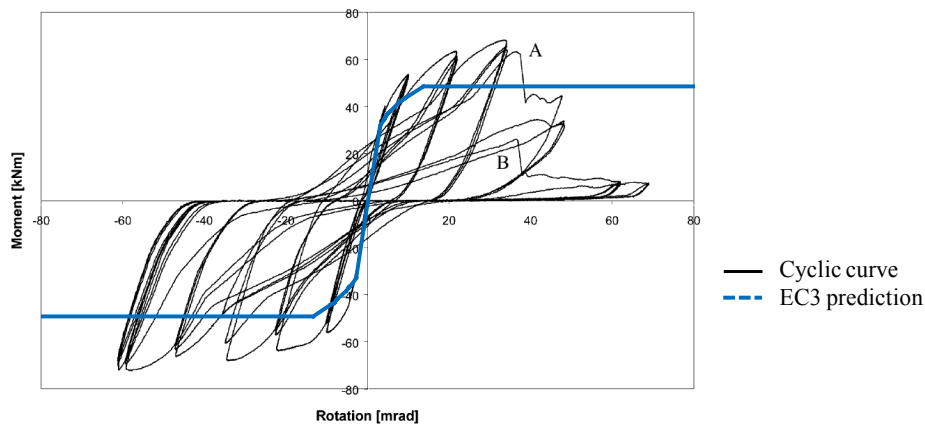


Figure 5.9. Theoretical vs. experimental results for specimen EP2 tested by Broderick and Thomson [2002].

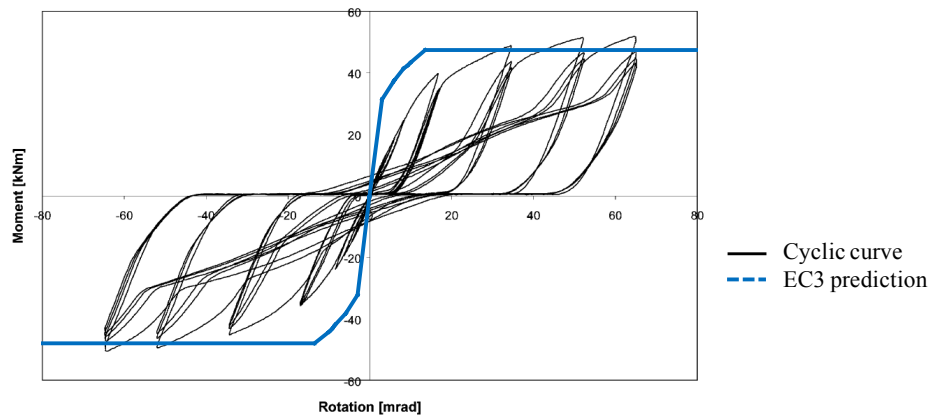


Figure 5.10. Theoretical vs. experimental results for specimen EP4 tested by Broderick and Thomson [2002].

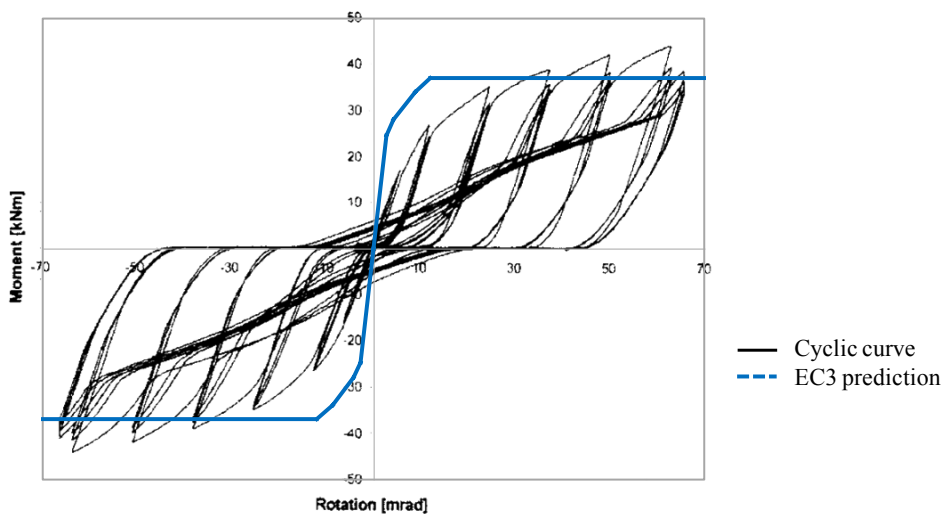


Figure 5.11. Theoretical vs. experimental results for specimen FP2 tested by Broderick and Thomson [2005].

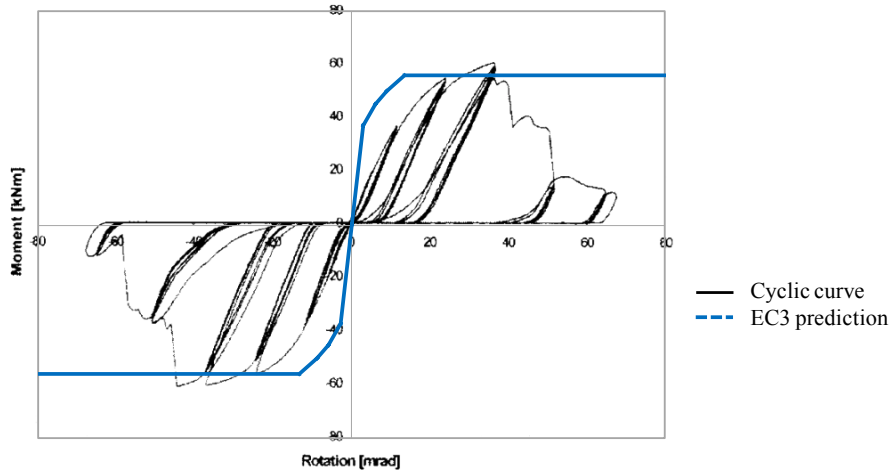


Figure 5.12. Theoretical vs. experimental results for specimen FP4 tested by Broderick and Thomson [2005].

5.3.1.1 Summary

For a generic test result, the experimental value of the plastic resistance ($M_{R,exp}$) was defined as the moment measured at a rotation such that the secant stiffness is 1/3 of the initial experimental stiffness. This definition is consistent with the theoretical moment-rotation relationship assumed by the EC3 model (Section 5.2). The experimental value of the initial stiffness ($S_{ini,exp}$) was obtained as the slope of a straight line drawn through the following two points:

- i) The first point has coordinates given by a moment equal to 2/3 of the theoretical plastic resistance ($2/3M_{R,th}$ = elastic limit) and a corresponding rotation from the experimental moment-rotation response curve.
- ii) The second point is determined in a similar manner, but the moment is taken equal to 1/10 of the plastic resistance.

This procedure generally eliminates any possible initial settling of the connections. Figure 5.13 is an illustrative diagram showing the procedure described above.

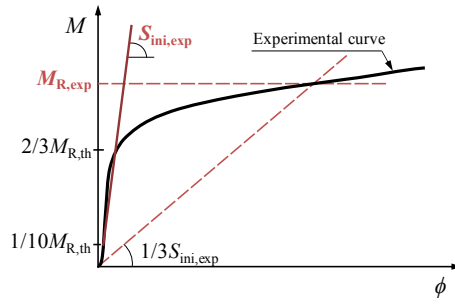


Figure 5.13. Experimental value of initial stiffness and plastic resistance.

Figure 5.14 illustrates the comparison between experimental results and theoretical predictions for all the considered extended end-plate connections. Figure 5.14(a) shows the comparison in terms of initial stiffness, while Figure 5.14(b) is for the plastic resistance. In both Figures, the vertical axis plots the ratio between the theoretically predicted parameter (initial stiffness, $S_{\text{ini},\text{th}}$, or plastic resistance, $M_{\text{R},\text{th}}$) and the experimental result (initial stiffness, $S_{\text{ini},\text{exp}}$, or plastic resistance, $M_{\text{R},\text{exp}}$), while the horizontal axis plots a simple numbering of specimens. Figure 5.14(a) shows that the mean value of the ratio between theoretical and experimental values of the initial stiffness is 1.46, while the standard deviation of the ratio is equal to 0.84. Figure 5.14(b) shows that the mean and the standard deviation of the plastic resistance ratio are equal to 0.87 and 0.18, respectively. Hence, the ability to theoretically predict the plastic resistance appears more accurate than the ability to predict the initial stiffness of the connection, where the uncertainty in the prediction of initial stiffness is large.

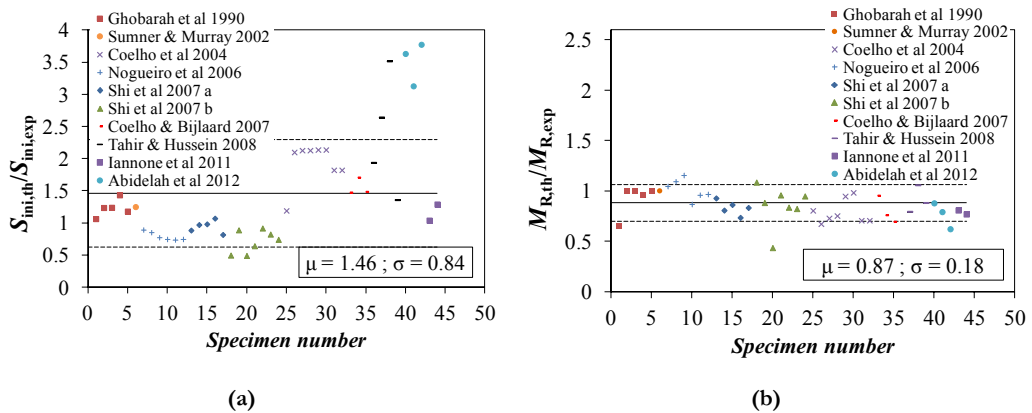


Figure 5.14. Theoretical vs. experimental results for extended end-plate joints: (a) initial stiffness (b) plastic resistance.

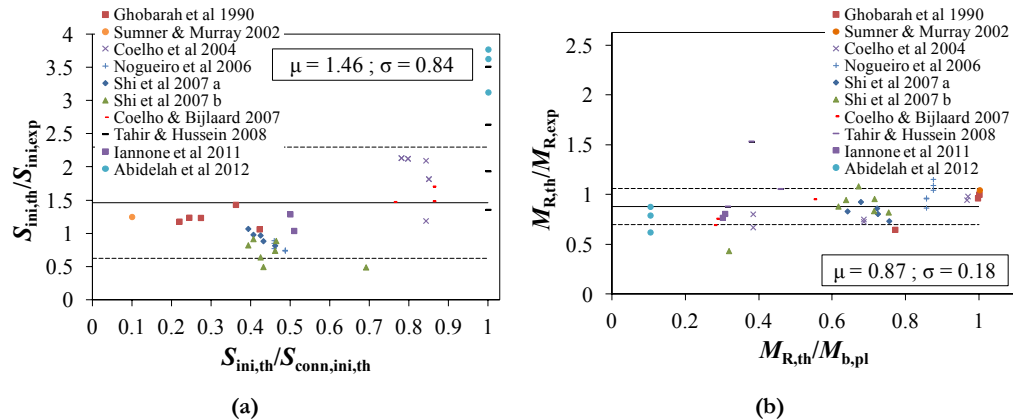


Figure 5.15. Theoretical vs. experimental results for extended end-plate joints: the role of joints.

Figure 5.15(a) plots on the vertical axis again the ratio between the theoretical and the experimental values of the initial stiffness, but the horizontal axis is the ratio between the theoretical value of the initial stiffness of the whole system experimentally tested ($S_{\text{ini,th}}$) and the initial stiffness of an ideal system constituted by the beam-to-column connection only ($S_{\text{conn,ini,th}}$). Considering that the reciprocal of stiffness is flexibility and that the total system flexibility is obtained by the addition of the flexibility of the different components constituting the beam-to-column assemblage, the horizontal axis in Figure 5.15(a) represents the relative influence of the beam-to-column connection on the whole system flexibility. The ratio varies between 0 (ideally rigid connections) and 1 (ideally the connection only). Figure 5.15(a) clearly shows a trend to obtain large overestimation of the system stiffness when the connection deformations are governing the system response, i.e. when the ratio $S_{\text{ini,th}}/S_{\text{conn,ini,th}}$ approaches a value of 1. Therefore, the largest source of uncertainty to the total variance observed from Figure 5.14(a) is due to the modelling of the connections' initial stiffness. Figure 5.15(b) is a plot of the theoretical to experimental plastic resistance ratio, as function of the ratio of the connection theoretical plastic resistance and the beam plastic moment. Figure 5.15(b) shows that there is no special relationship between the ability to predict theoretically the plastic resistance and the degree of plastic resistance, i.e. the resistance of weak connections is predicted to the same level of accuracy as the resistance of strong connections.

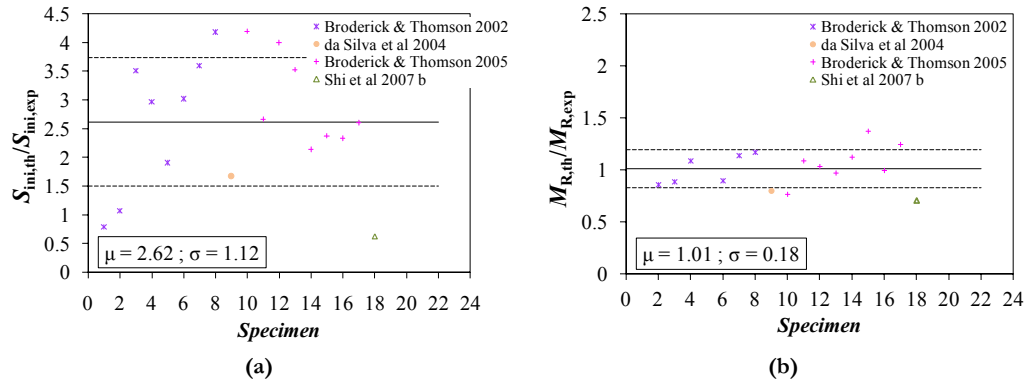


Figure 5.16. Theoretical vs. experimental results for flush end-plate joints: (a) initial stiffness; (b) plastic resistance.

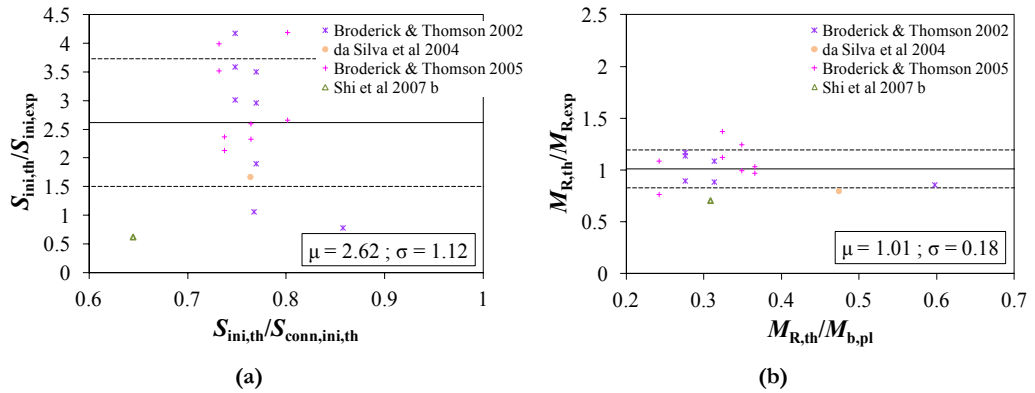


Figure 5.17. Theoretical vs. experimental results for flush end-plate joints: the role of joints.

Figure 5.16 illustrates data for flush end-plate connections similar to that shown in Figure 5.14 for extended end-plate connections. Figure 5.16(a) illustrates that the mean value of the ratio of theoretical and experimental initial stiffness is much larger than unity (2.62) and the standard deviation is also very large (1.12). Observing Figure 5.16(b), the mean value of the ratio between the theoretical and the experimental resistance is now slightly larger than unity (1.01). The standard deviation of the above ratio is 0.18, equal to the value observed for extended end-plate connections. Therefore, the flush end-plate connections appear to have response characteristics similar to the extended end-plate connections. It is noted that most of the available experimental data for flush end-plate connections in this study was obtained from the experimental campaigns carried out by a single research group [Broderick and Thomson, 2002, 2005]. Therefore, additional and independent results are needed for flush end-plate connections, in order to ascertain the validity of these preliminary statistical results.

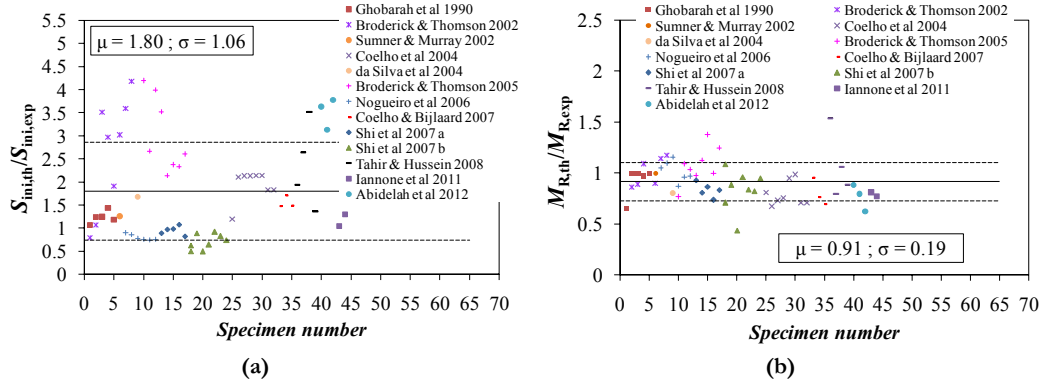


Figure 5.18. Theoretical vs. experimental results for end-plate joints: (a) initial stiffness (b) plastic resistance.

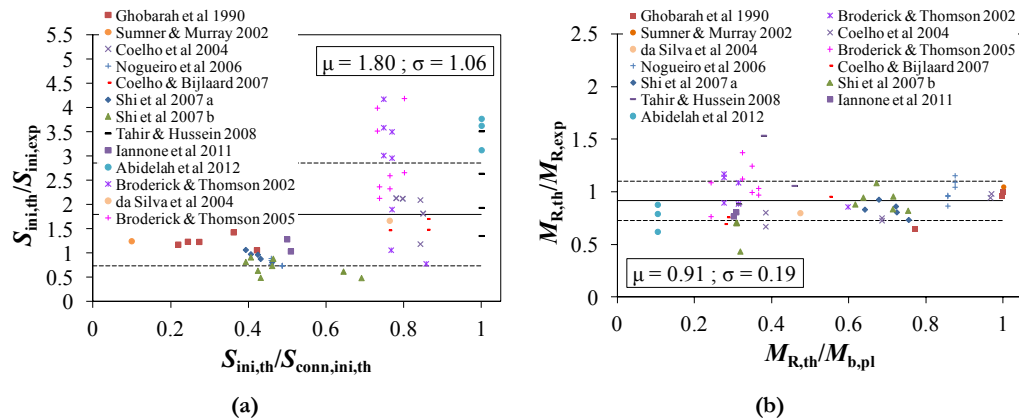


Figure 5.19. Theoretical vs. experimental results for end-plate joints: the role of joints.

Considering the similarity of results from the statistical assessment of the EC3 component method for extended and flush end-plate connections, the results for both types of connections have been put together in Figure 5.18 and Figure 5.19. This is advantageous in terms of the statistical assessment, in order to have a larger database. Figure 5.18(a) shows that the stiffness comparison's statistical parameters change when also flush end-plates are included in the database in addition to extended end-plates. The mean value of the theoretical to experimental initial stiffness ratio is now equal to approximately 1.80, while the standard deviation is approximately 1.06. This is an expected worsening of the comparison, due to the fact that flexible connections worsen the ability to predict the system elastic response. Figure 5.19(a) confirms this last

conclusion, but also shows that the scattering of response is large if systems with similar relative influence of connections are considered. In fact, for a given ratio $S_{\text{ini,th}}/S_{\text{conn,ini,th}}$, the theoretical stiffness can vary from being almost equal to 1 up to being almost 4 times larger than the experimental result.

Finally, Figure 5.18(a) and Figure 5.19(b) show that there is not a significant effect of the inclusion of flush end-plate connections on the statistical comparison in terms of plastic resistance (compare statistical data given in panels (b) of Figure 5.18 to Figure 5.19).

5.3.2 Plastic Rotation Capacity

5.3.2.1 Overview

The joint rotation capacity ($\phi_{j,c}$) was conventionally evaluated as the maximum rotation corresponding to the intersection of the horizontal line to $M=M_{j,R,\text{exp}}$ with the experimental moment-rotation response curve (Figure 5.20). The ultimate rotation ($\phi_{j,u}$) was defined as the rotation corresponding to joint failure, e.g. rupture of bolts, fracture of plates or welds and/or very large loss of strength (Figure 5.20).

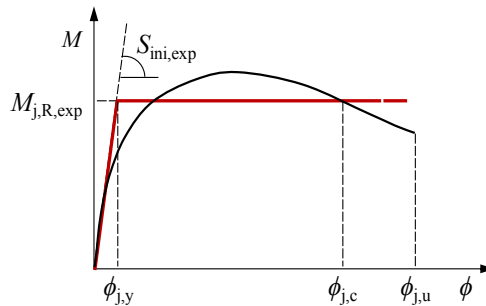


Figure 5.20. Definitions of rotation capacity and ultimate rotation.

Consequently, the plastic rotation capacity ($\phi_{j,pc}$) and the ultimate plastic rotation ($\phi_{j,pu}$) were defined as follows:

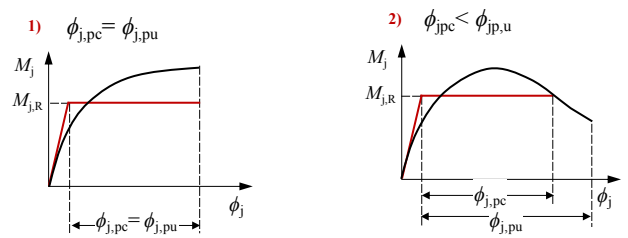
$$\phi_{j,pc} = \phi_{j,c} - \phi_{j,y,\text{exp}} \quad (5.7)$$

$$\phi_{j,pu} = \phi_{j,u} - \phi_{j,y,\text{exp}} \quad (5.8)$$

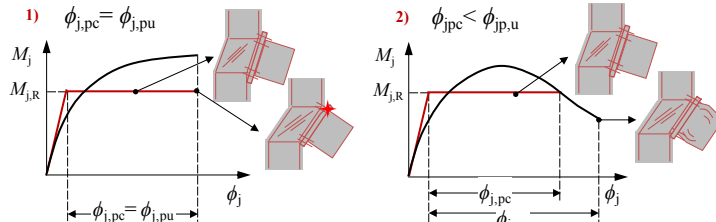
where $\phi_{j,y,\text{exp}}$ is the experimental yield rotation defined as the ratio of the plastic resistance and the initial stiffness measured in the experiment.

The definition of the rotation capacity according to Figure 5.20 is intended to establish limits to the perfectly plastic joint resistance model. At rotations larger than the capacity,

the joint resistance becomes smaller than the assumed value and the reliability of the model is lost. The ultimate rotation can be larger than the defined rotation capacity, when the system exhibits gradual and smooth loss of strength. When a sudden failure occurs, e.g. a bolt rupture or a weld fracture, the ultimate rotation coincides with the above defined rotation capacity. The difference between the ultimate rotation and the rotation capacity allows for consideration of consequences of joint failure when exceeding the rotation capacity, i.e. larger consequences should be associated with the case of an ultimate rotation being equal to the assumed capacity. On the other hand, economic consequences of exceeding a threshold of plastic rotation, in terms of repairing costs, are not dealt with in this report, although they are highlighted as potential future research developments in this area.



A: Failure occurs in the component which first yields



B: Failure occurs in a component different from the one that starts yielding

Figure 5.21. Analysis criteria for rotation capacity.

In general, joint failure can occur either in the component that first reaches the yield resistance or in a different component. In fact, due to strain hardening, the rupture can move from the weaker and more ductile component to a stronger and less ductile component. For example, this situation occurs when plastic deformations appear first in the column web panel in shear. The high ductility of the shear mode of deformation is associated with significant strain hardening of the panel zone, eventually leading to either connection failure or beam flexural yielding. From the above discussion, Figure 5.21 shows the analysis criteria considered in the evaluation of the rotation capacity and the plastic rotation capacity based on experimental results. The experimental results were

divided in two different classes, designated A and B. The A class includes all cases where the ultimate failure mode coincides with the plastic mechanism. Class B includes the cases where differences are observed between the ultimate failure mode and the plastic mechanism. For each class, two subclasses (1 and 2) were identified corresponding to $\phi_{j,pc} = \phi_{j,pu}$ and $\phi_{j,pc} < \phi_{j,pu}$, respectively.

5.3.2.2 Experimental data on extended end-plate joints

Examination of the plastic rotation capacity of joints with extended end-plate connections is briefly summarised in this section using the available experimental test results. The values obtained for the rotation capacity are summarised firstly based on the experimental test series. For each test series, the values are shown in order of increasing plastic rotation capacity and each specimen was classified according to the criteria presented in Figure 5.21.

Figure 5.22 shows the plastic rotation capacity of specimens tested by Ghobarah *et al.* [1990]. In these tests, the column web panel was restrained from shear deformations and hence, the results exclude any contribution from the column web panel in shear. The tests were performed on extended end-plate connections with different details. Specimens A-1 and A-4 were extended end-plate configurations without beam flange continuity plates and end-plate rib stiffeners. The two specimens differed for the end-plate thickness (Figure 5.22) but both specimens behaved as partial strength joints. According to the analysis criteria (Figure 5.21), they both belong to class A1 because failure occurred in the component which first yielded (end-plate in bending) and the plastic rotation capacity ($\phi_{j,pc}$) is equal to the ultimate rotation capacity ($\phi_{j,pu}$), because of fracture of the end plate. Specimens A-2, A-3 and A-5 were characterised by the presence of beam flange continuity plates; in case of A-3 and A-5 end-plate rib stiffeners were also included. These three configurations were full-strength joints with the formation of a beam plastic hinge. In specimens A-2, A-3 and A-5, failure occurred in the component which first yielded, i.e. the beam end. The measured rotation capacity ($\phi_{j,pc}$) is smaller than the ultimate plastic rotation ($\phi_{j,pu}$) for these specimens due to the gradual strength deterioration associated with the flexural plastic hinge. Therefore, specimens A2, A3 and A5 were classified as A2 with reference to criteria shown in Figure 5.22. It is worth mentioning that the results for full-strength joints are reported herein just for completeness, as well as for comparison purposes, even if the rotation capacity is not strictly that of the joint.

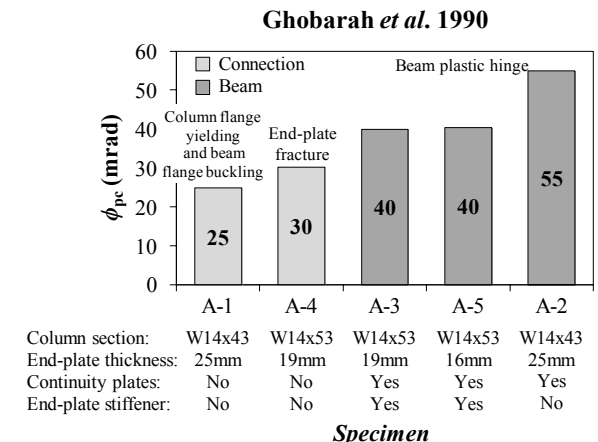


Figure 5.22. Plastic rotation capacities for Ghabbarah et al. [1990] specimens.

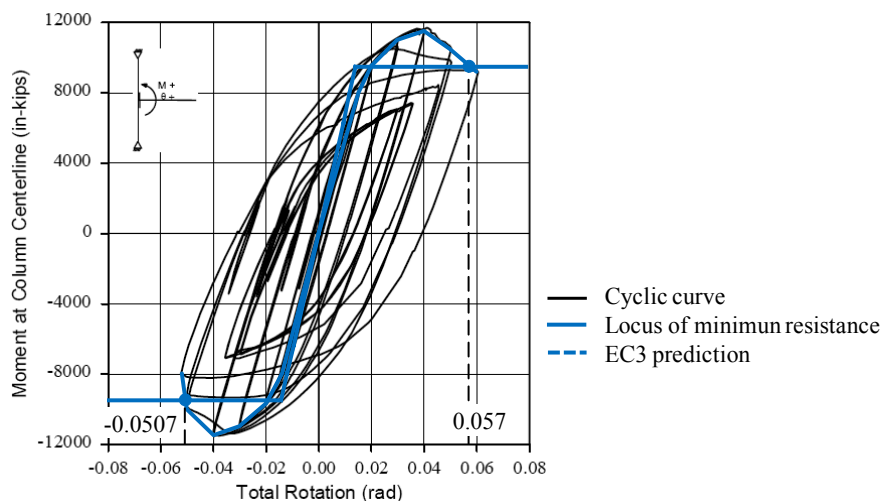


Figure 5.23. Plastic rotation capacities for Sumner and Murray [2002, 2003] specimens.

One of the specimens tested by Sumner and Murray [2002, 2003] (Figure 5.23) was an extended end-plate connection with beam continuity plates and a column web reinforcing plate. This is one additional case where the joint exhibited full-strength, allowing for the formation of a plastic hinge in the beam. This test is classified as A2 as the plastic mechanism coincides with the ultimate failure mode and the rotation capacity is smaller than the ultimate rotation of the joint. The plastic rotation capacity ($\phi_{pc} = 37$ mrad, average of the values from positive and negative deformation excursions) is comparable to the one exhibited in the tests by Ghabbarah *et al.* [1990] shown in Figure 5.22.

Figure 5.24 displays the plastic rotation capacities of joints tested by Coelho *et al.* [2004]. Eight extended end-plate joints were tested under monotonic loads. The specimens were grouped into four series named FS1, FS2, FS3, and FS4. Each set was different from the other for the end-plate thickness and/or the steel grade. The authors designed the specimens to produce the failure of the end-plate or bolts in order to investigate the effect of the geometry and material properties on the joint response. All the tested specimens behaved as expected. In series FS1, large plastic deformations in the end-plate were observed, even if the beam-to-plate weld failure produced the premature cracking of specimen FS1a. For series FS2, FS3 and FS4 bolt fracture produced the joint failure. In such cases, nut stripping or bolt fracture was observed. According to the analysis criteria of Figure 5.21 all specimens are classified as A1 except for FS1b, which is classified as A2. As shown in Figure 5.24 the plastic rotation capacity increases significantly when the end-plate thickness is decreased, i.e. when failure by end-plate yielding is favoured.

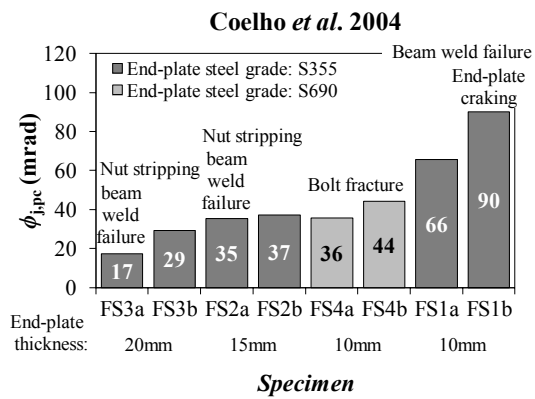


Figure 5.24. Plastic rotation capacities for Coelho *et al.* [2004] specimens.

Figure 5.25 displays the plastic rotation capacity measured for specimens J-1.1 and J-3.1, which were tested by Nogueiro *et al.* [2006] under monotonic loads. The specimens are extended end-plate joints provided with beam flange continuity plates and these specimens differ only for the column shape. According to the authors of the tests, in both specimens yielding occurred in the column web panel in shear. While for specimen J-1.1 the experimental test was continued up to the end-plate fracture, this was not the case for specimen J-3.1. Specimens J-1.1 and J-3.1 can be classified as B1 and A1, respectively.

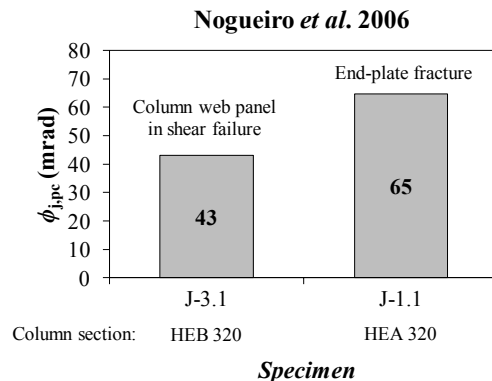


Figure 5.25. Plastic rotation capacities for Nogueiro *et al.* [2006] specimens.

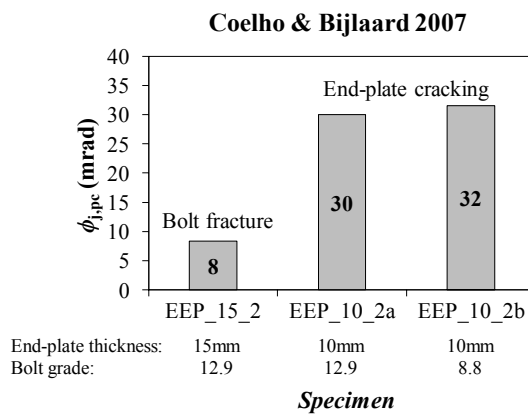


Figure 5.26. Plastic rotation capacities for Coelho and Bijlaard [2007] specimens.

Coelho and Bijlaard [2007] analysed three cases of extended end-plate joints with the end-plate made of high strength steel, under monotonic loads. Figure 5.26 shows the plastic rotation capacities of such specimens. Both the end-plate thickness and the bolt grade were varied from one specimen to the other and these specimens behaved as partial strength joints. The ultimate failure modes were bolt fracture and end-plate cracking. According to the analysis criteria of Figure 5.25, EEP_15_2, EEP_10_2a and EEP_10_2b belong to class A1. In fact, failure occurred in the component which first yielded and the plastic rotation capacity (ϕ_{ipc}) was equal to the ultimate rotation capacity (ϕ_{ipu}). The experimental program confirmed that larger rotation capacities are associated with joint arrangements characterised by strong bolts and weak end-plate.

The plastic rotation capacities of the specimens tested by Shi *et al.* [2007a, 2007b] are given in Figure 5.27 and Figure 5.28, which are relevant to the two different experimental

investigations carried out by the authors. In both cases, extended end-plate connections with beam flange continuity plates and end-plate rib stiffeners were analysed. Differences between the two sets of experimental tests were the loading protocols and the investigated joint parameters. In the first experimental activity, the specimens were tested under monotonic loads and the influence of the end-plate thickness and/or the bolt diameter on the joint behaviour was studied. The second test series considered cyclic loading protocols and in addition to the geometrical parameters studied with the former tests, the effect of continuity plates and end-plate stiffeners was also evaluated.

Figure 5.27 shows the rotation capacities evaluated for the specimens belonging to the first test series. The authors of the tests provided data for the contribution to the whole joint response from both connections and column web panels in shear. As shown in the figure, a large part of the plastic rotation capacity is due to the ductility of the column web panel in shear. The latter is the component predicted to yield and to determine the joint plastic resistance. However, because of the large deformation capacity and associated strain hardening, either connection failure (EPC-1, EPC2, EPC5) or the development of a beam plastic hinge (EPC3, EPC4) was observed as the ultimate failure mode. All specimens were therefore classified as B1, according to the classification criteria of Figure 5.21.

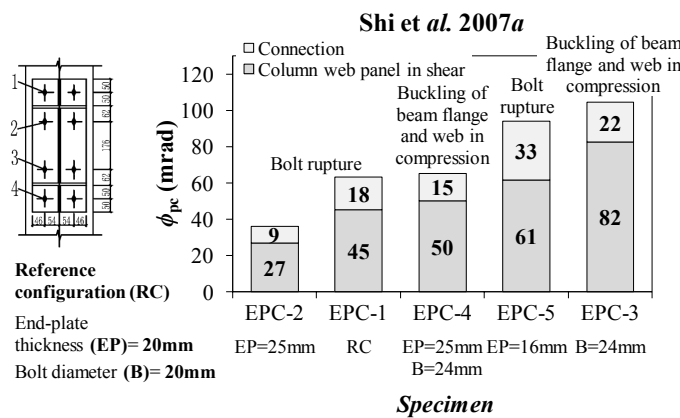


Figure 5.27. Plastic rotation capacities for Shi et al.[2007a] specimens.

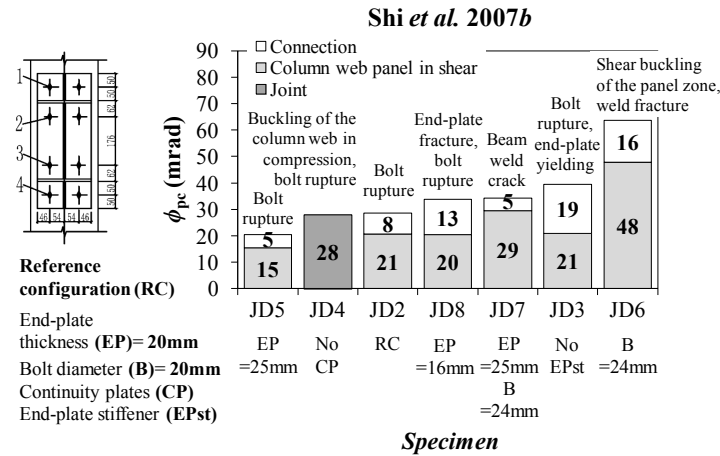


Figure 5.28. Plastic rotation capacities for Shi et al. [2007b] specimens.

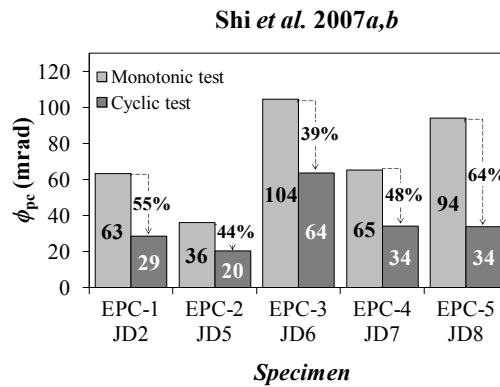


Figure 5.29. Comparison of plastic rotation capacities of Shi et al. [2007a, 2007b] specimens.

Similar observations can be derived from the analysis of the results obtained with the second experimental testing activity (Figure 5.28). In addition, observations on the influence of both the end-plate stiffener and the beam flange continuity plates can be derived. The removal of the end-plate rib stiffener produced the increase of the connection contribution to the plastic rotation capacity because of the larger deformability of the end-plate. The removal of the continuity plates introduced at the compression side of the connection the buckling of the column web as an additional failure mechanism. The plastic rotation capacity contains significant contributions from the column web panel in shear, as much in percentage to the total rotation as more the connection is made full strength.

The plastic rotation capacities of the specimens belonging to the two test series were compared to evaluate the effects of cyclic loads on plastic rotation capacity of extended end-plate joints. This comparison is possible because the two test series include couples of nominally identical specimens (Figure 5.27 and Figure 5.28). The results of this comparison are presented in Figure 5.29. As expected, larger values of the rotation capacity are associated with the monotonic tests. The difference between the monotonic and cyclic test results is equal to 50% on average.

Figure 5.30 shows the plastic rotation capacities of four extended end-plate connections tested by Tahir and Hussein [2008]. End-plate thickness, bolt diameter and end-plate width were varied from one specimen to the other. Specimens EEP6 and EEP7 were characterised by the end-plate failure. For specimens EEP8 and EEP9 column flange failure was observed. As shown in Figure 5.30, larger plastic rotation capacities were measured for thinner end-plates. For all specimens, failure occurred in the component where yielding started and the plastic rotation capacity is equal to the ultimate plastic rotation; therefore, these specimens can be classified as A1.

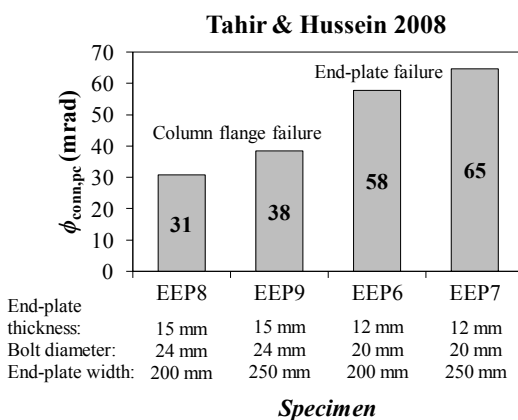


Figure 5.30. Plastic rotation capacities for Tahir and Hussein [2008] specimens.

Iannone *et al.* [2011] tested two extended end-plate joints under cyclic loads. Figure 5.31 shows the plastic rotation capacities obtained from the analysis of the published results. The specimens, identified as EEP-CYC-01 and EEP-CYC-02, were designed to produce yielding of either the column web panel in shear (EEP-CYC-01) or the end-plate in bending (EEP-CYC-02). EEP-CYC-01 is an extended end-plate without any column reinforcement, while EEP-CYC-02 is characterised by the presence of beam flange continuity plates and column web supplementary plates. Ultimate failure of EEP-CYC-01 occurred because of the brittle fracture of the beam-to-plate welds, but only after large yielding of column web panel in shear. In case of EEP-CYC-02, the ultimate failure mode was the end-plate fracture. The measured plastic rotation capacity of specimen EEP-CYC-01 is equal to the ultimate plastic rotation. Conversely, for specimen EEP-CYC-02

the plastic rotation capacity is smaller than the ultimate plastic rotation. Therefore, the specimens EEP-CYC-01 and EEP-CYC-02 were classified as B1 and A2, respectively.

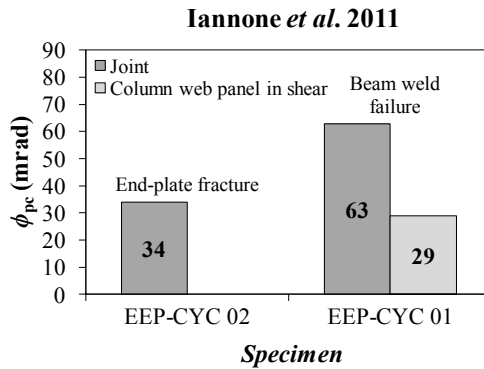


Figure 5.31. Plastic rotation capacities for Iannone et al. [2011] specimens.

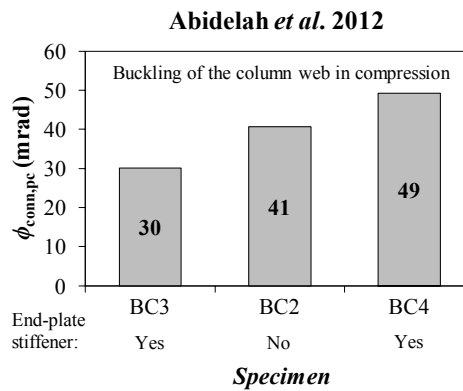


Figure 5.32. Plastic rotation capacities for Abidelah et al. [2012] specimens.

Figure 5.32 shows the plastic rotation capacities of the specimens tested by Abidelah *et al.* [2012]. The specimens are internal extended end-plate beam-to-column joints tested under monotonic loading. The experimental tests aimed to investigate the influence of the end-plate rib stiffener on the whole joint response. The column was chosen to be weak in order to localise plastic deformations in the column components. BC2 is an extended end-plate connection with unstiffened end-plate. Specimen BC3 is obtained from BC2 by providing the end-plate with a rib stiffener in the tension zone of the connection. Specimen BC4 is obtained from BC2 by stiffening the end-plate both on the tension and the compression side. For all the specimens, failure occurred due to buckling of the column web in compression, even if the component which started first yielding was the column flange in bending. Since the plastic rotation capacity is equal to the

ultimate plastic rotation, BC2, BC3 and BC4 are classified as B1 (Figure 5.21). The plastic rotation capacity of specimen BC3 is smaller than that measured for specimen BC2 because of the end-plate stiffener on the tension side, which reduced the deformations of the end-plate. A larger value of the plastic rotation capacity was measured for specimen BC4; therefore, it seems that stiffening the end-plate in the compression zone had a beneficial effect on the response in this case where the ultimate failure was due to buckling of the column web in compression.

The analysed experimental data clearly shows that the plastic rotation capacity is influenced by the ultimate failure mode. In general, full strength joints were characterised by larger values of the plastic rotation capacity compared with partial strength joints. Even if the column web panel provides large rotation capacity, sometimes comparable or even larger than that obtained in case of a beam plastic hinge, considerations regarding the consequences in terms of possibility to repair the damaged column should be taken into account. Besides, the large strain hardening of the column web panel in shear can lead to requirements in terms of large overstrength of the bolted end-plate connection in order to avoid relatively brittle ultimate failure modes (e.g. bolt rupture). The latter mode of failure corresponds to the easiest way to repair the joint, but also to the largest consequences in terms of deterioration of the joint mechanical performance.

In addition to the above comments, it is noted that when strain hardening is responsible for the ultimate failure mode being different from the main (initial) plastic mechanism, then it is difficult to associate a plastic rotation capacity to the joint response, unless large variations of the actual values are accepted. This is because of the many different potential ultimate failure modes and the small quantity of available experimental data. Therefore, a characterisation of the strain hardening of joint components is a necessary requisite in view of the development of rational methods to assess the joint rotation capacity. In Section 5.3.3, the strain-hardening of column web panels in shear is examined further.

5.3.2.3 *Experimental data on flush end-plate joints*

Figure 5.33 shows the plastic rotation capacities of specimens tested by Broderick and Thomson [2002]. Flush end-plate joints were tested under both monotonic and cyclic loading conditions. The geometry of the specimens was varied to ensure that three failure modes characterising the end-plate equivalent T-stub were activated. The specimens differ in the beam shape, the end-plate thickness and the bolt size. The specimen labelled EP2 failed due to end-plate yielding and bolt failure, while EP3 and EP4 were characterised by complete end-plate yielding. Bolt failure was observed for specimens EP6, EP7 and EP8. For all specimens failure occurred in the component which first yielded and the plastic rotation capacity is equal to the ultimate plastic rotation and

therefore, the specimens are labelled class A1. Larger plastic rotation capacities are associated with end-plate yielding, a more ductile failure mode, such as the mode exhibited by specimens EP3 and EP4. Conversely, smaller plastic rotation capacities were measured for specimens EP6, EP7 and EP8 due to the bolt failure. Observing Figure 5.33, the effect of the cycling loading on the plastic rotation capacity can be evaluated. For a given geometrical configuration (EP6, EP7 and EP8 or EP3 and EP4), the plastic rotation capacity measured in the monotonic test is comparable to that evaluated in the cyclic test. This is a consequence of the large pinching effects characterising the hysteresis response curve: the system degradation is largely dominated by the peak deformation demand, while the repetition of loading cycles at given amplitude produces relatively small additional degradation.

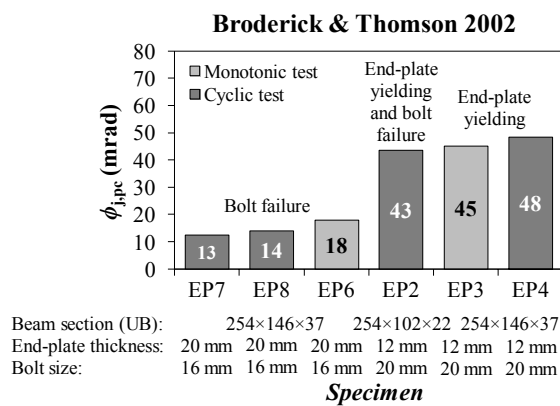


Figure 5.33. Plastic rotation capacities for Broderick and Thomson [2002] specimens.

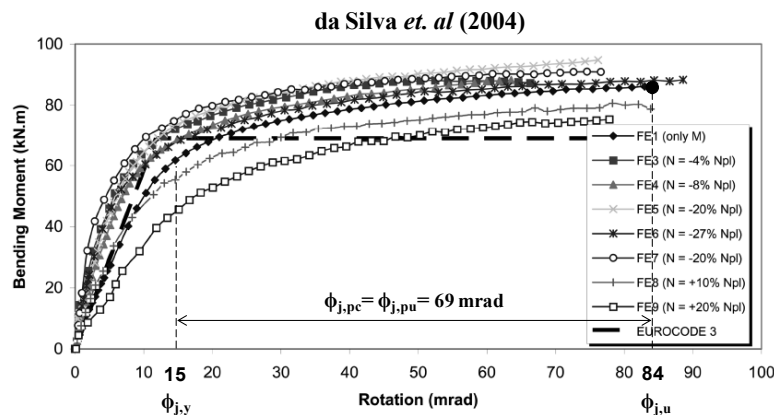


Figure 5.34. Plastic rotation capacity for da Silva et al. [2004] specimen.

Figure 5.34 provides a summary of the results in terms of plastic rotation capacity from one test on a flush end-plate joint tested by da Silva *et al.* [2004]. The specimen, labelled FE1, belongs to class A1, according to the classification criteria of Figure 5.21. The plastic rotation capacity is reported in Figure 5.34, and it is relevant to a mixed mode of end-plate yielding and bolt failure. As displayed in Figure 5.34, the plastic rotation capacity is equal to 69 mrad, which is a value comparable to those measured for extended end-plate joints and a similar failure mode.

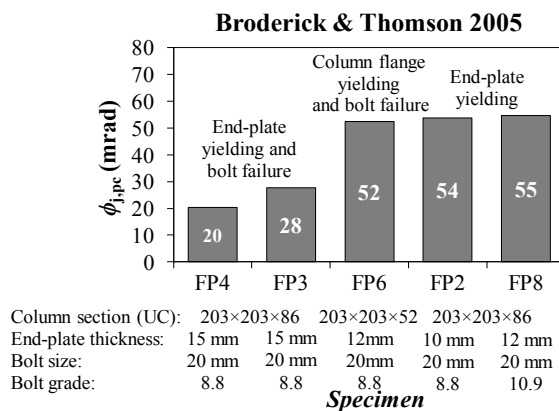


Figure 5.35. Plastic rotation capacities for Broderick and Thomson [2005] specimens.

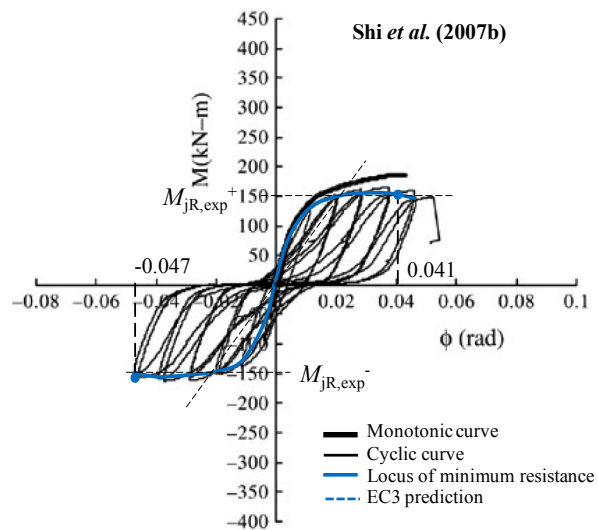


Figure 5.36. Plastic rotation capacity for Shi et al. [2007b] specimen.

The plastic rotation capacities of flush end-plate joints tested by Broderick and Thomson [2005] are presented in Figure 5.35. Similarly to previous experiments, Broderick and Thomson [2002] carried out tests on flush end-plate joints to investigate their structural performances by varying the connection details. The end-plate thickness and the bolt properties were varied, in addition to the column shape. The specimens were designed to exhibit the following failure modes: end-plate yielding for specimens FP2 and FP8; end-plate yielding and bolt failure for specimens FP3 and FP4; column flange yielding and bolt failure for specimen FP6. These expectations in terms of failure modes were all confirmed by experimental observations. According to the classification of Figure 5.21, the specimens can be classified as A1 and again, larger values of plastic rotation capacity are associated with the end-plate yielding mechanism.

Figure 5.36 shows evaluation of the rotation capacity for the specimen labelled JD1, which was tested by Shi *et al.* [2007b] under cyclic loads. Failure was expected in the connection according to a mixed failure mode of end-plate yielding and bolt failure, which was confirmed during the test. As shown in Figure 5.36, the ultimate plastic rotation coincides with the plastic rotation capacity, and therefore JD1 is a class A1 specimen.

5.3.2.4 Plastic rotation capacity and failure modes

In this section, the plastic rotation capacities of end-plate joints are grouped according to the failure mode, where distinction between tests is made in terms of connection type (extended or flush end-plate), contribution from the column web panel in shear to the joint plastic rotation (presence or absence of such contribution) and loading protocol (monotonic or cyclic loading). The data is always presented in order of increasing plastic rotation capacity.

Figure 5.37 displays the plastic rotation capacities in case of bolt failure, where values from 5 mrad up to 9 mrad are associated with the extended end-plate connections named JD5, JD2 and EPC-2 tested by Shi *et al.* [2007a, b]. JD5 and JD2 belong to the same test series (Figure 5.28). They differ in their end-plate thickness, which is 20 mm in case of JD2 and 25 mm for JD5. The comparison of such specimens provides information about the influence of the bolt diameter to end-plate thickness ratio (t_p/d) on the connection behaviour. These results suggest that the plastic rotation capacity increase with the ratio d/t_p . A similar plastic rotation capacity (8 mrad) was measured for the extended end-plate joint EEP_15_2 [Coelho and Bijlard, 2007], which was characterised by small (but non zero) web panel shear deformations. In this particular case, the plastic deformation of the joint almost coincides with that of the connection. Flush end-plate joints exhibited larger values of the plastic rotation capacities, which is expected because the tensile deformation

at a bolt level is approximately proportional to the distance from the bolt row axis to the compression centre, for a given connection rotation. In case of flush end-plate connections, the distance of the (single) bolt row is less than that of the outer bolt row in the corresponding extended configuration. Consequently, flush end-plate connections develop larger rotations to reach the same level of tensile bolt deformations. Values of the plastic rotation capacity varying from 13 mrad up to 18 mrad were evaluated from test results of specimens EP6, EP7 and EP8 [Broderick and Thomson, 2002]. These specimens were nominally identical (Figure 5.33), while they were tested under different loading protocols: EP6 was tested under monotonic loads, while EP7 and EP8 were tested under cyclic loads.

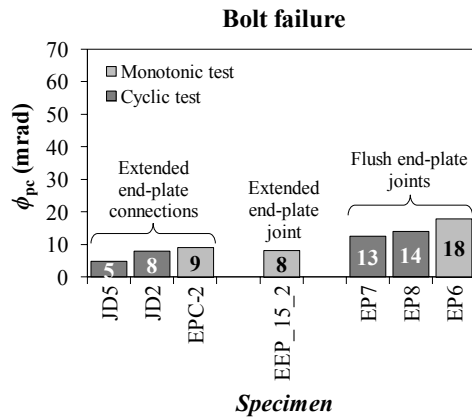


Figure 5.37. Plastic rotation capacity in case of bolt failure.

The plastic rotation capacities corresponding to equivalent T-Stub failure modes 1 are shown in Figure 5.38. Figure 5.38(a) illustrates the plastic rotation capacity for specimens in which the component that yielded first was also the one that failed first. As shown, the plastic rotation capacities of extended end-plate connections vary from 25 mrad up to 65 mrad. Within this group two subclasses can be identified. A-1, A-4, EEP8 and EEP9 constitute the first class. They are characterised by a concentration of plastic deformation either in the column flange or in the end-plate. EEP6 and EEP7 constitute the second class, characterised by contributions to the total plastic deformation from both the end-plate and the column flange. The experimental test on specimen A-1 [Ghobarah *et al.*, 1990] was stopped because of the excessive deformation of the column flange. Regarding the specimens EEP6-EEP9 [Tahir and Hussein, 2008], tests were also stopped because of excessive displacements. This implies that the plastic rotation capacity of specimens A-1, EEP6 and EEP7 could be larger than the reported values. The extended end-plate joints labelled EEP_10_2a, EEP_10_2b and EEP-CYC 02 are characterised by similar plastic rotation capacity. For all these specimens, end-plate cracking occurred around the weld

heat-affected zone. With regards to the flush end-plate joints, FP2 and FP8 belong to the set of specimens tested by Broderick and Thomson [2005]. The two specimens differ for the bolt grade only and exhibited similar plastic rotation capacity (Figure 5.35). The authors of the tests documented that end-plate yielding occurred in both specimens, but they did not provide details on damage distribution among joint components. Figure 5.38(b) displays the plastic rotation capacities of specimens where failure was caused by either column web buckling in compression (BC2, BC3 and BC4) or weld failure (FS1a and FS1b).

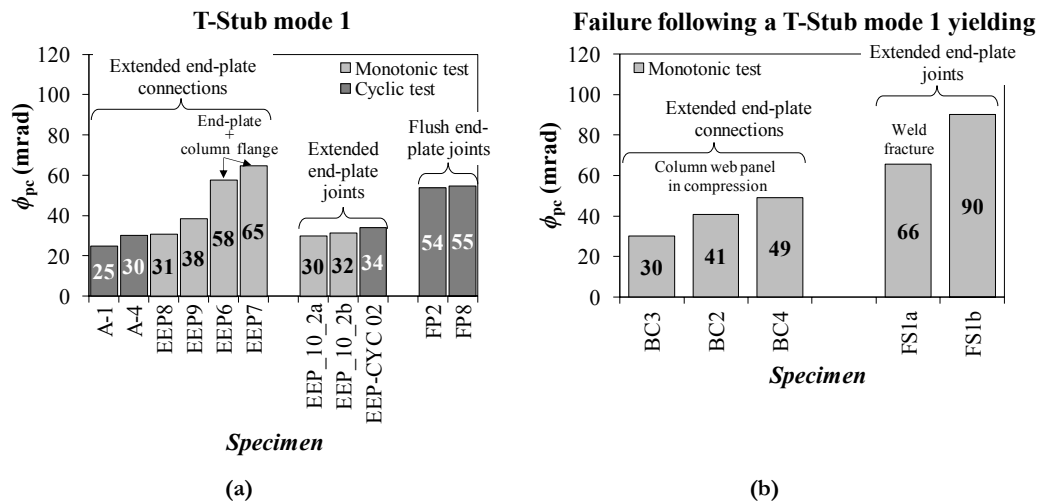


Figure 5.38. Plastic rotation capacity in case of the T-Stub mode 1 mechanism.

The plastic rotation capacities of end-plate joints showing equivalent T-Stub mode 2 plastic mechanisms are provided in Figure 5.39. If results for only extended end-plate connections are considered, values of plastic rotation capacity ranging from 18 mrad up to 33 mrad were obtained from the analysis of the available experimental tests. These results are shown in Figure 5.39 as the first group of data on the left hand side of the horizontal axis in the plot. When the contribution of the column web panel in shear is also included in the data, the plastic rotation capacity generally increases, as illustrated by the values provided with the group of data in the middle of the plot in Figure 5.39. Values ranging from a minimum of 17 mrad up to a maximum of 44 mrad can be observed.

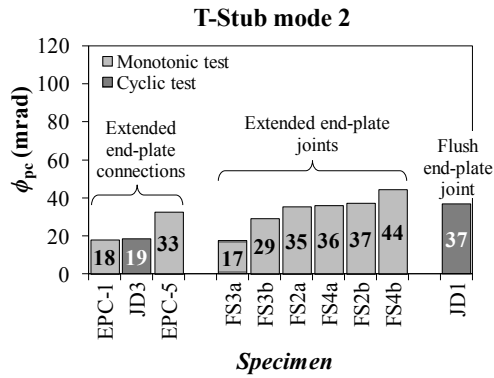


Figure 5.39. Plastic rotation capacity in case of T-Stub mode 2 mechanism.

The last specimen reported on the right hand side in the plot of Figure 5.40 is a flush end-plate joint with 37 mrad plastic rotation capacity. As expected, the plastic rotation capacity increases with the ratio (d/t_p) of the bolt diameter to the end-plate thickness. For instance, one can compare the specimens EPC-1 and EPC-5 [Shi *et al.*, 2007a] (Figure 5.40): the plastic rotation capacity increases from 18 mrad (EPC1) to 33 mrad (EPC5). Similar comparisons can be done for extended end-plate joints.

Figure 5.40 shows the plastic rotation capacities in case of shear buckling of the column web panel. Figure 5.40(a) refers to specimens where first yielding and failure occurred in the same component. Figure 5.40(b) shows all cases in which strain hardening of the column web panel, beyond shear buckling, produced the connection failure (JD2-JD8 and EPC-1, EPC-2, EPC-5) or the formation of a beam plastic hinge (EPC-3, EPC-4).

The plastic rotation capacities of the specimens characterised by the full development of a beam plastic hinge are provided in Figure 5.41 and as shown, the plastic rotation capacity varies from 37 mrad to 55 mrad.

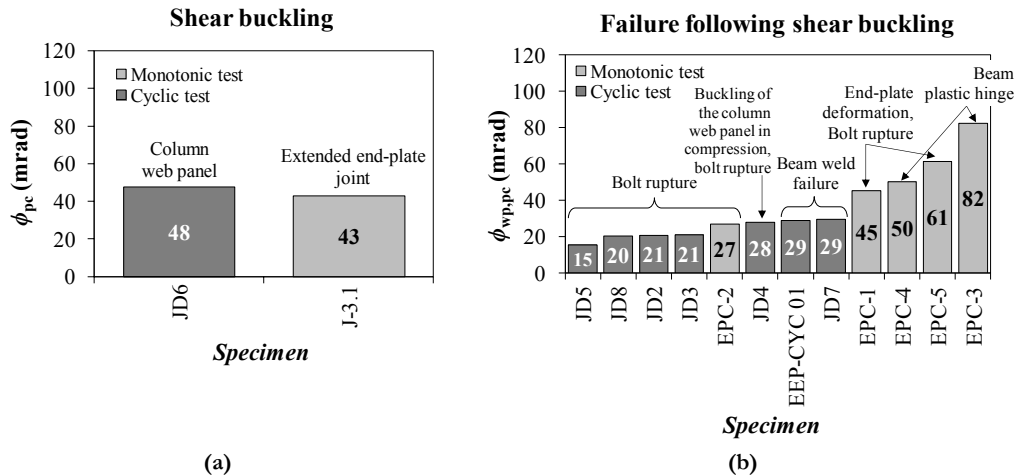


Figure 5.40. Plastic rotation capacity in case of shear buckling.

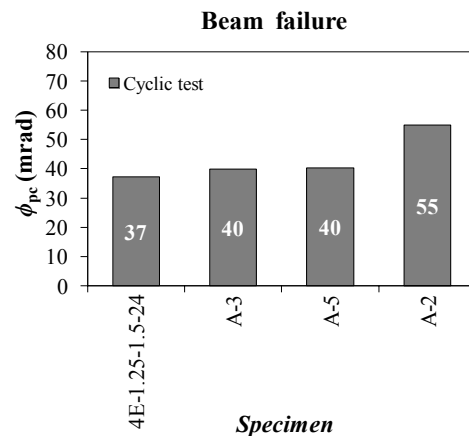


Figure 5.41. Plastic rotation capacity in case of beam plastic hinge.

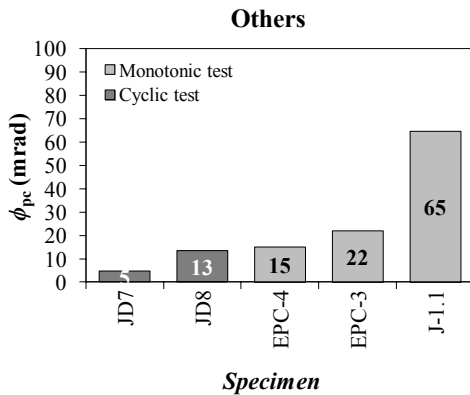


Figure 5.42. Plastic rotation capacity for other particular cases.

Figure 5.42 shows the plastic rotation capacities of extended end-plate connections and joints not included in the previous groups. These specimens are characterised by either end-plate stiffener fracture (JD7), beam welds failure (JD8), buckling of the beam web and beam flange in compression (EPC-3, EPC-4). In addition, J-1.1 is an extended end-plate joint tested by Nogueiro *et al.* [2006] in which the column web panel first yielded in shear, but due to strain hardening failure occurred in the end-plate. It is not included in any group defined above because the yielding mode is different from the failure mode. Unfortunately, the authors of the experimental test did not provide individual deformations of the connection and the column web panel in shear.

5.3.2.5 Strain-hardening of the column web panel in shear

Test results presented in Shi *et al.* [2007a, 2007b], Calado and Mele [2000] and Iannone *et al.* [2011] were used to investigate the strain hardening response of column web panels in shear. The actual shear force-deformation response was schematized by means of a bilinear relationship. The initial linear elastic response was limited by the plastic resistance, which was obtained by summing up the contributions from both the column web and the column flanges (EC3). The shear area was evaluated as $(b_c - 2t_{fc})t_{wc}$, where b_c , t_{fc} and t_{wc} are the column cross section height, the column flange thickness and the column web thickness. The post-yielding branch was obtained by connecting the point of the theoretical plastic resistance to the point of the actually measured peak resistance. Figure 5.43 shows two examples of such bilinear approximation: Figure 5.43(a) is for a monotonic loading test; Figure 5.43(b) is for a cyclic loading test. Consequently, the strain-hardening ratio has been defined as the ratio $k_{wp,sh}/k_{wp,e}$, where $k_{wp,sh}$ and $k_{wp,e}$ are the post- and pre-yielding stiffness respectively.

Figure 5.44(a) and Figure 5.44(b) illustrate the approximate bilinear relationships in case of monotonic and cyclic loading, respectively. Average ratios $k_{wp,sh}/k_{wp,e}$ are also

illustrated by means of the dashed lines. The mean strain-hardening ratios resulted equal to 4.6% and 7% in case of monotonic and cyclic loading, respectively. Ranges of variation of the strain hardening ratio were (3.5%, 5.8%) and (5%, 9.8%) in case of monotonic and cyclic loading, respectively.

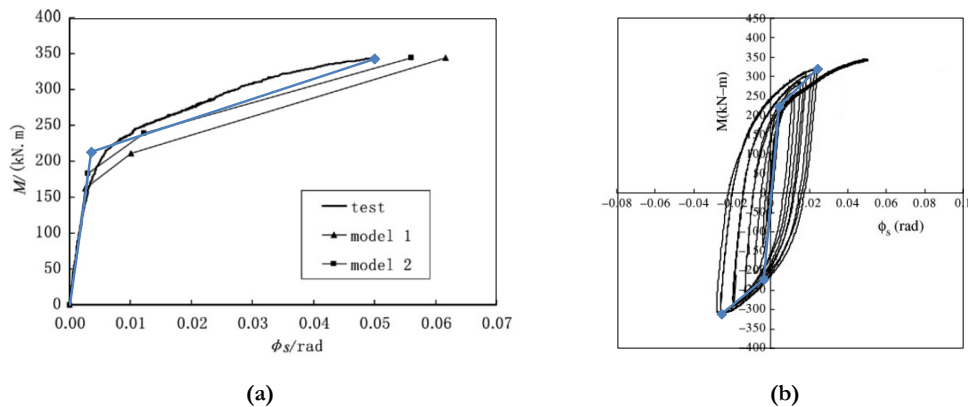


Figure 5.43. Bilinear modelling of shear force-deformation behaviour of the column web panel (test results from Shi et al. [2007a, 2007b]).

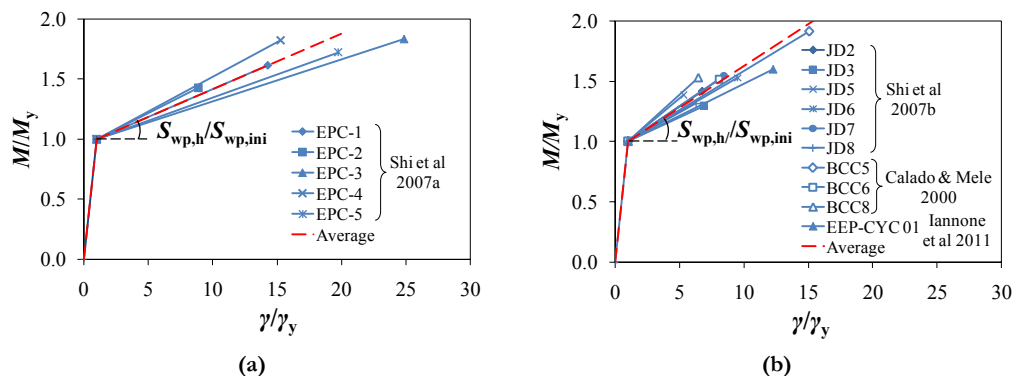


Figure 5.44. Normalised bilinear modelling of column web panel in shear: (a) monotonic loading; (b) cyclic loading.

Results of the type shown in Figure 5.44 are useful in order to evaluate the total joint plastic rotation capacity as a function of the ratio of connection to panel zone moment resistance, in case of joints yielding in the column web panel in shear and ultimately failing in connections. Starting with the ratio between the moment resistances of the connection and the column web panel in shear and using an assumed design value for the strain hardening ratio of the column web panel in shear, one could easily find the plastic deformation developing in the column web panel up to yielding of the connection. Then,

the design value of the plastic rotation capacity of the connection could be added to the plastic rotation developed in the column web panel, so that the total plastic rotation capacity is obtained.

The obtained bilinear models were also compared with a well-known model presented by Krawinkler *et al.* [1971]. Such example comparisons are shown in Figure 5.45.

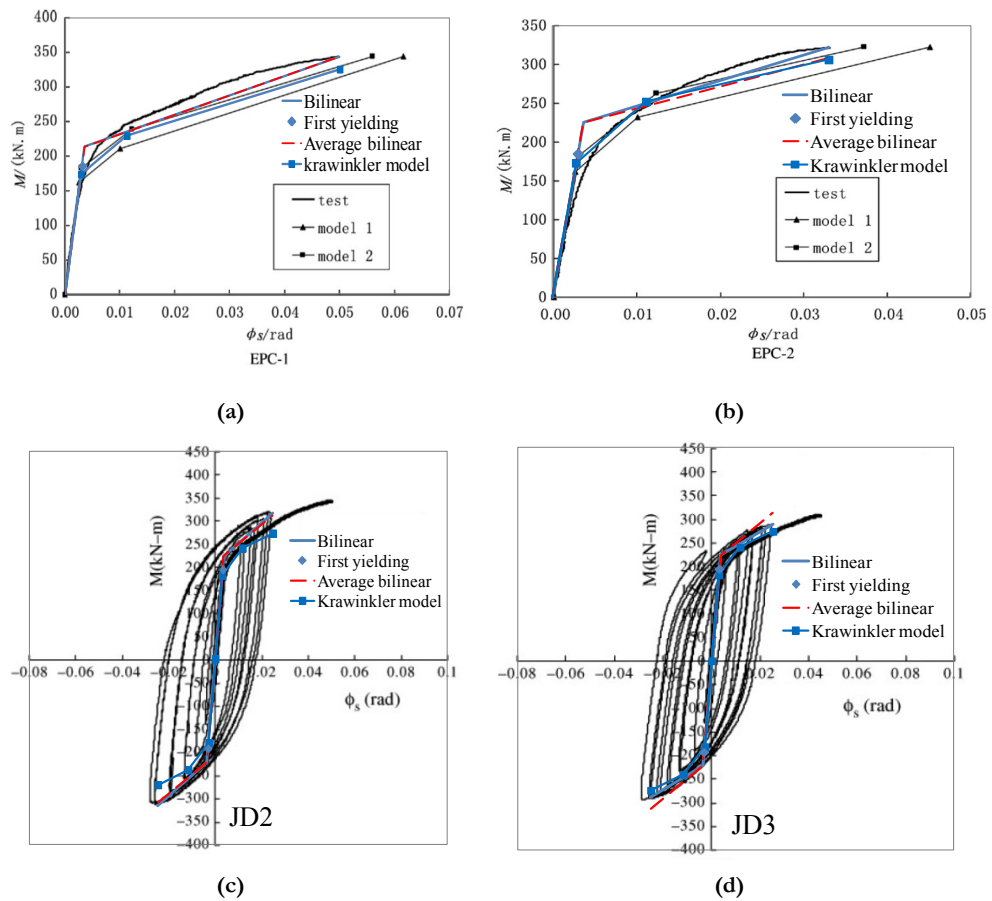


Figure 5.45. Example comparisons of approximate models.

5.3.2.6 Review and interpretation of experimental data

A collection of experimental results in terms of plastic rotation capacity of bolted end-plate beam-to-column joints has been reported in the preceding sections. The following discussion is based on a different organisation of the experimental data, such as to highlight the main factors affecting the plastic rotation capacity.

The detailed description of the available experimental results, as provided in preceding sections, shows clearly that the plastic rotation capacity is primarily a function of the type of plastic mechanism. The latter obviously depends on the relative resistance of components comprising the joint. Ideally, one should possess sufficient experimental data on the plastic rotation capacity of individual joint components and obtain the total joint rotation capacity by an assemblage of the individual components, in a manner similar to the one used for calculating the joint initial stiffness and resistance based on corresponding component characteristics. This approach has been already proposed and partially explored [da Silva and Coelho, 2001; da Silva *et al.* 2002; Beg *et al.* 2004]. However, such detailed experimental data on components is not currently available, while several experimental results on beam-to-column joint sub-assemblages are. The use of sub-assemblage tests to derive general information regarding the plastic rotation capacity of joints requires caution, because of the essential role played by the relative strength of components in the resulting value of the plastic rotation capacity. The role of the relative strength of components and the way as to how its effect should be managed is further discussed at the next paragraph.

If the components belonging to the joint have a relative plastic resistance close each to other, then evaluation of the plastic rotation capacity is difficult and the experimental results might exhibit significant scattering from one specimen to the other. Indeed, in case of two or more components having a plastic resistance close each to other, there will be two or more competing plastic mechanisms. In such a case, the actual plastic mechanism shares characteristics of different types of mechanisms and this will affect the plastic rotation capacity of the whole system. Therefore, only those test results for which the plastic mechanism is well identifiable, i.e. where different joint components have well separated plastic resistances, are considered in the following. Once the type of plastic mechanism is clearly identified, the plastic rotation capacity of a joint may still depend on the ratio of ultimate to plastic resistance of different joint components. Indeed, the component that initiates the yielding of the joint will generally also exhibit strain hardening. While the resistance of the yielding component increases more force demand is transferred to other components, thus eventually leading to an involvement of other components in the plastic range. Therefore, in order to find a clear relationship between the plastic rotation capacity and the type of plastic mechanism in the joint, it is necessary to consider only cases where the ratio of the ultimate resistance of the yielding component to the yield resistance of the non-yielding components is large enough to avoid that strain-hardening of the yielding component subsequently leads to yielding of any other component. These criteria regarding the relative resistance of different joint components may lead to discard some of the available experimental data, but it is deemed to be essential for a clear understanding of the relationship between the plastic rotation capacity and the type of plastic mechanism.

In addition, and as a complement, to the above issues, it is also noted that, frequently, researchers measure separately the contribution to the total joint rotation from the column web panel shear deformations. In these cases, the component “column web panel in shear” can be considered separately from the connection. Considering that the shear plastic mechanism exhibits significant strain-hardening (Section 5.3.2.5), which generally leads to subsequent failure of the connection, separation of the column web panel contribution from the connection response is very important for a rational evaluation of the plastic rotation capacity of the whole joint sub-assemblage.

Finally, when evaluating the plastic rotation capacity, the effect of the type of loading protocol should be accounted for. This effect could be significant in case of a response with small to negligible pinching of hysteresis loops, such as in case of column web panel shear yielding. However, the effect of the loading protocol is moderate to negligible when the response is characterised by hysteresis loops having moderate to large pinching, such as in case of end-plate connections, especially those failing according to a mode 3. In fact, if the system exhibits large pinching of hysteresis loops, then damage is mainly due to peak deformations. Therefore, in case of end-plate connections, experimental results from monotonic loading were added to those from cyclic loading, where scarcity of experimental data made it mandatory. On the contrary, in case of column web yielding in shear, only cyclic test results were considered. This approach introduced some, but expectedly not large, uncertainty in the evaluation of the plastic rotation capacity, as described in the following sections.

The following paragraphs discuss first the plastic rotation capacity of connections followed by the behaviour of column web panels in shear. Considering the strain-hardening response of the column web panel in shear described in Section 5.3.2.5. Section 5.3.2.7 proposes a procedure to consider both the contributions from the column web panel in shear and the connection to the total joint plastic rotation in case of a mixed plastic mechanism.

Plastic rotation capacity of connections

The case of connections failing in the compression components is excluded from the following analysis, as failure in the compression zone is generally characterised by low ductility, due to local buckling, and consequently it is considered a non-desirable plastic mechanism for seismic applications. Therefore, the plastic rotation capacity of a connection is considered to depend on the deformation capacity of the components forming the equivalent T-stubs on the tension side.

At a given bolt row in tension, two equivalent T-stubs are generally defined, one considering the column flange in bending and the other considering the end-plate in

bending. If the relative plastic resistance of the two equivalent T-stubs are well separated, then the plastic mechanism is well identified and plastic deformations are confined to one of the two T-stubs. As a first approach and trying to simplify the problem, it is preliminarily assumed that the location of the yielding mechanism does not affect the rotation capacity, i.e. yielding of either the column flange or the end-plate are considered equivalent each to other. However, it is clear that cases where yielding occurs both in the column flange and the end-plate will be characterised by a larger deformation capacity. Ideally, if there is no difference between the two T-stubs, then yielding starts for the same load level in both T-stubs and the plastic rotation capacity of the connection is doubled as respect to the plastic rotation capacity measured in case of yielding of only one of the two T-stubs. Therefore, in the following discussion, only those test results for which yielding is observed to be mainly located in one equivalent T-stub are considered.

It is known that three plastic mechanisms of the equivalent T-stub in tension are possible: complete flange yielding, also known as mode 1; bolt yielding, up to fracture, also known as mode 3; mixed flange and bolt yielding, up to bolt fracture, also known as mode 2. Generally, the type of failure mode may change from one bolt row to the other. However, it is here assumed that either there is no change of the plastic mechanisms of different bolt rows or the less ductile plastic mechanism is used for evaluating the connection plastic rotation capacity. For instance, in case of an extended end-plate connection, if the plastic mechanisms are of type 1 at the outer bolt row and of type 2 at the inner bolt row, then the plastic mechanism of type 2, which is less ductile, is considered to determine the connection plastic rotation capacity.

Given the equivalent T-stub characteristics and consequent plastic mechanism, the plastic rotation capacity could be approximately evaluated as the ratio of the plastic displacement capacity at the tension zone divided by the internal lever arm. Consequently, the connection rotation capacity is expected to be a function of the internal lever arm. In particular, the plastic rotation capacity of the connection is expected to decrease while the internal lever arm increases (having fixed characteristics of the equivalent T-stubs). Besides, it is noted that in case of a plastic mechanism of type 3, given the lever arm, the tensile deformation capacity depends only on the type of bolt. Similarly, in case of a plastic mechanism of type 1, the plastic displacement capacity of the equivalent T-stub depends on the plastic rotation capacity at the flexural plastic hinges forming in the T-stub flanges and the relative distance of plastic hinges forming close to the web and to the bolt axis (i.e. parameter m according to EC3 terminology). The local plastic rotation capacity of the T-stub flanges depends on the material plastic strain capacity and the length of the plastic hinge zone (i.e. strain-hardening properties of the steel). Such dependences cannot be appreciated with experimental data collected here and will not be included in the following analysis. Any relevant effect is treated here as (epistemic)

variability, but further research could be addressed to improve knowledge of these aspects. Therefore, for a plastic mechanism of type 1 or type 3, the plastic rotation capacity of the connection is considered to depend essentially on the internal lever arm. Using the available experimental results and looking for all the cases where a plastic mechanism 1 or 2 is clearly identifiable in the equivalent T-stub, the plot shown in Figure 5.46 has been obtained. In Figure 5.46 the variable z on the horizontal axis represents the connection internal lever arm (evaluated using the approximate value suggested by EC3), while the vertical axis plots the experimental value of the plastic rotation capacity. There is a clear trend of the plastic rotation capacity to decrease while the internal lever arm increases. The plot shows also a fitting curve based on average values of the plastic rotation capacities. In addition, curves corresponding to mean plus or minus one standard deviation are also provided. Unfortunately, there are few data points, due to the need of discarding results from tests exhibiting spurious or uncertain plastic mechanisms. Although the data is scarce (hence the statistical validation of the interpolating functions is weak), the plot of Figure 5.46 indicates a strong relationship between the plastic rotation capacity and the internal lever arm. Similarly, Figure 5.47 is obtained by considering all the data points corresponding to a plastic mechanism of type 3. Also in this case a strong relationship between the plastic rotation capacity and the internal lever arm appears, with a decreasing capacity while there is an increase of the lever arm. The dispersion of the results from the collected experimental tests appears larger for a mechanism of type 3 (compare Figures 5.46 and 5.47). The observed variability of the plastic rotation capacity could be attributed to some variability of the actual bolt response, depending on the specific technological features (e.g. length and type of the bolt threads).

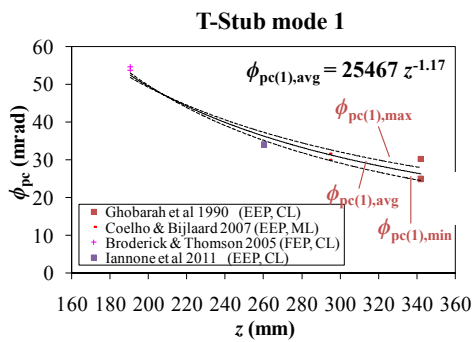


Figure 5.46. Plastic rotation capacity as a function of the internal lever arm in case of an equivalent T-stub plastic mechanism 1.

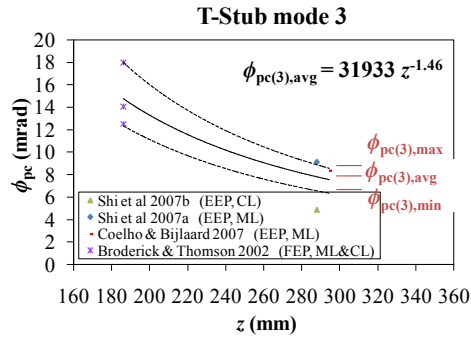


Figure 5.47. Plastic rotation capacity as a function of the internal lever arm in case of an equivalent T-stub plastic mechanism 3.

Ideally, given the material properties, the equivalent T-stub plastic mechanism 1 is occurring when the T-stub flange is thin relative to the bolt diameter, while the plastic mechanism 3 is expected to occur when the bolt diameter is small as respect to the flange thickness. Intermediate geometrical proportions are expected to lead to formation of a plastic mechanism 2. In this intermediate case, the ratio of bolt diameter (d) to flange thickness (t_p) is expected to affect the plastic rotation capacity: while the ratio d/t_p increases, the plastic rotation capacity is expected to increase too. Therefore, two geometrical parameters are expected to affect the plastic rotation capacity in case of a type 2 plastic mechanism: the internal lever arm, z , and the ratio d/t_p . For any given value of z , at small values of the ratio d/t_p the plastic rotation capacity should approach the value found for the plastic mechanism 3. Similarly, for any given value of z , at large values of the ratio d/t_p the plastic rotation capacity should approach the value found for a plastic mechanism 1. Extracting from the experimental database those results for connections with equivalent T-stubs exhibiting a plastic mechanism 2, the plot shown in Figure 5.48(a) is obtained. Unfortunately, the available experimental data is all related to the same value of approximately $z = 290$ mm, except for one additional case at approximately $z = 230$ mm. The plot of Figure 5.48(a) is anyway useful to see that there is large dispersion of plastic rotation capacities at a given value of z , thus indicating that additional factors must have a role in case of a plastic mechanism 2. Considering the experimental data points at $z = 290$ mm, and plotting the corresponding plastic rotation capacity as a function of the ratio d/t_p , the plot shown in Figure 5.48(b) is obtained. The figure shows a trend of the plastic rotation capacity to increase while the ratio d/t_p increases. The plot in Figure 5.48(b) shows also a proposed piecewise linear interpolating function: the lower horizontal line represents a theoretical lower bound provided by the plastic rotation capacity of a mode 3, while the upper horizontal line is a theoretical upper bound corresponding to a type 1 plastic mechanism. The inclined line is obtained by interpolating the experimental data points that show intermediate values of the plastic

rotation capacity. Both mean and mean minus one standard deviation curves are provided in the plot.

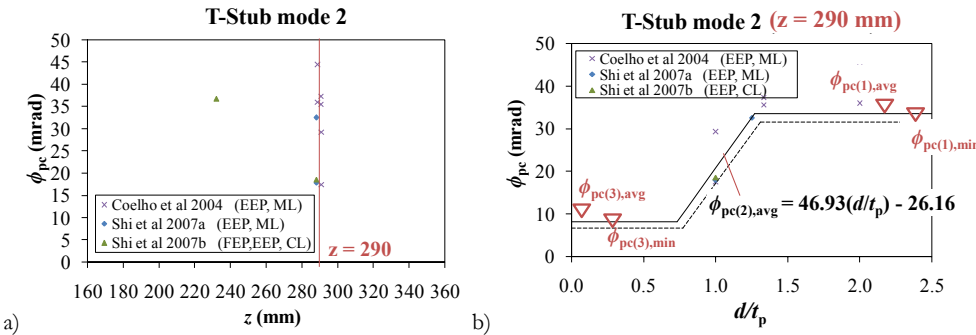


Figure 5.48. Plastic rotation capacity as a function of the internal lever arm (a) and the ratio d/t_p (b) in case of an equivalent T-stub plastic mechanism 2.

Figures 5.46 to 5.48 show clearly that the available experimental data is scarce. Frequently, results from the available database had to be disregarded, because of multiple reasons: (i) there is no measure provided regarding the separate connection and column web panel deformations; (ii) the plastic deformations involve both the column flange and the end-plate (i.e. two equivalent T-stubs); (iii) mixed and/or undesired failure modes are exhibited, e.g. failure in the connection compression zone. More research should be conducted to enrich the experimental database, with a more specific target on the plastic rotation capacity for the selected plastic mechanisms. Particularly, the experimental data appears to be insufficient to fully characterise the plastic rotation capacity of connections failing in a mode 2. In fact, the plot in Figure 5.48 is for a single value of ζ . However, one might argue that the variables ζ and d/t_p have an independent effect on the plastic rotation capacity. While increasing ζ for any given d/t_p , the plastic rotation capacity is expected to be a function of the type $a\zeta^{-1}$, where a is a function of the ratio d/t_p . However, this theoretical expectation is based on the assumption that a linear deformed shape can be assumed for the end-plate, which could be not accurate, as demonstrated by the interpolating functions in Figures 5.46 and 5.47. Therefore, additional research is recommended to obtain a more accurate statistical assessment, especially in case of a plastic mechanism 2.

The interpolating functions provided in Figures 5.46 and 5.47 are characterised by an exponent of the power function different from -1, what makes its use restrained to the same units used to derive it (i.e. ζ in mm and ϕ_{pc} in mrad). Besides, the very simple theoretical model based on a linear displacement pattern of the end-plate would suggest that the exponent should be -1. By forcing the exponent to be equal to -1, new interpolating functions can be derived as shown in the plots of Figures 5.49 and 5.50.

Dispersion of experimental data with respect to the interpolating function is larger than in case of Figures 5.46 and 5.47, obviously because of the restraint placed on the exponent of the power function. Eventually, analysis of the rotation capacity in case of a plastic mechanism 2 can be repeated by considering that the lower and upper bounds to the rotation capacity are now provided by the new interpolating functions shown in Figures 5.49 and 5.50. The plot shown in Figure 5.51 is then obtained. Although dispersion of data is slightly increased, the more simple form of the equations in Figures 5.49 and 5.50 suggest use of them, also considering the need to enlarge the data ensemble in the future.

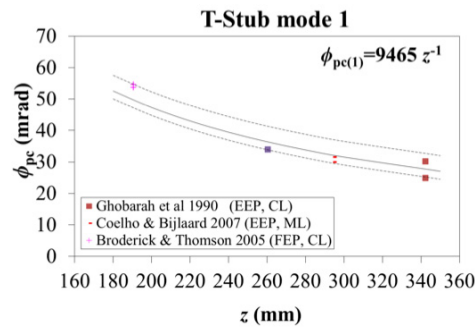


Figure 5.49. Plastic rotation capacity as a function of the internal lever arm in case of an equivalent T-stub plastic mechanism 1 – Interpolating data with a function type αz^{-1} .

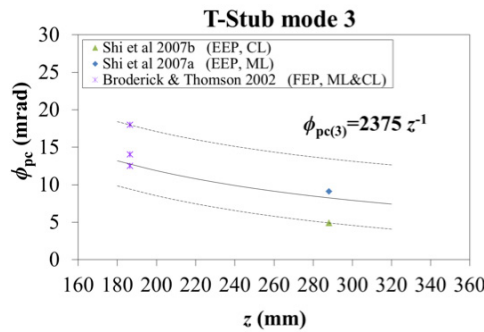


Figure 5.50. Plastic rotation capacity as a function of the internal lever arm in case of an equivalent T-stub plastic mechanism 3 – Interpolating data with a function type αz^{-1} .

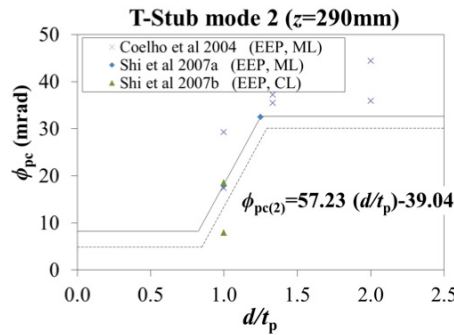


Figure 5.51. Plastic rotation capacity as a function of the internal lever arm (a) and the ratio d/t_p (b) in case of an equivalent T-stub plastic mechanism 2.

Plastic rotation capacity of the column web panel in shear

Figure 5.52 shows the plastic rotations associated to column web panel shear deformations and developed up to failure in the joints tested by Shi *et al.* [2007a and 2007b]. Failure of the tested joint sub-assemblages occurred in different components, depending on the characteristics of the tested joints. But, in all cases the column web panel continued to deform until failure occurred in a connection component, due to the increased force demand caused by the column web panel strain-hardening in shear. Therefore, the measured plastic rotation at joint failure is not the plastic rotation capacity of the column web panel in shear, which could have been deformed more than represented in the plot of Figure 5.52. These results, together with all the other cases investigated in this study, suggest that the column web panel shear deformations are normally not determining failure of the joint by themselves, but only because of the increased force demand to other joint components. This is the reason why Section 5.3.2.5 was specifically dedicated to characterise the strain-hardening behaviour of column web shear panels. The subsequent Section 5.3.2.7 will propose a method to account for both the plastic rotation due to the column web panel shear yielding and the plastic rotation of connections, in cases where a mixed yielding mode occurs.

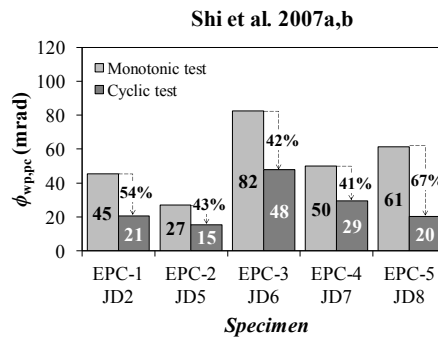


Figure 5.52. Plastic rotations associated to column web panel deformations in shear and developed up to failure in the joint sub-assemblages tested by Shi et al. [2007a and 2007b].

5.3.2.7 Total joint plastic rotation consider both the column web panel and connection plastic deformation

Section 5.3.2.6 summarised the results from experimental observations in terms of plastic rotation capacity of connections and column web panels. While the plastic rotation capacity corresponding to the column web panel shear yielding mechanism was found so large as to assume that it is virtually infinite, failure can ultimately occur because of excessive strain hardening and corresponding force demand to the adjacent beam-to-column connections. The following paragraphs discuss a procedure to consider both the column web panel and connection plastic deformations to the total joint plastic rotation.

Two cases need to be distinguished: (i) the connection starts yielding, followed by the column web panel because of strain-hardening of the connection; (ii) the column web panel starts yielding in shear, followed by the connection because of strain-hardening of the column web panel in shear. Section 5.3.2.5 discussed the strain-hardening of the column web panel in shear. Strain hardening of connections has not yet been completely studied and work is in progress on this aspect. Clearly, strain-hardening of connections is more difficult to be characterised because of the multiple components and plastic mechanisms that can affect response of connections. Therefore, for the time being, connections are assumed to have a perfectly plastic response, similar to the current modelling assumption of EC3. This assumption leads to safe-side estimations of the plastic rotation capacity, as described in detail in the following paragraphs.

In case of plastic deformations starting in the connection, then the column web panel could be also engaged in the plastic range of deformation if sufficient strain-hardening of the connection takes place. After yielding and due to strain-hardening, the total joint plastic rotation increases because of both the increase of the plastic rotation in the connection and the additional contribution from the column web panel in shear. As

explained above, since sufficient information on the strain-hardening of connections is still not available, the connection response is assumed to be perfectly plastic. Under this hypothesis, the plastic rotation capacity of joints where yielding starts in the connection coincides with the plastic rotation capacity of the connection itself, i.e. the additional contribution from the column web panel is neglected. Therefore, a safe-side estimation of the joint plastic rotation is obtained.

In case of plastic deformations starting in the column web panel in shear, the plastic rotation capacity of the joint will depend on the ratio of connection to column web panel plastic resistance (plastic over-strength of the connection). If the strain-hardening ratio of the column web panel is known (Section 5.3.2.5), then using the ratio of the plastic resistance of the connection to the plastic resistance of the column web panel, the plastic rotation due to column web panel shear deformations, and developed up to the attainment of the plastic resistance of the connection, can be readily calculated. This calculation procedure is shown, for example, in Figure 5.53(a). After reaching the plastic resistance of the connection, significant plastic deformation will also start developing in the connection itself. The connection itself is characterised by some strain-hardening response, which will produce an increase of the shear deformation in the column web panel. However, neglecting such an additional effect simplifies evaluation of the response and is on the side of safety, because the additional contribution to the total joint plastic rotation is neglected. Therefore, assuming that the connection is elastic-perfectly plastic, the total joint plastic rotation capacity can be obtained as the sum of two contributions: (i) the plastic rotation corresponding to the column web panel shear deformations and developed up to the attainment of the plastic resistance of the connection and (ii) the plastic rotation capacity of the connection. This is schematically illustrated in Figure 5.53(b).

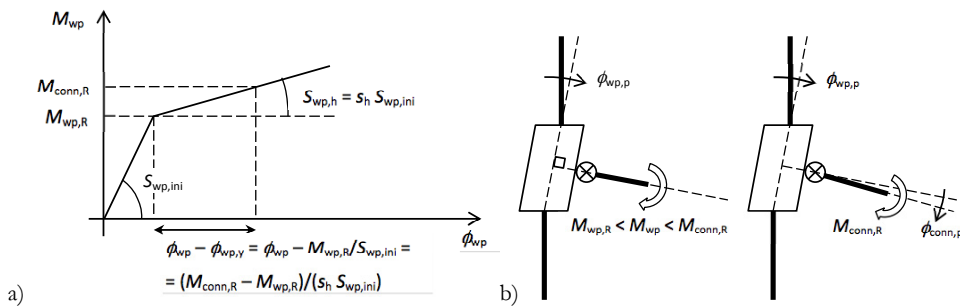


Figure 5.53. Plastic rotations of joints where yielding starts in column web panels and ultimate failure occurs in connections.

Therefore, the following Equations (5.9), (5.10) and (5.11) are proposed to calculate the plastic rotation capacity of joints where yielding starts in the column web and is followed by yielding of the connection:

$$\phi_{j,pC} = \phi_{wp,p} \left(M_{conn,R} / M_{wp,R} \right) + \phi_{conn,pC} \quad (5.9)$$

$$\phi_{wp,p} \left(M_{conn,R} / M_{wp,R} \right) = \frac{M_{conn,R} - M_{wp,R}}{s_b S_{wp,ini}} \quad (5.10)$$

$$\phi_{conn,pC,2} = \phi_{conn,pC,3} + \delta_2 \left(\frac{d}{t_p} - \left(\frac{d}{t_p} \right)_2 \right) \leq \phi_{conn,pC,1} \quad (5.11)$$

where:

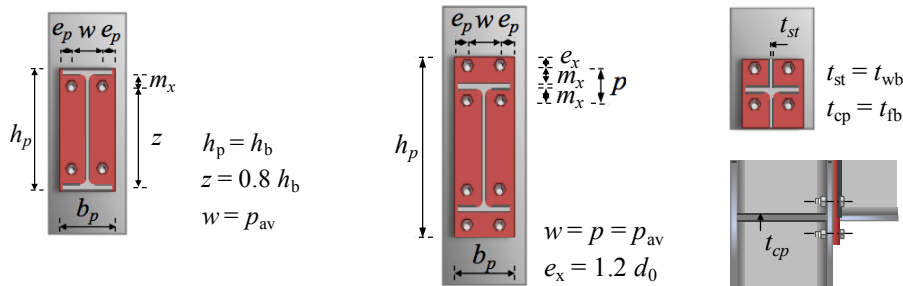
- $\phi_{wp,p} \left(M_{conn,R} / M_{wp,R} \right)$ = plastic rotation due to the column web panel shear deformations and developed up to the attainment of the plastic resistance of the connection;
- $\phi_{conn,pC}$ = plastic rotation capacity of the connection;
- $M_{conn,R}$ and $M_{wp,R}$ = plastic resistance of connection and column web panel, respectively;
- $S_{wp,ini}$ = initial (elastic) joint rotational stiffness of the joint due to the component “column web panel in shear” only;
- $s_b = S_{wp,b} / S_{wp,ini}$ = ratio of strain-hardening to initial (elastic) rotational stiffness of the joint due to the component “column web panel in shear” only;
- $\phi_{conn,pC,1}$, $\phi_{conn,pC,2}$ and $\phi_{conn,pC,3}$ = plastic rotation capacity of the connection for a plastic mechanism 1, 2 or 3, respectively;
- δ_2 = gradient of the plastic rotation capacity in case of a plastic mechanism 2 due to the increase of the ratio d/t_p (e.g. Figure 5.51);
- $\left(d/t_p \right)_2$ = value of the ratio (d/t_p) corresponding to the transition from a plastic mechanism 3 to a plastic mechanism 2 (e.g. Figure 5.51).

Values of the plastic resistances ($M_{conn,R}$ and $M_{wp,R}$) as well as the initial rotational stiffness of the column web panel ($S_{wp,ini}$) are evaluated according to the component method, as implemented by EC3, without considering partial safety factors. Statistical values of the strain-hardening ratio (s_b) are provided in Section 5.3.2.5. The mean value of s_h could be used or the mean minus one standard deviation, if more safe estimations are looked for.

The plastic rotation capacity of a connection failing either in a mode 1 ($\phi_{\text{conn,pC},1}$) or in a mode 3 ($\phi_{\text{conn,pC},3}$), as well as the value of the parameters δ_2 and $(d/t_p)_2$, were discussed in Section 5.3.2.6 (Figures 5.46, 5.47, 5.48(b), 5.49, 5.50 and 5.51), where also tentative values are provided based on the available experimental data.

5.4 PARAMETRIC ANALYSIS USING THE COMPONENT METHOD

The component method of EC3 was used for a parametric analysis of beam-to-column joints made of I-shaped beam and column and extended end-plate connections. For any given beam and column shape, the end-plate thickness (t_p) and the bolt diameter (d) were varied. The range of variations was defined in normalised terms, using the column flange thickness (t_{fc}) for normalising both the end-plate thickness and the bolt diameter. Both parameters were varied in the range (0.5-1.5). Figure 5.54 describes additional assumptions about the joint geometry. Bolts were positioned so as to generate an internal lever arm equal to 80% of the beam cross-section depth. In case of extended end-plates, the vertical spacing of bolts in the tension zone (p) was assumed equal to the horizontal spacing (w) (square bolt arrangement). The horizontal bolt spacing was selected as the average value between the minimum and maximum values compatible with the selected column shape (i.e. considering distances from edges and round corners at web to flange junctions). For any given beam and column shape, the bolt-holes needed for each bolt diameter and plate thickness were checked in order to satisfy bolt geometric limitations provided by EC3. Those combinations violating one or more of the code requirements were excluded. Beam-to-column joints including continuity plates and/or end-plate rib stiffeners were also considered. In such cases, the thickness of continuity plates was assumed equal to the beam flange thickness, while the rib stiffener plate thickness was considered equal to the beam web thickness. Eventually, beam-to-column joints having a rigid column web panel in shear were considered, assuming that diagonal plate stiffeners were provided. Material properties were fixed at the beginning of each parametric analysis.

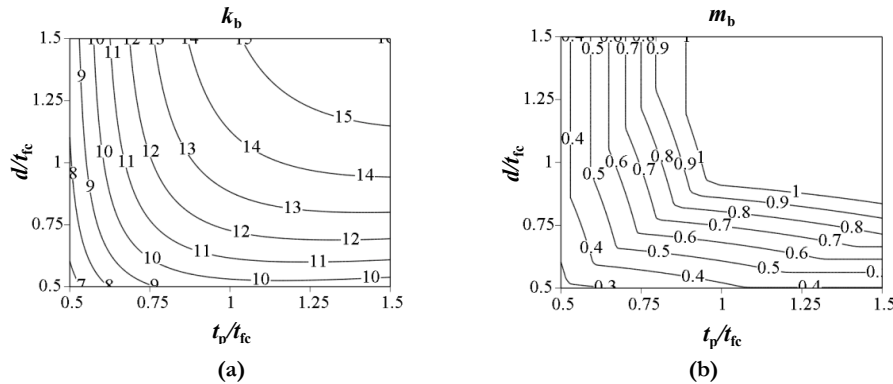


(a) (b)

Figure 5.54. Summary of assumptions about the geometry of joints for parametric analyses.

The joint response was represented in terms of normalised stiffness (k_b) and normalised resistance (m_b), as they are defined by EC3. Namely, $k_b = S_{j,ini}L_b/(25EI_b)$ and $m_b = M_{j,R}/M_{b,pl}$, where L_b = beam length, I_b = beam cross section moment of inertia, $M_{b,pl}$ = beam plastic moment, and E = Young's modulus of steel. In addition, the joint yield rotation (ϕ_{iy}) and plastic mechanisms were analysed for each selected joint. Results of parametric analyses were summarised in the form of graphs, showing the variation of k_b , m_b , ϕ_{iy} , and plastic mechanism with the two assumed geometrical parameters (t_p/t_{fc} and d/t_{fc}). Samples of such graphs are provided hereafter.

Figure 5.55 shows the results of the parametric analysis in the case of IPE 550 beam, HEM 280 column, S275 steel grade, 8.8 grade bolts, continuity plates, no rib stiffener, no column web panel stiffener. The beam length L_b was assumed equal to 25 times the beam cross-section depth. Figure 5.55(a) gives contour lines of k_b for varying values of t_p/t_{fc} (horizontal axis) and d/t_{fc} (vertical axis). In the examined range of end-plate thickness and bolt diameter, the normalised stiffness k_b varies from 7 through 15, implying that the joint is always semi-rigid according to EC3 classes. Figure 5.55(a) clearly shows that a rigid joint for moment resisting frames ($k_b > 25$) is practically impossible in this case.



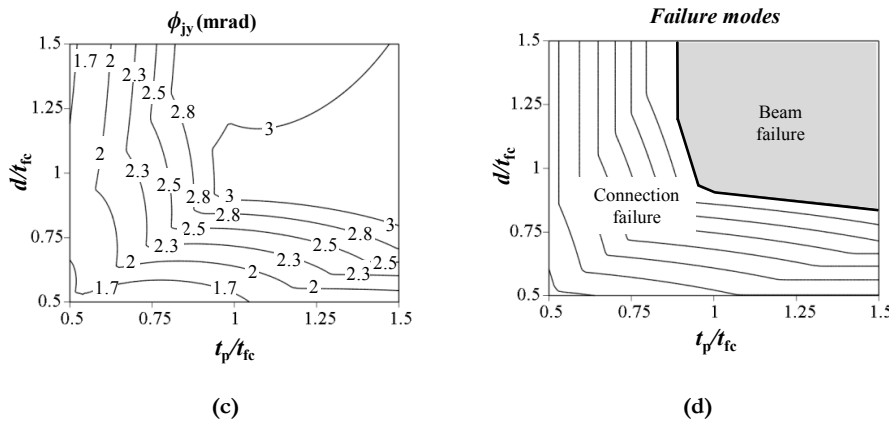


Figure 5.55. Variation of normalised stiffness (a), normalised resistance (b), yield rotation (c), failure mode (d) for extended end plate joints with: IPE 550 beam, HEB 280 column, continuity plates, no rib stiffener, no column web panel stiffener.

Figure 5.55(b) illustrates variations of the normalised resistance m_b ; for the larger values of t_p and d it is possible to obtain a full-strength joint ($m_b > 1$), though in most of the cases the joint resistance is significantly smaller than the beam plastic resistance ($m_b < 1$). Figure 5.55(c) shows variations of the joint yield rotation; the range of such variations is relatively small, with a minimum observed value of 1.7 mrad, up to a maximum of 3 mrad. This relatively small variation of the yield rotation is expected and is also advantageous from the viewpoint of the displacement-based methods of design and assessment. Figure 5.55(d) illustrates the ranges of geometrical parameters in which failure occurs by either connection or beam failure (there is no shear yielding of the column web panel in the specific case). Plots similar to the one shown in Figure 5.55(d) can provide more details about the mode of failure inside the connection (bolt failure, end-plate yielding, or mixed mode, in the column flange or the end-plate). In case of extended end-plate connections, the type of failure mode can change from one bolt-row to another. Figure 5.56 shows such type of more detailed graphs. Figure 5.56(a) illustrates variation of failure modes with the considered connection parameters, for the first bolt-row, while Figure 5.56(b) is similar but relevant to the second bolt row. Using such graphs, values of end-plate thickness and bolt diameter required to have one type of failure mode can be derived. By comparing Figure 5.56(a) and Figure 5.56(b), a superposition of different modes of failure for the two bolt rows is noted in certain regions of the design parameters. The response of a beam-to-column joint identical to the one of Figure 5.55, but with flush end-plate connection is provided in Figure 5.57. Subfigures (a), (b) and (c) of Figure 5.57 are conceptually similar to the corresponding panels of Figure 5.55. Clearly, the level of stiffness and resistance obtained in case of flush end-plates are both smaller than in case of extended end-plates. Subfigure (d) of Figure 5.57 is different from panel (d) of Figure 5.55 because of flush end-plate

connections having one single bolt row: consequently, the two plots shown in Figure 5.56 are not needed in case of flush end-plates.

Plots of the type shown in Figure 5.55 to Figure 5.57 were developed for many combinations of beam and column shapes and other structural details. They are useful design/analysis tools, allowing quick and easy inspection of the joint mechanical response for varying values of the end-plate thickness and the bolt diameter. Such plots can be used in two ways: (i) with fixed values of the end-plate thickness and the bolt diameter, the joint performance is readily assessed; (ii) with fixed target requirements in terms of k_b , m_b , yield rotation and failure mechanism, one can look for values of the end-plate thickness and the bolt diameter allowing satisfaction of those requirements.

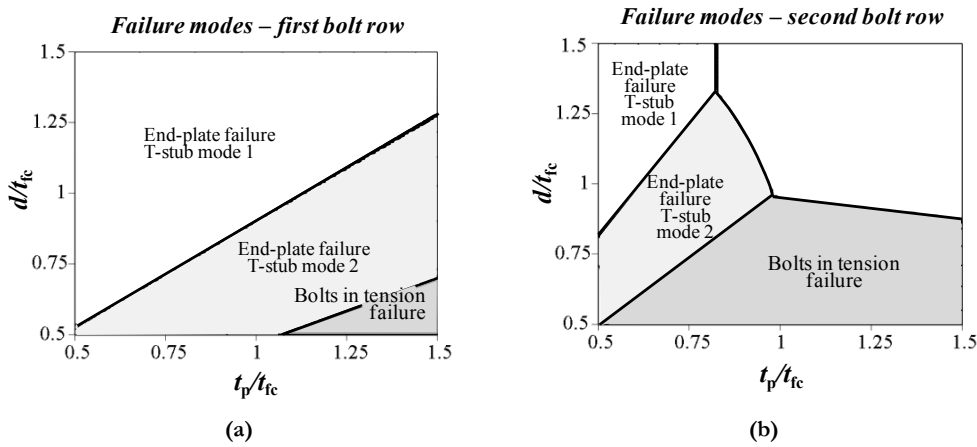
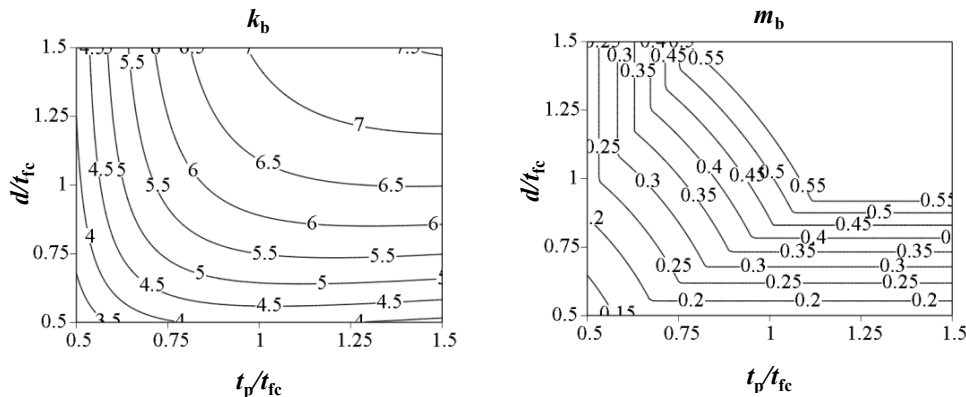


Figure 5.56. Variation of connection failure mode for the example case of Figure 12: (a) first bolt row; (b) second bolt row.



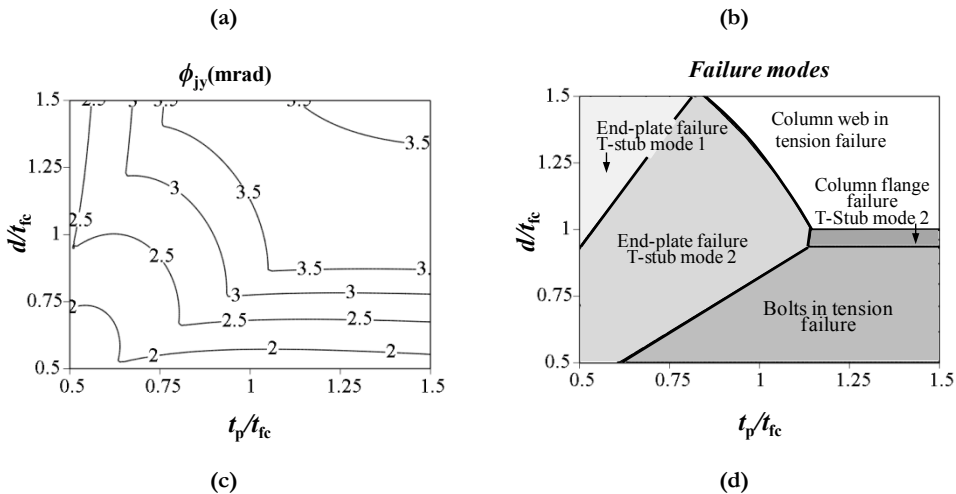


Figure 5.57. Variation of normalised stiffness (a), normalised resistance (b), yield rotation (c), failure mode (d) for flush end plate joints with: IPE 550 beam, HEB 280 column, continuity plates, no rib stiffener, no column web panel stiffener.

5.5 SIMPLIFIED DESIGN EXPRESSIONS

The parametric study described in the previous section permitted evaluation of relationships such as k_b vs. d/t_{fc} and m_b vs. d/t_{fc} , given the ratio t_p/t_{fc} . The comparison of such curves corresponding to several different beam-to-column joints allowed developing simplified analytical expressions for the normalised stiffness (k_b) and resistance (m_b) of extended end-plate joints.

European I section beams and wide flange section columns have been considered in this study. Beam cross-sections have been varied from IPE 200 through IPE 750, while column cross sections have been considered in the range from HEM 120 to HEM 400. The end-plate thickness has been assumed equal to the column flange thickness (i.e. $t_p/t_{fc} = 1$). Continuity plates have been eventually included.

According to the theoretical study, the normalised stiffness of end-plate joints can be approximately evaluated by means of Equation 5.9:

$$k_b = \left[8.343 \left(\frac{d}{t_{fc}} \right)^3 - 33.3 \left(\frac{d}{t_{fc}} \right)^2 + 47.32 \left(\frac{d}{t_{fc}} \right) + 0.865 \right] k_{ref} \quad (5.9)$$

Where k_{ref} is a reference coefficient which depends on the column and beam shape and it is obtained through Equations 5.10, 5.11 and 5.12, where b_b and b_c are the beam and column cross section depth, respectively.

$$k_{\text{ref}} = \alpha_{\text{kref}} b_b + \beta_{\text{kref}} \quad (5.10)$$

$$\alpha_{\text{kref}} = -5 \cdot 10^{-8} b_c^2 + 4 \cdot 10^{-5} b_c - 0.0075 \quad (5.11)$$

$$\beta_{\text{kref}} = 1 \cdot 10^{-5} b_c^2 - 0.0075 b_c + 2.133 \quad (5.12)$$

Two different Equations are proposed for the normalised resistance, depending on the column section size. Equation 5.13 can be used to estimate m_b in the case of beam-to-column joints having HEM 120 or HEM 140 column cross section. Equation 5.14 gives the normalised resistance in case of column cross sections varying from HEM 160 to HEM 400.

$$m_b = \left[2.205 \left(\frac{d}{t_{fc}} \right) - 0.524 \right] m_{\text{ref}} \leq m_{\text{ref}} \quad (\text{HEM 120 - HEM 140}) \quad (5.13)$$

$$m_b = \left[1.690 \left(\frac{d}{t_{fc}} \right) - 0.371 \right] m_{\text{ref}} \leq m_{\text{ref}} \quad (\text{HEM 160 - HEM 400}) \quad (5.14)$$

In both cases m_b cannot be larger than m_{ref} as provided by Equations 5.13 and 5.14.

Based on the examination of the numerical results from the parametric analysis, the parameter m_{ref} has been expressed as a linear function of the beam depth Equation 5.15.

$$m_{\text{ref}} = \alpha_{\text{mref}} b_b + \beta_{\text{mref}} \quad (5.15)$$

The linear combination parameters, α_{mref} and β_{mref} , depends on the column shape and depth of the cross section, as given by Equations 5.16 - 5.19.

$$\alpha_{\text{mref}} = -1.404 \cdot 10^{-7} b_c^2 + 9.466 \cdot 10^{-5} b_c - 0.0169 \quad (\text{HEM 120 - HEM 280}) \quad (5.16)$$

$$\alpha_{\text{mref}} = 9.282 \cdot 10^{-4} \quad (\text{HEM 300 - HEM 400}) \quad (5.17)$$

$$\beta_{\text{mref}} = -5.799 \cdot 10^{-3} b_c + 3.142 \quad (\text{HEM 120 - HEM 280}) \quad (5.18)$$

$$\beta_{\text{mref}} = 0.003 b_c + 0.344 \quad (\text{HEM 300 - HEM 400}) \quad (5.19)$$

The accuracy of these equations was evaluated comparing predictions with results from the component method. Figure 5.58(a) and Figure 5.58(b) show the k_b vs. d/t_{fc} and m_b vs. d/t_{fc} relationships obtained for the beam-to-column joints having a HEM 200 column cross section. Figure 5.59 and Figure 5.60 illustrate the normalised resistance and stiffness of several beam-to-column joints obtained by means of both the component method and

the proposed closed-form equations for given values of the ratio d/t_{fc} , chosen to obtain maximum differences between the two procedures. The accuracy of the equation providing the normalised stiffness was evaluated comparing the results obtained for d/t_{fc} equal to 0.5 and 0.8, as shown in Figure 5.59(a) and Figure 5.59(b) respectively. In the analysed cases, the maximum differences between the simplified equations and the component method are about 17% in case of d/t_{fc} equal to 0.5 (Figure 5.59(c)) and 18% if d/t_{fc} is equal 0.8 (Figure 5.59(d)). The proposed equations result into a normalised moment resistance, which differs from the theoretical value, obtained by the component method, 7% on average. Figure 5.60(a) and Figure 5.60(b) are relevant to the normalised stiffness and assume d/t_{fc} ratio equal to 0.5 and 1.5, respectively. As shown in Figure 5.60(c) and Figure 5.60(d), maximum differences approximately of 24% resulted in such comparisons. The difference in term of normalised stiffness is approximately 10% on average (Figure 5.60). Such differences are well within the range of differences found from the theoretical vs. experimental results comparison.

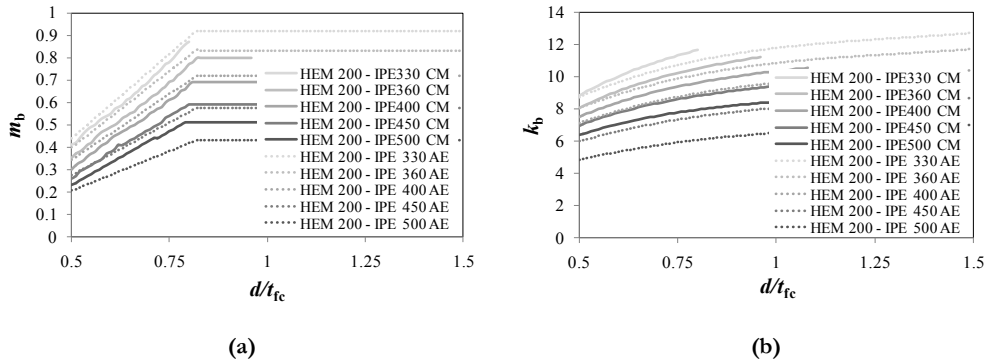
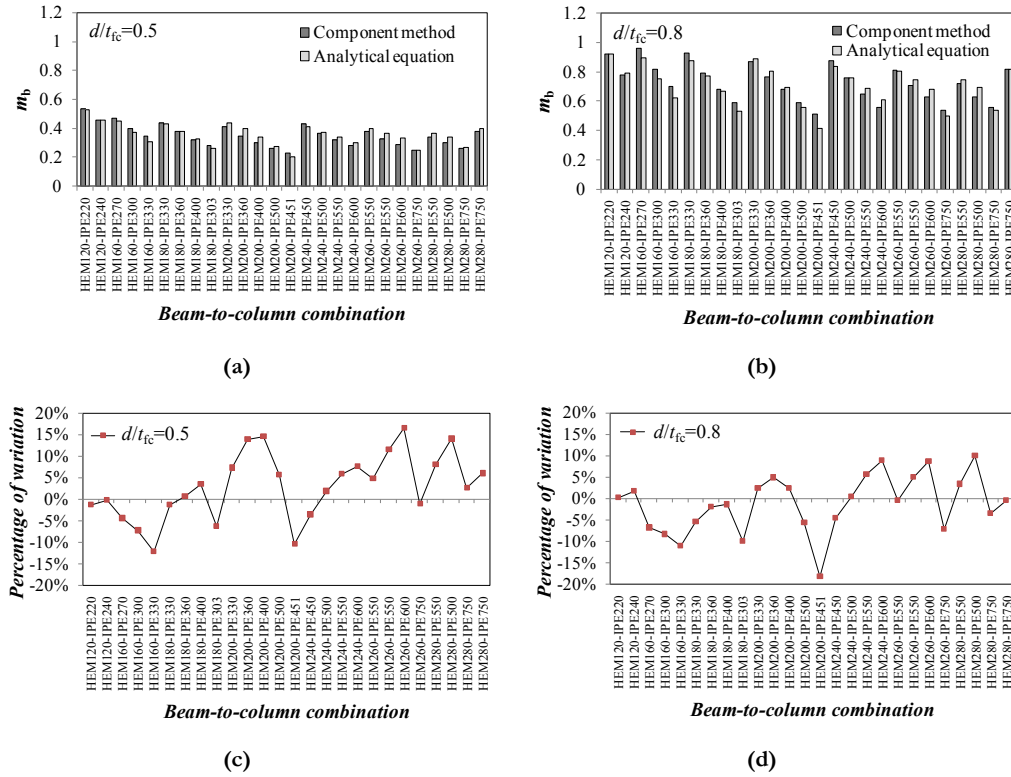


Figure 5.58. (a) m_b vs. d/t_{fc} and (b) k_b vs. d/t_{fc} relationships for beam-to-column combinations having HEM 200 column shape.


 Figure 5.59. Accuracy of approximate closed-form Equations: m_b .

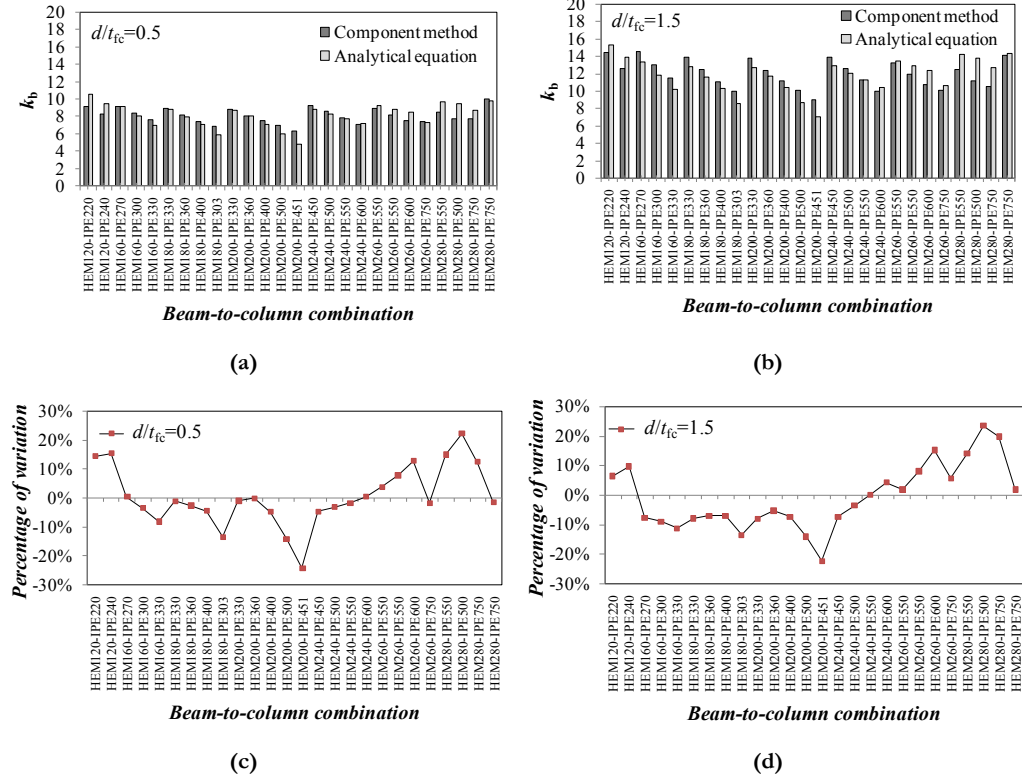


Figure 5.60. Accuracy of approximate closed-form Equations: k_b .

5.6 EQUATION FOR THE YIELD DRIFT OF STEEL FRAMES ACCOUNTING FOR THE JOINT CHARACTERISTICS

The yield drift ratio (or angle, θ_y , Figure 5.61) is essential in the displacement-based design and analysis of structures. The value of θ_y depends on the geometric and mechanic characteristics of the frame, including the characteristics of the beam-to-column joints (stiffness and resistance). Typically, full-strength joints with fully welded connections have been studied and equations are available for such case, where the only contribution from the joints to the total drift is the elastic deformation of the column web panels in shear. If the connection is flexible and/or partial strength, then the yield-drift ratio is modified because of both the change in the total system stiffness and plastic resistance.

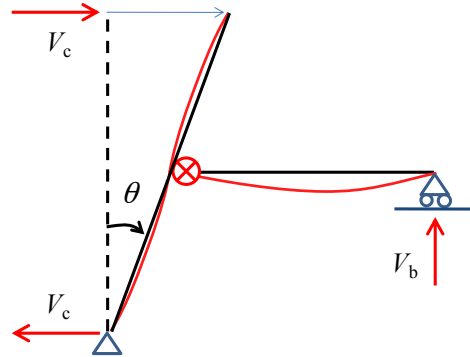


Figure 5.61. Drift ratio (or angle).

Using the structural model of Figure 5.61, it can be proved that the yield drift ratio is obtained as given by Equation 5.20.

$$\theta_y = M_{b,R} \left(\frac{L_{vb}}{3EI_b} + \frac{1}{GA_{vb}L_{vb}} + \frac{b}{12EI_c} + \frac{1}{GA_{vc}b} + \frac{1}{GA_{vc}\zeta} + \frac{1}{S_{conn}} \right) \quad (5.20)$$

where the symbols have the following meaning:

- $M_{b,R}$ is the plastic resistance at the beam end and it is the minimum of four quantities:
 - $M_{b,R} = \min\{M_{b,pl}; M_{R,conn}; M_{R,pz}; M_{R,c}\}$
 - where $M_{b,pl}$ = plastic moment of the beam cross section; $M_{R,conn}$ = plastic resistance of the beam-to-column connection; $M_{R,pz}$ = moment at the beam end corresponding to the plastic resistance of the column web panel in shear; $M_{R,c}$ = moment at the beam end corresponding to the plastic resistance of the column cross sections.
- L_{vb} = distance from the beam end to the point of zero moment along the beam.
- I_b and A_{vb} = second moment of area and shear area, respectively, of the beam cross section.
- b = distance between the two points of zero moment along the column length.
- I_c and A_{vc} = second moment of area and shear area, respectively, of the column cross section.
- ζ = internal lever arm at the beam-to-column connection = height of the column web panel zone in shear.
- $S_{conn,ini}$ = initial rotational stiffness of the connection.
- E, G = Young's modulus and shear modulus, respectively, of steel.

Following yielding, the drift ratio increases because of the plastic deformations taking place in the yielding zone. Figure 5.62 illustrates the plastic drift ratio developing as a consequence of plastic deformations in the yielding zone. Since the model assumes that the joint deformability is concentrated at the end of the beam, there is no difference in the frame kinematics whether yielding occurs in the beam or in the joint. In both cases, Equation 5.21 applies, where θ_p is the plastic drift ratio. In case of yielding taking place in the beam-to-column joint, then the plastic drift ratio coincides with the plastic rotation at the beam-to-column joint, as indicated by Equation 5.22, and the moment of resistance to be used into Equation 5.20 is the plastic resistance of the joint, $M_{j,R}$ (Equation 5.23) which is in turn the minimum of $M_{R,conn}$ and $M_{R,pz}$ as previously defined.

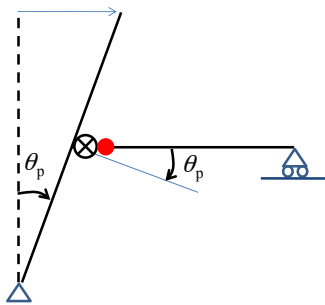


Figure 5.62. Plastic drift.

$$\theta = \theta_y + \theta_p \quad (5.21)$$

$$\theta_p = \phi_{j,p} \quad (5.22)$$

$$M_{b,R} = M_{j,R} \quad (5.23)$$

The form of Equation 5.20 is not very convenient, because a non-dimensional quantity θ_y is expressed as a function of dimensional parameters. To improve the form of this Equation, the following algebraic manipulations are carried out.

As a first step, the right-hand side of Equation 5.20 is multiplied and divided by the plastic moment of the beam cross-section as shown by Equation 5.24.

$$\theta_y = \frac{M_{b,R}}{M_{b,pl}} \left(\frac{M_{b,pl} L_b}{6EI_b} + \frac{2M_{b,pl}}{GA_{vb}L_b} + \frac{M_{b,pl} h}{12EI_c} + \frac{M_{b,pl}}{GA_{vc}h} + \frac{M_{b,pl}}{GA_{vc}\zeta} + \frac{M_{b,pl}}{S_{conn}} \right) \quad (5.24)$$

It is noted that L_{vb} has been substituted with $L_b/2$, which is a usual and convenient simplification for the purposes of the displacement-based seismic design.

As a second step, the contribution from the connection and column web panel zone flexibilities are grouped together and a single parameter is used, as follows:

$$\frac{1}{S_{j,ini}} = \frac{1}{S_{cws}} + \frac{1}{S_{conn,ini}} = \frac{1}{GA_{vc}z} + \frac{1}{S_{conn,ini}} \quad (5.25)$$

where $S_{j,ini}$ is the initial stiffness of the beam-to-column joint. Besides, the joint contribution is grouped together with the beam flexural contribution, as shown by Equation 5.26.

$$\theta_y = m_{b,R} \left(\frac{M_{b,pl}L_b}{6EI_b} \left(1 + 6 \frac{EI_b}{S_{j,ini}L_b} \right) + \frac{2M_{b,pl}}{GA_{vb}L_b} + \frac{M_{b,pl}b}{12EI_c} + \frac{M_{b,pl}}{GA_{vc}b} \right) \quad (5.26)$$

where $m_{b,R}$ is the resistance of the joint relative to the beam cross section (Equation 5.27).

$$m_{b,R} = \frac{M_{b,R}}{M_{b,pl}} \quad (5.27)$$

The contribution from the joint flexibility in Equation 5.26 is represented as a contribution relative to the beam flexural deformability. The parameter k_{jb} (defined by EC3) is then introduced, by means of the following Equation 5.28:

$$k_{jb} = \frac{S_{j,ini}L_b}{EI_b} \quad (5.28)$$

Consequently, the yield drift ratio is expressed by Equation 5.29:

$$\theta_y = m_{b,R} \left(\frac{M_{b,pl}L_b}{6EI_b} \left(1 + 6 \frac{1}{k_{jb}} \right) + \frac{2M_{b,pl}}{GA_{vb}L_b} + \frac{M_{b,pl}b}{12EI_c} + \frac{M_{b,pl}}{GA_{vc}b} \right) \quad (5.29)$$

Therefore, using the following additional definitions:

$$\varphi_{b,y} = \frac{M_{b,pl}L_b}{EI_b} \quad (5.30)$$

$$\psi_{jb} = 1 + 6 \frac{1}{k_{jb}} \quad (5.31)$$

The yield drift ratio can be written in the form provided by Equation 5.32.

$$\theta_y = m_{b,R} \left(\frac{\psi_{jb}\varphi_{b,y}}{6} + \frac{2M_{b,pl}}{GA_{vb}L_b} + \frac{M_{b,pl}h}{12EI_c} + \frac{M_{b,pl}}{GA_{vc}h} \right) \quad (5.32)$$

Using again Equation 5.30 and introducing the following ratio:

$$\alpha_{vb} = \frac{A_{vb}}{A_b} \quad (5.33)$$

Equation 5.32 is then transformed easily into Equation 5.34:

$$\theta_y = m_{b,R} \left(\frac{\psi_{jb}\varphi_{b,y}}{6} + \frac{4(1+\nu)\varphi_{b,y}}{\alpha_{vb}} \frac{r_b^2}{L_b^2} + \frac{M_{b,pl}h}{12EI_c} + \frac{M_{b,pl}}{GA_{vc}h} \right) \quad (5.34)$$

where ν is the Poisson's ratio and r_b is the radius of gyration of the beam cross section.

At this point, repeating the same transformation that has been done for the beam shear contribution but applied to the column shear contribution, and introducing the following non-dimensional parameters:

$$\psi_{vb} = \frac{24(1+\nu)}{\alpha_{vb}} \frac{r_b^2}{L_b^2} \quad (5.35)$$

$$\psi_{vc} = \frac{24(1+\nu)}{\alpha_{vc}} \frac{r_c^2}{h^2} \quad (5.36)$$

Equation 5.34 is written in the form of Equation 5.37.

$$\theta_y = m_{b,R} \left(\frac{\varphi_{b,y}}{6} (\psi_{jb} + \psi_{vb}) + \frac{M_{b,pl}h}{12EI_c} (1 + \psi_{vc}) \right) \quad (5.37)$$

Using once again Equation 5.30, and after simple additional manipulations, a new form can be obtained, as shown by Equations 5.38 and 5.39.

$$\theta_y = m_{b,R} \left(\frac{\varphi_{b,y}}{6} (\psi_{jb} + \psi_{vb}) + \varphi_{b,y} \frac{1}{12} \frac{I_b}{I_c} \frac{h}{L_b} (1 + \psi_{vc}) \right) \quad (5.38)$$

$$\theta_y = \frac{m_{b,R} \varphi_{b,y}}{6} \left(\psi_{jb} + \psi_{vb} + \frac{1}{2} \frac{I_b}{I_c} \frac{h}{L_b} (1 + \psi_{vc}) \right) \quad (5.39)$$

Eventually, the parameter $\varphi_{b,y}$ defined by Equation 5.30 can also be rewritten as follows:

$$\varphi_{b,y} = \frac{M_{b,pl}L_b}{EI_b} = \frac{f_y W_{b,pl}}{E} \frac{L_b}{I_b} = \frac{f_y}{E} \psi_b W_{b,el} \frac{L_b}{I_b} = 2\epsilon_y \psi_b \frac{L_b}{d_b} \quad (5.40)$$

where f_y and ϵ_y are the steel yield stress and strain, respectively.

Using the EC3 component method, the joint rotational stiffness can be expressed more explicitly, as follows:

$$S_{j,ini} = \frac{Ez^2}{\sum_i \frac{1}{k_i}} = \frac{Ez^2}{\frac{1}{k_1} + \sum_i \frac{1}{k_i}} = \frac{1}{\frac{1}{Ez^2 k_1} + \sum_i \frac{1}{Ez^2 k_i}} \quad (5.41)$$

where the left-hand side term at the denominator of Equation 5.41 is the column web shear contribution (Equation 5.42) and the second term on the right hand-side at the denominator of Equation 5.41 is the connection contribution to the total joint flexibility (Equation 5.43).

$$\frac{1}{S_{cws}} = \frac{1}{Ez^2 k_1} \quad (5.42)$$

$$\frac{1}{S_{conn,ini}} = \sum_i \frac{1}{Ez^2 k_i} \quad (5.43)$$

If the beam-to-column joint is an internal one, i.e. two beams are framing into a central column, Equation 5.39 is still valid at each side of the column, i.e. it is valid for both of the two joints originated by cutting the column in two halves and considering alternatively the left and right beams and relevant connections. However, the contribution from the column moment of inertia has to be divided by a factor of 2, and similarly for the contribution of the column web panel shear deformations a factor equal to 2 is needed (Equation 5.44).

$$\frac{1}{S_{cws}} = \frac{1}{Ez^2 k_1} = \beta \frac{1}{GA_{vc}z} \quad (5.44)$$

where β is a coefficient equal to 2 for internal joints and equal to 1 for external joints.

In order to further simplify the equation for the yield drift ratio, one might willing to neglect the shear deformations of beams and columns. Under this assumption, the equation for the yield drift ratio is as follows:

$$\theta_y \approx \frac{m_{b,R} \varphi_{b,y}}{6} \left(\psi_{jb} + \frac{1}{2} \frac{I_b}{I_c} \frac{b}{L_b} \right) \quad (5.45)$$

The last form provided by Equation 5.45 is relatively simple to be used. It only requires the preliminary estimation of non-dimensional parameters. The Equation covers all the types of beam-to-column joints, from rigid and full-strength to semi-rigid and partial strength.

5.7 REFERENCES

- Abidelah, A., Bouchaïr, A., Kerdal, D.E. [2012] "Experimental and analytical behavior of bolted end-plate connections with or without stiffeners", *Journal of Constructional Steel Research*, Vol. 76, pp. 13–27.
- Broderick, B.M., Thomson, A.W. [2002] "The response of flush end-plate joints under earthquake loading", *Journal of Constructional Steel Research*, Vol. 58, No.5, pp. 1161-1175.
- Broderick, B.M., Thomson, A.W. [2005] "Moment-rotation response of flush end-plate joints under cyclic loading", *International Journal of Steel and Composite Structures*, Vol. 5, No. 5, pp. 441-451.
- Calado, L., Mele, E.[2000] "Experimental behaviour of steel beam-to-column joints: Fully welded vs bolted connections", *Proceeding of the 12th World Conference on Earthquake Engineering*, Auckland, New Zealand, January 30 – February 4.
- CEN, European Committee for Standardization, [2005]. *Eurocode 3: Design of steel structures - Part 1-8: Design of joints*.
- Coelho, A.M.G., Bijlaard, F.S.K., da Silva, L.S. [2004] "Experimental assessment of the ductility of extended end plate connections", *Engineering Structures*, Vol. 26, pp. 1185–1206.
- Coelho, A.M.G., Bijlaard, F.S.K. [2007] "Experimental behaviour of high strength steel end-plate connections", *Journal of Constructional Steel Research*, Vol. 63, pp. 1228–1240.
- da Silva, L.S., De Lima, L.R.O., da S.Vellasco, P.C.G., de Andrade, S.A.L. [2004] "Behaviour of flush end-plate beam-to-column joints under bending and axial force", *Steel and Composite structures*, Vol. 4, No. 2, pp. 77–94.

- Della Corte, G., De Matteis, G., Landolfo, R., Mazzolani, F.M. [2002] "Seismic analysis of MR steel frames based on refined hysteretic models of connections", *Journal of Constructional Steel Research*, Vol. 58, pp. 1331-1345.
- Faella, C., Piluso, V., Rizzano, G. [2000] *Structural Steel Semirigid Connections - Theory, design and software*, CRC Press, Florida, ISBN 0-8493-7433-2.
- Ghobarah, A., Osman, A., Korol, R.M. [1990] "Behaviour of extended end-plate connections under cyclic loading", *Engineering Structures*, Vol. 12, pp. 15–27.
- Iannone, F., Latour, M., Piluso, V., Rizzano, G. [2011] "Experimental analysis of bolted steel beam-to-column connections: Component identification", *Journal of Earthquake Engineering*, Vol. 15, No. 2, pp. 214-244.
- Jaspart, J.P. [2000] "General report: session on connections", *Journal of Constructional Steel Research*, Vol. 55, pp. 69-89.
- Lemonis, M.E., Gantes, C.J. [2009] "Mechanical modelling of the nonlinear response of beam-to-column joints", *Journal of Constructional Steel Research*, Vol. 65, pp. 879-890.
- Nogueiro, P., Simões da Silva, L., Bento, R., Simões R. [2006] "Experimental behaviour of standardised European end-plate beam-to- column steel joints under arbitrary cyclic loading", *Proceeding of Stability and Ductility of Steel Structures*, Lisbon, Portugal, September 6-8.
- SCI [1995] *Joints in Steel Construction. Moment Connections*. The Steel Construction Institute (publication no. 207/95), Silwood Park, Ascot, UK.
- Shi, G., Shi, Y., Wang, Y. [2007a] "Experimental and theoretical analysis of the moment- rotation behaviour of stiffened extended end-plate connections", *Journal of Constructional Steel Research*, Vol.63, pp. 1279–1293.
- Shi, G., Shi, Y., Wang, Y. [2007b] "Behaviour of end-plate moment connections under earthquake loading", *Engineering Structures*, Vol. 29, pp. 703–716.
- Sumner, E.A., Murray, T.M. [2002] "Behavior of Extended End-Plate Moment Connections Subject to Cyclic Loading", *Journal of Structural Engineering*, Vol. 128, No. 4, pp. 501-508.

Sumner, III, E.A. [2003] "Unified design of extended end-plate moment connections subject to cyclic loading", *PhD Thesis in Civil Engineering*, Virginia Polytechnic Institute, Blacksburg, Virginia.

Tahir, M., Hussein, A. [2008] "Experimental tests on extended end-plate connections with variable parameters", *Steel Structures*, Vol. 8, pp. 369-381.

Terracciano, G. [2013] "Yield and ultimate rotations of beam-to-column end-plate joints", *PhD Thesis in Construction Engineering*, University of Naples Federico II.

Terracciano G., Della Corte G., Di Lorenzo G., Landolfo R. [2011] "Progetto agli spostamenti di telai con nodi semirigidi – Studio preliminare sulla modellazione dei collegamenti", *Atti del XXIII Congresso CTA (Collegio dei Tecnici dell'Acciaio)*, Ischia, 9-12 ottobre.

Terracciano G., Della Corte G., Di Lorenzo G., Landolfo R. [2013] "Simplified methods of analysis for end-plate beam-to-column joints", *Atti del XXIV Congresso CTA (Collegio dei Tecnici dell'Acciaio)*, Torino, 9-12 Ottobre.

Zoetemeijer, P. [1974] *A design method for the tension side of statically-loaded bolted beam-to-column joints*, Heron, Vol. 20, No. 1, pp. 1-59.

6. CHARACTERISING PARTIAL-STRENGTH JOINTS USING FINITE ELEMENT ANALYSIS

Hugo Augusto, José Miguel Castro, Carlos Rebelo & Luís Simões da Silva

6.1 INTRODUCTION

Although for static design, modern codes of practice allow the use of partial-strength and/or semi-rigid joints, provided that all other code requirements are met, the consideration of this type of joints in seismic resistant structures is not thoroughly addressed in design codes and is currently a topic of intensive research. Advantages of partial-strength/semi-rigid connections can be pointed out in terms of lower construction costs and simple fabrication. Previous studies have shown that, if adequately detailed, these connections can also be attractive to be used in structures located in seismic regions, allowing control of the actual location and response of energy dissipative elements [Bernuzzi *et al.*, 1996].

To ensure an adequate frame design, the structural engineer must be able to predict the joint behaviour. Many studies have been carried out with the objective of characterising the behaviour of steel connections (e.g. Jaspart [1991], Steenhuis *et al.* [1996], Faella *et al.* [2000]). The classification of steel joints can be divided into three categories, according to the following criteria:

- i) Strength – Full-strength or partial-strength;
- ii) Stiffness – Rigid, semi-rigid or pinned;
- iii) Rotation capacity – Ductile or non-ductile.

Figure 6.1 illustrates the joint behaviour for a connection subjected to bending moment. Each one of the properties has a direct impact on the joint behaviour and consequently, on the structural behaviour. The strength requirement determines if the joint is capable of transferring the full level of internal forces, classified as a full-strength connection, or if the joint is only able to transfer a fraction of the internal forces. In the latter case the joint is classified as partial-strength. In the case of partial-strength joints, even if the internal forces resulting from the structural analysis can be resisted by the connection, as in the case of seismic loading, there is a shift of the inelastic regions from the elements connected to the joint and hence, it is necessary to ensure that the additional

requirements for the connections are met, such as the energy dissipation and the rotation capacity.

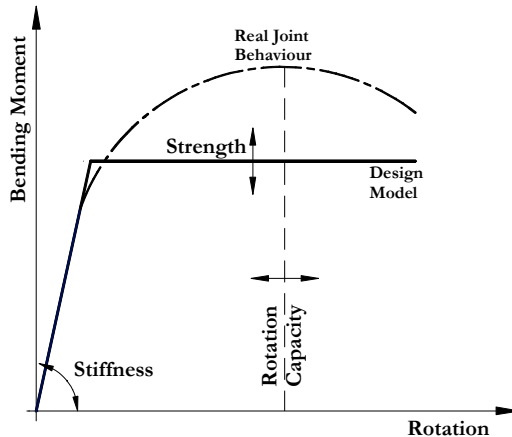


Figure 6.1. Joints moment-rotation behaviour.

The most common partial-strength joints configurations used in European buildings are that composed of an end-plate welded to the beam and which is then bolted to the steel column (Figure 6.2(a)) and the top and seat angle connection (Figure 6.2(b)).

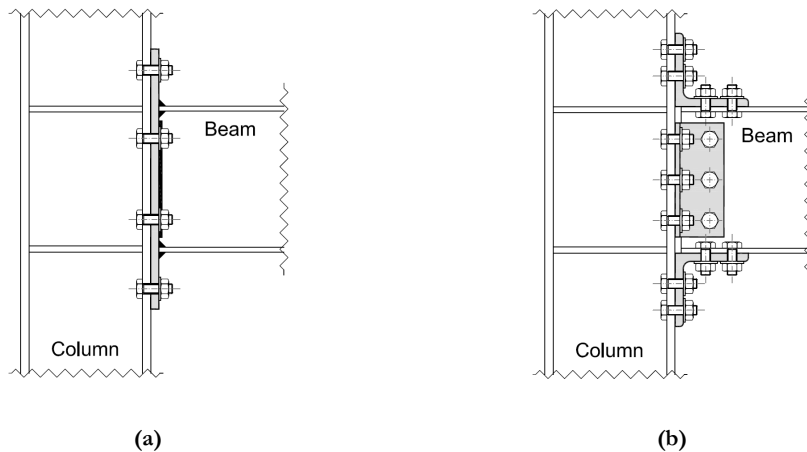


Figure 6.2. Common partial strength joints configurations: (a) end-plate connections; (b) top and seat angle connection.

Normally, partial-strength connections (Figure 6.3) are relatively flexible and hence, are classified as semi-rigid in terms of stiffness. Therefore, the use of this type of connection in seismic zones requires an adequate balance between strength, stiffness and ductility, as

they become the main dissipative components in the structure and therefore, additional requirements have to be met in the design process. Hence, as explained in subsequent sections, the joint typology to be discussed in this chapter is the extended end-plate, Figure 6.2(a), mainly due to its higher stiffness and strength in comparison with the top and seat angle typology.

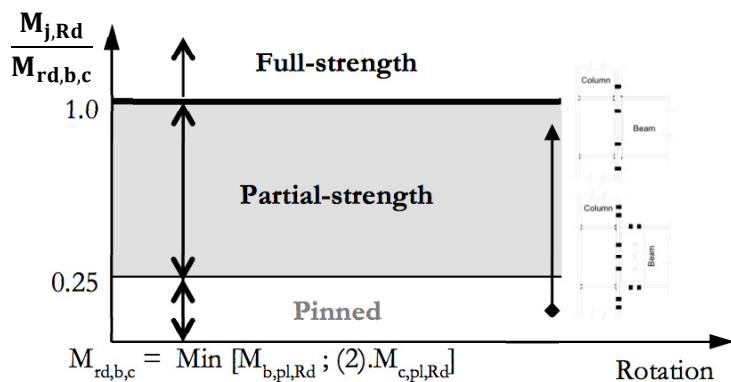


Figure 6.3. Strength classification.

It can be easily understood that the inelastic behaviour of a bolted joint is far more complex than a welded connection because more components, such as bolts, plates and angles, are introduced into the connection zone. The nonlinear interaction between the connection elements, and the variety of possible failure modes, greatly increases the complexity of the design and the analysis of the joints. Although, as realised by Shen and Astaneh-Asl [1999], when designed properly the bolted connection may exhibit high ductility and good energy-dissipation capacity under cyclic loading, provided that the proper overstrength is given to the brittle components.

From a survey of the literature, it was possible to identify that the hysteretic behaviour of partial-strength connections can be described by existing hysteretic models, such as the Ramberg-Osgood model [Ramberg and Osgood, 1943], which consist of mathematical relations that express strain (generalised displacement) as a nonlinear function of stress (generalised force). A valid alternative is the Richard and Abbott [1975] model that relates the generalised force (stress) with generalised displacement (strain). As demonstrated by Nogueiro *et al.* [2007] these two mathematical models have provided the basis for most of the models that have been proposed in the literature, like the Mazzolani [1988] comprehensive model, based on the Ramberg-Osgood expressions, but allowing for pinching effects and later modified further by Simões *et al.* [2001] to allow for pinching in the unloading zone. Based on the Richard-Abbott expressions, Della Corte *et al.* [2000]

also proposed a model that was able to simulate the pinching effect. Ramberg-Osgood expressions present the disadvantage of expressing strain as a function of stress which, in the context of finite element analysis, clearly complicates the integration in displacement-based, or for the calibration of tests results generally carried out under displacement-control once they reach the nonlinear stage. It is a widely known that predicting the cyclic behaviour of steel bolted joints is quite complex, due to the number of phenomena involved, such as material nonlinearity (plasticity, isotropic and kinematic strain-hardening), nonlinear contact and slip, geometrical nonlinearity, residual stress conditions, complicated geometrical configurations and also phenomena like pinching, the Bauschinger effect, ratchetting effect, among others. All these issues turn the prediction of the connection behaviour into an intricate task. Therefore, experimental testing represents the best way to concisely characterise joint behaviour. However, when extensive parametric studies are required, the limited resources in terms of time and money can be a real problem when one considers performing experimental tests. Allied to the experimental tests, and with the significant development in the computers technology and optimised algorithms provides the opportunity to extend the application of the numerical models to perform parametric studies, as demonstrated by Adány and Dunai [2004], the finite element method (FE) proved so far to be the best numerical approach to simulate the cyclic behaviour of steel joints. However, a large set of experimental tests is therefore required for the calibration of numerical models developed in order to overcome the enumerated difficulties and to validate the accuracy of the results obtained.

In the following section, a brief overview of past numerical studies will be described and the numerical models used to characterise the beam-to-column end-plate joints will be described and compared with the results of collected experimental data. Following this, the parametric study carried out to examine the cyclic behaviour of end-plate joints will be described, intending to characterise the several behaviours present in the ductile failure modes listed in Part 1-8 of Eurocode 3 [CEN, 2005b].

6.2 REVIEW OF PAST NUMERICAL STUDIES

As discussed in the previous sections, intensive experimental research work has been conducted on the cyclic behaviour of steel joints. The results of the research studies has allowed the development of empirical models, relating the parameters found in the response to the geometrical and mechanical properties of the joints, or on the other hand, the validation of mechanical models based on rigid and flexible components that when correctly assembled, predicts the joints behaviour main features and allows for the extension of the experimental results to a wider range of joints and applications. There are several examples of models available in the literature that are proposed based on experimental results, with Frye and Morris [1975] being one of the first empirical models known in which the representation of the $M-\theta$ rotation curve is obtained by an odd-

power polynomial function, where the rotation depends on parameters that are defined by the geometrical and mechanical properties of the structural details and also relies on curve-fitting constants. Ten years later, Azizinamini *et al.* [1985] improved the model to tackle the undesirable problem of in some cases, having a negative $M-\theta$ slope. In the field of using empirical relations or curve fitting, experimental or numerical curves, mathematical expressions, several works followed such as that by Krishnamurthy [1978] or the Kukreti [1987] model, or even the model developed by Faella, Piluso and Rizzano [Faella *et al.*, 1997] that used the same component based approach of that implemented in Eurocode 3 [CEN, 2005b] to develop a mechanical model capable of obtaining the data for reliable regression analyses for all the parameters affecting the joint rotation behaviour requiring less computational effort. Also, the work of Jaspart [1991] on the mechanical models based on the components approach should be pointed out, contributing significantly to the development of the Eurocode 3 methodology for the characterisation of joint behaviour and the strength, stiffness and rotation capacity design. More recent models have been proposed over the years, such as the Flejou and Colson [2002] model which followed a different approach to characterise the behaviour of several joint typologies and materials, associating to each type of joint the phenomena involved in the constitutive material, like the kinematic hardening for steel and the damage for concrete and timber, using then a multi-surface model to activate each one of the phenomena. Furthermore, with that model it is possible to simulate the joint cyclic behaviour. Also in the cyclic loading field, several works have been developed to characterise the joints or its components behaviour, like the mathematical models of Bernuzzi *et al.* [1992, 1996] or Bursi and Calvi [1997]. The former relates the stiffness values for several $M-\theta$ branches to the energy dissipation, and the second relates the strength obtained in the monotonic tests to the degradation and pinching of the cyclic ones and both are based on experimental evidence. Mechanical models such as those developed by Madas and Elnashai [1992] can be considered one of the first attempts to apply the component approach to characterise the cyclic behaviour of beam-to-column joints. Calado and Ferreira [1994] considered the monotonic behaviour of the component to assess the cyclic response. However, the model does not account for pinching or strength and stiffness degradation. A few years later, Calado [2003] also proposed a model for top and seat web angle for steel beam-to-column connections with damage accumulation, considered in the stress-strain relationship of the material, and including also the behaviour of the bolts in cyclic shear, taking into account the slip between the connected elements, although it disregards the ovalisation of the hole and the changes in preloading force. An important issue affecting the connection behaviour is the internal force interaction, namely the axial and bending moment interaction. The work of da Silva and Coelho [2001] resulted in a proposal of an equivalent elastic mechanical model replacing the bi-linear springs with equivalent elastic springs using an energy formulation to evaluate the behaviour of steel joint. More recently, Del Salvio *et al.* [2009] proposed a

component-based mechanical model for semi-rigid beam-to-column connections that combine the effect of axial force and bending moment by assuming a tri-linear characterisation of the joint response.

Although the prediction of the joint behaviour by analytical procedures is a subject with remarkable advances in the last few decades, and despite a large number of proposed models to predict the moment-rotation relationship of the joints, there are always some limitations associated with those, in order to find a generalised procedure able to characterise every type of joints or loading (monotonic, cyclic, dynamic, etc.). This is why the finite element analyses represent a powerful technique to study joint behaviour.

Numerous publications can be found in the literature, which use finite element (FE) models to predict the behaviour of different joint types. Krishnamurthy and Graddy [1976] was the earliest work that used the FE method to predict the behaviour of end-plate connections. Due to the limited computer resources available at the time, there were several limitations in the analyses performed. The authors attempted to correlate the results from an elastic three-dimensional FE analysis to those from an elastic two-dimensional FE analysis. Also in the early use of the FE method to model connections, Kukreti *et al.* [1987] used a similar approach developing moment-rotation relationships for bolted steel end-plate connections, focusing the research on the prediction of maximum end-plate separation through parametric analyses covering the various geometric and force related variable found in practical ranges. Later, with the development of computational resources and tools, several works have been conducted in the field of bolted beam-to-column behaviour characterization using 3D FE models, an improvement that was well accepted due to the proved inadequacy of the 2D displacement-based FE models to characterise the behaviour of bolted connections, which were known to predict stiffer and stronger solutions in comparison with the corresponding 3D models [Bursi and Jaspart, 1997a]. Ziomek *et al.* [1992] used 3D models with several types of shell and modelling approaches to simulate the one side extended end-plate experimental tests and to determine the best modelling approaches to be used in the behaviour assessment. The authors concluded mostly what is nowadays taken for granted, namely the influence of the material, mesh refinement, the bolts loading and the influence of nonlinearities on the results. A similar approach was adopted by Sherbourne and Bahaari [1994] using the ANSYS software package to develop 3D shell models trying to overcome the limited ability of the 2D models to deal with thin plates in which yielding occurs due to biaxial bending. The authors aimed to study the distribution and magnitude of the prying forces at the free edge of the end-plate and concluded that the extended end-plate connections can be successfully simulated with complete 3D model up to the ultimate load, and that the model developed was adequate for thin plates but also gave satisfactory results for thick plates. In the same line of research, and using the same techniques, Sherbourne and Bahaari [Sherbourne and

Bahaari, 1996, Bahaari and Sherbourne, 1996] conducted the first study on bolted T-stub connections, and also on complete extended end-plate connections in order to study the stiffness and strength of the joints with unstiffened column flanges. The authors concluded that only a 3D model could satisfactorily predict the interaction between the T-stub and the column flange, since the maximum bending stresses were perpendicular to each other, and that the prying forces in the T-hanger increased with the decrease in relative stiffness of flange to bolt. It was also concluded that the lack of the stiffeners changed the behaviour of the connections in the tensile and compression zones of the column flange. A few years later, Bahaari and Sherbourne [2000] used the same modelling approach and conducted a study on eight-bolt extended end-plate connections to analyse the large capacity of this solution, in terms of stiffness and strength, when no stiffeners in either tension or compression region were used in the column. Later, Maggi *et al.* [2003, 2005] performed some parametric analyses on the behaviour of bolted extended end-plate connections using FE modelling tools that were validated by the experimental tests performed. Studying the interaction between the end-plate and bolts, the authors concluded that the T-stub failure mode type 2 presented levels of interaction between the end-plate and bolts that is difficult to predict accurately. It was also found that there are some limitations in the T-stub analogy for the yield lines representation at the end-plate, leading to limitations both in accounting for prying action and in predicting values for strength and stiffness of the connection. Also in the field of the end-plate joints loaded monotonically, Shi *et al.* [2008] presented the development of a FE model to simulate the mechanical behaviour of different types of beam-to-column joints with pretensioned bolts. With the intention of providing a basis for developing mechanical models consistent with the Eurocode component method, since using FE results can provide additional valuable data for the joint's behaviour which are difficult to measure in experimental tests, such as the distribution of pressure caused by bolt pretension, the friction between the end-plate and the column flange and the principal stress flow in the connection.

In the field of composite end-plate joints, the work of Ahmed and Nethercot [1995] can be pointed out, which used the ABAQUS software package to simulate semi-rigid composite connections, aiming to develop a FE model that realistically represents all aspects of the physical behaviour of composite end-plate connections, observed in tests, and examine the effects of varying the reinforcement ratio and the shear interaction.

The achievements in FE modelling and analyses by Bursi and Jaspart [1997a, 1997b, 1998] in the field of end-plate joints and T-stub component behaviour assessment should also be pointed out. Trying to deal with and overcome the complex nonlinear phenomena which are commonly observed in the FE connections models, and study the best ways to

improve the degree of accuracy of the FE models, using their simulations as benchmarks in the validation process of FE software packages.

Regarding the field of beam-to-column top and seat-angle connections, Kishi *et al.* [2001] modelled four FE connections using different techniques aiming to find the one that best estimates M- θ relationship. Furthermore, a three-parameter power model was also used based on the Richard and Abbott's power function [Richard and Abbot, 1975], to compare the nonlinear M- θ curves. This concluded that the three-parameter power model and the FE model can be used as an efficient and reasonably accurate prediction of the joints behaviour, but with considerable differences at the computing time. In the same field of work, Pirmoz *et al.* [2008a, 2008b and 2009] studied the effect of the web angle dimensions on moment-rotation behaviour of bolted top and seat angle connections. Studying also the connections behaviour under combined axial and tension force, it was concluded that the axial tension load reduces the initial connection stiffness and moment capacity. A tri-linear semi-analytical method was proposed to estimate the connection response under combined tension and monotonic moment loading demonstrating sufficient accuracy, especially for relatively low levels of axial tension loads. In the same research group, Danesh *et al.* [2007] studied the moment-rotation behaviour of bolted top and seat angles with double web angle connections under the combination of shear force and bending moment and concluded that connections with low shear capacity of their web angles are more sensitive to shear force and have a large value for the initial stiffness reduction factor.

In another typology of joints, which are not so common in European countries is the half laminated H sections, T-stubs were used to connect the flanges of the beam and the column, using four columns of bolts. Takhirov and Popov [2002] studied, by means of FE analysis, a specimen with rectangular-shaped stems. Using this, a solid element analysis of the T-stub under tension in the stem was performed and a shell element modelling with buckling and instability analysis.

In the field of cyclic loading simulations, far less work can be found in the literature. For example, Nemati *et al.* [2000] presented a methodology based on FE techniques with a combination of several other methods to extend the component-based design philosophy of EC3 to the cyclic behaviour of end-plate connections. In that study, monotonic and cyclic loaded models of T-stubs were performed following the geometry of the experimental tests and comparing their results. Following that, a mathematical energy balance model was proposed by approximating the nonlinear response by six lines representing the slopes of the unloading and reloading branches. By using the FE curves, it was possible to find the common points in the hysteresis and use the energy balance method again. To extend the model to a mechanical model for the end-plate connection, the connection was divided into independent T-stubs, which can be replaced by a spring

with the constitutive law of the mathematical energy balance model, adopted for the isolated T-stub. Also in the field of T-stubs behaviour assessment, Bursi *et al.* [2002] presented some work based on numerical analysis of the low-cycle fracture behaviour of T-stubs with partial fillet welds which attempted to assess the seismic performance of bolted partial strength beam-to-column joints under seismic loading. Several FE models were undertaken in order to tune model material parameters connections in FE models, because the cyclic response was much more difficult to model than the monotonic one due to the nonlinear hardening behaviour involved. In this case, the nonlinear isotropic/kinematic hardening model available in the ABAQUS code was used. This model was proposed by Lemaitre and Chaboche [1990] and relies on small deformations and associate flow rule. Lastly, a parametric study was conducted in order to define details able to reduce loading-induced toughness demands, namely the effects of the weld-to-base metal yield strength ratio, the residual stress influence and the end-plate yield-to-ultimate strength ratio. The conclusions showed that the overall behaviour of the specimens was governed by the material provided with the lowest strength, which is the base metal, in which yielding occurs effectively. In addition, Ádány and Dunai [2004] presented some work in the field of FE modelling and analysis of end-plate joints in steel frames under monotonic and cyclic loading conditions which tried to deal with the main features involved in the joints modelling and validation, such as the applicable material models or the nonlinear solution algorithms. The main conclusion was that the models cannot be tested in a single step but instead, a multi-step verification is recommended, presenting a step-by-step checking procedure for the cyclic models and computational methods. Recently, Gerami *et al.* [2011] conducted a series of FE simulations using the experimental tests of Summer and Murray [2000] which looked at end-plate and rectangular-shaped T-stub connections to compare the cyclic behaviour of fourteen specimens by changing the horizontal and vertical arrangement of bolts. It was intended to study the cyclic behaviour influence when the parameters used in the design of bolted connections suffer undesirable changes such as the imperfections in construction. The objective of this study was to help the designers to choose appropriate connections according to the construction conditions. The results revealed that moment capacity and rotational stiffness of T-stubs bolted connections are higher than that of end-plate bolted connections, considering the total energy dissipation of both groups to be approximately the same. It was also concluded that under cyclic loading the probability of failure mode change is higher in T-stub connections than that of the end-plate ones, due to the arrangement variation of bolts; as such end-plate connections are suggested for conditions where the imperfections in construction are probable.

It can be concluded from the above that much work still can be performed in the field of the assessment of joints behaviour when subjected to cyclic loadings, although the advances in this area have greatly improved the state of knowledge.

6.3 SURVEY OF EXPERIMENTAL RESULTS

The objective of this section is to identify the characteristic hysteresis of the considered joint typology and to choose the most suitable tests to use in the calibration/validation of parametric numerical models, which will then be used to study joint hysteretic behaviour. Thirty-two experimental tests were analysed and the results compared.

Firstly, the relevant features of each test found in the literature will be described and a quantitative analysis will be performed using the available data, allowing to conclusions needed to move forward in the research to be drawn.

6.3.1 Beam-to-Column Joints Tests

Three typologies of joints were analysed: top and seat angles connections, flush end-plate connections and extended end-plate connections, described in the next sub-sections organised by authors.

6.3.1.1 *Bernuzzi et al. [1996]*

The paper reports a research project that aimed at developing simple design criteria for semi-rigid steel frames in seismic zones. A simple prediction model was proposed taking into account the results of the tests under reversal loading. The main parameters identified, in the first series, were the influence of the loading history and the main stiffness and strength parameters, whereas in the second series the study focused on the influence of the key geometrical and mechanical parameters in the cyclic performance, and also on the energy dissipation capacity. The research work focused on joints with extended end-plates and with cleat connections. The work on extended end-plate connections intended to study the overall joint response and the individual contribution of the individual components. On the other hand, the study on cleat connections intended to assess the problem of the cumulative damage. The European Convention for Constructional Steel Work [ECCS, 1986] and an additional three loading histories were used for the cyclic loading pattern, and a parametric study was undertaken in the connection components. All specimens consisted of a long beam stub with IPE 300 section, attached through the connection to be tested to a rigid counter-beam. All bolts were grade 8.8. For the first series it was adopted the preloaded according to the Italian code and in the second series the preload was limited to 40% of the actual yield strength. From the top and seat angles connections (TSC), the results showed that the correlation between the monotonic tests and the envelopes of the cyclic ones correlate well in the initial elastic range and in the final inelastic ranges, whereas in the intermediate range differences were remarkable mostly because of the slippage. Failure was always characterised by fracture of one bolt on the side in tension at very high connection rotation (more than 60 mrad). For the flush end-plate connections (FPC) the correlation between the monotonic tests and the envelop of the cyclic ones differ remarkably,

although this difference was explained by the earlier plastic deformation of the end-plate in the vicinity of the beam flanges affecting the contact with the counter-beam, where this appends just after a few cycles. The main contribution to the rotation of nodal zone is the end-plate deformation (close to 90%). The conclusions of the first test series, albeit for limited data, were that the flush end-plates are more sensitive to the loading history with differences up to 40% and that the ECCS procedure may provide a rather conservative assessment of joint ductility. The contribution of the deformation of the cleats to the overall rotation of the top and seat angles connection was minimal, and negligible for most of the response. For the second series of tests, the steel grade was changed among other parameters. For the flush end-plate connections, such influence appeared to be insignificant, but the deformation of the cleats in the TSC specimens was fairly affected by the steel beam grade and also the fracture mechanism changed to one occurring in the cleats. In addition, the TSC connections showed lower pinching and higher resistance (of about 14%). The change of the bolts in the flush end-plate appeared to have a considerable impact in the connection's stiffness and strength but, on the other hand, the connection showed lower ductility. For the extended end-plate connections (EPBC), the results revealed that the plate extension ensures a noticeable increase in the stiffness and strength when compared to the FPC connections. The key features of the behaviour were nonetheless the same, with the plate contributing the most to the response in both the elastic and inelastic range. If the thickness of the end-plate increased, the behaviour of the connection changed, with bolt inelastic elongation and pinching behaviour becoming more prominent. The failure mode differed also for the lower end-plate thickness, where failure occurred in the plate welds and with the thickness increase, the bolts were seen to fail first. As for the energy dissipation capacity, TSC and EPBC-1 connections exhibited remarkably higher energy dissipation compared to both flush end-plate connections, but only in the high rotation range. The EPBC1 connection therefore showed the better balance between the stiffness and rotation ductility. As a general conclusion, the cyclic response of semi-rigid connections can be generally considered quite satisfactory in terms of stiffness, strength and rotational ductility.

6.3.1.2 Kim and Yang [2007]

This work presented an experimental study on the cyclic behaviour of the steel sub-assemblages with fully welded (FW), bolted web angles (DWA) and top and seat with web angles (TSD) connections. It was intended to compare the cyclic behaviour of the bolted joints with the welded one. The tests revealed that the bolted connections have lower initial stiffness than the welded one, 95.5% less for the DWA and 61% less for the TSD and lower ultimate moment, obtained for the moment-rotation relationship, 72% less for the DWA connection and 41.4% less for the TSD connection. DWA specimens are composed of two web angles L50x50x6 bolted to the column flange and beam web.

The semi-rigid joint TSD comprised top and seat angles L75x75x6 bolted to the flanges of the beam and column and L50x50x6 bolted to the beam web and to the column flange. It was concluded that the total energy dissipated of the TSD frame was about 5 times bigger than of the DWA frame at a total drift ratio of 3%. The percentage of energy dissipation of the TSD to the FW was high until yielding occurred, due to joint slip, and then the percentage dropped as inelastic deformation of the panel zone and the column increased.

6.3.1.3 *Dubina et al. [2002]*

Experimental testing was carried out in the “Politehnica” University of Timisoara, Romania on three connections typologies, extended end-plate (EP), welded (W) and with cover plates (CWP). The beam-to-column joints were double-sided and each typology was tested twice under symmetrical (XS) and anti-symmetrical (XU) cyclic loading. The main parameters considered in the study were the initial stiffness, moment capacity and plastic rotation capacity and the results of the experiment were compared with the Eurocode 3 [CEN, 1992], Annex J. In addition, the anti-symmetric loading tests were compared with the symmetrical loaded ones due to the panel zone plastic mechanism developed in the anti-symmetrical ones. This resulted in the following differences for the XU tests: increase of ductility; decrease of moment capacity; and initial stiffness; and more stable energy dissipation through hysteretic loops. The test specimens were composed of HEB 300 for the columns and IPE360 for the beams with a steel grade S235, although the coupon tests revealed that the steel properties are more likely to be of a S275 steel grade, the steel plates presented a lower yield strength compatible to the S235 steel grade. The ECCS [1986] procedure was used for the applied loading history. The failure of the specimens was defined as when the force applied to the joint fell below 50% of the maximum load applied during the loading history. The test results for the SX-EP specimens showed that the end-plate was the weakest component with visible deformation in the vicinity of the beam flanges. Cracks began to appear in the root of the end-plate to beam bottom flange welds until complete rupture. Also a bolt failed in tension during the XS-EP2 test, leading to large deformations of the end-plate. For the XU-EP specimens, the contribution of the column panel zone for the inelastic behaviour was commonly observed to be the first zone to yield. The deformations of the end-plate started only after the $\pm 2\epsilon_y$ cycle, where ϵ_y is the yield displacement according to ECCS [1986] procedure. Again, cracks on the bottom flange welds to the end-plate appeared, with some bolts failure contributing to the decrease of the connection stiffness. After a number of plastic excursions, complete rupture of the extended part of the end-plate occurred. The main source of ductility was the column panel zone with stable hysteretic loops over the entire loading history, with an important strain hardening. A degradation of strength and stiffness was observed throughout the entire loading history of the extended end-plate tests. In the case of XU-EP2 specimen, failure occurred by fracture of the beam web and top flange, and cracks started in the heated affected zone of the beam

flange. The main conclusions were that the loading type (symmetrical and anti-symmetrical) significantly affected the connection response, where the column panel zone was the component that differentiated their behaviour. Unbalanced moments affect the column panel zone by reducing the stiffness and strength of the connection. A joint classified as rigid and full-strength in a symmetrical loading case can be classified as semi-rigid and partial-strength in an anti-symmetrical loading case. In the comparison with Annex J of EC3, similar values were found for the XS series for the plastic moments. On the other hand for the XU series, all experimental values were lower than the ones computed with the Annex J of EC3. For what concerns the initial stiffness, numerical and experimental results agreed for the XU series, but were very different for the XS series. In general, bolted end-plate connections showed good rotation capacity and more ductile behaviour when compared to welded connections, but with a reduced initial stiffness. The plastic rotation of the XU series showed to be higher than the values generally accepted by codes (30%).

6.3.1.4 Dubina et al. [2002]

This research consisted of experimental tests carried out at the “Politehnica” University of Timisoara, Romania. As mentioned in the previous section, this study consisted of an experimental programme with the objective of examining the effect of the symmetrical and anti-symmetrical loading on double sided beam-to-column joints, but in this case the purpose was only to evaluate the performance of extended end-plate connections. Special attention was given to the fracture of beams and end-plates. Two types of structural members were considered for the X series hot rolled profiles and for the BX series built-up sections. The tests referred in the document for the X series are the ones already described in the previous section [Dubina et al., 2001], hence this section will focus on the BX series tests. For the BX series, the built-up beam was a typical “I” section, while the column was an “X” section. The use of an “X” section for the column, combined with the web stiffeners, increased the effective shear area resulting in an increase in stiffness and moment capacity when subjected to seismic loading. Six experimental tests were carried out, three under symmetrical loading (BX-SS) and three under anti-symmetrical loading (BX-SU). The ECCS [1986] procedure was used for the applied loading history. The first test of each series was monotonically loaded to evaluate the yield displacement. During the tests, the symmetrical loaded specimens revealed an initial plastic deformation of the end-plate and column flanges and after a few cycles, a sudden brittle failure of the lower left beam flange to end-plate weld occurred on the inter flange width. During the reversal load, cracking of beam web to end-plate weld led to upper flange failure. For the anti-symmetrical loaded specimens, the deformation of the column panel zone was the first signal in the test, followed by the bending of the end-plate and column flanges. During the plastic deformation, cracks appeared in the lower left beam flange to end-

plate weld, which propagated into the end-plate for the BX-SU-C1 specimen. For the BX-SU-C2 specimen the first cracks initiated in the top right beam flange to end-plate welds and after cracks appeared in the lower weld leading to lamellar tearing of the end-plate. With increasing deformation, successive bolt failure occurred. The proposed recommendations for the weld design and manufacture were: full penetration welds should be used if reversal loading is expected; notch-tough weld rods; use of base material with guaranteed through-thickness quality to avoid the lamellar tearing. The main conclusions revealed the importance of a proper welding procedure and design. The loading type (symmetrical and anti-symmetrical) was seen to affect significantly the beam-to-column joint behaviour due to the influence of the column panel zone in shear. Hence, it is very important to choose the appropriate model for interior (double-sided) beam-to-column joints. The use of X-shaped columns increases the stiffness and moment resistance for the anti-symmetrical loading when compared to the usual I and H shaped columns.

6.3.1.5 Nogueiro [2009]

This publication presented a set of 13 tests performed on external beam-to-column extended end-plate joints under monotonic and cyclic loads. The aim of the research was to characterise the behaviour of the connections under cyclic loading and the numerical implementation of a mathematical model capable of simulating real connections behaviour. The model was incorporated into the SeismoStruct software package [SeismoSoft, 2011] to enable the understanding of the global behaviour of the structure with the real connections behaviour modelled. The model was calibrated with the experimental tests performed, in addition to other tests collected from the literature. Three steel structure typologies were studied and subjected to seismic loading by means of artificial accelerograms, where the real behaviour of the steel connections were incorporated. The tested specimens attempted to represent real sub-assemblages of real buildings and were composed by HEA320 and HEB320 for the columns and IPE360 and HEA 280 for the beams. The tests were divided in four groups: J1, J2, J3 and J4 series. Of the three tested specimens, the first was monotonically loaded and the other two subjected to cyclic loading. The steel grade for the structural elements and plates was S355 while M24 bolts of grade 10.9 were used. The loading protocol was in accordance with the ECCS [1986] procedure but with two variants. The test results for the J1 series, with the HEA320 for the column and the IPE360 for the beam, revealed good agreement of the monotonically tested specimen to the values predicted by the EC3-1-8, albeit on the safe-side. The cyclic tests presented stable hysteresis loops without pinching. The failure mode was characterised by rupture occurring at the interface of the weld to the end-plate. The lower load amplitudes in the J1.2 lead to both a higher energy dissipation and number of cycles. For the energy dissipation, the column web panel provided a large contribution. For the J2 series using the same structural elements with the introduction of the axial load on the column and for the monotonically loaded tests once more the

computed values by the EC3-1-8 were closer to the experimental ones, but in this case the initial stiffness of the test was lower than the EC3-1-8 prediction. As in the previous series, the cyclic tests presented stable hysteresis loops without pinching and rupture occurred at the interface between the weld and the beam flange. Once again, the high contribution of the column web panel to the energy dissipations was pronounced. For the J3 series that used a HEB320 for the column and an IPE360 for the beam, the monotonically loaded tests presented higher values of moment resistance and initial stiffness than the ones computed by the EC3-1-8. For the cyclic loaded tests, the J3.3 presented a similar behaviour compared to the other tests but with less energy dissipation due to the lower contribution of the column web panel. In the case of the J3.2, the rupture of the extended part of the end-plate led to behaviour of a flush end-plate with degradation of stiffness and strength and pinching behaviour. For the J4 series, where the column consisted of a HEA320 and the beam HEA 280, the results computed with EC3-1-8 were closer to the test results but the EC3-1-8 values were a little lower than the tests values. During the cyclic tests, the pinching behaviour was prominent due to lack of pre-loading in the bolts with the rupture occurring at the weld that connects the beam flange to the end-plate.

6.3.2 Organisation and Data Processing

6.3.2.1 Relevant Properties

In order to make adequate use of the collected test data, it is necessary to choose the tests that best fit the needs of the adopted methodology for the assessment of the partial-strength joints characterisation, and consequently lead to justifiable outcome in this research.

Firstly, it was important to determine the relevant properties in the tested specimens, so that they could be properly grouped.

The main properties of the collected tests that are relevant to this study are:

- Initial stiffness (K_0) - it is important to know the elastic stiffness of the joint since this is a key parameter to ensure adequate behaviour of a MRF structure when subject to seismic loads and other horizontal loads, such as wind.
- Strength ($M_{max}/M_{pl,Rd,b}$) - as stated before, strength is an important factor to take into account in the design of a connection because its relation with ductility is crucial for a good connection behaviour under seismic actions.
- Rotation capacity (θ_u) - this is an important property associated to the dissipative elements in an MRF; it is necessary to ensure that connections have sufficient

rotational capacity in order to withstand the acceptable demands without collapse.

- Ductility (e_u/e_y or θ_u/θ_y) - this property represents the capacity of the connection for dissipating energy and for sustaining plastic deformations. Hence, it is an important factor to take into account in the selection of connections.

By focusing these properties, it was possible to determine the most suitable joints based on the following comparisons.

6.3.2.2 Stiffness Comparison

In order to compare the test results, a beam span L_b of 6m was assumed and the Young's modulus was taken equal to 210GPa. Figure 6.4 and Table 6.1 show the stiffness of the connections tested and also the EC3-1-8 limits for the connections classification as rigid or pinned.

This classification is as follows:

- Rigid: $S_{j,ini} \geq 25 EI_b / L_b$
- Pinned: $S_{j,ini} \leq 0.5 EI_b / L_b$

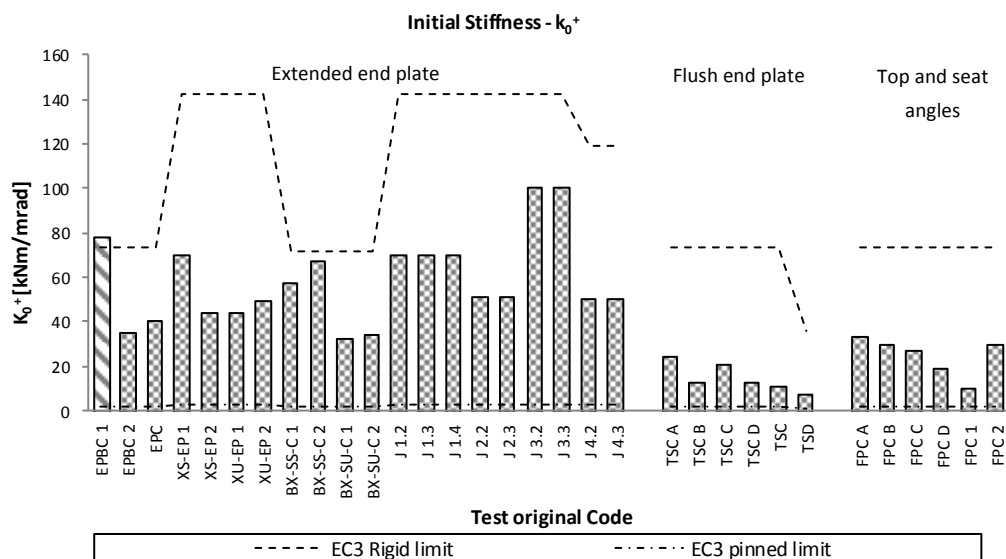


Figure 6.4. Initial stiffness comparison.

It is possible to see that the majority of the joints analysed exhibited a semi-rigid nature based on their initial stiffness.

Table 6.1. Initial stiffness comparison.

Test code	Author	Typology	$K_0^+ [kNm/mrad]$	Classif.
EPBC 1	Bernuzzi <i>et al.</i> [1996]	Extended End-plate	78.00	Rigid
EPBC 2	Bernuzzi <i>et al.</i> [1996]	Extended End-plate	35.40	Semi-rigid
EPC	Bernuzzi <i>et al.</i> [1996]	Extended End-plate One Side	40.50	Semi-rigid
XS-EP 1	Dubina <i>et al.</i> [2001]	Extended End-plate	69.54	Semi-rigid
XS-EP 2	Dubina <i>et al.</i> [2001]	Extended End-plate	44.21	Semi-rigid
XU-EP 1	Dubina <i>et al.</i> [2001]	Extended End-plate	44.08	Semi-rigid
XU-EP 2	Dubina <i>et al.</i> [2001]	Extended End-plate	49.00	Semi-rigid
BX-SS-C 1	Dubina <i>et al.</i> [2002]	Extended End-plate	57.76	Semi-rigid
BX-SS-C 2	Dubina <i>et al.</i> [2002]	Extended End-plate	67.37	Semi-rigid
BX-SU-C 1	Dubina <i>et al.</i> [2002]	Extended End-plate	32.08	Semi-rigid
BX-SU-C 2	Dubina <i>et al.</i> [2002]	Extended End-plate	34.18	Semi-rigid
J 1.2	Nogueiro [2009]	Extended End-plate	69.50	Semi-rigid
J 1.3	Nogueiro [2009]	Extended End-plate	69.50	Semi-rigid
J 1.4	Nogueiro [2009]	Extended End-plate	69.50	Semi-rigid
J 2.2	Nogueiro [2009]	Extended End-plate	51.50	Semi-rigid
J 2.3	Nogueiro [2009]	Extended End-plate	51.50	Semi-rigid
J 3.2	Nogueiro [2009]	Extended End-plate	100.00	Semi-rigid
J 3.3	Nogueiro [2009]	Extended End-plate	100.00	Semi-rigid
J 4.2	Nogueiro [2009]	Extended End-plate	50.00	Semi-rigid
J 4.3	Nogueiro [2009]	Extended End-plate	50.00	Semi-rigid
TSC A	Bernuzzi <i>et al.</i> [1996]	Top and Seat Angles	24.20	Semi-rigid
TSC B	Bernuzzi <i>et al.</i> [1996]	Top and Seat Angles	12.50	Semi-rigid
TSC C	Bernuzzi <i>et al.</i> [1996]	Top and Seat Angles	21.00	Semi-rigid
TSC D	Bernuzzi <i>et al.</i> [1996]	Top and Seat Angles	12.80	Semi-rigid
TSC	Bernuzzi <i>et al.</i> [1996]	Top and Seat	11.00	Semi-rigid
TSD	Yang and Kim (2007b)	Top and Seat Angles	6.98	Semi-rigid
FPC A	Bernuzzi <i>et al.</i> [1996]	Flush End-plate	32.90	Semi-rigid
FPC B	Bernuzzi <i>et al.</i> [1996]	Flush End-plate	29.20	Semi-rigid
FPC C	Bernuzzi <i>et al.</i> [1996]	Flush End-plate	27.10	Semi-rigid

Test code	Author	Typology	$K_0^+ [kNm/mrad]$	Classif.
FPC D	Bernuzzi <i>et al.</i> [1996]	Flush End-plate	19.00	Semi-rigid
FPC 1	Bernuzzi <i>et al.</i> [1996]	Flush End-plate	9.70	Semi-rigid
FPC 2	Bernuzzi <i>et al.</i> [1996]	Flush End-plate	30.00	Semi-rigid

6.3.2.3 Strength Comparison

Figure 6.5, Figure 6.6 and Table 6.2 show a comparison of the envelope of maximum bending moments for the positive and negative branches of the moment-rotation response. The EC3-1-8 limits for the full-strength and pinned classification are also depicted in the charts. In addition, it is also depicted a reference line for a proposed minimum strength of 70% of the beam strength needed for a joint be able to fulfil the seismic design requirements of a medium-rise building i.e. the 0.7 to 1.0 range considered for the strength ratio was deemed to be acceptable in regions of moderate to high seismicity.

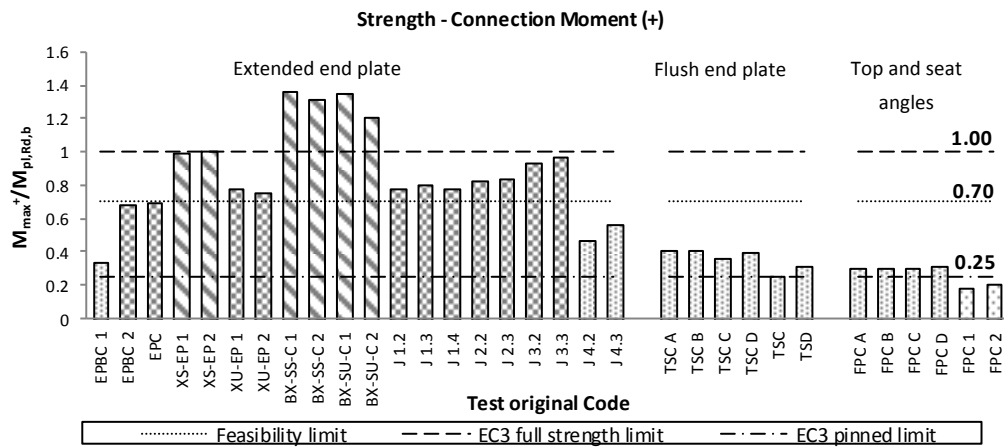


Figure 6.5. Strength comparison for the envelope maximum positive moments achieved.

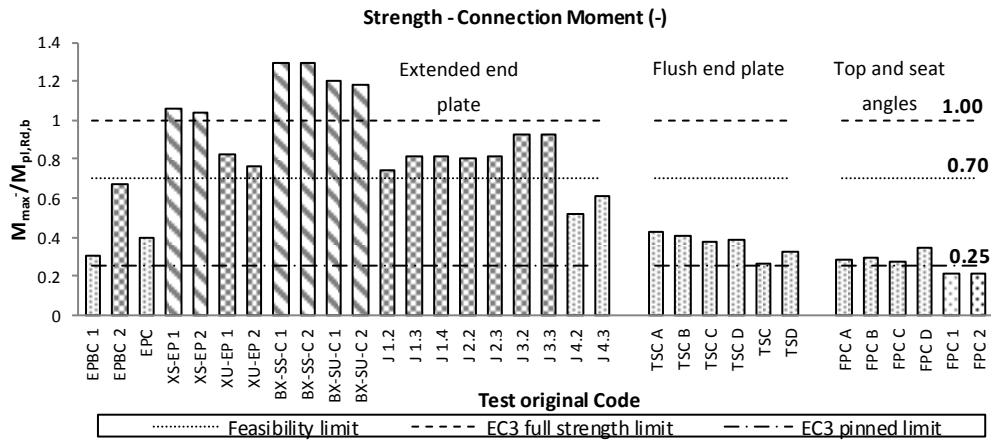


Figure 6.6. Strength comparison for the envelope maximum negative moments achieved.

There are only nine joints that fulfil the imposed requirements.

Table 6.2. Strength comparison for the envelope maximum moments achieved.

Test ID	Author	Typology	$M_{\max}^+ / M_{pl,Rd,b}$	$M_{\max}^- / M_{pl,Rd,b}$
XS-EP 1	Dubina <i>et al.</i> [2001]	Extended End-plate	0.99	1.06
XS-EP 2	Dubina <i>et al.</i> [2001]	Extended End-plate	1.01	1.04
BX-SS-C 1	Dubina <i>et al.</i> [2002]	Extended End-plate	1.36	1.30
BX-SS-C 2	Dubina <i>et al.</i> [2002]	Extended End-plate	1.32	1.31
BX-SU-C 1	Dubina <i>et al.</i> [2002]	Extended End-plate	1.35	1.21
BX-SU-C 2	Dubina <i>et al.</i> [2002]	Extended End-plate	1.21	1.19
EPBC 2	Bernuzzi <i>et al.</i> [1996]	Extended End-plate	0.69	0.68
XU-EP 1	Dubina <i>et al.</i> [2001]	Extended End-plate	0.78	0.83
XU-EP 2	Dubina <i>et al.</i> [2001]	Extended End-plate	0.76	0.76
J 1.2	Nogueiro [2009]	Extended End-plate	0.78	0.75
J 1.3	Nogueiro [2009]	Extended End-plate	0.80	0.82
J 1.4	Nogueiro [2009]	Extended End-plate	0.78	0.82
J 2.2	Nogueiro [2009]	Extended End-plate	0.83	0.80
J 2.3	Nogueiro [2009]	Extended End-plate	0.84	0.82
J 3.2	Nogueiro [2009]	Extended End-plate	0.94	0.93
J 3.3	Nogueiro [2009]	Extended End-plate	0.98	0.93
EPBC 1	Bernuzzi <i>et al.</i> [1996]	Extended End-plate	0.34	0.31
EPC	Bernuzzi <i>et al.</i> [1996]	Extended End-plate One Side	0.70	0.40

Test ID	Author	Typology	$M_{max}^+ / M_{pl,Rd,b}$	$M_{max}^- / M_{pl,Rd,b}$
J 4.2	Nogueiro [2009]	Extended End-plate	0.47	0.52
J 4.3	Nogueiro [2009]	Extended End-plate	0.57	0.61
TSC A	Bernuzzi <i>et al.</i> [1996]	Top and Seat Angles	0.41	0.43
TSC B	Bernuzzi <i>et al.</i> [1996]	Top and Seat Angles	0.41	0.41
TSC C	Bernuzzi <i>et al.</i> [1996]	Top and Seat Angles	0.37	0.38
TSC D	Bernuzzi <i>et al.</i> [1996]	Top and Seat Angles	0.40	0.39
TSC	Bernuzzi <i>et al.</i> [1996]	Top and Seat	0.26	0.27
TSD	Yang and Kim (2007b)	Top and Seat Angles	0.31	0.33
FPC A	Bernuzzi <i>et al.</i> [1996]	Flush End-plate	0.31	0.29
FPC B	Bernuzzi <i>et al.</i> [1996]	Flush End-plate	0.31	0.30
FPC C	Bernuzzi <i>et al.</i> [1996]	Flush End-plate	0.31	0.28
FPC D	Bernuzzi <i>et al.</i> [1996]	Flush End-plate	0.32	0.35
FPC 1	Bernuzzi <i>et al.</i> [1996]	Flush End-plate	0.18	0.22
FPC 2	Bernuzzi <i>et al.</i> [1996]	Flush End-plate	0.21	0.22

6.3.2.4 Rotation Capacity Comparison

A comparison of the rotational capacity can be seen in Figure 6.7, Figure 6.8 and Table 6.3. Also shown in the charts are the 25 mrad and 35 mrad, which correspond to the minimum limits required in EC8 [CEN, 2004] for medium and high ductility connections, respectively.

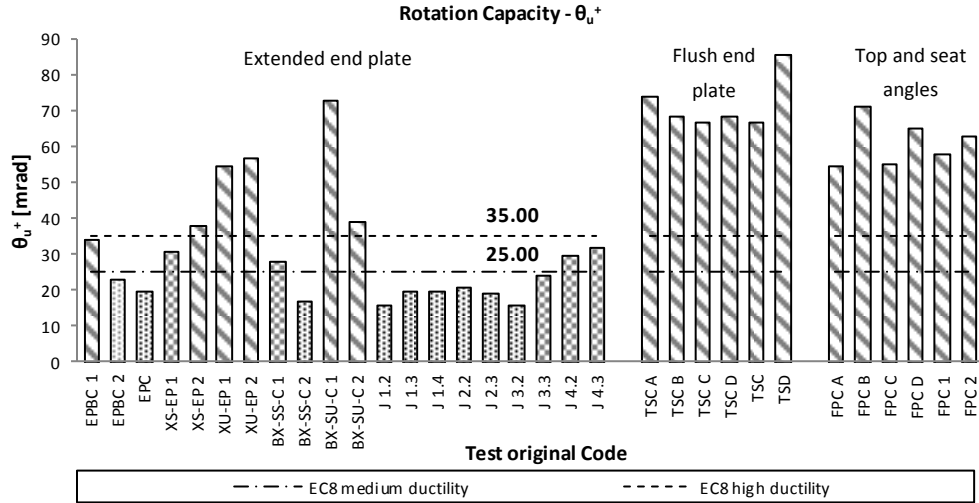


Figure 6.7. Rotation comparison for the positive envelope.

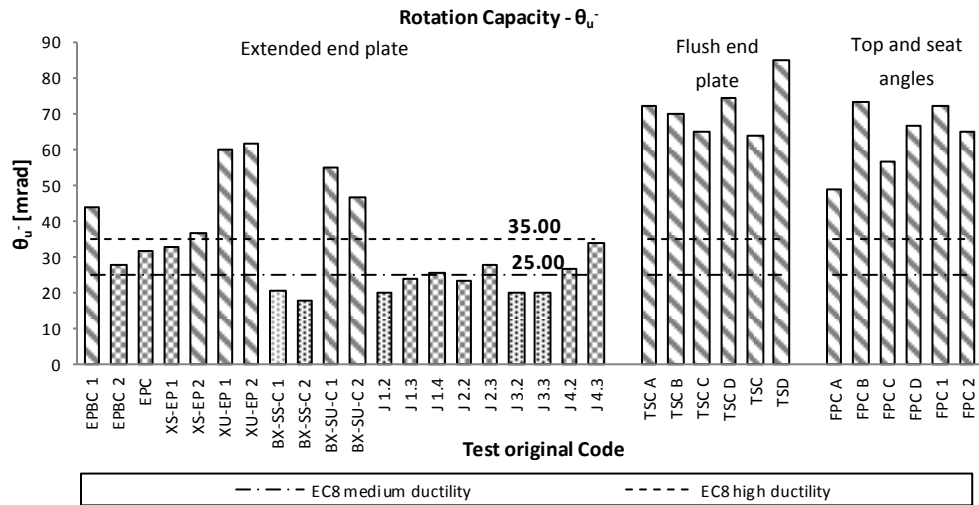


Figure 6.8. Rotation comparison for the negative envelope.

Table 6.3. Rotation comparison.

Test ID	Author	Typology	θ_u^+ [mrad]	θ_u^- [mrad]
EPBC 1	Bernuzzi <i>et al.</i> [1996]	Extended End-plate	34.20	44.40
XS-EP 2	Dubina <i>et al.</i> [2001]	Extended End-plate	38.00	37.00
XU-EP 1	Dubina <i>et al.</i> [2001]	Extended End-plate	55.00	60.00
XU-EP 2	Dubina <i>et al.</i> [2001]	Extended End-plate	57.00	62.00
BX-SU-C 1	Dubina <i>et al.</i> [2002]	Extended End-plate	73.00	55.00
BX-SU-C 2	Dubina <i>et al.</i> [2002]	Extended End-plate	39.00	47.00
TSC A	Bernuzzi <i>et al.</i> [1996]	Top and Seat Angles	74.20	72.70
TSC B	Bernuzzi <i>et al.</i> [1996]	Top and Seat Angles	68.80	70.10
TSC C	Bernuzzi <i>et al.</i> [1996]	Top and Seat Angles	67.10	65.50
TSC D	Bernuzzi <i>et al.</i> [1996]	Top and Seat Angles	68.70	74.60
TSC	Bernuzzi <i>et al.</i> [1996]	Top and Seat	67.00	64.10
TSD	Yang & Kim [2007b]	Top and Seat Angles	85.60	85.40
FPC A	Bernuzzi <i>et al.</i> [1996]	Flush End-plate	55.00	49.00
FPC B	Bernuzzi <i>et al.</i> [1996]	Flush End-plate	71.40	73.40
FPC C	Bernuzzi <i>et al.</i> [1996]	Flush End-plate	55.40	56.70
FPC D	Bernuzzi <i>et al.</i> [1996]	Flush End-plate	65.10	67.20
FPC 1	Bernuzzi <i>et al.</i> [1996]	Flush End-plate	58.00	72.60
FPC 2	Bernuzzi <i>et al.</i> [1996]	Flush End-plate	63.20	65.30
XS-EP 1	Dubina <i>et al.</i> [2001]	Extended End-plate	31.00	33.00
J 4.2	Nogueiro [2009]	Extended End-plate	30.00	27.00
J 4.3	Nogueiro [2009]	Extended End-plate	32.00	34.00
EPBC 2	Bernuzzi <i>et al.</i> [1996]	Extended End-plate	23.30	28.00
EPC	Bernuzzi <i>et al.</i> [1996]	Extended End-plate One Side	19.90	31.90
BX-SS-C 1	Dubina <i>et al.</i> [2002]	Extended End-plate	28.00	21.00
BX-SS-C 2	Dubina <i>et al.</i> [2002]	Extended End-plate	17.00	18.00
J 1.2	Nogueiro [2009]	Extended End-plate	16.00	20.00
J 1.3	Nogueiro [2009]	Extended End-plate	20.00	24.00
J 1.4	Nogueiro [2009]	Extended End-plate	20.00	26.00
J 2.2	Nogueiro [2009]	Extended End-plate	20.78	23.50
J 2.3	Nogueiro [2009]	Extended End-plate	19.00	28.00
J 3.2	Nogueiro [2009]	Extended End-plate	16.00	20.00
J 3.3	Nogueiro [2009]	Extended End-plate	24.00	20.00

As expected, the joints with the highest rotation capacities are also the ones that achieved the lowest values of strength. A balance between these two properties is always needed to be able to fulfil the codes requirements in seismic regions.

6.3.2.5 Ductility Capacity

The ductility of a connection can be evaluated in many ways and it is inherent that different authors report ductility using different calculation approaches. Figure 6.9 and Table 6.4 shows the different ductility demands achieved for the different connections. Although a direct comparison cannot be made, it allows visualising the evolution of the ductility in the various groups.

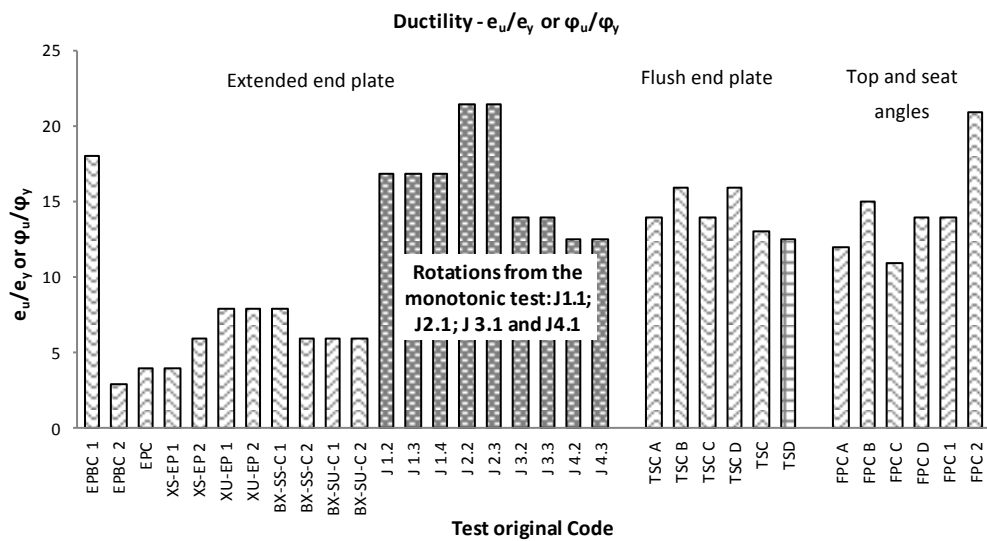


Figure 6.9. Ductility capacity.

Table 6.4. Ductility capacity.

Test ID	Author	Typology	e_u/e_y or θ_u/θ_y
EPBC 1	Bernuzzi <i>et al.</i> [1996]	Extended End-plate	18.00
EPBC 2	Bernuzzi <i>et al.</i> [1996]	Extended End-plate	3.00
EPC	Bernuzzi <i>et al.</i> [1996]	Extended End-plate One Side	4.00
XS-EP 1	Dubina <i>et al.</i> [2001]	Extended End-plate	4.00
XS-EP 2	Dubina <i>et al.</i> [2001]	Extended End-plate	6.00
XU-EP 1	Dubina <i>et al.</i> [2001]	Extended End-plate	8.00

Test ID	Author	Typology	ϵ_u/ϵ_y or θ_u/θ_y
XU-EP 2	Dubina <i>et al.</i> [2001]	Extended End-plate	8.00
BX-SS-C 1	Dubina <i>et al.</i> [2002]	Extended End-plate	8.00
BX-SS-C 2	Dubina <i>et al.</i> [2002]	Extended End-plate	6.00
BX-SU-C 1	Dubina <i>et al.</i> [2002]	Extended End-plate	6.00
BX-SU-C 2	Dubina <i>et al.</i> [2002]	Extended End-plate	6.00
J 1.2	Nogueiro [2009]	Extended End-plate	16.90
J 1.3	Nogueiro [2009]	Extended End-plate	16.90
J 1.4	Nogueiro [2009]	Extended End-plate	16.90
J 2.2	Nogueiro [2009]	Extended End-plate	21.42
J 2.3	Nogueiro [2009]	Extended End-plate	21.42
J 3.2	Nogueiro [2009]	Extended End-plate	13.95
J 3.3	Nogueiro [2009]	Extended End-plate	13.95
J 4.2	Nogueiro [2009]	Extended End-plate	12.50
J 4.3	Nogueiro [2009]	Extended End-plate	12.50
TSC A	Bernuzzi <i>et al.</i> [1996]	Top and Seat Angles	14.00
TSC B	Bernuzzi <i>et al.</i> [1996]	Top and Seat Angles	16.00
TSC C	Bernuzzi <i>et al.</i> [1996]	Top and Seat Angles	14.00
TSC D	Bernuzzi <i>et al.</i> [1996]	Top and Seat Angles	16.00
TSC	Bernuzzi <i>et al.</i> [1996]	Top and Seat	13.00
TSD	Yang and Kim (2007b)	Top and Seat Angles	12.50
FPC A	Bernuzzi <i>et al.</i> [1996]	Flush End-plate	12.00
FPC B	Bernuzzi <i>et al.</i> [1996]	Flush End-plate	15.00
FPC C	Bernuzzi <i>et al.</i> [1996]	Flush End-plate	11.00
FPC D	Bernuzzi <i>et al.</i> [1996]	Flush End-plate	14.00
FPC 1	Bernuzzi <i>et al.</i> [1996]	Flush End-plate	14.00
FPC 2	Bernuzzi <i>et al.</i> [1996]	Flush End-plate	21.00

The ductility demands represented in the figure were obtained directly from the cyclic tests, and this corresponds to the ratio between the maximum displacement/rotation and the elastic displacement/rotation, with an exception for the darker bars where the ductility demands were obtained from the monotonic tests according to the same ratio.

6.3.2.6 Final Remarks

From the above comparisons, it is possible to state that there are clearly a wide range of behaviours for the different connection typologies examined, with the extended end-

plates being the ones that exhibited improved properties to be used in steel moment resisting frames of medium to high-rise buildings. For that reason, in the subsequent studies only the extended end-plate joints will be addressed.

In order to choose the most feasible joints to validate and subsequently calibrate the numerical models, a binary classification was assigned for each one of the tests analysed according to their performance, where 1 represented the joint behaviour achieving the imposed criteria and 0 if not, and these are shown in Table 6.5. It is highlighted in the table that the connections which presented the best classification are those that are most suitable for the validation of the FE models.

Table 6.5. Joints ranking table.

Test ID	Author	K_0^+	$M_{max}^+ / M_{pl,Rd,b}$	$M_{max}^- / M_{pl,Rd,b}$	θ_u^+	θ_u^-	e_u/e_y	Sum
EPBC 1	Bernuzzi <i>et al.</i> (1996)	1	0	0	1	1	1	4
EPBC 2	Bernuzzi <i>et al.</i> (1996)	0	1	1	0	1	0	3
EPC	Bernuzzi <i>et al.</i> (1996)	1	1	0	0	1	0	3
XS-EP 1	Dubina <i>et al.</i> [2001]	0	0	1	1	1	0	3
XS-EP 2	Dubina <i>et al.</i> [2001]	0	0	1	1	1	0	3
XU-EP 1	Dubina <i>et al.</i> [2001]	0	1	1	1	1	0	4
XU-EP 2	Dubina <i>et al.</i> [2001]	0	1	1	1	1	0	4
BX-SS-C 1	Dubina <i>et al.</i> [2002]	1	0	0	1	0	0	2
BX-SS-C 2	Dubina <i>et al.</i> [2002]	1	0	0	0	0	0	1
BX-SU-C 1	Dubina <i>et al.</i> [2002]	0	0	0	1	1	0	2
BX-SU-C 2	Dubina <i>et al.</i> [2002]	0	0	0	1	1	0	2
J 1.2	Nogueiro [2009]	0	1	1	0	0	1	3
J 1.3	Nogueiro [2009]	0	1	1	0	1	1	4
J 1.4	Nogueiro [2009]	0	1	1	0	1	1	4
J 2.2	Nogueiro [2009]	0	1	1	0	1	1	4
J 2.3	Nogueiro [2009]	0	1	1	0	1	1	4
J 3.2	Nogueiro [2009]	1	1	1	0	0	1	4
J 3.3	Nogueiro [2009]	1	1	1	1	0	1	5
J 4.2	Nogueiro [2009]	0	0	0	1	1	1	3
J 4.3	Nogueiro [2009]	0	0	0	1	1	1	3

6.4 CALIBRATION OF THE FINITE-ELEMENT MODELS

As previously mentioned, the numerical modelling of the joints requires the interaction of various domains of high complexity, such as solving the complex geometry of the connections, material nonlinearity and nonlinearity in the interface between elements, mainly through the contact between the end-plate and the column flange and the contact between bolts and end-plate or column flanges. When the cyclic behaviour is considered, new requirements have to be taken into account as recommended by Ádány and Dunai [2004] who pointed out the following:

- The model should consider the complex 2D or 3D geometry of the joint.
- The load model should represent appropriately the cyclic loading history.
- The material model should take into account the cyclic behaviour of the steel material (isotropic and kinematic hardening).
- The model should be able to represent the local buckling of the slender plate elements subjected to load reversal.
- The conditional connections between the joint components should be modelled under cyclic effects (contact-separation-re-contact).

For this task the ABAQUS [2011] finite element software package was used to achieve the following objectives:

- Perform parametric simulations based on the calibrated model of the connection.
- Generate global hysteretic moment-rotation curves to use in the derivation of ductility-equivalent viscous damping relationships for the direct displacement-based seismic design procedure.

The dissipative behaviour of the connections is achieved by means of the main dissipative components, i.e. the end-plate in bending and the column web panel in shear. For the resistance of the remaining components, an adequate level of overstrength is assumed in order to ensure that the dissipative response is observed.

6.4.1 Description of the Finite Element Models

In this section, various aspects related with the development of the FE models are discussed, such as the element types, the constraints, the interactions and the nonlinear solver, which have also been documented in Augusto *et al.* [2013].

In general the standard volume elements of ABAQUS were used. Mainly the quadrilateral and hexahedra C3D8RH element is used, which is an 8-node linear brick element, with a hybrid formulation, featuring constant pressure, reduced integration and hourglass control. However, in specific situations where the hexahedra formulation was not

possible to use, element C3D6H was used which is a 6-node linear triangular prism, hybrid and constant pressure element. The preferential use of quadrilateral and hexahedral elements was due to the higher convergence rate of these elements in comparison with the triangular and tetrahedral elements, thus providing equivalent accuracy at lower computational cost for regular meshes, which is the case in most part of the models. Due to the size and complexity of the models of the complete end-plate connections, reduced integration elements were adopted using a lower-order integration to form the element stiffness matrix, with the intention of saving computational time. Although in this case the numerical problem concerning the shear locking is overcome, the hourglass can be a real problem for the linear reduced-integration elements. As the elements have just one integration point, it is possible to have distortion deformation modes in such a way that their stiffness is severely reduced. In problems governed by bending deformations this effect may influence the accuracy of the results. To avoid this problem at least three layers were considered in the connections members' thickness and the hourglass control formulation was activated for the elements. The elements chosen also have a hybrid formulation normally used for fully incompressible materials behaviour. When severe plastic deformation is expected, as it is the case in the present situation, the rate of total deformation becomes incompressible as the plastic deformation starts to dominate the response [ABAQUS, 2011]. The column and beam parts where solid elements were not necessary a three-dimensional first-order linear beam element with 2 nodes is used, i.e. the ABAQUS element B31. This element is based on the Timoshenko beam theory which allows for transverse shear strains, also allowing for large strains and rotations in its formulation.

The models are composed by several parts as shown in Figure 6.10 and Figure 6.11, which interact with each other through constraints or interactions. The beam elements are constrained to the solid column and beam parts using multi-point constraint that uses the concept of slave and master nodes to define the same degrees of freedom between both nodes. Between the end-plate and the solid beam, a tie constraint is imposed using the same master and slave philosophy and the degrees of freedom of the dependent nodes are eliminated, i.e. the two surfaces will have common degrees of freedom. The interactions between the end-plate and the column flange and the interactions between the bolts and the end-plate or column flange are achieved using the general contact algorithm based on "hard contact" formulation that acts in the normal direction to resist penetration and also accounts for tangential behaviour considering the friction between surfaces.

Monotonic and cyclic analyses were performed using the Abaqus/Standard solver that iteratively solves a system of equations implicitly at each solution increment [ABAQUS,

2011]. The geometric nonlinear effects from large displacement theory were taken into account in all FE models.

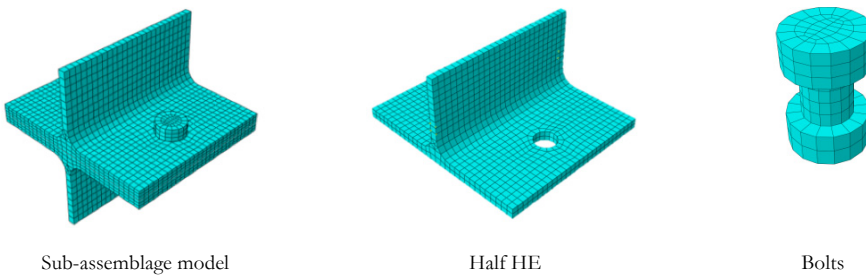


Figure 6.10. T-stub meshed parts of the FE model.

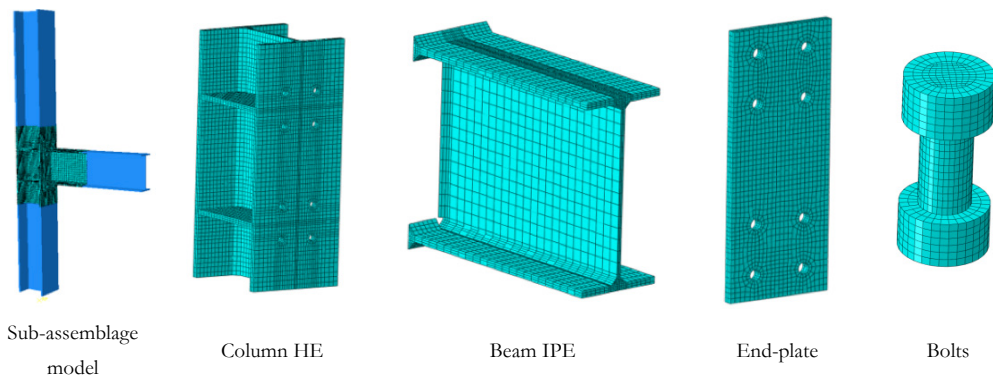


Figure 6.11. End-plate joint meshed parts of the FE model.

6.4.2 T-stub Models

To understand the cyclic behaviour of the dissipative components of the partial-strength connections, it is important to study and calibrate each component separately. A set of models of isolated bolted T-Stubs that represent the flange of the column and the end-plate in bending were developed to calibrate their behaviour. The numerical models are in accordance with the experimental tests performed by Piluso and Rizzano [2008] at the Material and Structures Laboratory of the Department of Civil Engineering of Salerno University. Furthermore, the authors kindly provided the results of the coupons materials tests for use in this study. The objective is to calibrate the three typical bolted T-Stub failure modes shown in Figure 6.12 and also to calibrate the hysteretic behaviour of those connections.

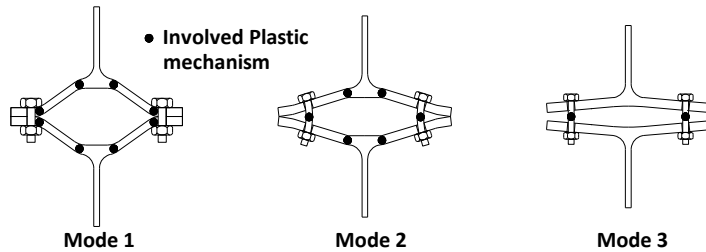


Figure 6.12. Failure modes of bolted T-stubs.

Two types of “T” were used, namely laminated and welded as shown in Figure 6.13. For the laminated profiles, half HEA180 and HEB180 profiles were used and for the welded profiles, plates with thicknesses of 18mm for the flanges and 12mm for the webs were used. The bolts were M20 (class 8.8) in all cases, and the geometrical properties are listed in Table 6.6.

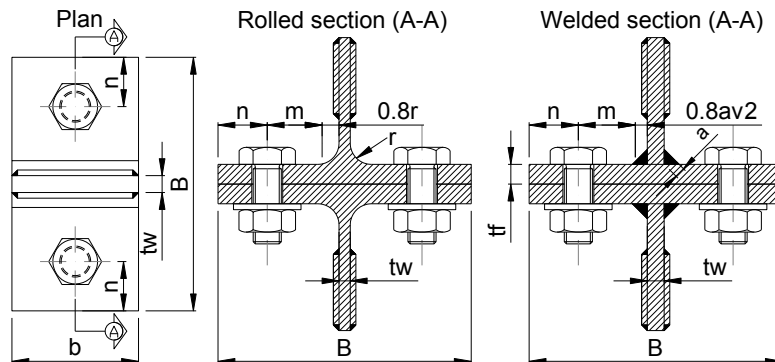


Figure 6.13. Geometry of bolted T-Stubs (Adapted from Piluso and Rizzano [2008]).

Table 6.6. Measured geometrical properties of tested specimens.

Series	Test	B (mm)	b (mm)	t_f (mm)	t_w (mm)	r (a) (mm)	m (mm)	n (mm)
A: HEA 180	A1	181.25	158.75	9.71	6.78	15.00	37.39	37.85
	A2	181.75	158.25	9.68	6.83	15.00	37.23	38.24
B: HEB 180	B1	180.00	159.00	14.14	8.10	15.00	36.76	37.19
	B7	180.00	158.25	14.19	8.15	15.00	36.71	37.21
D: W18	D1	231.00	90.25	18.64	12.25	7.50	52.31	51.07

6.4.2.1 Material Modelling

An important feature in a numerical model is the material definition using constitutive stress-strain models. These models can be more or less elaborated depending on the material behaviour and generally, for sharp knee material types, bi-linear idealisations can be used without impairing accuracy.

Two types of loading protocol were used in these models: monotonic and cyclic loading. It is recognised that the material property definition needs to be different to account for the difference in behaviour associated with the cyclic plasticity.

For the HEA 180, HEB 180 and plates, the material stress-strain data from Piluso and Rizzano [2008] were adopted and for the bolts, the nominal values for the 8.8 class were used. Table 6.7 shows the coupons tests material properties, which reports values in terms of true stress and true strain.

Table 6.7. Measured mechanical properties of tested specimens.

Series	A_0 [mm ²]	ϵ_u [%]	f_y [MPa]	f_u [MPa]
A: HEA 180	207.82	98.28	334.67	530.62
B: HEN 180	106.28	109.92	280.10	464.56
D: W18	373.13	98.32	307.34	464.94

The use of theoretical stress-strain relationships for the material definition, and their validation through real tests, revealed to be an important help in the standardisation of the data collected from the several experimental tests. Three theoretical expressions were used in the T-Stub models: a bilinear approach, the Ramberg-Osgood approach and the Menegotto-Pinto approach. To define each expression the following material properties have been used: the yielding strength, f_y , ultimate strength, f_u and young's modulus, E .

The bilinear approach is a simple material model definition represented by two linear expressions where the initial stiffness governs the first one, until the yield strength and the second one is the hardening stiffness, typically defined as a ratio b to the initial stiffness. Due to its linearity and simplicity, this approach requires relatively little computational effort and is very attractive for use in numerical and analytical simulations. For the bilinear model's definition, the following data are required: f_y , f_u , ϵ_y , E and b .

The Ramberg-Osgood approach is a stress-strain relationship normally used for materials of round-house type and it is based on the observation that a representation in a log-log coordinates of the true stress against true plastic strain results is a straight line and can be represented by a power function:

$$\sigma = K(\varepsilon_p)^n \quad (6.1)$$

where ε_p is the true plastic strain, σ is the true stress, K is the strength coefficient and n is the strain hardening exponent. If the elastic strain, ε_e , is included and the total strain, ε , the relationship proposed by Ramberg and Osgood [1943] is obtained:

$$\varepsilon = \varepsilon_e + \varepsilon_p = \frac{\sigma}{\varepsilon} + \left(\frac{\sigma}{K} \right)^{1/n} \quad (6.2)$$

According to De Martino *et al.* [1990] the exponent n is determined in accordance to the reference points for the elastic limit and the ultimate stress, or other two intermediate points. In this case n is determined as follows:

$$n = \frac{\log(\varepsilon_u / \varepsilon_y)}{\log(f_u / f_y)} \quad (6.3)$$

The Menegotto-Pinto model consists of an expression that relates inelastic stress-strain in the hardening phases of sharp knee metals at yielding and is represented by:

$$\sigma = \left\{ E_\infty + (E_0 + E_\infty) \Big/ \left[1 + \left(\frac{\varepsilon}{\varepsilon_0} \right)^R \right]^{1/R} \right\} \varepsilon \quad (6.4)$$

where E_0 is the initial tangent modulus of the stress-strain curve, E_∞ is the secondary tangent modulus of the stress-strain curve, R is a material constant and $\varepsilon_0 = \sigma_0/E_0$ is the strain at the stress σ_0 as shown in Figure 6.14. According to Kato *et al.* [1990], when the gradient of the nominal engineering stress-strain curve becomes zero at the maximum load, the secondary tangent modulus E_∞ is set to zero at the maximum stress $\sigma_{0(MP)} = E\varepsilon_0 = f_{max}$, as shown in Figure 6.15. Furthermore, the initial tangent modulus E_0 can be assumed to be equal to the modulus of elasticity E . The previous equation is then simplified as follows:

$$\sigma = \left\{ E \Big/ \left[1 + \left(\frac{\varepsilon}{\varepsilon_0} \right)^R \right]^{1/R} \right\} \varepsilon \quad (6.5)$$

Using the $\varepsilon_0 = f_{max}/E$ introduces a large error at the maximum load, as can be seen in Figure 6.15, and therefore another material constant is introduced to improve the fitness of the Equation 6.5, becoming $\varepsilon_0 = \gamma_{MP}f_{max}/E$ or:

$$\sigma_{0(MP)} = \gamma_{MP} f_{\max} = E \epsilon_0 \quad \gamma_{MP} > 1 \quad (6.6)$$

To determine the parameters R and γ_{MP} it is sufficient to use the coordinates of two points of the strain-hardening curve P_A (σ_A, ϵ_A) and P_B (σ_B, ϵ_B), R can be determined with the following equation:

$$\left(\frac{\sigma_A \sigma_B}{E} \right)^R \left[\left(\frac{1}{\epsilon_A} \right)^R - \left(\frac{1}{\epsilon_B} \right)^R \right] + (\sigma_A^R - \sigma_B^R) = 0 \quad (6.7)$$

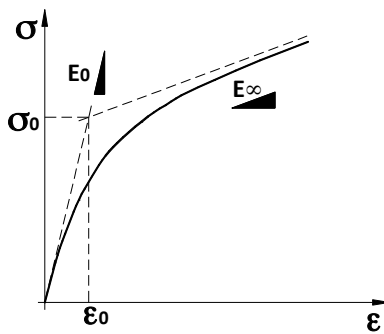


Figure 6.14. Menegotto-Pinto model.

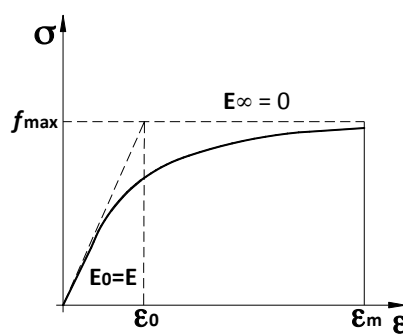


Figure 6.15. The case of $E_0 = E$ and $E_\infty = 0$.

Figure 6.16 to Figure 6.18 illustrates the stress-strain relationships for the models adopted for the A1, B1 and D1 tests.

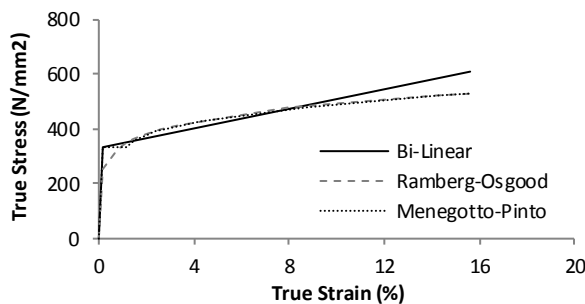


Figure 6.16. Stress-strain relationships for the A1 test.

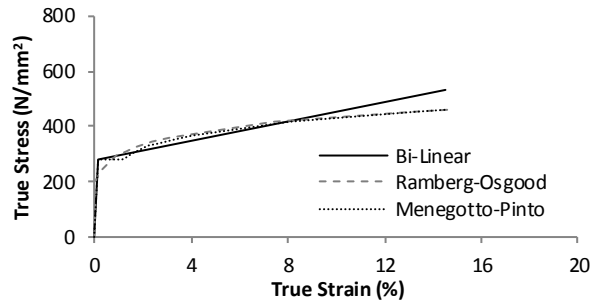


Figure 6.17. Stress-strain relationships for the B1 test.

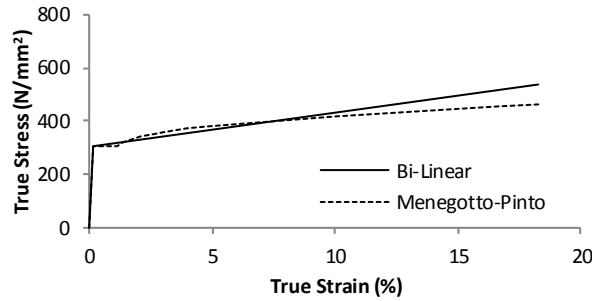


Figure 6.18. Stress-strain relationships for the D1 test.

For the cyclic models, the combined isotropic/kinematic model available in ABAQUS was used for the simulation of the material hardening when subjected to cyclic loads. This constitutive model is based on the work of Chaboche [1986] and uses the Von Mises [1913] yield criterion and an associative flow rule is assumed.

The isotropic component of the model defines the change of the size of the yield surface σ^0 as a function of equivalent plastic strain ε^p , and is given by:

$$\sigma^0 = \sigma|_0 + Q_\infty \left(1 - e^{-b_{iso} \varepsilon^p} \right) \quad (6.8)$$

Where $\sigma|_0$ is the yield stress at zero equivalent plastic strain, Q_∞ is the maximum change in the size of the yield surface and b_{iso} is the rate at which the size of the yield surface changes as plastic strain increases.

The kinematic component of the model defines the changes of backstress α , which is expressed as:

$$\alpha = \frac{C_{kin}}{\gamma} + (1 - e^{-\gamma\epsilon^P}) + \alpha_1 e^{-\gamma\epsilon^P} \quad (6.9)$$

where C_{kin} and γ are material constants. The ratio C_{kin}/γ is the maximum change in backstress and γ determines the rate at which the backstress varies as the plastic strain increases.

To determine the C_{kin} and γ parameters of the combined model, using known points of the curve, as for the monotonic calibration, the curve was adjusted by those points, minimising the error between the points and the analytical kinematic expression. Table 6.8 lists the procedure for the A2 test and Figure 6.19 and Figure 6.20 illustrate the adjustment for the A2 and B7 tests.

Table 6.8. Kinematic hardening determination for the A2 test.

$$\begin{array}{ll} C_{kin} = & 3179.401 \\ \gamma = & 14.47243 \end{array} \quad C_{kin}/\gamma = 219.6867 \text{ N/mm}^2$$

ϵ (true)	σ (true)	ϵ_{pl} (true)	α (test)	α	error
0.162857559	334.6746	0	0	0	0
7.54	478.0844	0.073074	143.3885	143.4098	0.000457
15.64907968	530.6737	0.153908	196.0034	195.9991	1.81E-05
Σ					0.000475

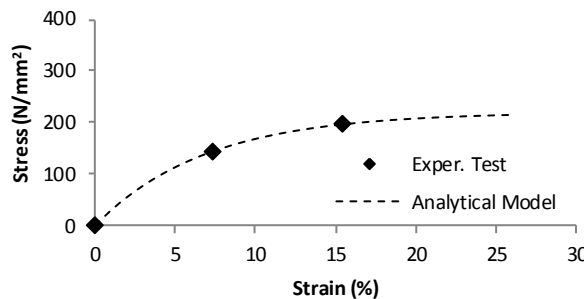


Figure 6.19. Chaboche model for kinematic hardening for the A2 test.

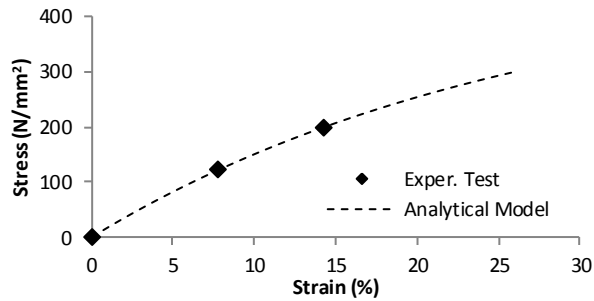


Figure 6.20. Chaboche model for kinematic hardening for the B7 test.

6.4.2.2 Results of the T-stub Numerical Models

For the monotonic models, the bilinear (B-L) approach achieved a good agreement with the experimental results. For the Ramberg-Osgood (R-O) approach the agreement was not so good, and the best correlation was achieved with the Menegotto-Pinto (M-P) model, due to its similarities with the measured stress-strain relationship, as shown in Figure 6.21 to Figure 6.27. As stated before, the objective of the monotonic study was to calibrate the various failure modes of bolted T-stubs, according to EC3-1-8. Thus, the A1 tests exhibited failure mode 1, the B1 tests showed failure mode 2 and the D1 tests presented a failure mode 3.

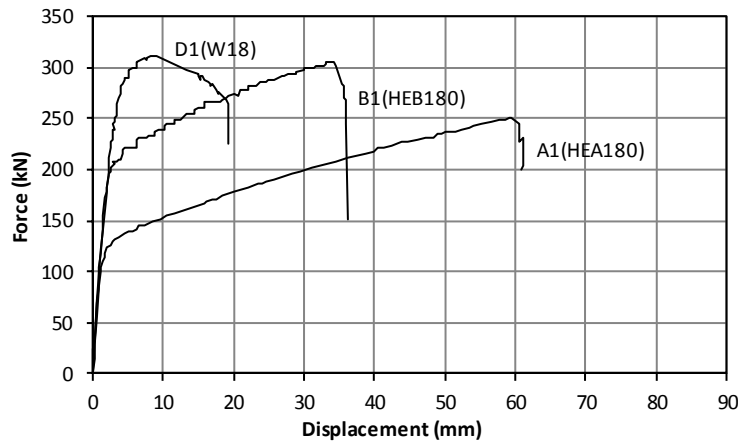


Figure 6.21. Monotonic force-displacement experimental results [Piluso and Rizzano, 2008].

The numerical results are compared with the experimental test results in terms of force-displacement relationship. Only the relevant part of the chart will be presented in Figure 6.23, Figure 6.25 and Figure 6.27. The numerical results are presented in dashed lines and

the experimental results are depicted in solid lines. In Figure 6.22, Figure 6.24 and Figure 6.26, the Von Mises stresses are plotted, highlighting the development of the three failure modes previously outlined. For the A1 test, it is possible to observe the formation of the complete yielding of the flange, which is characteristic of the first mode plastic mechanism. In the case of the B1 test, the second mode plastic mechanism can be observed with the yielding of the plates and bolts. For the D1 test, the early yielding of the bolts indicates failure mode 3 behaviour.

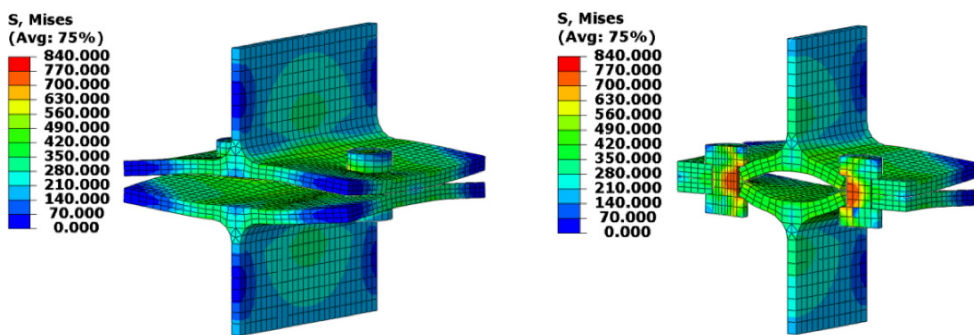


Figure 6.22. A1 test – Von Mises stress results for a 20mm displacement.

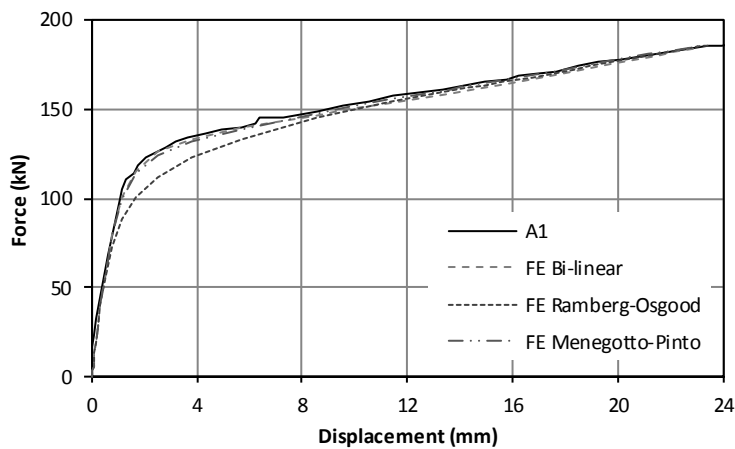


Figure 6.23. A1 model results comparison with different material characterisations.

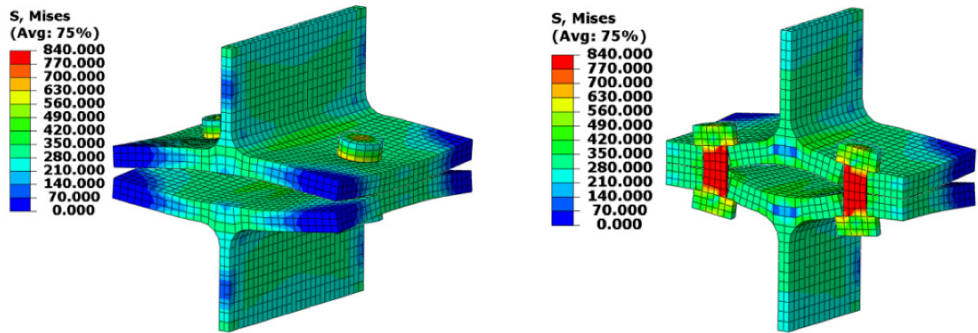


Figure 6.24. B1 test – Von Mises stress results for a 20mm displacement.

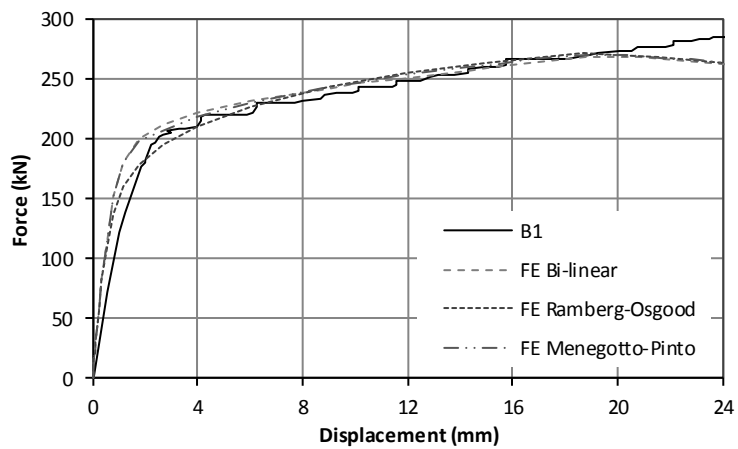


Figure 6.25. B1 model results comparison with different material characterisations.

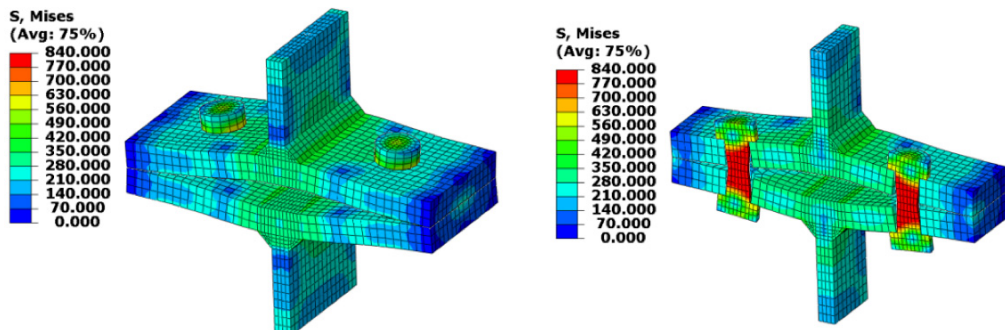


Figure 6.26. D1 test – Von Mises stress results for a 20mm displacement.

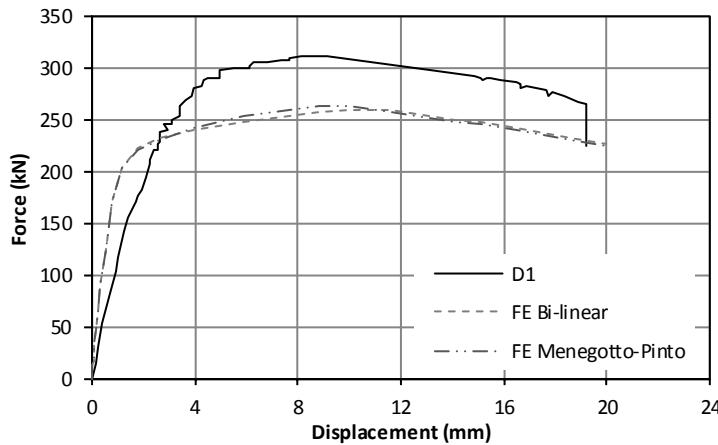


Figure 6.27. D1 model results comparison with different material characterisations.

For the D1 simulation, the numerical model did not fit well with the experimental results. According to EC3, this connection should exhibit failure mode type 2 but the test revealed a type 3 mode of failure, as observed also by the Piluso and Rizzano [2008] who remarked:

"The application of the formulations suggested by Eurocode 3, for predicting the resistance and the collapse mechanism of bolted T-stubs, provides for such specimens a type-2 collapse mechanism, i.e. flange yielding with bolt fracture. However, it is important to underline that, according to experimental evidence, W18 specimen exhibits a type-3 collapse mechanism, i.e. bolt fracture only."

A further objective of the present study is the calibration of the cyclic hysteretic behaviour of the bolted T-Stubs for the two dissipative failure modes type 1 and type 2.

The loading histories applied to both the tests and models consisted of 57 cycles of constant amplitude (10 mm) for the A2 test and 13 cycles of constant amplitude (20 mm) for the B7 test, which were applied to the upper support of the web.

For the cyclic response, the numerical results show good agreement with the experimental results, mainly in the A2 tests. For the B7 tests, the results were acceptable, but with less agreement. The comparison of results observed in Figure 6.28 and Figure 6.29 show good agreement between the numerical and experimental behaviour.

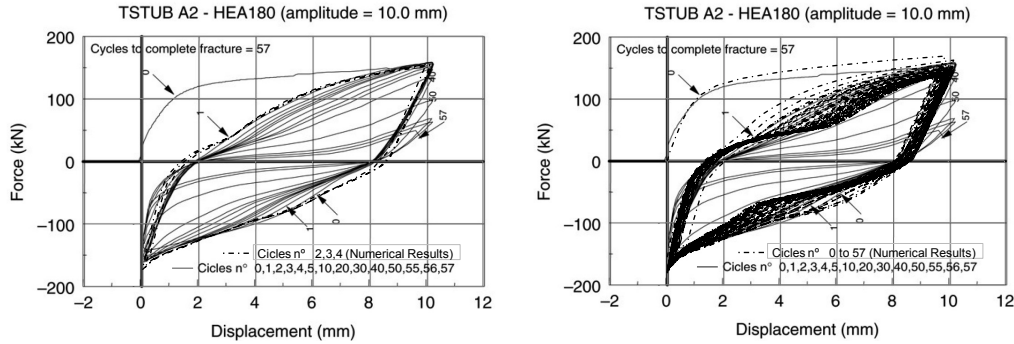


Figure 6.28. A2 model results comparison, on the left only cycles 2 to 5 and on the right the complete results.

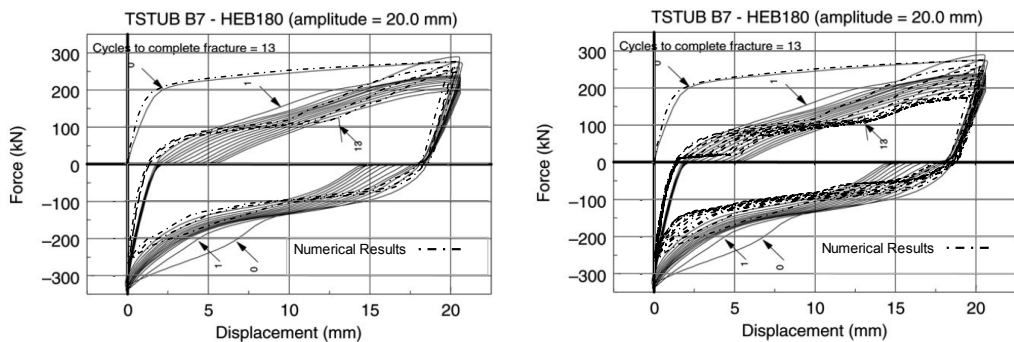


Figure 6.29. B7 model results comparison, on the left the first 3 cycles and on the right the complete results.

6.4.3 Full Connection Models

After the calibration of the end-plate and column flange T-Stubs the numerical behaviour of full end-plate joint can be simulated. Two of the previously collected experimental tests were chosen, the J1 and J3 series specimens, tested by Nogueiro *et al.* [2006a, 2006b] at the Materials and Structures Laboratory of the Civil Engineering Department, Faculty of Science and Technology, University of Coimbra (DEC-FCTUC). This consisted of an external extended end-plate connection between a HEA320 or HEB320 column profile and an IPE360 beam profile. A schematic view of the test setup is shown in Figure 6.30.

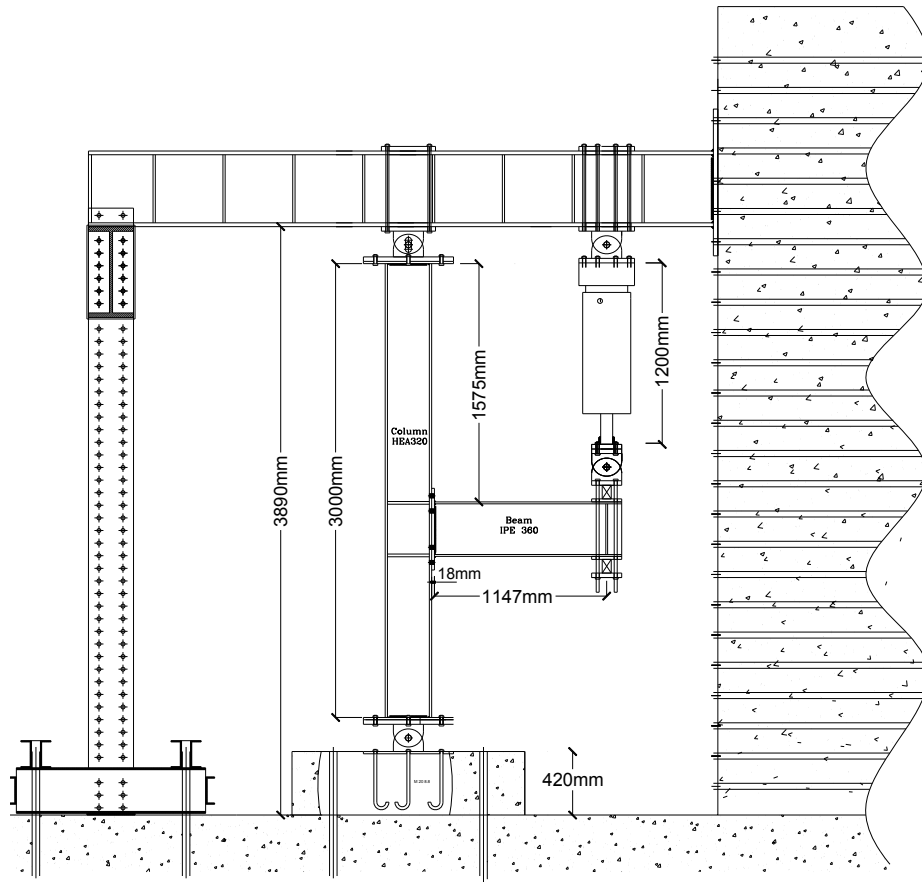


Figure 6.30. Experimental test setup (Adapted from Nogueiro *et al.* [2006b]).

6.4.3.1 Material Modelling

As for the T-stub models, the material properties obtained from the coupon tests were used, which are shown in Table 6.9. As previously highlighted, the use of a simple elastoplastic isotropic hardening model can be adequate for the monotonically loaded models. However, this is not the case for cyclic loaded models due to the reversal load. Therefore, the material definition used was the combined isotropic/kinematic hardening model available in ABAQUS. Using the same methodology adopted for the T-stub, the kinematic hardening parameters were assessed, converting the stresses to the backstress (α) and using the Equation 6.9 to obtain the C_{kin} and γ parameters by matching the computed values to the experimental ones.

Table 6.9. Material properties for the J1 and J3 series.

Components		Modulus of elasticity (GPa)	Yield strength (MPa)	Yield strain (%)	Ultimate strength (MPa)	Ultimate strain (%)	Strain at failure (%)
		E_m	f_{ytm}	ϵ_{ytm}	f_{utm}	ϵ_{utm}	ϵ_{rtm}
IPE360	Flanges	206.0	430.0	0.209	554.2	15.00	25.00
	Web	213.6	448.2	0.210	552.9	16.00	26.00
HEA320	Flanges	204.9	414.8	0.202	531.4	17.00	29.00
	Web	207.4	449.6	0.217	553.4	15.00	24.00
HEB320	Flanges	208.8	393.9	0.189	520.7	17.00	30.00
	Web	210.3	398.8	0.190	521.1	17.00	27.00
End-plate		208.4	392.9	0.189	523.0	14.00	24.00
Stiffeners		205.9	286.4	0.139	451.8	20.00	30.00
Bolts		213.0	990.0	0.465	1170.0	1.10	3.40
Welds		213.0	440.0	0.207	540.0	22.20	26.00

6.4.3.2 Loading Protocol

The loading protocol considered in the analyses was the same applied in the experimental tests, i.e., a loading protocol based on the ECCS recommendations [ECCS, 1986]. For J1.3, a cyclic displacement was imposed at the tip of the beam, beginning with increasing amplitudes of single cycles of $(\theta_y \times 3)/4$; (ii) $2(\theta_y \times 3)/4$; (iii) $3(\theta_y \times 3)/4$, where θ_y denotes the yield rotation of the connection. This was followed by a constant cyclic displacement corresponding to $\theta_y \times 3$ until the connection reached the cycle corresponding to failure observed in the experimental test. In the case of J3.2, the load strategy also began with single cycles applied according to $(\theta_y \times 3)/4$; (ii) $2(\theta_y \times 3)/4$; (iii) $3(\theta_y \times 3)/4$, followed by 20 cycles at constant amplitude of $\theta_y \times 3$ and afterwards another 20 cycles with an increasing amplitude of more 2.5 mrad in each direction, until the connection reached the cycle corresponding to failure observed in the experimental test. It is also important to note that the bolts were preloaded with 20% of the ultimate bolt strength in the FE models, as per the experimental test procedure.

6.4.3.3 Data Collection and Treatment

In the case of the experimental tests, the relevant data is collected by instrumenting the sub-assemblage with displacement transducers, strain gauges and load cells to measure displacements, strains and forces, respectively, which are recorded in such a way that

allows the assessment of the connection main properties, such as the moment-rotation relationship for the joint and its components. The instrumentation of J1.1 can be seen in Figure 6.31.

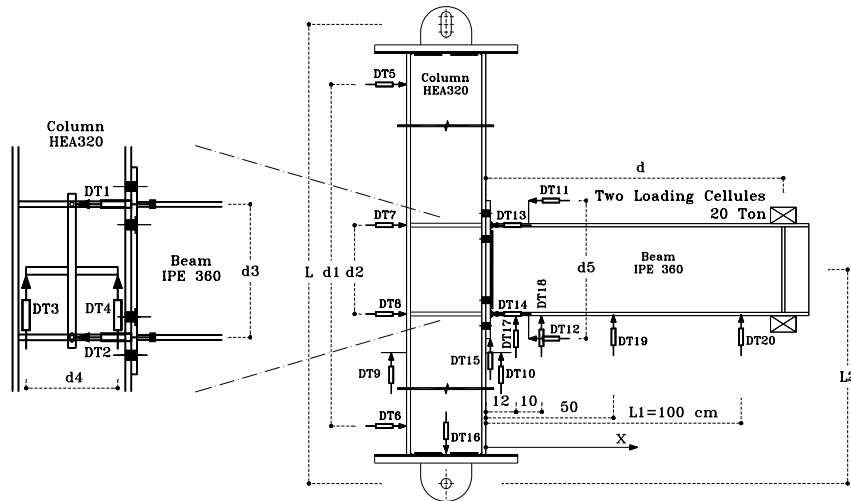


Figure 6.31. Experimental test setup for J1.1 (Adapted from Nogueiro *et al.* [2006b]).

To be able to compare the results from the FE models to those obtained in the experimental tests, namely the moment-rotation relationships, a similar procedure was followed in the models by adopting a similar definition of some predefined mesh nodes where the displacements and forces are collected. The points are indicated in Figure 6.32 and named according to the experimental tests. The data collected is computed using the expressions provided in Table 6.10. To assess the bending moment, Equation 6.10 was used, where d_{DT20} is the distance between the point where the imposed displacement take place ($DT20$) and the column flange, and $R2_{DT20}$ is the reaction force obtained in the same point; the total rotation of the joint is obtained by the Equation 6.11., the sum of the column web contribution with the other components contributions (end-plate, column flanges and bolts), Equation 6.12 is used for the experimental test data and the Equation 6.13 for the numerical models data. The column web contribution is obtained by Equation 6.14 for the experimental tests data and Equation 6.15 for the numerical models data. The end-plate and column flange contribution is given by Equation 6.16 and Equation 6.17 for the experimental test data and for the numerical data, respectively. Equation 6.18 represents the analytical elastic deformation of the column and Equation 6.19 of the beam, used according to the way that the rotations are computed and Equation 6.20 is rotation in block of the tested system.

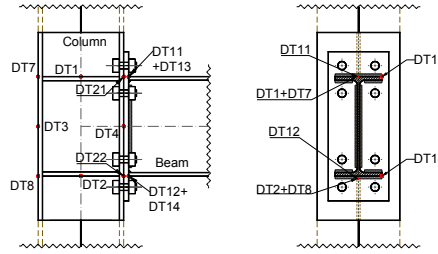


Figure 6.32. Points where the data is collected.

Table 6.10. Equations for the M-θ curves determination.

Experimental	Numerical models
$M_{Ed} = R2_{DT20} \cdot d_{DT20}$	(6.10)
$\theta_{Total} = \theta_{Column_Web} + \theta_{End-Plate} - \theta_{elast_column} - \theta_{elast_beam} - \theta_{block}$	(6.11)
$\theta_{Total} = a \tan\left(\frac{DT3_{U3} - DT4_{U3}}{DT3DT4}\right) + \\ + a \tan\left(\frac{DT1_{U3} - DT2_{U3}}{DT1DT2}\right) - \\ - \theta_{elast_column} - \theta_{block}$	$\theta_{Total} = a \tan\left(\frac{DT11_{U3} - DT12_{U3}}{DT11DT12}\right) - \\ - \theta_{elast_column}$
$\theta_{Column_web} = a \tan\left(\frac{DT3_{U3} - DT4_{U3}}{DT3DT4}\right) - \\ - \theta_{elast_column} - \theta_{block}$	$\theta_{Column_web} = a \tan\left(\frac{DT1_{U3} - DT2_{U3}}{DT1DT2}\right) - \\ - \theta_{elast_column}$
$\theta_{EP+flange} = a \tan\left(\frac{DT1_{U3} - DT2_{U3}}{DT1DT2}\right) - \\ - \theta_{elast_beam}$	$\theta_{EP+flange} = a \tan\left(\frac{DT13_{U3} - DT14_{U3}}{DT13DT14}\right) - \\ - \theta_{Column_web}$
$\theta_{elast_column} = \frac{\frac{R2_{DT20} \cdot d_{DT20} \cdot L^2}{L} + \frac{2 \cdot R2_{DT20} \cdot d_{DT20} \cdot L}{6} - R2_{DT20} \cdot d_{DT20} \cdot L^2}{E \cdot I_{y(Column)}}$	(6.18)
$\theta_{elast_beam} = \frac{R2_{DT20} \cdot d_{DT20} \cdot x - R2_{DT20} \cdot \frac{x^2}{2}}{E \cdot I_{y(Beam)}}$	(6.19)

$$\theta_{block} = a \tan\left(\frac{DT5 - DT6}{d1}\right) \quad (6.20)$$

6.4.3.4 Results of the J1 Series Specimens

The J1 series joints consisted of an external double extended end-plate connection between a HEA320 column profile and an IPE360 beam profile. A schematic view of the connection is shown in Figure 6.33.

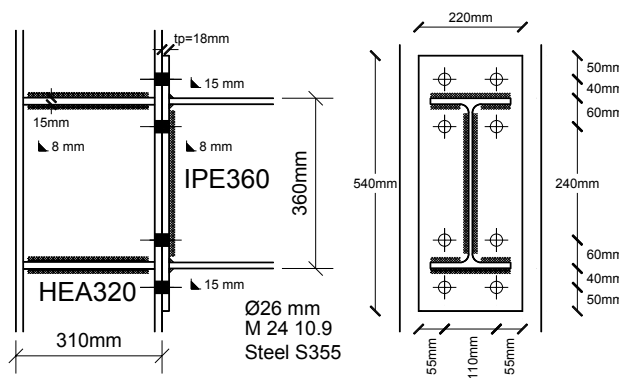


Figure 6.33. J1 Nogueiro's test series – scheme of the connections (Adapted from Nogueiro *et al.* [2006b]).

The moment-rotation relationship is depicted in Figure 6.34 along with a comparison between the experimental results and the ones obtained from the monotonically and cyclically loaded analyses performed in ABAQUS. The Von Mises stresses are plotted in Figure 6.35 for a level of rotation closer to the maximum obtained in the experimental test. Examining this figure it is obvious that the column web panel reached a plastic stress state. Also for the end-plate in the tension zone, the yielding of the plate and bolts is observed.

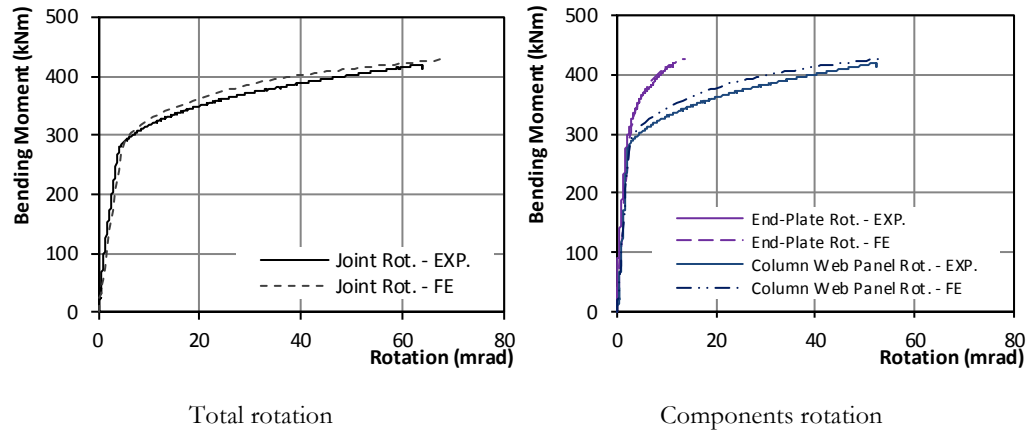


Figure 6.34. J1.1 Joint moment-rotation comparisons.

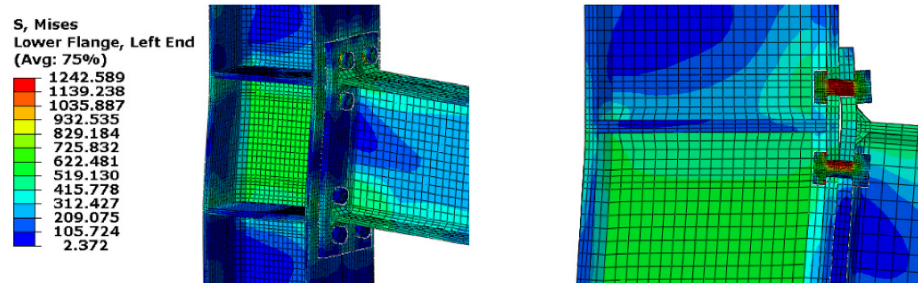


Figure 6.35. J1.1 Von Mises stress field.

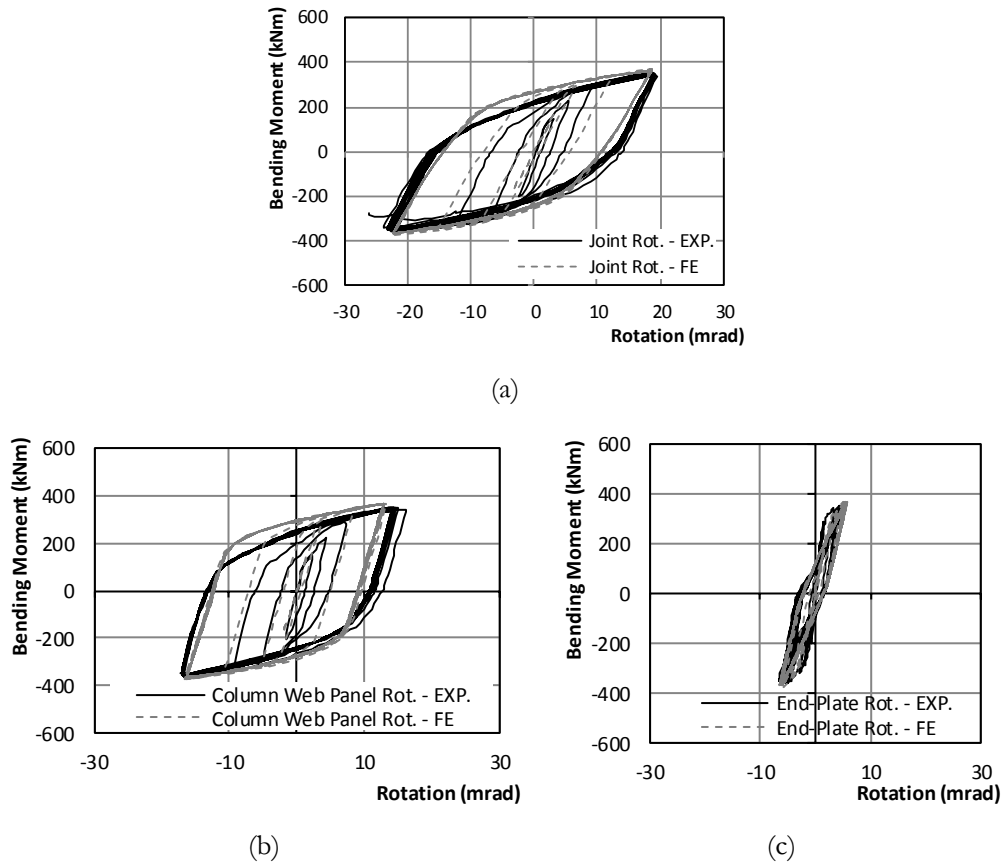


Figure 6.36. J1.3 Connection moment-rotation comparisons, (a) total rotation of the sub-assemblage, (b) rotation of the component column web, (c) rotation of the component end-plate.

The energy dissipated during the experimental tests and the FE models was determined by the area delimited by the moment-rotation relationship. In the case of the cyclic models the dissipated energy was obtained adding the area of each cycle. The comparison can be seen in Figure 6.37 and Figure 6.38.

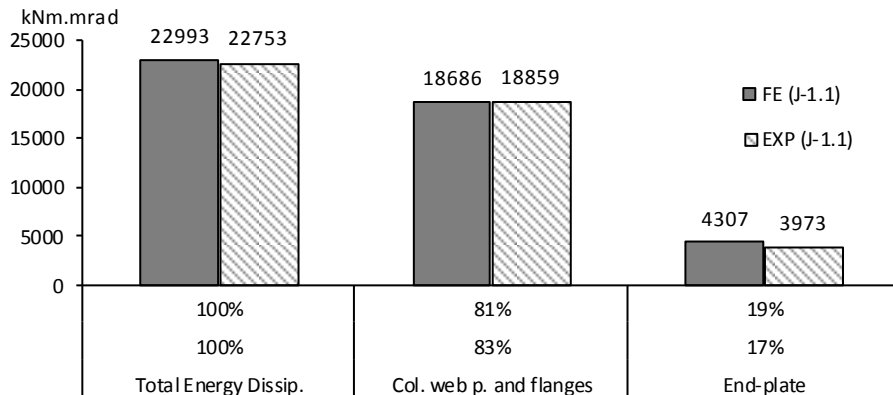


Figure 6.37. Energy dissipation comparison for the monotonic loaded model.

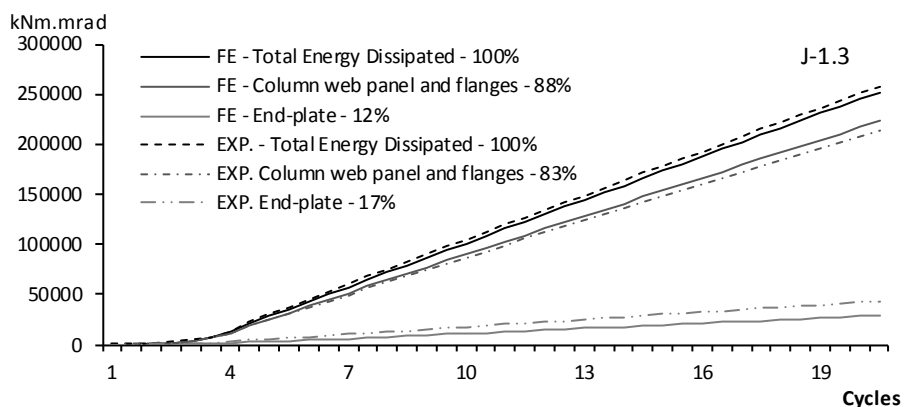


Figure 6.38. Cumulative energy dissipation comparison for the cyclic loaded model.

The results obtained from FE analysis show good agreement with the experimental ones and it is therefore concluded that the numerical models for the J1 series are representative of the real behaviour.

6.4.3.5 Results of the J3 Series Specimens

Similar to the J1 connection series, the J3 series consisted of an external extended end-plate connection but used a HEB320 section for the column and also an IPE360 section for the beam. The schematic view of the test setup is the same as for the J1 series, and the connection geometry is shown in Figure 6.39.

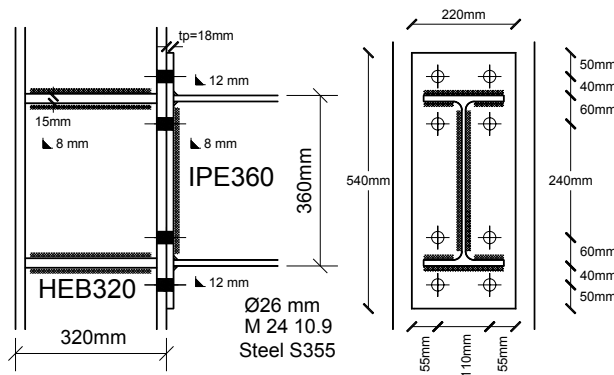


Figure 6.39. J3 Nogueiro's test series – scheme of the connections (Adapted from Nogueiro *et al.* [2006b]).

Figure 6.40 and Figure 6.42 depict the moment-rotation relationship allowing the comparison between experimental results and those obtained from the monotonically and cyclically loaded analyses performed in ABAQUS. The Von Mises stresses are depicted in Figure 6.41 for a rotation close to the one obtained by the experimental test before the test was stopped. It is possible to see that the column web panel reached a plastic stress state although, as expected, with less incidence comparing to the J1.1 connection, as well as for the end-plate tension zone with the yielding of the plate and bolts. In Figure 6.43 and Figure 6.44, the energy dissipated between the experimental and numerical results is compared.

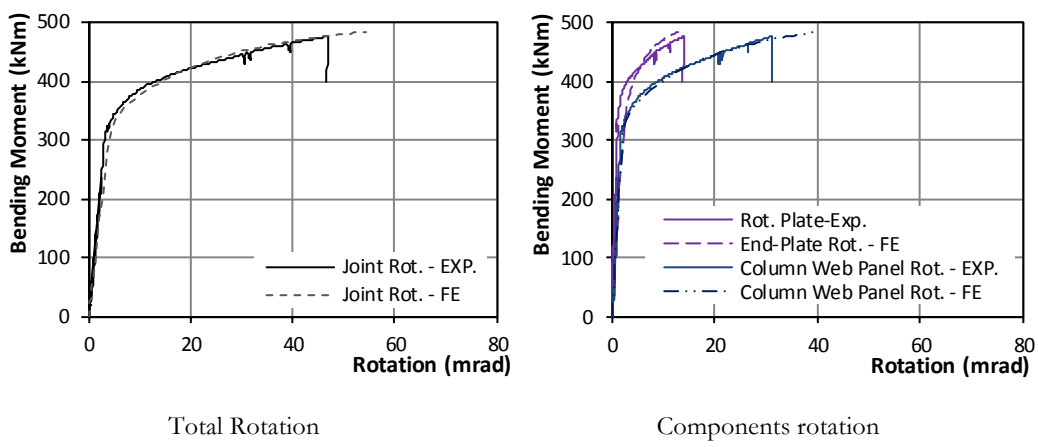


Figure 6.40. J3.1 Joint moment-rotation comparisons.

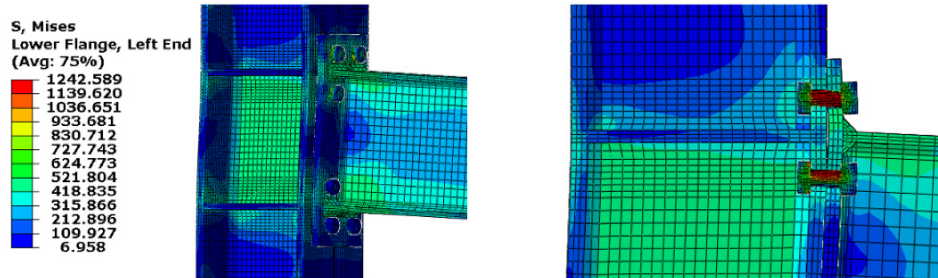
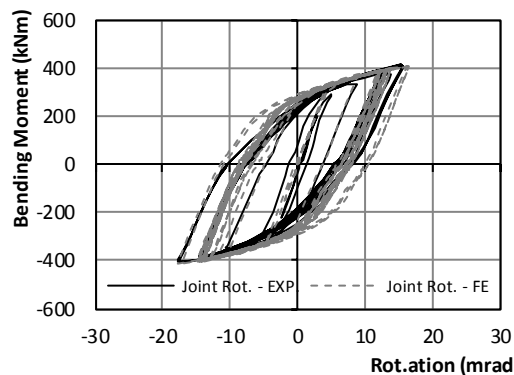
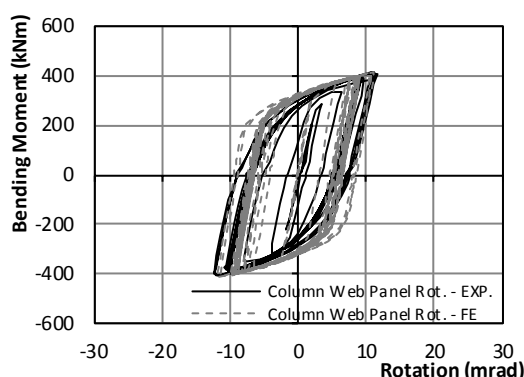


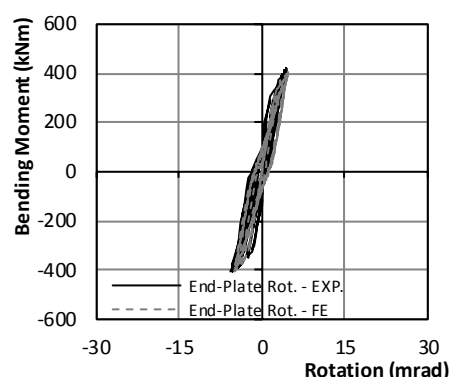
Figure 6.41. J3.1 Von Mises stress field.



(a)



(b)



(c)

Figure 6.42. J3.2 Connection moment-rotation comparisons, (a) total rotation of the sub-assemblage, (b) rotation of the component column web, (c) rotation of the component end-plate.

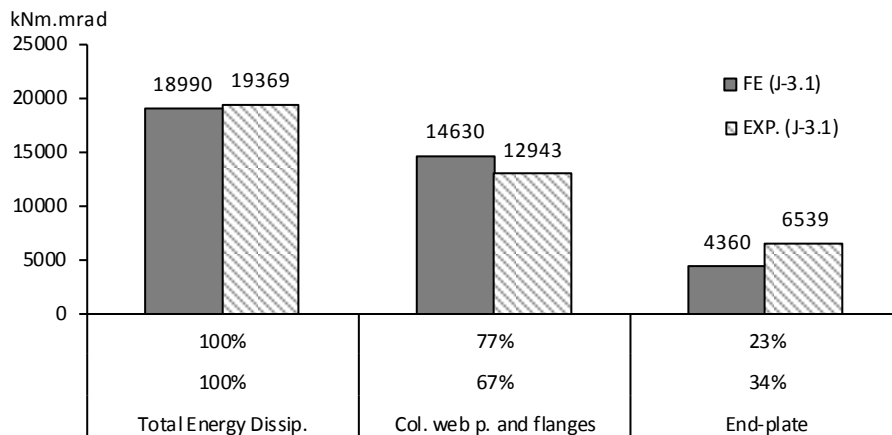


Figure 6.43. Energy dissipation comparison for the monotonic loaded model.

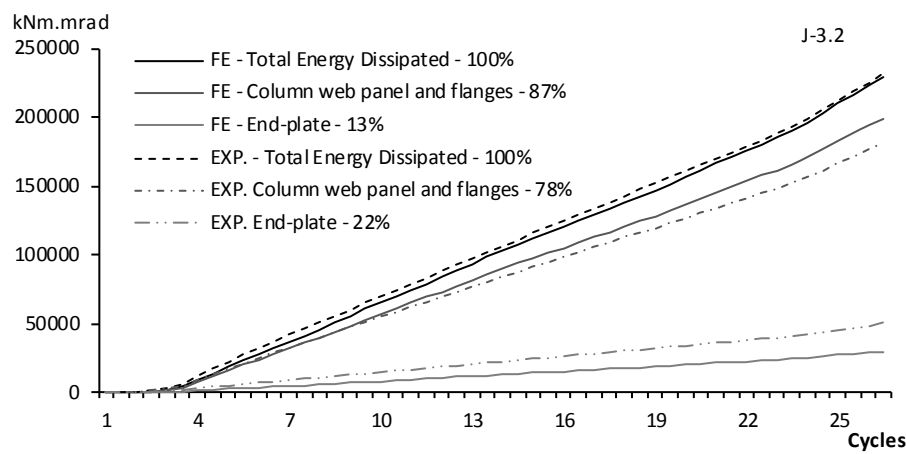


Figure 6.44. Cumulated energy dissipation comparison for the cyclic loaded model.

From the figures above it is possible to conclude that the results of the numerical models are in very good agreement with the experimental data, both for the J1 connections series that presented a connection governed mainly by the column web panel in shear and also for the J3 series, which is a more balanced connection between the column web panel in shear and the end-plate in bending.

From the results presented here, it is possible to state that the developed numerical models are reliable to predict the beam-to-column end-plate bolted joints behaviour.

6.4.3.6 Further Validation of the FE Models

In addition to the static and cyclic analyses, the FE models are to be employed also in extensive NLTH analyses for the derivation of ductility-equivalent viscous damping relationships, which are needed for the DDBD procedure. For the validation of the dynamic analyses, the results of the ABAQUS model were compared with those obtained with a “simpler” model developed in the SeismoSoft [2011] structural analysis program, which was based on the J1.3 experimental test setup, see Figure 6.45(a). To model the cyclic behaviour of the joint a special spring link between the beam and column was used with a modified Richard-Abbott hysteretic behaviour [Della Corte et al., 2000], which can simulate the cyclic path of a curve through the calibration of a set of parameters. Using the previously calibrated parameters for the J1.3 connection [Nogueiro et al., 2005] shown in Table 6.11, the NLTH analyses were run by applying the seismic time-history acceleration shown in Figure 6.46 to the model and also using an additional point mass of 440 tonnes at the end of the beam, as illustrated in Figure 6.45(b).

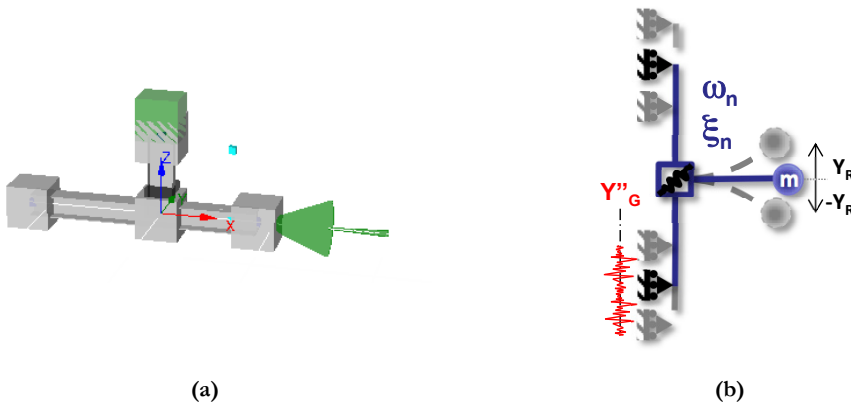


Figure 6.45. (a) SeismoStruct model for the J1.3; (b) analysis representation.

Table 6.11. Modified Richard-Abbott model parameters for the J1-3 connection.

K_a	M_a	K_{pa}	n_a	K_{ap}	M_{ap}	K_{pap}	n_{ap}	t_{1a}	t_{2a}	C_a	i_{Ka}	i_{Ma}	H_a	E_{maxa}
55600	285	5500	1.0	55600	285	5500	1.0	1.0	1.0	1E-5	0.5	1E-5	1E-5	0.1
K_d	M_d	K_{pd}	n_d	K_{dp}	M_{dp}	K_{pdp}	n_{dp}	t_{1d}	t_{2d}	C_d	i_{Kd}	i_{Md}	H_d	E_{maxd}
55600	285	5500	1.0	55600	285	5500	1.0	1.0	1.0	1E-5	0.5	1E-5	1E-5	0.1

With reference to the values specified in Table 6.11, stiffness related parameters are given in kNm/rad, bending moment related parameters in kNm and the rotations are in radians.

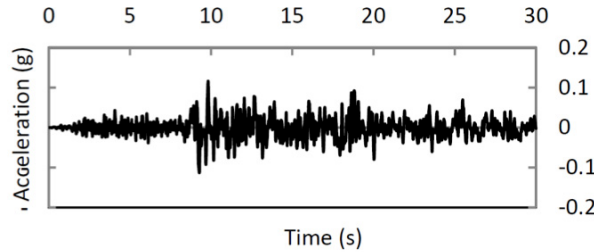


Figure 6.46. Record used in the validation of the NLTH analyses.

To run the NLTH analysis using the FE model developed in ABAQUS, the column boundary conditions were changed to allow the movement along the column axis. As shown in Figure 6.45(b), a point mass of 440 ton was added to the beam end, generating an inertia force and consequently bending moments and rotations at the connection. The system was subjected to the record shown in Figure 6.46. The analysis was performed using an implicit time integration algorithm. The results are plotted in Figure 6.47, along with the results obtained with the SeismoStruct model. The results obtained with the simplified model are in good agreement with those obtained with the more complex and realistic 3D model, thus confirming the adequacy of the proposed model to perform dynamic analyses.

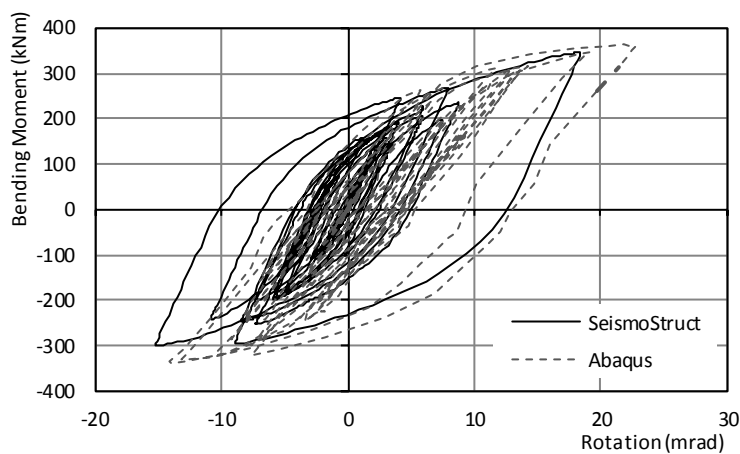


Figure 6.47. NLTH analysis of the sub-assemblage.

6.4.3.7 Final Remarks

A series of FE models were developed and validated based on a set of experimental test results. Several modelling techniques, namely in the field of the material modelling, were considered and the ones that best fit the modelling needs were adopted. The numerical and experimental results were compared and a good correlation was found, both for the monotonic and cyclic loading cases. It was concluded that in the case of the cyclic analyses, the material properties should take into account the combined effect of the isotropic and kinematic hardening effect, in order to capture the Bauschinger effect during loading reversal. In the case of the monotonic tests, the use of the isotropic hardening effect is sufficient to model the behaviour of the joints, since no reversal of loads or stresses occur. Nevertheless, the combined hardening model available in ABAQUS is an excellent choice to use in the monotonic analyses.

The FE model was modified to enable performing nonlinear time-history analyses, where the results were compared with simpler SeismoStruct models revealing a good agreement.

The results obtained in the calibration and subsequent validation of the FE models revealed that they are a powerful and viable option to investigate the behaviour of partial-strength extended end-plate joints. Therefore, they can be employed in the conduction of parametric studies aiming to obtain the relevant properties needed for subsequent studies, namely the derivation of ductility-viscous damping relationships to be adopted in DDBD.

6.5 PARAMETRIC STUDY OF PARTIAL-STRENGTH JOINTS USING FE ANALYSIS

In this section a series of representative partial-strength connections covering the different features of their behaviour are numerically simulated. The criteria adopted allow the connections to exhibit the following features:

- Similar properties to those already studied and analysed.
- Partial-strength behaviour.
- One of the following:
 - Post-elastic behaviour governed by column panel zone in yielding;
 - Post-elastic behaviour governed by yielding of the end-plate in bending – plastic mechanism according to failure mode 1;
 - Post-elastic behaviour governed by yielding of the end-plate in bending – plastic mechanism according to failure mode 2.

Five different connections were chosen to fulfil the previous criteria. Table 6.12 summarises the details of each connection.

Table 6.12. Connections description.

Connection	% of beam moment resistance	Description
C1	~90%	J3.2 [Nogueiro <i>et al.</i> , 2006a, 2006b]
C2	~120%	Modified to fulfil the EC3 requirements, strengthening the web and the end-plate
C3	~75%	Based on the C2, reduction of the column strength (HEB320 to HEA320)
C4	~75%	Based on the C2, reduction of the end-plate, failure mode 1 according to the EC3
C5	~75%	Based on the C2, reduction of the end-plate, reduction of the bolts diameter and strength class, failure mode 2 according to the EC3

One of the previously calibrated connections should be used as reference, which is the C1 connection that shows the same properties as the J3.2 specimen tested by Nogueiro *et al.* [2006a, 2006b]. The C2 connection is a full-strength full-rigid connection, due to the presence of web stiffeners and end-plate thickness, being a control connection for the partial-strength ones. The geometry of the C2 connection will be changed, in the next connections, to achieve the required strength level and failure modes desired. The other three connections are designed to achieve the same level of strength, but with different governing failure modes, in order to understand their influence. C3 is a partial-strength connection governed by yielding of the column web panel zone. To ensure the web column panel yielding, the column was changed to an HEA 320 and the column stiffeners were removed. On the other hand, C4 and C5 connections have the same level of strength as C3, but in this case, the governing plastic mechanism is the end-plate in bending. A smaller end-plate thickness ensures the plastic mechanism type one according to the EC3 for the C4 connection. In addition, a balanced reduction of the end-plate thickness, bolt diameter and bolt class ensures a plastic mechanism type two for the C5 connection. The sub-assemblage with the joint's geometrical properties, for the FE model sub-assemblage are listed in Table 6.13 and the geometry of the joints are provided in Table 6.14 and the geometrical parameters are represented in Figure 6.48.

The connections were calculated analytically, according to the rules prescribed in EC3-1-8 [CEN, 2005b] and also numerically using ABAQUS models. The results obtained from the two approaches were compared and are presented in the following sections.

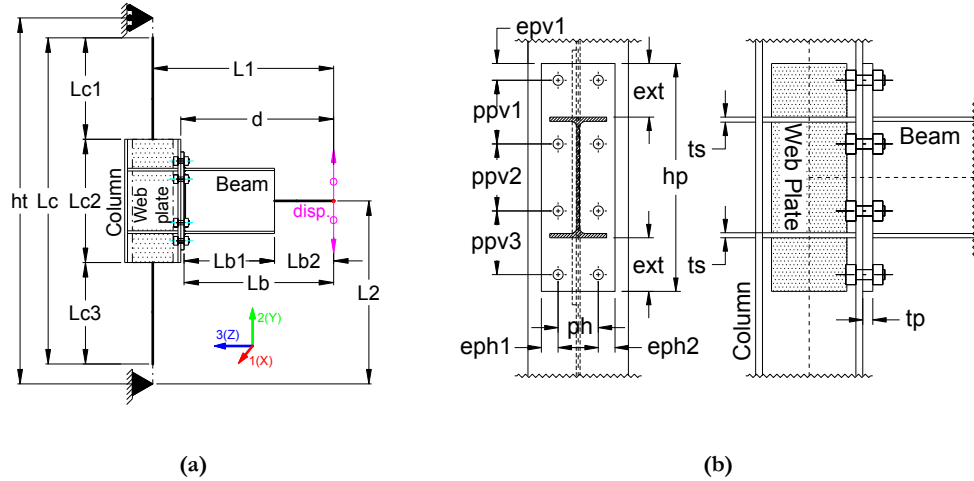


Figure 6.48. (a) Sub-assemblage geometric properties for the FE models (b) Joint geometry.

Table 6.13. FE model geometric properties.

	Column	Beam	ht	Lc	Lc1	Lc2	L1	L2	Lb	Lb1	d
C1	HEB320	IPE360	3229	3009	1207	840	1338	1492	1160	468	1178
C2	HEB320	IPE360	3500	3250	1290	920	1320	1625	1100	468	1160
C3	HEA320	IPE360	3500	3250	1260	980	1315	1625	1100	468	1160
C4	HEB320	IPE360	3500	3250	1290	920	1278	1625	1100	468	1118
C5	HEB320	IPE360	3500	3250	1290	920	1287	1625	1100	468	1127

Note: Dimensions in mm.

Table 6.14. Joint geometrical properties.

	Column	Beam	hp	bp	tp	epv1	ppv1	ppv2	ppv3	eph1	ph	eph2	d_{bolt}	b_{class}	ext	ts	$t(\text{wp})$
C1	HEB320	IPE360	540	220	18	50	100	240	100	55	110	55	24	10.9	90	15	no
C2	HEB320	IPE360	680	220	60	50	190	200	190	50	120	50	30	10.9	160	15	12
C3	HEA320	IPE360	680	220	60	50	190	200	190	50	120	50	30	10.9	160	no	no
C4	HEB320	IPE360	680	215	18	50	190	200	190	50	115	50	30	10.9	160	15	12
C5	HEB320	IPE360	680	220	27	50	190	200	190	50	120	50	24	8.8	160	15	12

6.5.1 Analytical Calculations

The analytical calculations were performed with the partial safety factors $\gamma_M = 1.00$ in order to be possible to compare with the numerical calculations. For the stiffness classification, a beam length of 7.5m was considered. In the case of the C2 and C3 joints, due to the end-plate thickness larger than 40mm, the steel properties should be reduced in accordance with EC3-1-1 [CEN, 2005a], but for the sake of the joints results comparison, the steel properties were kept equal for all the specimens. Table 6.15 summarises the main results obtained when the EC3-1-8 procedure is followed.

Table 6.15. Analytical calculation main results.

	C1		C2		C3		C4		C5	
Moment resistance: $M_{j,Rd}$ (kNm)	337.00		437.98		263.85		255.58		281.59	
Initial stiffness: $S_{j,ini}$ (kNm/rad)	74464		105733		55499		52525		71516	
Stiffness class:	Semi-rigid (65.38%)		Semi-rigid (92.84%)		Semi-rigid (48.73%)		Semi-rigid (46.12%)		Semi-rigid (62.79%)	
Class of strength:	Partial strength (93.16%)		Full strength (121.07%)		Partial strength (72.94%)		Partial strength (70.65%)		Partial strength (77.84%)	
Dominant compression component:	BFW: $F_{c,fb,Rd}$ (kN)	1041.59	BFW: $F_{c,fb,Rd}$ (kN)	1041.59	CWT: $F_{c,wc,Rd}$ (kN)	592.10	BFW: $F_{c,fb,Rd}$ (kN)	1041.59	BFW: $F_{c,fb,Rd}$ (kN)	1041.59
Dominant tension components:	Bolts row 1		Bolts row 1		Bolts row 1		Bolts row 1		Bolts row 1	
	EP: $F_{t1,Rd}$ (kN)	459.41	CF: $F_{t1,Rd}$ (kN)	805.00	CF: $F_{t1,Rd}$ (kN)	535.89	EP: $F_{t1,Rd}$ (kN)	123.87	EP: $F_{t1,Rd}$ (kN)	264.65
	Mode 2		Mode 2		Mode 1		Mode 1		Mode 2	
	Bolts row 2		Bolts row 2		Bolts row 2		Bolts row 2		Bolts row 2	
	EP: $F_{t2,Rd}$ (kN)	520.50	CF: $F_{t2,Rd}$ (kN)	236.59	CF: $F_{t2,Rd}$ (kN)	56.22	EP: $F_{t2,Rd}$ (kN)	652.76	EP: $F_{t2,Rd}$ (kN)	508.32
	Mode 2		Mode 2		Mode 1		Mode 1		Mode 3	
	Bolts row 3		Bolts row 3		Bolts row 3		Bolts row 3		Bolts row 3	
	EP: $F_{t3,Rd}$ (kN)	61.69	CF: $F_{t3,Rd}$ (kN)	0	CF: $F_{t3,Rd}$ (kN)	0	EP: $F_{t3,Rd}$ (kN)	264.96	EP: $F_{t3,Rd}$ (kN)	268.62
	Mode 2		Mode 2		Mode 1		Mode 1		Mode 3	

In the compression and tension dominant components, BFW stands for beam or column flange and web in compression, CWT stands for column web in transverse compression, EP stands for end-plate in bending and CF stands for column flange in bending. Connection C1 is governed by the end-plate in bending, which is failure mode type 2. Bolt failure with yielding of the flange, only in the third row the resistance has to be reduced to avoid overcome the beam flange or web in compression resistance and in the end, it is the beam that governs the joint behaviour. In the case of the C2 connection, it is also the beam that governs the connection strength, as the first bolts-row the column flange in bending is the weakest component, with a type 2 failure mode although the second bolts-row resistance has to be reduced to avoid overcoming the beam flange or web in compression resistance, line three is inactive. For the C3 connection, the first bolts-row is governed by the column flange in bending in failure mode type 1, complete yielding of the flange, but for the second bolts-row the column web in transverse compression resistance limits the resistance and the third bolts-row is inactive. In the case of the C4 connection, the end-plate in bending governs the first two bolts-rows, in a failure mode type 1, and for the third bolts-row the beam flange or web in compression resistance limits the resistance. Connection C5 is able to develop the resistance of the two first bolts-rows allowed by the end-plate, in a failure mode type 2 for the first bolts-row and type 3 for the second row, equivalent to bolt failure, the third bolts-row resistance is limited by the beam flange or web in compression.

6.5.2 Numerical Calculations

The steel grade used in the analyses was S355 and for the material properties definition, the minimum values imposed by the section 3 of the EC3-1-1 [CEN, 2005a] were adopted:

- Ratio between the ultimate and yielding strength $f_u/f_y = 1.10$
- Ration between the ultimate and yield strain $\epsilon_u/\epsilon_y = 15$
- Elongation at failure $\epsilon_{r(\min)} = 0.15$

For the ratio between the ultimate strength and failure strength, $f_u/f_r = 1.031$ was adopted, which is a value omitted in the EC3 and is taken as the median value from the experimental coupon tests performed by Nogueiro [2009].

6.5.3 Numerical Results

For the monotonically loaded models, the moment-rotation relationship is plotted in the following figures. A comparison with the analytical results depicting in the charts the

moment-rotation envelope obtained by the clause 6.3.1(6) of the EC3-1-8 is also performed. In Figure 6.50 the response of the isolated components, for the several connections, is depicted allowing the comparison of the main dissipative components in the joints.

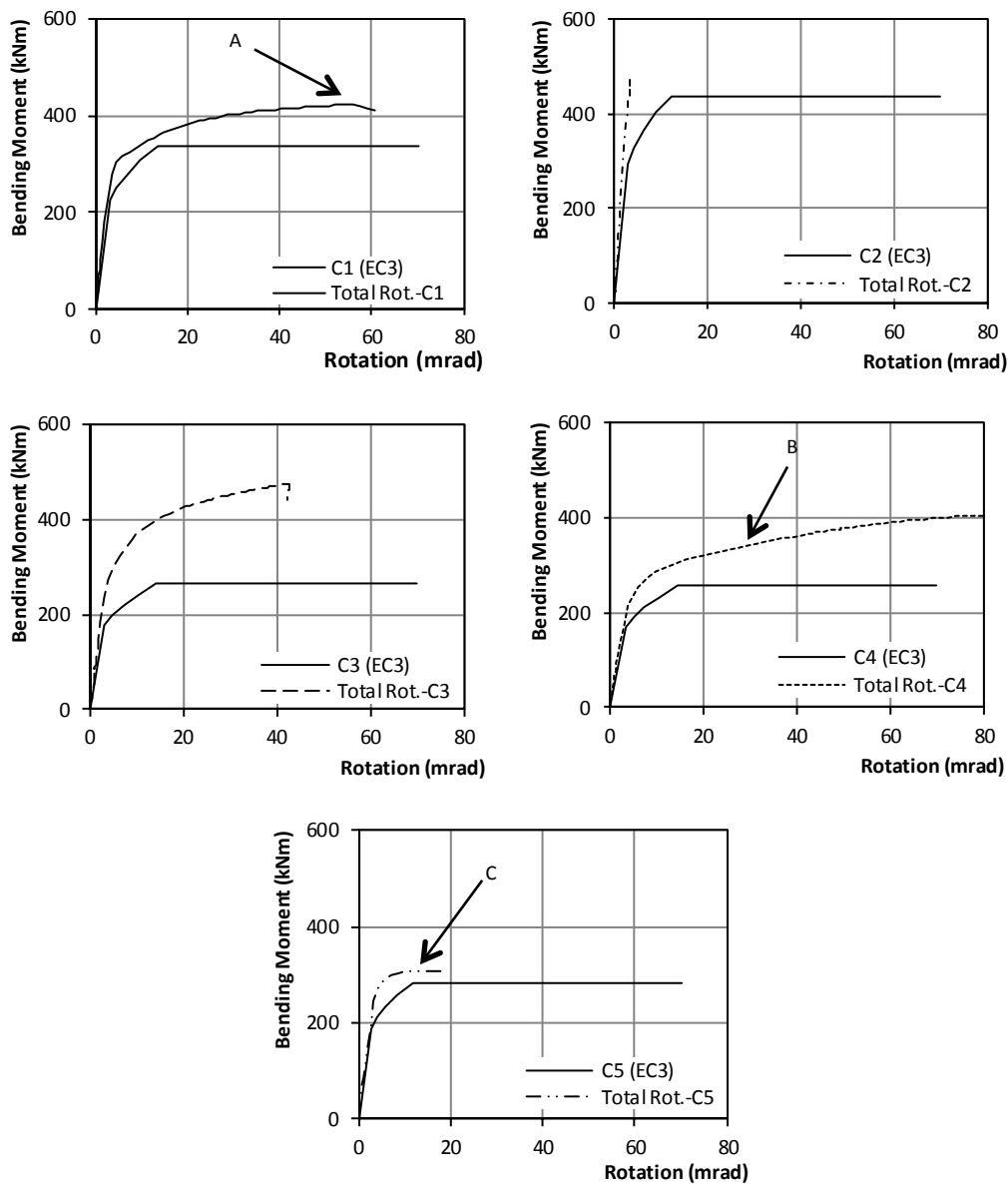


Figure 6.49. Monotonic results for the C1 to C5 joints.

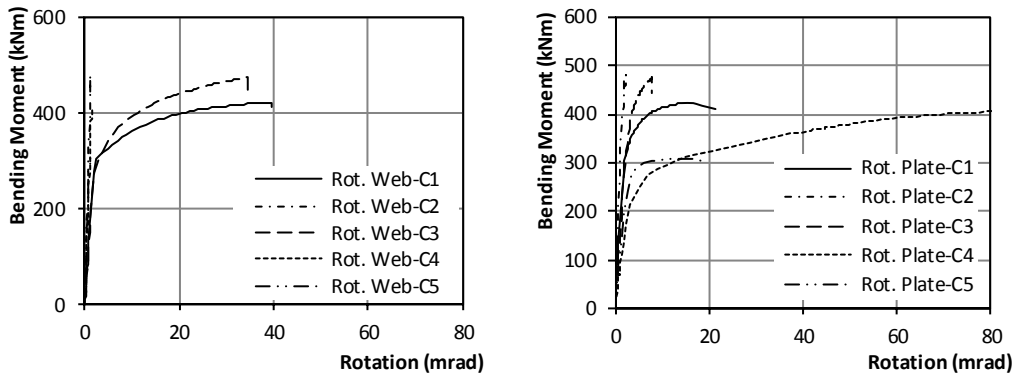


Figure 6.50. Monotonic results for the C1 to C5 components.

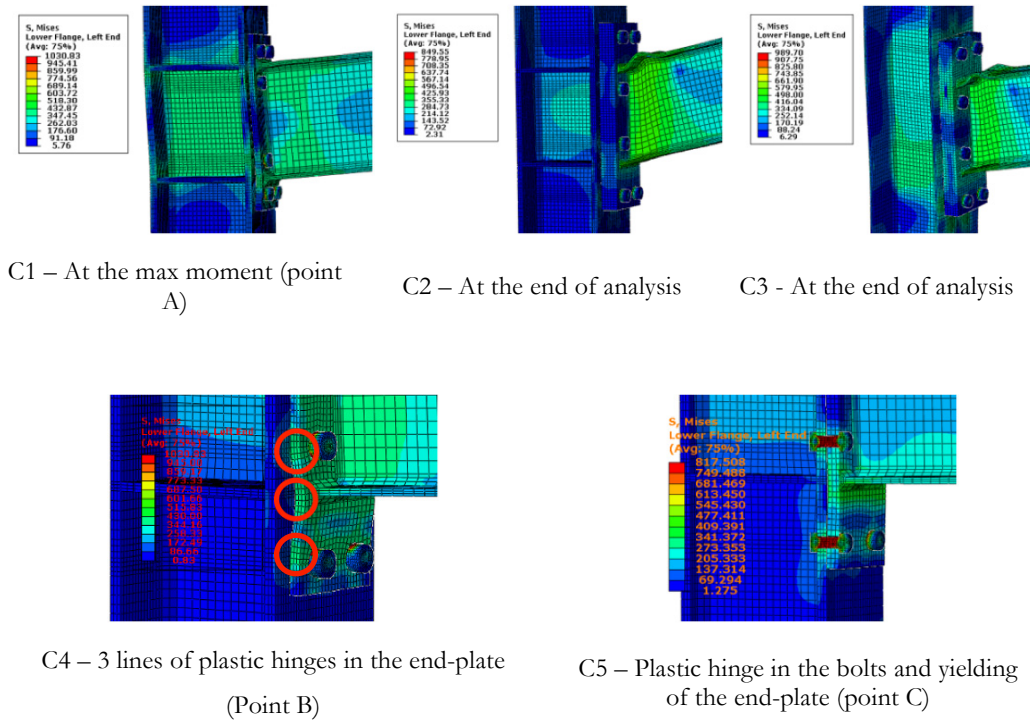


Figure 6.51. Von Mises stress representation for the identified situations.

From these figures, it is possible to state that connection C1 exhibited a plastic mechanism similar to the failure mode type 2, showing a plastic hinge line near the lower

beam flange and plastic hinges in the bolts in tension that may lead to rupture. As expected, connection C2 responded in the elastic range with a plastic hinge forming in the beam. Connection C3 was clearly governed by the column web panel in shear. Connection C4 exhibited a plastic mechanism of type 1, with the formation of three plastic hinges in the end-plate before the bolts yield in tension. Connection C5 exhibited a plastic mechanism of type 2, similar to that developed in connection C1, but with a clearly lower rotation capacity due to the stiffened column web.

To perform an analytical comparison of the results, the ECCS procedure was applied to the numerical results to assess the joints strength and stiffness, as illustrated in Figure 6.54 for the C1 connection. The comparison between the analytical and numerical responses reveals, on one hand, a balanced agreement in terms of strength and in the case of the initial stiffness and, on the other hand, an apparent difficulty of the EC3-1-8 to reach the higher values obtained in the numerical approach. The comparisons are presented in Table 6.16, Table 6.17 and in Figure 6.52. The most significant differences occurred in joints C2 and C3 in terms of stiffness, with differences of around 40% and for the other joints, the differences were lower than 15%. In terms of strength, the C3 joint presented the most obvious difference where an increase of around 23% was observed with the numerical model, which could be justified by the higher non linearity of the C3 joint as it is essentially governed by the column web in shear, which makes the determination of the yield point difficult to assess. The C1 joint also showed considerable difference of over 12%, but in this case, a lower strength value in the numerical response was recorded. The strength results obtained for the joints C4 and C5 revealed good agreement between the numerical and the analytical results.

Table 6.16. Analytical results summary.

Analytical calculations								
Joints results			Classification				Failure mode	
M _{J,Rd} (kN.m)	S _{j,ini} (kN.m)	S _{j,ini} Rigid limit	Strength		Stiffness		Weakest Comp.	Failure mode (EC3)
337.00	74464.08	113890	Partial-strength	93.16%	Semi-rigid	65.38%	End-plate	2
437.98	105733.01	113890	Full-strength	121.07%	Semi-rigid	92.84%	Column flange	2
263.85	55499.06	113890	Partial-strength	72.94%	Semi-rigid	48.73%	End-plate	1
255.58	52525.01	113890	Partial-strength	70.65%	Semi-rigid	46.12%	End-plate	1
281.59	71515.69	113890	Partial-strength	77.84%	Semi-rigid	62.79%	End-plate	2

Table 6.17. Numerical results summary.

Numerical calculations									
Joints results			Classification				Failure mode		
M _{J,Rd} (kN.m)	S _{j,ini} (kN.m)	S _{j,ini} Rigid limit	Strength		Stiffness		Weakest Comp.	Failure mode (EC3)	
293.76	83384	113890.00	Partial-strength	81.21%	Semi-rigid	73.21%	End-plate	2	
479.64	143340	113890.00	Full-strength	132.59%	Rigid	125.86%	Beam	-	
324.80	78480	113890.00	Partial-strength	89.79%	Semi-rigid	68.91%	Web-panel	-	
252.53	59925	113890.00	Partial-strength	69.81%	Semi-rigid	52.62%	End-plate	1	
272.71	78814	113890.00	Partial-strength	75.39%	Semi-rigid	69.20%	End-plate	2	

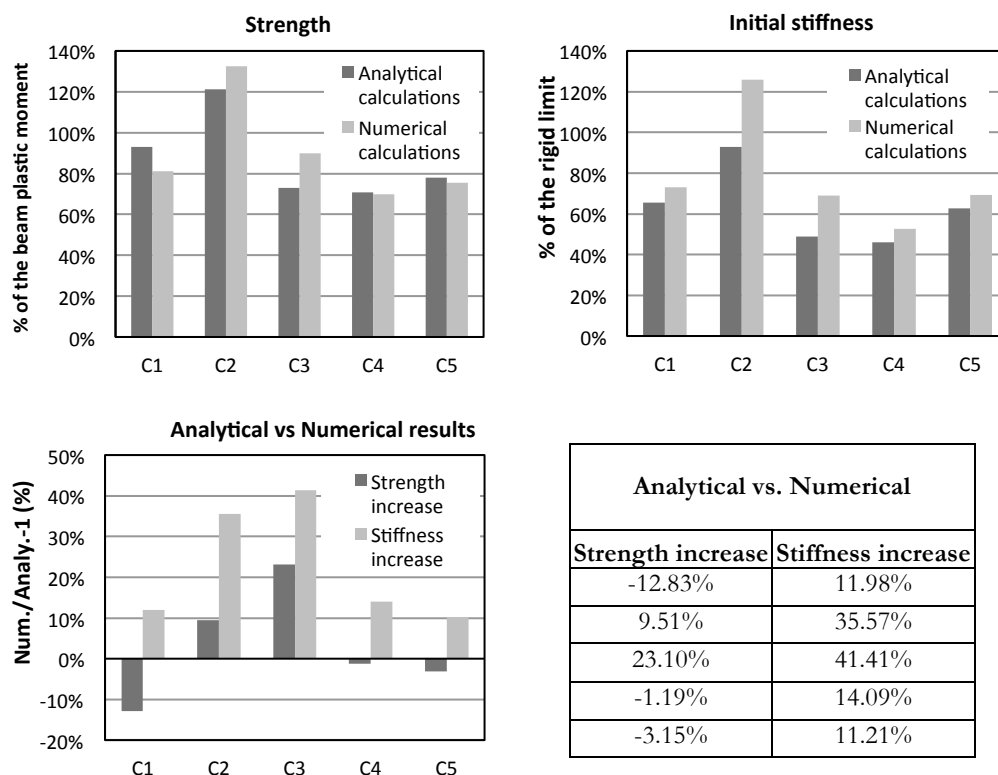


Figure 6.52. Comparison of strength and stiffness results.

The cyclic loading cases were analysed using the same joint geometry and material properties and using the loading protocol depicted in Figure 6.53. The yield rotation (θ_y) was derived from the monotonic results employing the ECCS procedure [ECCS, 1986], which is illustrated for the C1 joint in Figure 6.54. The yield rotation and the beam tip relative displacement (Δ_y) can be also observed in the same figure, disregarding and considering the elastic deformation of the column and beam, respectively.

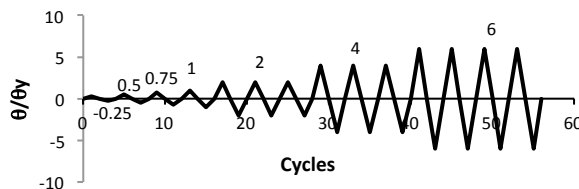


Figure 6.53. ECCS load protocol.

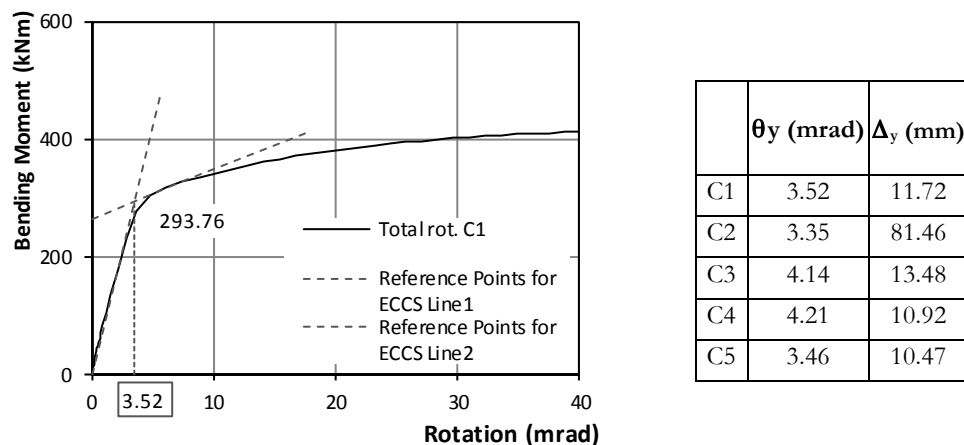


Figure 6.54. Assessment of the θ_y according to the ECCS procedure for the C1 joint.

The results can be seen in Figure 6.55, for the global joint rotation and for the main dissipative components column web in shear and the end-plate in bending. The results from the cyclic analyses confirm that the model is capable of representing different types of behaviour governed by the main dissipative components in the connections, namely the end-plate in bending and the column web panel in shear.

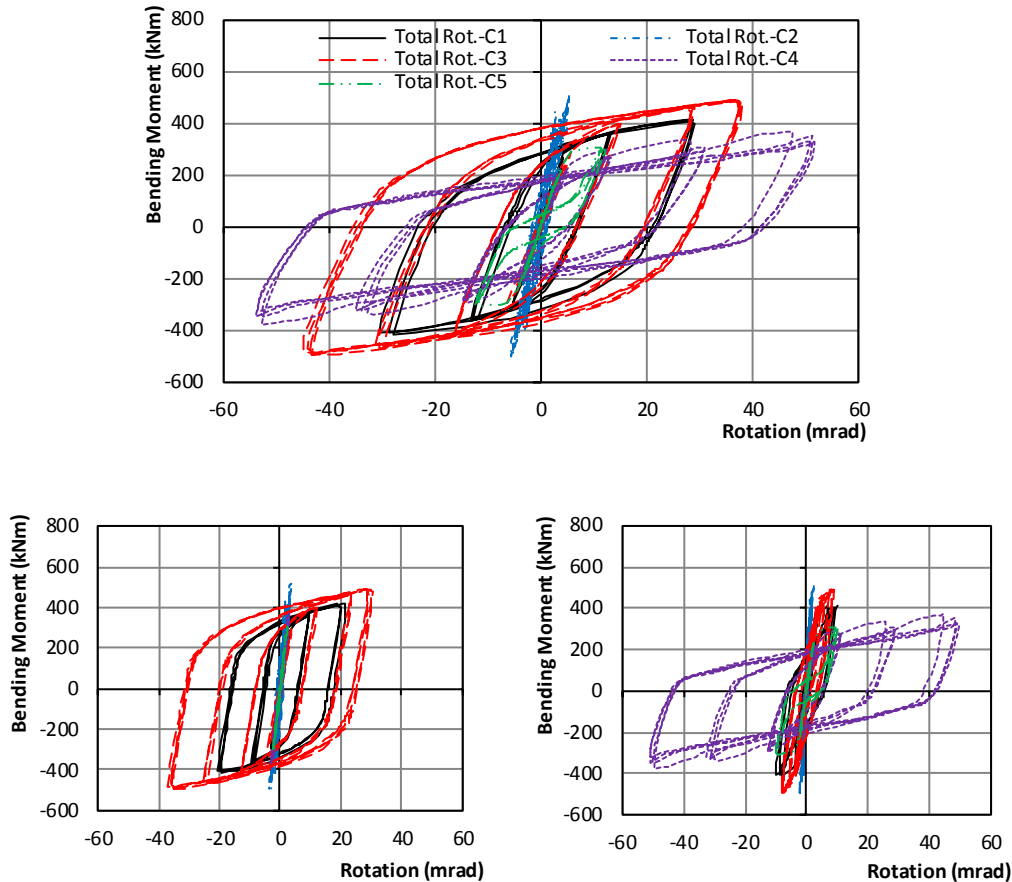


Figure 6.55. Cyclic response comparison for the joints C1 to C5.

6.5.3.1 *Final Remarks of the Parametric Study*

A parametric study was undertaken using the modelling techniques described in previous sections. A comparison between the numerical and analytical results, obtained by means of the component method prescribed in Eurocode 3, revealed a good agreement in terms of the failure modes obtained and also, a reasonable agreement in the strength achieved for each joint. However, concerning the initial stiffness, some discrepancies were found in the results, which indicate some possible limitations regarding the application of the component method to determine the initial stiffness of the joints which was mainly observed in the ones governed by yielding of the web column in shear, C3, and the ones that exhibited elastic behaviour, C2.

In terms of the cyclic loaded models, it became evident from the results obtained that the FE models are capable of representing different types of behaviour governed by the main dissipative components in the connections, namely the end-plate in bending and the column web panel in shear.

6.6 DERIVATION OF EQUIVALENT VISCOS DAMPING AND DISPLACEMENT REDUCTION FACTORS

As described in Section 2.1, the direct displacement based design (DDBD) procedure accounts for the energy dissipation of a structure subjected to a seismic event by considering an equivalent elastic single degree of freedom (SDOF) system that has an equivalent viscous damping (EVD) coefficient and an effective period that results in a maximum displacement equal to that of the inelastic system. This section aims to extend the validity of the procedure to steel MRF structures with partial-strength beam-to-column joints, as previously encountered for the case of full strength joints in Section 4.6. For this purpose, it is necessary to determine the EVD for several levels of ductility demand.

The equivalent viscous damping, ξ_{eq} , consists of the elastic viscous damping, ξ_{el} , and the damping associated with the energy dissipated (hysteretic damping ξ_{hyst}) during the inelastic response, given by:

$$\xi_{eq} = \xi_{el} + \xi_{hyst} \quad (6.21)$$

where the hysteretic damping, ξ_{hyst} , depends on the hysteresis characteristics of the structure. The elastic viscous damping, ξ_{el} , represents the energy dissipated by internal friction within the material particles and is typically given as a fraction of the critical damping, ξ , which is the damping used in the dynamic equation of equilibrium given by:

$$m\ddot{x} + c\dot{x} + k_0x = -m\ddot{x}_g \quad (6.22)$$

where x is the response relative displacement, \ddot{x}_g is the ground acceleration, m and k_0 are the mass and the initial stiffness, respectively, and the damping coefficient, c is given by:

$$c = 2\xi\sqrt{mk} \quad (6.23)$$

The damping coefficient and consequently the damping force, depends on the stiffness value adopted in Equation 6.23. Generally, for inelastic analysis, the initial stiffness is used, but several authors [e.g., Priestley et al., 2007] argue that this approach results in large and spurious damping forces and that tangent stiffness should be used instead.

Normally, for concrete structures, the elastic viscous damping ratio is taken as 5% of the critical damping, but a lower value is often used for steel structures. In this work, a value of 3% of the critical damping is adopted.

To derive the ductility-equivalent viscous damping relationships needed for the DDBD procedure, a set of sub-assemblages representing SDOF systems with hysteretic characteristics representative of partial-strength connections were analysed using the NLTH procedure for a wide range of ductility levels and effective periods. The connections were subjected to sets of accelerograms with different levels of intensity, in order to achieve different levels of system ductility. Calibration was carried out by identifying, for a given record, the level of damping that resulted in the same displacement demand of an elastic system with effective period T_e as an inelastic system with the partial-strength flexible joint hysteretic characteristics and with elastic viscous damping levels only. The procedure adopted and validated for this task is explained in detail in the next sub-sections.

6.6.1 Procedure Developed for the EVD Assessment

The linearization of the inelastic response of the partial-strength end plate connection is obtained by the developed procedure explained in detail as follows:

- i) the maximum response of the FE model sub-assemblage, calibrated in the previous sections, is determined from the NLTH analysis using a given record, for a given mass, m , elastic period, T_e , and setting the level of elastic viscous damping ξ_{el} (see Figure 6.56);

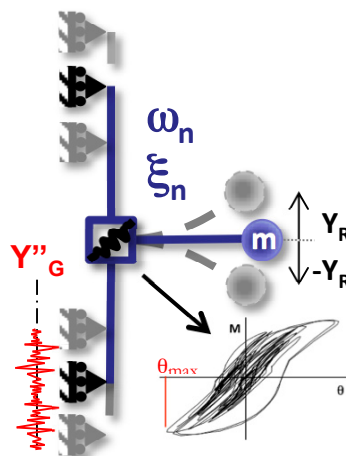


Figure 6.56. NLTH analysis of the sub-assemblage.

- ii) the yield point ($\theta_y; M_{\text{y}}$) is determined by the linearization of the monotonic response curve (Figure 6.57);

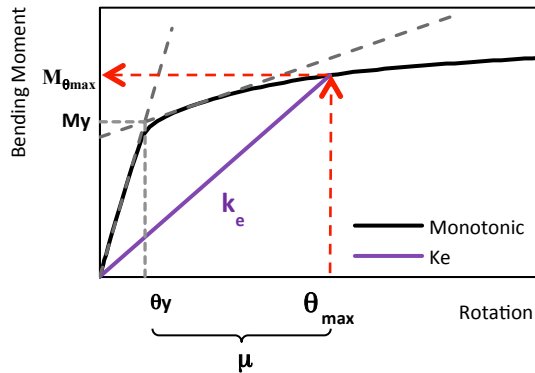


Figure 6.57. Determination ductility and yield moment.

- iii) the achieved ductility μ is calculated by evaluating the ratio between the maximum displacement / rotation and the yield displacement / rotation, given by:

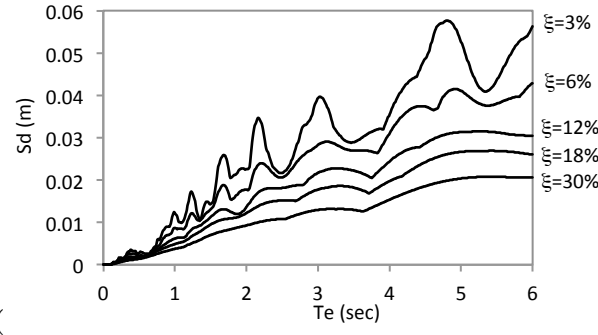
$$\mu = \theta_{\text{max}} / \theta_y \quad (6.24)$$

- iv) using the monotonic response curve (pushover) of the connection, the bending moment corresponding to the maximum rotation is obtained and the secant stiffness, k_e , is determined using the following expressions:

$$k_e = \frac{M_{(\theta_{\text{max}})}}{\theta_{\text{max}}} \quad (6.25)$$

$$T_e = \frac{2\pi}{\sqrt{k_e/m}} \quad (6.26)$$

- v) the displacement spectra are determined for several values of viscous damping



- vi) Figure 6.58); in this study, the SeismoSignal [SeismoSoft, 2012] software package was used to determine the displacement spectra of the several records, for several elastic damping levels;

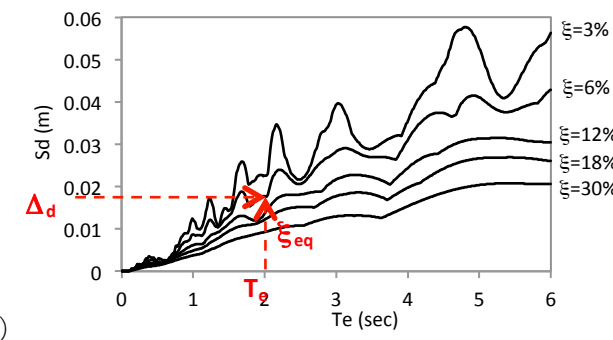


Figure 6.58. EVD assessment in the elastic displacement spectra.

- viii) with the effective period, T_e , and the target displacement, Δ_d , (corresponding to the max rotation, θ_{max}) the equivalent viscous damping, ξ_{eq} , is determined interpolating a more precise value in the displacement spectra.

By applying the procedure described above to a wide range of periods and a range of ductility demands it is possible to determine the ductility-EVD relationships need for the different joints behaviours found in practice, namely the ones that lead to the several failure modes according to EC3-1-8 [CEN, 2005b], and implement them in the DDBD procedures for MRF structures with partial-strength joints, as illustrated in

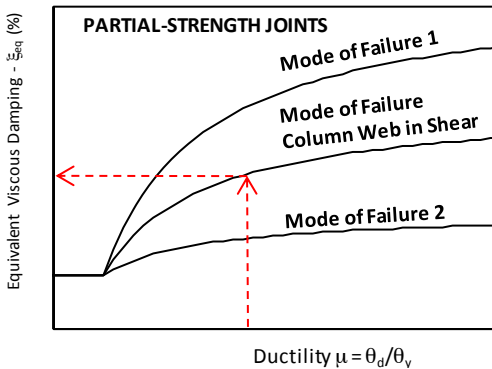
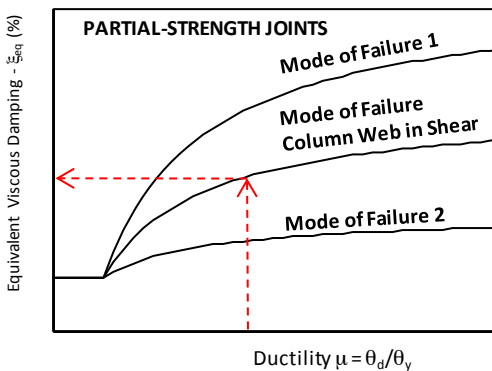


Figure 6.59.

Figure 6.59. Example of μ -EVD relationship chart.

6.6.2 Joints Properties Adopted for the EVD Assessment

The partial-strength joints chosen for the parametric study were the same studied in Section 6.5, C1 to C5, including the material properties described in Section 6.5.2. The geometric properties are described in Table 6.12, Table 6.13, Table 6.14 and in Figure 6.48. As explained before, the connections were designed to develop different plastic mechanisms corresponding to the various failure modes defined in EC3-1-8 [CEN, 2005b], where C1 and C5 governed by the plastic mechanism type 2, C4 is governed by the plastic mechanism type 1 due to the reduced end-plate thickness and C3 is governed by the column web in shear plastic mechanism. C1 has the same geometry as the J3.2 used in the FE models validation, where the contribution of the column web in shear is also significant in this joint.

In the procedure presented in the previous section, the monotonic behaviour of the joints is used firstly to determine the elastic deformation limit, θ_j , and secondly, to

determine the corresponding bending moment for the maximum rotation achieved in the NLTH analysis. For each joint, the monotonic response for positive and negative bending moment was determined, imposing a positive or negative displacement on the beam end, and the yield rotations were derived from the monotonic results employing the ECCS procedure [ECCS, 1986] which is illustrated in Figure 6.57. The results are presented in Table 6.18. The bending moments were obtained with Equation 6.10, and the rotations were obtained using Equations 6.13 and 6.18.

For the generation of significant inertia force and, consequently, bending moments and rotations at the connection during the NLTH analyses it was necessary to consider a concentrated mass, m , to the model, applied in the beam end. The masses were determined in an iterative process using frequency analyses in the several joints, see Figure 6.60, in order to obtain, for the elastic periods of the system, $T_{el} = 1.0\text{ s}$ and $T_{el} = 0.5\text{ s}$. The masses considered are provided in Table 6.17.

Table 6.18. Connections properties for the EVD assessment.

	$M_{y(j)}^+$	$M_{y(sys)}^+$	$\theta_{y(j)}^+$	$\theta_{y(sys)}^+$	$\Delta_{y(sys)}^+$	M_y^-	$M_{y(sys)}^-$	θ_y^-	$\theta_{y(sys)}^-$	$\Delta_{y(sys)}^-$	m (ton)	
											$T_{el} = 1.0\text{ (s)}$	$T_{el} = 0.5\text{ (s)}$
C1	294	303	3.52	4.91	11.72	-293	-302	-3.49	-4.86	-11.57	637.500	159.375
C2	480	480	3.35	5.54	79.46	-480	-480	-3.35	-5.54	-77.87	837.500	209.375
C3	327	349	4.28	6.70	13.71	-325	-346	-4.22	-6.62	-13.61	634.375	158.750
C4	253	260	4.22	5.53	10.92	-253	-262	-4.12	-5.47	-10.87	545.313	136.250
C5	273	276	3.46	4.77	10.51	-273	-279	-3.60	-4.96	-10.79	696.875	174.063

Bending Moments in kNm, rotations in mrad, displacements in mm, periods in seconds and mass in tones.

The elastic damping, ξ_{el} , is incorporated in the models through the use of Rayleigh damping with a value of 3% of critical damping. Stiffness-proportional damping according to Equation 6.27 was used and applied to the first elastic period, which is determined with a modal analysis performed in ABAQUS ($T_{el} \approx 1.0\text{ s}$ and $T_{el} \approx 0.5\text{ s}$). In ABAQUS, the stiffness-proportional damping coefficient, β_k , is requested in the material properties definition for the model parts.

$$\beta_k = \frac{T_{el}\xi_{el}}{\pi} \quad (6.27)$$

The material properties adopted for the joints were the same as those used in the cyclic analyses in the parametric study conducted in Section 6.5 to be able to account for the reversal re-loading.

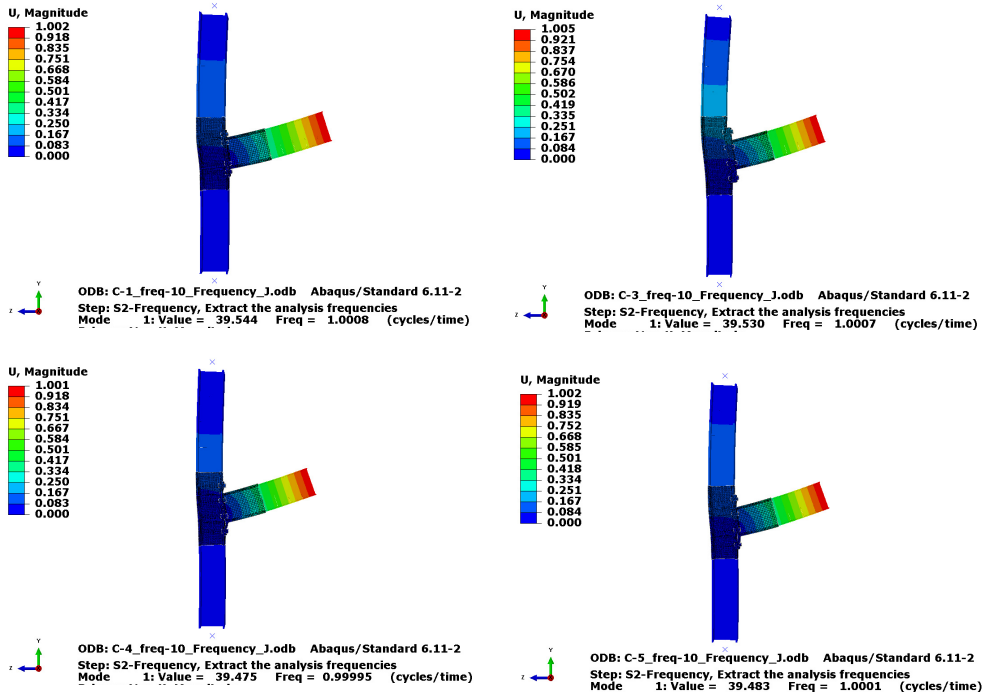


Figure 6.60. Frequency analyses for $T_{el} = 1.0s$.

6.6.3 Records Adopted in the NLTH Analyses

A set of twenty records of real earthquakes were used, which are representative of soils type A (LA1r to LA10r) and soils type C (LC1r to LC10r), according to the EC8 [CEN, 2004]. The LA record set, shown in Table 6.19, was selected to be compatible with the EC8 spectrum for soil type A and corner period, T_D , of at least 8s, as described in Maley *et al.* [2013]. The LC record set, presented in Table 6.20, was also selected to be compatible with the EC8 spectrum for soil type C and corner period, T_D , of at least 8s, as described in Maley *et al.* [2013]. To save some computational time, the records were cut in the time domain by eliminating the initial or the tail part with lower seismic activity when possible, while still maintaining the original acceleration and displacement spectra. The differences obtained from the original spectra and the reduced ones were lower than 1%. The acceleration and displacement spectra, for 3% of elastic damping, are represented in Figure 6.61 for soil type A and in Figure 6.62 for soil type C.

Table 6.19. Record set for the soil type A (LA).

	Record Sequence Number	Earthquake	Station Name	Earthq. Mag.	CstD (km)	Vs30 (m/s)	Scaling Factor ⁺
LA1	2111	Denali, Alaska	R109 (temp)	7.9	43	964	6.5
LA2	1518	Chi-Chi, Taiwan	TCU085	7.62	58	1000	5.8
LA3	1440	Chi-Chi, Taiwan	TAP065	7.62	122	1024	6.1
LA4	1352	Chi-Chi, Taiwan	KAU003	7.62	114	914	5.2
LA5	-	Darfield, NZ	Rata Peats (RPZ)	7.1	93*	**	13.4
LA6	804	Loma Prieta	So. San Francisco, Sierra Pt.	6.93	63	1021	7.2
LA7	804	Loma Prieta	So. San Francisco, Sierra Pt.	6.93	63	1021	6.8
LA8	284	Irpinia, Italy-01	Auletta	6.9	10	1000	7.9
LA9	1074	Northridge-01	Sandberg - Bald Mtn	6.69	42	822	6.2
LA10	946	Northridge-01	Antelope Buttes	6.69	47	822	12.7

+ In order to match the EC8 design spectrum constructed with a ground acceleration of $a_g=0.40g$

* Epicentral distance

** No reference to shear wave velocity over the first 30m of soil profile is provided for this record

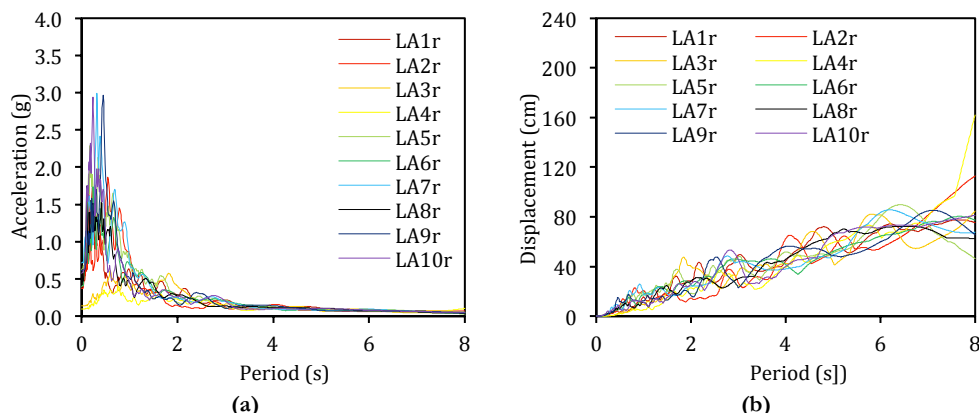


Figure 6.61. (a) Acceleration response spectra for LA set (b) Displacement response spectra for LA set.

Table 6.20. Record set for the soil type C (LC).

	Record Sequence Number	Earthquake	Station Name	Earthq. Mag.	CstD (km)	Vs30 (m/s)	Scaling Factor ⁺
LC1	1233	Chi-Chi, Taiwan	CHY082	7.62	36	194	2.1

	Record Sequence Number	Earthquake	Station Name	Earthq. Mag.	ClstD (km)	Vs30 (m/s)	Scaling Factor ⁺
LC2	1153	Kocaeli	KOERI Botas	7.51	127	275	7.9
LC3	851	Landers	CDMG 14368 Downey - Co Maint Bldg	7.28	157	272	4.0
LC4	1810	Hector	Mecca - CVWD Yard	7.13	92	345	2.9
LC5	1629	St Elias, Alaska	USGS 2728 Yakutat	7.54	80	275	1.5
LC6	777	Loma Prieta*	USGS 1028 Hollister City Hall	6.93	28	199	1.8
LC7	1043	Northridge-01	Neenach - Sacatara Ck	6.69	52	309	5.8
LC8	728	Superstition Hills-02	Westmorland Fire Sta	6.54	13	194	2.3
LC9	172	Imperial Valley-06	El Centro Array #1	6.53	22	237	5.1
LC10	2615	Chi-Chi, Taiwan-03*	TCU061	6.2	40	273	5.6

+ In order to match the EC8 design spectrum constructed with a ground acceleration of $a_0=0.40g$

* Additional record for used with pair set for 3D analyses with 7 3-component sets

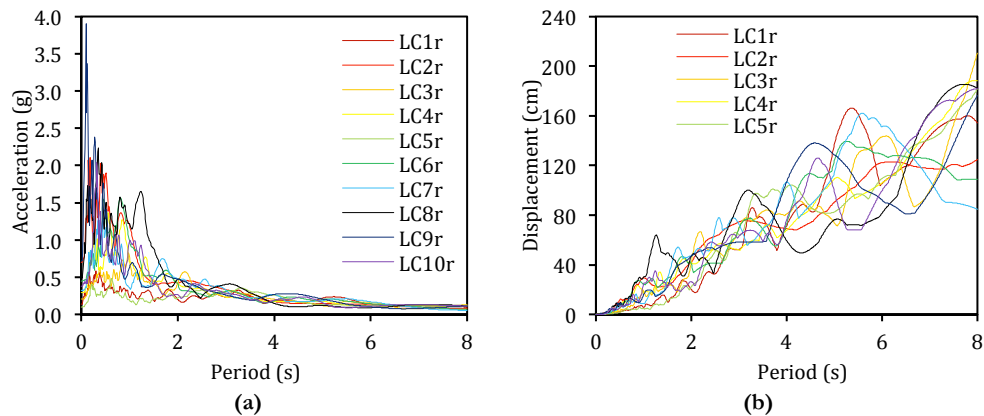


Figure 6.62. (a) Acceleration response spectra for LC set (b) Displacement response spectra for LC set.

The record set used in the NLTH analyses for the soil type A can be seen in Figure 6.63 and for the soil type C in Figure 6.64.

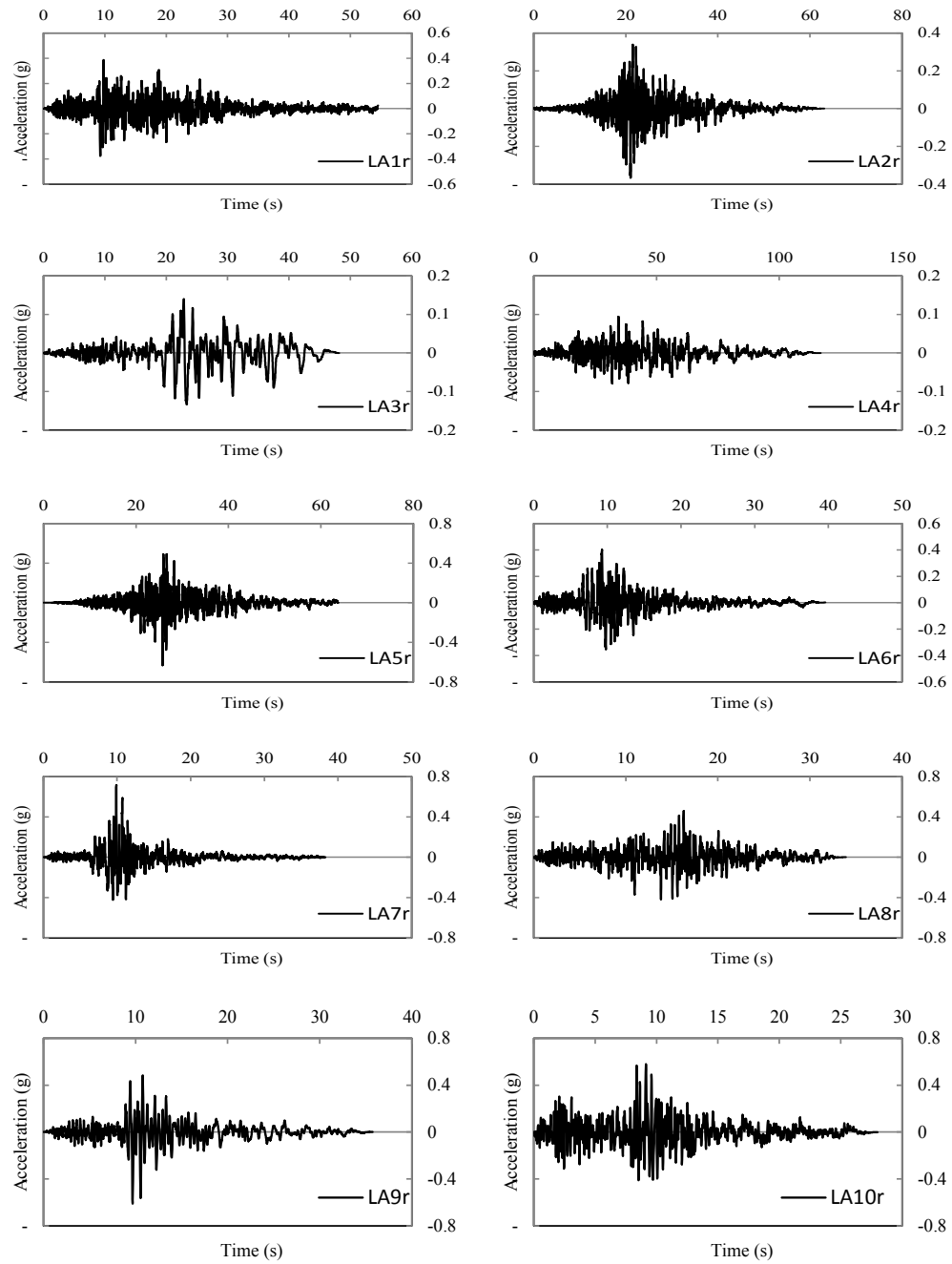


Figure 6.63. Records for the soil type A.

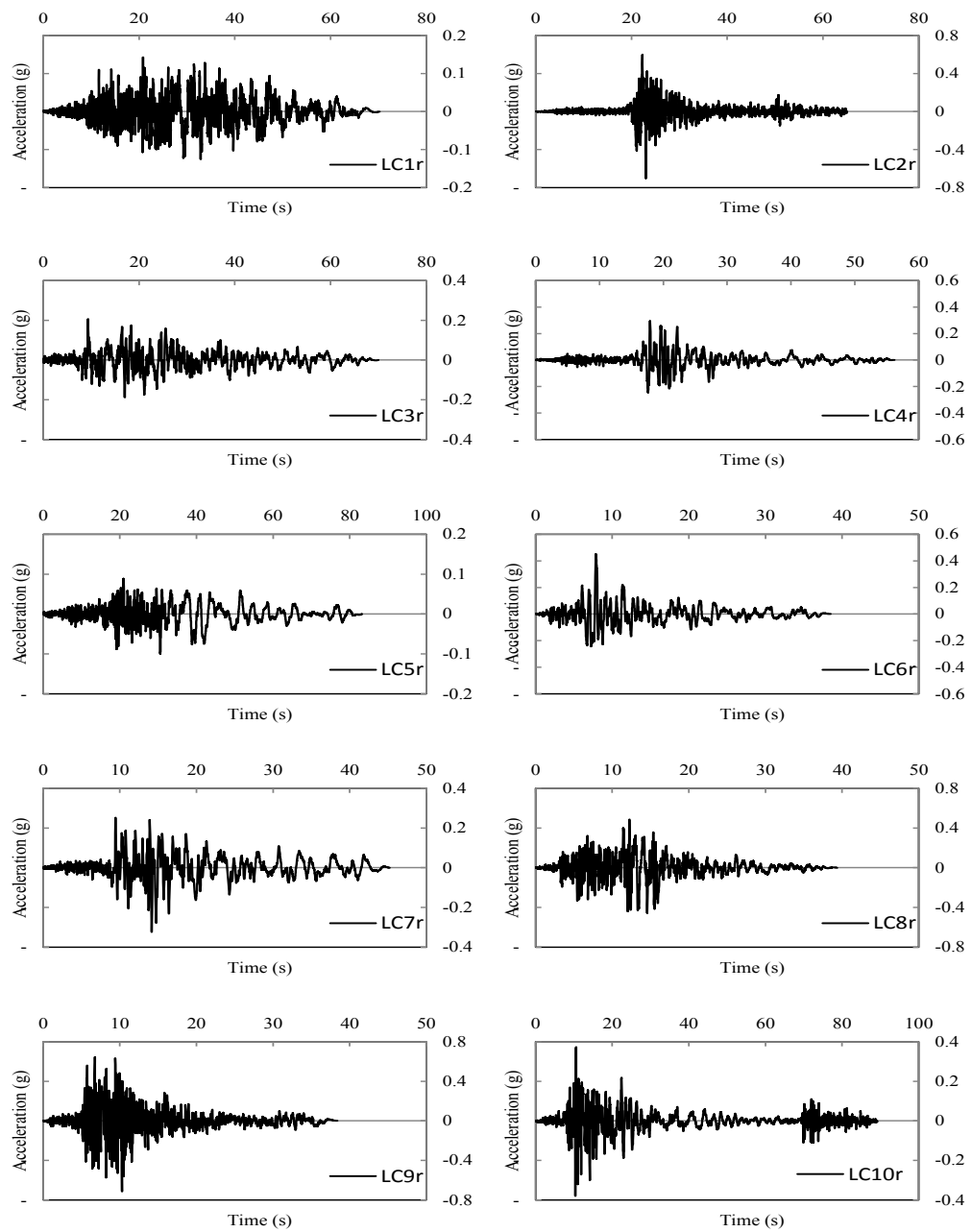


Figure 6.64. Records for the soil type C.

6.6.4 Results from the NLTH Analyses and EVD Assessment

A large parametric study was undertaken with the objective of deriving ductility-EVD relationships. Joints C1, C3, C4 and C5 were subjected to successive NLTH analyses using the previously presented records. The records were scaled to achieve five levels of ductility demand for each connection. The equal-displacement rule (see Figure 6.65(a)) was used in the prediction of the scaling factors (SF) using the displacement spectra obtained from each record shown in Figure 6.61(b) and Figure 6.62(b). The calculated yield displacement, Δ_y , from the monotonic response of each connection shown in Table 6.18 for each elastic period, T_e , is used to determine the SF. Due to the inadequacy of the equal displacement rule in some cases, some analyses turned out to be subjected to ductility demands, μ , lower than 1 or higher than 5.

The procedure described in Section 6.6.1 was then applied to each one of the NLTH analysis results considering or neglecting the column elastic deformation (CCED or NCED, respectively) according to Equation 6.13 and 6.18. When the column elastic deformation is removed by using Equation 6.18, it was considered that the elastic deformation increases only until the yield moment is reached, M_y , and afterwards θ_{elast_column} reaches a plateau. This assumption had the elastic-perfectly-plastic behaviour into consideration for the several components involved in the system, namely the connection the column and the beam, when the connection reaches the yield moment the moment of the system does not increase any more, see Figure 6.65(b).

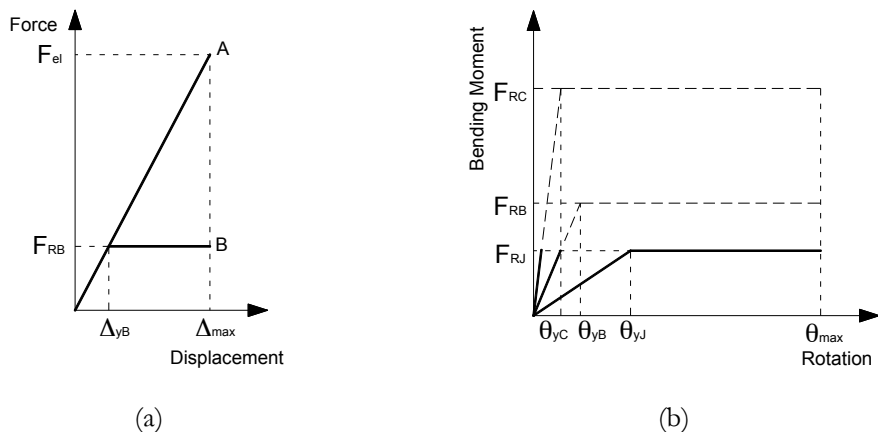


Figure 6.65. (a) Equal-displacement rule; **(b)** Elasto-plastic idealised behaviour for the sub-assemblage components, column, beam and joint.

A recent study conducted by Dwairi *et al.* [2007] on the EVD assessment to be used in the DDBD method presented as an extensive evaluation of Jacobson's damping

approach [Jacobsen, 1930] combined with the secant stiffness method, using a large number of real earthquake accelerograms (100 ground motion records) and four hysteresis rules (Ring-Spring, Large Takeda, Small Takeda and Elasto-plastic) resulted in the proposal of new EVD expressions dependent on the ductility and the period. Successive NLTH analyses were undertaken for each individual record, ductility level, effective period and hysteresis rule separately, concluding that on average, the EVD is overestimated and consequently, the displacement is underestimated for intermediate and long periods. It was also evident that on average, the EVD is largely underestimated for short effective periods, in particular less than 0.4 seconds. The scatter range obtained was between 20% and 40% for intermediate and long periods. The resulting expressions proposed for the EVD have the form:

$$\xi_{eq} = \xi_{el} + C \left(\frac{\mu - 1}{\mu\tau} \right) \quad (6.28)$$

where the coefficient C depends on the hysteretic shape and is a constant for periods greater or equal to one, but for shorter periods ($T_e < 1.0s$) is presented as a function of the effective period itself (see Equation 6.29), which complicates the direct design of the structure. Although, it is stated by Priestley *et al.* [2007] that if Equation 6.28 is adopted in the DDBD procedure, the vast majority of the structures will have effective periods greater than one second and hence, the adoption of an expression non-dependent of the effective period will generally be adequate, and even conservative if a period lower than one is achieved because a low estimate of damping will be obtained.

$$\xi_{eq} = \xi_{el} + (c + d(1 - T_e)) \left(\frac{\mu - 1}{\mu\tau} \right) \quad \text{for } T_e < 1.0s \quad (6.29)$$

Based on the previous study, Priestley *et al.* [2007] proposed a series of equations for several types of structures, materials and hysteretic response, only valid for elastic viscous damping of 5% ($\xi_{el} = 0.05$). For steel frame buildings with a Ramberg-Osgood hysteresis rule, the following equation was proposed:

$$\xi_{eq} = 0.05 + 0.577 \left(\frac{\mu - 1}{\mu\tau} \right) \quad (6.30)$$

6.6.4.1 Equivalent Viscous Damping

Figure 6.66 and Figure 6.67 shows the results CCED and NCED, respectively, where the results are presented in a ductility, μ , EVD, ξ_{eq} , relationship, with each point representing the EVD procedure applied to a joint typology for a given record, effective period and a given global ductility demand considering a viscous damping of 3%. The EVD for the ductility demands achieved are compared for each connection and record.

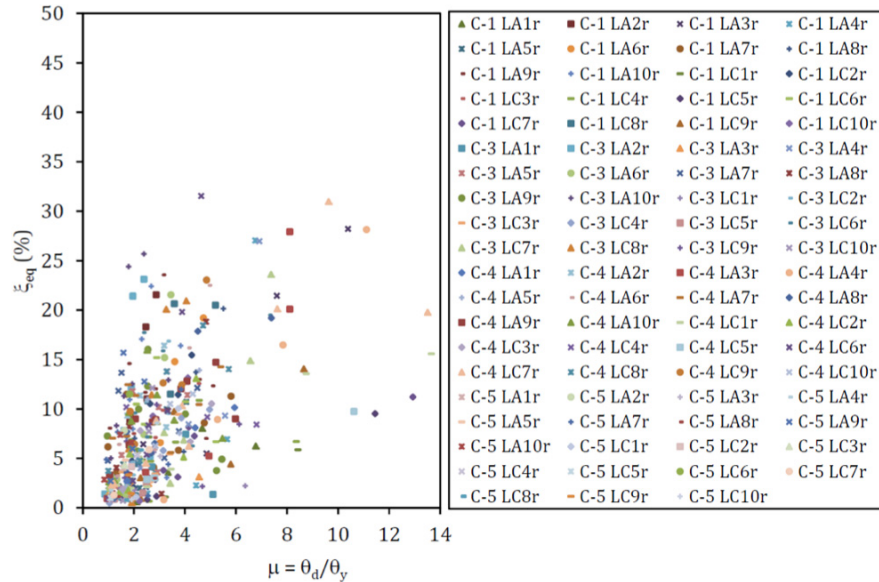


Figure 6.66. EVD results using the NLTHA (CCED).

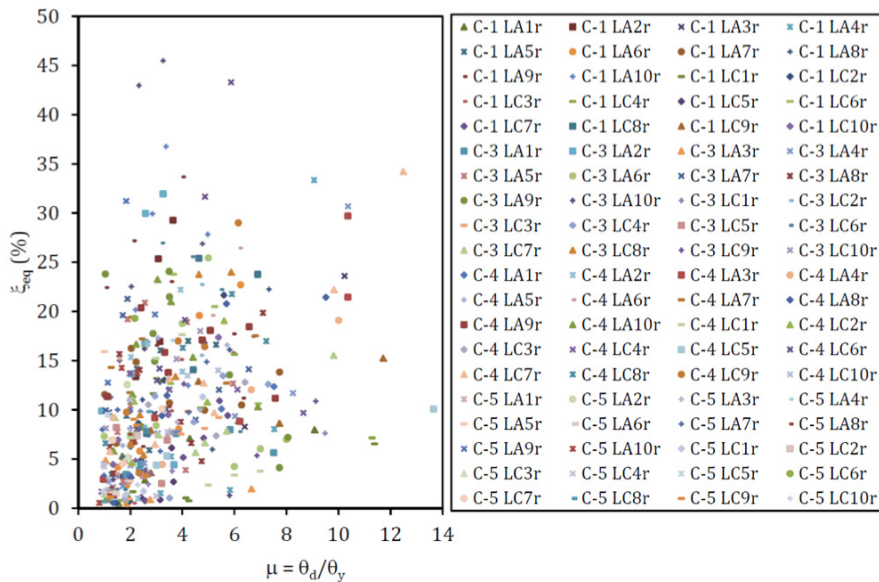


Figure 6.67. EVD results using the NLTHA (NCED).

Some dispersion of the results is observed. It is worth noting that the ductility demands reached in some of the analyses are almost three times the initial prediction, proving the inadequacy of the equal-displacement rule.

To achieve the type of relationships illustrated in

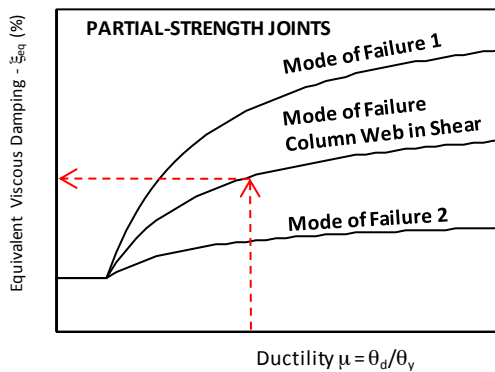


Figure 6.59 for steel partial-strength joints, a modification to Equation 6.30 was proposed. Equation 6.31 was derived using the ordinary least squares to determine the constant C . The results obtained with the proposed expression are depicted in Figure 6.68 and Figure 6.69 for CCED and NCED, respectively, for each connection which is identified by (D-K), along with the predictions obtained with Equation 6.30, identified by P(R-O).

$$\xi_{eq} = 0.03 + C \left(\frac{\mu - 1}{\mu \pi} \right) \quad (6.31)$$

In order to achieve a better curve fitting for the EVD results, a new empirical expression based on a natural logarithm formulation was evaluated, that is given by:

$$\xi_{eq} = b + K \cdot \ln(\mu) \quad (6.32)$$

where b is considered to be the elastic viscous damping and K is a constant determined again by applying the ordinary least squares. The equations predictions are also included in the figures, identified by (ln).

The determined coefficients for the previous equations are provided in Figure 6.70 and Figure 6.71. From the results, it is possible to observe that several analysis reached effective periods lower than one second. According to what was stated previously, it is possible that those results are better described by an effective period dependent equation, similar to Equation 6.29. In order to determine the c and d constants, the ordinary least

squares was applied using Equation 6.28 and 6.29 for the analysis with effective period higher or lower than one second, respectively and considering also $c = C$. For all the cases, the values determined for the constant d were zero, except for the C5 connection CCED a value of 0.014 was derived. For this reason, Equation 6.31 with the derived coefficients is proposed for the DDBD of partial-strength connections.

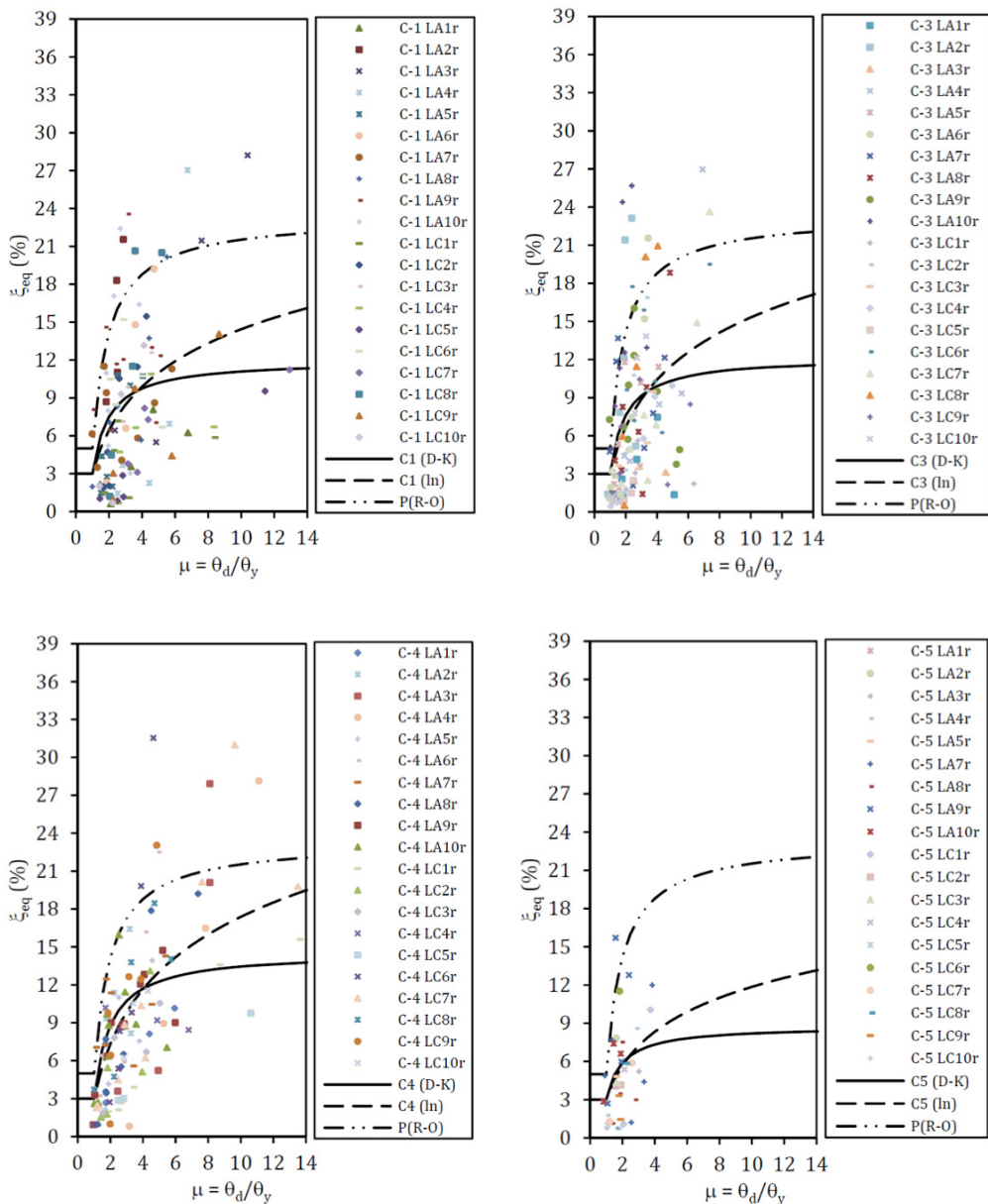


Figure 6.68. Ductility-EVD relationships (CCED).

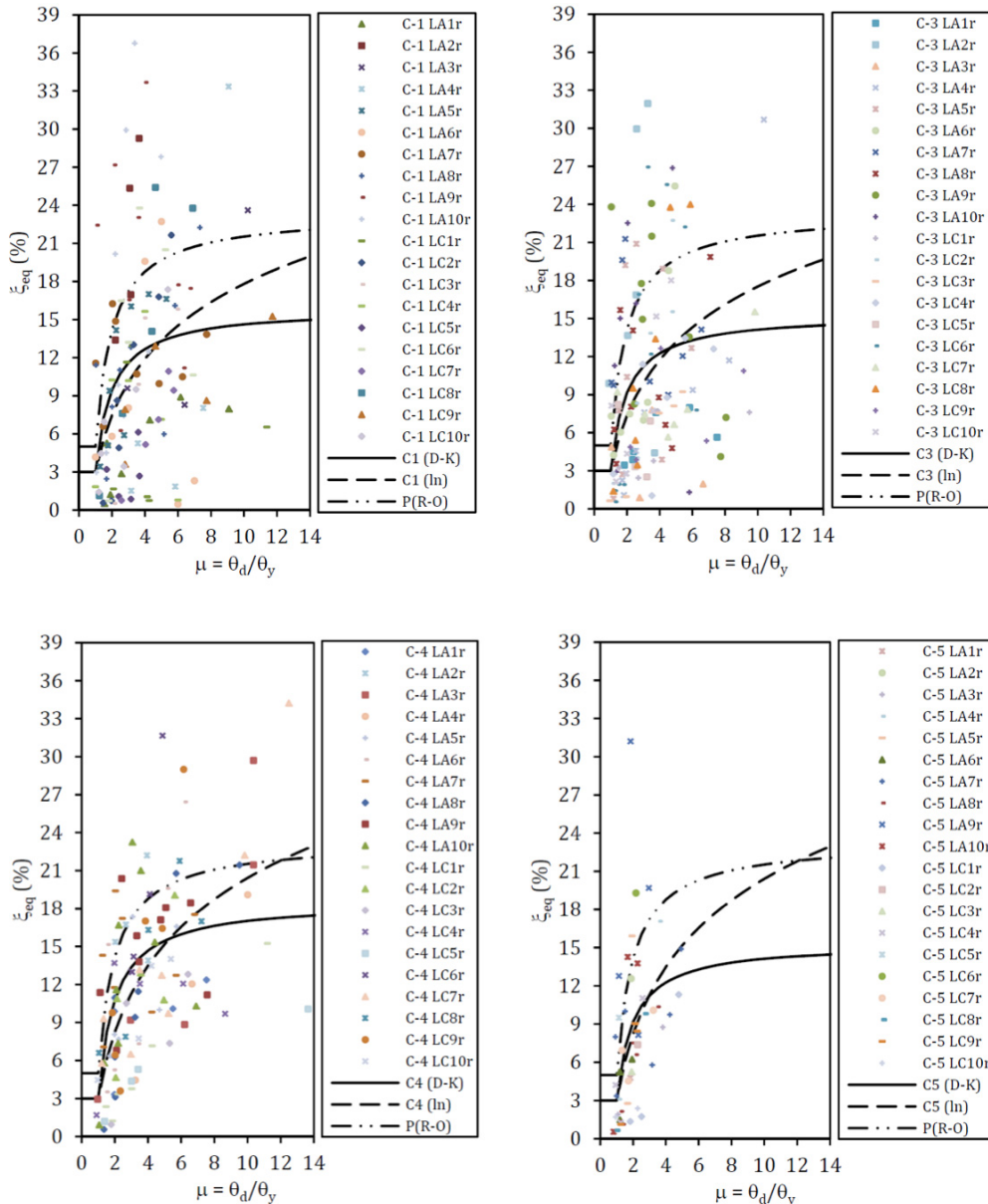


Figure 6.69. Ductility-EVD relationships (NCED).

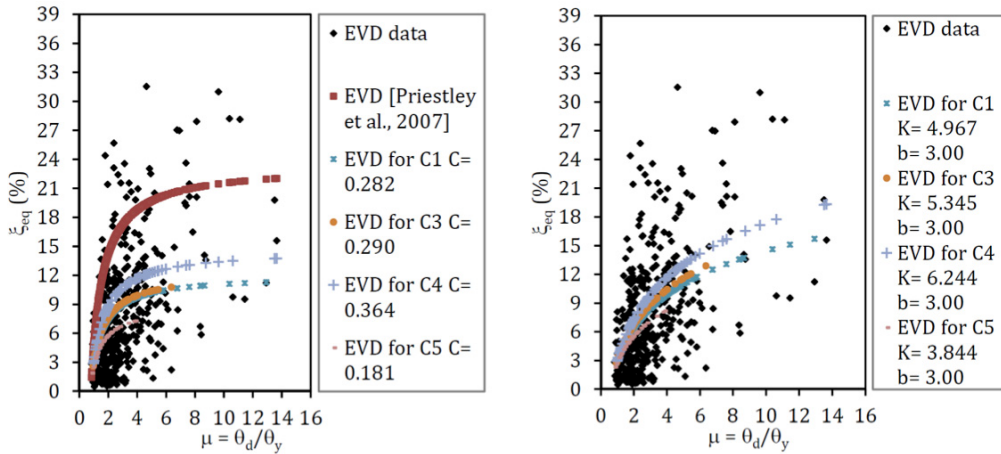


Figure 6.70. Coefficients for the derived equations CCED.

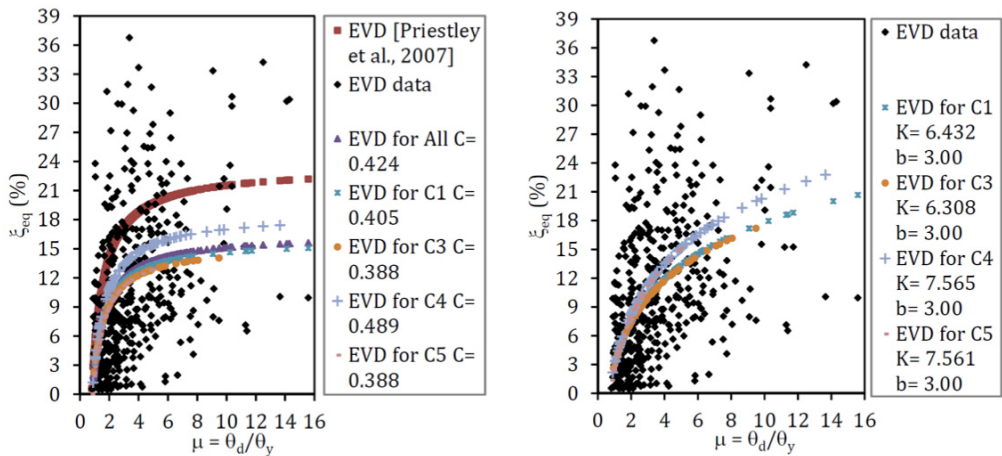


Figure 6.71. Coefficients for the derived equations NCED.

The results revealed a significant scatter and, for that reason, any linear law will always provide a poor fitting of the data. Nevertheless, Equation 6.31 performed better in the cases where the column elastic deformation was neglected, although, for the connection C4, Equation 6.32 presented a better accuracy (reducing the error between the analytical and NLTH results in 8.5%). In the cases where the elastic deformation was taken into account, Equation 6.32 performed better (reaching 22% decrease in the error between the analytical and the NLTH results), though a better fitting in the connection C4 was achieved. The ductility-EVD relationships proposed for the several connections analysed, representative of the several plastic mechanisms considered in EC3-1-8 are depicted in the

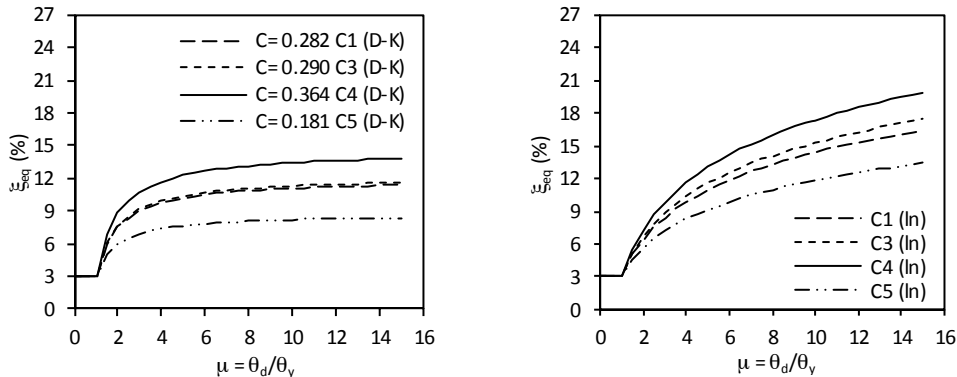


Figure 6.72 (CCED) and in

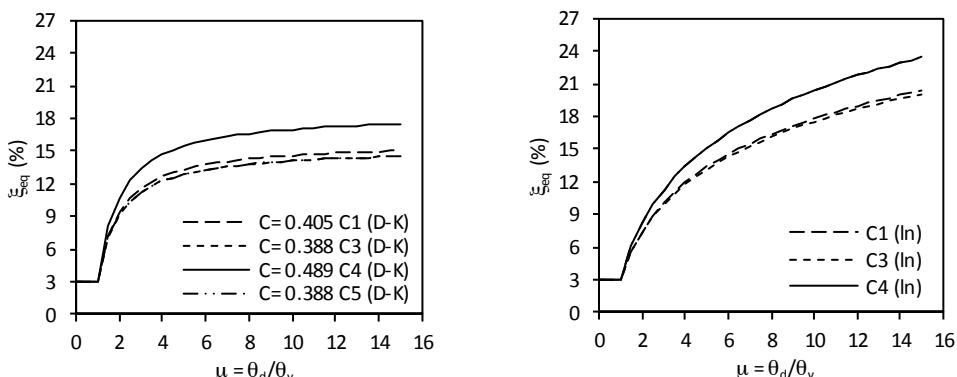


Figure 6.73 (NCED).

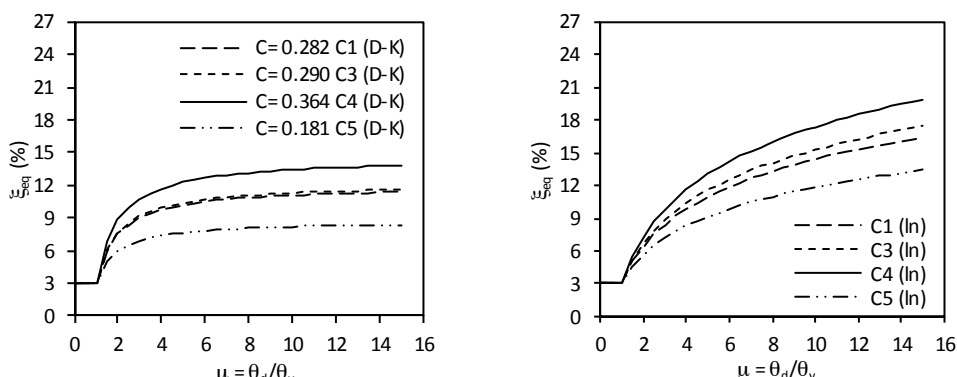


Figure 6.72. Derived ductility-EVD relationships, CCED.

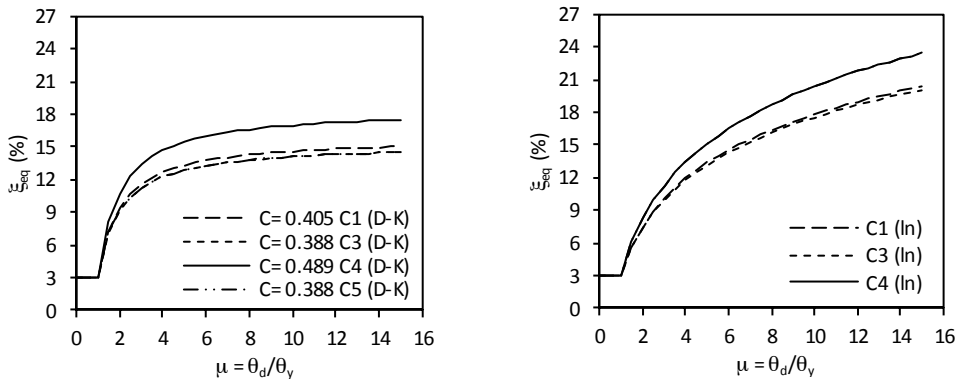


Figure 6.73. Derived ductility-EVD relationships, NCED.

6.6.4.2 Modification Factor for the Spectral Displacement Response

Due to the fact that the DDBD procedure uses the effective period for the representation of the structural response, a modification factor is required to be applied to the displacement response spectrum to account for ductile response [Priestley *et al.*, 2007].

The recent developments in the DDBD approach, namely the latest model code [Sullivan *et al.*, 2012] suggest that in order to take the effects of the energy dissipation and/or non-linear structural response into account, the displacement spectrum should be reduced by a modification factor, R_s , which is a function of the EVD. This way, the EVD represents a simplified means of identifying the inelastic displacement spectra associated with the effective period.

It is therefore important to have a robust damping modifier R_s to be applied to the elastic spectrum for different levels of damping. The problem is that there have been some uncertainties in this area, where there are several expressions presented thus far, like the EC8 expression presented earlier [CEN, 1994], which is given by:

$$R_{\xi} = (0.07 / (0.02 + \xi))^{0.5} \geq 0.7 \quad (6.33)$$

where ξ is a ratio of the elastic critical damping. In the 2003 revision of EC8, this expression was replaced by:

$$R_{\xi} = (0.1 / (0.05 + \xi))^{0.5} \geq 0.55 \quad (6.34)$$

Newmark and Hall [1982] proposed a different expression, which is given as:

$$R_{\xi} = (1.31 - 0.19 \ln(100\xi)) \quad (6.35)$$

However, this expression revealed to be very conservative in comparison with that proposed in EC8. Priestley [2003] proposed another expression, based on limited data, for sites where forward directivity velocity pulse characteristics might be expected (Equation 6.36) and it is similar to the expression of EC8 [CEN, 1994] but with a change of power from 0.5 to 0.25 in this case, as shown below:

$$R_{\xi} = (0.07 / (0.02 + \xi))^{0.25} \quad (6.36)$$

Recent studies, through numerous NLTH analyses, such as that conducted by Pennucci *et al.* [2011], revealed that for structures responding in the inelastic range, the use of expressions that relate directly the ductility and inelastic reduction factor, which essentially bypasses the EVD expression step, leads to an improvement in the displacement estimates. These expressions were subsequently included in the most recent version of the model code [Sullivan *et al.*, 2012].

To determine the displacement reduction factor, the ratio between the inelastic displacement and the elastic displacement for the same effective period is computed as follows:

$$\eta = \frac{\Delta_{in}}{\Delta_{el,T_e}} \quad (6.37)$$

Figure 6.74 and Figure 6.76 show the comparison of the results using Equation 6.37, from NLTH analyses to determine the maximum inelastic displacement Δ_{in} , and using the elastic displacement spectra with 3% of elastic damping to determine the elastic displacement, Δ_{el,T_e} , with the analytical expressions found in literature and presented previously. Note that the analytical expressions were used without the limitations imposed in the codes, i.e., only the first part of Equation 6.33 and 6.34 were used in the next comparisons. Figure 6.75 and Figure 6.77 present the ratio between the reduction factors obtained from the NLTH analyses and the reduction factors obtained using Equations 6.33 to 6.36.

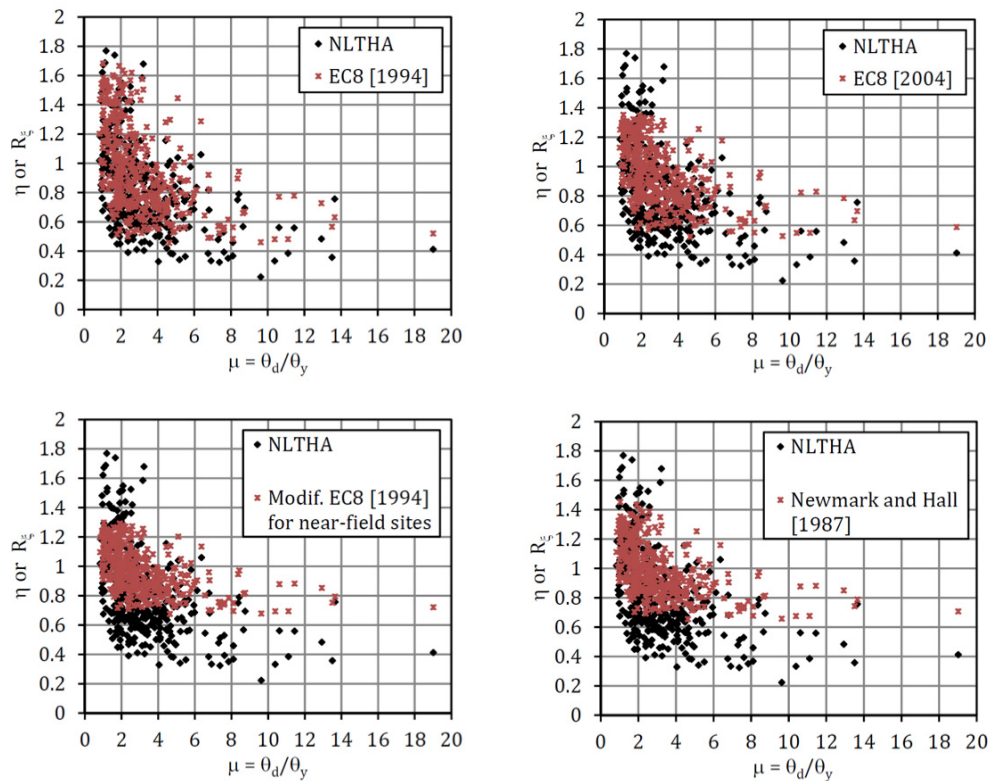


Figure 6.74. Damping modifier comparison (CCED).

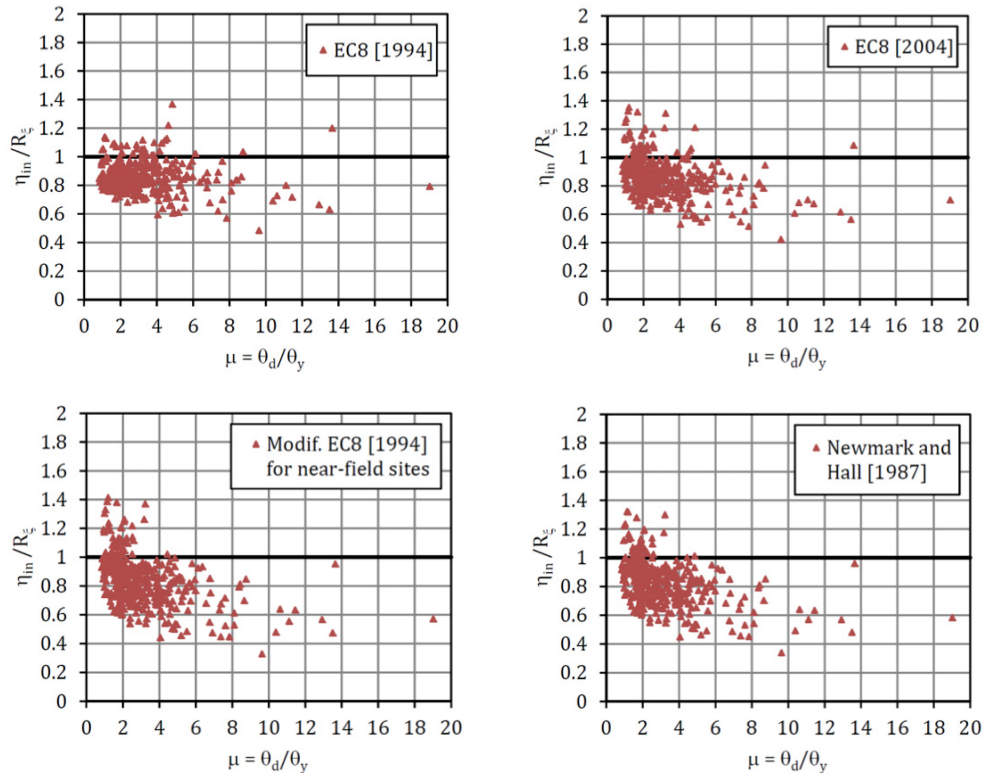


Figure 6.75. Deviation from the “real” and analytical reduction factors (CCED).

From a detailed inspection of the figures, it is possible to conclude that the most accurate analytical values are obtained with Equation 6.33, although the predictions obtained with the expression proposed in the current version of the EC8 [CEN, 2004] are also reasonable. In the case of Equations 6.35 and 6.36, the poor correlation of the results indicates some inadequacy to deal with partial-strength joints and hence, they will be discarded in this study.

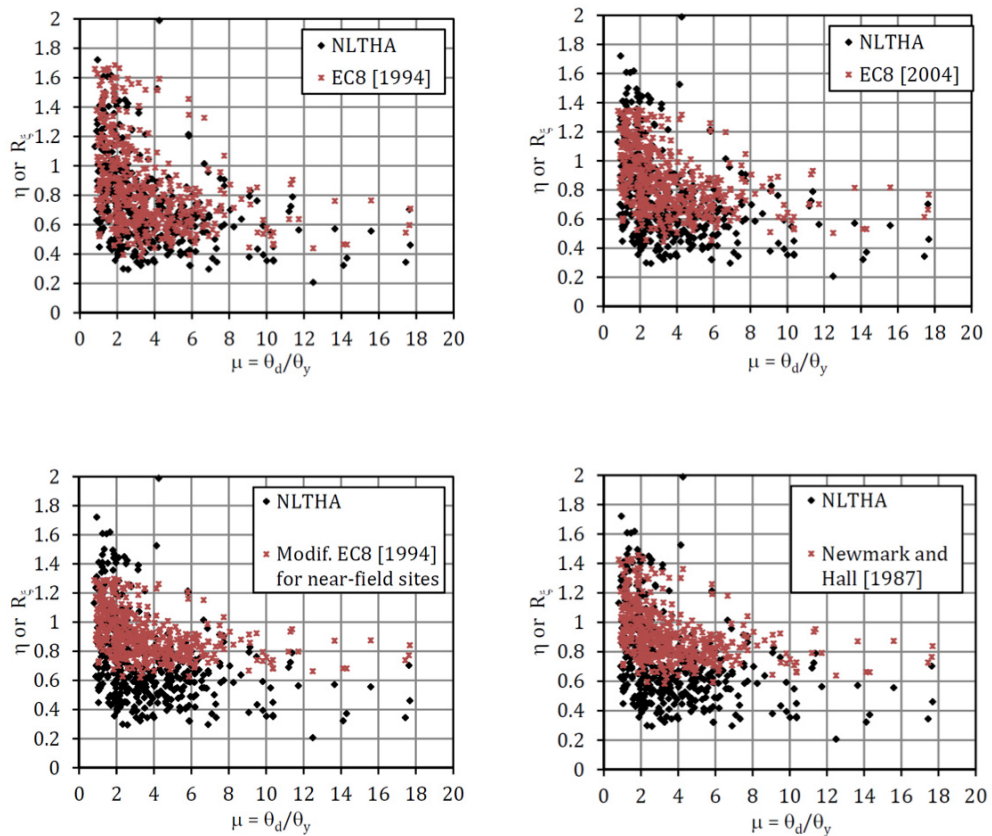


Figure 6.76. Damping modifier comparison (NCED).

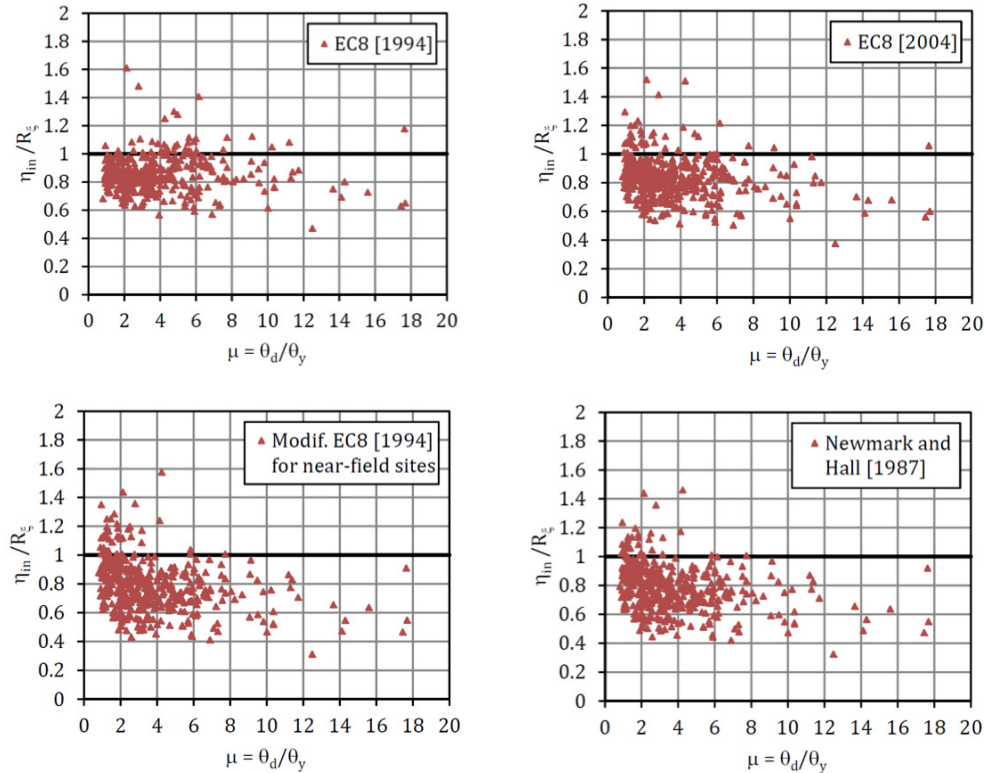


Figure 6.77. Deviation from the “real” and analytical reduction factors (NCED).

Seeking for a better adjustment, a modification to Equation 6.33 was undertaken (Equation 6.38) by using again the ordinary least squares to determine the constant x . The results can be seen in Figure 6.78 for the CCED and NCED cases. In Figure 6.79, the ratio between the reduction factors obtained from the NLTH analyses and the reduction factors obtained with Equations 6.38 are plotted.

$$R_{\xi} = (x/(3 + \xi))^{0.5} \quad (6.38)$$

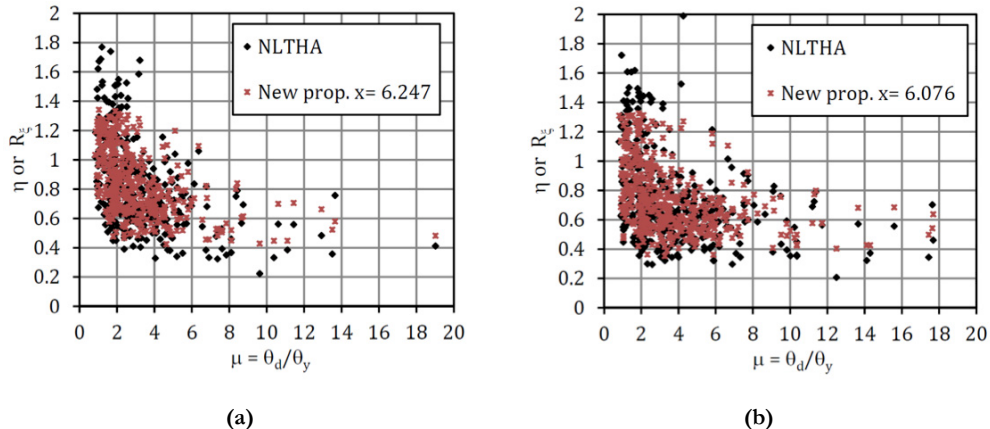


Figure 6.78. Proposition for an improvement in the expression for the damping modifier: (a) CCED
(b) NCED.

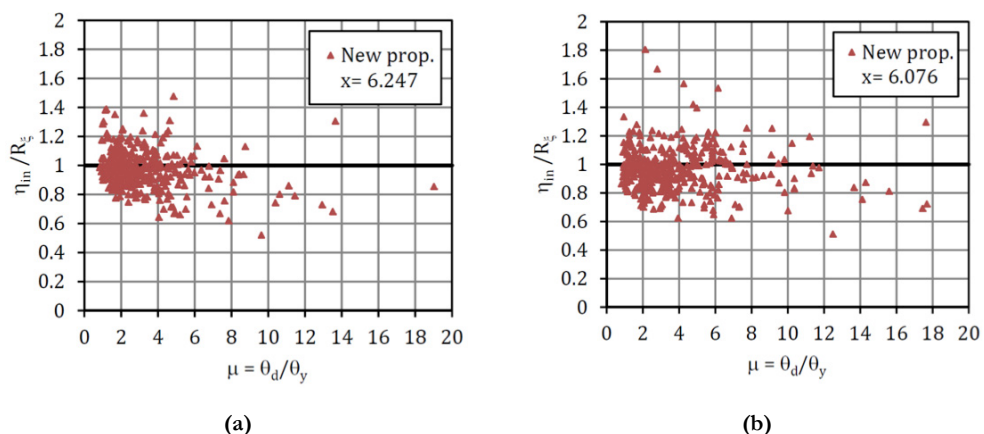


Figure 6.79. Deviation from the "real" and analytical reduction factors: (a) CCED (b) NCED.

An improvement of almost 60% was reached for the CCED case and, in the case of NCED, the improvement was around 54% in the overall error between the adjustments of the analytical values to the NLTH analyses values.

If the derived Equations 6.31 and 6.32 are used to determine the EVD for the same ductility demand of the NLTH analyses and including those results in the Equation 6.38, the analytical approach recommended for the DDBD in the recent model code [Sullivan et al., 2012] is obtained. The comparison with η is shown in Figure 6.80.

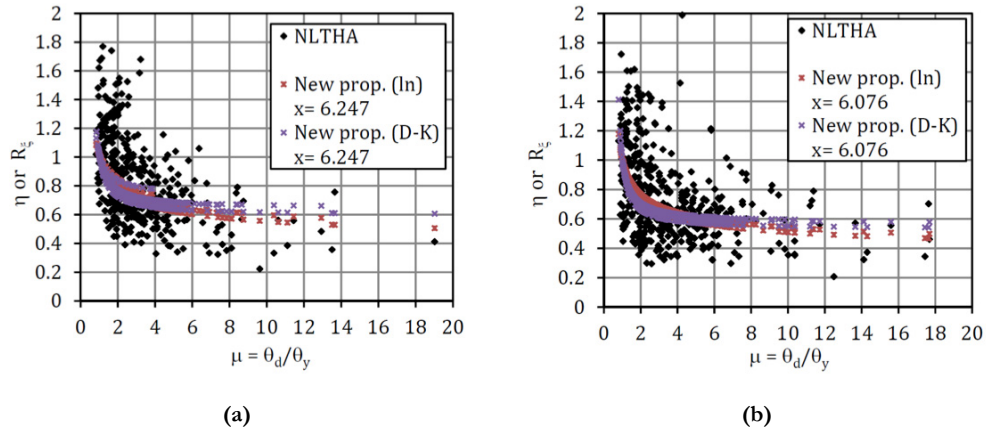


Figure 6.80. Comparing the combined new EVD expressions with the new damping modifier expressions to the NLTH analyses ductility demands: (a) CCED (b) NCED.

Relating now the damping modifier with the effective period for the results of the NLTH analyses, see Figure 6.81, it is possible to observe that there is a considerable dispersion for the lower periods and a lower dispersion for the higher periods. However, the displacement values are overestimated.

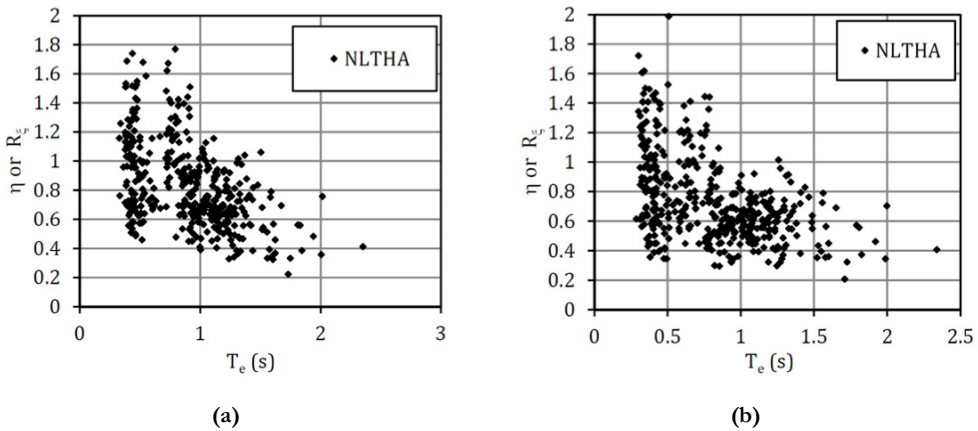


Figure 6.81. NLTH analyses to elastic displacement ratio: (a) CCED (b) NCED.

6.7 INTERPRETATION OF THE RESULTS OF THE EVD STUDY

The study has been conducted using a set of real ground motions. Partial-strength bolted extended end-plate connections have been examined through consideration of four different yielding mechanisms. Distinction has also been made as to whether column elastic deformations are included in the formulation or not. After fitting EVD curves to the results of NLTH analyses, the following expression was proposed for the EVD:

$$\xi_{eq} = 0.03 + C \left(\frac{\mu - 1}{\mu\pi} \right) \quad (6.39)$$

where the coefficient C adopts the values reported in Table 6.21 for various joint typologies (assuming that column elastic deformations should be included in the formulation):

Table 6.21. C-values determined for various joint typologies.

Failure Mechanism of the 1 st bolts row	Joint Reference Number	C (for Eq.6.35)
Mode 2 End Plate	C1	0.282
Column Web Panel + Mode 1 Column Flange	C3	0.290
Mode 1 End Plate	C4	0.364
Mode 2 End Plate	C5*	0.181

*Joint with low rotation capacity should be avoided in the design.

Furthermore, it was found that the best correlation with inelastic displacement-reduction factors was obtained when Equation 6.39 was used in combination with Equation 6.38, in which x was set to 6.247. Given that the damping-dependent spectral scaling factor should give a value of 1.0 when the equivalent viscous damping is equal to 3% (the elastic damping value assumed in the analyses) then the following spectral scaling expression is assumed to lead to the best displacement-reduction factors for the results obtained:

$$R_\xi = (6.0 / (3 + \xi))^{0.5} \quad (6.40)$$

Moreover, the final displacement reduction factor expression can therefore be found as:

$$\eta = \left(0.06 / \left(0.06 + C \left(\frac{\mu - 1}{\mu\pi} \right) \right) \right)^{0.5} \quad (6.41)$$

$$\eta = \left(\frac{1}{\left(1 + \frac{C}{0.06} \left(\frac{\mu - 1}{\mu \pi} \right) \right)} \right)^{0.5} \quad (6.42)$$

$$\eta = \left(\frac{1}{\left(1 + C_\eta \left(\frac{\mu - 1}{\mu \pi} \right) \right)} \right)^{0.5} \quad (6.43)$$

Considering Equation 6.43, the final coefficients required to compute the inelastic displacement reduction factors are therefore those indicated in Table 6.22:

Table 6.22. C_η -values determined for various joint typologies.

Failure Mechanism of the 1 st bolts row	Joint Reference Number	C_η (for Eq.6.39)
Mode 2 End Plate	C1	4.7
Column Web Panel + Mode 1 Column Flange	C3	4.8
Mode 1 End Plate	C4	6.1
Mode 2 End Plate	C5*	3.0

*Joint with low rotation capacity should be avoided in the design.

As mentioned in the beginning of Section 6.6, the partial-strength joints of MRF structures chosen for the EVD and displacement spectra modification factors expressions improvement should be representative of the several plastic mechanisms defined in EC3-1-8 [CEN, 2005b], especially those with improved energy dissipation capacity, namely the column web in shear and the end plate in bending. In the case of the end plate in bending the T-stubs failure modes type one or type two can be considered. From the results obtained in Table 6.21 and Table 6.22 it is possible to conclude that the C1 and C3 joints achieved similar coefficients, because they are both governed predominantly by the column web in shear, although joint C1 exhibited a higher contribution from the other dissipative components. So the two joints can be considered governed by the column web in shear. With that in mind, the previous results can be grouped according to Table 6.23, and Equation 6.43 can be represented in the

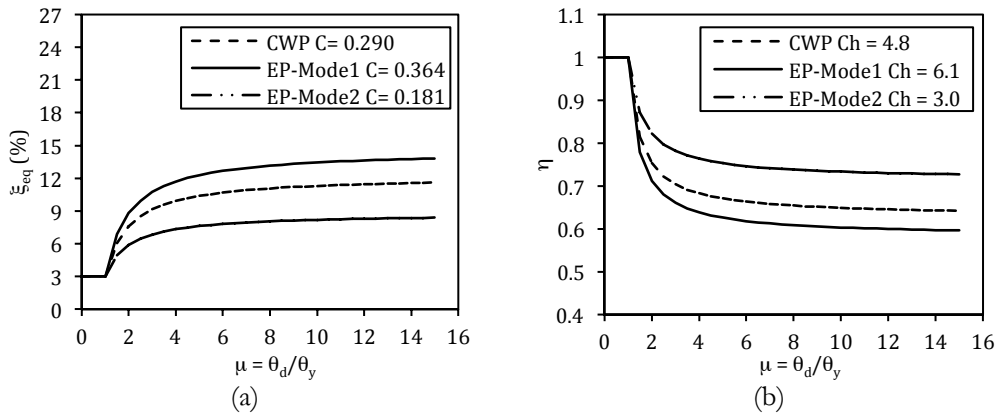


Figure 6.82.

Table 6.23. C and C_n -values determined for the several dissipative plastic mechanisms found in the end plate partial-strength joints.

Predominant Plastic Mechanism	C (for Eq.6.35)	C_n (for Eq.6.39)
Column web panel (predominant component) (CWP)	0.290	4.8
Mode 1 - end plate in bending (EP-Mode1)	0.364	6.1
Mode 2 – end plate and/or column flange in bending (EP-Mode2)	0.181	3.0*

*Joint with low rotation capacity should be avoided in the design.

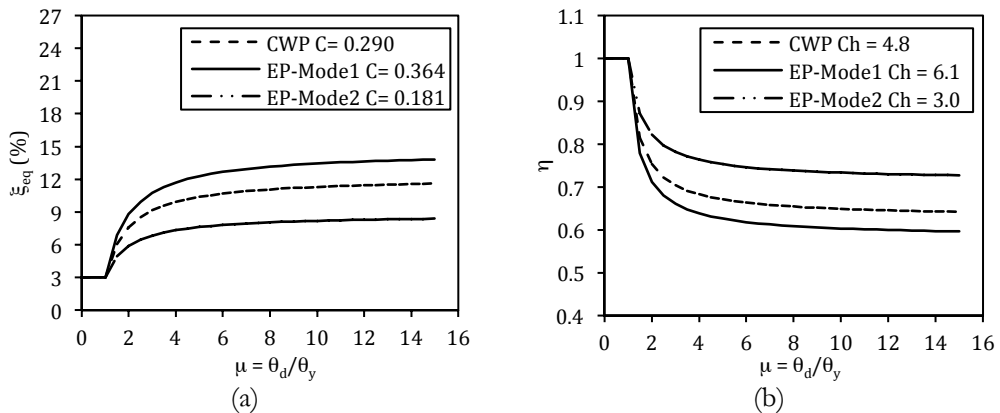


Figure 6.82. (a) Derived equivalent viscous damping factors; and (b) derived modification factors for the spectral displacement response for the several joints plastic mechanisms.

6.8 SUMMARY AND CONCLUSIONS

In this chapter, a review of the most relevant studies available in the literature in the field of end-plate beam-to column joints was carried out. The reviewing process involved the collection of experimental test data made available by several authors from numerous publications available in the literature. There is a considerable amount of work already undertaken in what concerns FE modelling of partial-strength joints. However, most of the research performed in the past focused essentially on studying monotonic behaviour, with very few studies addressing cyclic loading scenarios. A number of complex phenomena are associated with cyclic loading of joints, namely the loading protocol to consider, the kinematic hardening effect, re-contact effects, the potential for pinching, the stiffness and strength degradation, among others.

Although several approaches and different proposals can be found in the literature, there is a consensus within the scientific community regarding the use of the FE method to assess joint behaviour, provided that the models are previously validated against experimental test data. The FE models developed in this research were subjected to an extensive calibration with a selected set of experimental tests that were identified in the reviewing process. During the selection process, priority was given to the tests that considered beam-to-column joints with properties that were found to be realistic to be employed in medium to high-rise buildings located in seismic regions. Two types of FE models were developed, namely models of T-stub components and models of full connections.

Overall, the results obtained from the FE analyses revealed a good agreement with the experimental tests. The results allowed concluding that the plastic mechanism of type one, as defined in EC3-1-8, can be reproduced by FE analysis. However, in the case of the plastic mechanism of type two, due to the complex interaction between the connection elements, the results obtained with FE analysis showed some discrepancy with analytical predictions.

A parametric study was then conducted in a set of five joints with different behaviour characteristics, namely in terms of plastic mechanisms. The joints were modelled using the approaches that were previously validated. In one of the joints that was adopted for the calibration of the FE model, which served as a reference case, several geometrical properties were changed in order to obtain a full-strength joint, and three additional cases with partial-strength properties, designed to achieve the same level of strength, but with different governing plastic mechanisms. The results of the numerical models, using the ECCS procedure to determine the strength and stiffness of the joints were compared with the analytical results obtained using the component method. The comparison

revealed a relatively good agreement in terms of strength, but considerable differences were found for the joint case that was governed by the yielding of the column web in shear. In the case of the initial stiffness, some limitations were found in the application of Eurocode 3. The values of initial stiffness obtained with the code were significantly below the values obtained in the numerical models, with differences of 40% for the joint governed by the column web in shear and 35% for the full-strength joint.

In conclusion, the validation of the FE models revealed that they are able to reproduce the behaviour of the end-plate partial strength joints and also the several failure modes behaviour, therefore demonstrating the adequacy of the models to be employed in the behaviour assessment of beam-to-column connections using extended end-plate joints.

The models used in the parametric study were then used in the derivation of the ductility-equivalent viscous damping relationships needed for the direct displacement-based design procedure for MRF structures with partial-strength joints. A set of twenty records were used for several ductility demands in numerous non-linear time history (NLTH) analyses. A procedure to determine the equivalent viscous damping was proposed and then applied to the results from NLTH analyses, resulting in new expressions being proposed based on the better adjustment of the curves to the data obtained. In addition, an improvement to damping modifier expressions was proposed based on the ratio between the maximum inelastic displacement of the NLTH analyses and the elastic displacement obtained in the displacement spectra for 3% of elastic viscous damping, obtaining a reduction of the overall differences between the analytical values and the results of the NLTH analyses of 55 to 60 %. This resulted in the proposal of a new expression for spectral displacement-reduction factors that account for joint typology.

In conclusion, the improved expressions proposed in this work reduce the error in the adjustment to the results of the NLTH analyses and represent a contribution to the overall improvement of the DDBD procedure for steel MRF structures with partial strength joints.

6.9 REFERENCES

ABAQUS User's Manual – Version 6.11 and 6.12 (2011). ABAQUS, Inc., Dassault Systèmes Simulia Corp., Providence, USA.

Ádány, S., Dunai, L. [2004]. "Finite element simulation of the cyclic behaviour of end-plate joints," *Computers & Structures*, Vol. 82, pp. 2131-2143.

Ahmed, B., Nethercot, D.A. [1995] "Modelling composite connection response," *Proceedings of Connections in Steel Structures III*, Trento, Italy, pp. 259-268.

- Augusto, H., Castro, J.M., Rebelo, C., Simões da Silva, L. [2013] “Numerical simulation of partial-strength steel beam-to-column connections under monotonic and cyclic loading,” *Proceedings of the Congress on Numerical Methods in Engineering*, Bilbao, Spain, pp. 121-140.
- Azizinamini, A., Bradburn, J.H., Radziminski, J.B. [1985] “Static and cyclic behaviour of steel beam-column connections,” *Structural Research Studies*, Civil Engineering Department, University of South Carolina, USA.
- Bahaari, M.R., Sherbourne, A.N. [1996] “3D simulation of bolted connections to unstiffened columns - II. Extended endplate connections,” *Journal of Constructional Steel Research*, Vol. 40, No. 3, pp. 189-223.
- Bahaari, M.R., Sherbourne, A.N. [2000] “Behaviour of eight-bolt large capacity endplate connections,” *Computers and Structures*, Vol. 77, pp. 315-325.
- Bernuzzi, C. [1992] “Cyclic response of semi-rigid steel joints,” *Proceedings of 1st COST Workshop*, Strasbourg, France, pp. 194–2009.
- Bernuzzi, C., Zandonini, R., Zanon, P. [1996] “Experimental analysis and modelling of semi-rigid steel joints under cyclic reversal loading,” *Journal of Constructional Steel Research*, Vol. 38, No. 2, pp. 95-123.
- Burzi, O.S., Ferrario, F., Fontanari, V. [2002] “Nonlinear analysis of the low-cycle fracture behaviour of isolated Tee stub connections,” *Computers and Structures*, Vol. 80, pp. 2333-2360.
- Bursa, O.S., Galvani, M. [1997] “Low cycle behaviour of isolated bolted Tee stubs and extended end plate connections,” *Proceedings of CT4, Italian Conference on Steel Construction*, Ancona, Italy.
- Burzi, O.S., Jaspart, J.P. [1997a] “Benchmarks for finite element modelling of bolted steel connections,” *Journal of Constructional Steel Research*, Vol. 43, Nos. 1-3, pp. 17-42.
- Burzi, O.S., Jaspart, J.P. [1997b] “Calibration of a finite element model for isolated bolted end-plate steel connections,” *Journal of Constructional Steel Research*, Vol. 44, No. 3, pp. 225-262.
- Burzi, O.S., Jaspart, J.P. [1998] “Basic issues in the finite element simulation of extended end plate connections,” *Computers and Structures*, Vol. 69, pp. 361-382.

Calado, L. [2003] "Nonlinear cyclic model of top and seat with web angle for steel beam-to-column connections," *Engineering Structures*, Vol. 25, pp. 1189-1197.

Calado, L., Ferreira, J. [1994] "A numerical model for predicting the cyclic behaviour of steel beam-to-column joints," *Proceedings of 10th European Conference on Earthquake Engineering*, Vienna, Austria.

CEN [1992] "General rules and rules for buildings," *EN 1993 part 1-1. Eurocode 3*, European Committee for Standardization, Brussels.

CEN [1994] "Design of structures for earthquake resistance: General rules," *EN 1998 part 1. Eurocode 8*, European Committee for Standardization, Brussels.

CEN [2004] "Design of structures for earthquake resistance: General rules," *EN 1998 part 1. Eurocode 8*, European Committee for Standardization, Brussels.

CEN [2005a] "Design of steel structures: General rules and rules for buildings," *EN 1993 part 1-1. Eurocode 3*, European Committee for Standardization, Brussels.

CEN [2005b] "Design of steel structures: Design of joints," *EN 1993 part 1-8. Eurocode 3*, European Committee for Standardization, Brussels.

Chaboche, J. L. [1986] "Time independent constitutive theories for cyclic plasticity," *International Journal of Plasticity*, Vol. 2, No. 2, pp. 149-188.

Danesh, F., Pirmoz, A., Daryan, A.S. [2007] "Effect of shear force on the initial stiffness of top and seat angle connections with double web angles," *Journal of Constructional Steel Research*, Vol. 63, pp. 1208-1218.

Della Corte, G., De Matteis, G. and Landolfo, R. [2000] "Influence of connection modelling on seismic response of moment resisting steel frames," In: Mazzolani FM (ed.). *Moment Resistant Connections of Steel Buildings Frames in Seismic Areas*, E. & F.N. Spon, London, UK.

Del Salvio, A.A., Nethercot, D.A., Vellasco, P.C.G.S., Andrade, S.A.L., Martha, L.F. [2009] "Generalised component-based model for beam-to-column connections including axial versus moment interaction," *Journal of Constructional Steel Research*, Vol. 65, pp. 1876-1895.

De Martino, A., Landolfo, R., Mazzolani, F. M. [1990] "The use of the Ramberg-Osgood law for materials of round-house type," *Materials and Structures*, Vol. 23, pp. 59-67.

- Deng, C.G., Bursi, O., Zandonini, R. [2000] "A hysteretic connection element and its applications," *Computers and Structures*, Vol. 78, pp. 93-110.
- Dubina, D., Ciutina, A.L., Stratan, A. [2001] "Cyclic Tests of Double-Sided Beam-to Column Joints," *Journal of Structural Engineering*, Vol. 127, No. 2, pp. 129-136.
- Dubina, D., Ciutina, A.L. and Stratan, A. [2002] "Cyclic testes on bolted steel and composite double-sided beam-to-column joints," *Steel and Composite Structures*, Vol. 2, No. 2, pp. 147-160.
- Dunai, L., Kovács, N., Calado, L. [2004] "Analysis of Bolted End-plate Joints: Cyclic Test and Standard Approach," Proceedings of the V International Workshop in Connections in Steel Structures, Amsterdam, Netherlands, pp. 191-200.
- Dwairi, H.M., Kowalsky, M.J., Nau, J. M. [2007] "Equivalent Damping in Support of Direct Displacement-Based Design," *Journal of Earthquake Engineering*, Vol.11, No. 4, pp. 512-530.
- ECCS [1986] "Recommended Testing Procedure for Assessing the Behaviour of Structural Steel Elements Under Cyclic Loads," *Technical Committee 1, TWG 1.3 – Seismic Design*, publ. n.º 45, European Convention for Constructional Steelwork, Brussels, Belgium.
- Faella, C., Piluso, V., Rizzano, G. [1997] "A new method to design extended end plate connections and semirigid braced frames," *Journal of Constructional Steel Research*, Vol. 41, pp. 61-91.
- Faella, C., Piluso, V., Rizzano, G. [2000] *Structural steel semirigid connections: Theory, design and software*, CRC Press, USA.
- Flejou, J.L., Colson, A. [1992] "A general model for cyclic response of structural civil engineering connections," *Proceedings of 1st COST Workshop*, Strasbourg, France, pp. 419–430.
- Frye, M.J., Morris, G.A. [1975] "Analysis of flexibly connected steel frames," *Canadian Journal of Civil Engineering*, Vol. 2, pp. 280-291.
- Gerami, M., Saberi, H., Daryan, A.S. [2011] "Cyclic behaviour of bolted connections with different arrangement of bolts," *Journal of Constructional Steel Research*, Vol. 67, pp. 690-705.

Jacobsen, L.S. [1930] "Steady forced vibrations as influenced by damping," *ASME Transactione*, Vol. 52, No. 1, pp. 169–181.

Jaspart, J.P. [1991]. "Étude de la Semi-Rigidité des Noeuds Poutre-Colonne et son Influence sur la Resistance et la Stabilité des Ossatures en Acier," *Phd thesis*, Faculty of Applied Sciences, University of Liège, Belgium

Kato, B., Aoki, H., Yamanouchi, H. [1990] "Standardized mathematical expression for stress-strain relations of structural steel under monotonic and uniaxial tension loading," *Materials and Structures*, Vol. 23, pp. 47-58.

Kishi, N., Ahmed, A., Yabuki, N. [2001] "Nonlinear finite element analysis of top- and seat-angle with double web-angle connections," *Structural Engineering and Mechanics*, Vol. 12, No. 2, pp. 201-214.

Korol, R.M., Ghobarah, A., Osman, A. [1990] "Extended End-plate Connections Under Cyclic Loading : Behaviour and Design," *Journal of Constructional Steel Research*, Vol. 16, pp. 253-280.

Krishnamurthy, N. [1978]. "Fresh look at bolted end-plate behaviour and design," *Engineering Journal, AISC*, Vol. 15, No. 2, pp. 39-49.

Krishnamurthy, N., Graddy, D.E. [1976]. "Correlation between 2- and 3-Dimensional Finite Element Analysis of Steel Bolted End-Plate Connections," *Computers & Structures*, Vol. 6, No. 4-5, pp. 381-389.

Kukreti, A.R., Murray, J.M., Abolmaali, A. [1987]. "End-plate connections moment-rotation relationship," *Journal of Constructional Steel Research*, Vol. 8, pp. 137-157.

Lemaître, J., Chaboche, J.L. [1990] *Mechanics of solid materials*, Cambridge University Press, UK.

Madas, P.J., Elnashai, A.S. [1992] "A component-based model for beam-to-column connections," *Proceedings of 10th World Conference on Earthquake Engineering*, Vol. 8, Madrid, Spain.

Maggi, Y.I., Gonçalves, R.M., Calado, L. [2003] "Numerical and experimental behaviour of beam-to-column extended end plate connections," *Proceedings of the 4th International Conference STESSA 2003*, Naples, Italy.

- Maggi, Y.I., Gonçalves, R.M., Leon, R.T., Ribeiro, L.F.L. [2005] "Parametric analysis of steel bolted end plate connections using finite element modeling," *Journal of Constructional Steel Research*, Vol. 61, pp. 689-708.
- Maley, T., Roldán, R., Lago, A., and Sullivan, T.J. [2013] "Characterising the Seismic Behaviour of Steel MRF Structures," *Research Report EUCENTRE 2013/02*, IUSS Press, Pavia, Italy.
- Mazzolani, F.M. [1988] "Mathematical model for semi-rigid joints under cyclic loads," In R. Bjorhovde et al. (eds) *Connections in Steel Structures: Behaviour, Strength and Design*, Elsevier Applied Science Publishers, London, UK, pp. 112-120.
- Nemati, N., Le Houedec, D., Zandonini, R. [2000] "Numerical modelling of the cyclic behaviour of the basic components of steel end plate connections," *Advances in Engineering Software*, Vol. 31, pp. 837-849.
- Newmark, N.M., Hall, W.J. [1982] *Earthquake Spectra and Design*, EERI Monograph, Oakland, USA.
- Nogueiro, P., Simões da Silva, L., Bento, R. and Simões, R.. [2005] "Numerical implementation and calibration of a hysteretic model with pinching for the cyclic response of steel and composite joints", *Proceedings of Fourth International Conference on Advances in Steel Structures*, Vol. 1, pp. 767-774.
- Nogueiro, P., Simões da Silva, L., Bento, R. [2006(a)] "Numerical implementation and calibration of a hysteretic model for cyclic response of end-plate beam-to-column steel joints under arbitrary cyclic loading," *Proceedings of Computational Methods in Engineering and Science*, Sanya, China.
- Nogueiro, P.; Simões da Silva, L.; Bento, R.; Simões, R. [2006(b)] "Experimental behaviour of standardised European end plate beam-to-column steel joints under arbitrary cyclic loading,". *Proceedings of the Stability and Ductility of Steel Structures*. 2, Lisbon, Portugal, pp.951-960.
- Nogueiro, P., Simões da Silva, L., Bento, R. Simões, R. [2007] "Numerical implementation and calibration of a hysteretic model with pinching for the cyclic response of steel joints," *Advanced Steel Construction*, Vol. 3, No. 1, pp. 459-484.
- Nogueiro, P. [2009] "Comportamento Dinâmico de Ligações Metálicas," *PhD Thesis in Civil Engineering*, University of Coimbra, Portugal.

- Pennucci, D., Sullivan, T.J., Calvi, G.M. [2011] "Displacement Reduction Factors for the design of medium and long-period structures" *Journal of Earthquake Engineering*, Vol. 15, Supplement 1, pp. 1-29.
- Piluso, V., Rizzano, G. [2008] "Experimental analysis and modelling of bolted T-stubs under cyclic loads," *Journal of Constructional Steel Research*. Vol. 64, No.1, pp. 655–669.
- Pirmoz, A., Daryan, A.S., Mazaheri, A., Darnandi, H.E. [2008a] "Behaviour of bolted angle connections subjected to combined shear force and moment," *Journal of Constructional Steel Research*, Vol. 64, pp. 436-446.
- Pirmoz, A.; Mohammadrezapour, E. [2008(b)] "Behaviour of bolted top-seat angle connections under combined axial tension and moment loading,". *Proceedings of the 14th World Conference on Earthquake Engineering*, Beijing, China.
- Pirmoz, A., Khoei, A.S., Mohammadrezapour, E., Daryan, A.S. [2009] "Moment_rotation behaviour of bolted top-seat angle connections," *Journal of Constructional Steel Research*, Vol. 65, pp. 973-984.
- Plumier, A., Schleich, J.B. [1993] "Seismic Resistance of Steel and Composite Frame Structures," *Journal of Constructional Steel Research*, Vol. 27, pp. 159-176.
- Popov, E.P. [1987] "Panel Zone Flexibility in Seismic Moment Joints," *Journal of Constructional Steel Research*, Vol. 8, pp. 91-118.
- Priestley, M.J.N., Calvi, G.M., Kowalsky, M.J., [2007]. *Displacement-Based Seismic Design of Structures*, IUSS Press, Instituto Universitario de Studi Superiori de Pavia, Italy.
- Ramberg, W., Osgood, W.R. [1943] "Description of stress-strain curves by three parameters," *Monograph N.^o 4*, Publicazione Italsider, Nuova Italsider, Genova, Italy.
- Richard, R.M. and Abbott, B.J., (1975). "Versatile elastic-plastic stress-strain formula;," *Journal of the Engineering Mechanics Division, ASCE*, Vol. 101, No. 4, pp. 511-515.
- SeismoSoft srl [2012] SeismoSignal, SeismoSoft Ltd., Inc., Earthquake Engineering Software Solutions, Greece, [online]. Available from URL: <http://www.seismosoft.com>.
- SeismoSoft srl [2011] SeismoStruct, SeismoSoft Ltd., Inc., Earthquake Engineering Software Solutions, Greece, [online]. Available from URL: <http://www.seismosoft.com>.

- Shen, J., Astaneh-Asl, A. [1999] "Hysteretic behaviour of bolted-angle connections," *Journal of Constructional Steel Research*, Vol. 51, pp. 201-218.
- Sherbourne, A.N., Bahaari, M.R. [1994] "3D simulation of end-plate bolted connections," *Journal of Structural Engineering*, Vol. 120, No. 11, pp. 3122-3136.
- Sherbourne, A.N., Bahaari, M.R. [1996] "3D simulation of bolted connections to unstiffened columns - I. T-stub connections," *Journal of Constructional Steel Research*, Vol. 40, No. 3, pp. 169-187.
- Shi, G., Shi, Y., Wang, Y., Bradford, M.A. [2008] "Numerical simulation of steel pretensioned bolted end-plate connections of different types and details," *Engineering Structures*, Vol. 30, pp. 2677-2686.
- Simões da Silva, L., Girão Coelho, A.M [2001] "An analytical evaluation of the response of steel joints under bending and axial force," *Computers and Structures*, Vol. 79, pp. 873-881.
- Simões, R., Simões da Silva, L. and Cruz, P. [2001] "Cyclic behaviour of end-plate beam-to-column composite joints," *International Journal of Steel and Composite Structures*, Vol. 1, No. 3, pp. 355-376.
- Steenhuis, M., Evers, H., Gresnigt, N. [1996] "Conceptual design of joints in braced steel frames," *Proceedings of LABSE Semi-Rigid Structural Connections Colloquium*, Istanbul, Turkey, pp 327- 336.
- Sullivan, T.J., Priestley, M.J.N., Calvi, G.M., Editors [2012]. *A Model Code for the Displacement-Based Seismic Design of Structures, DBD12*, IUSS Press, Pavia.
- Sumner, E.A., Murray, T.M. [2002] "Behaviour of extended end-plate moment connections subjected to cyclic loading", *Journal of Structural Engineering*, Vol. 128, No. 4, pp. 501-508.
- Takhirov, S.M., Popov, E.P. [2002] "Bolted large seismic steel beam-to-column connections Part 2: numerical nonlinear analysis," *Engineering Structures*, Vol. 24, pp. 1535-1545.
- Von Mises, R. [1913] "Mechanik der festen Körper im plastisch-deformablen Zustand," *Nachrichten von der Gesellschaft der Wissenschaften zu Göttingen, Mathematisch-Physikalische Klasse*, Vol. 1913, pp. 582-592.
- Yang, C.M., Kim, Y.M. [2007] "Cyclic behaviour of bolted and welded beam-to-column joints", *International Journal of Mechanical Sciences*, Vol. 49, No. 5, pp. 635-649.

Zandonini, R., Bursi, O.S. [2002] "Monotonic and hysteretic behaviour of bolted endplate beam-to-column joints," *Proceedings of Advanced in Steel Structures, Vol. 1*, Hong Kong, China.

Ziomek, D., Tomana, A., Waszczyszyn, Z. [1992] "Finite element modeling of end plate connection versus experimental results," *Proceedings of 1st COST Workshop*, Strasbourg, France, pp. 433-442.

7. SUMMARY OF THE DISTEEL PROJECT RECOMMENDATIONS FOR THE CHARACTERISATION OF STEEL BEAM-COLUMN JOINTS

Timothy J. Sullivan, Gerard J. O'Reilly, Francesco Morelli, Walter Salvatore, Gaetano Della Corte, Giusy Terraciano, Gianmaria Di Lorenzo, Raffaele Landolfo, Hugo Augusto, José Miguel Castro, Carlos Rebelo & Luís Simões da Silva

7.1 SUMMARY

This document has reported on a detailed study of steel beam-column assemblages, with careful consideration of how the joint typology can be accounted for when characterising a steel MRF. The work has focused on identifying characteristics (deformation capacity, yield drift and equivalent viscous damping expressions) required for displacement-based design (DBD), but has also permitted an examination of cyclic behaviour that is sure to prove very useful in general for performance-based earthquake engineering of steel MRFs.

The first two chapters of the report provided the motives for a study into the behaviour of beam-column joints, with a review of the DBD approach and identification of aspects needing more research. Chapter 3 provided a valuable summary of experimental data currently available in the literature for what regards fully welded and bolted extended end-plate connections.

Chapter 4 then proceeded to use existing experimental data to assist in characterising steel MRFs with full-strength rigid joints. The Richard-Abbot hysteretic model was calibrated to experimental test results and the calibrated models were used to calibrate expressions for the equivalent viscous damping of steel frames by conducting NLTH analyses on SDOF systems subject to a number of accelerograms. Finally, by comparing displacement-reduction factors obtained from the new approach with the equivalent expression from Priestley et al. [2007] for steel MRFs with full-strength rigid joints, it was found that existing expressions for equivalent viscous damping of steel frames work well, provided they are used in conjunction with an appropriate spectral scaling expression.

Chapter 5 explored the possibilities of characterising beam-column assemblages using the component-method, which is a method permitted by the European standard EC3. After explaining the basis of the component method, experimental results obtained from the literature (listed in Chapter 3) were examined and various response quantities were compared with those predicted using the component method. This comparison found that overall the component method provides a good estimate of the strength of bolted end-plate joints, with the ratio of predicted to experimentally observed strength equal to 0.91 on average, with a coefficient of variation (COV) of 0.21, as shown in Table 7.1. In contrast, the component method does not currently appear to be very effective in estimating the connection initial stiffness, tending to overestimate with Table 7.1 showing an average mean ratio of predicted to experimental values of 1.80, with a coefficient of variation of 0.59. The experimental results were also examined in order to identify the typical deformation capacity of bolted end-plate joints and this was found to be significantly influenced by the ultimate failure mode. Provided that bolt-failure is avoided (i.e. EC3 mode 1 type failure), then extended end plate connections appear to be able to sustain a plastic rotation demand around 25mrad (with some test results indicating more than 50mrad capacity). A parametric analysis was then undertaken that assisted in the formulation of simplified design expressions for the strength and stiffness of bolted extended end-plate joints. Finally, a new simplified expression for the yield drift of beam-column assemblages was derived that is able to consider either full-strength or partial-strength joints and also accounts for the connection stiffness.

Table 7.1. Ratio of component method predicted to experimental values of stiffness and resistance.

	Initial Stiffness			Plastic Resistance		
	Mean	Std Dev	COV	Mean	Std Dev	COV
Extended End-Plates	1.46	0.84	0.58	0.87	0.18	0.21
Flush End-Plates	2.62	1.12	0.43	1.07	0.17	0.16
Extended & Flush End Plates	1.8	1.06	0.59	0.91	0.19	0.21

Chapter 6 explored the possibilities of characterising beam-column assemblages used advanced finite-element (FE) models subject to cyclic analyses. After reviewing the state-of-the-art for what regards FE modelling and analysis, experimental results were examined in detail to consider the observed strength, stiffness, rotation capacity and ductility capacity of a large number of partial-strength connections. This review of experimental results indicated that extended end-plate connections offer reasonably good characteristics that could be suitable for use in seismic regions. Subsequently, a selection of experimental test results were used to calibrate finite element models of bolted extended end-plate joints, with a detailed description of the modelling assumptions provided. This chapter therefore provided useful guidance for the FE modelling and analysis of beam-column joints and the results of experimental tests showed that the approach can accurately predict the strength, stiffness and different possible failure

modes of extended end-plate beam-column joints. The chapter also included a study of the equivalent viscous damping and spectral displacement reduction factors (to be used to scale elastic displacement spectra to inelastic displacement spectra) for a selection of partial-strength extended end-plate beam-column joints. The results obtained from this study will be summarised in Section 7.5.

7.2 EXPRESSION FOR THE INITIAL STIFFNESS AND PLASTIC RESISTANCE OF STEEL BEAM-COLUMN ASSEMBLAGES

Following the characterisation of the component method for beam-column joints using experimental test results, an additional parametric study was carried out in Chapter 5 to develop a set of expressions to represent the initial stiffness and plastic resistance of the connections.

In terms of the initial stiffness, the expression developed in Chapter 5 is as follows:

$$k_b = \left[8.343 \left(\frac{d}{t_{fc}} \right)^3 - 33.3 \left(\frac{d}{t_{fc}} \right)^2 + 47.32 \left(\frac{d}{t_{fc}} \right) + 0.865 \right] k_{ref} \quad (7.1)$$

where k_{ref} is a reference coefficient which depends on column and beam shapes given by:

$$k_{ref} = \alpha_{kref} b_b + \beta_{kref} \quad (7.2)$$

$$\alpha_{kref} = -5 \cdot 10^{-8} b_c^2 + 4 \cdot 10^{-5} b_c - 0.0075 \quad (7.3)$$

$$\beta_{kref} = 1 \cdot 10^{-5} b_c^2 - 0.0075 b_c + 2.133 \quad (7.4)$$

where b_b and b_c are the beam and column cross section depth, respectively, where all dimensions are in terms of mm, kN and mrad. The expression described above has been developed with the assumptions that the thickness of the end-plate is equal to that of the column flange and continuity plates have been employed in the detailing of the columns. As can be noted above, this expression depends on relatively few terms, namely the height of both beam and column sections and the thickness of the column flange, making it a relatively simple expression to use when evaluating the initial stiffness offered by a bolted end-plate connection.

For the estimation of the plastic resistance provided by connections using European section sizes, the following two expressions have been proposed in Chapter 5:

$$m_b = \left[2.205 \left(\frac{d}{t_{fc}} \right) - 0.524 \right] m_{ref} \leq m_{ref} \quad (\text{HEM 120 - HEM140}) \quad (7.5)$$

$$m_b = \left[1.690 \left(\frac{d}{t_{fc}} \right) - 0.371 \right] m_{ref} \leq m_{ref} \quad (\text{HEM 160 - HEM 400}) \quad (7.6)$$

where the term m_{ref} is given by:

$$m_{ref} = \alpha_{mref} h_b + \beta_{mref} \quad (7.7)$$

which is further aggregated depending on the section sizes being employed, with the terms α_{mref} and β_{mref} given by:

$$\alpha_{mref} = -1.404 \cdot 10^{-7} h_c^2 + 9.466 \cdot 10^{-5} h_c - 0.0169 \quad (\text{HEM 120 - HEM 280}) \quad (7.8)$$

$$\alpha_{mref} = 9.282 \cdot 10^{-4} \quad (\text{HEM 300 - HEM 400}) \quad (7.9)$$

$$\beta_{mref} = -5.799 \cdot 10^{-3} h_c + 3.142 \quad (\text{HEM 120 - HEM 280}) \quad (7.10)$$

$$\beta_{mref} = 0.003 h_c + 0.344 \quad (\text{HEM 300 - HEM 400}) \quad (7.11)$$

Again, the expression provided for the estimation of the plastic resistance offered by steel beam-column connections with bolted end-plates is a function of relatively few terms. These are again the height of both the beam and column section sizes and also the thickness of the column flange. Again, the assumptions regarding end-plate thickness and continuity plates have been used in the development of this expression.

7.3 DESIGN EXPRESSION FOR THE DEFORMATION CAPACITY OF STEEL BEAM-COLUMN ASSEMBLAGES

The plastic deformation capacity of beam-column assemblages has been examined in chapters 4, 5 and 6 of this report through examination of existing experimental data. Ranges of plastic rotation capacities were observed, and it was concluded that the plastic rotation capacity in partial-strength joints was heavily dependent on the failure mechanism (e.g. end-plate yielding versus bolt failure versus a mixed mechanism in which both end-plates and bolts yield). With the objective of arriving at a set of plastic rotation capacities for beam-column joints that could be used for seismic design, the results in the various chapters have been reviewed and the plastic rotation limits provided in Table 7.2 are proposed.

Table 7.2. Design plastic rotation capacity for different beam-column joint typologies.

Joint Typology	Local mechanism	Plastic Rotation Capacity θ_p (mrad) ¹
Full-strength Fully Welded	Beam yielding	35
Partial-strength Bolted Extended End-Plate	Mode-1 type T-stub yielding	$9465/\zeta$
Partial-strength Bolted Extended End-Plate	Mode-2 type T-stub yielding ²	$53.23(d/t_p) - 39.04$
Partial-strength Bolted Extended End-Plate	Mode-3 type T-stub yielding ³	$2375/\zeta$

¹ The term ζ is the effective lever arm depth in mm (evaluated according to the simplified method of EC3), d is the bolt diameter in mm and t_p is the thickness of the end-plate in mm.

² Joints with Mode-3 type T-stub yielding are not recommended for use in seismic regions.

³ This expression for mode 2 type yielding is only considered valid for ζ equal to 290mm. Furthermore, θ_p should not be taken greater than the θ_p for mode 1 type mechanisms or less than the θ_p value for mode 3 type mechanisms.

The limits indicated in Table 7.2 are supported by the results of experimental testing but nevertheless, should be considered relatively preliminary since the number of experimental test results was fairly limited, particularly in the case of partial strength extended end-plate failure mode type 2, and because a large number of factors can affect the final deformation capacity, as discussed in Chapters 4, 5 and 6. While the relation between plastic rotation capacity and lever arm has been acknowledged in Table 7.2 for partial strength joints, further testing should be conducted to confirm this relation. In addition, it should be noted that for the plastic capacity of partial strength extended end-plate joints with failure mode type 2, the relation given in Table 7.2 is only valid for a lever arm of 290mm, since the available data was for a single value of ζ , despite the dependence of the plastic capacity on this parameter being noted in Section 5.3.2.6.

7.4 DESIGN EXPRESSION FOR THE YIELD DRIFT OF STEEL BEAM-COLUMN ASSEMBLAGES

As previously mentioned, an expression for calculation of the yield drift of connections is essential for displacement-based design of MRFs, as this allows for the design ductility to be determined and hence, the appropriate value of equivalent viscous damping to be used. Chapter 5 outlined that while expressions for the calculation of MRF yield drift have been previously developed, these typically focused on the deformation of full-strength connections with the only contribution coming from the elastic shear deformations provided by the column web. This study has advanced on such yield drift

expressions to include the additional deformations associated with flexible and partial-strength connections. Analytical developments in Chapter 5 now permit the consideration of the additional deformations associated with flexible and partial strength connections by:

$$\theta_y \approx \frac{m_{b,R}\varphi_{b,y}}{6} \left(\psi_{jb} + \frac{1}{2} \frac{I_b}{I_c} \frac{b}{L_b} \right) \quad (7.12)$$

where $m_{b,R}$ represents the ratio between the minimum connection resistance and the beam section plastic resistance, I_b and I_c and the second moments of area of the shear area of both beam and column sections, respectively, b is the distance between the two points of zero moment along the column length and L_b is the distance from the beam end to the point of zero moment along the beam. The parameters $\varphi_{b,y}$ and ψ_{jb} are given by:

$$\varphi_{b,y} = \frac{M_{b,pl}L_b}{EI_b} \quad (7.13)$$

$$\psi_{jb} = 1 + 6 \frac{EI_b}{S_{j,ini} L_b} \quad (7.14)$$

where $S_{j,ini}$ is the initial stiffness of the beam-to-column joint and E is the Young's modulus of steel.

7.5 EQUIVALENT VISCOUS DAMPING EXPRESSIONS AND SPECTRAL DISPLACEMENT REDUCTION FACTORS

For the design of steel MRF structures using the displacement-based design methodology outlined in Chapter 2, an expression for the equivalent viscous damping provided by both the elastic and hysteretic damping associated with the specific structural system being employed is required. Prior to this work, EVD expressions for full-strength connections were available in the form of Ramberg-Osgood or bilinear hysteresis rules, which were deemed representative of steel MRFs with full-strength joints. Following the development and validation of numerical models to represent both full strength and flexible/partial strength connections in Chapters 4 to 6, a set of equivalent viscous damping expressions have been developed to incorporate the specific characteristics of these connection types when designing steel MRFs. The general format of these expressions is:

$$\xi = \xi_{el} + \xi_{hyst} = \xi_{el} + C \left(\frac{\mu - 1}{\mu\pi} \right) \quad (7.15)$$

where the C factor represents a constant value depending on the type of structure and its associated hysteretic properties. In the DBD method, the value of EVD for a given ductility of a certain structure type is found and from this, a spectral displacement reduction factor (η) is found to reduce the design displacement spectrum for the appropriate amount of equivalent viscous damping. Since the EVD is a function only of the structure ductility, and the spectral displacement reduction factor is a function of the EVD, it may be considered more convenient to represent the spectral displacement reduction factor directly as a function of ductility by simply combining the expressions. Using the spectral displacement reduction factor relation provided by Eurocode 8 [CEN, 2004] and assuming 5% elastic damping, this can be achieved by:

$$\eta = \sqrt{\frac{0.10}{0.05 + \xi}} \quad (7.16)$$

and substituting in Eq. 7.15 gives:

$$\eta = \sqrt{\frac{0.10}{0.05 + 0.05 + C\left(\frac{\mu-1}{\mu\pi}\right)}} = \sqrt{\frac{1}{1 + C_\eta\left(\frac{\mu-1}{\mu\pi}\right)}} \quad (7.17)$$

where C_η is a coefficient that should be calibrated using the results of NLTH analyses. From the expression in Equation 7.17, it can be seen that the spectral displacement reduction factor is now expressed directly as a function of the system ductility. Importantly, Pennucci et al. [2011] showed that such ductility-dependent spectral displacement-reduction factors are more appropriate because calibrated equivalent viscous damping expressions are particularly sensitive to the ground motion characteristics used for their development.

For the cases of both full-strength and partial-strength connections for MRFs, extensive NLTH analyses reported on in Chapters 4 and 6 have lead to the spectral displacement reduction coefficients, C_η , summarised in Table 7.3. Note that the elastic damping used to derive the equations was set at 3% of critical damping, except for the full strength fully-welded case that adopted a 5% damping value.

Table 7.3. C_r -values determined for various joint typologies.

Type of Joint	Joint Strength Classification	Predominant Plastic Mechanism	C_r (for Eq. 7.17)
Fully welded	Full-strength	Beam and/or column web panel ⁽¹⁾	8.2
Bolted end plate	Partial-strength	Column web panel (predominant component) ⁽²⁾	4.8
Bolted end plate	Partial-strength	Mode 1 - end plate in bending ⁽³⁾	6.1
Bolted end plate	Partial-strength	Mode 2 - end plate and/or column flange in bending ⁽⁴⁾	3.0

- (1) For the case of fully welded full-strength joints, mixed beam and panel zone yielding is permitted for this typology. These values are appropriate for compact (Class 1) beam sections.
- (2) Although the predominant component for the energy dissipation in the joint is the column web panel in shear, other dissipative components can, and should, also be associated in the contribution to the energy dissipation, such as the end plate and/or the column flange in bending. However, these components may have limited rotation capacity, which in turn affects the amount of energy dissipated. The proposed coefficient was derived from two types of joints. The first presents a strong contribution from the column web in shear and only a small contribution of the end plate, working in a plastic mechanism type 2 with limited rotation capacity (the presence of continuity web stiffeners limits the deformation of the column flanges). The second joint is clearly governed by the column web panel with a small contribution of the column flanges in bending. Note that these two joint typologies had very different deformation capacities even though the effects of energy dissipation on seismic demands were similar.
- (3) The spectral displacement reduction coefficient, C_r , achieved for this kind of joint behaviour, taken as 6.1, was computed in Chapter 6 for joints with large rotation capacity (see Figure 6.55) dissipating a high amount of energy. However, this type of joint possessed reduced stiffness and strength, adopted to define an upper bound in the procedure as it may be prudent to adopt in practice.
- (4) In contrast to the previous typology (2), this type of joint presented lower rotation and energy dissipation capacity due to the influence of the bolts in the type 2 plastic mechanism, and so it can be considered a represent a lower bound for the reduction coefficient, $C_r = 3.0$.

7.6 UNCERTAINTIES AND AREAS FOR FUTURE RESEARCH

While the work presented in this report represents positive developments for the characterisation of the seismic behaviour of beam-column connections in MRFs, a number of uncertainties and areas of further development can be recognised.

One uncertainty arises from the definition of the yield point of the connection's moment-rotation behaviour, as this nonlinear behaviour is typically bilinearised (see for example, Figure 5.20). This demonstrates that the actual behaviour of beam-column connections demonstrate no obvious yield point that is traditionally assumed and is more of a gradual change in stiffness when going from initial elastic to plastic behaviour. As such, the precise definition of the yield point is a matter of convention being employed, and should an alternative definition be used, designers ought to be aware of the implications of this with respect to the work presented here.

The effects of fatigue on a connection's behaviour have not been incorporated into the work presented here. This could be particularly relevant in the case of seismic design, as systems susceptible to the effects of low-cycle fatigue could be adversely affected by the occurrence of foreshocks before the main seismic event and may exhibited a different behaviour to that observed without the inclusion of fatigue. Hence, this is an area of future research that should be considered in the characterisation of beam-column connections in MRFs.

For the equivalent viscous damping expressions developed for the various joint typologies studied, a major limitation of these expressions is the limited number of ground motions used for establishing these expressions. As observed in Chapter 4 and 6, a fair amount of scatter was observed in the calibration of such expressions. This was partly due to the computation time require to evaluate and calibrate the equivalent system's response to be representative of the actual nonlinear behaviour and as a number of ground motions were used for this calibration of these expressions.. Nevertheless, the general trend of the data available is clear and hence, the expressions previously discussed are proposed. However, further analysis that incorporates a larger ground motion set could be used to better calibrate these expressions as part of future studies.

Uncertainty also arises in the definition and justification of elastic damping to be used in the calibration of equivalent viscous damping expressions. A nominal value of 3% has been used here for the MRFs with partial strength joints (Chapter 6) whereas 5% damping was adopted for the studies of MRFs with full-strength welded joints (Chapter 4). The actual elastic damping is likely to be structural configuration dependent, with bolted and riveted connections typically providing more frictional energy dissipation than welded connections. The actual quantification of damping values is not so straightforward, however, it is also affected by other sources of energy dissipation, as explained in Priestley *et al.* [2007]. Whilst 3% damping is currently considered reasonable for steel frames, the exact values represent an important uncertainty and should be investigated as part of future studies.